Platinum Complexes of Bicyclopropylidene and Related Ligands

by

Sarah Amy Hoyte

Victoria
UNIVERSITY OF WELLINGTON
Te Whare Wānanga
o te Ūpoko o te Ika a Māui

A thesis
submitted to the Victoria University of Wellington
in fulfilment of the requirements for the degree of
Doctor of Philosophy
in Chemistry

Victoria University of Wellington
2014

Abstract

The coordination chemistry of the cyclopropyl-substituted alkenes, bicyclopropylidene (BCP) and methylenecyclopropane (MCP), with platinum was explored. A range of complexes with η^2-alkene ligands were synthesised by the displacement of a ligand, typically ethene, from a precursor complex. These complexes are [Pt(L)(P—P)] (L = BCP, MCP; P—P = $Ph_2P(CH_2)_3PPh_2$, $Cy_2P(CH_2)_2PCy_2$, $^tBu_2P(CH_2)_2P^tBu_2$, $^tBu_2PCH_2(o\text{-}C_6H_4)CH_2P^tBu_2$), [Pt(L)(P—S)] (L = BCP, MCP; P—S = $^tBu_2PCH_2(o\text{-}C_6H_4)CH_2S^tBu$), [Pt($C_2H_4$)(L)($PR_3$)] (L = BCP, MCP; PR_3 = PPh_3, PCy_3), [Pt(MCP)$_2$(PR_3)] (PR_3 = PPh_3, PCy_3) and [$PtCl_2$(L)(L′)] (L = BCP, MCP; L′ = Py, DMSO). These were the first examples of platinum complexes with η^2-BCP ligands, and the first bis-MCP Pt complexes.

BCP underwent ring-opening reactions with both Pt(0) and Pt(II) complexes to form the 1,3-diene allylidenecyclopropane (ACP). The first transition metal complexes of ACP [Pt(ACP)(P—P)] (P—P = $Ph_2P(CH_2)_3PPh_2$, $Cy_2P(CH_2)_2PCy_2$, $^tBu_2P(CH_2)_2P^tBu_2$) were synthesised. Some of these complexes rearranged to form η^2:σ^2-metallacyclopentene complexes, the first instances of the formation of η^2:σ^2-metallacyclopentene complexes from η^2:π-diene complexes. With MCP, the ring-opening reaction only occurred with [$PtEt_2$(COD)], as a result of the anti-Markovnikov addition of Pt–H, generated by the β-hydride elimination of an Et group, across the double-bond. The major products of this reaction were the 1-methylcyclopropyl complexes [Pt($C(CH_2)_2CH_3$)Et(COD)] and [Pt($C(CH_2)_2CH_3$)$_2$(COD)], the first examples of such complexes.

Protonation of [Pt(L)(P—P)] resulted in a ring-opening reaction to form both the 2-substituted and 1-methyl allyl complexes, [Pt(η^3-CH_2CRCH_2)(P—P)]$^+$

(R = ^{c}Pr, Me; P—P = $Ph_2P(CH_2)_3PPh_2$, $^{t}Bu_2PCH_2(o\text{-}C_6H_4)CH_2P^{t}Bu_2$) and $[Pt(\eta^3\text{-}CR_2CHCHMe)(P—P)]^+$ (R = ^{c}Pr, Me; P—P = $Ph_2P(CH_2)_3PPh_2$, $^{t}Bu_2PCH_2(o\text{-}C_6H_4)CH_2P^{t}Bu_2$). The analogous 1-methyl complexes were also formed from [Pt(L)(P—S)], wherein the alkene reacted with a hydride formed by the *ortho*-metallation of the P—S ligand. Computational models were used to investigate the formation of the allyl structures and it was found that the activation energy had a more significant effect than complex stability on product distributions.

Complexes with β-chloroalkyl ligands $[Pt(C(CH_2)_2CR_2Cl)Cl(L)_2]$ (R = CH_2, H, L = SEt_2, $NC^{t}Bu$, Py) were formed by the addition of Pt–Cl across the alkene double bond. Phosphine complexes were formed by the displacement of a ligand from *cis*–$[Pt(C(CH_2)_2CR_2Cl)Cl(Py)_2]$ (R = CH_2, H). These are the first examples of stable Pt(II) β-haloalkyl complexes. It was found using computational models that the presence of cyclopropyl rings had a stabilising effect on these complexes.

Acknowledgments

Writing the acknowledgments section has turned out to be a difficult task. There are so many people who have helped and supported me over the years, I'm sure I'll miss some. The most important person to thank would have to be my supervisor Prof. John L. Spencer, for all of the support and guidance over the years.

I would like to thank the members of my research group, both past and present – Kathryn, Teresa, Melanie, Brad, Chris, Rosie, Almas, David and Jacqui. Climbing Mount PhD with you has been exhilarating, heartbreaking and everywhere in between, but ultimately rewarding. Thank you for all of your support, ideas, proofreading and the myriad of other ways you have helped me.

I am grateful for the help and support that numerous other people at SCPS have provided me with. Dr. Joanne Harvey, my second supervisor; Dr. Matthias Lein, for the computational chemistry guidance; Ian Vorster, Dr. John Ryan, Dr. Jono Singh and Assoc. Prof. Peter Northcote, for NMR-related assistance; Helen, Jaime-Anne, Jackie, Teresa, Gordon, Sally, Lisa, Kara, Dan and other general staff, for all manner of things. Also thank you to Dr. Jan Wikaira at the University of Canterbury for collection of the single-crystal X-ray data.

Thank you to both my chemistry and non-chemistry friends for all of the support, distraction, entertainment and sanity. Thank you to my family, particularly my Grandad, for help and support over the years. A huge thank you to Mel Abbott of Empower Therapies for teaching me how to be healthy again.

Lastly, thank you to the Curtis-Gordon Research Scholarship in Chemistry and the Victoria University Doctoral Scholarship/Assistantship for funding.

Contents

List of Figures

List of Schemes

List of Tables

Glossary

acac	acetylacetonate
ACP	allylidenecyclopropane
BCP	bicyclopropylidene (cyclopropylidenecyclopropane)
br	broad
COD	cycloocta-1,5-diene
Cp	cyclopentadiene
Cp#	2-(di-*tert*-butylphosphanyl)-P-ethyl)cyclopentadienyl
^{c}Pr	cyclopropyl (C_3H_5)
Cy	cyclohexyl (C_6H_{11})
cyp	cyclopentyl (C_5H_9)
d	doublet
dbpe	1,2-bis(di-*tert*-butylphosphino)ethane
dbpx	1,2-bis[(di-*tert*-butylphosphino)methyl]benzene
DBU	1,8-Diazabicycloundec-7-ene
dcyppe	1,2-bis(dicyclopentylphosphino)ethane
DMSO	dimethylsulfoxide
dppe	1,2-bis(diphenylphosphino)ethane
dppp	1,3-bis(diphenylphosphino)propane
Et	ethyl (C_2H_5)
EWG	Electron-Withdrawing Group
HOMO	Highest Occupied Molecular Orbital
IR	infrared

^{i}Pr	*iso*-propyl ($HC(CH_3)_2$)
LUMO	Lowest Unoccupied Molecular Orbital
m	multiplet
M	metal
MCP	methylenecyclopropane
Me	methyl (CH_3)
nb	norbornene (dicyclo[2.2.1]hept-2-ene)
NMR	Nuclear Magnetic Resonance
Nu	nucleophile
Ph	phenyl (C_6H_5)
P—C	C_6H_3-*o*-$CH_2P^tBu_2$-*m*-CH_2S^tBu
P—S	$^tBu_2PCH_2$(*o*-C_6H_4)CH_2S^tBu
PTA	1,3,5-triaza-7-phosphaadamantane
4-Py	4-pyridyl (4-C_5H_5N)
Py	pyridine (C_5H_5N)
q	quartet
quint	quintet
s	singlet
t	triplet
^{t}Bu	*tert*-butyl ($C(CH_3)_3$)
TFP	trifurylphosphine
TM	transition metal
4-Tol	4-tolyl (4-$C_6H_4CH_3$)

Chapter 1

Introduction

1.1 Transition Metal Chemistry of Alkenes

1.1.1 Introduction

Alkene complexes of transition metals, particularly platinum, are among the most extensively studied organometallic compounds.[1] The first transition metal-alkene complex was $K[PtCl_3(C_2H_4)].H_2O$, or Zeise's salt, which was synthesised in 1830.[2] Alkene complexes are common intermediates in catalytic cycles, and several model complexes have been synthesised over the years in order to lend insight into the processes that occur during catalysis.[1]

1.1.2 Bonding

When the X-ray crystal structure of Zeise's salt was solved in 1953, it was found that the alkene ligand was bound to the metal *via* the π electrons, rather than by a σ-bond to just one of the carbon atoms, an arrangement now known to be typical of transition metal-alkene complexes.[3] The currently accepted model for the bonding between alkene ligands and transition metal complexes is the Dewar-Chatt-Duncanson model. This was first proposed by Dewar in relation to silver-ethene complexes[4] and later applied to platinum-ethene complexes by Chatt and Duncanson.[5] In this model, there is a synergistic bond between the metal and the ligand, involving the donation of electron density from the

highest occupied molecular orbital (HOMO) of the ligand, the π-orbital, into an empty metal orbital with σ-type symmetry, coupled with the back-donation from a filled π-type metal d-orbital into the lowest unoccupied molecular orbital (LUMO) of the ligand, the π^*-orbital (Figure 1.1).[5–8] As a result of the back-donation, the double-bond is weakened and lengthened, and there is a partial rehybridisation of the carbon centres, with the sp^2 carbon atoms becoming more sp^3-like.[8] With the change in hybridisation, the substituents on the double-bond carbon atoms are bent away from the bond, with the angle increasing with the degree of back-bonding.[8] The effect of back-donation can be seen in the infrared spectra of the complexes, with the coordinated alkene having a C=C bond stretch at lower wavenumber.[5]

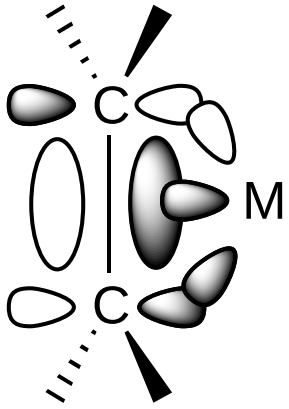

Figure 1.1. Schematic of the synergistic bonding between a metal atom and an alkene ligand.[5–8]

In general, the attenuation of the bond strength, and therefore the increase in bond length is correlated to the extent of back-bonding. In the case of a weak π-base, such as the Pt(II) in Zeise's salt, the back-bonding is minimal. The ethene C=C bond length is similar to that in free ethene, and it can therefore be described as a simple π-complex. This is typical of alkene complexes with the metal in a high oxidation state.[8] Conversely, when an electron-deficient alkene is coordinated to a strongly π-basic metal, as in the formally Pt(0) complex $[Pt(C_2(CN)_4)(PPh_3)_2]$, the back-bonding is maximised. The alkene double-bond is significantly lengthened, and the complex can best be described as a metallacyclopropane species.[8] Most transition metal-alkene complexes fall between the above extremes.

As late transition metals have more filled orbitals than the earlier ones, the ability of the alkene ligand to act as a π-acceptor determines the strength of the binding to the metal, and stronger complexes are therefore formed with electron-deficient alkenes.[8–10] Early transition metals, on the other hand, tend to have more empty orbitals, so it is the ability of the ligand to act as a σ-donor that predominantly affects the binding strength, and stronger complexes are formed with electron-rich alkenes.[8,11–13] In general, alkenes are weak σ-donors but very good π-acceptors.[8]

The high π-accepting ability of alkene ligands mean that they have a strong *trans*-effect.[2] Electron deficient alkenes, which have lower LUMOs, have stronger *trans*-effects.[8] The *trans*-influence of the alkene ligand, however, is highly dependent on the nature of the ligand *trans* to the alkene.[2]

The coordination strength of an alkene ligand is not just dependent on the electronic properties of the ligand. The structure of the alkene also plays a significant role in determining the stability of a complex. In general, the stability decreases with the number of substituents on the alkene, and *cis* isomers tend to be more tightly bound than the corresponding *trans* isomer.[8,9,14,15] Ring strain is also a very important factor in complex stability. Strained alkenes such as norbornene (nb) form particularly stable complexes as coordination and the subsequent rehybridisation of the carbon atoms alleviates the strain.[8,15] Strained alkenes also have a lower π*-molecular orbital and a higher π-orbital than unstrained alkenes, which leads to a more favourable overlap with metal d-orbitals and therefore more stable complexes.[16]

1.1.3 Group 10 Alkene Complexes

By far the most common class of alkene complexes are those of the Group 10 metals nickel, palladium and platinum. These range from monoalkene complexes with a variety of auxiliary ligands, to complexes with three alkene ligands. There are several ways of synthesising Group 10 alkene complexes. Complexes with the metal in the +2 oxidation state can be made either by reacting a metal salt directly with an alkene (Scheme 1.1 (i)),[17] or by displacing a ligand such as another alkene (Scheme 1.1 (ii)).[2,18] Complexes

(i)

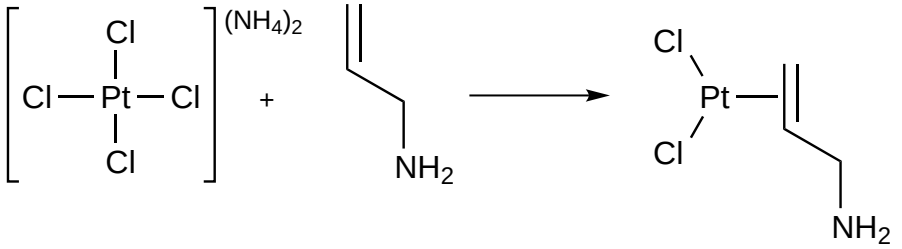

(ii)

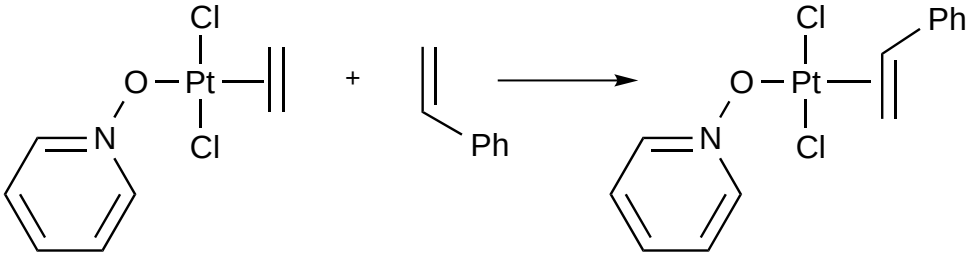

(iii)

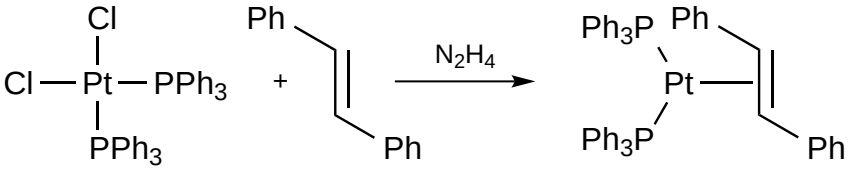

(iv)

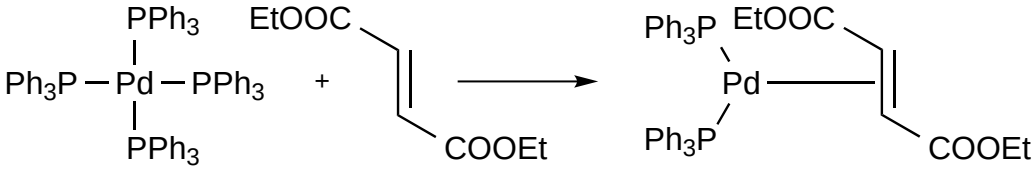

(v)

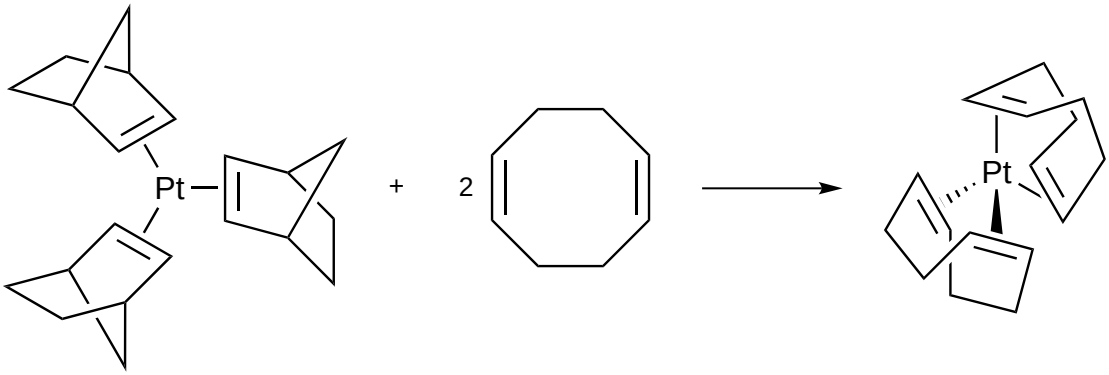

Scheme 1.1. Synthesis of alkene-transition metal complexes.[17–21]

with the metal in the zero oxidation state can be synthesised by the reduction of a M(II) complex in the presence of an alkene (Scheme 1.1 (iii)),[19] or by the displacement of other ligands such as phosphines or other alkenes (Scheme 1.1 (iv) and (v)).[2,20,21]

The first complexes containing purely alkene ligands were made with nickel, [Ni(cycloocta-1,5-diene)$_2$] and [Ni(*trans*,*trans*,*trans*–cyclododeca-1,5,9-triene)].[16] Pure alkene complexes of platinum and palladium have also been synthesised. These are commonly used as precursors in the synthesis of other complexes, as alkenes are relatively easily displaced by other ligands. They are also used as catalysts and pre-catalysts.

The orientation of the coordinated alkene ligands is dependent on the oxidation state of the metal. In M(II) complexes, the alkene ligand usually sits perpendicular to the metal coordination plane (Figure 1.2 (i)),[2,22] while in M(0) complexes, the alkene usually lies parallel to the coordination plane (Figure 1.2 (ii)).[2,23] In cases where the ligands are constrained, the geometry of the complex differs from the ideal. The coordination geometry means that a maximum of three monoalkenes can coordinate to the metal in pure alkene complexes, although it is possible for four individual double-bonds to coordinate.[16] Bis(cycloocta-1,5-diene)platinum, for example, has four coordinated double-bonds and a Pt(0) metal centre, and is almost tetrahedral at the metal.[24]

1.2 Methylenecyclopropane

1.2.1 Synthesis and Properties

Methylenecyclopropane (MCP) (Figure 1.3) is a four-carbon molecule that contains a cyclopropane ring with an external double-bond. It is a gas at room temperature, with a boiling point of 10 °C. As cyclopropane rings have some analogous reactivities to double-bonds,[25] MCP can be considered analogous to allene. Methylenecyclopropane was first synthesised in 1952 from 3-chloro-2-(chloromethyl)-1-propene using magnesium (Scheme 1.2 (i)).[26] In this synthesis, the 3-chloro-2-(chloromethyl)-1-propene first had to be prepared by the chlorination of 3-chloro-2-methyl-1-propene (methallyl chloride). A second synthetic method enabled the transformation of methallyl chloride directly into

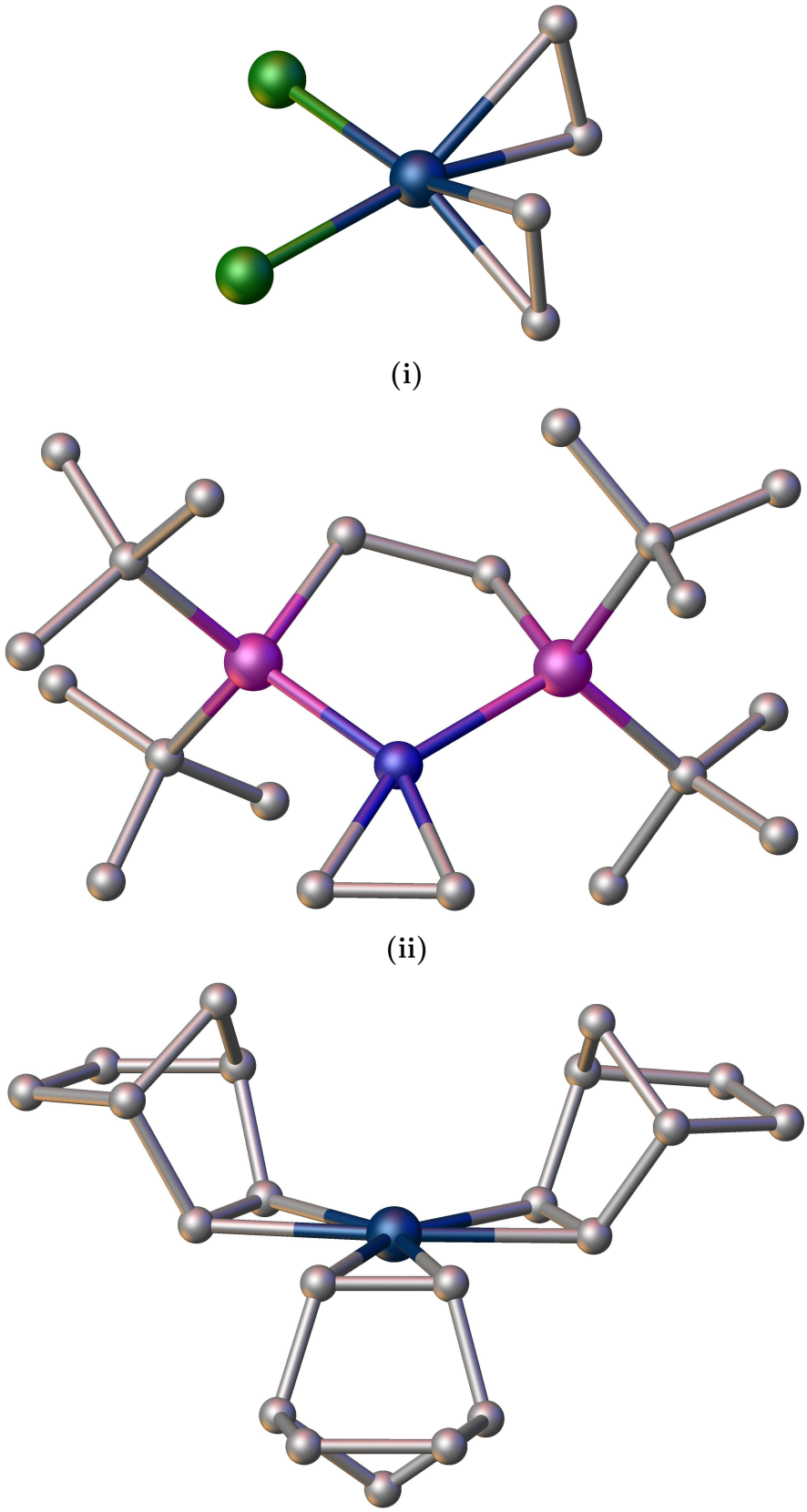

Figure 1.2. X-ray crystal structures of some metal-alkene complexes: (i) $[PtCl_2(C_2H_4)_2]$,[22] (ii) $[Ni(C_2H_4)(^tBu_2P(C_2H_4)P^tBu_2)]$[23] and (iii) $[Pt(nb)_3]$.[16]

MCP using potassium amide (Scheme 1.2 (ii)).[27] The equivalent reaction with sodium amide produced 1-methylcyclopropene, which means that the choice of base is important. This method was further modified to use a $KO^tBu/NaNH_2$ base system.[28]

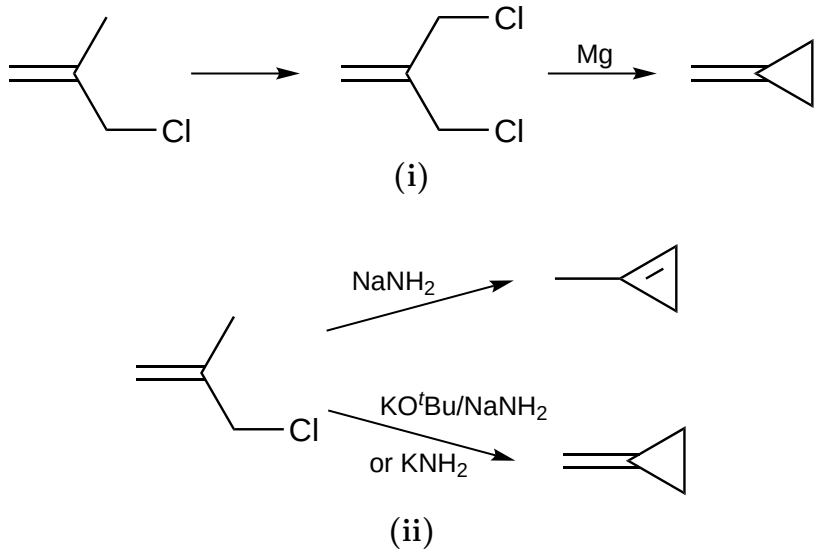

Scheme 1.2. Methods of synthesising methylenecyclopropane.[26,27]

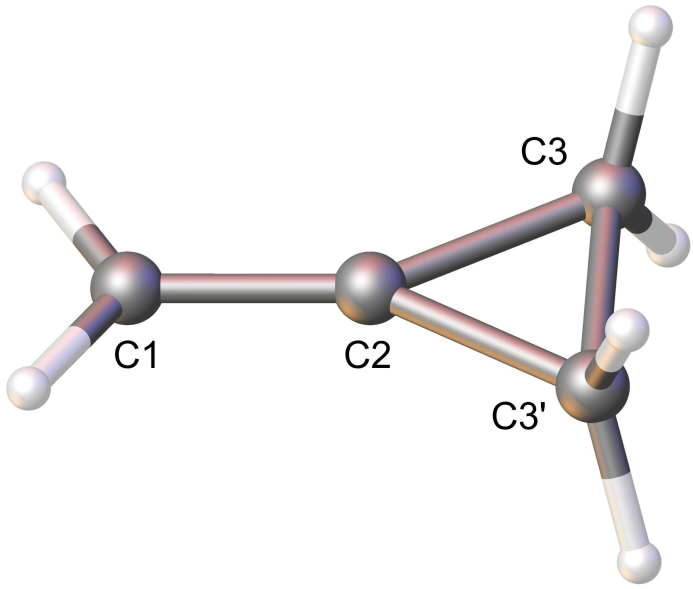

Figure 1.3. Methylenecyclopropane.[29]

While a crystal structure of MCP has not been obtained, the structural properties have been calculated from the microwave spectrum.[29] The length of the double-bond (1.332 Å) is comparable to that of ethene (1.330 Å)[30] and 2-methylpropene (1.330 Å).[29] The

proximal (C2–C3) bond lengths (1.457 Å) are shortened relative to the ideal cyclopropane bond lengths of 1.514 Å,[29] while the distal bond length (1.542 Å) is lengthened. The proximal bond shortening is due to the fact that the bonding is between formally sp^3 and sp^2 carbon atoms, which typically means a shorter bond length than that of a bond between two sp^3 carbon atoms.[29] This trend can also be observed in 2-methylpropene and cyclopropanone, with proximal bonds shortened to 1.507 and 1.475 Å respectively, while in methylcyclopropane the bond lengths are 1.517 Å, closer to the ideal.[29,31] The C3–C2–C3′ angle is larger than that of cyclopropane (60°)[32] at 63.9°, while the remaining angles in the ^{c}Pr ring are 58.0°.[29]

The first ionisation energy of methylenecyclopropane is 9.6 eV, similar to 2-methylpropene (9.2 eV), but significantly less than ethene (10.5 eV).[33] MCP shows a strong C=C stretch at 1742 cm^{-1} in the infrared spectrum, which is at a higher wavenumber than that of ethene, 1623 cm^{-1}.[34,35] In the NMR spectra, there are three different carbon and two proton environments.[28,36] The double-bond methylene carbon has a proton resonance at 5.35 ppm and a carbon resonance at 103.0 ppm, while the ring methylenes have resonances at 1.00 and 2.6 ppm in the ^{1}H NMR and ^{13}C NMR spectra respectively ($CDCl_3$). The ring sp^2 carbon has a signal at 130.7 ppm. The ^{13}C–^{1}H coupling constant of the ring carbons, 162 Hz, is indicative of the long-range effect of the increased s-character of the double-bond relative to cyclopropane, which has a coupling constant of 160.3 Hz.[36,37]

1.2.2 Organometallic Chemistry

1.2.2.1 Transition Metal-Catalysed Reactions

The transition metal chemistry of methylenecyclopropane and its derivatives has been explored since the 1970s. There are four different ways that MCPs react with transition metal species (Scheme 1.3).[38] When the metal reacts with the cyclopropane ring, there can be insertion into either the distal (Scheme 1.3 (i)) or the proximal bonds (Scheme 1.3 (ii)) of the ring. When the double-bond reacts with an organotransition metal species (R–ML_n), this can yield either the Markovnikov product (Scheme 1.3 (iii)), with the metal

bound to the ^{c}Pr carbon atom, or the anti-Markovnikov product (Scheme 1.3 (iv)), with the metal bound to the methylene carbon atom.

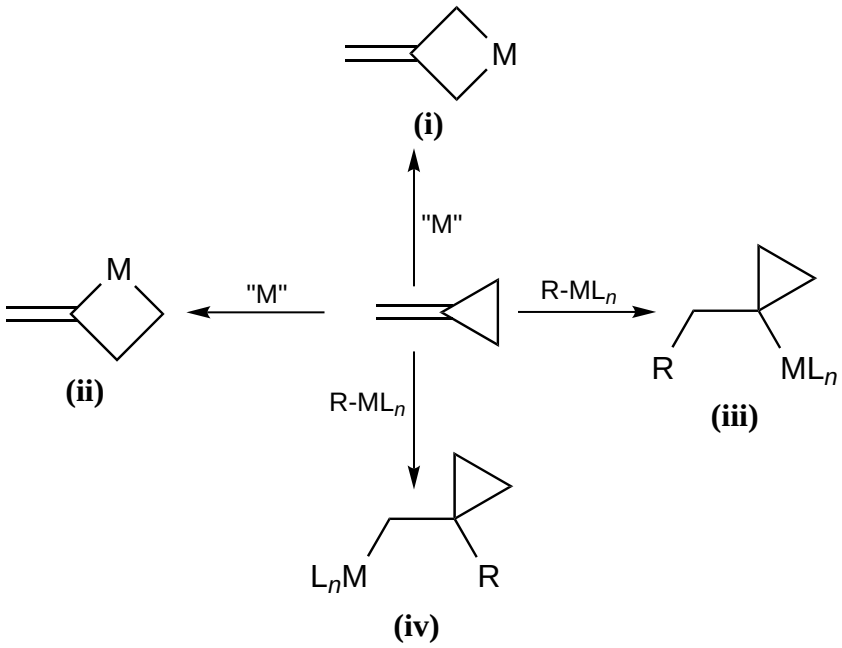

Scheme 1.3. The four reaction modes of methylenecyclopropanes with transition metals.[38]

The transition metal-catalysed reactions of MCPs which have been previously studied can be divided into four types, which involve at least one of the above transformations: Transition metal-catalysed [3+2] cycloadditions, Heck-type reactions with organopalladium species, additions of metal hydrides (M–H) and pronucleophiles (Nu–H), and the addition of bis-metallic species.[38]

1.2.2.2 Transition Metal-Catalysed [3+2] Cycloadditions

Methylenecyclopropane can act as a three-carbon unit in transition metal catalysed [3+2] cycloadditions.[38–40] These reactions always involve the cleavage of one of the bonds in the ^{c}Pr ring. In the case of distal bond cleavage (Scheme 1.4), the reaction proceeds *via* the formation of a metallacyclobutane species, followed by the insertion of an X=Y multiple bonded species. This forms a 5-membered carbo- or hetero-cycle, depending on the nature of X=Y.[38,41]

Alternatively, in the case of proximal bond cleavage, the reaction can proceed *via* one

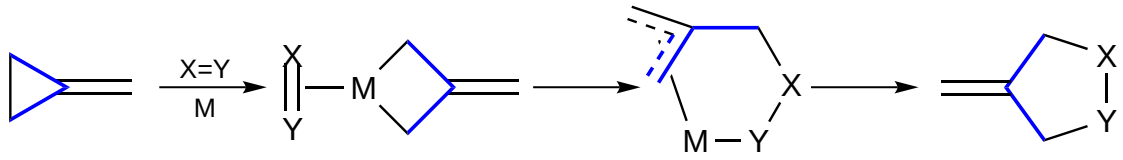

Scheme 1.4. TM catalysed [3+2] cycloaddition of MCP involving distal bond cleavage.[38]

of two routes. (Scheme 1.5). The first, the direct attack of the catalyst on the proximal bond, is similar to distal bond cleavage, involving a metallacyclobutane intermediate. In the second route, a metallacyclopentane species is formed, incorporating X=Y. This then undergoes a cyclopropyl to homoallyl rearrangement, yielding 5-membered carbo- or hetero-cycles with different regiochemistry to the distal bond cleavage product. The mode of ring opening is catalyst dependent.[38,41]

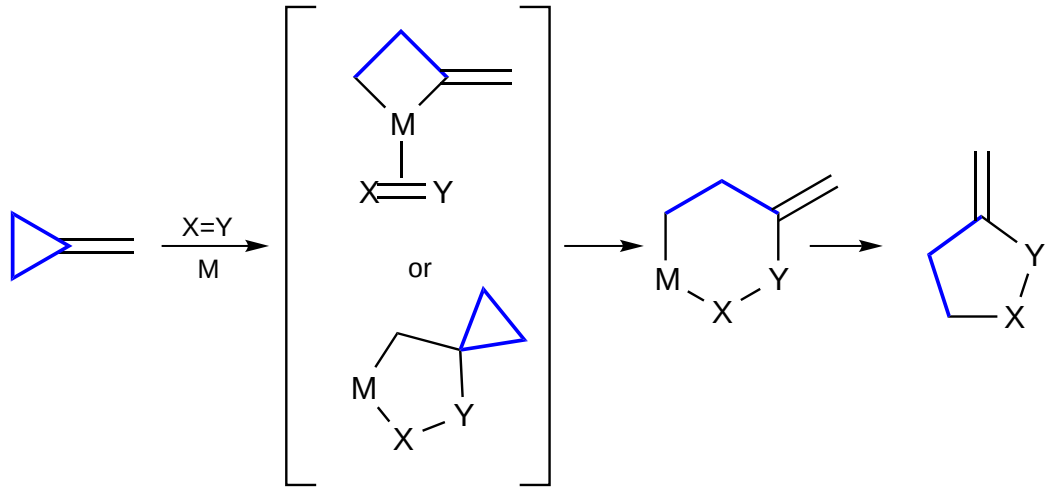

Scheme 1.5. TM catalysed [3+2] cycloaddition of MCP involving proximal bond cleavage.[38]

There are several species that can behave as X=Y in these [3+2] cycloadditions. Reactions where X=Y is a carbon-carbon multiple bond have been extensively investigated, particularly for nickel- and palladium-catalysed reactions.[38–40] A variety of MCP derivatives have been utilised as the three-carbon component, and the reaction has been extended to intramolecular versions.[42–44]

Reactions with carbon-heteroatom bonds have been successful with heterocumulenes such as carbon dioxide and ketenimines, producing lactones and pyrrolidine derivatives

respectively.[41,45] MCPs can also be reacted with aldehydes to produce substituted tetrahydrofurans,[46] and with imines to produce 3-methylenepyrrolidine derivatives.[47] These reactions are reasonably high yielding, ranging from 38% to 94%, depending on the nature of both the MCP derivative and the carbon-heteroatom species.[38]

1.2.2.3 Heck-Type Reactions

Methylenecyclopropanes can undergo palladium-catalysed Heck-type reactions with alkyl or aryl halides (Scheme 1.6).[38] These reactions predominantly involve the cleavage of one of the proximal bonds of the ^{c}Pr ring.[38,48,49] Initially, a previously formed R–Pd–X species adds across the double-bond in an anti-Markovnikov fashion. The proximal bond is then cleaved in a cyclopropyl to homoallyl rearrangement, generating a homoallylpalladium species. When this undergoes β-hydride elimination, the product is a 2-alkylated 1,3-diene. However, in some cases the homoallylpalladium species rearranges to a π-allylpalladium intermediate, which can then be trapped by an appropriate nucleophile.[38]

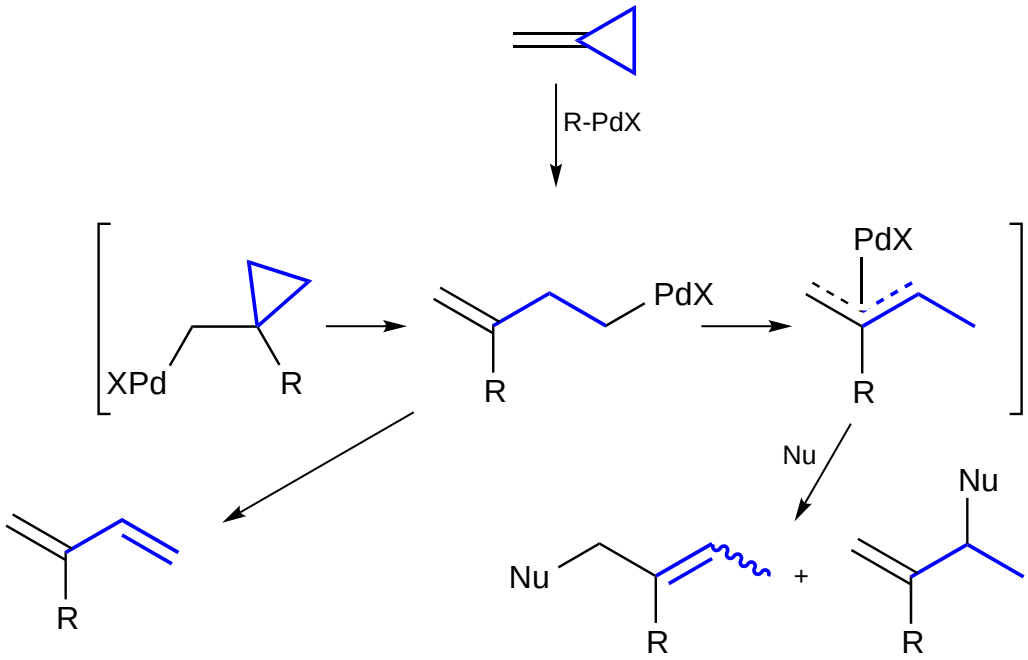

Scheme 1.6. Palladium-catalysed Heck-type reaction with MCP.[38]

1.2.2.4 Addition of Metal Hydrides and Pronucleophiles

The palladium-catalysed reactions of methylenecyclopropanes with either metal hydrides (M–H) or pronucleophiles (Nu–H) are of considerable use, as this can introduce a functional group into unsaturated molecules in an atom-economical manner.[38] These reactions involve the cleavage of one of the ^{c}Pr bonds. The type of bond cleaved is dependent upon the substrate.[38] In the reaction with metal hydrides such as stannyl hydrides ($HSnR_3$) and hydrosilanes ($HSiR_3$), it is usually one of the proximal bonds that is cleaved.[38,50] First, the palladium atom inserts into the M–H bond, and then, as with the Heck-type reactions, the resulting H–Pd–M species undergoes anti-Markovnikov addition across the MCP double-bond. The proximal bond is cleaved, forming a homoallylpalladium species. The product is formed by reductive elimination from the palladium (Scheme 1.7). Proximal bond cleavage also occurs in the addition of a boron-boron bond.[38]

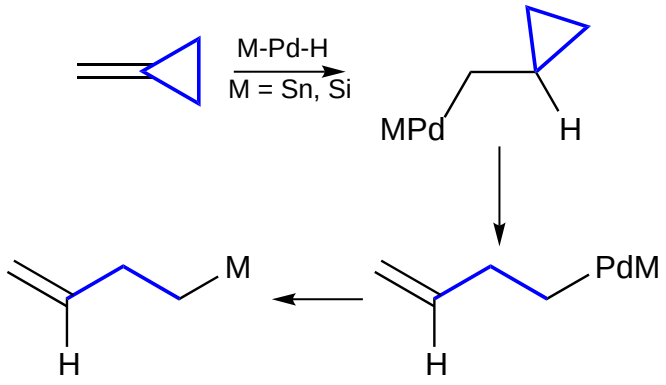

Scheme 1.7. Palladium-catalysed addition of metal hydrides to MCP.[38]

In the reaction with pronucleophiles such as carbo-pronucleophiles ($HC(EWG)_nR_{3-n}$), amines (HNR_2) and alcohols (HOR), it is mainly the distal bond that is cleaved.[38] There are two mechanistic possibilities in this reaction. The palladium atom could first insert into the Nu–H bond, generating a H–Pd–Nu species, which then adds across the double-bond in a Markovnikov fashion. The cyclopropylpalladium species undergoes β-carbon palladium elimination to give a π-allylpalladium intermediate that is attacked by the nucleophile to yield the product (Scheme 1.8). Alternatively, the Pd can insert into the distal ^{c}Pr bond, forming a metallacyclobutane. This then reacts with the pronuclophile

to give the same π-allylpalladium species as before.

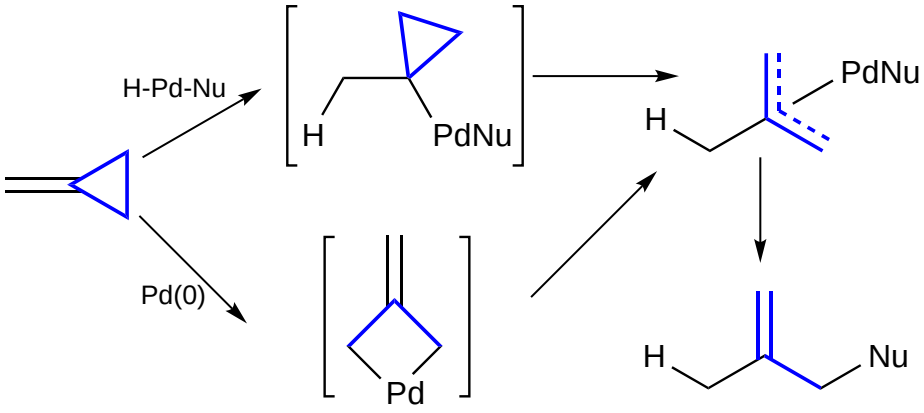

Scheme 1.8. Palladium-catalysed addition of pronucleophiles to MCP.[38]

1.2.2.5 Bismetallation

Catalytic bismetallation is an attractive methodology to introduce two metal atoms into a carbon framework by directly adding the metals across a carbon-carbon multiple bond. This chemistry has previously been demonstrated using alkenes, alkynes, 1,3-dienes and allenes. More recently, methylenecyclopropanes have been used as acceptors as they impart unique structural properties to the products.[38]

The palladium- and nickel-catalysed bismetallation of substituted MCPs has been achieved using trimethylsilyl cyanide.[51] This can be done either with retention of the ring, or with cleavage of the distal bond. Unsubstituted MCP has been bismetallated by a diborane using a platinum catalyst, with cleavage of the proximal ring bond to yield a ring-opened product.[52] Most extensively studied has been the palladium- and platinum-catalysed silaboration of MCPs.[53] These reactions can involve either distal or proximal bond cleavage. The mechanism of the silaboration reaction has not been fully explored, and there are several possible reaction pathways (Scheme 1.9).[38,53] Firstly, there is the possibility that it proceeds similar to the Heck type reactions and Nu–H additions, with the addition of a R_2B–M–SiR'_3 species across the double-bond, followed by a rearrangement to yield a homoallyl product. However, this does not completely explain the product distribution. An alternative mechanism is possible, with the oxidative

addition of the proximal bond onto the metal forming a metallacyclobutane, followed by reductive elimination of the borane and the double-bonded carbon atom to generate the same homoallyl species. The metallacyclobutane mechanism can also be applied to the case of distal bond cleavage.

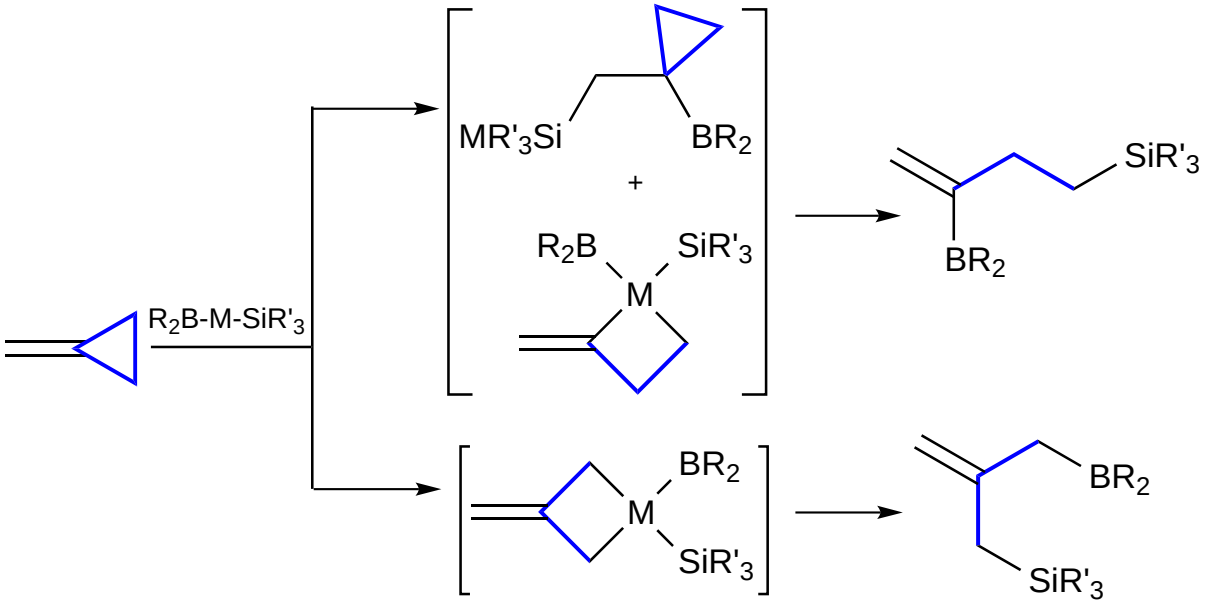

Scheme 1.9. Possible mechanisms for the metal-catalysed silaboration of MCP.[38,53]

1.2.2.6 Transition Metal Complexes

The transition metal chemistry of methylenecyclopropane is dominated by ring opening reactions, which has somewhat limited the isolation of η^2-methylenecyclopropane complexes. A common occurrence upon the coordination of MCP is the ring-opening of the distal ^{c}Pr bond to form η^4-trimethylenemethane complexes. Complexes of this ligand formed from MCP have been isolated for molybdenum,[54] iron,[39] nickel[39,55] and palladium.[56,57] Despite this propensity to ring-open, there are several instances of transition metal-catalysed reactions of MCP in which the ring is retained, and as such there have been a few η^2-methylenecyclopropane complexes isolated. As MCP has a high HOMO compared to other alkenes such as ethene, and is highly strained, it should be able to both effectively donate electron density into empty metal orbitals and accept back donation.[58,59] Due to the sensitivity of MCP to ring-opening reactions, the precursor complexes and the

ancillary ligands need to be carefully chosen. Complexes of nickel and platinum with phosphine ligands have been successfully synthesised by starting from the equivalent ethene complexes. In the presence of an excess of MCP, the ethene is displaced to yield [Ni(η^2-MCP)(PPh_3)$_2$][60] and [Pt(η^2-MCP)(PPh_3)$_2$].[61] (Scheme 1.10).

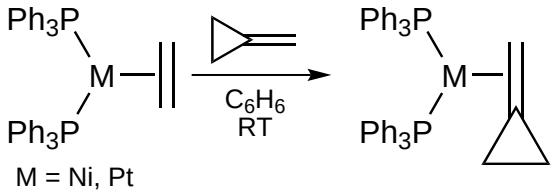

Scheme 1.10. Synthesis of Ni and Pt complexes of MCP.[60,61]

A rhodium-bis-MCP complex has also been isolated by the displacement of ethene from [Rh(acac)(C_2H_4)$_2$].[61] The variable temperature NMR data of this complex shows that the MCP ligands undergo rapid propeller rotation at room temperature.[61] Also, the NMR data showed that coupling to ^{103}Rh only occurs to the olefinic carbon atoms and protons, not to those in the ^{c}Pr ring. This is also the case for the above Pt complex. An X-ray crystal structure of [Rh(acac)(MCP)$_2$] was obtained (Figure 1.4).[61] This shows that the coordination geometry of the rhodium atom is almost perfectly square planar. The two MCP ligands are anti-parallel to each other, and perpendicular to the metal coordination plane. The double-bond ring carbon is closer to the metal than the double-bond methylene carbon atom carbon atom (2.07 and 2.13 Å respectively), and the coordination plane intersects the double-bond closer to the ring carbon atom. This can also be inferred from the ^{103}Rh–^{13}C coupling constants, with that of the ring carbon atom larger than that of the methylene carbon atom (20 Hz vs. 14 Hz). The plane of the ^{c}Pr ring is bent away from that of the double-bond by 23°, indicative of back bonding from the metal. The double-bond itself is at an angle of 80° relative to the metal plane. This distortion is similar to that observed in allene complexes.[61,62]

MCP complexes can be synthesised by methods other than the displacement of an ethene ligand. The above nickel-phosphine complex ([Ni(MCP)(PPh_3)$_2$]) can also be synthesised from [Ni(acac)], $Et_2Al(OEt)$, PPh_3 and MCP.[60] A cobalt complex has been synthesised by reductive complexation from a chloro complex. The Co(II) complex

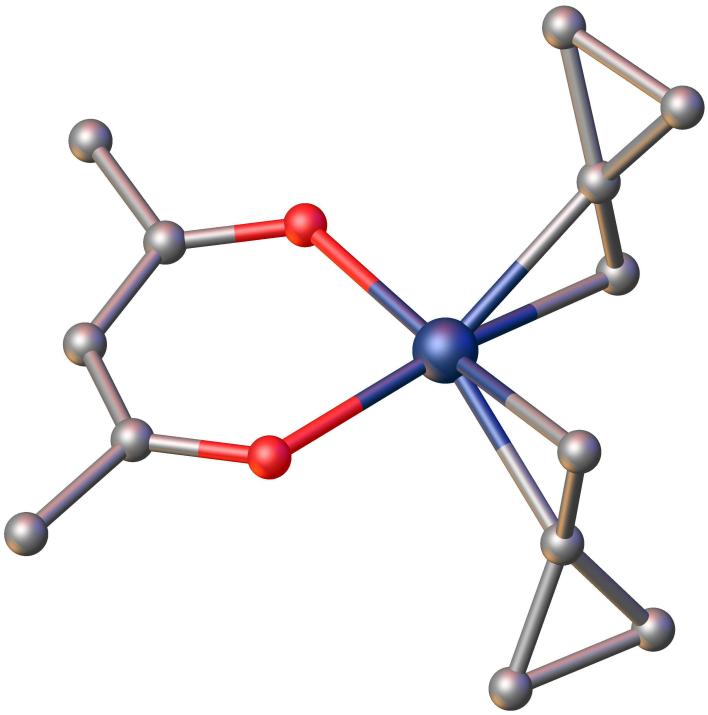

Figure 1.4. X-ray crystal structure of $[Rh(acac)(MCP)_2]$.[61]

((2-(di-tert-butylphosphanyl)-P-ethyl)cyclopentadienyl)chlorocobalt(II) ([CoCl(Cp#)]) was treated with sodium amalgam and MCP at −50 °C to yield [Co(Cp#)(MCP)] (Scheme 1.11).[58,59]

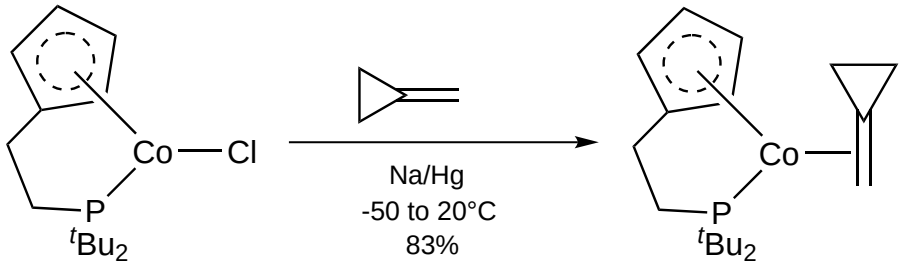

Scheme 1.11. Synthesis of a Co-MCP complex.[58,59]

1.3 Bicyclopropylidene

1.3.1 Synthesis of Bicyclopropylidene

Bicyclopropylidene (BCP) is a unique tetra-substituted alkene, consisting of two cyclopropylidene units joined by a common double-bond. It was originally conceived

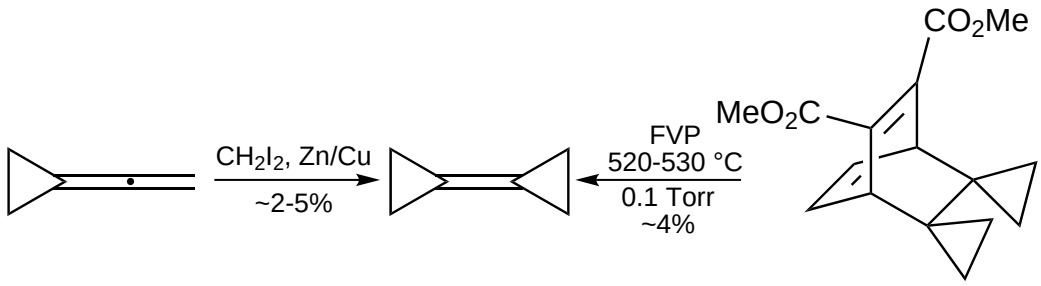

Scheme 1.12. First syntheses of bicyclopropylidene.[63]

by two independent groups as a molecule of mainly theoretical interest.[37] The first syntheses (Scheme 1.12), either a Simmons-Smith-type monocyclopropanation of the terminal double-bond in ethenylidenecyclopropane[64] or a retro-Diels-Alder cleavage of dispiro[cyclopropane-1,2′-bicyclo[2.2.2]octa[5,7]diene-3′,1″-cyclopropane]-5′,6′-dimethyl ester,[65] did not yield enough compound to perform a full structural and spectroscopic characterisation. Later syntheses were higher yielding, but still too convoluted to be synthetically useful.[63] It was not until the Kulinkovich reaction enabled the transformation of an ester to a cyclopropanol group using an ethylmagnesium bromide/titanium tetraisopropoxide reagent that BCP could be easily made in useful quantities.[63] This enabled the transformation of methyl cyclopropanecarboxylate to 1-cyclopropylcyclopropanol quantitatively, which could then be simply converted to the bromide followed by dehydrobromination to form the double-bond (Scheme 1.13).[66,67] This efficient synthesis method allowed the properties and chemistry of BCP to be studied extensively.

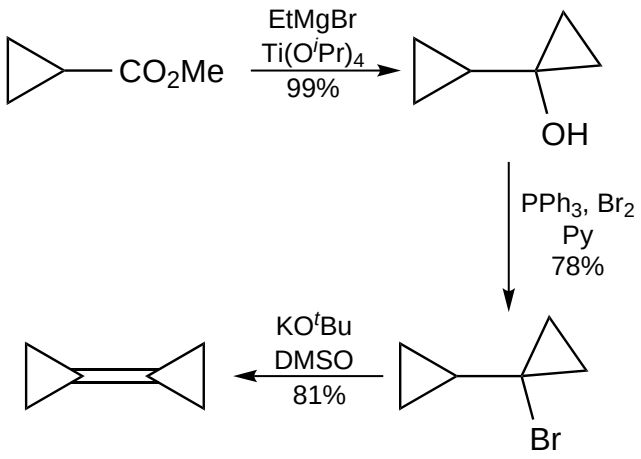

Scheme 1.13. Highest yielding synthesis of bicyclopropylidene.[66,67]

1.3.2 Properties of Bicyclopropylidene

1.3.2.1 Structural Properties

Bicyclopropylidene can be thought of as comprising two joined methylenecyclopropane units. The double-bond has increased s-character due to the presence of the ^{c}Pr rings and the carbon atoms are therefore close to sp-hybridised.[29,32,68] As a result of this, in the X-ray crystal structure the length of the double-bond is 1.304 Å (Figure 1.5),[30] shorter than the double-bonds in ethene (1.330 Å)[30] and MCP (1.332 Å).[29] It is noteworthy that the presence of one terminal ^{c}Pr on a double-bond does not make much of a difference to the bond length, as in the case of MCP, while the presence of two significantly shortens the bond. The double-bond in BCP is comparable to the central bond in butatriene, and has properties approaching those of an acetylenic triple bond.[63] The length of the bonds in the ^{c}Pr rings, 1.472 and 1.549 Å for proximal (C1–C2, C1–C3) and distal (C2–C3) respectively, are comparative to the equivalent bonds in MCP, 1.457 and 1.542 Å, although the BCP proximal bond is somewhat longer.[30] As with MCP, the shortening of the proximal bonds relative to the bonds in cyclopropane (1.541 Å)[29] has been attributed to the fact that these bonds are nominally sp^2-sp^3, which tend to be shorter than sp^3-sp^3 bonds.[29]

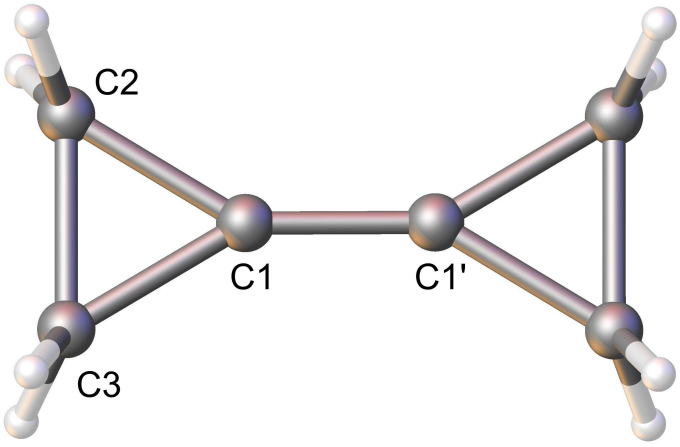

Figure 1.5. X-ray crystal structure of BCP at 173 K.[30]

The C2–C1–C3 angle is 63.1°,[30] approximately the same as that in MCP (63.9°)[29] and larger than that in cyclopropane (60°).[32] Correspondingly, the C1–C2–C3 and C1–C3–C2 angles are smaller than those in cyclopropane at 58.4°. The two ^{c}Pr rings are coplanar

with the double-bond to within 0.002°.[30]

1.3.2.2 Spectroscopic and Electronic Properties

There have been several IR and Raman spectra of bicyclopropylidene reported by different groups, and not all are in agreement.[37] The most relevant vibrational mode with respect to its bonding properties is the double-bond stretch, a weak band at 1836 cm^{-1} in the Raman.[37] The NMR data show a peak at 1.16 ppm in the ^{1}H NMR spectrum and peaks at 2.9 and 110.2 ppm in the ^{13}C NMR spectrum ($CDCl_3$).[67] The ^{13}C–^{1}H coupling constant, 162.3 Hz, is indicative of a slightly increased s character of the C–H bonds relative to those in cyclopropane, which has a coupling constant of 160.3 Hz.[37] Bicyclopropylidene has a relatively high-lying HOMO, 0.64 eV higher than that of MCP.[37] While the first ionisation energy of BCP (8.93 eV)[68] is higher than that of tetramethylethene (8.27 eV),[69] BCP is significantly more reactive towards additions across the double-bond.[63] This is in part due to the decreased steric bulk of the ^{c}Pr rings relative to the methyl groups, but mostly due to the difference in hybridisation of the double-bond carbon atoms.[63] There is significant electronic interaction between the two ^{c}Pr rings, which can be approximated as double-bonds,[70] meaning that BCP has been described as a 'bishomobutatriene'.[37] This, and the high HOMO mean that BCP has a uniquely enhanced reactivity towards a wide range of electrophiles and cycloaddends.[37]

1.3.2.3 Reactivity

BCP is reactive towards cycloadditions and additions across the double-bond. Due to the high HOMO, BCP is nucleophilic.[32] While most monoalkenes are limited in their cycloadditions, the uniqueness of BCP is evident in the fact that it undergoes a wider range of reactions towards cycloaddends, comparable to cross-conjugated polyenes.[71] For example, thermal cyclodimerisations of monoalkenes are rare, but BCP dimerises at high temperatures.[64] Some of the chemistry of BCP is similar to that of cumulenes, namely that it undergoes high temperature dimerisations and [2+2] cycloadditions with conjugated dienes.[32] This is to be expected from the fact that it is a 'bishomobutatriene'.

BCP can be deprotonated easily, leading to the formation of a wide range of substituted bicyclopropylidenes.[37,63] This enhanced kinetic acidity is due not so much to the polarity of the C–H bond, but rather to the stabilisation of the carbanion.[37] BCP can also undergo reactions in which either the proximal or distal bonds of the ^{c}Pr rings are cleaved.[37,63]

1.3.3 Organometallic Chemistry

1.3.3.1 Transition Metal-Catalysed Reactions

Bicyclopropylidene is active in several transition metal-catalysed reactions. These tend to be analogous to the transition metal-catalysed reactions of methylenecyclopropanes. To date, the bulk of the catalysis has involved the use of a palladium catalyst, although there are some examples of nickel-catalysis.[37,63]

1.3.3.2 Transition Metal-Catalysed Cycloadditions

As with other methylenecyclopropanes, BCP can undergo palladium-catalysed [3+2] cycloadditions as the C_3-building block.[72] When reacted with electron-deficient alkenes such as those in Scheme 1.14, two regioisomers that possess the 4-methylenespiro[2.4]heptane skeleton are produced.

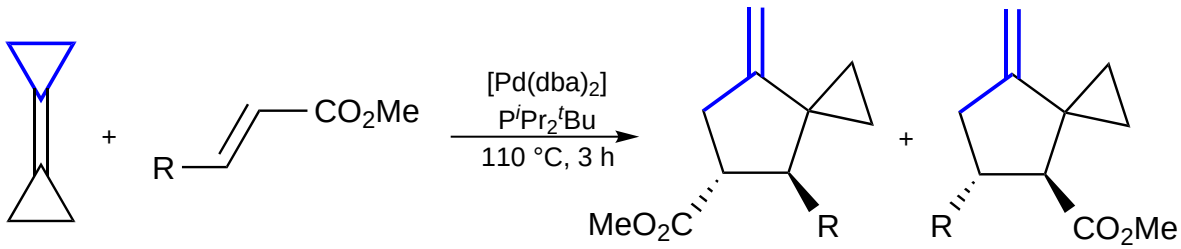

R	Yield %	(i):(ii)
H	54	74:26
Me	58	90:10
Ph	81	89:11

Scheme 1.14. Pd-catalysed reactions of BCP with electron-deficient alkenes.[72]

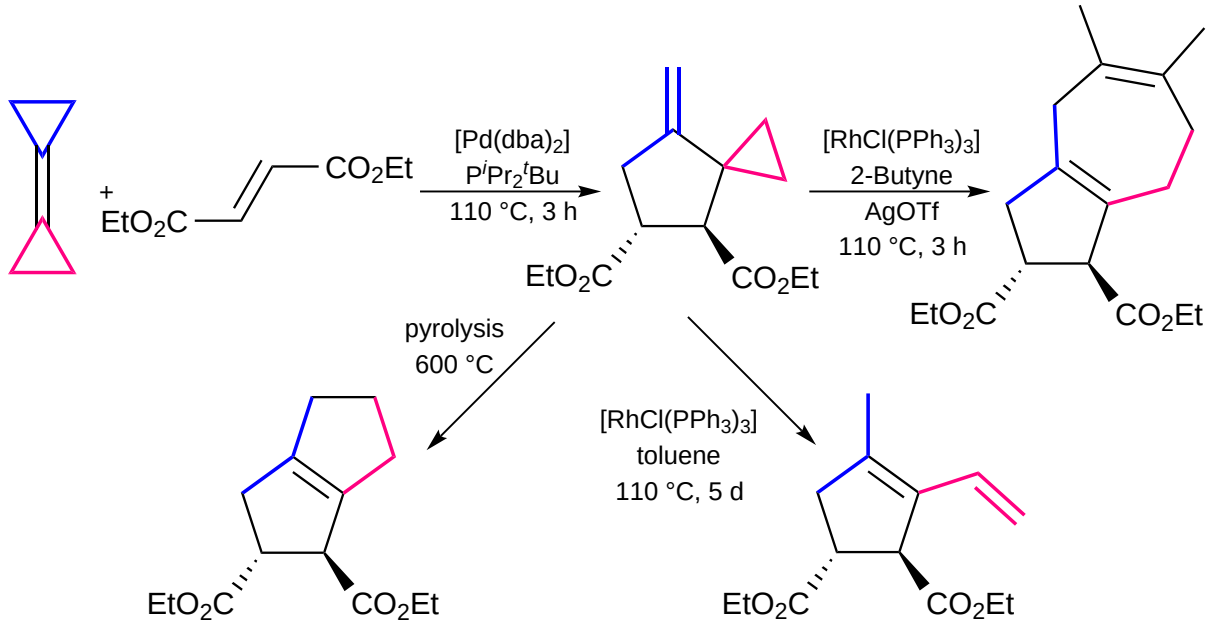

Scheme 1.15. Pd-catalysed reactions of BCP with diethyl fumarate.[72]

These reactions are regioselective, both with respect to BCP, in that only methylene-spiro[2.4]heptane derivatives are produced, and with respect to the positioning of the carboxylate relative to the ^{c}Pr ring in the product, with 75–90% of the products having the carboxylate group in the γ-position (Scheme 1.14 (i)). In equivalent reactions with isopropylidene- and cyclopentylidene cyclopropane, the alkylidene group is retained, while Pd(0) catalysed reactions of 2-(1-trimethylsilyl-1-cyclopropyl)alkyl pivalate with electron deficient alkenes give a solvent-dependent distribution of products. Calculations involving MCP and ethene[73] predict that the regioisomers with the carboxylate in the β-position (Scheme 1.14 (ii)) should be the sole products.[72] However, these are the minor products, with the γ-carboxylate products being favoured. While the mechanism for the product formation is not completely understood, Scheme 1.16 shows the proposed mechanisms.[72] Alternatively, a '(trimethylenemethane)palladium' intermediate with charge separation could account for the observed regiochemistry.[72]

In the case of the reaction of BCP with diethyl fumarate (Scheme 1.15), there is only one possible isomer formed. Several further reactions of this product have been explored, and the rhodium-catalysed cocyclisation with an alkyne yielding a further seven-membered ring, the first intermolecular case of this reaction, may have applications in

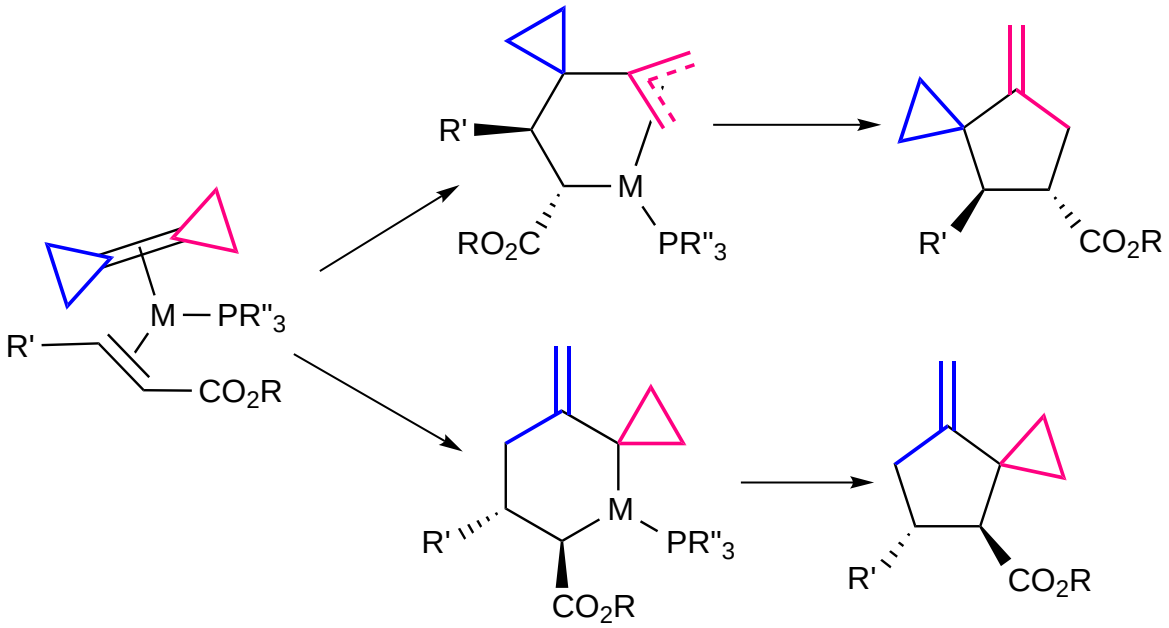

Scheme 1.16. Mechanisms for the formation of [3+2] cycloaddition products of BCP.[72]

terpene total synthesis.[72]

BCP can also undergo palladium(0)-catalysed [3+2] cycloadditions with strained alkenes such as norbornene and norbornadiene to give products similar to those in Scheme 1.14 in good yields (Scheme 1.17).[72] In the case of nb, there are also a number of 2:1 nb:BCP cotrimers formed. As BCP is itself a strained alkene, it can also can also undergo a [3+2] cycloaddition to form a dimer.[74] This involves the cleavage of a distal ring bond (Scheme 1.18).

When a nickel(0) rather than a palladium(0) catalyst is used, the reaction is no longer a simple [3+2] cycloaddition. When BCP was reacted with diethyl fumarate under Ni(0)-catalysis conditions, there were three products formed (Scheme 1.19).[72] The major product was the [2+2] cycloaddition product (Scheme 1.19 (i)), in 23-46% yield, depending on the proportion of phosphine used in the catalyst mixture.[72] The [3+2] addition product (Scheme 1.19 (ii)), resulting from distal bond cleavage, was still produced in 10-25% yield, and a cotrimer, generated by the [3+2] cycloaddition of two molecules of diethyl fumarate onto the two ^{c}Pr rings of BCP, with proximal cleavage (Scheme 1.19 (iii)) was also produced. Nickel(0) can also catalyse the [2+2] cycloaddition between cyclobutene and BCP to give dispiro[cyclopropane-1,2′-bicyclo[2.2.0]hexane-3′,1″-

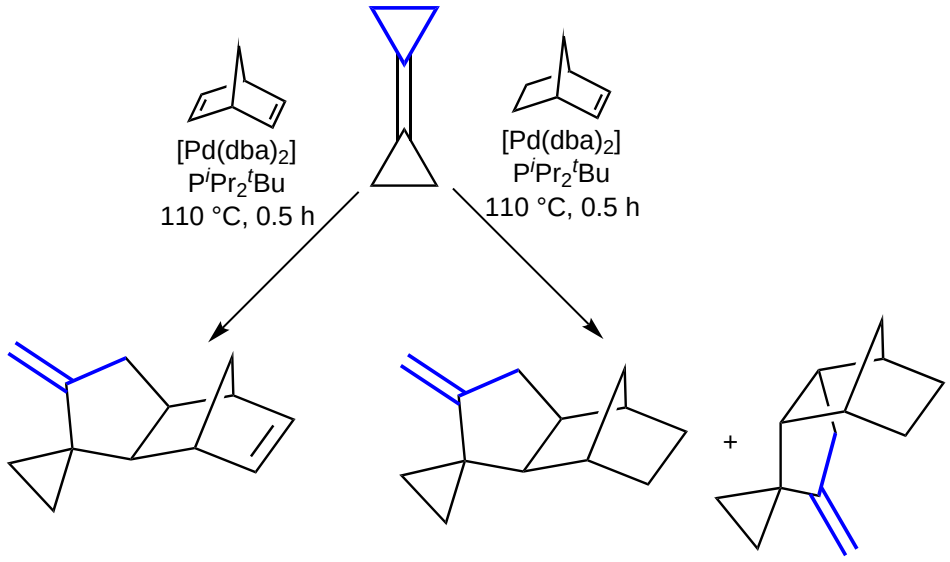

Scheme 1.17. Pd(0)-catalysed cyclodimerisation of BCP with norbornene and norbornadiene.[72]

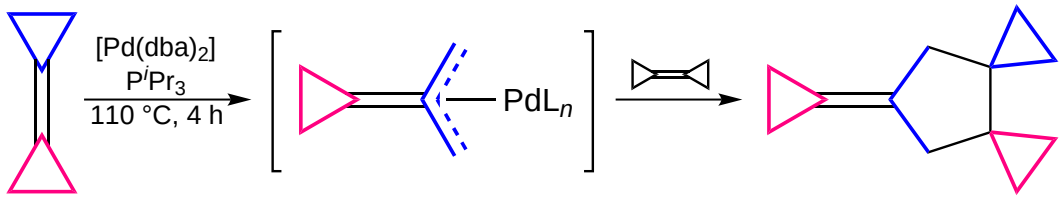

Scheme 1.18. Pd(0)-catalysed cyclodimerisation of bicyclopropylidene.[74]

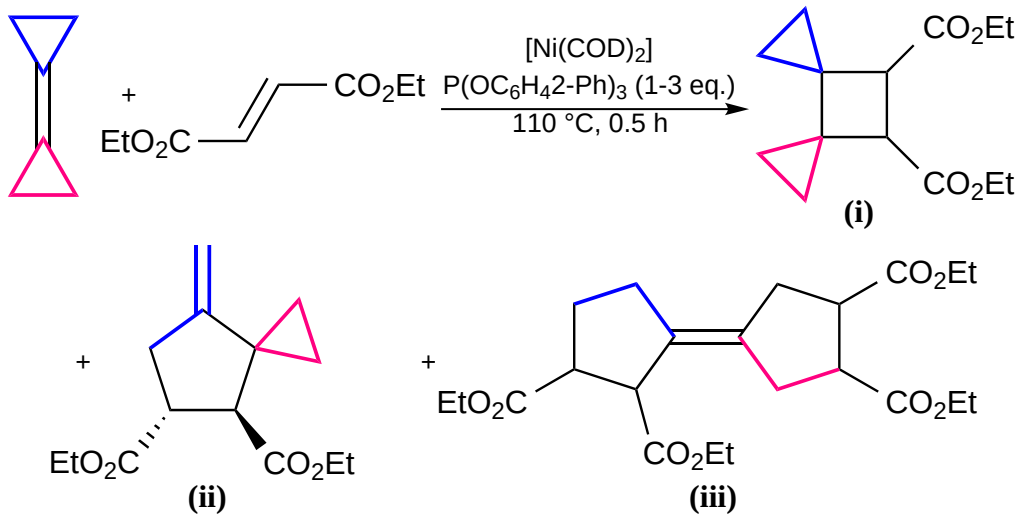

Scheme 1.19. Ni(0)-catalysed cycloaddition of bicyclopropylidene with diethyl fumarate.[74]

cyclopropane] (Scheme 1.20).[37,75] This reaction also produces cycloocta-1,5-diene *via* the dimerisation of cyclobutene and subsequent rearrangement.

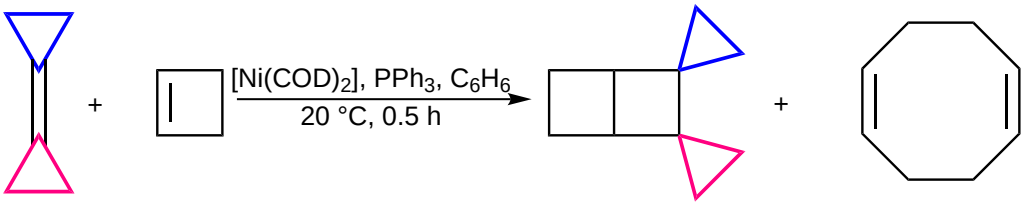

Scheme 1.20. Ni(0)-catalysed [2+2] cycloaddition of BCP with cyclobutene.[37,75]

1.3.3.3 Heck-Type Reactions

BCP undergoes reactions with Heck-type reagents in a similar fashion to methylenecyclopropanes. First an organopalladium species adds across the BCP double-bond, after which one of the ^{c}Pr rings opens up to a homoallylpalladium species. This then undergoes β-hydride elimination to yield a cross-conjugated diene (Scheme 1.21).[74] While the resulting diene can be isolated, it is more often used in further reactions, usually Diels-Alder reactions with a dieneophile.[44,74,76] This can lead to a series of domino Heck-Diels-Alder reactions, creating a range of spiro[2.5]octane derivatives. (Scheme 1.22).[63,74] These reactions tend to be high yielding, and the reactions have been carried out on a robotic system to generate several small-molecule libraries of compounds.[74]

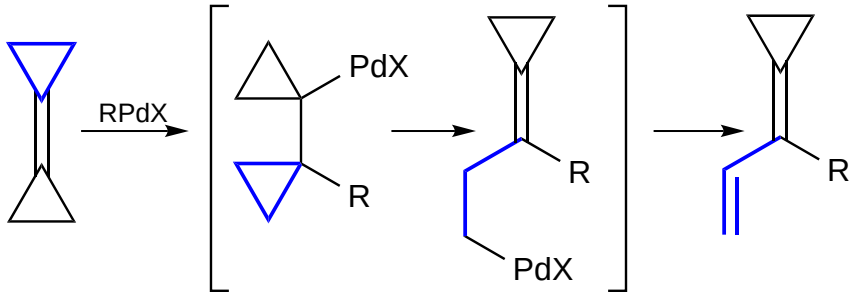

Scheme 1.21. The reaction of BCP with Heck-type reagents.[74]

The domino reaction can be extended to create a variety of carbon skeletons containing a cyclopropane ring. In the case of the reaction with iodoethene, the cross-conjugated triene product can undergo two sequential Diels-Alder reactions to give a tricyclic product

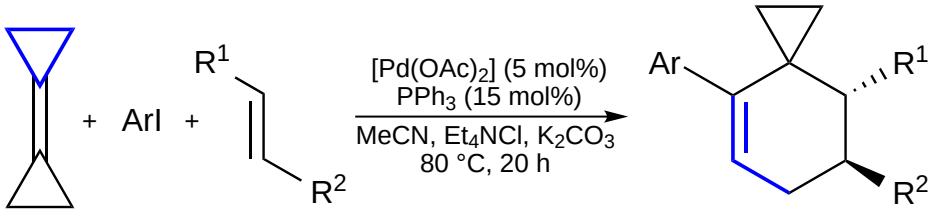

Ar	R^1	R^2	Yield %
Ph	H	CO_2Me	100
Ph	H	$CO_2{}^tBu$	87
Ph	CO_2Me	CO_2Me	97
4-Tol	CO_2Me	CO_2Me	
4-Py	H	$CO_2{}^tBu$	81
4-Py	CO_2Me	CO_2Me	60

Scheme 1.22. Domino Heck-Diels-Alder reactions of BCP.[63,74]

(Scheme 1.23).[74] When the reaction involves oligoiodoarenes, there is the possibility of creating up to 12 new C–C bonds in a single synthetic operation in at least 47% yield (Scheme 1.24).[74]

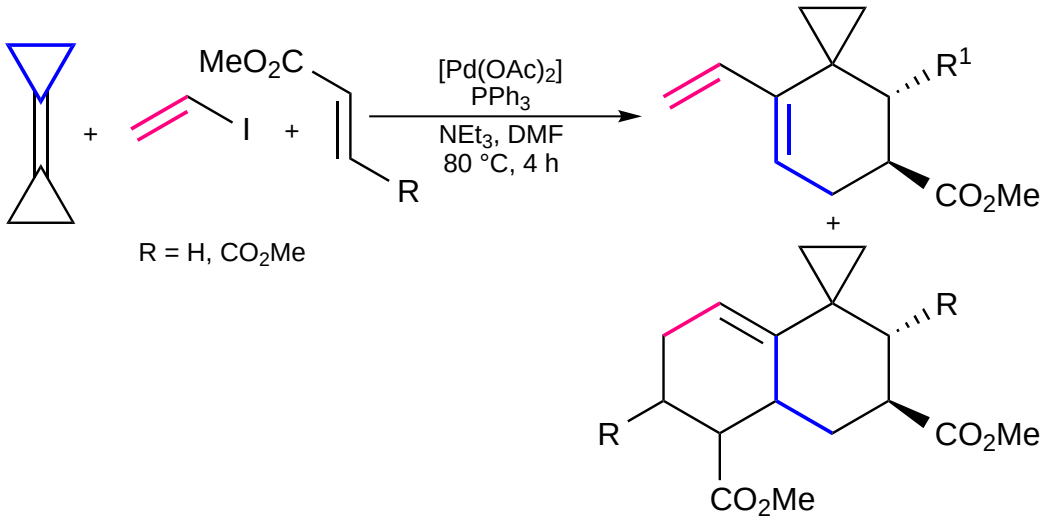

Scheme 1.23. Domino Heck-Diels-Alder reaction of BCP with iodoethene and dienophiles.[37,75]

An alternative sequence of reactions is observed when, instead of undergoing β-hydride elimination after the formation of the homoallylpalladium species, the intermediate rearranges to form a π-allylpalladium species.[74] This is favoured by the use of electron-rich ligands such as trifurylphosphine (TFP), which is known to retard β-hydride

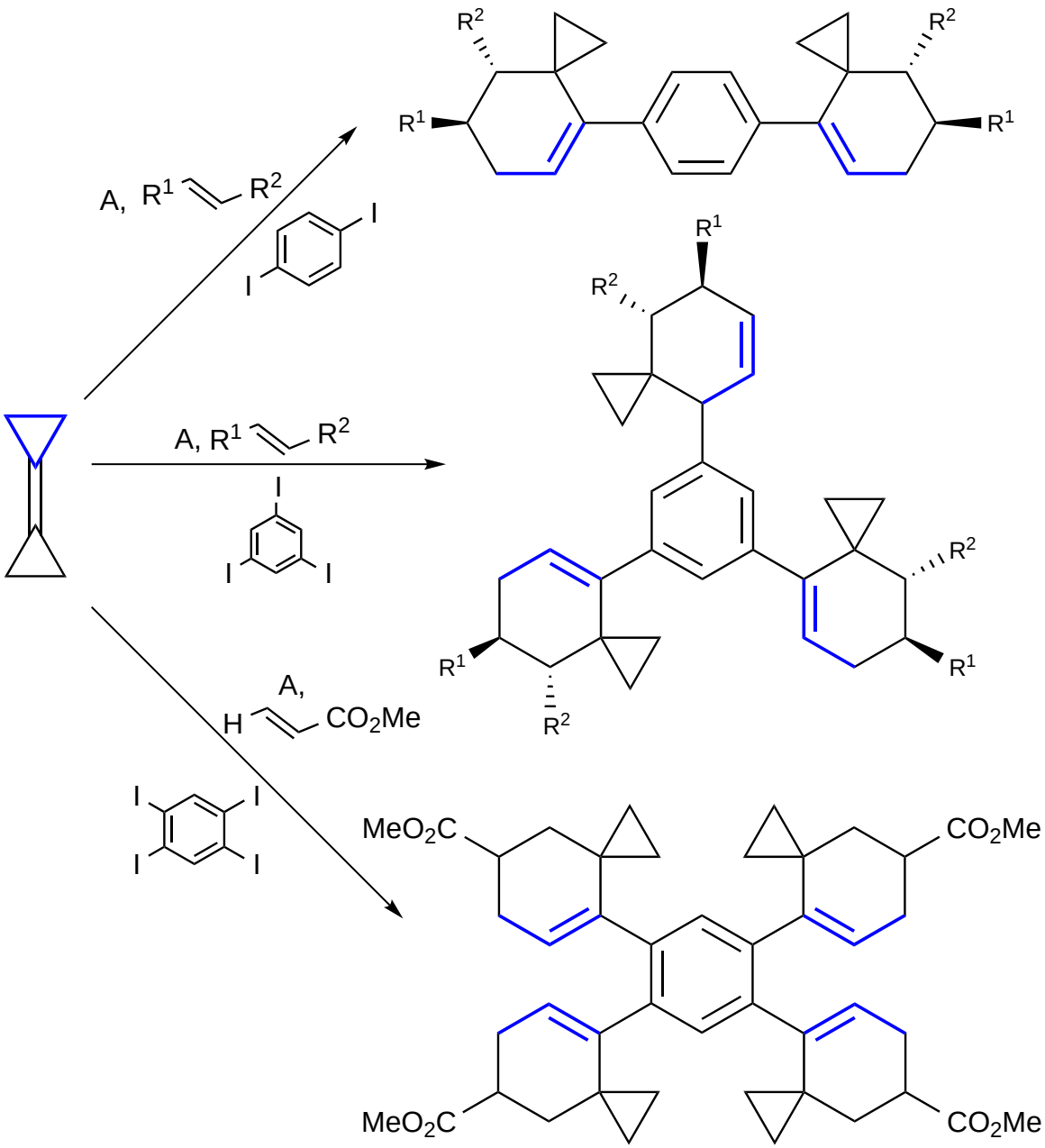

R^1	R^2
CO_2Me	H
$CO_2{}^tBu$	H
CO_2Me	CO_2Me

A = $[Pd(OAc)_2]$, PPh_3, MeCN, Et_4NCl, K_2CO_3, 80 °C, 2–3 d

Scheme 1.24. Multicomponent domino reactions of BCP.[74]

elimination.[63] The π-allylpalladium species can then undergo either inter- or intramolecular attack by a nucleophile (Schemes 1.25 and 1.26, *c.f.* Scheme 1.6).[63]

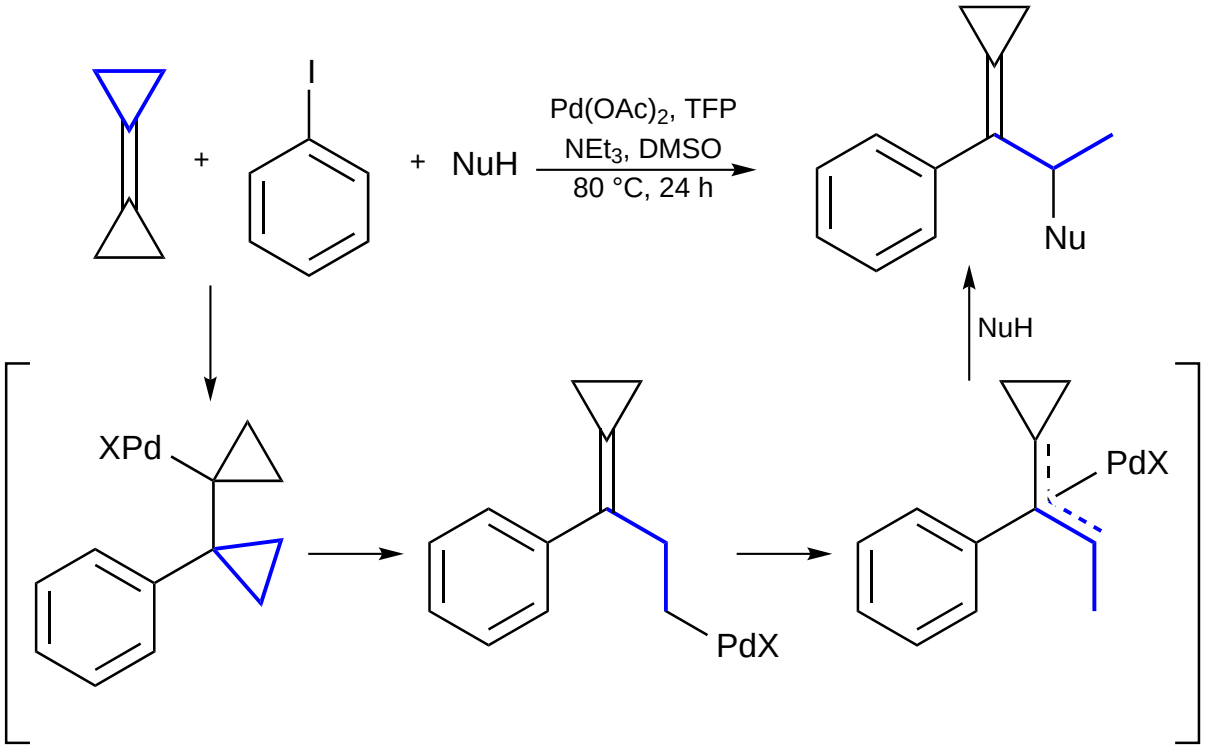

Scheme 1.25. Domino reaction of BCP involving a homoallyl- to π-allyl palladium rearrangement with an intermolecular nucleophile.[63]

When BCP is reacted with a Heck catalyst in the absence of another activated alkene, it undergoes Pd-catalysed isomerisation to form allylidenecyclopropane (Scheme 1.21, R = H). This then slowly reacts further to form several different dimeric species (Scheme 1.27).[74]

1.3.3.4 Bismetallation

As is the case with methylenecyclopropane, bicyclopropylidene can undergo palladium catalysed bismetallations. In particular, the additions of silyl-containing species, such as disilanes, silylboranes and silylstannanes, have been studied.[77] Disilanes, both intra- and inter-molecular, can be added across the bond with retention of both ^{c}Pr rings (Scheme 1.28).[77] The retention of both rings has also been achieved with silylstannanes (Scheme 1.29).[77] Tributyl(trimethylsilyl)stannane adds directly across the

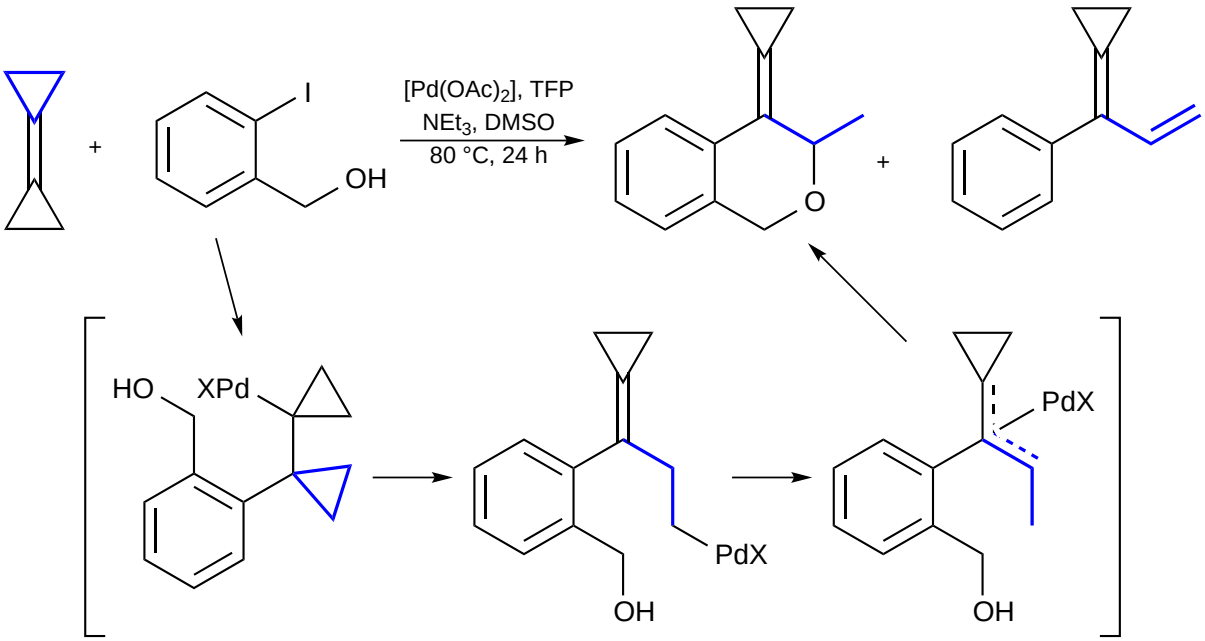

Scheme 1.26. Domino reaction of BCP involving a homoallyl- to π-allyl palladium rearrangement with an intramolecular nucleophile.[63]

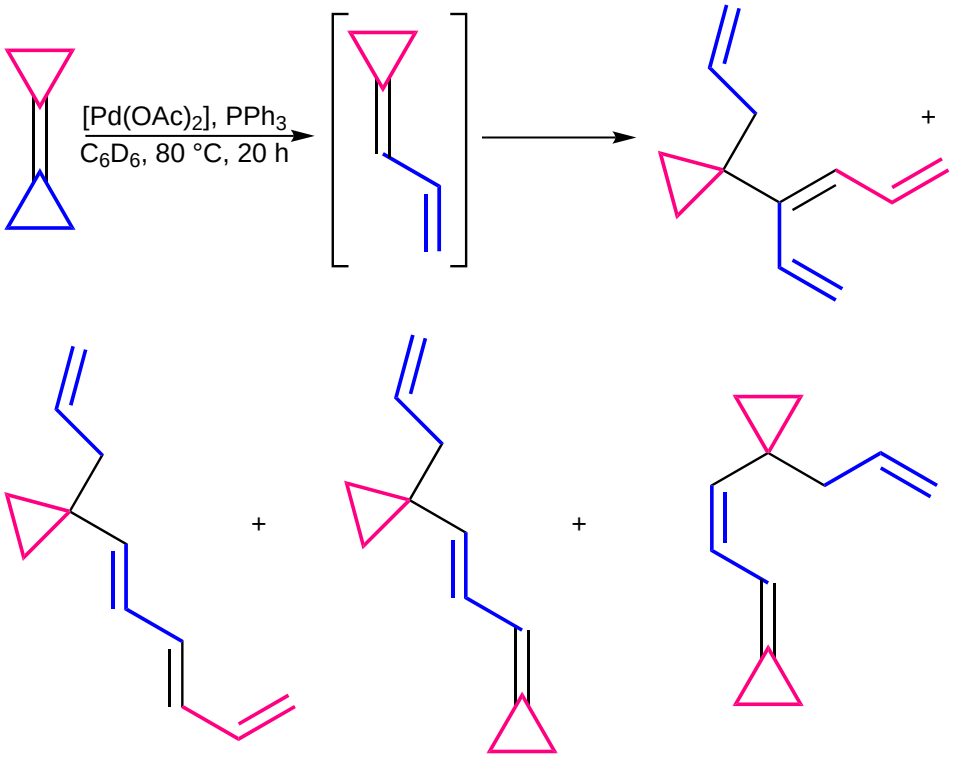

Scheme 1.27. Palladium-catalysed isomerisation of BCP.[74]

double-bond to give tributyl[1′-(trimethylsilyl)[1,1′-bicyclopropyl]-1-yl]-stannane. However, trimethyl(trimethylsilyl)stannane underwent Pd-catalysed disproportionation to form disilanes and distannanes, and the distannane subsequently added across the double-bond.[77]

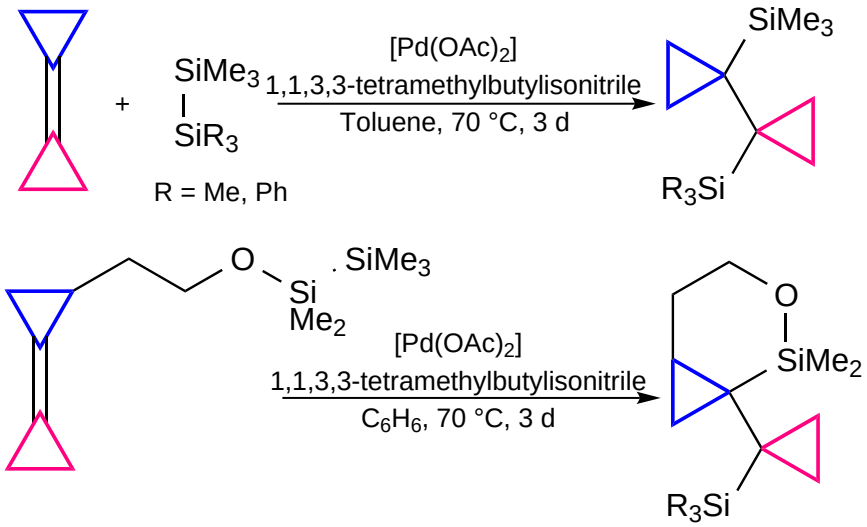

Scheme 1.28. Inter- and intra-molecular examples of the addition of a disilane to BCP with retention of both ^{c}Pr rings.[77]

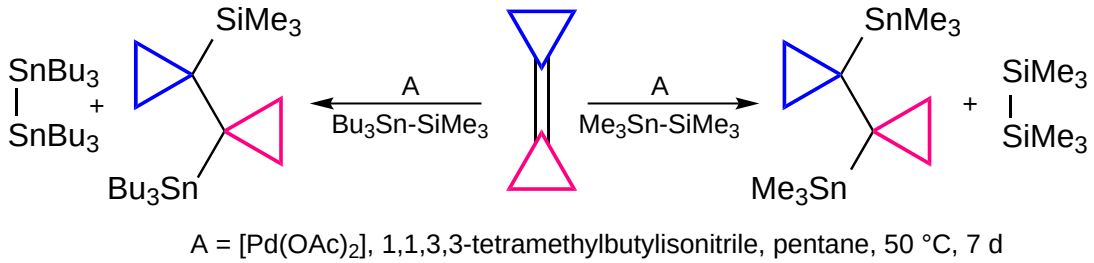

Scheme 1.29. Pd-catalysed addition of silylstannanes to BCP.[77]

Bismetallation reactions which involve the cleavage of one of the ^{c}Pr bonds can also occur.[77] This occurs with disilanes for which at least one of the silanes is halogenated, as well as for silylboranes and silylstannanes. The reaction seems to initially proceed by the insertion of a palladium atom into the silyl-metal bond, then by the addition of this silylpalladium species across the BCP double-bond. In the case where the ^{c}Pr rings are retained, the next step is reductive elimination to form the bicyclopropyl products. However, in most cases, instead of a reductive elimination there is a rearrangement to

generate a homoallylpalladium intermediate. This intermediate then undergoes reductive elimination to generate the ring-opened products (Scheme 1.30). It is thought that the deciding factor as to whether the product is the ring-opened or ring-retained product is the electrophilicity of the organopalladium species formed by the addition of the silylpalladium species across the double-bond (Scheme 1.30 (i)), with more electrophilic species favouring the ring-opened product.[77]

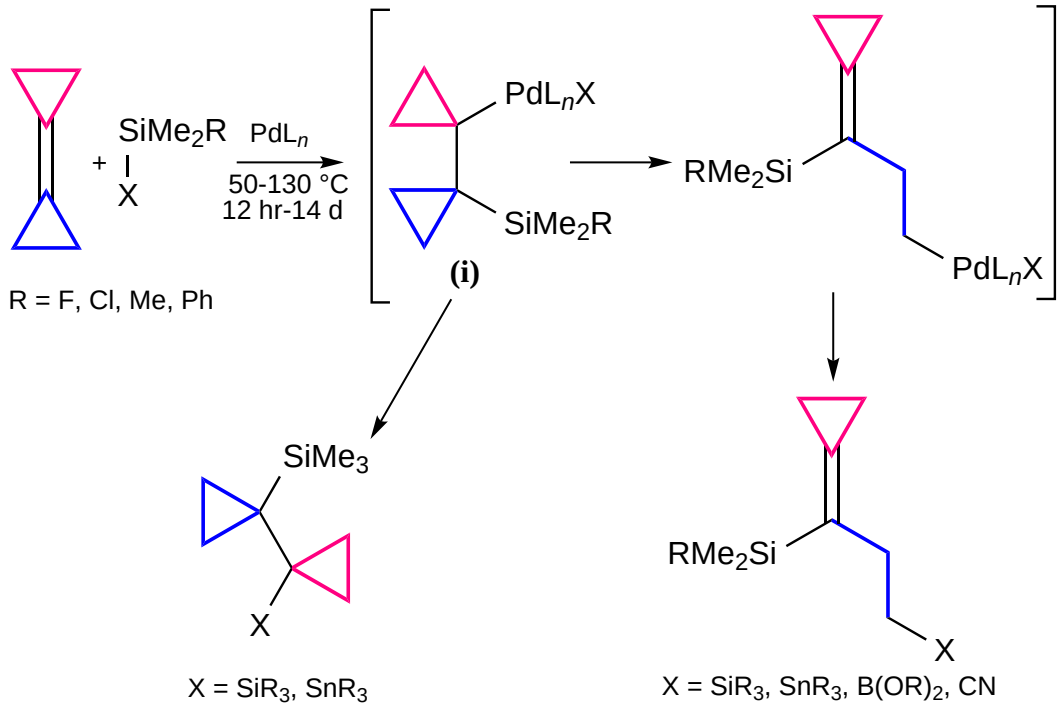

Scheme 1.30. Mechanism for the Pd catalysed bismetallation of BCP.[77]

1.3.3.5 Transition Metal Complexes

To date, there have been only two isolated transition metal complexes which have bicyclopropylidene as a ligand in η^2-coordination.[58] Most of the organometallic research involving BCP thus far has been focused on its behaviour in metal-catalysed reactions, rather than on the organometallic intermediates themselves. BCP has the potential to be a good ligand towards transition metals for a number of reasons. The high-lying HOMO means that it should be able to effectively donate electron density into the empty metal orbitals. Also, as it is a highly strained system, it should be able to accept back-bonding, stabilising the system by alleviating ring strain upon complexation.

The first transition metal complex of BCP was made from a bis(cyclopentadienyl)-bis(trimethylphosphine)titanium(II) precursor by reaction with BCP in pentane (Scheme 1.31).[58] The product with ligated BCP was obtained as a green solid in 79% yield. The precursor complex was chosen because titanocene complexes with alkene ligands are known 16-electron species. As such, if a BCP ligand was prone to ring-opening by oxidative addition, it would be likely to happen in this complex.[58] The isolation of this BCP complex shows that this does not happen with titanium.

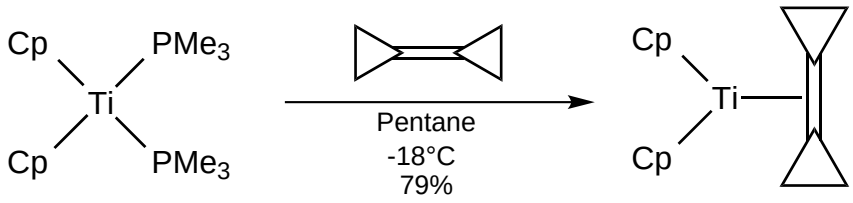

Scheme 1.31. Synthesis of the first Ti complex of BCP.[58]

The second BCP complex was made by reacting ((2-(di-tert-butylphosphanyl)-P-ethyl)cyclopentadienyl)chlorocobalt(II) ([CoCl(Cp#)]) with sodium amalgam and BCP (Scheme 1.32).[58,59] The Cp# ligand prevents potential oligomerisation reactions because the phosphine arm wins competition for the coordination site, preventing the complexation of another ligand and therefore reaction with the existing BCP ligand.[58]

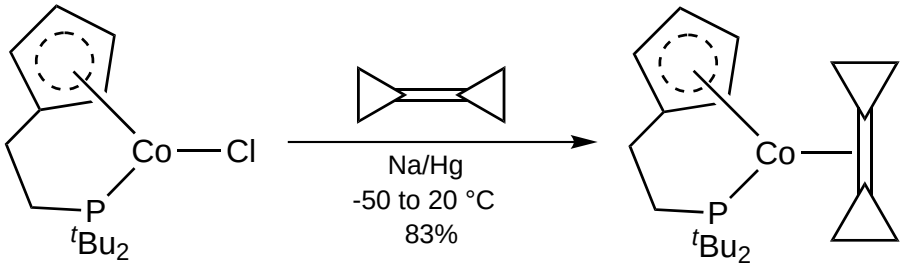

Scheme 1.32. Synthesis of the first Co complex of BCP.[58,59]

The X-ray crystal structure of the [Co(Cp#)(BCP)] complex (Figure 1.6)[58] shows that the ^{c}Pr rings of the BCP ligand are bent away from the double-bond by 40°. This and the increase of the length of the double-bond to 1.401 Å indicate that there is a high degree of back bonding, as predicted. The percentage change in the bond length upon complexation is greater in the case of BCP (7.4%) than for free ethene (5.0%), implying

a greater degree of back bonding to BCP.[78] As the character of the double-bond carbon atoms has become more sp^3-like, the proximal bonds in the two ^{c}Pr rings have shortened from 1.544 to 1.499 Å.

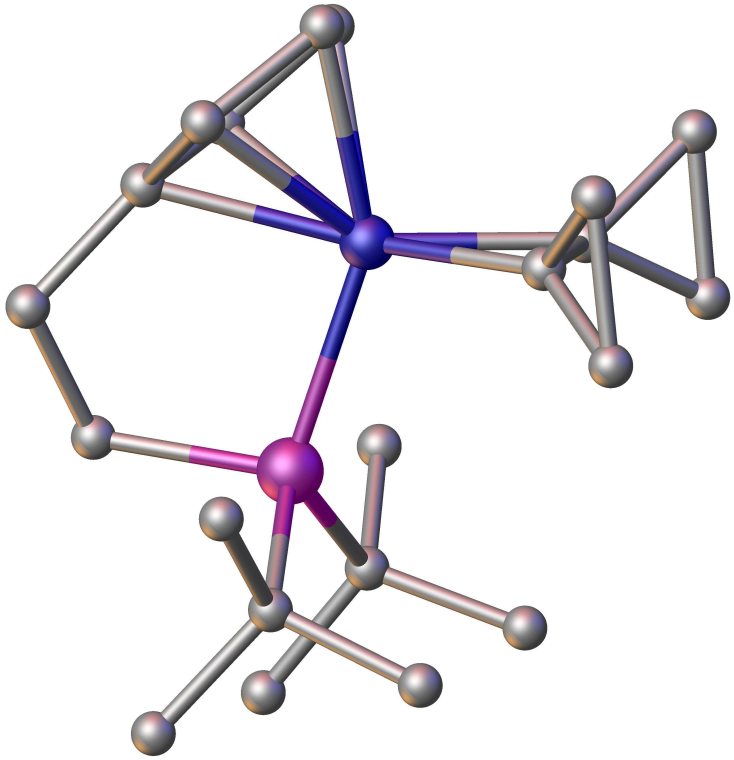

Figure 1.6. X-ray crystal structure of [Co(Cp#)(BCP)].[58]

These two complexes show that BCP is a good ligand toward transition metals. As such, there is much potential for the synthesis of complexes containing this ligand with other transition metals. As there is a dearth of isolated η^2-alkene complexes of both BCP and MCP, the initial focus of this project was on the synthesis of platinum complexes with these ligands. The reactivity of these complexes was then investigated. During the exploration of the reactivity of BCP and MCP towards platinum, a range of reactivity patterns were observed. Complexes with ligands derived from these reactions were also synthesised.

Chapter 2

Platinum(0) Phosphine Complexes

The reactions of methylenecyclopropane and bicyclopropylidene with Pt(0) alkene complexes produced η^2-MCP and BCP complexes. Complexes with both mono- and di-phosphine auxillary ligands were synthesised. BCP underwent a ring-opening reaction to form the 1,3-diene allylidenecyclopropane, and the coordination chemistry of ACP was explored.[79]

2.1 [Pt(L)(P—P)] Complexes

A range of Pt(0) complexes containing chelating diphosphines as auxiliary ligands were chosen as precursors. These complexes were chosen because chelating phosphines not only stabilise transition metal complexes, particularly those in low oxidation states, but also allow the coordination of only one alkene ligand, thus preventing possible oligomerisation reactions. The diphosphines used in this research were 1,3-bis(diphenylphosphino)propane (dppp), 1,2-bis(dicyclopentylphosphino)ethane (dcyppe), 1,2-bis(di-*tert*-butylphosphino)ethane (dbpe) and 1,2-bis[(di-*tert*-butylphosphino)methyl]benzene (dbpx), representing a variety of electronic properties and backbone sizes (Figure 2.1).

As discussed in Section 1.1.3, one of the ways of synthesising alkene complexes is by the displacement of another ligand such as another alkene. Ethene complexes were chosen as suitable precursors due to the ease of displacement of the ethene ligand as well

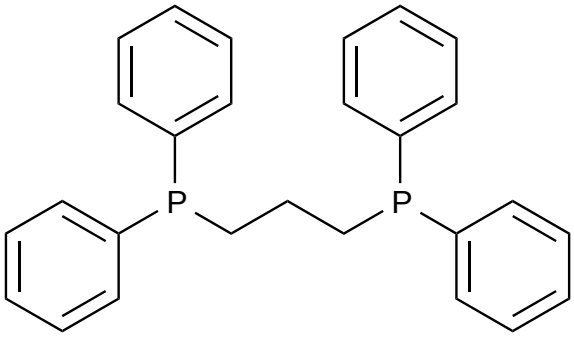

dppp

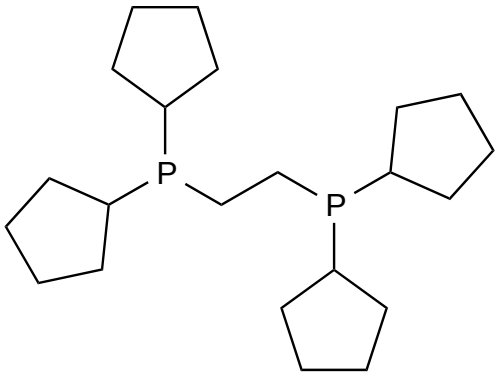

dcyppe

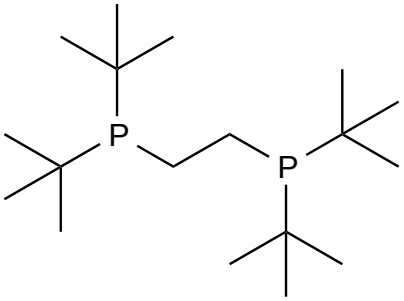

dbpe

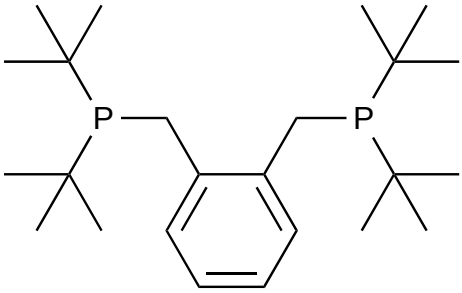

dbpx

Phosphine	***θ*** **(°)**	***ν*** **(cm^{-1})**
dppp	127	2067 (PPh_2Et)
dcyppe	*	*
dbpe	115[80]	2058 (PEt^tBu_2)
dbpx	138[81]	2060 ($P(o\text{-tol})^tBu_2$)

θ = Tolman cone angle. Calculated from the cone formed between the metal and the outer hydrogens of the ligand with an M–P bond length of 2.28 Å.[82]
ν = Tolman electronic parameter. Calculated from the C≡O stretching frequency in $[Ni(CO_3)(L)]$.[82]
* No data available.

Figure 2.1. Structures and properties of diphosphine ligands.[82]

as the simplicity of the NMR spectra of both the free and the coordinated alkene, which facilitated the monitoring of the reactions. Free ethene is observed at δ_H 5.2 and δ_C 123 ppm, while the resonances of coordinated ethene occur at approximately δ_H 2–3 ppm and δ_C 20–30 ppm.

A range of methods were used to synthesise the various ethene complexes, with the choice of method dictated by the diphosphine ligand. The complexes $[Pt(C_2H_4)(dbpe)]$ and $[Pt(C_2H_4)(dbpx)]$ were synthesised by adding adding the appropriate diphosphine to $[Pt(C_2H_4)_3]$, generated *in situ* from $[Pt(COD)_2]$.[83] This method was unsuitable for the synthesis of $[Pt(C_2H_4)(dppp)]$, as the coordination of a second dppp ligand to form $[Pt(dppp)_2]$ is very facile. Instead, the ethene complex was generated by the reduction of $[PtCl_2(dppp)]$ under an ethene atmosphere using $NaBH_4$.

While the reaction of dcyppe with $[Pt(C_2H_4)_3]$ yielded $[Pt(C_2H_4)(dcyppe)]$, problems with purification meant that this was not a viable synthetic method. Reduction with $NaBH_4$ was attempted, but was not successful. Instead, $[Pt(C_2H_4)(dcyppe)]$ was synthesised by the reduction of $[PtCl_2(dcyppe)]$ using sodium amalgam. Complexes of 1,2-bis(diphenylphosphino)ethane (dppe) were considered, as these would have made a good comparison for the dppp complexes. However, $[Pt(C_2H_4)(dppe)]$ could not be synthesised from $[Pt(C_2H_4)_3]$ due to the facile formation of $[Pt(dppe)_2]$, while reduction methods yielded only $[Pt_3H_3(dppe)_3]^+$. $[Pt_3H_3(dppe)_3]^+$ forms because the intermediate hydride complex in the reduction reaction is dimeric for dppe, rather than monomeric as for dppp.[84,85] While the synthesis of $[Pt(C_2H_4)(dppe)]$ using sodium naphthalenide has been reported,[86] this method did not involve the isolation of the pure ethene complex, which meant that this synthesis was not suitable for the NMR-scale studies undertake here.

Methylenecyclopropane was made by the reaction of methallyl chloride with sodium amide and potassium *tert*-butoxide (Scheme 1.2 (ii)),[28] while the synthesis of bicyclopropylidene made use of the Kulinkovich reaction to produce cyclopropylcyclopropanol from methyl cyclopropanecarboxylate, which was then converted to the bromide followed by dehydrobromination to produce the alkene (Scheme 1.13).[67] Whereas BCP is an easily handled liquid, MCP is a gas at room temperature, with a boiling point of 10 °C. For this

research, it was generally deemed most practical to use MCP by cooling a glass syringe in the freezer and then rapidly inject a small amount of the liquid alkene into the reaction vessel. However, standard solutions in both C_6D_6 and $CDCl_3$ were occasionally used.

Carbon-13 enriched bicyclopropylidene was synthesised in order to increase the sensitivity of the double-bond carbons toward ^{13}C NMR spectroscopy (Scheme 2.1). First, cyclopropanecarboxylic acid was synthesised using a Grignard reagent formed from cyclopropyl bromide and CO_2 generated from $BaCO_3$ (70% ^{13}C). This was then converted to methyl cyclopropanecarboxylate using methyl iodide and DBU.[87] The ^{c}PrCOOMe was then diluted with the carbon-12 variant to 12% enrichment of carbon-13, and the BCP synthesis continued as previously. The overall yield of this process was 0.8% based on $BaCO_3$. This was both due to the small scale of the ^{c}PrCOOMe to BCP synthesis (the yield of this stage was 7%, compared to 27% for larger scale) and to difficulties in the ^{c}PrCOOH synthesis. While the literature method reported yields of 82% for the synthesis of ^{c}PrCOOH, it was not possible to obtain yields of greater than 30%.[88]

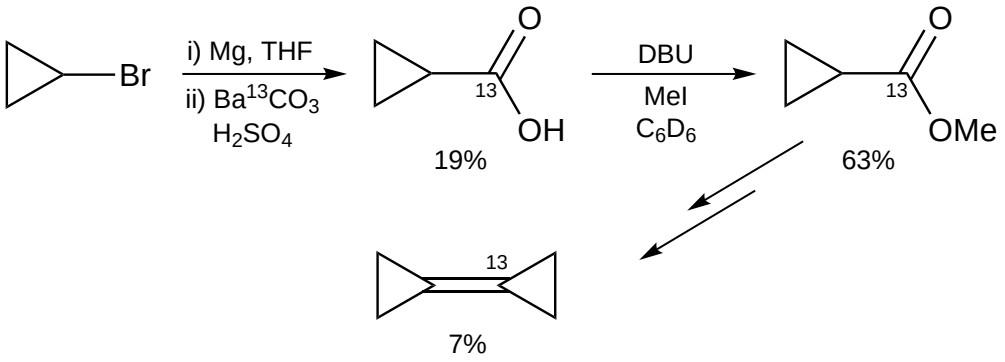

Scheme 2.1. Synthesis of carbon-13 enriched bicyclopropylidene.

BCP and MCP complexes were synthesised *via* the displacement of the ethene ligand from the precursor complexes. This was done by dissolving the ethene complex in either toluene or d_6-benzene and adding an excess of the appropriate alkene, producing the diphosphine complexes [Pt(BCP)(P—P)] (P—P = dppp (**1a**), dcyppe (**1b**), dbpe (**1c**) and dbpx (**1d**)) and [Pt(MCP)(P—P)] (P—P = dppp (**2a**), dcyppe (**2b**), dbpe (**2c**) and dbpx (**2d**)) (Scheme 2.2).

The formation rates of the complexes were found to depend on both the size of the

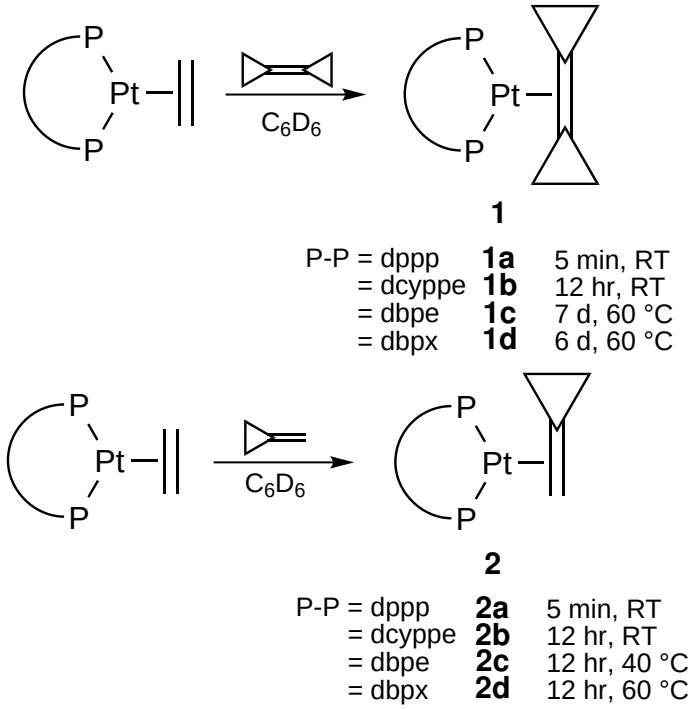

Scheme 2.2. Synthesis of [Pt(BCP)(P—P)] (**1**) and [Pt(MCP)(P—P)] (**2**).

alkene and the size of the diphosphine ligand. MCP, with only one ^{c}Pr ring, coordinated more rapidly than BCP, with two rings. The steric bulk of the substituents on the phosphine ligands had a more significant effect on the formation rates. Complexes of dppp formed most rapidly, with the reaction occurring almost instantly at room temperature. Complexes of dcyppe reacted more slowly, forming overnight at room temperature. Both of the ^{t}Bu phosphine complexes required heating, at 40 and 60 °C overnight for **2c** and **2d**, respectively, and for up to 7 days for **1c** and **1d**. The dependence of reaction rate on steric bulk points to an associative rather than dissociative exchange mechanism.

X-ray quality crystals of **1a** were grown by recrystallisation from hot toluene, and an X-ray crystal structure was obtained (Figure 2.2, Table 2.1). The BCP C=C bond length increased from 1.304(2) Å in the free alkene to 1.427(3) Å in **1a**, an increase of 9.4%.[30] This was greater than the 7.4% increase observed for [Co(Cp#)(BCP)], which had a C=C bond length of 1.401(5) Å.[59] The bond length of **1a** was closer to that of the comparable C–C bond in bicyclopropyl (1.487(4) Å, differing from **1a** by 0.06 Å) than to the C=C bond length of free BCP (differing from **1a** by 0.123 Å).[89] The two ^{c}Pr rings in **1a** were bent by 36.02° and 37.14° away from the plane of the double-bond. The

corresponding angles in the cobalt complex were 39.33° and 41.04°, while in bicyclopropyl the rings were at 54.72° to the central C–C bond. There was a decrease in the ^{c}Pr ring angle centered on the double-bond carbon atom from 63.3(1)° to 61.40(14)° and 61.37(15)° upon coordination and a concomitant shortening of the distal ring bond from 1.539(2) Å to 1.516(3) and 1.519(3) Å. This effect was greater in the Co complex, with angles and distal bond lengths of 61.15° and 1.499(12) Å, respectively. The increase in the C=C bond length, the out-of-plane bend of the ^{c}Pr rings, and the shortening of the ring bond and angle were all indicative of the large degree of back-donation and subsequent rehybridisation of the double-bond carbon atoms upon coordination.[8,59]

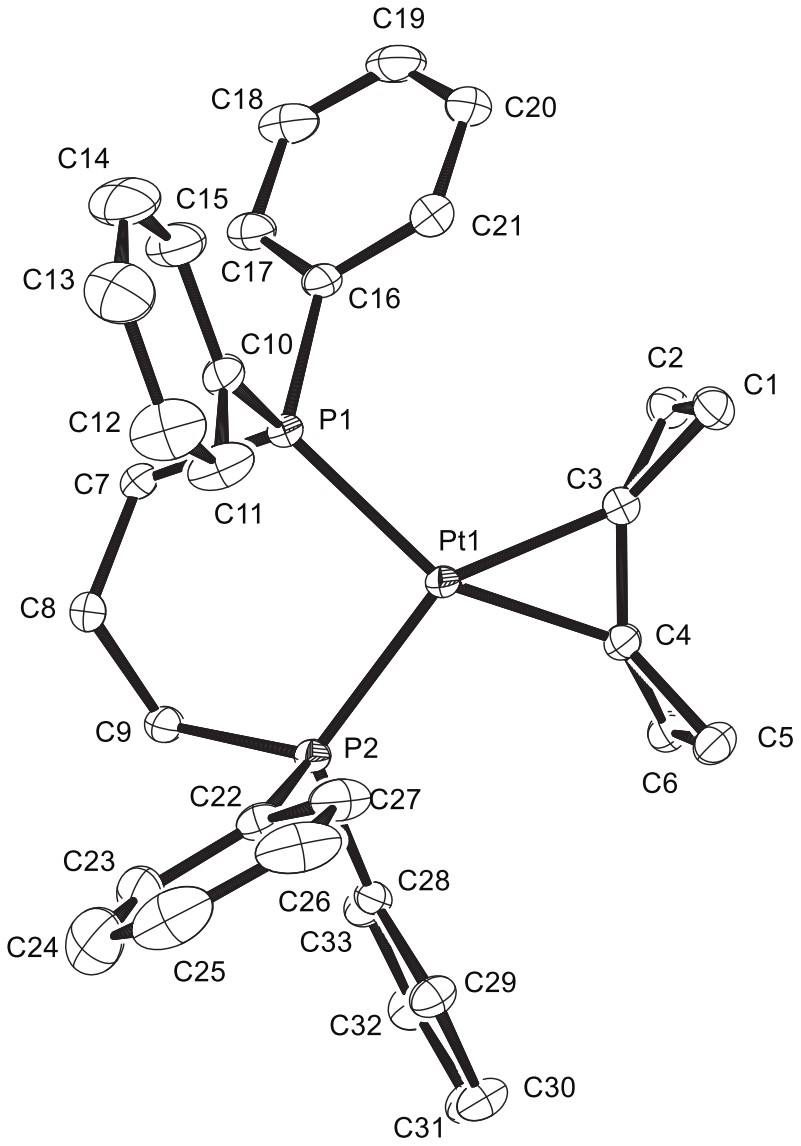

Figure 2.2. ORTEP diagram of [Pt(BCP)(dppp)] (**1a**) showing 50% probability thermal ellipsoids. H atoms have been omitted for clarity.

Table 2.1. Crystallographic Data for [Pt(BCP)(dppp)] (**1a**).

Chemical formula	$C_{33}H_{34}P_2Pt$
Formula weight	687.63
a, Å	16.8042(6)
b, Å	9.6338(3)
c, Å	17.7241(6)
α, deg	90.00
β, deg	106.904(2)
γ, deg	90.00
V, Å^3	2745.35(16)
Z	4
Space group	$P2_1/n$
T, K	119.0
λ, Å	0.71073
D_{calcd}, g cm^{-3}	1.664
μ, mm^{-1}	5.248
R_1, [I$> 2\sigma$(I)]^a	0.0252
wR_2 (all data)^a	0.0502

^{a} Definition of R indices: $R_1 = \Sigma||F_o|-|F_c||/\Sigma|F_o|$; $wR_2 = [\Sigma w({F_o}^2-{F_c}^2)^2/\Sigma w({F_o}^2)^2]^{1/2}$.

The dppp backbone adopted a chair conformation, with a P–Pt–P angle of 96.762(19)°. A search of the Cambridge Crystallographic Database in March 2011 showed that of 81 dppp complexes with one or two platinum atoms, 86% adopted a chair and 9% adopted a boat conformation, while 5% were not sufficiently resolved to determine the conformation. Four of the 81 complexes were Pt(0) species, and of the four, three were trigonal planar complexes. All four Pt(0) complexes had dppp in a chair conformation.[90–92] These complexes had P–Pt–P angles of 90.99–97.76°, with that of **1a** falling at the top end of the range.

2.1.1 NMR Characterisation

For representative NMR spectra, see Figures A.1–A.11. The magnitude of the platinum–phosphorus $^1J_{Pt–P}$ coupling constants in the $^{31}P\{^1H\}$ NMR spectra of **1** and **2** showed that

the alkenes were in η^2-coordination. In the BCP complexes, $^1J_{\text{Pt–P}}$values were between 2731 and 2983 Hz (Table 2.2), ∼450 Hz less than those in the parent ethene complex. The ^{31}P{^{1}H} NMR spectra of **2** had second-order ABX (A, B = ^{31}P, X = ^{195}Pt) peak patterns due to the unsymmetrical alkene and the rigid coordination geometry (Figure 2.3 (i)). The $^1J_{\text{Pt–P}}$values could be used to distinguish the P *trans* to the ^{c}Pr group from that of the P *trans* to the methylene in the MCP complexes, as the two coupling constants were comparable to those of **1** and the parent ethene complexes, respectively.

The ^{13}C{^{1}H} NMR spectra also clearly showed that the alkenes were in η^2-coordination. The cyclopropyl double-bond carbons showed large $^1J_{\text{Pt–C}}$ values, 410–456 Hz for **1** and 455–538 Hz for **2** (Table 2.2), while the methylene carbon in **2** had $^1J_{\text{Pt–C}}$ several hundred Hz less (164–173 Hz). There was also a large upfield shift of the ^{c}Pr double-bond carbon resonances upon coordination, from 110.6 to 29–34 ppm for **1** and from 131.0 to 33–43 ppm for **2**. The methylene carbon was typically ∼15 ppm upfield of the ^{c}Pr carbon, expect for in **2d**, where the difference was only 5.8 ppm. For comparison, the methylene chemical shift differed from that of the parent ethene ligand by 0.6–6.6 ppm. A stronger Pt–C bond is formed to the cyclopropyl carbons in **1** and **2** than to the methylene carbons in **2** and the parent ethene complexes. This is evidenced by the lower $^1J_{\text{Pt–P}}$ of the P *trans* to the cyclopropyl carbons and the higher $^1J_{\text{Pt–C}}$ coupling constants of these carbons and is a result of the decrease in strain energy of the ^{c}Pr rings by rehybridisation upon coordination.[8,93–97]

For the double-bond carbons in **1**, the line shape was characteristic of a "false AA′X" spin system (A, A′ = ^{31}P, X = ^{13}C) with ^{195}Pt satellites due to both the magnetic inequivalence of the two chemically equivalent carbons when one was ^{13}C and to the two ^{31}P atoms having the same chemical shift (Figure 2.3).[98,99] The double-bond carbons in **2**, however were ABX systems with ^{195}Pt satellites, as the two ^{31}P atoms were in different chemical environments.[99] These ^{13}C NMR peaks, and the ^{31}P NMR spectra of **2**, indicate that the alkene ligands do not rotate at room temperature when coordinated, as rotation would result in the two ^{31}P atoms becoming equivalent.

The *endo*/*exo* geometry of the ^{c}Pr protons in **1a** and **2a** (Figure 2.4) was assigned

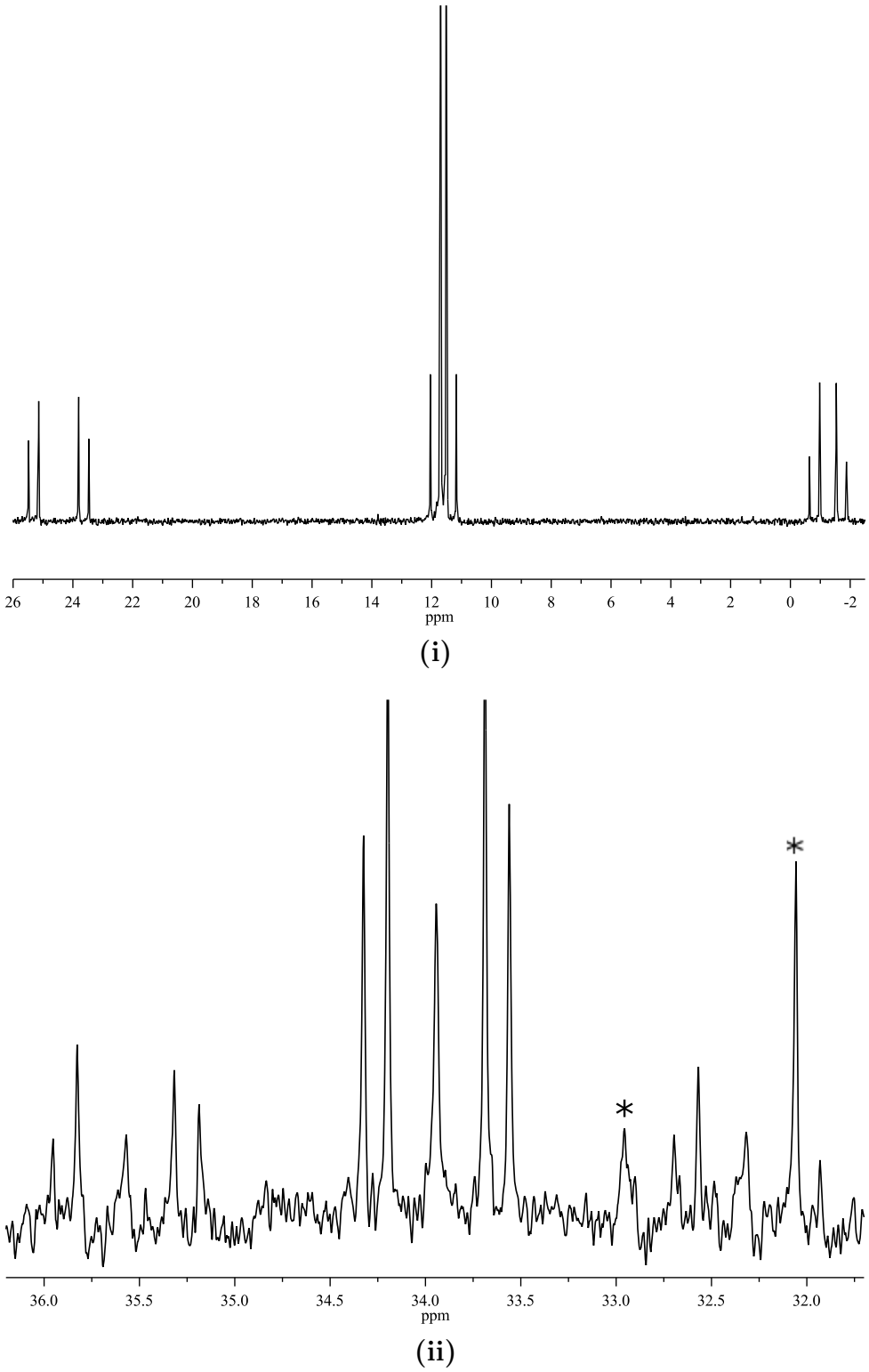

Figure 2.3. (i) $^{31}P\{^{1}H\}$ NMR spectrum of [Pt(MCP)(dppp)] (**2a**) (125 MHz, RT, 40 mg/mL, C_6D_6). (ii) $^{13}C\{^{1}H\}$ NMR spectrum of [Pt(BCP)(dppp)] (**1a**) (150 MHz, RT, 40 mg/mL, C_6D_6). * signifies peaks belonging to other species.

Table 2.2. Selected NMR Data of [Pt(L)(P—P)].[a]

Compound		δ_P	$^1J_{Pt-P}$	$^2J_{Pt-P}$		^cPr				=CHR				$=CR_2$	
						δ_H	J_{Pt-H}	δ_C	J_{Pt-C}	δ_H	$^2J_{Pt-H}$	δ_C	$^1J_{Pt-C}$	δ_C	$^1J_{Pt-C}$
BCP						1.18		3.3						110.6	
MCP						0.90		2.9		5.46		103.5		131.1	
ACP						0.93		2.6		6.53		136.9		129.3	
						0.85		2.3							
[Pt(BCP)(dppp)]	**1a**	9.3	2932			1.29	66.0	8.8	23.1					34.3	410.8
						1.18	37.7								
[Pt(BCP)(dcyppe)]	**1b**	70.8	2731			1.5–1.4	[b]	10.4	23.1					33.8	424.6
[Pt(BCP)(dbpe)]	**1c**	97.4	2798			1.57	[b]	9.9	23.7					31.8	428.9
						1.31	[b]								
[Pt(BCP)(dbpx)]	**1d**	43.3	2983			1.34	61.2	9.9	22.5					29.3	456.3
						0.99	32.0								
[Pt(BCP)(P—S)]	**8**	54.9	3383			[b]	[b]	9.0					*trans* P	28.1	579.0
								8.7					*trans* S	25.2	656.6
[Pt(MCP)(dppp)]	**2a**	11.7	3275	42	*trans* $=CH_2$	1.65	33.0	10.1	25.9	2.63	65.3	25.3	173.4	42.7	455.4
		11.4	2975		*trans* $=CR_2$	1.32	82.5								
[Pt(MCP)(dcyppe)]	**2b**	75.0	2751	63	*trans* $=CR_2$	1.95	[b]	12.3	23.0	2.40	60.5	22.4	169.0	38.3	501.0
		70.8	3107		*trans* $=CH_2$	1.80	[b]								
[Pt(MCP)(dbpe)]	**2c**	100.8	2807	66	*trans* $=CR_2$	1.89	33.6	11.8	24.5	2.39	60.6	23.5	171.6	36.8	511.4
		99.2	3167		*trans* $=CH_2$	1.79	60.0								
[Pt(MCP)(dbpx)]	**2d**	49.3	3362	30	*trans* $=CH_2$	1.60	[b]	11.4	25.0	2.12	56.2	27.8	164.2	33.6	537.6
		43.7	3025		*trans* $=CR_2$	1.60	[b]								
[Pt(MCP)(P—S)]	**9a**	58.8	3870		*trans* $=CH_2$	1.45	[b]	10.5	30.1	2.05	52.7	26.3	145.1	[b]	[b]
						1.37	[b]								
[Pt(MCP)(P—S)]	**9b**	55.3	3483		*trans* $=CR_2$	1.59		10.0	24.8	2.38	82.1	25.7	270.6	[b]	[b]
						1.50									
[Pt(ACP)(dppp)]	**3a**	10.3	3293	39	*trans* $=CHR$	1.3–0.8	[b]	[b]	[b]	3.78	67.8	[b]	[b]	[b]	[b]
		9.7	3003		*trans* $=CR_2$										
[Pt(ACP)(dcyppe)]	**3b**	70.0	3153	−59	*trans* $=CHR$	[b]	[b]	[b]	[b]	3.41	62.1	[b]	[b]	[b]	[b]
		68.6	2771		*trans* $=CR_2$										
[Pt(ACP)(dbpe)]	**3c**	96.4	2848	62	*trans* $=CR_2$	1.5	[b]	10.6	17.7	3.43	62.0	44.7	165.5	41.4	533.1
		96.4	3196		*trans* $=CHR$	1.0	[b]	9.5	15.5						
[Pt(C_2H_4)(dppp)]		13.8	3340							2.68	60.0	31.9	216.0		
[Pt(C_2H_4)(dcyppe)]		75.4	3170							2.38	58.0	23.2	227.4		
[Pt(C_2H_4)(dbpe)]		102.5	3230							2.41	59.4	25.0	229.0		
[P(C_2H_4)(dbpx)]		50.1	3493							2.20	57.3	27.2	217.0		

[a] δ values are given in ppm and J values in Hz. All spectra were measured in C_6D_6 at room temperature with 40 mg/mL sample. [b] NMR data could not be obtained.

using 1D NOESY correlations. When each proton resonance was selectively excited, those due to the *endo* protons showed correlations to the *o*-C_6H_5 protons on the phosphine substituents, as well as to the other ^{c}Pr protons, while the *exo* protons only correlated to the ^{c}Pr protons. It was also found that the *endo* protons had significantly higher $J_{\mathrm{Pt-H}}$ couplings (∼60 *vs.* ∼30 Hz), allowing the geometry of other complexes to be assigned by analogy.

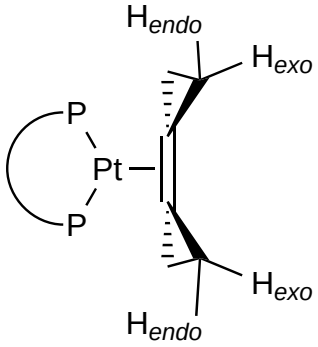

Figure 2.4. Geometry of the *endo*/*exo* protons in [Pt(BCP)(P—P)] (**1**).

Due to the complex nature of the ^{31}P NMR spectra of **2** and the ^{13}C NMR resonances of the double-bond carbons of **1**, the NMR modelling program gNMR was used to obtain chemical shift and coupling constant data reported in Table 2.2.

2.2 Allylidenecyclopropane

It was found that when BCP reacted with $[Pt(C_2H_4)_3]$, a ring-opening reaction occurred to form the 1,3-diene, allylidenecyclopropane (ACP) (Scheme 2.3). This reaction also occurred with $[Pt(COD)_2]$, $[Pt(nb)_3]$, $[PtMe_2(1,5\text{-hexadiene})]$ and $[PtEt_2(COD)]$. One previous instance of the formation of ACP from BCP has been reported, occurring in the reaction of BCP with $[Pd(OAc)_2]$ and PPh_3.[74] The proposed mechanism for this reaction involved the addition of a palladium hydride across the BCP double-bond, followed by a cyclopropylmethyl to homoallyl rearrangement and terminated by β-hydride elimination. Under the reported conditions, ACP went on to react with another molecule of BCP to form various oligomers (see Scheme 1.21, R = H). However, no oligomerisation reactions were observed with the above Pt complexes, even after several days at 60 °C.

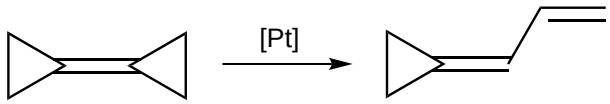

Scheme 2.3. Synthesis of allylidenecyclopropane from bicyclopropylidene.

As there were no published reports of any transition metal chemistry with ACP, the formation of Pt-diphosphine complexes containing ACP ligands was investigated. A solution of ACP was produced for these reactions by dissolving a few crystals of [$PtMe_2$(1,5-hexadiene)] in either $CDCl_3$ or C_6D_6 under inert atmosphere and adding a small amount of BCP. The reaction could then be monitored by NMR spectroscopy for completion, typically reaching ∼95% after 5 days. The solution was then used without further purification.

The first transition metal complexes of allylidenecyclopropane (**3a** and **3b**) formed immediately upon addition of the ACP solution to the parent ethene complex [$Pt(C_2H_4)$(P—P)] (P—P = dppp, dcyppe) (Scheme 2.4). ACP could also be generated *in situ* from small amounts of [$Pt(COD)_2$], and the addition of BCP and [$Pt(COD)_2$] to solutions of [$Pt(C_2H_4)$(dbpe)], followed by heating at 40 °C, was used to synthesise **3c** (Scheme 2.5). With 10% [$Pt(COD)_2$] present, the reaction reached 97% completion after heating overnight. The formation of **3c** still occurred when no detectable [$Pt(COD)_2$] was present; however, this reaction only reached 88% completion after 13 days. [Pt(ACP)(dbpx)] could not be synthesised, likely due to the steric bulk of the phosphine ligand making coordination of the alkene unfavourable.

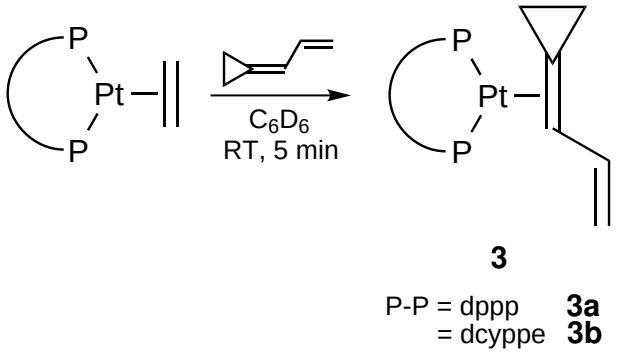

Scheme 2.4. Synthesis of [Pt(ACP)(P—P)] (**3**).

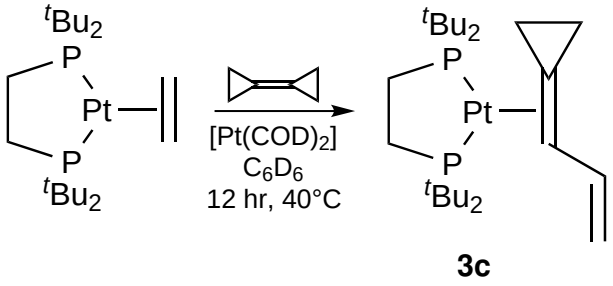

3c

Scheme 2.5. Synthesis of [Pt(ACP)(dbpe)] (**3c**).

It was found that when both ACP and BCP were present in the reaction mixture, ACP complexes formed initially. However, the ACP ligand in **3a** was slowly displaced by BCP over several hours at room temperature to form **1a**. For the dbpe complexes, **3c** was the only product at 40 °C, while at 60 °C, **3c** formed initially, before continued heating over several days produced **1c**. It was unclear whether this would also happen for the dcyppe complexes, as **3b** underwent a rearrangement that reached completion too rapidly for displacement to occur (see below), although it is considered likely. From this we infer that the complexes of the less bulky ACP were the kinetic products, while the BCP complexes, which had a degree of extra stabilisation afforded by alleviation of strain in the second cyclopropyl ring, were the thermodynamic products.

Complexes **3a** and **3b** were unstable in solution, undergoing a rearrangement to form the metallacyclic complexes **4a** and **4b** (Scheme 2.6). The rearrangement proceeded more rapidly for the dcyppe complex **3b**, with significant amounts of **4b** present within 5 min of addition of the ACP solution and the reaction proceeding to completion after 3 hr. For the dppp complex **3a**, the metallacycle appeared in the $^{31}P\{^{1}H\}$ NMR spectroscopy after 3 hr, reaching 96% completion after 7 days.

The formation of metallacyclo-3-pentenes from 1,3-dienes is well established. There are two possible binding modes for these ligands: the η^4:σ^2,π mode, where the double-bond is also coordinated to the metal, common for early transition and actinide metals,[100–102] and the planar η^2:σ^2 mode. Planar metallacyclopentene complexes are considered to be intermediates in ring-flipping mechanisms of η^4-diene complexes,[103] and complexes with η^2:σ^2-metallacyclopentene ligands formed from various 1,3-dienes have been reported for

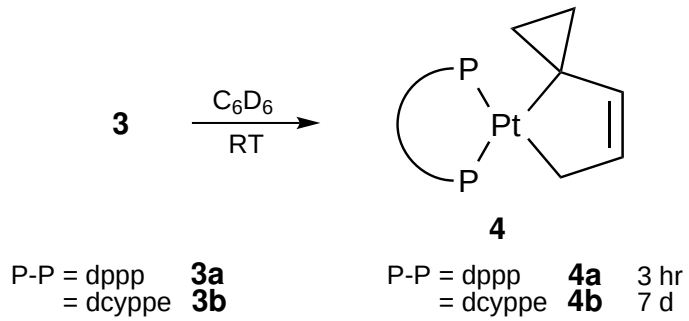

Scheme 2.6. Rearrangement of [Pt(ACP)(P—P)] (**3a**) to form metallocyclopentene complexes

Fe,[104,105] Co,[106] Mo[107] W,[107] Rh,[103,108–110] Ir,[111–114] Pt,[103,115] Ge,[116] and Mg.[117]

The rearrangements of **3** to **4** appear to be the first instances of the formation of η^2:σ^2-metallacyclopentene complexes from η^2:π-diene complexes. Previously reported η^2:σ^2-metallacyclopentenes were formed either directly upon addition of the 1,3-diene to a metal precursor[103–105,108–110,115–117] or by rearrangement of an η^4:π-diene complex, generally initiated by the addition of a species such as a Lewis base.[106,107,113,114]

2.2.1 NMR Characterisation

2.2.1.1 Allylidenecyclopropane Complexes

All ACP complexes exhibited second-order ABX $^{31}P\{^1H\}$ NMR spectra similar to the corresponding MCP complexes, with $^1J_{Pt–P}$ couplings for both phosphine environments within 40 Hz of those in **2** (Table 2.2). The ^1H NMR signal of the internal double-bond proton showed a large upfield shift from 6.6 ppm in free ACP to 3.4–3.8 ppm in **3** (Table 2.3). The magnitudes of the $^2J_{Pt–H}$ coupling constants of these protons, 62–68 Hz, were typical of coordination through this bond. The protons of the terminal double-bond have chemical shifts much closer to those in the free alkene. Both the ^1H and the ^{31}P NMR data indicated that ACP was coordinated *via* the internal rather than the terminal double-bond. This is to be expected given the stabilisation afforded by the alleviation of ring strain in the ^{c}Pr upon coordination.

The $^1J_{Pt–C}$ coupling constants of the internal double-bond carbons of **3c** further indicated that the alkene had coordinated *via* this bond. The coupling constant for

Table 2.3. ^{1}H and ^{13}C{^{1}H} NMR Data of [Pt(ACP)(P—P)].[a]

Compound		δ_H				δ_C				
		^{c}Pr	=CH$_2$	terminal =CHR	internal =CHR	^{c}Pr	=CH$_2$	terminal =CHR	internal =CHR	=CR$_2$
ACP		0.93	5.18	6.49	6.58	2.6	115.2	120.2	136.9	129.3
		0.85	5.05			2.3				
[Pt(ACP)(dppp)]	**3a**	1.3–0.8	5.04	6.47	3.78	[b]	[b]	[b]	[b]	[b]
			4.69		$^2J_{Pt-H}$ = 67.8 Hz					
[Pt(ACP)(dcyppe)]	**3b**	[b]	4.85	6.11	3.41	[b]	[b]	[b]	[b]	[b]
			4.37		$^2J_{Pt-H}$ = 62.1 Hz					
[Pt(ACP)(dbpe)]	**3c**	1.5	4.98	6.20	3.43	10.6	102.7	147.5	44.7	41.4
			4.64		$^2J_{Pt-H}$ = 62.0 Hz	9.5				

[a] δ values are given in ppm and J values in Hz. All spectra were measured in C_6D_6 at room temperature with 40 mg/mL sample. [b] NMR data could not be obtained.

the cyclopropyl carbon was 533 Hz, while that of the methyne was 166 Hz, both of which were within 20 Hz of the corresponding value for **2c** (Table 2.2). The chemical shifts of the carbons of the terminal double-bond were also much closer to those of the free alkene than the internal double-bond carbons (Table 2.3). In **3c**, the double-bond carbons had an AA′X coupling pattern with ^{195}Pt satellites similar to those of the BCP complexes. This was due to the two phosphorus atoms in this complex coincidentally having the same chemical shift.[99] The effect could be seen throughout the carbon spectrum, with all of the resonances of the ACP ligands in **3a** and **3b** would have ABX spectra (with ^{195}Pt satellites) similar to the corresponding MCP complexes, as the phosphorus atoms have different chemical shifts. However, due to the short lifetimes of these complexes, ^{13}C NMR data could not be obtained.

2.2.1.2 Metallocyclopentene Complexes

For representative NMR spectra, see FIgures A.12–A.15. The NMR data of **4** were consistent with a planar η^2:σ^2-metallocyclopentene structure. The $^1J_{\mathrm{Pt–P}}$ coupling constants of **4** (1784–1856 Hz) were comparable to those of [Pt(CH$_2$CPh=CCHC=CMe$_2$)(dppe)] (1818 and 1842 Hz), which showed that there were Pt–C σ-bonds in **4**.[103] In the previously reported Pt metallacycles, the CH_2 groups directly bonded to the metal had δ_{H} at 2.8–3.2 ppm with $^2J_{\mathrm{Pt–H}}$ = 68–92 Hz and δ_{C} at 31–41 ppm with $^1J_{\mathrm{Pt–C}}$ = 603–787 Hz,[103,115] while the Ir metallacycles had 2.4–3.0 and −2–13 ppm for δ_{H} and δ_{C}, respectively.[113] The NMR data of both the Pt–CH_2 groups (δ_{H} = 2.9–3.2 ppm, $^2J_{\mathrm{Pt–H}}$ = 62–73 Hz, δ_{C} = 29–39 ppm, $^1J_{\mathrm{Pt–C}}$ = 297–450 Hz) and the Pt–CR_3 groups (δ_{C} = 32-33 ppm, $^1J_{\mathrm{Pt–C}}$ = 959 Hz for **4b**) in **4** agree well with the literature. The NMR data of the double-bond carbons and their attached protons (δ_{H} = 5.3–6.4 and δ_{C} = 131–154 ppm) also compared favourably to the literature values (δ_{H} = 5.0–5.6 and δ_{C} = 135.9–151.3 ppm).[103,113,115]

2.3 [Pt(L)$_2$(PR$_3$)] Complexes

Precursor complexes containing two ethene ligands and one phosphine ligand were also investigated. Bis-ethene complexes were chosen due to the possibility that oligomerisation

or isomerisation reactions similar to the formation of ACP from BCP might occur. Complexes of the type [M(L)(BCP)(PR_3)] (M = Ni, Pd, L = electron-deficient alkene, PR_3 = *tert*-butyldiisopropylphosphine, tris(*o*-phenylphenyl)phosphite) have been proposed as intermediates in the palladium- and nickel catalysed [3+2] co-cyclisation of BCP with various alkenes, but were not isolated (see Scheme 1.16).[72] Bis-BCP complexes have also been postulated to be intermediates in nickel-catalysed [3+2+2] co-cyclisations.[118]

Bis-ethene precursor complexes [Pt(C_2H_4)$_2$(PR_3)] (PR_3 = PPh_3, PCy_3) were synthesised by addition of the appropriate phosphine (Figure 2.5) to [Pt(C_2H_4)$_3$].[119] When BCP was added to [Pt(C_2H_4)$_2$(PR_3)], the product was [Pt(C_2H_4)(BCP)(PR_3)] (PR_3 = PPh_3 (**5a**), PCy_3 (**5b**)) (Scheme 2.8). For the bulkier PCy_3, complex **5b** was stable with an excess of BCP. However, **5a** was stable in solution only when 1 equiv. of BCP was used. When more than 1 equiv. was used, [Pt(BCP)(PPh_3)$_2$] began to form after 40 min and was the only phosphine-containing product after 24 hr. No other platinum-containing species were identified. The formation of a bis-BCP complex did not occur with either of the phosphines used in this work. This was likely due to the steric constraints of having the two alkenes in a planar coordination geometry as occurs with platinum(0).[2]

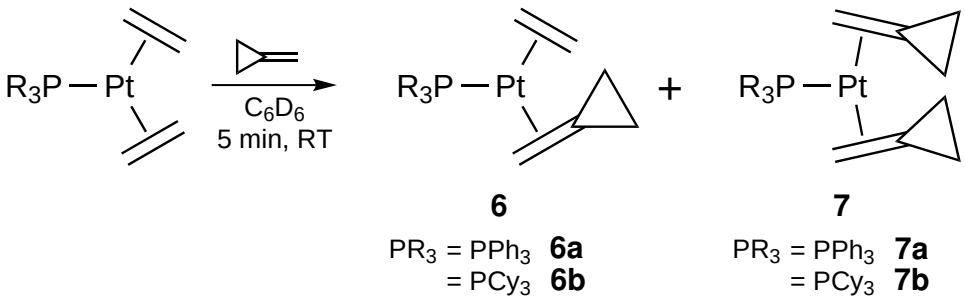

Scheme 2.7. Synthesis of [Pt(MCP)(C_2H_4)(PR_3)] (**6**) and [Pt(MCP)$_2$(PR_3)] (**7**).

Despite the large excesses of MCP used, both the mixed alkene [Pt(C_2H_4)(MCP)(PR_3)] (PR_3 = PPh_3 (**6a**), PCy_3 (**6b**)) and the bis-MCP complexes [Pt(MCP)$_2$(PR_3)] (PR_3 = PPh_3 (**7a**), PCy_3 (**7b**)) were always formed in a closed system (Scheme 2.7). The bis-MCP complexes **7** are the first examples of Pt-MCP complexes with more than one MCP ligand. When PPh_3 was used, the product ratio was 80:20 bis-MCP:mixed alkene. The ratio changed to 30:70 in favour of the mixed complex when PCy_3 was used, with the

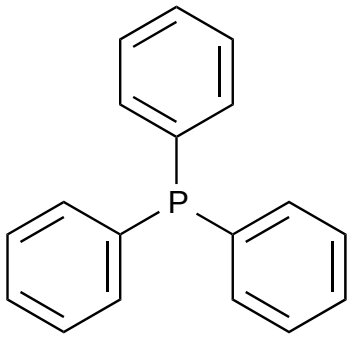

PPh_3

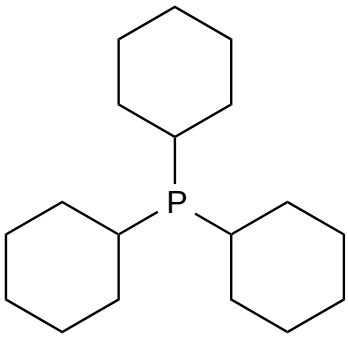

PCy_3

Phosphine	$\boldsymbol{\theta}$ **(°)**	$\boldsymbol{\nu}$ **(cm^{-1})**
PPh_3	145	2069
PCy_3	170	2056

θ = Tolman cone angle. Calculated from the cone formed between the metal and the outer hydrogens of the ligand with an M–P bond length of 2.28 Å.[82]
ν = Tolman electronic parameter. Calculated from the C≡O stretching frequency in $[Ni(CO_3)(L)]$.[82]

Figure 2.5. Structures and properties of monophosphine ligands.[82]

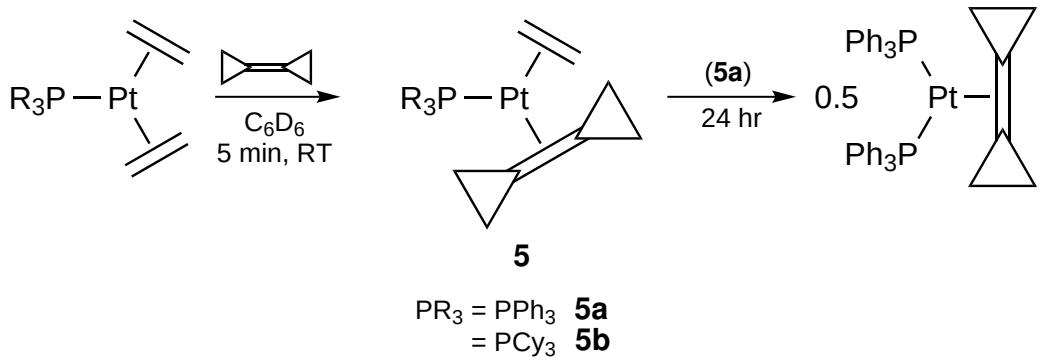

Scheme 2.8. Synthesis of $[Pt(BCP)(C_2H_4)(PR_3)]$ (**5**).

bulkier phosphine hindering but not preventing the coordination of the second MCP ligand. When ethene was allowed to diffuse out of the reaction, complex **7a** was formed in 90% yield. Yields could be improved and complex **7b** formed selectively when inert gas was bubbled through the reaction mixture. The mixed alkene complexes **6** became the major products when ethene was bubbled through the solution. However, the mixed alkene complexes were much less stable than the bis-MCP complexes, as large amounts of ethene regenerated the bis-ethene complexes, while in the presence of free MCP, **7** formed.

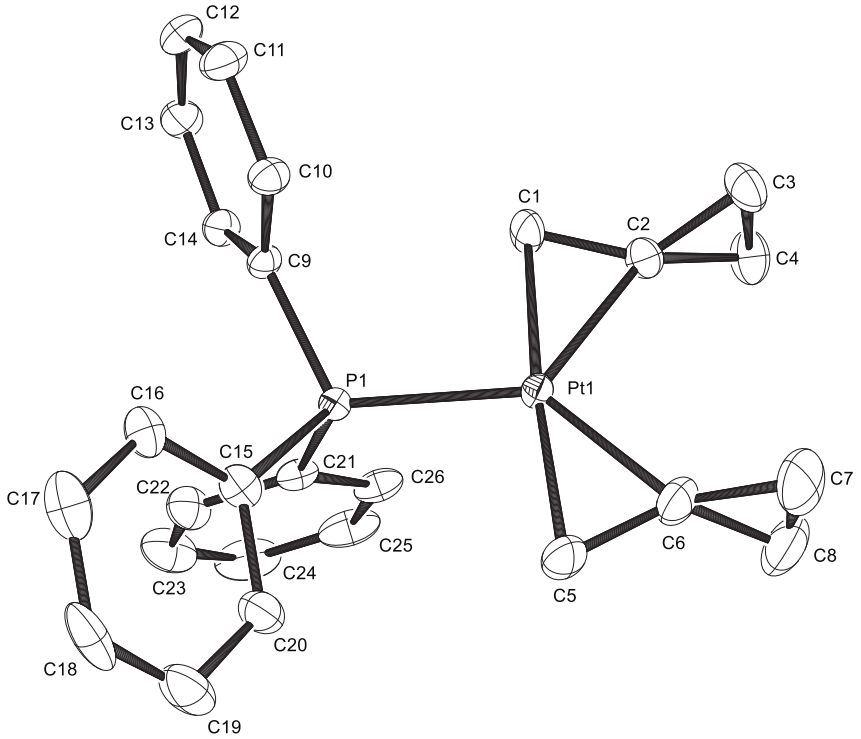

Figure 2.6. ORTEP diagram of $[Pt(MCP)_2(PPh_3)]$ (**6**a) showing 50% probability thermal ellipsoids. H atoms have been omitted for clarity.

X-ray quality crystals of **7a** were grown from cold hexane (Figure 2.6, Table 2.4). The MCP carbon–carbon double-bond length was increased by 5.7% upon coordination, from 1.332(1) Å in free MCP to 1.408(5) Å in **7a**.[29] In [Rh(acac)(MCP)$_2$], the only other MCP complex characterized by X-ray diffraction, the bond lengths were 1.405(19) and 1.440(19) Å, representing increases of 5.4% and 8.1%, respectively. The increase in MCP bond length upon coordination was much greater than the 1.5% increase in ethene C=C bond length in the related complex [Pt(C_2H_4)(C_2F_4)(PCy_3)], the only other [Pt(alkene)$_2$(PR_3)] complex with an X-ray crystal structure.[120,121] The C_2F_4 bond increased by 10.0% upon coordination.[122] The cyclopropyl rings in **7a** were bent by 35.49° and 35.86° away from the plane of the double-bond, a greater angle than those in the Rh complex (26.48° and 27.79°). Given the strain of the ^{c}Pr ring, it would be expected that there was a stronger bond from the platinum to the ring double-bond carbon than to the methylene carbon. This was evidenced by the shorter Pt–C distance to the ^{c}Pr carbon (2.087(3) and 2.093(3) Å) than to the methylene (2.130(3) and 2.123(3) Å). The Pt–P bond length was 2.3028(7) Å, shorter than that in [Pt(C_2H_4)(C_2F_4)(PCy_3)], which had a Pt–P distance of 2.343(2) Å.

2.3.1 NMR Characterisation

For representative NMR spectra, see Figures A.20–A.25. The double-bond carbons of the BCP ligands in **5** had similar chemical shifts (29–30 ppm) and $^1J_{\mathrm{Pt–C}}$ (431–483 Hz) to those in **1**, indicating that the ligands were in η^2-coordination (Table 2.5). The $^1J_{\mathrm{Pt–P}}$ coupling constants in both mixed alkene complexes were ∼330 Hz lower than those of the parent bis-ethene complexes, showing the same decrease in $^1J_{\mathrm{Pt–P}}$ upon coordination of BCP as was seen for the diphosphine complexes.

The mixed ethene–MCP complexes **6** had $^1J_{\mathrm{Pt–P}}$ couplings within 10 Hz of the ethene–BCP complexes **5** (Table 2.5). ^{13}C NMR data could not be obtained for these complexes due to their instability. However, their ^{1}H NMR spectra showed similar chemical shifts and $^2J_{\mathrm{Pt–H}}$ for the ethene ligands to **5**. The bis-MCP complexes **7** had $^1J_{\mathrm{Pt–P}}$ several hundred Hz lower than the parent ethene complexes and more than 150 Hz lower than

Table 2.4. Crystallographic Data for $[Pt(MCP)_2(PPh_3)]$ (**6**a).

Chemical formula	$C_{26}H_{27}PPt$
Formula weight	565.54
a, Å	10.4179(4)
b, Å	10.7385(4)
c, Å	11.3770(4)
α, deg	66.647(2)
β, deg	71.772(2)
γ, deg	70.542(2)
V, Å^3	1077.48(7)
Z	2
Space group	$P-1$
T, K	119.0
λ, Å	0.71073
D_{calcd}, g cm^{-3}	1.743
μ, mm^{-1}	6.594
R_1, [I$> 2\sigma$(I)]^a	0.0250
wR_2 (all data)^a	0.0601

^{a} Definition of R indices: $R_1 = \Sigma||F_o|-|F_c||/\Sigma|F_o|$; $wR_2 = [\Sigma w(F_o{}^2-F_c{}^2)^2/\Sigma w(F_o{}^2)^2]^{1/2}$.

the mixed alkene complex (Table 2.5). The MCP methylene resonances in the ^{1}H NMR were also at lower chemical shifts than in the mixed complex and had lower $^2J_{Pt-H}$ (50-55 Hz), closer to those of the ethene rather than the MCP ligand in **6**. Both the carbon and proton NMR data showed that the two MCP ligands were in the same chemical environment on the NMR time scale. While this could be due to rotation of the ligands, it was considered more likely that the ligands were arranged either head-to-head or tail-to-tail. The X-ray crystal structure of **7a** showed that in the solid state the two MCP ligands were tail-to-tail

Table 2.5. Selected NMR Data of $[Pt(L)_2(PR_3)]$.[a]

Compound		δ_P	$^1J_{Pt-P}$	^cPr				MCP $=CH_2$				C_2H_4 $=CH_2$				$=CR_2$	
				δ_H	J_{Pt-H}	δ_C	J_{Pt-C}	δ_H	$^2J_{Pt-H}$	δ_C	$^1J_{Pt-C}$	δ_H	$^2J_{Pt-H}$	δ_C	$^1J_{Pt-C}$	δ_C	$^1J_{Pt-C}$
$[Pt(BCP)(C_2H_4)(PPh_3)]$	**5a**	23.2	3094	1.2–0.8	[b]	9.2–6.8	[b]					2.71	51.0	54.8	102.2	30.2	431.5
$[Pt(BCP)(C_2H_4)(PCy_3)]$	**5b**	25.3	2976	1.17–1.05	[b]	8.3	23.8					2.68	50.0	50.7	101.8	29.1	482.9
$[Pt(MCP)(C_2H_4)(PPh_3)]$	**6a**	23.6	3085	1.64	60.0	[b]	[b]	2.58	61.5	[b]	[b]	2.61	56.0	[b]	[b]	[b]	[b]
				1.55	34.0												
$[Pt(MCP)(C_2H_4)(PCy_3)]$	**6b**	28.0	2978	1.5–0.9	[b]	[b]	[b]	2.52	61.2	[b]	[b]	2.49	48.1	[b]	[b]	[b]	[b]
$[Pt(MCP)_2(PPh_3)]$	**7a**	22.3	2932	1.31	[b]	7.8	24.5	2.39	55.0	38.9	100.3					54.1	352.9
$[Pt(MCP)_2(PCy_3)]$	**7b**	23.2	2695	1.47–1.29	[b]	7.2	25.0	2.27	50.0	32.0	[b]					48.5	385.6
$[Pt(MCP)_2(P—S)]$	**10**	40.6	2661	[b]	[b]	7.2	25.4	2.49	48.1	35.7	100.6					48.7	381.9
$[Pt(C_2H_4)_2(PPh_3)]$		24.6	3426									2.82	57.8	42.3	146		
$[Pt(C_2H_4)_2(PCy_3)]$		29.2	3296									2.72	56.7	36.9	146		

[a] δ values are given in ppm and J values in Hz. All spectra were measured in C_6D_6 at room temperature with 40 mg/mL sample. [b] NMR data could not be obtained.

Chapter 3

Phosphine-Thioether and Allyl Complexes

Phosphine-thioether (P—S) Pt(0) complexes with η^2-methylenecyclopropane and bicyclopropylidene ligands were synthesised by the displacement of the norbornene ligand from [Pt(nb)(P—S)]. These complexes rearranged to form allyl complexes through metallation of the P—S backbone. Analogous allyl complexes were also synthesised by the protonation of diphosphine MCP and BCP complexes.

3.1 [Pt(L)(P—S)] Complexes

The novel complex [Pt(nb)(P—S)] (nb = norbornene, P—S = ^{t}Bu$_2$PCH$_2$(*o*-C$_6$H$_4$)CH$_2$S^{t}Bu),[123] was used as a precursor complex because the P—S ligand is an analogue of 1,2-bis[(di-*tert*-butylphosphino)methyl]benzene (dbpx). Dbpx is used in a number of catalytic systems, including the commercial synthesis of methyl methacrylate.[124–128] The replacement of one of the phosphine groups with a thioether has the potential to affect the reactivity of complexes in catalysis, particularly as the sulfur is potentially hemilabile.[129–132] The synthesis of BCP and MCP complexes was undertaken to give insight into the effect of the different donor atoms, as well as to compare the P—S ligand to dbpx (see Section 2.1 for dbpx complexes).

[Pt(BCP)(P—S)] (**8**) was synthesised by the addition of a stoichiometric amount

of BCP to [Pt(nb)(P—S)] (Scheme 3.1). The formation of **8** was complete after one hour at room temperature. In the analogous reaction with MCP, two isomers of [Pt(MCP)(P—S)] formed over an hour at room temperature. In this case, two isomers were formed. The major isomer (**9a**), which formed in a 62:38 ratio relative to the minor isomer, had the cyclopropyl ring *trans* to the sulfur, while the minor isomer (**9b**) had the cyclopropyl ring *trans* to the phosphorus (Scheme 3.2). When one equivalent of MCP was added to [Pt(nb)(P—S)], **9** formed in only 80% yield by $^{31}P\{^{1}H\}$ NMR. However, the [Pt(nb)(P—S)] continued to react slowly, until it had reacted completely (see Section 3.2.1). When a large excess of MCP was used, all of the nb complex reacted immediately, and **9a**, **9b** as well as a new complex **10** formed, initially in a 40:24:36 ratio. This new complex (**10**) was determined to be [Pt(MCP)$_2$(P—S)] (Scheme 3.3).

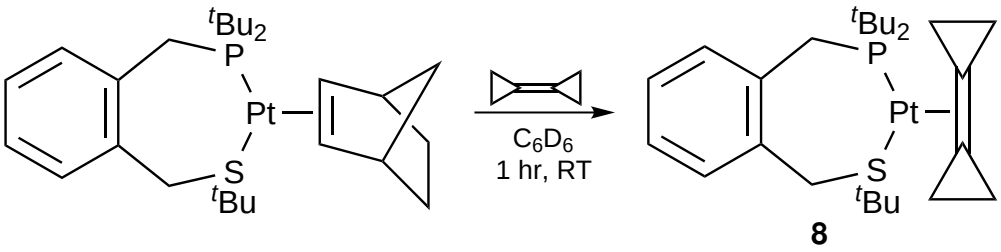

Scheme 3.1. Synthesis of [Pt(BCP)(^{t}Bu$_2$PCH$_2$(o-C$_6$H$_4$)CH$_2$S^{t}Bu)] (**8**).

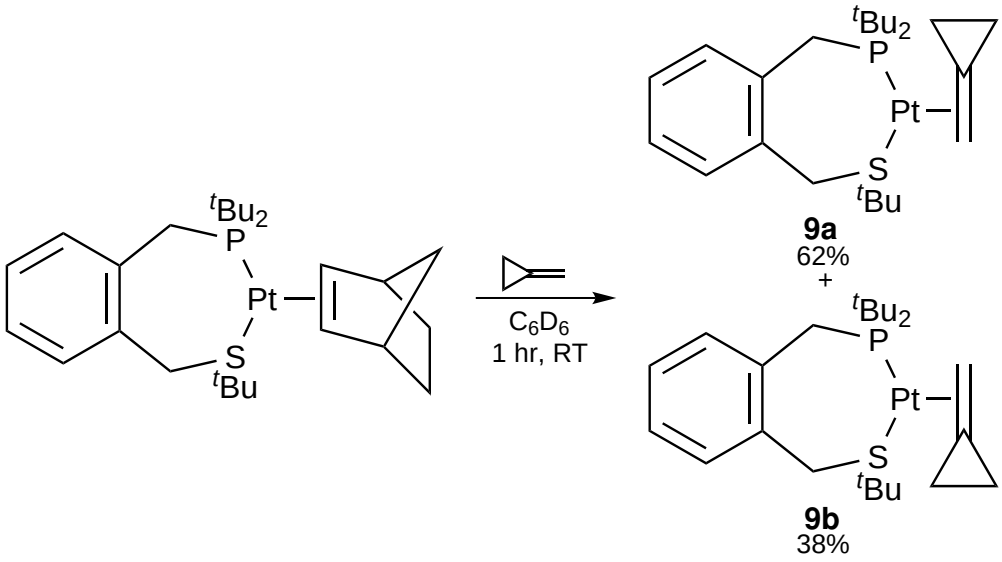

Scheme 3.2. Synthesis of [Pt(MCP)(^{t}Bu$_2$PCH$_2$(o-C$_6$H$_4$)CH$_2$S^{t}Bu)] (**9**).

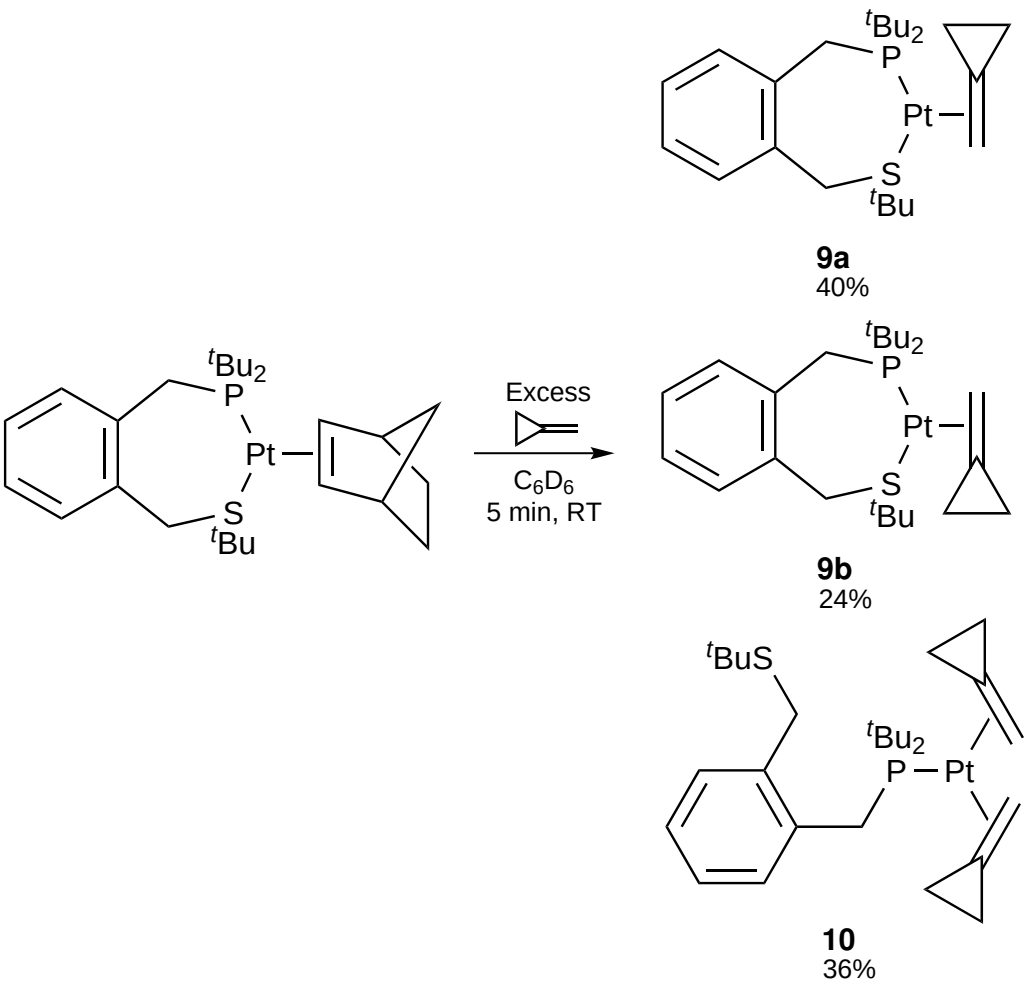

Scheme 3.3. Reaction of [Pt(nb)(^{t}Bu$_2$PCH$_2$(o-C$_6$H$_4$)CH$_2$S^{t}Bu)] with an excess of MCP.

3.1.1 NMR Characterisation

The η^2-BCP complex **8** formed from [Pt(nb)(P—S)] had the highest $^1J_{\text{Pt–P}}$ coupling constant of the BCP complexes synthesised in this study by a significant margin (3383 compared to 2983 Hz for [Pt(BCP)(dbpx)] (**1d**)); this was due to the nature of the P—S ligand, rather than the BCP ligand (Table 2.2). The nb starting material had a significantly higher $^1J_{\text{Pt–P}}$ coupling (3868 Hz) than both the ethene precursors used in Section 2.1 (∼3300 Hz) and [Pt(nb)(dbpx)] (3331 Hz).[133] The change in $^1J_{\text{Pt–P}}$ upon coordination of BCP was 485 Hz, similar to the average change of ∼450 Hz for **1**, and therefore consistent with the formation of a BCP complex.

The two different isomers of [Pt(MCP)(P—S)] could be easily distinguished by their

$^1J_{\text{Pt–P}}$ coupling constants. For **9a** $^1J_{\text{Pt–P}}$ was 3870 Hz, while for **9b** $^1J_{\text{Pt–P}}$ was 3483 Hz. These coupling constants were both higher than those in **2d** (3362 Hz for P *trans* to methylene, 3025 Hz for P *trans* to ^{c}Pr). However, the relative changes in $^1J_{\text{Pt–P}}$ upon coordination were similar enough to be consistent with the formation of MCP complexes (2 and 385 Hz for **9**, ∼70 and ∼425 Hz for **2**), particularly given that nb complexes tend to have lower $^1J_{\text{Pt–P}}$ than ethene complexes (3331 Hz for [Pt(nb)(dbpx)] *vs.* 3493 Hz for [Pt(C_2H_4)(dbpx)]). As with **2**, the P *trans* to the ^{c}Pr carbon had a lower coupling constant due to the higher *trans*-influence of the sp^2 carbon of the cyclopropyl ring.

The $^{13}C\{^1H\}$ NMR data for **8**, **9a** and **9b** confirmed the formation of η^2-BCP and η^2-MCP complexes. In particular, the values of the $^1J_{\text{Pt–C}}$ coupling constants were consistent with those of **1** and **2** (Table 2.2). These coupling constants showed the differing *trans*-influences of the two donor atoms of the P—S ligand. For **8**, the carbon atom *trans* to P had a $^1J_{\text{Pt–C}}$ of 579.0 Hz, while that *trans* to S had a $^1J_{\text{Pt–C}}$ of 656.6 Hz. In **9**, when the methylene was *trans* to P, $^1J_{\text{Pt–C}}$ was 145.1 Hz, while the $^1J_{\text{Pt–C}}$ *trans* to S was 270.6 Hz. The peak due to the ^{c}Pr carbon in **9** could not be found due to its low intensity. The higher $^1J_{\text{Pt–C}}$ coupling constant for the carbons *trans* to S demonstrates the weaker *trans*-influence of sulfur relative to phosphorus, resulting in a stronger Pt−C bond *trans* to S.[93] This effect was also evident in the ^1H NMR spectra in the relative sizes of the $^2J_{\text{Pt–H}}$ coupling constants of the methylene resonances in **9**. For the methylene *trans* to the P, $^2J_{\text{Pt–H}}$ was 52.7 Hz, slightly lower than those in **2** (∼60 Hz). The $^2J_{\text{Pt–H}}$ of the methylene *trans* to S was significantly larger at 82.1 Hz.

The NMR data for **10** were consistent with the other bis-MCP complexes **7** (Table 2.5). The $^1J_{\text{Pt–P}}$ coupling constant (2661 Hz) was closer to that of [Pt$(MCP)_2(PCy_3)$] (**7b**) (2695 Hz) than [Pt$(MCP)_2(PPh_3)$] (**7a**) (2932 Hz). This could be rationalised by the fact that the phosphine of the P—S ligand was more similar both sterically and electronically to PCy_3 than PPh_3.[82] For PCy_3, the cone angle θ is 170° and the Tolman electronic parameter ν is 2056 cm^{-1}, while for PPh_3, θ is 145° and ν is 2069 cm^{-1}. The cone angle of the P—S ligand was calculated to be 180° when in monodentate coordination through the P in *trans*–[PtH_2(P—S)],[123] while the P(*o*-tol)^{t}Bu$_2$ (ν = 2060 cm^{-1}) is a

close analogue for the electronic parameter. These show more similarity to PCy_3 than to PPh_3.

The $^{13}C\{^1H\}$ NMR data for the MCP ligands of **10** were very similar to those of **7**, particularly **7b**. The double-bond carbons had chemical shifts of 48.7 and 35.7 ppm and $^1J_{Pt–C}$ of 381.9 and 100.6 Hz for ^{c}Pr and methylene respectively, compared to 48.5–54.1 and 32.0–38.9 ppm, and 352.9–385.6 and 100.3 Hz for **7**. The cyclopropyl methylene carbons appeared at 7.18 ppm with $J_{Pt–C}$ coupling of 25.4 Hz, compared to 7.20–7.70 ppm and 24.5–25.0 Hz for **7**. The ^{1}H NMR data of **10** was also in agreement with **7**, with the methylene protons of **10** appearing at 2.49 ppm with a $^2J_{Pt–H}$ of 48.1 Hz, compared to 2.27–2.39 ppm and 50.0–55.0 Hz for **7**.

3.2 Allyl Complexes

3.2.1 Complexes Formed By Hydride Transfer

Both [Pt(BCP)(P—S)] (**8**) and the two isomers of [Pt(MCP)(P—S)] (**9a** and **9b**) (P—S = ^{t}Bu$_2$PCH$_2$(o-C$_6$H$_4$)CH$_2$S^{t}Bu) proved to be unstable in solution. In the case of **8**, two new complexes (**11a** and **11b**) began to form after one hour. The formation of these complexes was 99% complete by ^{31}P NMR spectroscopy after eight days at room temperature. For **9a** and **9b**, two new complexes (**12a** and **12b**) began to form overnight, reaching 91–95% completion after three weeks. When 1 eq. of MCP was used, 20% [Pt(nb)(P—S)] was still present initially, as well as **9a**, **9b** and free MCP. The [Pt(nb)(P—S)] was the slowest of the three alkene species to react, and the conversion to **12a** and **12b** reached 95% completion after 21 days. When [Pt(MCP)$_2$(P—S)] (**10**) was present (excess of MCP used), all three MCP complexes rearranged to form **12a** and **12b**. Complex **10** reacted more rapidly than **9a** or **9b** due to the sulfur already being displaced. The ratio of **9** to **10** changed from 64:36 to 78:22 after 10 days, all **10** had reacted after 13 days, and the reaction reached 91% completion after 21 days at room temperature.

The new complexes **11a**, **11b**, **12a** and **12b** were determined to be allyl complexes wherein the alkene ligand had undergone a reaction with a hydride, resulting in proximal

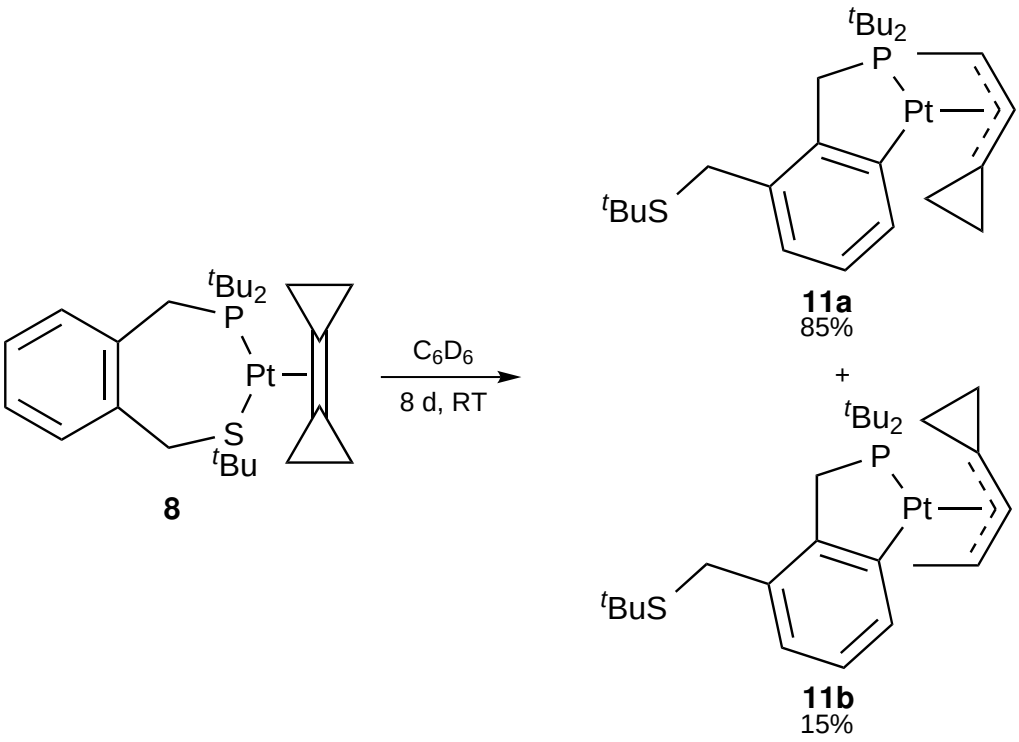

Scheme 3.4. Formation of allyl complexes from [Pt(BCP)(P—S)] (**8**).

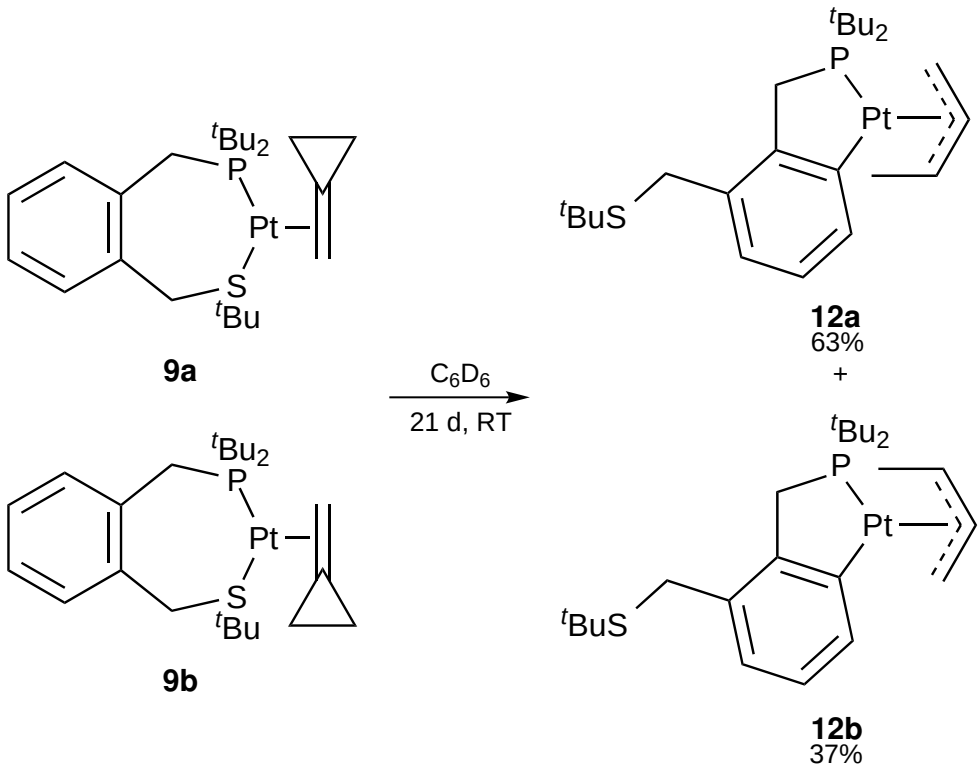

Scheme 3.5. Formation of allyl complexes from [Pt(MCP)(P—S)] (**9**).

bond cleavage of one of the cyclopropyl rings (Schemes 3.4 and 3.5). The hydride was generated by *ortho*-metallation of the P—S ligand, producing a P—C chelate ring. The formation of allyl complexes from coordinated MCP has been observed previously in the reaction of MCP with *trans*-$[PtH(NO_3)(L)_2]$ (L = PEt_3, PMe_2Ph, PPh_3)[134,135] and with $[PdCl_2(NCPh)_2]$.[136] The product of the reaction with *trans*-$[PtH(NO_3)(L)_2]$ was dependent on the phosphine ligand. When L = PEt_3 or PMe_2Ph, the product was entirely the 1-methylallyl complex. When L = PPh_3, an approximately 1:1 mixture of the 1-methylallyl and 2-methylallyl complexes was produced. With $[PdCl_2(NCPh)_2]$, the product was the 1-methylallyl complex, with a Cl at the 2-position. Allyl complexes are also intermediates in several of the transition metal catalysed reactions of both MCP and BCP, most notably in Heck-type reactions (see Schemes 1.6 and 1.21).[38,72,74,137,138]

The proposed mechanism for the formation of the 1-methyl allyl complexes involves the anti-Markovnikov addition of Pt–H across the double-bond, with the H attaching to the ^{c}Pr carbon. This was followed by the cleavage of the proximal ring bond to form an alkyl ligand, β-hydride elimination, then hydride attack at the methylene end of the coordinated double-bond (Scheme 3.6). This was supported by studies using *trans*-$[PtD(NO_3)(L)_2]$ and the reaction with $[PdCl_2(NCPh)_2]$, with, respectively, the deuterium or the chloride ending up in the 2-position. The proposed mechanism for the formation of the 2-methyl allyl complexes also began with the addition of Pt–H across the double-bond, except that in this case the H attached to the methylene carbon. The cleavage of the ring then occurred at the distal rather than the proximal bond, leading to the direct formation of the 2-methylallyl complex (Scheme 3.6). When *trans*-$[PtD(NO_3)(PPh_3)_2]$ was used, the deuterium ended up on the methyl carbon in the 2-substituted product.[134]

The P—S complexes in this work formed exclusively 1-methylallyls. Due to the lack of symmetry in both the allyl and the P—C ligand, in each case there were two possible isomers. The isomer which had the least substituted carbon *trans* to the C of the P—C ring formed in the largest amounts (**11a** and **12a**). For **11**, there was a pronounced difference in the proportions of the two isomers, 85:15 **11a** to **11b**. The isomer with the ^{c}Pr ring *trans* to the C was disfavoured due to the high *trans*-influences of both the

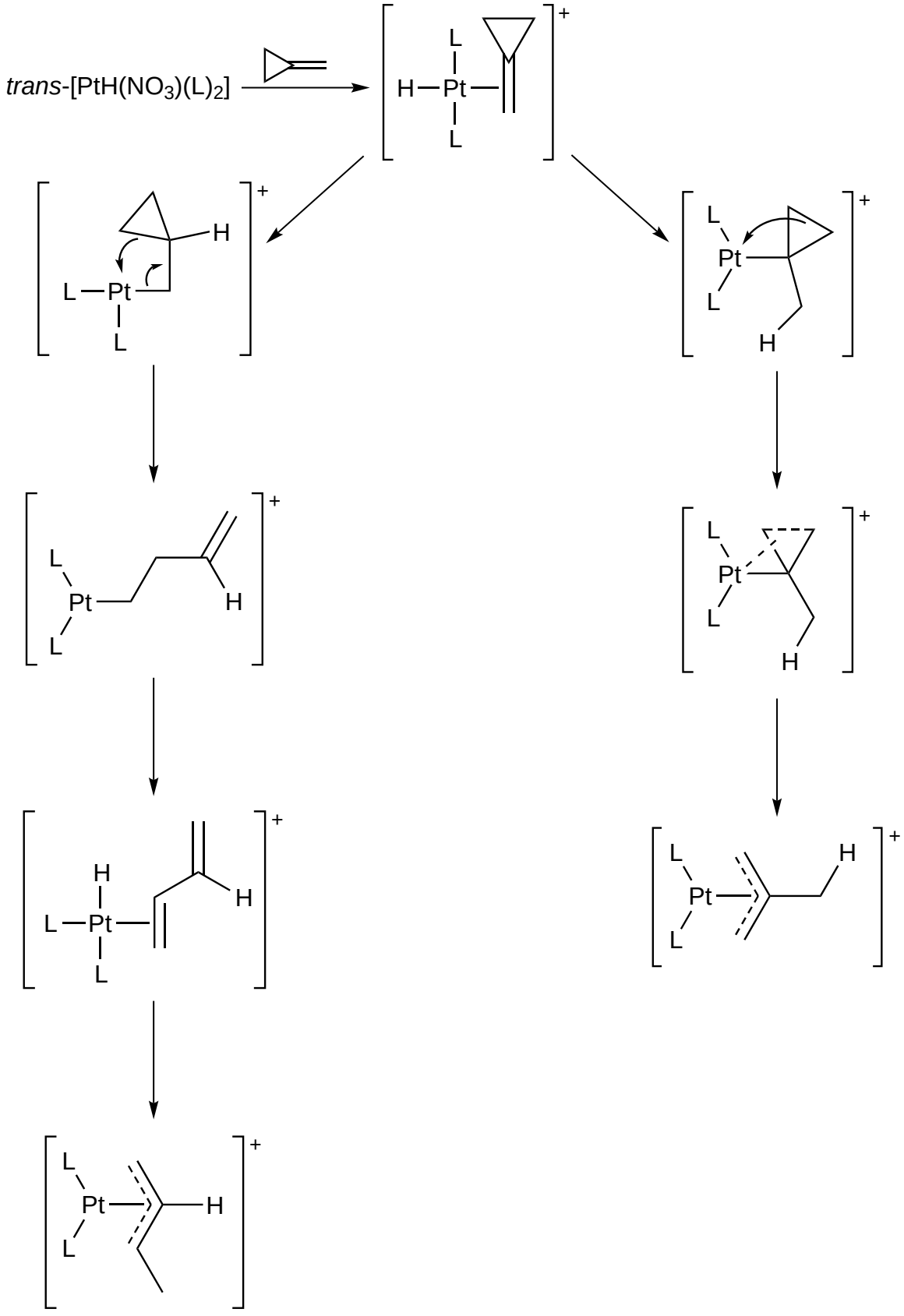

Scheme 3.6. Mechanism for the formation of allyl complexes from MCP.[135]

σ-bonded carbon and the ^{c}Pr ring.[93,139] The difference between the two isomers of **12** was less significant, 63:37 **12a**:**12b**. In this case, the proportions were more equal due to the steric and electronic similarity of the methylene to the CHMe group.[140]

The methyl groups in **11** and **12** were determined to be in the *anti* position based on ^{1}H NMR coupling constants (Section 3.2.1.1). In other systems, *anti* methyl groups were the kinetic products, while *syn* methyl groups were the thermodynamically stable isomer (Figure 3.1).[141,142] No rearrangement to the *syn*-methyl isomer was observed for **11** and **12**, even when the complexes were placed in d_6-acetone, which was found to facilitate the rearrangment of other allyl systems (Section 3.2.2).

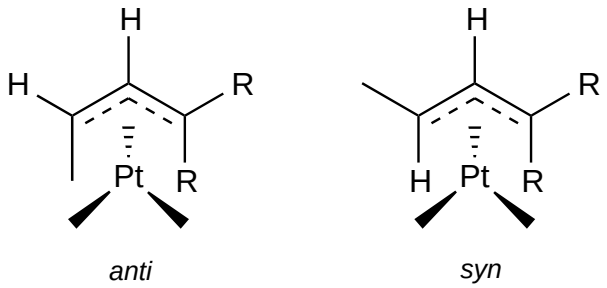

Figure 3.1. Geometry of allyl systems with *anti* and *syn* methyl groups.

3.2.1.1 NMR Characterisation

For representative NMR spectra, see Figures A.26–Figure A.35. As with other complexes (see Table 2.2), it was possible to distinguish between the two isomers of **11** based on their $^1J_{\text{Pt–P}}$ coupling constants (Table 3.1). The isomer with the P *trans* to the ^{c}Pr ring, **11a**, had a $^1J_{\text{Pt–P}}$ of 3141 Hz, while **11b**, with P *trans* to the CHMe, had a $^1J_{\text{Pt–P}}$ of 3893 Hz. The two isomers of **12** had very similar coupling constants; 3560 and 3590 Hz for **12a** and **12b** respectively.

The orientation of the allyl relative to the P—C chelate ring had an effect on the ^{13}C{^{1}H} NMR spectra. The most pronounced differences were in the resonances of the carbons of the allylic system (Table 3.2). The allyl carbon *trans* to the phosphorus donor had $^1J_{\text{Pt–C}}$ and $J_{\text{P–C}}$ couplings typical of other alkene/allyl complexes (see Table 2.2).[143] In **11a**, the quaternary ^{c}Pr carbon had a large *trans* $J_{\text{P–C}}$ coupling constant (76.3 Hz),

Table 3.1. Selected $^{31}P\{^{1}H\}$ and ^{1}H NMR Data of Allyl Complexes.[a]

Compound		δ_P	$^1J_{Pt-P}$	^{c}Pr	CH_2		CH		CHMe		CH_3
				δ_H	δ_H	$^2J_{Pt-H}$	δ_H	$^2J_{Pt-H}$	δ_H	$^2J_{Pt-H}$	δ_H
[Pt(η^3-C(CH_2)$_2$CHCHMe)(P—C)] [b]	**11a**	82.0	3141	1.56			4.54	39.0	4.85	13.0	1.63
				1.26							
[Pt(η^3-C(CH_2)$_2$CHCHMe)(P—C)] [b]	**11b**	80.1	3893	1.38			4.82	41.6	4.57	[c]	1.65
				1.26							
				1.1							
[Pt(η^3-CH_2CHCHMe)(P—C)] [b]	**12a**	84.1	3560		3.57	(*syn*)	4.61 (13.3, 7.7)	41.9	4.34		1.39
					2.27	38.1 (*anti*)					
[Pt(η^3-CH_2CHCHMe)(P—C)] [b]	**12b**	82.0	3590		3.6	(*syn*)	4.61 (13.3, 7.7)	41.9	4.39		1.29
					2.92	(*anti*)					
[Pt(η^3-C(CH_2)$_2$CHCHMe)(dppp)]$^+$	**13a**	1.4	3852	1.21			5.40 (8.2)	54.0	4.93		0.88
		−2.8	3259	0.86							
				0.37							
[Pt(η^3-C(CH_2)$_2$CHCHMe)(dppp)]$^+$	**13b**	1.0	4042	1.22			5.39 (12.5)	51.0	4.14		1.38
		−0.4	3267	0.65							
				0.39							
				0.14							
[Pt(η^3-CH_2CHCHMe)(dppp)]$^+$	**16a**	−1.2	3569		3.94	(*syn*)	5.32 (14.1, 7.6)	53.4	4.62		0.80
		−1.2	3625		2.99	(*anti*)					
[Pt(η^3-CH_2CHCHMe)(dppp)]$^+$	**16b**	1.4	3670		3.59	(*syn*)	5.23 (12.7, 7.3)	51.5	3.68		1.29
		−1.8	3693		2.54 (12.7, 10.0, 2.7)	(*anti*)					
[Pt(η^3-CH_2CHCHMe)(dbpx)]$^+$	**18b**	36.9	3844		4.53	(*syn*)	5.04 (12.2, 7.5)	51.9	6.28		[c]
					2.86 (11.1, 10.0, 2.2)	34.4 (*anti*)					
[Pt(η^3-CH_2C^{c}PrCH_2)(dbpx)]$^+$	**17**	33.9	3632	0.93	4.81	(*syn*)					
		32.1	3647	0.87	2.74 (8.1)	41.3 (*anti*)					
[Pt(η^3-CH_2CMeCH_2)(dppp)]$^+$	**15**	0.1	3521		3.56	(*syn*)					1.96
					2.95 (8.5)	32.0 (*anti*)					
[Pt(η^3-CH_2CMeCH_2)(dbpx)]$^+$	**18a**	33.9	3572		4.88	(*syn*)					[c]
		32.4	3641		2.80 (8.4)	39.4(*anti*)					

[a] δ values are given in ppm and J values in Hz. Values in parentheses are J_{H-H} couplings. All spectra were measured in d_6-acetone at room temperature with 40 mg/mL sample unless noted. [b] Spectra collected in C_6D_6. [c] NMR data could not be obtained.

Table 3.2. Selected $^{13}C\{^1H\}$ NMR Data of Allyl Complexes.[a]

Compound		Pt–C		^{c}Pr		CR_2		CH		CHMe		CH_3	
		δ_C	$^1J_{Pt-C}$	δ_C	J_{Pt-C}	δ_C	$^1J_{Pt-C}$	δ_C	$^1J_{Pt-C}$	δ_C	$^1J_{Pt-C}$	δ_C	$^2J_{Pt-C}$
[Pt(η^3-C(CH_2)$_2$CHCHMe)(P—C)] [b]	**11a**	152.9 (2.4)	1192.1	7.7 (4.3) 3.7	25.9 18.0	53.5 (76.3)	447.4	98.6 (4.3)	21.1	74.1	32.6	17.3	27.9
[Pt(η^3-C(CH_2)$_2$CHCHMe)(P—C)] [b]	**11b**	159.9 (2.8)	1043.3	9.0 6.6	15.0	48.1	202.3	102.8	7.1	84.3 (30.1)	130.6	16.8 (4.6)	41.6
[Pt(η^3-CH_2CHCHMe)(P—C)] [b]	**12a**	158.4 (2.3)	1142.7			42.5	52.0	108.2	8.4	73.4 (37.0)	173.4	15.3 (5.2)	39.9
[Pt(η^3-CH_2CHCHMe)(P—C)] [b]	**12b**	155.5 (2.4)	1132.8			53.1 (40.4)	182.6	108.7	11.0	62.5	48.6	15.6	26.6
[Pt(η^3-C(CH_2)$_2$CHCHMe)(dppp)]$^+$	**13a**			8.2 (4.0) 4.4	16.8 15.6	66.7 (54.4)	252.6	104.2 (3.4, 1.7)		91.2 (22.6)	65.9	15.5 (4.1)	33.2
[Pt(η^3-C(CH_2)$_2$CHCHMe)(dppp)]$^+$	**13b**			8.6 (4.0) 5.7	20.8	67.1 (53.2)	269.3	111.6 (4.1, 1.8)		92.6 (21.9)	29.0	15.9 (2.4)	
[Pt(η^3-CH_2CHCHMe)(dppp)]$^+$	**16a**					60.2	88.0	113.9 (3.2)	16.5	83.4	83.7	14.1 (2.8, 1.1)	23.1
[Pt(η^3-CH_2CHCHMe)(dppp)]$^+$	**16b**					62.3	100.1	119.3 (3.5)	26.6	84.3	54.4	15.9 (2.9)	3.8
[Pt(η^3-CH_2CHCHMe)(dbpx)]$^+$	**18b**					51.7	106.9	106.8		84.6	63.7	16.5	14.5
[Pt(η^3-CH_2C^{c}PrCH_2)(dbpx)]$^+$	**17**			8.9		59.1 (30.2, −2.1)	79.8	126.4	44.5				
[Pt(η^3-CH_2CMeCH_2)(dppp)]$^+$	**15**					66.4	85.0	135.9 (3.2)	24.8			24.8	30.0
[Pt(η^3-CH_2CMeCH_2)(dbpx)]$^+$	**18a**					63.3		127.1	56.7			21.6	28.4

[a] δ values are given in ppm and J values in Hz. Values in parenthesis are J_{P-C}. All spectra were measured in d_6-acetone at room temperature with 40 mg/mL sample unless noted. [b] Spectra collected in C_6D_6.

and a $^{1}J_{\mathrm{Pt–C}}$ of 447.4 Hz, similar to those in the alkene complexes **1** and **2**. For the allyl carbon attached to the methyl, when *trans* to the P in **11b** and **12a** $^{1}J_{\mathrm{Pt–C}}$ was 130.6 and 173.4 Hz, while $J_{\mathrm{P–C}}$ was 30.1 and 37.0 Hz respectively. The methylene in **12b** had a $^{1}J_{\mathrm{Pt–C}}$ of 182.6 Hz and a $J_{\mathrm{P–C}}$ of 40.4 Hz.

The $^{1}J_{\mathrm{Pt–C}}$ coupling constants for the allyl carbons dramatically decreased when *trans* to the carbon donor. For **11b**, the $^{1}J_{\mathrm{Pt–C}}$ coupling of the quaternary ^{c}Pr carbon was less than half that of **11a** at 202.3 Hz. The carbons attached to the methyls in **11a** and **12b** had couplings of 32.6 and 48.6 Hz respectively, 98–125 Hz less than their counterparts. In **12a**, the methylene carbon also had a significant decrease in $^{1}J_{\mathrm{Pt–C}}$ from **12b**, decreasing by 130 Hz to become 52.0 Hz. The effect on the central carbon of the allyl was less significant, but was still evident. In **11b** and **12a**, which had the methyls *trans* to the phosphorus, $^{1}J_{\mathrm{Pt–C}}$ was 7.1 and 8.4 Hz respectively, while in **11a** and **12b** $^{1}J_{\mathrm{Pt–C}}$ was 21.1 and 11.0 Hz respectively. There was also a decrease in the $^{2}J_{\mathrm{Pt–C}}$ coupling constants of the methyl carbons when they were *trans* to the C, from 41.6 and 39.9 Hz in **11b** and **12a** (*trans* P) to 27.9 and 26.6 in **11a** and **12b** (*trans* C). The low $J_{\mathrm{Pt–C}}$ coupling constants for the carbons *trans* to the C of the P—C chelate was due to the high *trans*-influence of the σ-bonded carbon.[93] This lowering of $^{1}J_{\mathrm{Pt–C}}$ *trans* to a σ-bonded carbon has been reported for a range of η^{3}-allyl complexes, both with P—C chelate rings and for [Pt(η^{3}-C_3H_5)Me(PPh_3)] complexes.[144]

The orientation of the allyl also had an effect on the chemical shift of the carbon resonances. There was some variation in the absolute chemical shift; when a particular carbon environment was *trans* to the phosphorus it had a shift 10.2–10.9 ppm higher than when it was *trans* to the carbon. The exceptions to this were the central allyl carbons, which did not sit *trans* to either donor and had differences of 0.5–4.2 ppm, and the ^{c}Pr CH_2 carbons, which again did not sit directly *trans*, only differed by 5.5 ppm.

The metallation of the aromatic ring was evident in the high chemical shift (152.9–159.9 ppm) and high $^{1}J_{\mathrm{Pt–C}}$ coupling constant (1043.3–1192.1 Hz) of one of the ring carbon atoms. The complex with the ^{c}Pr ring *trans* to the carbon, **11b**, had a $^{1}J_{\mathrm{Pt–C}}$ 100 Hz lower than the other complexes, signifying that the strong Pt−^{c}Pr bond caused

a weakening of the Pt−C σ-bond. The shifts of both of the S−^{t}Bu carbons were very similar to those of the free ligand, and showed no platinum or phosphorus coupling, unlike in **8** and **9**. This was consistent with the S no longer being coordinated.

The ^{1}H NMR spectra of **11a**–**12b** were typical of allyl complexes.[141,142,144,145] It was possible to assign the *syn* and *anti* protons of the methylenes of **12a** and **12b** both from the chemical shift and from the $J_{\text{H–H}}$ couplings. The *anti* protons had lower chemical shifts (2.27 and 2.97 ppm) than the *syn* (3.57 and 3.6 ppm), while the $J_{\text{H–H}}$ coupling of the *anti* protons to the central allyl protons was higher (∼13 *vs.* ∼8 Hz). It was also possible to determine the geometry at the CHMe carbon of **11** and **12** using $J_{\text{H–H}}$ couplings. The peak belonging to the central allyl proton in **11a** was a doublet with coupling of 8.0 Hz, while that of **11b** was a doublet with coupling of 7.5 Hz, corresponding to couplings to a proton in the *syn* position. The methyl groups were therefore in the *anti* position. In both **12a** and **12b**, the central allyl proton was a doublet of triplets, with a doublet coupling of 13.3 Hz and a triplet coupling of 7.7 Hz, indicating one proton in the *anti* position (from the CH_2) and two in the *syn* position (from the CH_2 and the CHMe). Again, the methyl groups were therefore in the *anti* position.

3.2.2 Complexes Formed By Protonation

The reactivity of a selection of η^2-alkene P—P complexes [Pt(BCP)(P—P)] (P—P = dppp (**1a**), dbpx (**1d**)) and [Pt(MCP)(P—P)] (P—P = dppp (**2a**), dbpx (**2d**)) with acids was explored. The acid predominantely used for these studies was $H_2C(SO_2CF_3)_2$ (pKa = 2.4 in DMSO).[146] The reactions with dppp complexes were also performed using $HCPh(SO_2CF_3)_2$ (pKa = 2.0 in DMSO)[146] and HBF_4 (pKa = 1.2 in 1,2-dichloroethane),[147] with no difference in product distributions observed.

When $H_2C(SO_2CF_3)_2$ was added to a suspension of **1a** in d_6-acetone, a reaction occurred immediately, resulting in the formation of two species in a approx. 75:25 ratio. The major product **13a** proved to be a 1-methylallyl complex similar to **11**, with the methyl in the *anti* position, formed by cleavage of the proximal ring bond, while the structure of the minor product (**14a**) could not be assigned. Overnight, **13a** began to

convert into the *syn*-methyl complex, **13b**. The conversion continued slowly, eventually stabilising at 27:73 *anti*:*syn* after two months at room temperature.

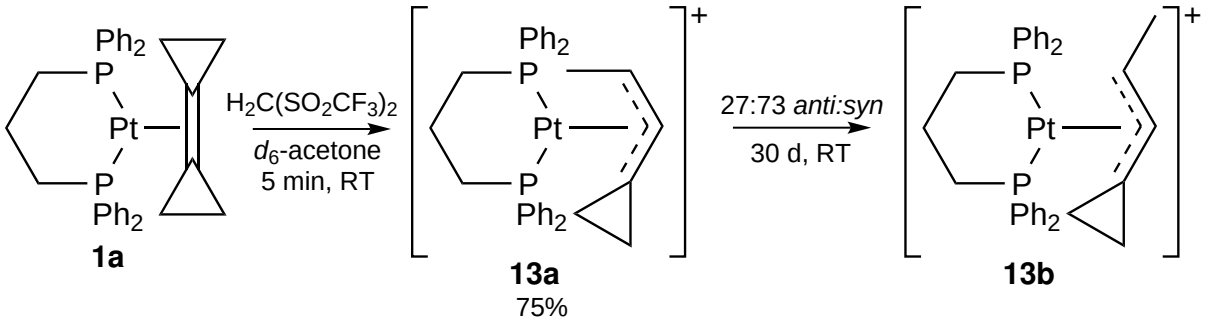

Scheme 3.7. Formation of allyl complexes by protonation of [Pt(BCP)(dppp)] (**1a**).

In the equivalent reactions with **2a**, there were two products formed initially (**15** and **16a**), in a 68:32 ratio (Scheme 3.8). In this case, the major product **15** was a 2-methylallyl complex, formed by the cleavage of the distal ring bond (Scheme 3.6). This complex had been synthesised previously by the addition of dppp to $[Pt(CH_2CMeCH_2)(acetone)_2]^+$.[148] The minor product **16a** was a 1-methylallyl complex with the methyl in the *anti* position. As with **13**, the conversion to the *syn*-methyl complex (**16b**) was evident within 12 hr, with the ratios stabilising at 16:84 *anti*:*syn* after 8 days. When the protonation reaction was done in CD_2Cl_2 rather than d_6-acetone, the ratio of **15** to **16a** was much higher in favour of the 2-methyl complex at 84:16. There was also no conversion of the *anti* 1-methyl complex into the *syn* form. This was ascribed to the ability of d_6-acetone to coordinate to the metal, filling a vacant coordination site while the allyl converted from η^3 (*anti*) to η^1 to η^3 (*syn*), which was not possible in non-coordinating CD_2Cl_2.

The reactivity of the dbpx complexes differed from that of the dppp complexes. The products of the reactions were again allyl complexes, but different isomers were favoured. In the reaction of **1d** with $H_2C(SO_2CF_3)_2$, the only species produced (**17**) was an allyl substituted in the 2-position with a cyclopropyl ring (Scheme 3.9). This species was not observed with **1a**, though the analogous 2-methylallyl complex was the major product with **2a**. The 2-methyl complex (**18a**) was also formed in the reaction with **2d**, as well as the 1-methylallyl complex with the methyl in the *anti* position (**18b**) (Scheme 3.10). Unlike the dppp complexes, in this case it was the 1-methylallyl complex that was the

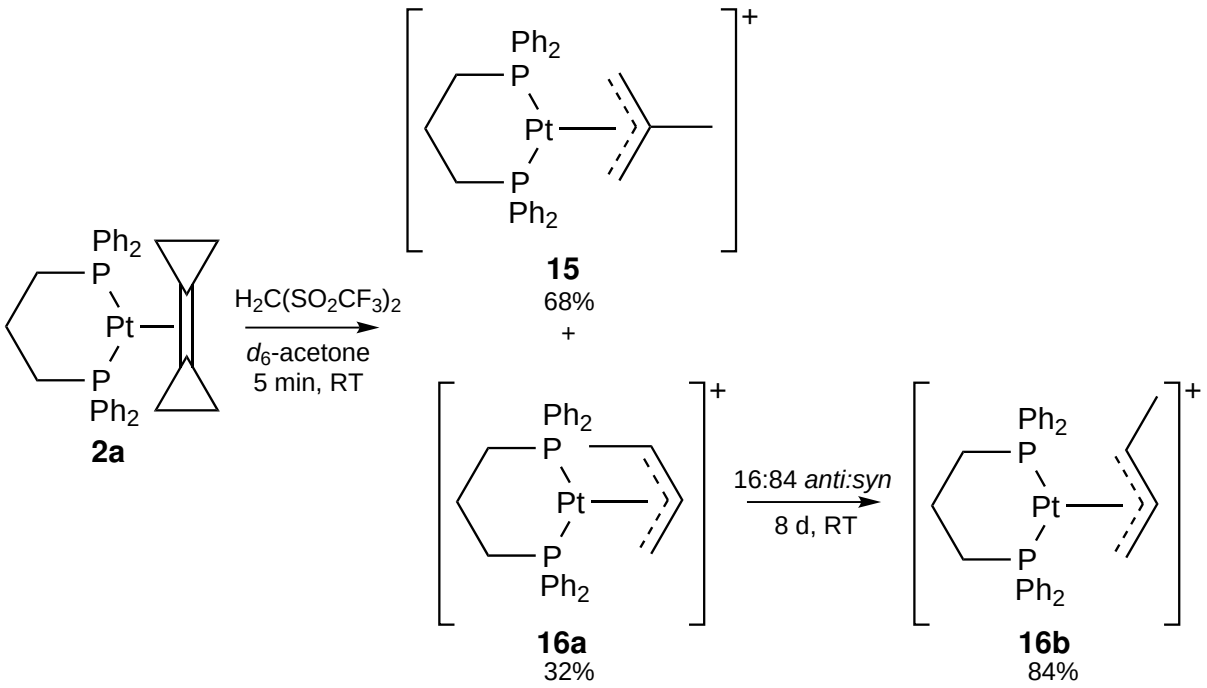

Scheme 3.8. Formation of allyl complexes by protonation of [Pt(MCP)(dppp)] (**2a**).

major isomer, with a ratio of 58:42 **18a**:**18b**. The dbpx complexes further differed from the dppp complexes with no rearrangement of the *anti*-methyl **18b** to the *syn*-methyl complex.

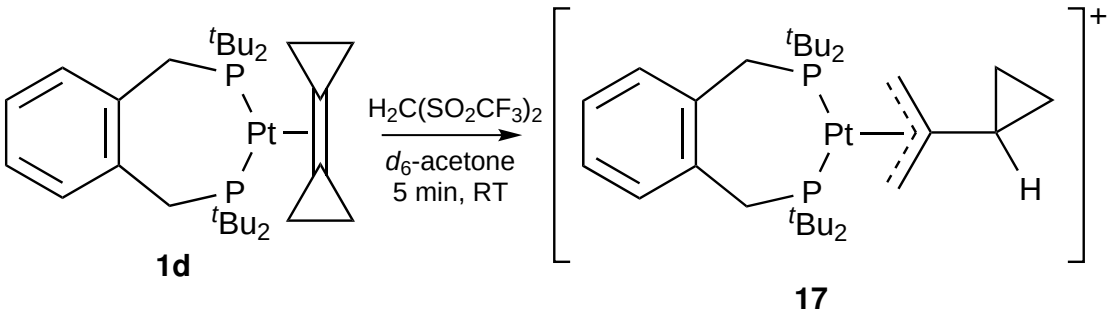

Scheme 3.9. Formation of an allyl complex by protonation of [Pt(BCP)(dbpx)] (**1d**).

3.2.2.1 NMR Characterisation

For representative NMR spectra see Figures A.36–A.70. The ^{1}H NMR resonances of the 1-methylallyl complexes as well as 1D NOESY correlations were used to assign the geometries of the allyl ligand. In **16a** and **18b**, the peak due to the central allyl proton was a doublet of triplets with couplings of 14.1 and 7.6 Hz for **16a** and 12.2 and 7.5 Hz

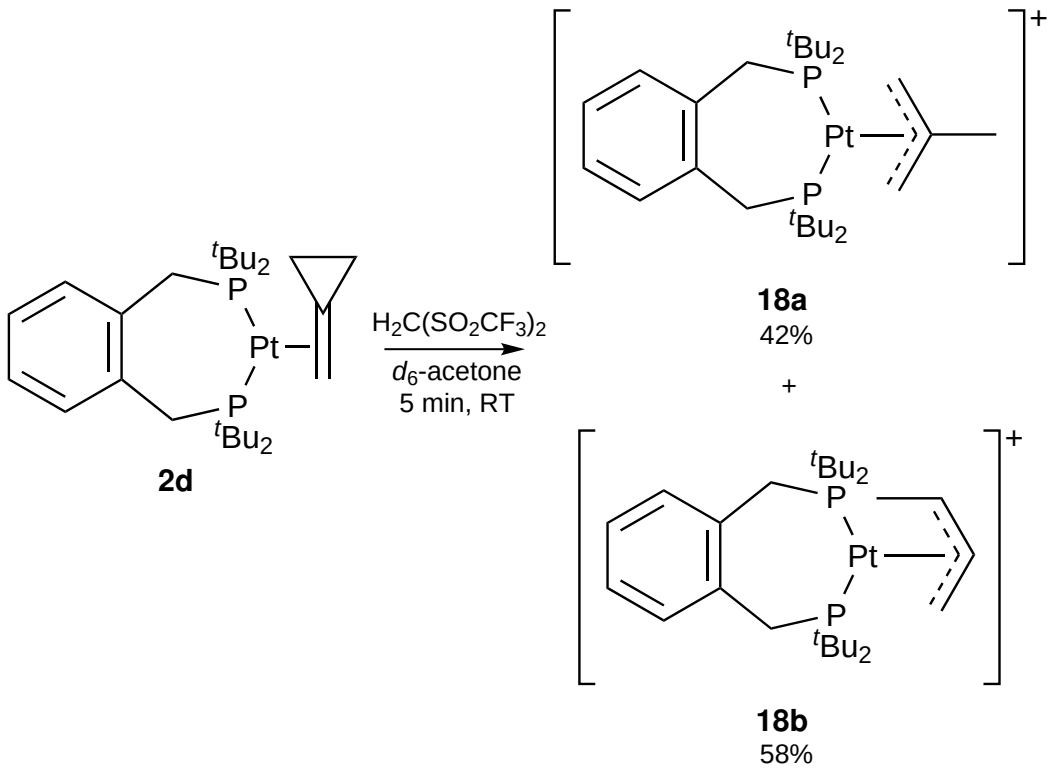

Scheme 3.10. Formation of allyl complexes by protonation of [Pt(MCP)(dbpx)] (**1d**).

for **18b**. This showed that there were two protons in the *syn* positions (from the CHMe and the CH_2), and one in the *anti* (from the CH_2), and that the methyl was therefore in the *anti* position (Figure 3.2).[141,142,144,145] The peak due to the central allyl proton in **16b**, however, was a triplet of doublets with couplings of 12.7 and 7.3 Hz, showing that there were now two *anti* protons, and the methyl was therefore *syn*. The central allyl protons in **13a** and **13b** were also used to assign the allyl geometries. In **13a**, the peak had a $J_{\mathrm{H-H}}$ coupling of 8.2 Hz to the CHMe proton, indicating that it was in the *syn* position, with the methyl group in the *anti*. The $J_{\mathrm{H-H}}$ coupling in **13a** was 12.5 Hz, and the methyl group was therefore *syn*.

There were several other differences between the *anti*- and *syn*-methyl allyl complexes in the NMR spectra (Tables 3.1 and 3.2). In the ^{1}H NMR spectrum, the chemical shifts for the methyl protons appeared at lower chemical shifts for the *anti* methyl groups (0.80 and 0.88 ppm) than for the *syn* (1.29 and 1.38 ppm). This differed from the other protons, with the chemical shifts of the protons in the *syn*-methyl allyl lower than the equivalent *anti*-methyl allyl. The $^2J_{\mathrm{Pt-H}}$ couplings on the central proton were also slightly larger for

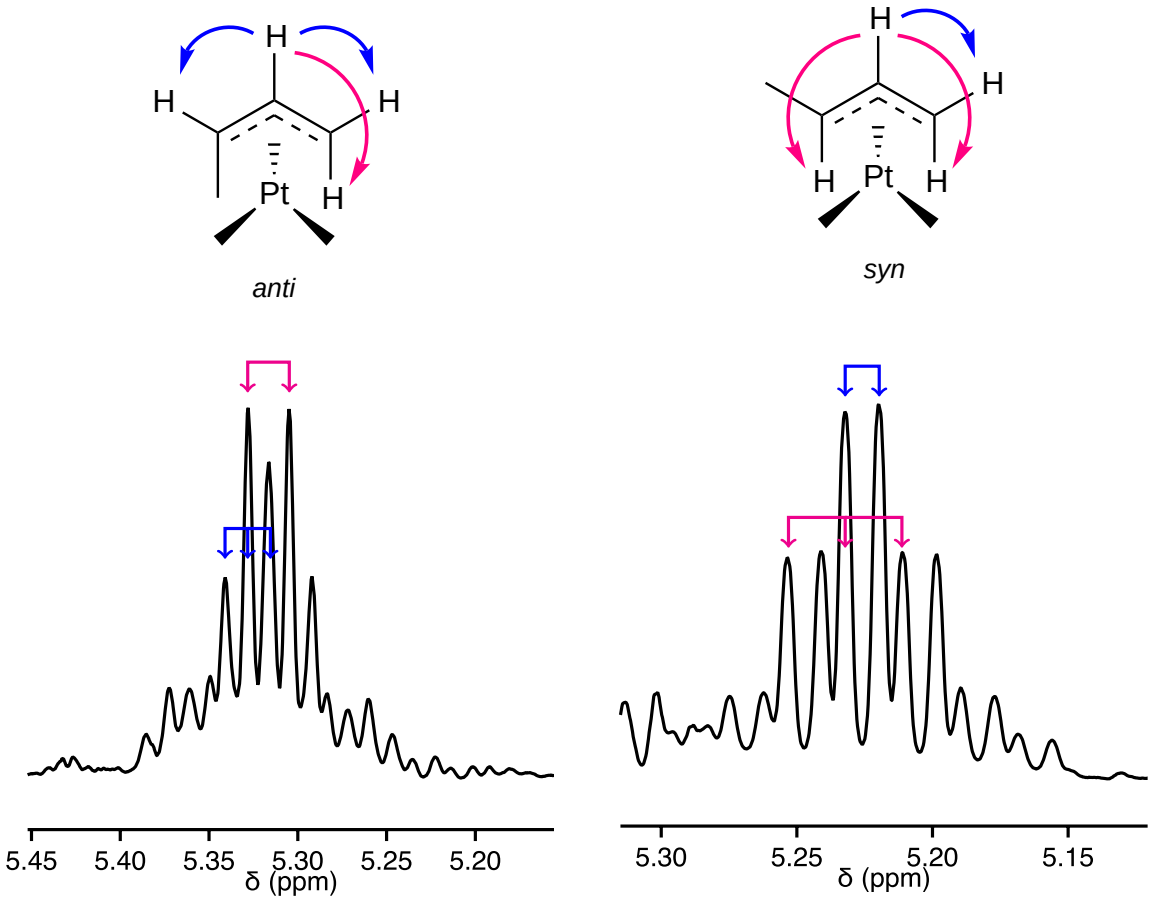

Figure 3.2. ^{1}H NMR resonances of the central allyl proton in [Pt(η^3-$CH_2CHCHMe$)(dppp)][$PhC(SO_2CF_3)_2$] **16a**[$PhC(SO_2CF_3)_2$] (*anti*) and **16b**[$PhC(SO_2CF_3)_2$] (*syn*).

the *anti* form (53.4 and 54.0 Hz) than for the *syn* form (51.0–51.9 Hz).

In the $^{13}C\{^1H\}$ NMR spectrum (Table 3.2), the differences in chemical shift had the opposite trend, with those of the *anti* isomers typically being at lower ppm than the *syn* isomer, by 0.4–7.4 ppm. Most of the $J_{Pt–C}$ coupling constants were also lower in the *anti* isomer by 10–17 Hz. The exception to this was the CHMe carbons, where the $^1J_{Pt–C}$ coupling constants were higher in the *anti* case by 36.9 Hz for **13** and 29.3 Hz for **16**. As with other complexes, the carbon with the cyclopropyl ring attached had a significantly higher $^1J_{Pt–C}$ than the equivalent methylene carbon due to the higher *trans*-influence of the ^{c}Pr ring, 252.6 and 269.3 *vs.* 88.0–106.9 Hz. However, the coupling constants of the ^{c}Pr allyl carbons in **13** were lower by ∼150 Hz than those in **1**. This decrease was consistent with the metal in the allyl complexes being Pt(II) rather than Pt(0), with less electron-density being available and therefore weaker bonds to the allyl system than to the alkene ligands.[140,149–151] In **11a**, which was also Pt(II) with the ^{c}Pr ring *trans* to P, the $^1J_{Pt–C}$ of the ^{c}Pr allyl carbon (447.4 Hz) was also larger than for **13**, though that of **11b**, with the ^{c}Pr *trans* to C, was lower (202.3 Hz). However, the P—P complexes had a positive charge, again leading to a lower electron density. As well as this, the allyl system in the P—C complexes would be affected by the significantly different strengths of the Pt–P and Pt–C bonds, leading to a comparatively stronger bond *trans* to the P. The lower $^1J_{Pt–C}$ coupling constants of the CHMe carbon compared to the CH_2 carbon in **16** and **18b** indicated that there was a greater interaction with the metal for the CH_2 group than for the CHMe, both in the P—P and the P—C complexes.[93] The differences varied between 3.4 Hz when *trans* to C in **12** and 45.7 Hz for **16b**.

In the $^{31}P\{^1H\}$ NMR spectra of **13**, there was a large difference between $^1J_{Pt–P}$ coupling constants, with that of the phosphorus *trans* to the ^{c}Pr ring significantly lower than the that of the P *trans* to CHMe at 3260 Hz. There was a nearly 200 Hz difference in the $^1J_{Pt–P}$ of the P *trans* to the CHMe group between the *anti*- and *syn*-methyl complexes, 3852 and 4042 Hz respectively. As with **11**, the P *trans* to the CHMe had a significantly higher $^1J_{Pt–P}$ in the complexes derived from BCP than from MCP. In **16**, the $^1J_{Pt–P}$ of the P *trans* to CHMe (3625 and 3695 Hz) were within 60 Hz of the $^1J_{Pt–P}$ of the P *trans*

to CH_2 (3569 and 3670 Hz).

The 2-substituted allyl complexes with dbpx (**17** and **18a**) both had NMR spectra that varied with temperature. At room temperature, the ^{31}P NMR spectra of both complexes showed two very broad peaks of uneven intensity, with the major peaks at 32.1 and 32.4 ppm with $^1J_{\text{Pt–P}}$ of 3647 and 3572 Hz and the minor peaks at 33.9 and 33.9 ppm with $^1J_{\text{Pt–P}}$ of 3632 and 3641 Hz for **17** and **18a** respectively (Figure 3.4). When NMR spectra were run at higher temperatures, the peaks coalesced into a sharp singlet (**17** δ_{P} = 33.4 ppm, $^1J_{\text{Pt–P}}$ = 3640 Hz, **18a** δ_{P} = 32.3 ppm, $^1J_{\text{Pt–P}}$ = 3598 Hz), beginning at 30 °C. This fluxional behaviour was due to flipping of the dbpx backbone.[152,153] When the temperature of **17** was decreased, the two broad peaks became four sharp peaks, beginning at 0 °C (δ_{P} = 34.2, 33.0, 31.0 and 30.7 ppm, $^1J_{\text{Pt–P}}$ = 3650, 3651, 3639 and 3642 Hz, with 8:34:12:46 intensity). This was ascribed to a combination of flipping of the dbpx backbone and different orientations of the cyclopropyl substituent, prevented from free rotation due to the large steric bulk of the ^{t}Bu substituents (Figure 3.3).

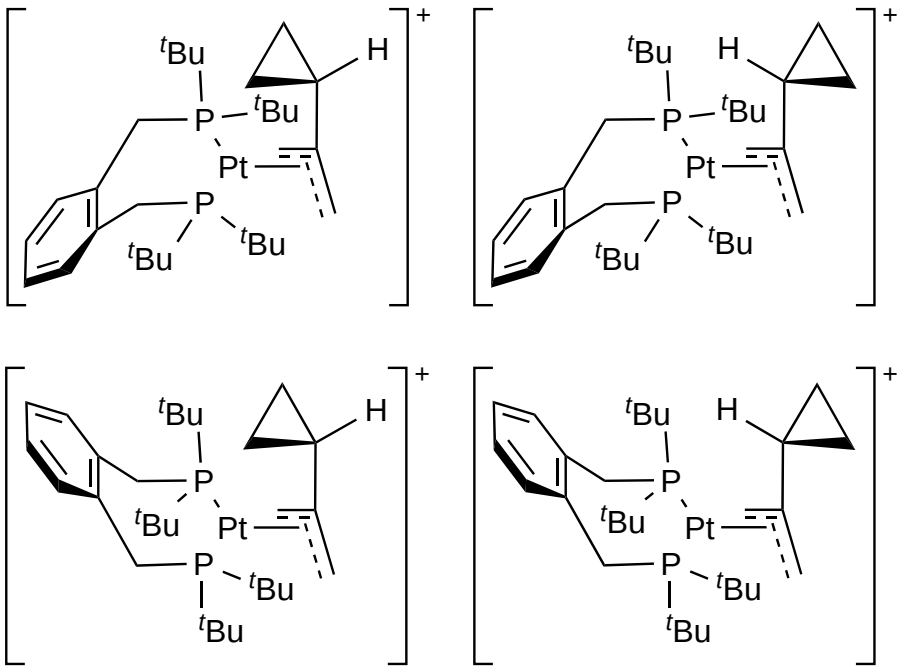

Figure 3.3. Possible conformations of [Pt(η^3-$CH_2C^cPrCH_2$)(dbpx)]$^+$ (**17**).

The coalescence temperature for the ^{1}H NMR of **17** was slightly lower than for the ^{31}P NMR, between 0 and −10 °C. (Figures 3.5 and 3.6). The room temperature proton spectra

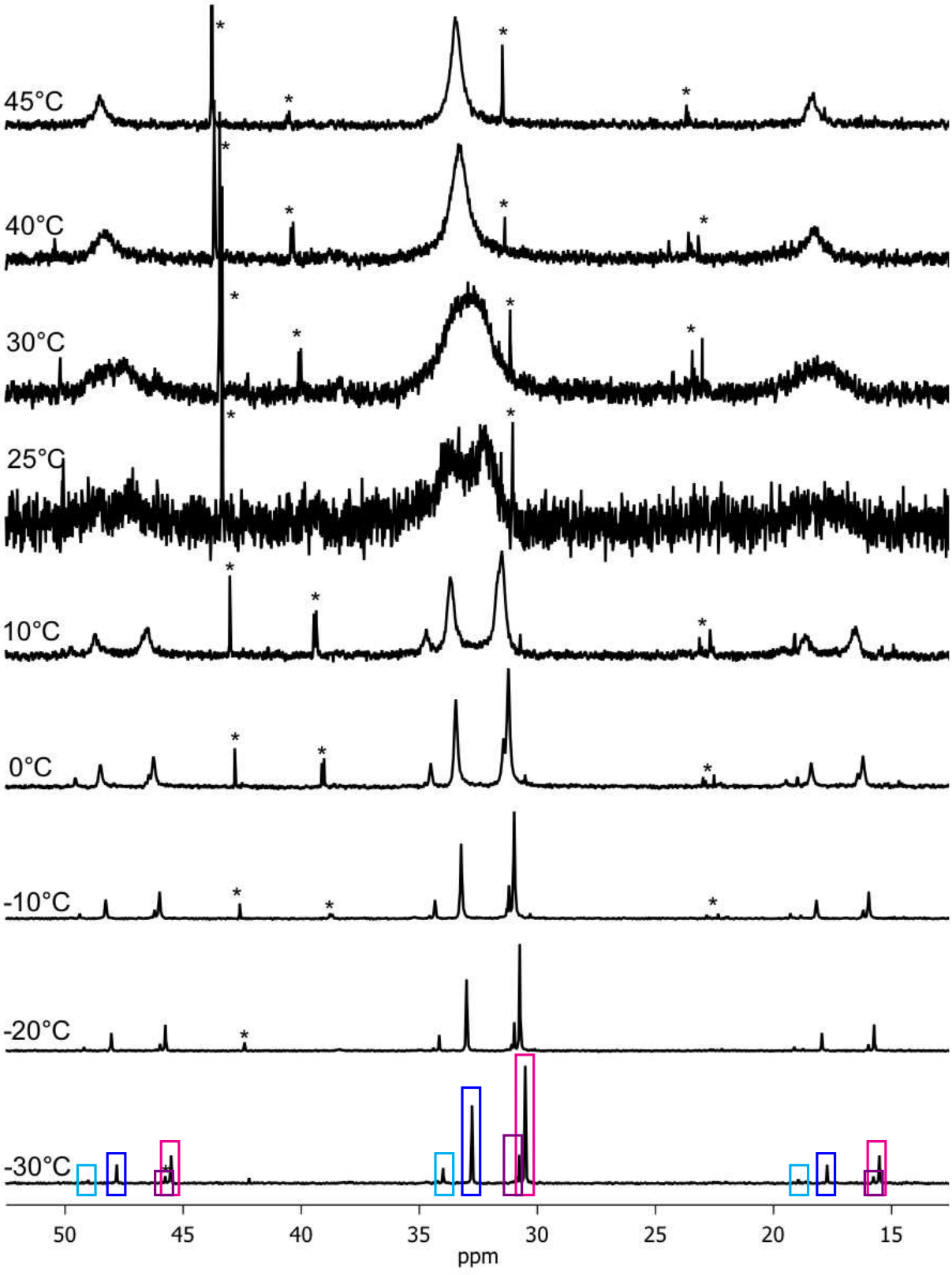

Figure 3.4. Temperature-dependent $^{31}P\{^{1}H\}$ NMR spectra of $[Pt(\eta^3\text{-}CH_2C^cPrCH_2)(dbpx)]^+$ (**17**) (125 MHz, 40 mg/mL, C_6D_6). * signifies peaks belonging to other species

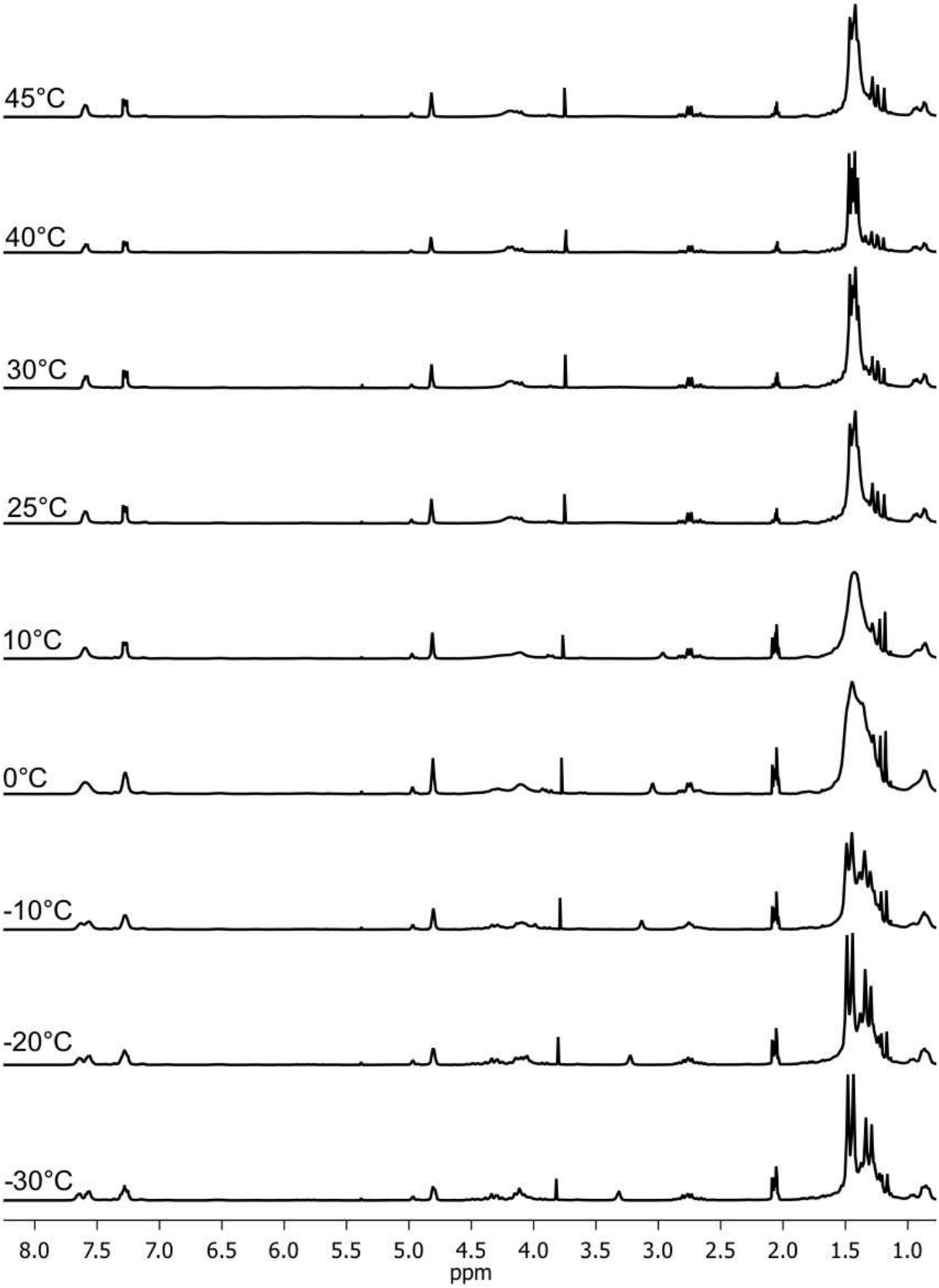

Figure 3.5. Temperature-dependent ^{1}H NMR spectra of [Pt(η^3-$CH_2C^cPrCH_2$)(dbpx)]$^+$ (**17**) (300 MHz, 40 mg/mL, C_6D_6).

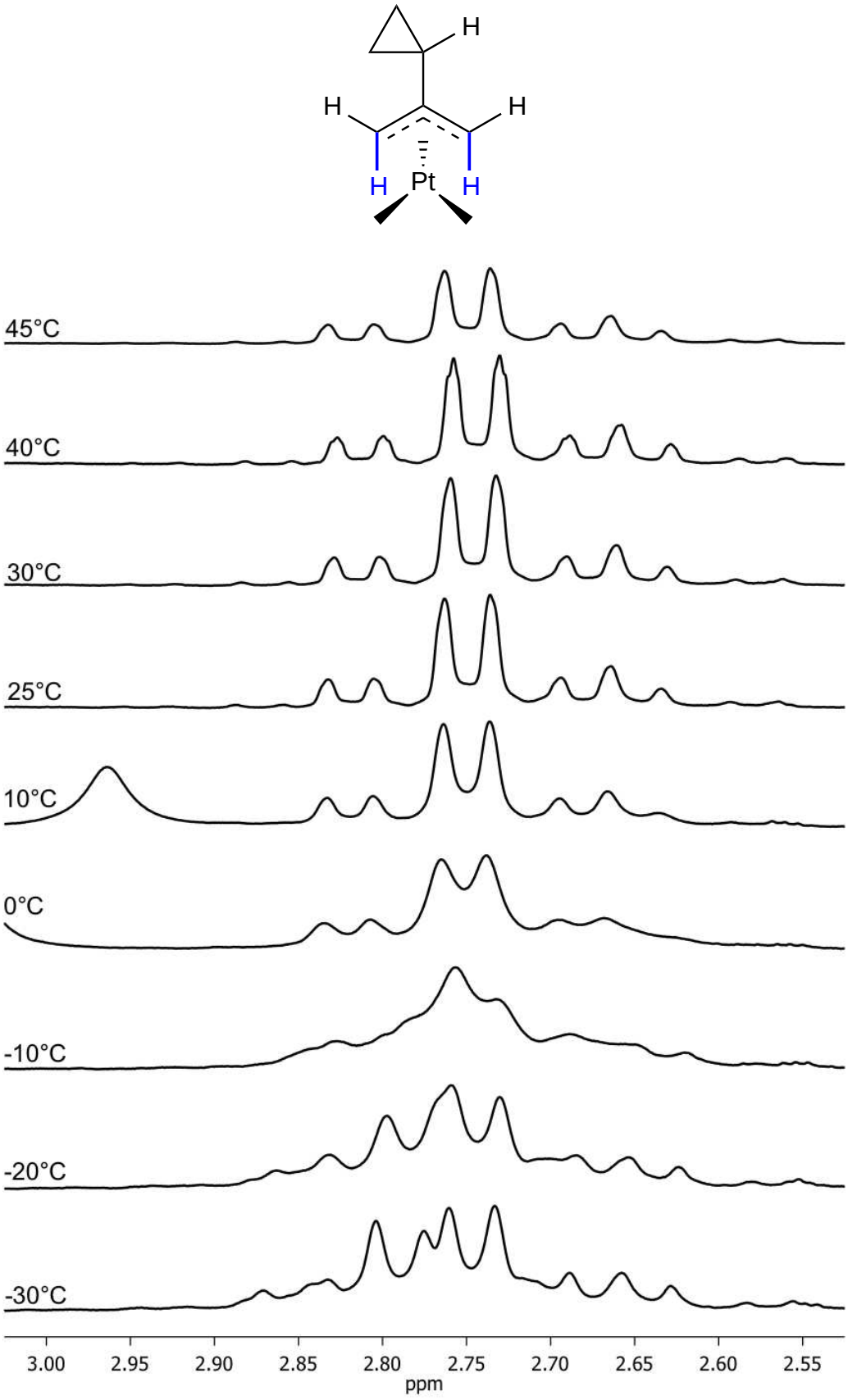

Figure 3.6. Temperature-dependent ^{1}H NMR spectra of the *anti* methylene proton of $[Pt(\eta^3\text{-}CH_2C^cPrCH_2)(dbpx)]^+$ (**17**) (300 MHz, 40 mg/mL, C_6D_6).

of the three 2-substituted allyl complexes **15**, **17** and **18a** showed good agreement. All three showed a broad singlet peak due to the *syn* CH_2 allyl peaks between 3.56–4.88 ppm, with only 0.07 ppm difference between the two dbpx complexes. The *anti* CH_2 allyl peaks appeared between 2.74–2.95 ppm, with $^2J_{Pt–H}$ between 32.0–41.3 Hz. Due to the presence of the large ^{t}Bu peaks, the methyl protons for **18a** could not be found, with those of **15** appearing at 1.96 ppm, higher than for the 1-methyl allyl complexes.

The room temperature $^{13}C\{^1H\}$ NMR spectra of **17** and **18a** showed the same broadness as the ^{31}P NMR spectra, although there was only one set of peaks. The central allyl carbon peak appeared at higher chemical shifts (126.4–135.9 ppm) than the corresponding carbon in the 1-methyl allyl complexes (98.59–119.33 ppm). The peak due to the methylene carbon appeared at similar chemical shifts to the 1-methyl methylene carbons (51.7–66.4 ppm), with the methylene in the 2-methyl complex at higher shifts than in the 1-methyl complex with the same phosphine backbone. The methyl carbons also appeared at higher ppm than in the 1-methyl complexes, at 21.6 and 24.8 ppm. The $^1J_{Pt–C}$ coupling constants of the 2-methyl complexes showed the same trends, with that of the methylene carbon of similar magnitude (79.8–85.0 *c.f.* 88.0–100.1 Hz) and that of the methyl carbon higher (28.4–30.0 *c.f.* 3.8–23.1 Hz) than for the 1-methyl allyl complexes.

The structure of the minor product in the protonation reaction of **1a** could not be fully determined. The complex formed initially (**14a**) converted into a second complex overnight (**14b**), and remained unchanged over several months. The same complexes formed in the same ratios when either $H_2C(SO_2CF_3)_3$, $HCPh(SO_2CF_3)_3$ or HBF_4 was used. From the $^1J_{Pt–P}$ coupling constants, 3439 and 3520 Hz for **14a**, 3512 and 3592 Hz for **14b**, both complexes had unsymmetrical allyl ligands, therefore were not the 2-substituted allyl similar to **17**. The similar size of the coupling constants indicated that the end of the allyl was not substituted with a cyclopropyl ring, as with **11** and **16**.

The $^{13}C\{^1H\}$ NMR data for **14b** suggested that it was a 2-substituted allyl, evidenced by the presence of a peak at 135.8 ppm, comparable to **15**, **17** and **18a**. There were peaks at 84.7 and 76.3 ppm with $^1J_{Pt–C}$ of 123.7 and 56.6 Hz respectively. When carbon-13 enriched BCP (enriched at the double-bond carbons) was used, it was the peak at

84 ppm which was enhanced, as well as the peak at 135 ppm. The peak at 76 ppm was at a much higher chemical shift and had a much smaller $^{1}J_{\mathrm{Pt–C}}$ coupling constant than the methylene resonances in the other allyl complexes (Table 3.2). Three other carbon resonances were identified, at 12.5, 27.4 and 30.6 ppm. None of these were in good agreement with the methyl peaks in either the 2-methyl (21.6 and 24.8 ppm) or 1-methyl (14.1–17.3 ppm) allyls. The presence of two phosphorus and three allyl carbon environments precludes a structure similar to **17**. A structure similar to that of **11** and **16** with the methyl in the 2-position was ruled out due to the similarities of the $^{1}J_{\mathrm{Pt–P}}$ coupling constants and the small size of the allyl $^{1}J_{\mathrm{Pt–C}}$ couplings compared to those of the ^{c}Pr allyl carbons. While it was evident that the second cyclopropyl ring had opened, there was no sign of a double-bond, which which would result from the ring-opening when the number of protons was conserved. The possibility of ring-opening with the gain of deuterium from the NMR solvent (d_6-acetone) was considered, but was deemed unlikely due to the lack of coupling to deuterium on any of the ^{13}C NMR peaks.

3.2.3 Computational Studies

Complexes with three allyl structural motifs were observed experimentally, with the proportions of these dependent on both the phosphine backbone and the solvent used. These were the allyl substituted in the 2-position, the 1-methyl allyl with the methyl in the *anti* position and the 1-methyl allyl with the methyl in the *syn* position. When formed from BCP, the 1-methyl allyls had a cyclopropyl ring in the 3-position. Computational models were used to investigate the formation of the allyl complexes. All structures were optimised and frequencies calculated using density functional theory calculations (B3LYP),[154–157] optimised using the def2-TZVP basis set,[158] of triple ζ quality.

Structures with a range of allyl systems were optimised for each of the three phosphine backbones used. The three phosphine backbones were the *ortho*-metallated phosphine-thioether ligand C_6H_3-*o*-$CH_2P^tBu_2$-*m*-CH_2S^tBu (P—C), dppp and dbpx. Six allyl complexes were used for both dppp and dbpx (Figures 3.9, 3.10, 3.11 and 3.12). These were the 2-substituted allyl complexes [Pt(η^3-$CH_2C^cPrCH_2$)(P—P)]

(P—P = dppp (**19**), dbpx (**17**)) and [Pt(η^3-CH_2CMeCH_2)(P—P)] (P—P = dppp (**15**), dbpx (**18a**)), the 1-methyl allyl complexes with the the methyl in the *anti* position [Pt(η^3-$C(CH_2)_2CHCHMe$)(P—P)] (P—P = dppp (**13a**), dbpx (**20a**)) and [Pt(η^3-$CH_2CHCHMe$)(P—P)] (P—P = dppp (**16a**), dbpx (**18b**)), and the 1-methyl complex with the methyl in the *syn* position [Pt(η^3-$C(CH_2)_2CHCHMe$)(P—P)] (P—P = dppp (**13b**), dbpx (**20b**)) and [Pt(η^3-$CH_2CHCHMe$)(P—P)] (P—P = dppp (**16a**), dbpx (**18c**)).

Due to the unsymmetrical phosphine ligand in the P—C complexes, there were 10 possible allyl structures (Figures 3.7 and 3.8). The 2-substituted complexes were [Pt(η^3-$CH_2C^cPrCH_2$)(P—C)] (**21**) and [Pt(η^3-CH_2CMeCH_2)(P—C)] (**22**). There were four 1-methyl allyl complexes with the methyl group in the *anti* position, [Pt(η^3-$C(CH_2)_2CHCHMe$)(P—C)] (Me *trans* C (**11a**), Me *trans* P (**11b**)) and [Pt(η^3-$CH_2CHCHMe$)(P—C)] (Me *trans* P (**12a**), Me *trans* C (**12b**)), and four 1-methyl complexes with the methyl in the *syn* position, [Pt(η^3-$C(CH_2)_2CHCHMe$)(P—C)] (Me *trans* C (**23a**), Me *trans* P (**23b**)) and [Pt(η^3-$CH_2CHCHMe$)(P—C)] (Me *trans* P (**24a**), Me *trans* C (**24b**)). Structures for the parent alkene complexes [Pt(BCP)(P—P)] (P—P = dppp (**1a**), dbpx (**1d**)), [Pt(MCP)(P—P)] (P—P = dppp (**2a**), dbpx (**2d**)), [Pt(BCP)(P—S)] (**8**), [Pt(MCP)(P—S)] (^{c}Pr *trans* S (**9a**), ^{c}Pr *trans* P (**9b**)), the acid used in the protonation reactions ($H_2C(SO_2CF_3)_2$) and its counter ion ($HC(SO_2CF_3)_2^-$) were also optimised.

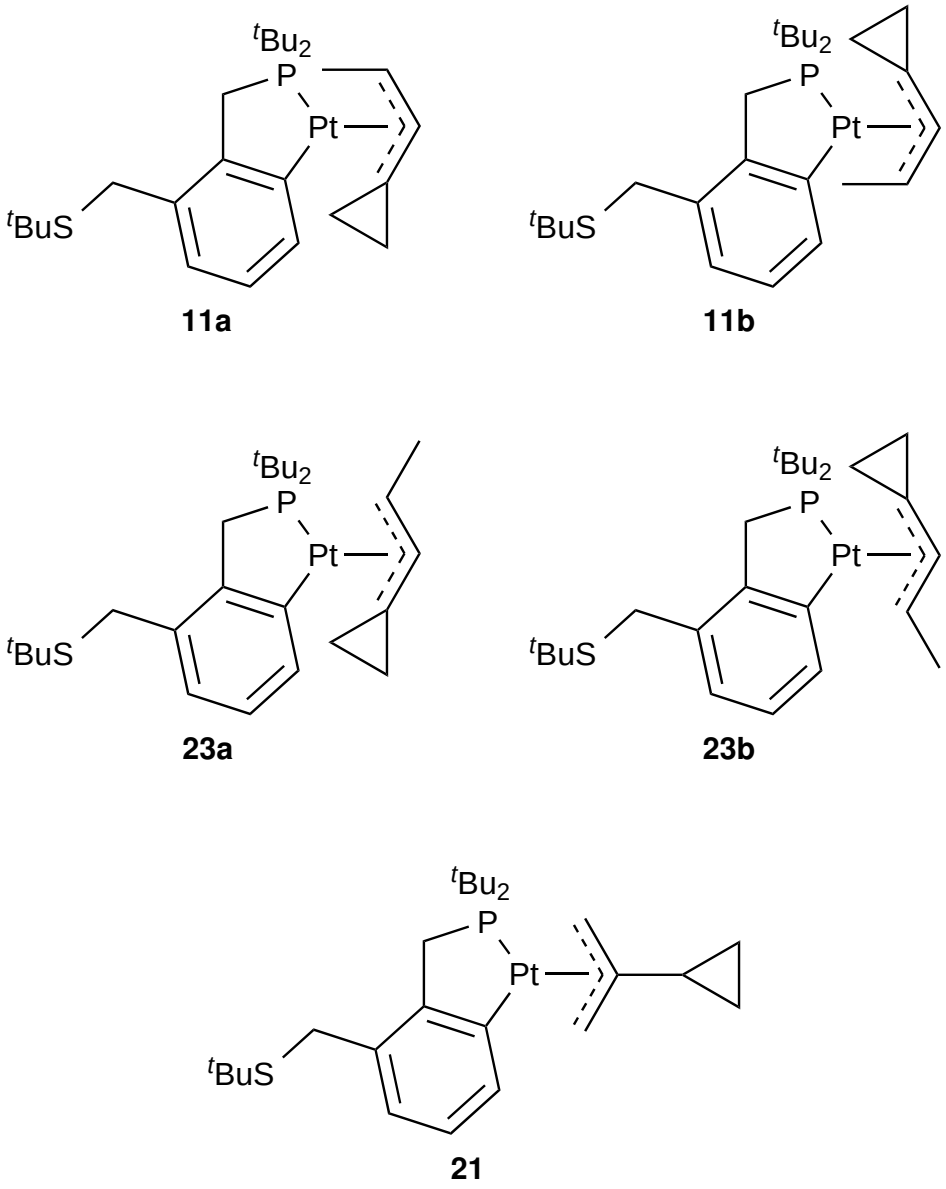

Figure 3.7. Allyl structural motifs derived from [Pt(BCP)(P—S)] (**8**).

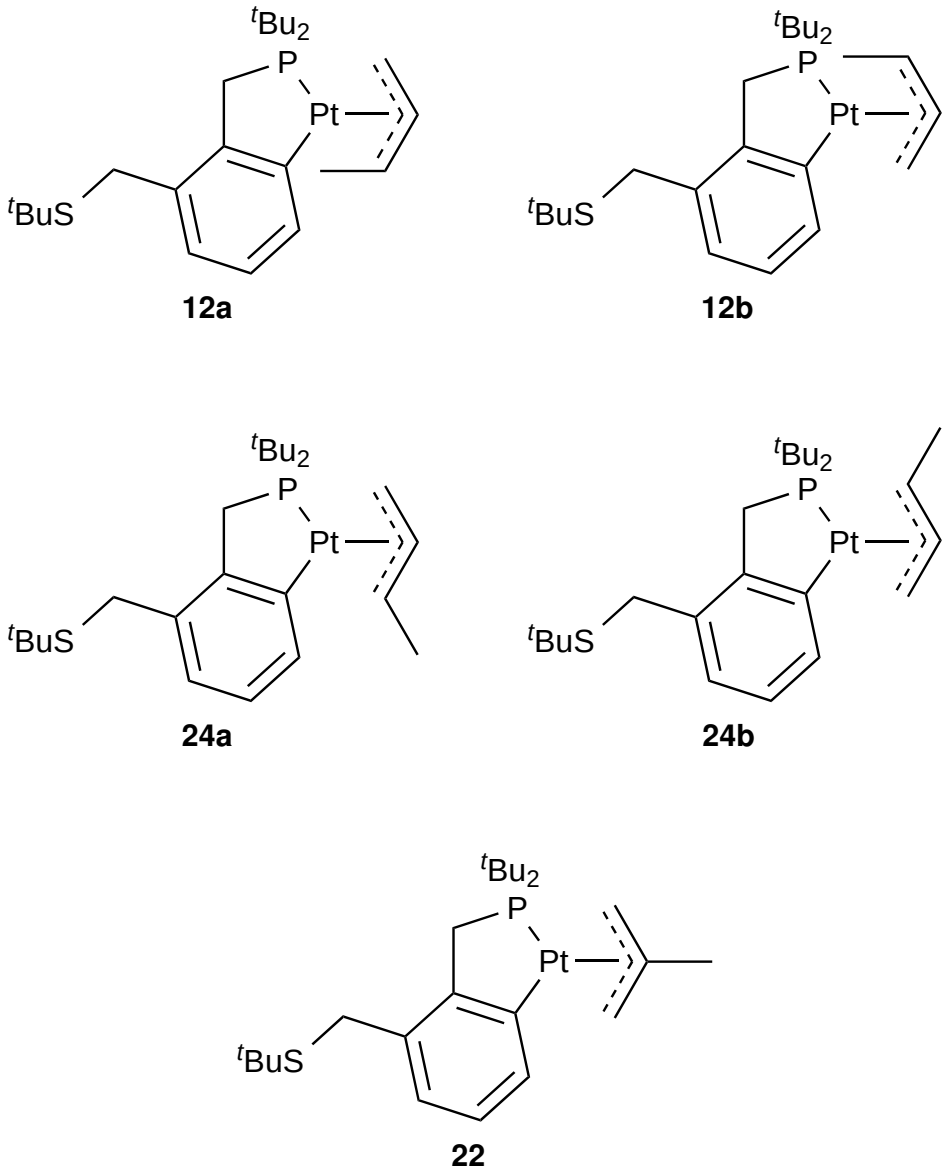

Figure 3.8. Allyl structural motifs derived from [Pt(MCP)(P—S)] (**9**).

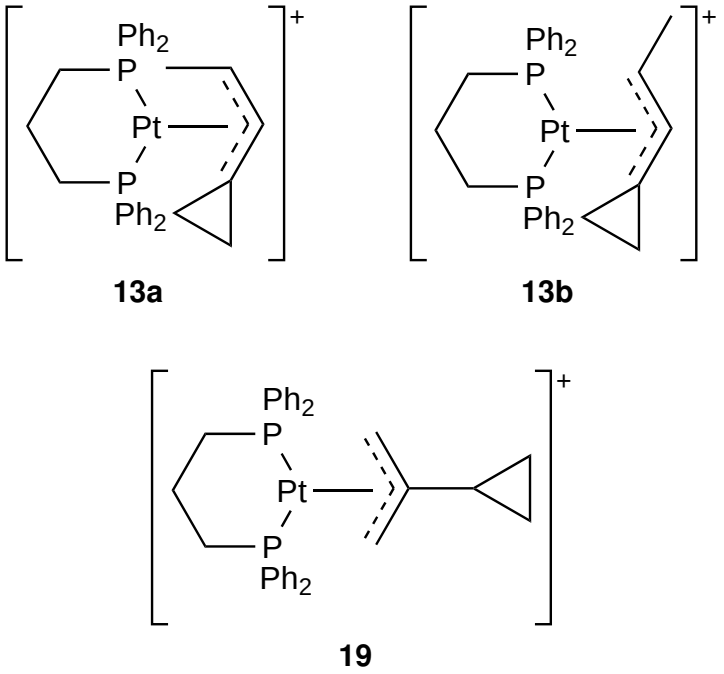

Figure 3.9. Allyl structural motifs derived from [Pt(BCP)(dppp)] (**1a**).

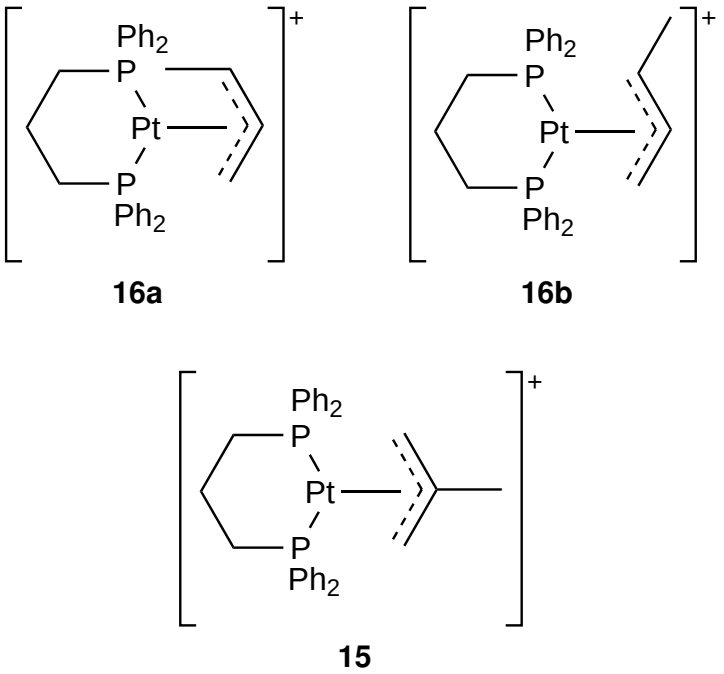

Figure 3.10. Allyl structural motifs derived from [Pt(MCP)(dppp)] (**2a**).

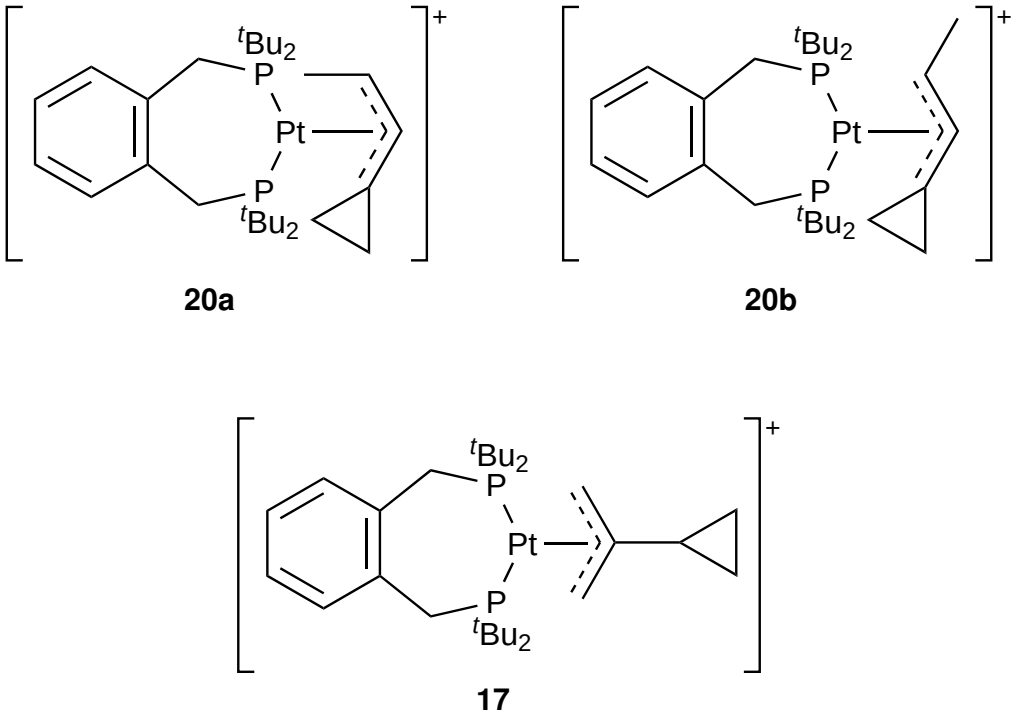

Figure 3.11. Allyl structural motifs derived from [Pt(BCP)(dbpx)] (**1d**).

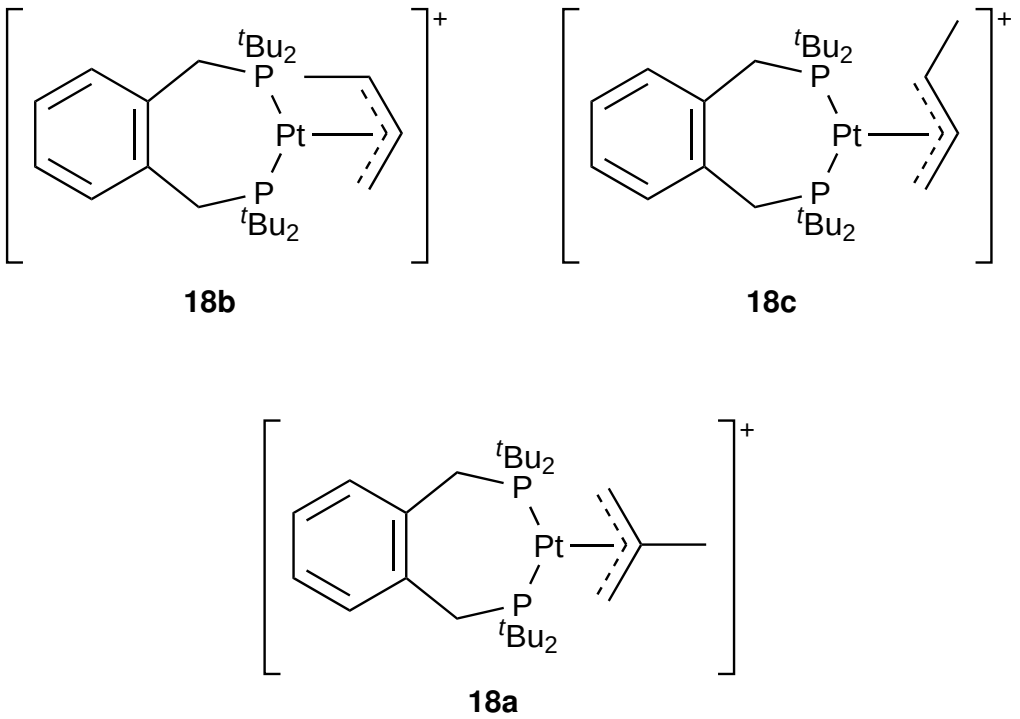

Figure 3.12. Allyl structural motifs derived from [Pt(MCP)(dbpx)] (**2d**).

The reaction ΔH values for the formation of the allyl complexes from the appropriate η^2-alkene complexes were calculated (Tables 3.3 and 3.4, Figures 3.13, 3.14 and 3.15). The reaction used for the P—C complexes was the rearrangement of the parent [Pt(L)(P—S)] complex to form the allyl complex (Scheme 3.11), with the isomers of [Pt(MCP)(P—S)] leading to two reaction possibilities. For the diphosphine complexes, the reaction used was the addition of $H_2C(SO_2CF_3)_2$ to [Pt(L)(P—P)], forming $[Pt(allyl)(P—P)]^+$ and $HC(SO_2CF_3)_2^-$ (Scheme 3.12). The species used in the calculations were isolated molecules in the gas phase, so the absolute values of ΔH thus obtained were not necessarily those for the experimental systems. However, the calculated values of reaction ΔH were considered to be accurate indicators of the trends in stability of the complexes, within the limits of the theoretical description. Transition state structures were not calculated, so no kinetic information was obtained.

In all systems, the reaction ΔH for the formation of the 2-substituted allyl complexes had the lowest value. The 2-cyclopropyl complexes with P—C (**21**) and dppp (**19**) (ΔH $= -172.6$ and 46.7 kJ mol^{-1} respectively) were not observed experimentally, despite the lower ΔH value indicating that these complexes were more stable than the corresponding 1-methyl complexes. The difference between ΔH for the 2-substituted and 1-methyl complexes was similar for both backbones (39.1–48.1 kJ mol^{-1}). The formation of the 2-substituted allyl complexes occurs *via* a different mechanism than for the formation of the 1-methyl allyls (Scheme 3.6). It is therefore likely that there was a larger activation energy for the formation of the 2-substituted complexes, leading to the formation of the 1-methyl complexes being favoured kinetically. The 2-cyclopropyl complex **17** was the only protonated product observed experimentally with dbpx. In this case, ΔH (56.3 kJ mol^{-1}) was significantly lower than for the 1-methyl complexes, with differences of 79.8 and 81.3 kJ mol^{-1} between the *anti* and *syn* methyl complexes respectively, nearly twice that of the P—C and dppp systems.

The 2-methyl substituted complexes **15**, **18a** and **22** also had lower reaction ΔH values than for the 1-methyl allyls, 69.0, 97.9, -141.5 and -145.4 kJ mol^{-1} respectively. In this case, there were smaller differences between the 2-substituted and 1-methyl complexes

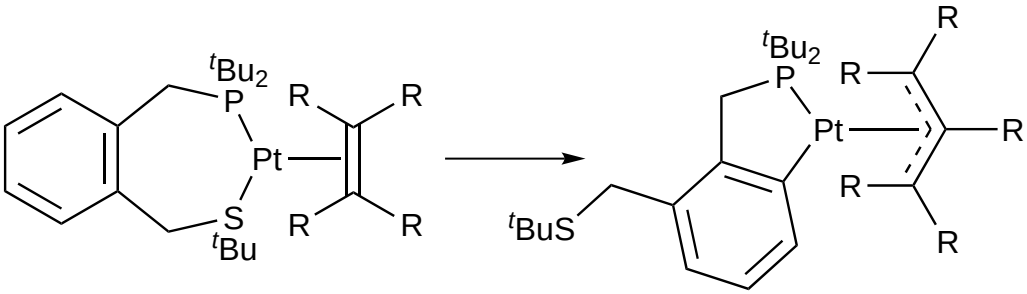

Scheme 3.11. Formation of P—C allyl complexes from [Pt(L)(P—S)].

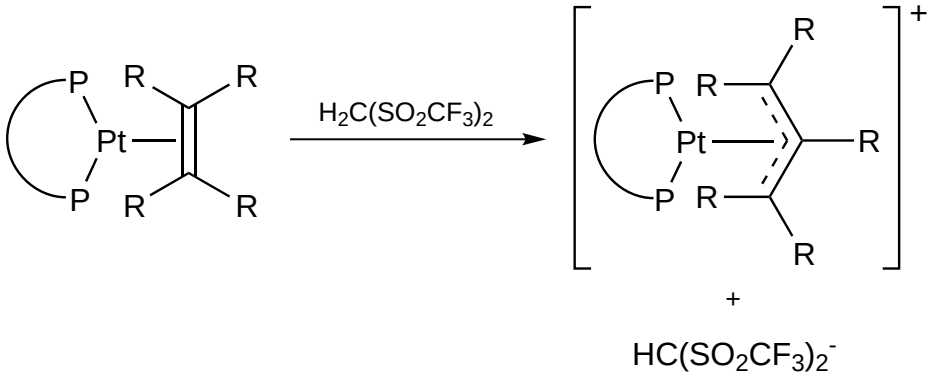

Scheme 3.12. Formation of P—P allyl complexes from [Pt(L)(P—P)].

Table 3.3. Reaction ΔH for the Formation of Allyl Complexes from η^2-BCP Complexes.

Compound				**ΔH (kJ mol^{-1})**
[Pt(η^3-$CH_2C^cPrCH_2$)(P—C)]			**21**	−172.6
[Pt(η^3-$C(CH_2)_2CHCHMe$)(P—C)]	Me *trans* C	*anti*	**11a**	−126.9
[Pt(η^3-$C(CH_2)_2CHCHMe$)(P—C)]	Me *trans* C	*syn*	**23a**	−133.6
[Pt(η^3-$C(CH_2)_2CHCHMe$)(P—C)]	Me *trans* P	*anti*	**11b**	−124.6
[Pt(η^3-$C(CH_2)_2CHCHMe$)(P—C)]	Me *trans* P	*syn*	**23b**	−124.5
[Pt(η^3-$CH_2C^cPrCH_2$)(dppp)]$^+$			**19**	46.7
[Pt(η^3-$C(CH_2)_2CHCHMe$)(dppp)]$^+$		*anti*	**13a**	93.0
[Pt(η^3-$C(CH_2)_2CHCHMe$)(dppp)]$^+$		*syn*	**13b**	86.2
[Pt(η^3-$CH_2C^cPrCH_2$)(dbpx)]$^+$			**17**	56.2
[Pt(η^3-$C(CH_2)_2CHCHMe$)(dbpx)]$^+$		*anti*	**20a**	136.0
[Pt(η^3-$C(CH_2)_2CHCHMe$)(dbpx)]$^+$		*syn*	**20b**	137.4

Table 3.4. Reaction ΔH for the Formation of Allyl Complexes from η^2-MCP Complexes.

Compound				ΔH (kJ mol^{-1})		
				From 9a	From 9b	From 2
[Pt(η^3-CH_2CMeCH_2)(P—C)]			**22**	−141.5	−145.4	
[Pt(η^3-$CH_2CHCHMe$)(P—C)]	Me *trans* P	*anti*	**12a**	−124.9	−128.7	
[Pt(η^3-$CH_2CHCHMe$)(P—C)]	Me *trans* P	*syn*	**24a**	−125.3	−129.2	
[Pt(η^3-$CH_2CHCHMe$)(P—C)]	Me *trans* C	*anti*	**12b**	−119.7	−123.6	
[Pt(η^3-$CH_2CHCHMe$)(P—C)]	Me *trans* C	*syn*	**24b**	−125.4	−129.3	
[Pt(η^3-CH_2CMeCH_2)(dppp)]$^+$			**15**			69.0
[Pt(η^3-$CH_2CHCHMe$)(dppp)]$^+$		*anti*	**16a**			86.0
[Pt(η^3-$CH_2CHCHMe$)(dppp)]$^+$		*syn*	**16b**			81.5
[Pt(η^3-CH_2CMeCH_2)(dbpx)]$^+$			**18a**			97.9
[Pt(η^3-$CH_2CHCHMe$)(dbpx)]$^+$		*anti*	**18b**			115.5
[Pt(η^3-$CH_2CHCHMe$)(dbpx)]$^+$		*syn*	**18c**			118.7

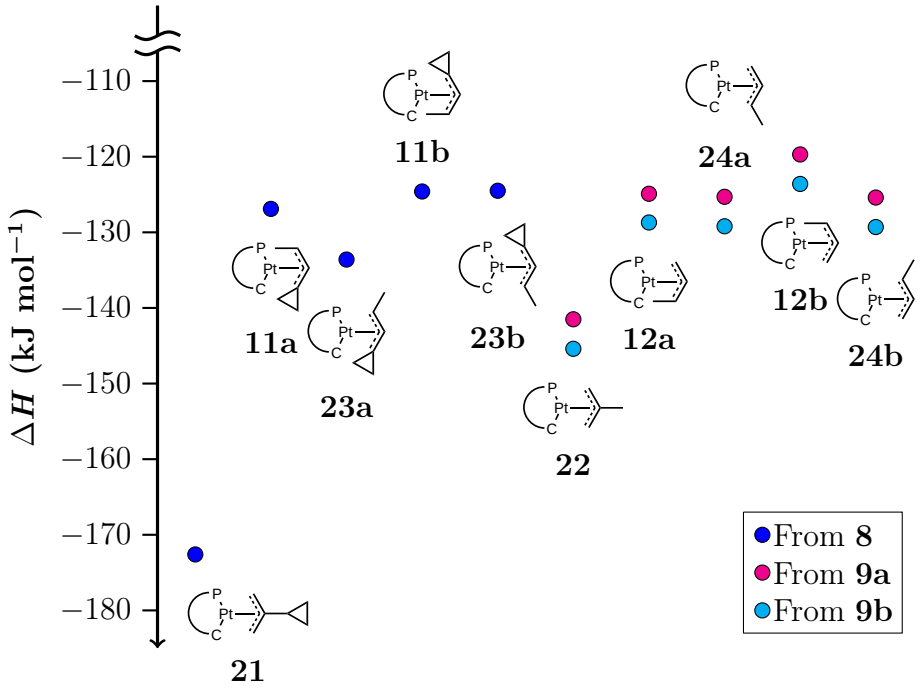

Figure 3.13. Reaction ΔH for the formation of allyl complexes from [Pt(L)(P—S)].

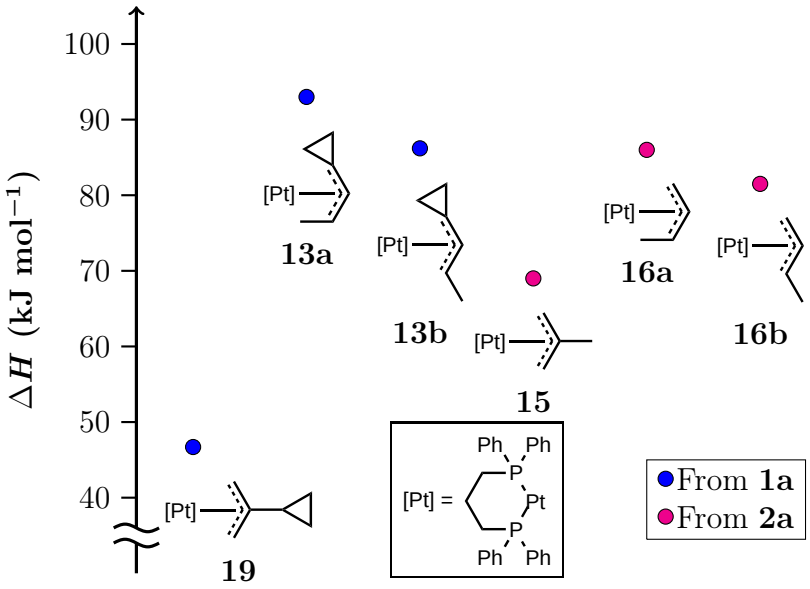

Figure 3.14. Reaction ΔH for the formation of allyl complexes from [Pt(L)(dppp)].

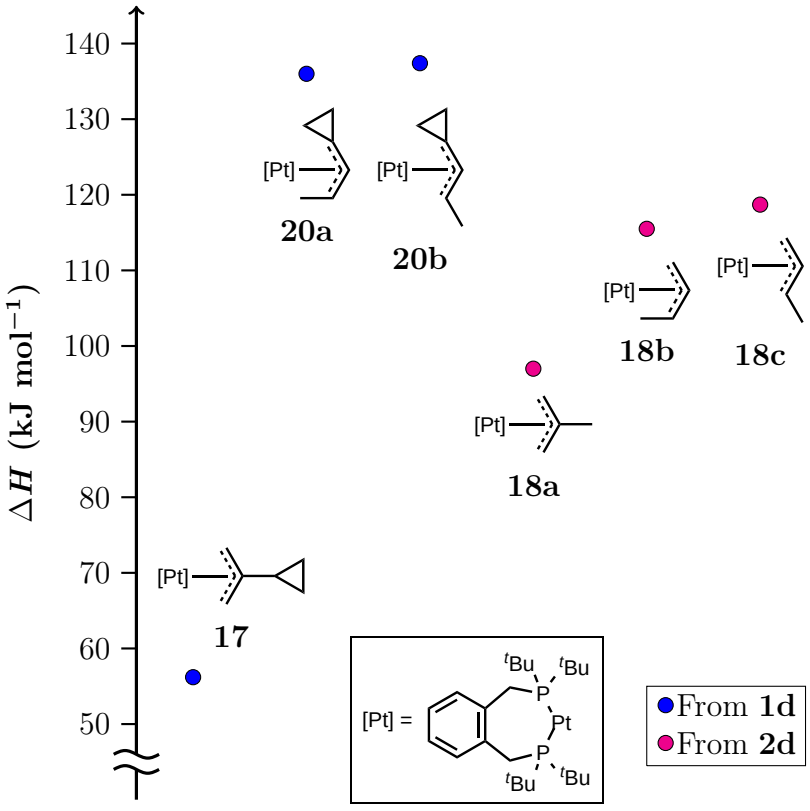

Figure 3.15. Reaction ΔH for the formation of allyl complexes from [Pt(L)(dbpx)].

(12.6–21.8 kJ mol^{-1}). Again, it was likely that the size of the activation barrier played a part in determining which isomers were formed. While the differences in ΔH for the P—C complexes (16.1–21.8 kJ mol^{-1}) was similar to those of the diphosphine complexes, **22** was not observed experimentally. A significantly larger proportion of **15** (68%) was produced than **18a** (42%), despite the similarity in the differences of ΔH (12.6–17.1 and 17.6–20.9 kJ mol^{-1} respectively). It was found experimentally that the solvent used in the reaction had a large effect on the proportion of **15** formed, with 68% **15** formed in *d*$_6$-acetone and 84% **15** formed in CD_2Cl_2 (Section 3.2.2), indicating that more factors affected the reaction outcome than were considered in this computational study.

The majority of the 1-methyl complexes with the methyl group in the *anti* position had enthalpy values higher than the corresponding complexes with the methyl group in the *syn* position, indicating that the *syn* isomer was thermodynamically more stable. The dbpx complexes and the P—C cyclopropyl allyl complexes with the methyl group *trans* to the P (**11b** and **23b**), which had lower values for the *anti* isomer, were the exception to this. The complexes of dppp (ΔH = 93.0, 86.0, 86.0 and 81.5 kJ mol^{-1} for **13a**, **13b**, **16a** and **16b** respectively) and P—C with the methyl group *trans* to C (ΔH = −126.9 for **11a**, −133.6 for **23a**, −119.7 and −125.4 for **12b**, and −123.6 and −129.3 kJ mol^{-1} for **24b**) had the largest differences between the *anti* and *syn* isomers, 4.5–6.8 kJ mol^{-1} in favour of the *syn* isomer. The P—C complexes with the methyl group *trans* to P had only small differences between the isomers; ΔH was −124.9 and −128.7 kJ mol^{-1} for **12a** and −125.3 and −129.2 kJ mol^{-1} for **24a**, 0.5 kJ mol^{-1} in favour of the *syn* isomer, −124.6 and −124.5 kJ mol^{-1} for **11b** and **23b**, 0.1 kJ mol^{-1} in favour of the *anti* isomer. The dbpx complexes (ΔH = 136.0, 137.4, 115.5 and 118.7 kJ mol^{-1} for **20a**, **20b**, **18b** and **18c** respectively) had differences of 1.5 and 3.2 kJ mol^{-1}, in favour of the *anti* isomer.

Experimentally, it was the *anti* isomer that was formed initially, for all cases except for the protonation of [Pt(BCP)(dbpx)] (**1d**), where only the 2-substitiuted allyl **17** was observed. While this was consistent with the lower *anti* reaction ΔH values for the dbpx complexes and **11b**/**23b**, for the other reactions it was the *syn* isomer which was thermodynamically the more stable. The *anti* isomer would therefore be the kinetic

isomer, with a lower activation energy for formation (not calculated in this study). Rearrangement to the *syn* isomer was observed for the dppp complexes, with *anti*:*syn* ratios stabilising at 27:73 for **13** and 58:42 for **16**. Other allyl systems showed similar reactivity, with the *anti* methyl isomers formed initially, followed by rearrangement to the *syn* isomer.[141,142] No rearrangement was observed for the P—C complexes, indicating that the energy barrier for rearrangement was higher in these systems.

In order to determine whether the atomic charges on the double-bond atoms had an effect on the site of protonation, NBO calculations were performed on the starting complexes (Table 3.5). For the P—S/P—C complexes, the reaction was with an internal hydride formed by the *ortho*-metallation of the backbone aromatic ring, rather than a proton. Structures of the likely intermediate complexes [PtH(L)(P—C)] were optimised, and the atomic charges calculated. A number of structures were possible due to the unsymmetrical backbone and the perpendicular coordination of the alkene (Figure 3.16), favoured in platinum(II) complexes.[2,22] Two isomers of [PtH(BCP)(P—C)] were used, with H *trans* to P (**25a**) and with H *trans* to C (**25b**). There were four isomers of [PtH(MCP)(P—C)] used, H *trans* to P with the ^{c}Pr ring up according to the coordination plane as drawn (**26a**), H *trans* to P with the ^{c}Pr ring down (**26b**), H *trans* to C with the ^{c}Pr ring down (**26c**) and H *trans* to C with the ^{c}Pr ring down (**26d**).

The atomic charges on the double-bond carbons in the dppp complexes (−0.20 *e* for **1a**, −0.22 (=CR_2) and −0.55 *e* (=CH_2) for **2a**) were found to be the same as for the dbpx complexes (−0.20 *e* for **1d**, −0.22 (=CR_2) and −0.55 *e* (=CH_2) for **2d**). The double-bond carbons *trans* to P in the P—S complexes had charges 0.2 *e* lower (more negative) than for the P—P complexes, −0.22 *e* for **8**, −0.24 *e* (=CR_2) for **9b** and −0.58 *e* (=CH_2) for **9a**. When *trans* to S, the carbons had charges higher (more positive) by 0.6 *e* than when *trans* to P, −0.16 *e* for **8**, −0.18 *e* (=CR_2) for **9a** and −0.52 *e* (=CH_2) for **9b**. For the hydride complexes, the atoms *trans* to P had higher charges. This difference was small for the double-bond carbons, 0.01–0.04 *e*, but larger for the hydride, 0.08–0.09 *e*. The methylene end of the MCP double-bond had a higher charge than the cyclopropyl end, −0.6 *vs.* −0.2 *e*, which indicated that protonation of the =CH_2 would be more likely. According

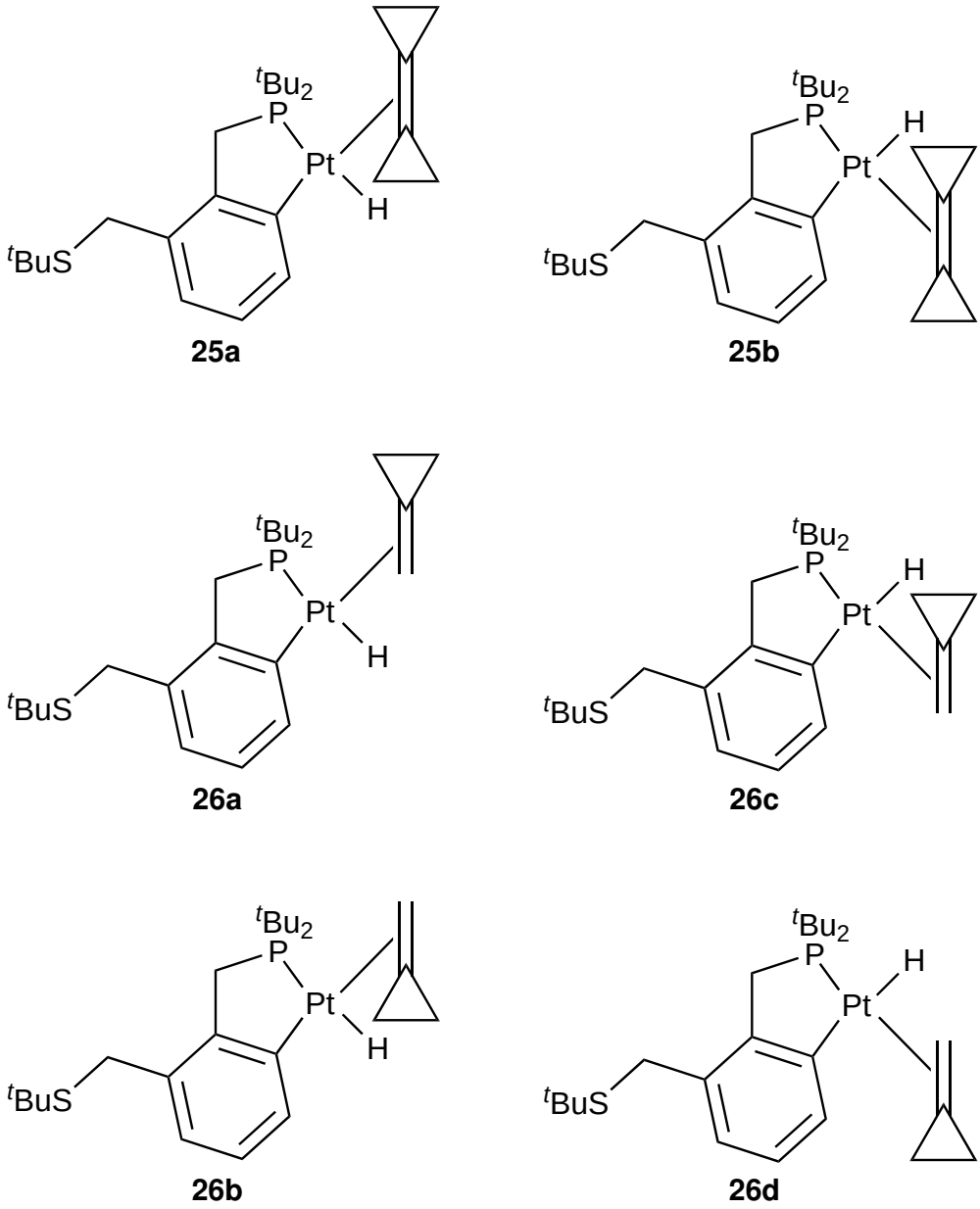

Figure 3.16. Structures of [PtH(L)(P—C)] complexes.

Table 3.5. Atomic Charges on the Double-Bond and Hydride Atoms of Alkene Complexes.

Compound			Charge (e, 1.602×10^{-19} C)		
			$=CR_2$	$=CH_2$	H
[Pt(BCP)(P—S)]	**8**		−0.22 (*trans* P)		
			−0.16 (*trans* S)		
[PtH(BCP)(P—C)]	**25a**	H *trans* P	−0.04 (up)		−0.05
			−0.06 (down)		
[PtH(BCP)(P—C)]	**25b**	H *trans* C	−0.03 (up)		−0.14
			−0.03 (down)		
[Pt(BCP)(dppp)]	**1a**		−0.20		
			−0.20		
[Pt(BCP)(dbpx)]	**1d**		−0.20		
			−0.20		
[Pt(MCP)(P—S)]	**9a**	^{c}Pr *trans* S	−0.18	−0.58	
[Pt(MCP)(P—S)]	**9b**	^{c}Pr *trans* P	−0.24	−0.52	
[PtH(MCP)(P—C)]	**26a**	H *trans* P	−0.05 (up)	−0.41 (down)	−0.07
[PtH(MCP)(P—C)]	**26b**	H *trans* P	−0.04 (down)	−0.42 (up)	−0.06
[PtH(MCP)(P—C)]	**26c**	H *trans* C	−0.03 (up)	−0.38 (down)	−0.15
[PtH(MCP)(P—C)]	**26d**	H *trans* C	−0.03 (down)	−0.38 (up)	−0.15
[Pt(MCP)(dppp)]	**2a**		−0.22	−0.55	
[Pt(MCP)(dbpx)]	**2d**		−0.22	−0.55	

to the literature mechanism for the allyl formation (Scheme 3.6), attack on the methylene carbon results in the formation of 2-methyl allyl complexes. While these isomers were observed experimentally, the fact that the dbpx complex, which formed 42% **18a**, had the same atomic charges as for the dppp complex, which formed 68% **15**, indicated that the factors affecting the product distribution were not simply electronic.

This is supported by the Tolman electronic parameters ν of the phosphines both in this study and in the reaction of *trans*-[PtH(NO_3)($L)_2$] (L = PEt_3 (ν = 2062 cm^{-1}), PMe_2Ph (ν = 2067 cm^{-1}), PPh_3 (ν = 2069 cm^{-1})) with MCP.[82,134,135] While there was no data available for dppp and dbpx, PPh_2Et (ν = 2067 cm^{-1}) and P(*o*-tol)^tBu_2 (ν = 2060 cm^{-1}) were reasonable approximations.[82] The electronic properties of the P—C ligand were more complicated. No 2-substituted allyl complex was observed with PEt_3 or PMe_2Ph, which were on the low and high end respectively of the range of electronic parameters. With

PPh_3, dppp and dbpx, 42–100% of the products were 2-substituted, with the ν values again at both ends of the range. There was therefore no correlation between the value of ν and the product distribution.

There was a stronger correlation between the product distribution and the cone angle of the phosphine ligand. In the reaction of *trans*-$[PtH(NO_3)(L)_2]$ with MCP, when the cone angle was small (PEt_3 $\theta = 132°$, PMe_2Ph $\theta = 122°$), only 1-methyl allyl complexes were formed.[82] With PPh_3, which had a larger cone angle of 145°, the products were 50:50 1-methyl to 2-methyl allyls. A similar trend was seen in the protonation of the BCP complexes of dppp ($\theta = 127°$) and dbpx ($\theta = 138°$),[81,82] where no 2-substituted complex was observed for dppp, and 100% 2-substituted was observed for dbpx. These trends indicated that steric factors had a significant effect on product distributions. The protonation of the MCP complexes did not fit this trend, with more 2-substituted complexes observed with dppp than with dbpx. This suggested that the factors affecting product distribution were more complicated than those discussed here, and it was likely that both steric and electronic factors played a part.

In summary, the reaction ΔH values indicated that the 2-substituted complexes were more stable than the corresponding 1-methyl substituted complexes. In most cases, the 1-methyl complex with the methyl in the *syn* position was more stable than the *anti* isomer, although it was the *anti* isomer that was formed initially experimentally. This indicated that the activation energy had a significant effect on complex formation.

Chapter 4

Platinum(II) Chemistry

4.1 Introduction

Three different types of reactivity were observed when bicyclopropylidene and methylenecyclopropane were reacted with platinum(II) complexes. These were (i) ring-opening reactions to form 1,3-dienes, (ii) the coordination of an alkene to form an η^2-alkene complex, and (iii) the formation of a β-chloroalkyl complex.

4.2 1,3-Dienes

Allylidenecyclopropane (ACP) is a 1,3-diene which has a cyclopropyl ring at the end of one of the double-bonds, and can be produced when bicyclopropylidene undergoes a single ring-opening reaction. As mentioned previously (Section 2.2), there has been one report of the formation of ACP from BCP, occurring in the reaction of BCP with [$Pd(OAc)_2$] and PPh_3.[74] The proposed mechanism for this reaction involved the addition of a palladium hydride across the BCP double-bond, followed by a cyclopropylmethyl to homoallyl rearrangement and termination by β-hydride elimination. Under the reported conditions, ACP went on to react with another molecule of BCP to form various oligomers (see Scheme 1.27).

In the reactions of BCP with the alkyl complexes [$PtMe_2$(1,5-hexadiene)] and [$PtEt_2$(COD)], ACP was produced (Scheme 4.1). This reaction was also observed with the

Pt(0) complexes [$Pt(C_2H_4)_3$], [$Pt(COD)_2$] and [$Pt(nb)_3$] (Section 2.2). With [$PtMe_2$(1,5-hexadiene)] the reaction was catalytic, converting a ∼1000 fold excess of BCP into ACP in three days at room temperature, although the [$PtMe_2$(1,5-hexadiene)] was largely unreacted. Only two equivalents of BCP were converted to ACP in the reaction with [$PtEt_2$(COD)]. This occurred over one day at room temperature, with the reaction mixture unchanged over several weeks. While approximately half of the [$PtEt_2$(COD)] reacted with BCP, no platinum-containing products could be characterised.

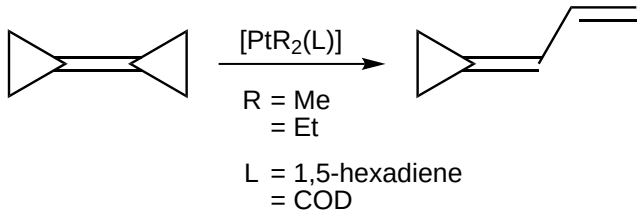

Scheme 4.1. Formation of allylidenecyclopropane from Pt(II) alkyl complexes.

The analogous ring-opening reaction of MCP would produce 1,3-butadiene. When MCP was combined with [$PtMe_2$(1,5-hexadiene)] at room temperature no reaction occurred. With [$PtEt_2$(COD)], there was a small amount of 1,3-butadiene formed (10% relative to the amount of [$PtEt_2$(COD)]). However, this was not the major product. After one day, two new complexes [$PtEt(C(CH_2)_2CH_3)$(COD)] (**27a**) and [$Pt(C(CH_2)_2CH_3)_2$(COD)] (**27b**) formed in an approximately 2:1 ratio (Scheme 4.2), with about a third of the [$PtEt_2$(COD)] still unreacted. All of the [$PtEt_2$(COD)] had reacted after 2 days. The mono-ethyl complex **27a** also continued to react with MCP, reaching a 15:85 **27a**:**27b** ratio after 30 days, even when 11 eq. of MCP was used.

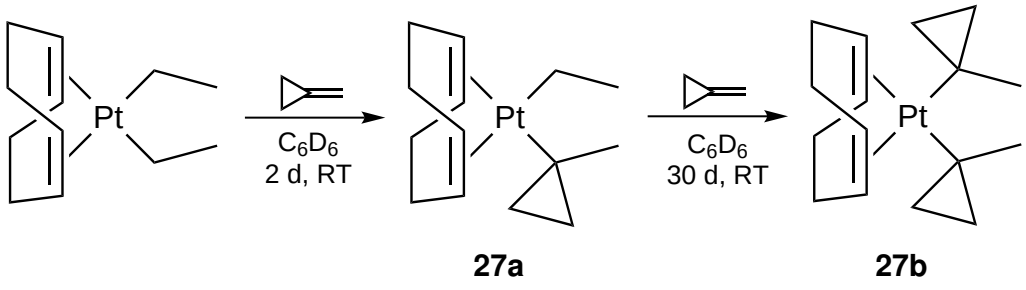

Scheme 4.2. Reaction of [$PtEt_2$(COD)] with MCP.

While the cyclopropylmethyl motif is fairly common (see Sections 2.2 and 4.4 for examples from this work), these complexes are the first examples of complexes with stable, unsubstituted cyclopropylmethyl ligands. The ligands were formed by the Markovnikov addition of Pt–H across the MCP double-bond, with **27a** formed from one equivalent of MCP, and **27b** formed from two equivalents (Scheme 4.2). The Pt–H was generated by the β-hydride elimination of an ethyl group, as evidenced by the presence of ethene in the reaction mixture.[159] The small amount of butadiene resulted from the anti-Markovnikov addition of the Pt–H, followed by a cyclopropylmethyl to homoallyl rearrangement and β-hydride elimination (Scheme 4.3). Allylidenecyclopropane would be produced in the corresponding reaction from BCP, with only one addition product possible due to the two identical ends of the double-bond (Scheme 4.4).

4.2.1 NMR Characterisation

For NMR spectra see Figures A.71–A.78. The peaks in the $^{13}C\{^1H\}$ NMR spectra of **27a** and **27b** due to the cyclopropyl carbon directly bound to the metal had very high $^1J_{Pt–C}$ coupling constants (1160.6 and 1178.5 Hz), characteristic of a Pt–C σ-bond (Table 4.2).[93,139] These coupling constants were greater than those of the platinum-bound carbon of the ethyl ligands in $[PtEt_2(COD)]$ and **27a** (847.2 and 854.8 Hz respectively). This indicated that the interaction with the metal was stronger for the ^{c}Pr ring than for the sp^3 methylene, which has also been observed previously in this work for sp^2 cyclopropyl carbons (see Sections 2.1 and 3.2). The remaining ^{13}C and ^1H NMR data (Table 4.1) were consistent with the assigned structures.

4.3 η^2-Alkene Complexes

Platinum(II) η^2-alkene complexes of BCP and MCP were synthesised by the displacement of a neutral ligand from a precursor complex, as with the platinum(0) complexes previously discussed (Chapter 2). For the Pt(0) complexes, it was an alkene ligand that was displaced. This was usually ethene, but in the case of the P—S complexes, a norbornene precursor

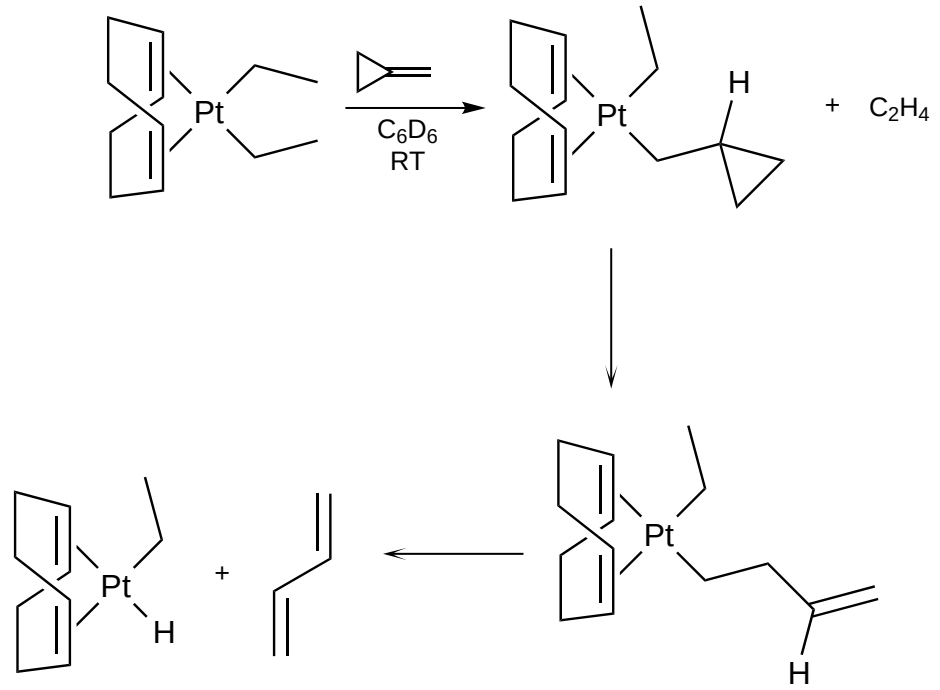

Scheme 4.3. Formation of butadiene from [$PtEt_2$(COD)].

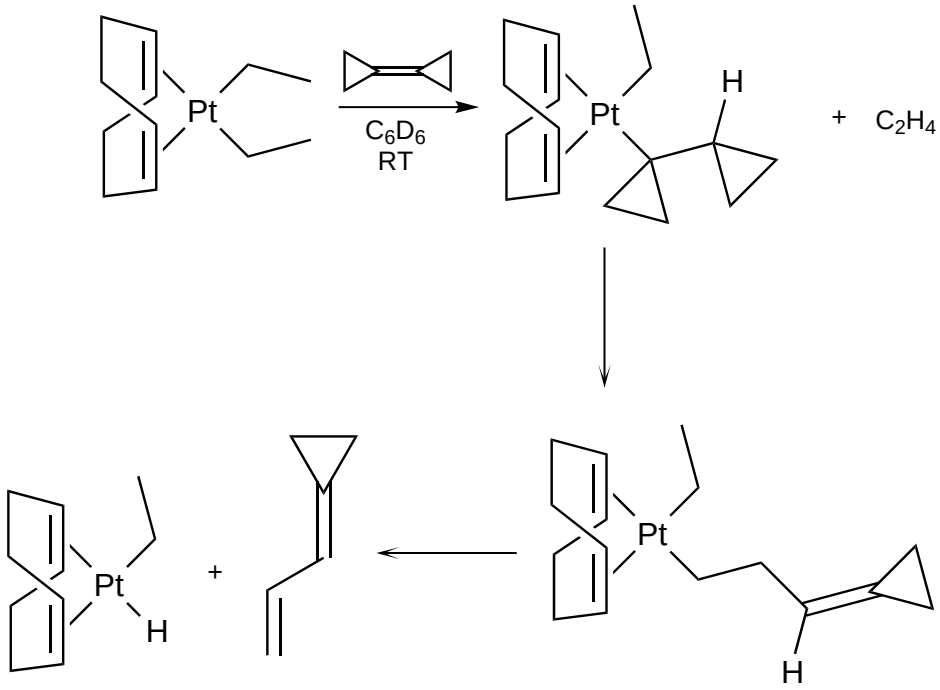

Scheme 4.4. Formation of ACP from [$PtEt_2$(COD)].

Table 4.1. Selected ^{1}H NMR Data of [Pt(L)$_2$(COD)].[a]

Compound		δ_H			
		^{c}Pr	CH_3	Et CH_2	Et CH_3
[$PtEt_2$(COD)]				1.89 (90.2)	1.54 (79.5)
[PtEt($C(CH_2)_2CH_3$)(COD)]	**27a**	0.73 (66.2)	1.35 (55.9)	1.96 (91.8)	1.51 (74.4)
		0.42 (46.5)			
[Pt($C(CH_2)_2CH_3)_2$(COD)]	**27b**	0.86 (66.2)	1.41 (53.5)		
		0.41 (44.4)			

[a] δ values are given in ppm and J values in Hz. All spectra were measured in C_6D_6 at room temperature with 40 mg/mL sample. Values in parentheses are platinum couplings.

Table 4.2. Selected ^{13}C{^{1}H} NMR Data of [Pt(L)$_2$(COD)].[a]

Compound		δ_C				
		Pt–C	^{c}Pr	CH_3	Et CH_2	Et CH_3
[$PtEt_2$(COD)]					20.4 (847.2)	16.6 (32.9)
[PtEt($C(CH_2)_2CH_3$)(COD)]	**27a**	17.4 (1160.6)	14.9	31.2 (27.2)	21.8 (854.8)	16.4 (35.2)
[Pt($C(CH_2)_2CH_3)_2$(COD)]	**27b**	17.2 (1178.5)	15.9	31.5 (21.3)		

[a] δ values are given in ppm and J values in Hz. All spectra were measured in C_6D_6 at room temperature with 40 mg/mL sample. Values in parentheses are platinum couplings.

was used (Section 3.1). It was found that both BCP and MCP were able to displace ethene from the Pt(II) complex *trans*–[$PtCl_2(C_2H_4)$(Py)] to form the η^2-alkene complexes *trans*–[$PtCl_2$(L)(Py)] (L = BCP (**28**), MCP (**29**)) (Scheme 4.5). The ethene complex was synthesised *in situ* by the addition of two equivalents (one per Pt) of pyridine to Zeise's dimer ([$Pt_2Cl_4(C_2H_4)_2$]). The formation of **28** and **29** occurred immediately upon the addition of the appropriate alkene to *trans*–[$PtCl_2(C_2H_4)$(Py)] at room temperature. Both of these complexes were unstable, decomposing after approximately 1 hour.

When *cis*–[$PtCl_2(DMSO)_2$] was used, it was one of the DMSO ligands that was displaced by the alkene to form *cis*–[$PtCl_2$(L)(DMSO)] (L = BCP (**30**), MCP (**31**)) (Scheme 4.6). The reactions occurred over the course of several hours, and did not go to completion. Unlike the pyridine complexes, these were stable for several days.

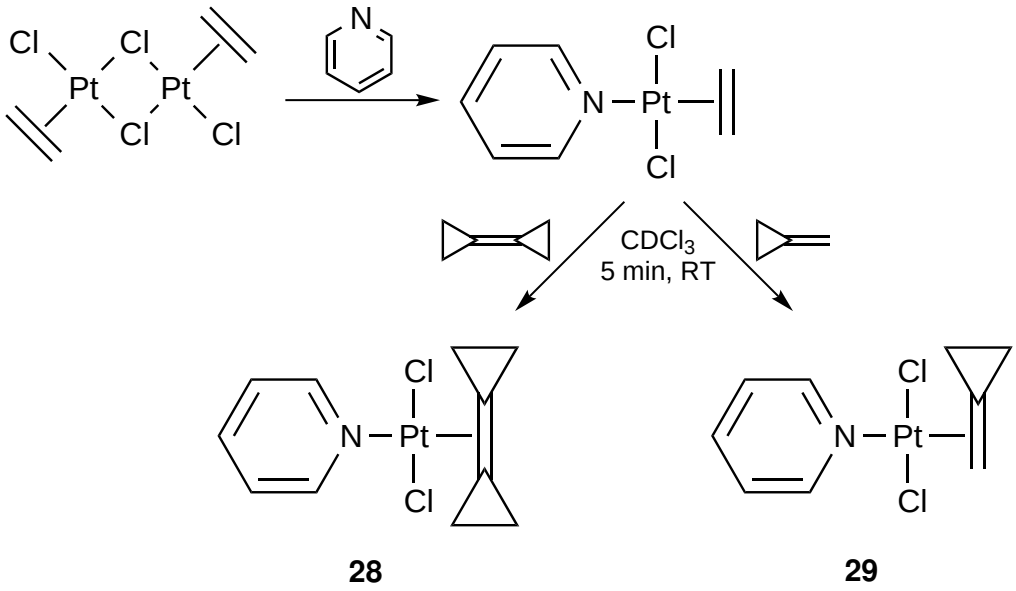

Scheme 4.5. Synthesis of *trans*–[$PtCl_2$(L)(Py)] (**28** and **29**) from *trans*–[$PtCl_2(C_2H_4)$(Py)].

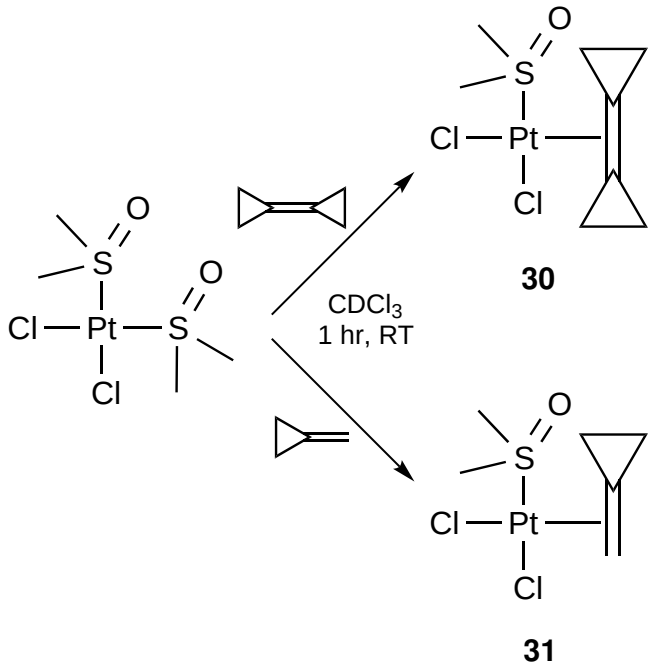

Scheme 4.6. Synthesis of *cis*–[$PtCl_2$(L)(DMSO)] (**30** and **31**) from *cis*–[$PtCl_2(DMSO)_2$].

4.3.1 NMR Characterisation

For representative NMR spectra, see FIgures A.79–A.81. Compared to the platinum(0) η^2-alkene complexes, the alkene carbons in the Pt(II) complexes had significantly higher chemical shifts in the $^{13}C\{^1H\}$ NMR spectra and therefore smaller changes in chemical shift ($\Delta\delta$) between the free and coordinated alkene (Tables 2.2 and 4.3). In the BCP complexes **28** and **30**, the chemical shifts of the double-bond carbons were 75.3 and 82.3 ppm respectively, representing $\Delta\delta$s of 35.3 and 28.3 ppm. For [Pt(BCP)(P—P)] (**1**), the chemical shifts were between 29–34 ppm, while in [Pt(BCP)(P—S)] (**8**), the two double-bond carbons had shifts at 25.2 and 28.1 ppm, with an average $\Delta\delta$ of 81 ppm. For the Pt(II) MCP complexes **29** and **31**, the cyclopropyl double-bond chemical shifts (91.6 and 97.34 ppm) were ∼30 ppm higher than the methylene double-bond carbons (59.8 and 67.5 ppm), twice the ∼15 ppm difference in [Pt(MCP)(P—P)] (**2**). The ^{c}Pr carbons also had a lower $\Delta\delta$ (39.5 and 33.7 ppm) than the methylene carbons (43.7 and 36.0 ppm). Again, the same resonances in the Pt(0) MCP complexes **2** and [Pt(MCP)(P—S)] (**9**) appeared at significantly lower shifts, 33–43 ppm for the ^{c}Pr double-bond carbon and 22–28 ppm for the methylene carbon (due to the low intensity of the signal, the NMR data for the ^{c}Pr carbon in **9** could not be obtained). The average $\Delta\delta$ was therefore 93 ppm for the ^{c}Pr carbon and 78 ppm for the methylene carbon.

The magnitude of $\Delta\delta$ gives a good estimate of the electron density around the alkene carbons, with a larger upfield shift of the resonance upon coordination (larger $\Delta\delta$) indicative of a greater electron density.[140,149–151] A larger $\Delta\delta$ also indicates that there is a larger degree of π back-bonding. Between the Pt(0) and Pt(II) complexes, there was a ∼50 ppm difference in $\Delta\delta$ for the ^{c}Pr double-bond carbons and a ∼44 ppm difference for the methylene double-bond carbons. This was consistent with there being a higher metal electron density to be shared through back-donation in d^{10} Pt(0) complexes than in d^8 Pt(II) complexes.

There was a similar lowering of the magnitude of the $^1J_{Pt–C}$ coupling constants in the Pt(II) complexes compared the the Pt(0) complexes. In the BCP complexes **28** and **30**, $^1J_{Pt–C}$ of the ^{c}Pr double-bond carbons were 248.5 and 251.8 Hz respectively. In **1**,

Table 4.3. Selected NMR Data of [$PtCl_2$(η^2-alkene)(L)].[a]

Compound		^{c}Pr		=CH_2			=CR_2	
		δ_H	δ_C	δ_H	δ_C	$^1J_{Pt-C}$	δ_C	$^1J_{Pt-C}$
trans–[$PtCl_2$(BCP)(Py)]	**28**	1.58	10.6				75.3	248.5
		1.12						
cis–[$PtCl_2$(BCP)(DMSO)]	**30**	1.25	12.5				82.3	251.8
		0.85	11.5					
trans–[$PtCl_2$(MCP)(Py)]	**29**	1.62	10.2	5.02	59.8		91.6	
		1.32						
cis–[$PtCl_2$(MCP)(DMSO)]	**31**	1.88	12.6	4.81	67.5	141.0	97.3	277.5
		1.55		4.64				
		1.38						
		1.28						

[a] δ values are given in ppm and J values in Hz. All spectra were measured in $CDCl_3$ at room temperature with 40 mg/mL sample.

$^1J_{Pt-C}$ was 410–456 Hz, ~200 Hz larger, while in **8** $^1J_{Pt-C}$ was even higher (579.0 and 656.6 Hz), a difference of as much as 400 Hz. For the ^{c}Pr double-bond carbon in the MCP complex **31**, $^1J_{Pt-C}$ was slightly higher than in the BCP complexes, 277.5 Hz, an average of ~220 Hz lower than **2**. Due to the broadness of the spectra of **29**, no coupling data could be obtained. The $^1J_{Pt-C}$ of the methylene carbon in **31** was also lower than those of **2** at 141.0 Hz, a difference of ~27 Hz, a smaller difference than for the ^{c}Pr carbons.

4.4 β-Chloroalkyl Complexes

The polymerisation of halogenated monomers such as vinyl chloride typically occurs through a radical mechanism.[160–163] However, this method is problematic as it can lead to a range of "defect sites", which decrease the thermal stability of the resulting polymer. An alternative pathway involves insertion of the alkene monomer into a metal alkyl bond, forming a halogenated alkyl ligand. Chain propagation would then occur with the coordination of another monomer molecule, followed by another insertion step. It is thought that this mechanism would lead to a polymer that contains fewer defects, as well as allowing greater control over polymer structure by using tailored catalysts.[160,162]

When vinyl chloride was reacted with a variety of both early- and late-transition metal catalysts, it was found that the insertion step was followed by a rapid β-chloride elimination to form a M–Cl bond.[160–163] There are two possible modes of insertion of vinyl chloride into a M–R bond (Scheme 4.7). For 2,1-insertion, the R group attaches to the methylene carbon, leading to an α-chloroalkyl ligand. For 1,2-insertion, the R group attaches to the same carbon as the Cl, and a β-chloroalkyl ligand is produced. While the 2,1-insertion is favoured theoretically, this product was never observed. Either the 1,2-insertion product was the only one that formed, or the 2,1-product underwent a facile isomerisation to form the 1,2-product.[162,164,165] A very fast β-chloride elimination reaction then occurred. The elimination proceeded more rapidly than the coordination of a second monomer, preventing the propagation of the polymer chain. Complexes of the early transition metals are more prone to β-halogen elimination than those of the late transition metals due to the relative strengths of the M–X and M–C bonds.[160,162] Calculations on a palladium phosphine species also showed that β-halide elimination is both thermodynamically and kinetically more favourable than β-hydride elimination.[166]

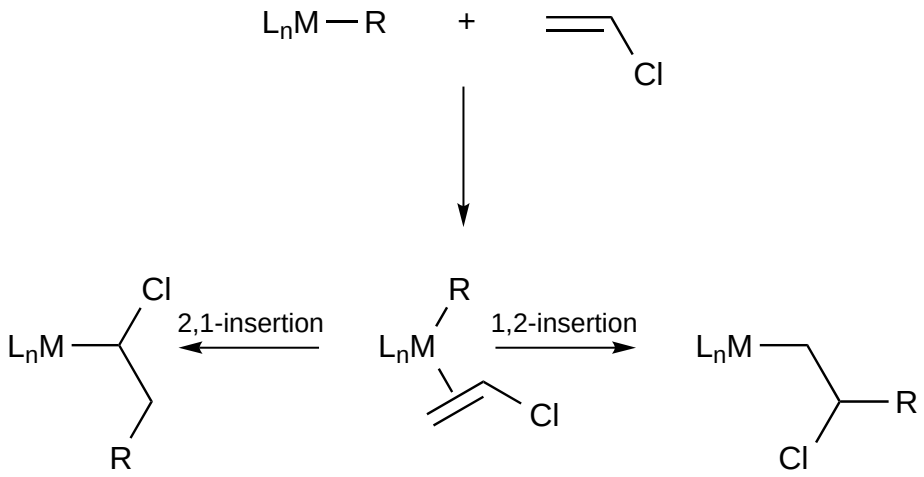

Scheme 4.7. Vinyl chloride insertion into M–R.

Due to the facile nature of β-halide elimination, only a handful of complexes that contain β-haloalkyl ligands have been synthesised.[167] The majority were platinum(IV) complexes, $[PtCl_5(CH_2CH_2Cl)]^{2-}$[168] and a range of complexes of the formula $[PtX_3(CH_2CHRX)(2,9\text{-}Me_2\text{-phen})]$ (X = Cl, Br, 2,9-Me_2-phen = 2,9-dimethyl-1,10-

phenanthroline).[169] An iridium complex, $[IrBr_2(CH_2CH_2Br)(CO)(PMe_2Ph)_2]$,[170] has also been synthesised, as well as complexes with ligands that contain multiple halogens,[171] particularly perfluorinated ligands.[172–177] Except for the perfluorinated complexes, these β-haloalkyl complexes were synthesised by the addition of X_2 to an alkene complex.

4.4.1 Synthesis From Dichloro Complexes

It was found that when bicyclopropylidene was reacted with a range of platinum precursors that contained chloride ligands, BCP inserted into the Pt–Cl bond to form complexes with stable β-chloroalkyl ligands. The reactions with $[PtCl_2(SEt_2)_2]$ (a mixture of isomers),[178] *trans*–$[PtCl_2(NC^tBu)_2]$ and *trans*–$[PtCl_2(Py)_2]$ yielded the complexes *trans*–$[Pt(C(CH_2)_2C(CH_2)_2Cl)Cl(L)_2]$ (L = SEt_2 (**32**), NC^tBu (**33**), Py (**34a**)) respectively (Scheme 4.8). The formation of **32** takes up to 5 days with an excess of BCP, while the formation of **33** takes 2 days with 1 eq. BCP. The formation of **34a** occurred over 2 days. However, the reaction did not go to completion, with **34a** making up 30% of the species in solution by ^{1}H NMR spectroscopy, and a large amount of undissolved solid remaining. After two weeks, a second new complex formed from the *trans*–$[PtCl_2(Py)_2]$ in a 1:3 ratio relative to **34a**. This complex could not be characterised.

When *cis*–$[PtCl_2(NC^tBu)_2]$ and *cis*–$[PtCl_2(Py)_2]$ were used, no reaction occurred. Given this, it is likely that only the *trans* form of $[PtCl_2(SEt_2)_2]$ undergoes a reaction with BCP. The *cis* and *trans* forms of $[PtCl_2(SEt_2)_2]$ can interconvert in the presence of SEt_2, forming an equilibrium mixture.[179] The need for the interconversion of the isomers could explain the long reaction time with BCP.

When two equivalents of BCP (one per Pt) was reacted with Zeise's dimer ($[Pt_2Cl_4(C_2H_4)_2]$) and two equivalents pyridine (one per Pt), initially an η^2-alkene complex, *trans*–$[PtCl_2(BCP)(Py)]$ (**28**) was formed (Section 4.3). This complex was unstable, and decomposed after an hour. When a second equivalent of Py was added after the formation of **28**, the alkene complex reacted immediately formed the β-chloroalkyl complex *cis*–$[Pt(C(CH_2)_2C(CH_2)_2Cl)Cl(Py)_2]$ (**34b**). Complex **34b** could also be synthesised directly by the addition of two equivalents of BCP (one per Pt) and

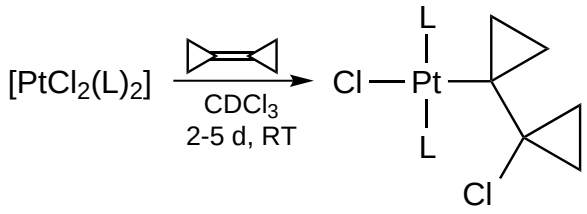

L = SEt_2 **32**
= NC^tBu_2 **33**
= Py **34a**

Scheme 4.8. Synthesis of *trans*–[$Pt(C(CH_2)_2C(CH_2)_2Cl)Cl(L)_2$] from [$PtCl_2(L)_2$] (**32**–**34a**).

four equivalents of Py (two per Pt) to Zeise's dimer. This reaction occurred immediately upon the mixing of the reagents (Scheme 4.9).

Comparable reactivity was observed with MCP. Again, when only two equivalents of Py was used a η^2-alkene complex formed, *trans*–[$PtCl_2$(MCP)(Py)] (**29**). When a further two equivalents of Py (one per Pt) was added, *cis*–[$Pt(C(CH_2)_2CH_2Cl)Cl(Py)_2$] (**34c**) was formed (Scheme 4.10). The corresponding reaction of [$Pt_2Cl_4(C_2H_4)_2$] with two equivalents of MCP (one per Pt) and four equivalents of Py (two per Pt) also produced **34c**). The analogous reactions of MCP with [$PtCl_2(SEt_2)_2$], *cis*– and *trans*–[$PtCl_2(NC^tBu)_2$] and *cis*– and *trans*–[$PtCl_2(Py)_2$] did not occur.

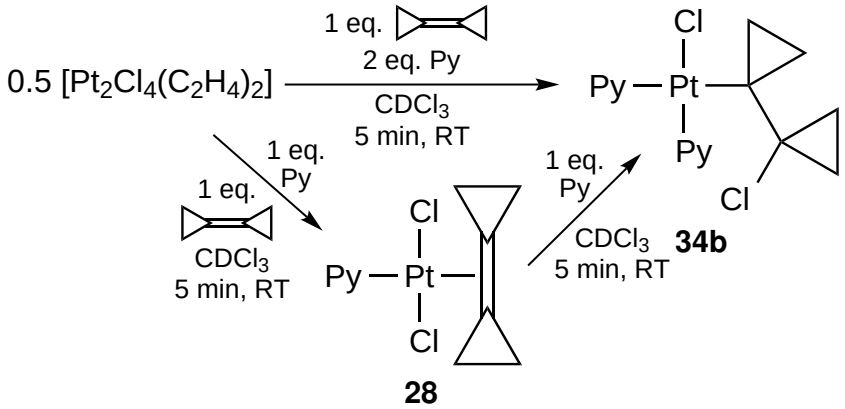

Scheme 4.9. Synthesis of *cis*–[$Pt(C(CH_2)_2C(CH_2)_2Cl)Cl(Py)_2$] (**34b**) from [$Pt_2Cl_4(C_2H_4)_2$].

The ethene complex [$PtCl_2(C_2H_4)$(Py)] in the presence of pyridine is in equilibrium with the 5-coordinate complex [$PtCl_2(C_2H_4)(Py)_2$].[180] The availability of the 5-coordinate

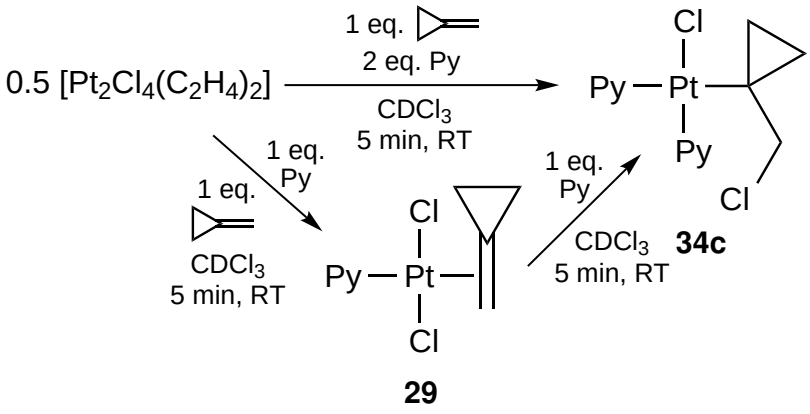

Scheme 4.10. Synthesis of *cis*–[Pt(C$(CH_2)_2CH_2$Cl)Cl$(Py)_2$] from [$Pt_2Cl_4(C_2H_4)_2$] (**34c**).

complex suggests that the mechanism for the formation of the β-chloroalkyl complexes would be associative, rather than dissociative. Initially, BCP or MCP would coordinate to form an intermediate η^2-alkene complex (as with **28** and **29**). This would be followed by the addition of the second equivalent of pyridine and insertion of the alkene into the Pt–Cl bond. The *cis*-pyridine complexes formed the most rapidly of the β-chloroalkyl complexes (by several days), and had isolatable alkene complex intermediates, **28** and **29**, which were able to be converted to **34b** and **34c** by the addition of pyridine, supporting this mechanism.

4.4.2 Synthesis of Phosphine Complexes

The synthesis of a phosphine complex containing a β-chloroalkyl ligand was considered desirable due to the inclusion of another NMR-active nuclei, increasing the amount of characterisation data available. However, no reaction occurred when either BCP or MCP was combined with [$PtCl_2(PR_3)_2$] complexes. Instead, phosphine complexes were synthesised by the addition of the phosphine to a complex with a β-chloroalkyl ligand already installed.

The thioether complex *trans*–[Pt(C$(CH_2)_2$C$(CH_2)_2$Cl)Cl$(SEt_2)_2$] (**32**) was treated with a number of phosphines, both mono- and bi-dentate. When triphenylphosphine was used, the SEt_2 was successfully displaced by the PPh_3. However, a β-chloride elimination occurred, forming *cis*–[$PtCl_2(PPh_3)_2$] as well as free BCP. The chelating phosphines

1,3-bis(diphenylphosphino)propane (dppp) and 1,2-bis(diphenylphosphino)ethane (dppe) were also used. In these reactions, there was again a β-chloride elimination, producing the Pt(II) bis-diphosphine complexes $[Pt(P—P)_2]Cl_2$ (P—P = dppp (**35a**), dppe (**35b**)) and free BCP. The phosphine-chloride complexes were identified by ^{31}P NMR data.[181,182]

Single crystals of **35a** were grown by layering a frozen solution of **32** in $CDCl_3$ with a solution of dppp in $CDCl_3$ and allowing to warm to room temperature, and an X-ray crystal structure obtained (Figure 4.1, Table 4.4).[183] The asymmetric unit contained only half of the molecule, consisting of a complete dppp ligand as well as one of the chloride counter ions and three of the six $CDCl_3$ solvent molecules. The platinum coordination geometry was close to square planar, with a P1–Pt–P2 angle of 87.23(3)°. This is smaller than the corresponding angle in the quasi-tetrahedral Pt(0) complex $[Pt^0(dppp)_2]$ (97.76(4)°).[90] The Pt–P bond lengths in **35a** were 2.3647(8) and 2.3790(8) Å, longer than those in $[Pt^0(dppp)_2]$ (2.286(1) Å). The chelate ring had a 'chair' conformation, typical for dppp complexes. In **35a**, the two chelate rings were rotated by 180° relative to each other, while in $[Pt^0(dppp)_2]$ the rings were rotated by 87.20(2)°, according to the P1–Pt–P2 planes. While **35a** crystallised as a $CDCl_3$ solvate in the orthorhombic *Pccn* space group, $[Pt^0(dppp)_2]$ crystallised solvent-free in the monoclinic $C2/c$ space group. The Cl^- counter ion was separated by 4.197 Å from the Pt, indicating that it was not coordinated. The $[Pt^{II}(dppp)_2]^{2+}$ ions were arranged in 2D layers, with the Cl^- anions and solvent between the layers (Figure 4.2).

When 1,3,5-triaza-7-phosphaadamantane (PTA) was added to **32**, the SEt_2 ligands were again successfully displaced by the phosphine. As with the other phosphines, *cis*–$[PtCl_2(PTA)_2]$ and free BCP were formed.[184] However, in this case a short-lived (approx. 1 hr) complex formed inititally. This complex is believed to be *trans*–$[Pt(C(CH_2)_2C(CH_2)_2Cl)Cl(PTA)_2]$ (**36a**) (Scheme 4.11). The reaction of PTA with *trans*–$[Pt(C(CH_2)_2C(CH_2)_2Cl)Cl(NC^tBu)_2]$ (**33**) also resulted in the formation of **36a** and subsequently *cis*–$[PtCl_2(PTA)_2]$.

The synthesis of *cis*–phosphine complexes proved to be more successful than *trans*–phosphine complexes. When *cis*–$[Pt(C(CH_2)_2C(CH_2)_2Cl)Cl(Py)_2]$ (**34b**) was treated

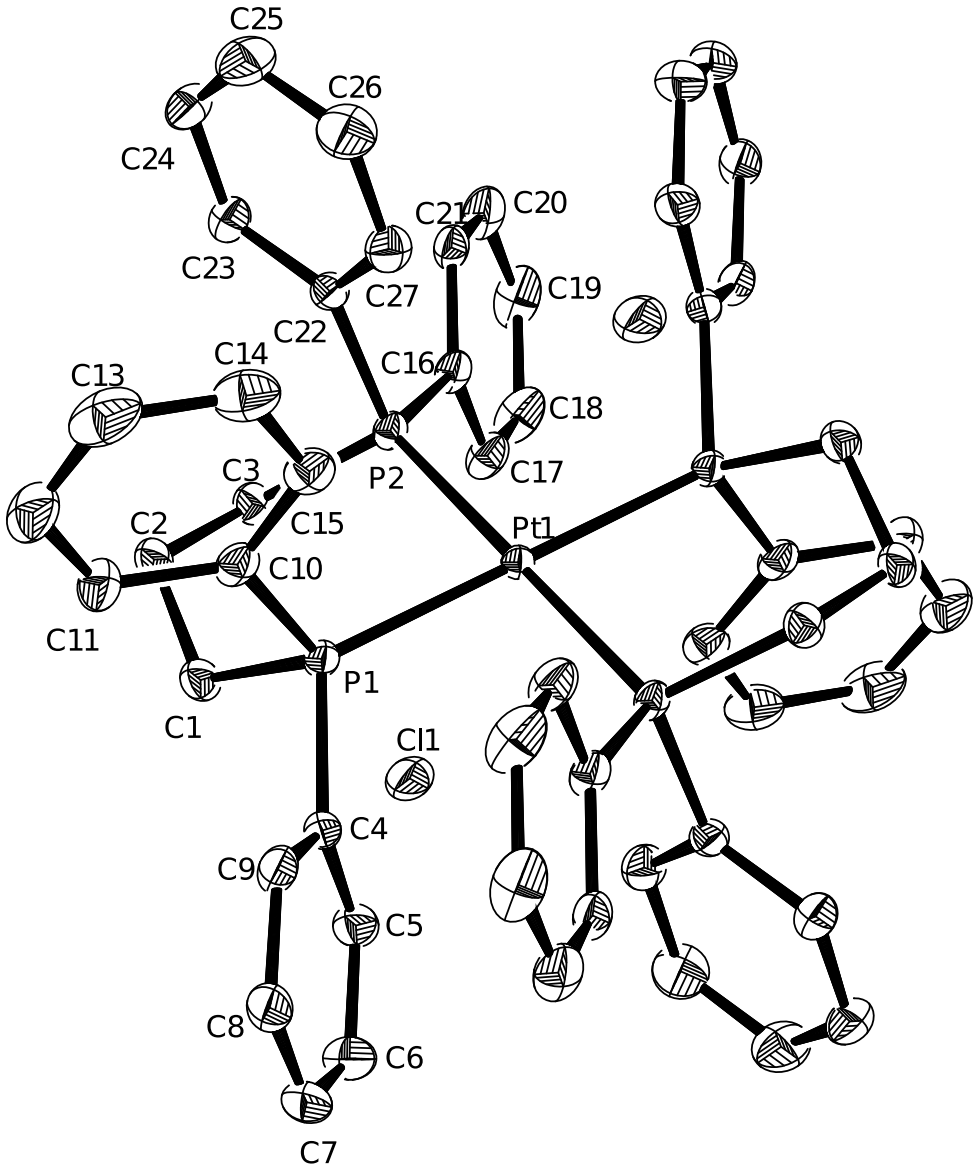

Figure 4.1. ORTEP diagram of $[Pt(dppp)_2]Cl_2 \cdot 6\,CDCl_3$ (**35a**) showing 50% probability thermal ellipsoids. H atoms and $CDCl_3$ solvent molecules have been omitted for clarity.

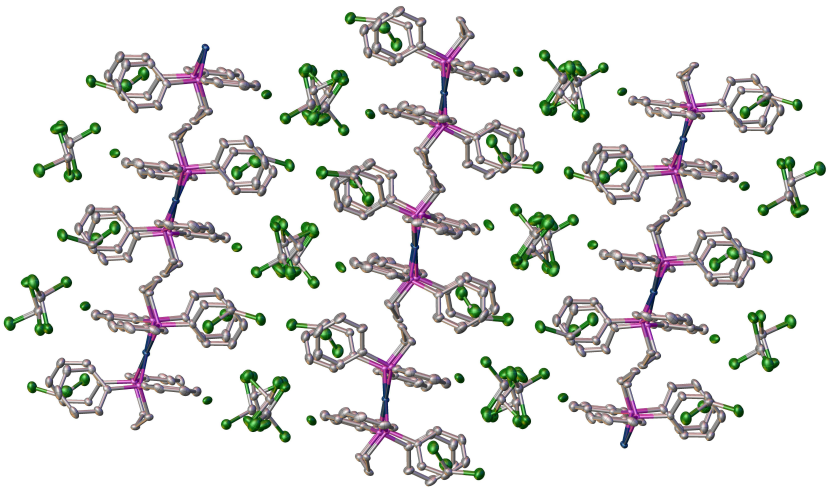

Figure 4.2. Layered packing of $[Pt(dppp)_2]Cl_2 \cdot 6\,CDCl_3$ (**35a**).

Table 4.4. Crystallographic Data for $[Pt(dppp)_2]Cl_2 \cdot 6\,CDCl_3$ (**35a**).

Chemical formula	$C_{60}H_{58}Cl_{20}P_4Pt$
Formula weight	1687.77
a, Å	26.2042(9)
b, Å	15.3120(5)
c, Å	16.7930(5)
α, deg	90.00
β, deg	90.00
γ, deg	90.00
V, Å^3	6738.0(4)
Z	4
Space group	*Pccn*
T, K	160
λ, Å	0.71073
D_{calcd}, g cm^{-3}	1.664
μ, mm^{-1}	2.890
R_1, [I$> 2\sigma$(I)][a]	0.0373
wR_2 (all data)[a]	0.0745

[a] Definition of R indices: $R_1 = \Sigma||F_o|-|F_c||/\Sigma|F_o|$; $wR_2 = [\Sigma w(F_o^2-F_c^2)^2/\Sigma w(F_o^2)^2]^{1/2}$.

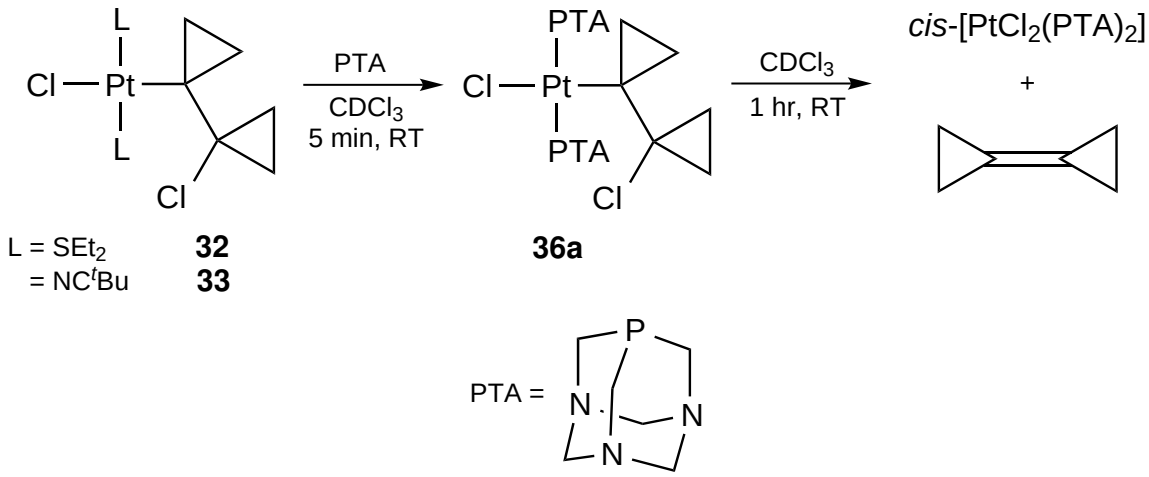

Scheme 4.11. Synthesis of *trans*–[Pt(C(CH$_2$)$_2$C(CH$_2$)$_2$Cl)Cl(PTA)$_2$] (**36a**) from *trans*–[Pt(C(CH$_2$)$_2$C(CH$_2$)$_2$Cl)Cl(L)$_2$] (**32** and **33**).

with either PTA, dppp or PPh$_3$, the products were β-chloroalkyl complexes *cis*–[Pt(C(CH$_2$)$_2$C(CH$_2$)$_2$Cl)Cl(P)$_2$] ((P)$_2$ = (PTA)$_2$ (**36b**), dppp (**37a**), (PPh$_3$)$_2$ (**38a**)) which were stable in solution over several weeks (Scheme 4.12). The reactions also generated a small amount of *cis*–[PtCl$_2$(P)$_2$]. The amount of *cis*–[PtCl$_2$(PTA)$_2$] produced was significantly greater than for the other phosphines. As *cis*–[PtCl$_2$(PTA)$_2$] was only partially soluble, the exact amount was not calculated, while there was 30% *cis*–[PtCl$_2$(PPh$_3$)$_2$] and 11% *cis*–[PtCl$_2$(dppp)$_2$].

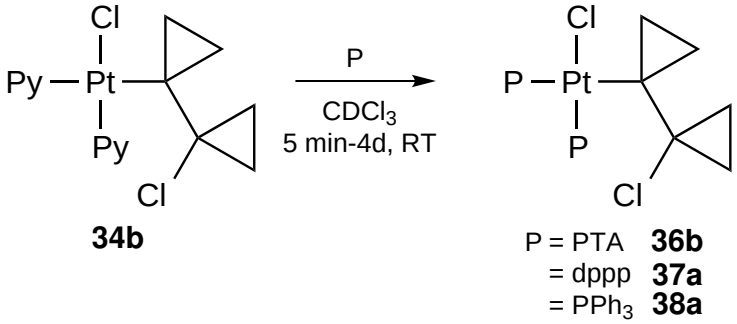

Scheme 4.12. Synthesis of *cis*–[Pt(C(CH$_2$)$_2$C(CH$_2$)$_2$Cl)Cl(P)$_2$] from *cis*–[Pt(C(CH$_2$)$_2$C(CH$_2$)$_2$Cl)Cl(Py)$_2$] (**34b**).

In the reaction of **34a** with PPh$_3$, a complex with only one phosphine ligand was formed initially (**38b**). The ^{31}P{^{1}H} and ^{13}C{^{1}H} NMR data (see below) indicated that it was the pyridine *trans* to the chloride that was displaced. The bis(phosphine) complex

38a began to form after an hour. The reaction did not reach completion; after 4 days there was 53% **38a**, 8.5% monophosphine complex, 8.5% PPh_3 and 30% *cis*–$[PtCl_2(PPh_3)_2]$, with the ratios remaining stable over several weeks. With dppp, **37a** formed initially, reaching 85% with 11% $[PtCl_2(dppp)]$ after 2 days.

The addition of phosphines to the β-chloroalkyl complex formed from MCP (*cis*–$[Pt(C(CH_2)_2CH_2Cl)Cl(Py)_2]$, **34c**) also resulted in the formation of phosphine complexes *cis*–$[Pt(C(CH_2)_2CH_2Cl)Cl(P)_2]$ ($(P)_2$ = $(PTA)_2$ (**36c**), dppp (**37b**)), as well as *cis*–$[PtCl_2(P)_2]$ (Scheme 4.13). These complexes were all unstable, decomposing into the dichloride complexes over 1 (dppp) to 5 (PTA) days. Again, due to the insolubility of *cis*–$[PtCl_2(PTA)_2]$, the exact amount formed was not calculated, with **36c** comprising approximately 50% of the species in solution after 24 hrs. With dppp, the solution contained 58% **37b**, 26% *cis*–$[PtCl_2(dppp)]$ and 16% $[Pt(dppp)_2]Cl_2$ after 10 min. There was no bisphosphine β-chloroalkyl complex formed in the reaction with PPh_3. Instead, the monophosphine complex with the phosphine *cis* to the β-chloroalkyl ligand (**38c**) was formed, decomposing to form *cis*–$[PtCl_2(PPh_3)_2]$ over 4 hours (Scheme 4.14).

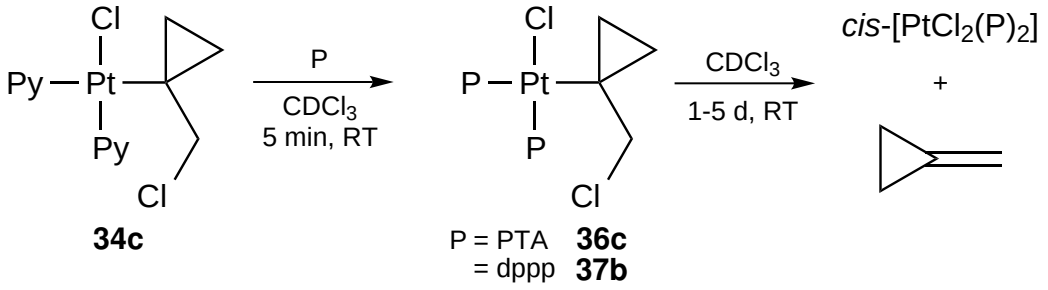

Scheme 4.13. Synthesis of *cis*–$[Pt(C(CH_2)_2CH_2Cl)Cl(P)_2]$ from *cis*–$[Pt(C(CH_2)_2CH_2Cl)Cl(Py)_2]$ (**34b**).

It appeared that the stability of the β-chloroalkyl complexes was dependent on the cone angle, θ, of the phosphine ligand. Complexes of the smallest phosphine, PTA (θ = 115°)[185] were the most stable. The *trans* complex **36a** was the only β-chloroalkyl complex with *trans* phosphines to be formed. For the complexes formed from MCP, the PTA complex **36c** was stable for several days longer than the dppp complex **37b** (θ = 127°),[82] while no bisphosphine complex was observed with PPh_3 (θ = 145°).[82]

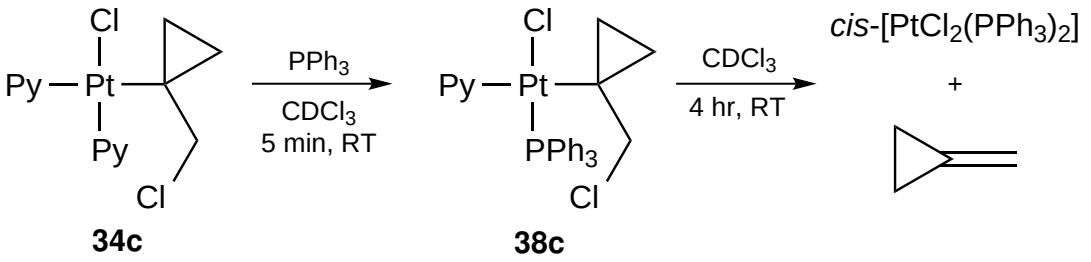

Scheme 4.14. Synthesis of $[Pt(C(CH_2)_2CH_2Cl)Cl(Py)(PPh_3)]$ (**38c**) from *cis*–$[Pt(C(CH_2)_2CH_2Cl)Cl(Py)_2]$ (**34b**).

4.4.3 NMR Characterisation

For representative NMR spectra, see Figures A.83–A.105. The various NMR spectra of the β-chloroalkyl complexes were distinctive. The $^{31}P\{^1H\}$ NMR spectra of **36b**–**38b** showed two doublets with $^2J_{P–P}$ couplings in the range of 14.9–25.9 Hz, typical for *cis* couplings. The peak due to the phosphorus *trans* to the β-chloroalkyl ligand had a low $^1J_{Pt–P}$ coupling constant of 1522–1684 Hz, with those of the complexes from MCP having values larger by ∼30 Hz. This low value was consistent with being *trans* to a σ-bound ^{c}Pr ring.[93,139] The $^1J_{Pt–P}$ coupling constant of the other peak was very large, 3884–4490 Hz, significantly larger than the $^1J_{Pt–P}$ of the phosphines *trans* to Cl in *cis*–$[PtCl_2(P)_2]$ (3350–3674 Hz).[181,184] This difference can be ascribed to the difference in *cis*-influence between Cl and ^{c}Pr. While the *cis*-influence has not been reported for ^{c}Pr, it was found that a *cis*-influence series was approximately the reverse of the corresponding *trans*-influence series.[186] The $^1J_{Pt–P}$ coupling constant for the phosphines *cis* to Cl in $[PtX(PPh_3)_3]$ was 444 Hz smaller than that of Me, which has a lower *trans*-influence than ^{c}Pr.[139] It would therefore be expected that $^1J_{Pt–P}$ would be significantly higher in *cis*–$[Pt(C(CH_2)_2C(CH_2)_2Cl)Cl(P)_2]$ and *cis*–$[Pt(C(CH_2)_2CH_2Cl)Cl(P)_2]$ than in *cis*–$[PtCl_2(P)_2]$.

For the mono-phosphine complexes $[Pt(C(CH_2)_2C(CH_2)_2Cl)Cl(Py)(PPh_3)]$ and $[Pt(C(CH_2)_2CH_2Cl)Cl(Py)(PPh_3)]$, $^1J_{Pt–P}$ were 4735 and 4661 Hz, respectively. As these values were more similar to those *trans* to the chloride than those *trans* to the β-chloroalkyl ligands in **36**–**38**, it was therefore the pyridine *trans* to the Cl that was displaced by the phosphine.

Table 4.5. Selected NMR Data of $[Pt(C(CH_2)_2CR_2Cl)Cl(L)_2]$.[a]

Compound		Pt ^{c}Pr			Cl ^{c}Pr		Pt−C		Cl−C	δ_P	$^1J_{Pt-P}$
		δ_H		δ_C	δ_H	δ_C	δ_C	$^1J_{Pt-C}$	δ_C		
trans–$[Pt(C(CH_2)_2C(CH_2)_2Cl)Cl(SEt_2)_2]$	**32**	0.36 (29.4)	*exo*	16.4	0.83	14.3	−0.4	1011	57.1		
		0.21 (63.0)	*endo*		0.77						
trans–$[Pt(C(CH_2)_2C(CH_2)_2Cl)Cl(NC^tBu)_2]$	**33**	0.30		14.7	1.03	15.8	0.0	953	55.2		
					0.73						
trans–$[Pt(C(CH_2)_2C(CH_2)_2Cl)Cl(Py)_2]$	**34a**	−0.03 (37.9)	*exo*	13.1	0.41	12.9	1.1	1202	56.2		
		−0.15 (50.8)	*endo*		−0.25						
cis–$[Pt(C(CH_2)_2C(CH_2)_2Cl)Cl(Py)_2]$	**34b**	0.50	*endo*	15.0	1.34	11.0	−11.1	970	65.9		
		0.36	*exo*		1.05						
cis–$[Pt(C(CH_2)_2CH_2Cl)Cl(Py)_2]$ [b]	**34c**	0.52 (29.6)	*endo*	14.3			−15.6	[c]	76.8		
		0.32 (19.6)	*exo*								
trans–$[Pt(C(CH_2)_2C(CH_2)_2Cl)Cl(PTA)_2]$	**36a**	0.44		[c]	1.03	[c]	[c]	[c]	[c]	−59.2	3000
		0.27			0.76						
cis–$[Pt(C(CH_2)_2C(CH_2)_2Cl)Cl(PTA)_2]$	**36b**	0.92		13.4	1.69	16.7	15.5 [121.8, 8.6]	809	64.8	−57.9 [15.6]	3949
		0.80		8.7	1.31	15.7				−65.8 [15.6]	1522
		0.49			0.92						
		0.27			0.85						
cis–$[Pt(C(CH_2)_2CH_2Cl)Cl(PTA)_2]$	**36c**	[c]		[c]			[c]		[c]	−58.9 [14.9]	3884
										−64.8 [14.9]	1530
cis–$[Pt(C(CH_2)_2C(CH_2)_2Cl)Cl(dppp)]$	**37a**	0.48		13.3	1.05	17.1	15.6 [124.5, 6.8]	789	63.6	−1.8 [25.9]	1654
		0.35		6.1	0.71	12.2				−2.7 [25.9]	4133
		0.20			0.48						
		−1.22			−0.46						
cis–$[Pt(C(CH_2)_2CH_2Cl)Cl(dppp)]$	**37b**	[c]		[c]			[c]		[c]	0.4 [25.2]	4051
										0.2 [25.2]	1684
cis–$[Pt(C(CH_2)_2C(CH_2)_2Cl)Cl(PPh_3)_2]$	**38a**	0.77		13.3	1.34	19.2	15.7 [126.7, 8.0]	798	63.3	22.7 [15.6]	4490
		0.57		8.1	0.85	15.8				16.7 [15.6]	1646
		0.41			0.69						
		−0.85			−0.14						
$[Pt(C(CH_2)_2C(CH_2)_2Cl)Cl(Py)(PPh_3)]$	**38b**	[c]		[c]	[c]	[c]	−8.7 [9.2]	940	[c]	10.8	4738
$[Pt(C(CH_2)_2C(CH_2)_2Cl)Cl(Py)(PPh_3)]$	**38c**	[c]		[c]			[c]		[c]	13.5	4661

[a] δ values are given in ppm and J values in Hz. All spectra were measured in $CDCl_3$ at room temperature with 40 mg/mL sample unless otherwise noted. Values in parentheses are ^{195}Pt couplings, values in square brackets are ^{31}P couplings. [b] Spectra collected in d_6-acetone. [c] NMR data could not be obtained.

The $^{13}C\{^1H\}$ NMR data of the β-chloroalkyl ligands in **32**–**38** was characteristic of these complexes (Table 4.5). Due to the short lifetimes, $^{13}C\{^1H\}$ NMR data could not be obtained for **36a**, **36c**, **37b**, **38b** and **38c**. The sp^3 carbons directly bound to the platinum in **32**–**38** had very large $^1J_{Pt-C}$ coupling constants ($^1J_{Pt-C}$ = 989–1202 Hz), indicative of Pt–C σ-bonds.[93,139] The magnitude of these coupling constants reflected the *trans*-influence of the *trans* ligand, with Cl and Py approximately the same while the phosphines, with higher *trans*-influences, had lower $^1J_{Pt-C}$.[93] The nature of the *trans* ligand also had a significant effect on the chemical shift of the platinum-bound carbon. When *trans* to P, the chemical shift appeared at 15 ppm. In contrast, when *trans* to Cl, the chemical shift dropped by 15 ppm to 0 ppm and by about 25 ppm to approximately −11 ppm when *trans* to Py. While the majority of the NMR data for **38b** could not be obtained due to the reactivity of this species, the use of carbon-13 enriched BCP enabled the detection of the peak due to the carbon bound to the platinum. Both the chemical shift (−8.7 ppm) and $^1J_{Pt-C}$ (940 Hz) was consistent with the β-chloroalkyl ligand being *trans* to Py rather than PPh_3, as indicated by the ^{31}P NMR data.

The carbons attached to the chlorines had resonances at δ_C = 55–66 ppm, except for **34c**, which had a resonance at 76.8 ppm. This was due to the fact that this was a methylene rather than a cyclopropyl carbon. None of these resonances showed $^2J_{Pt-C}$ couplings. The cyclopropyl methylene carbons appeared at 6–19 ppm, within the typical range for ^{c}Pr carbons.

The ^1H NMR resonances of the CH_2 protons of the ^{c}Pr ring bound to the Pt in **32**–**38** appeared at low chemical shifts, between −1.22 and 0.92 ppm. The protons of the ^{c}Pr ring bound to the Cl appeared between −0.46 and 1.34 ppm, at shifts more typical of organic cyclopropyl protons, except in **34a** and the phosphine complexes. For **34a**, all of the shifts were lower than in the other complexes, with the Cl ^{c}Pr protons appearing at 0.41 and −0.25 ppm. In the phosphine complexes, the ^{c}Pr peaks were spread over a wider range than for the other complexes, although the range of the Pt ^{c}Pr peaks was lower than the Cl ^{c}Pr peaks. Generally, the resonances appeared as four sharp peaks, each integrating for two protons, corresponding to the *exo* and *endo* environments of

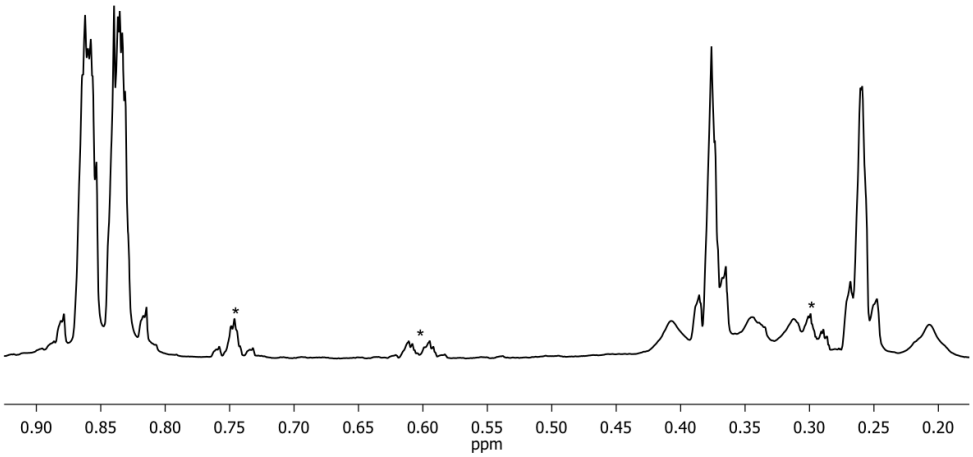

(i)

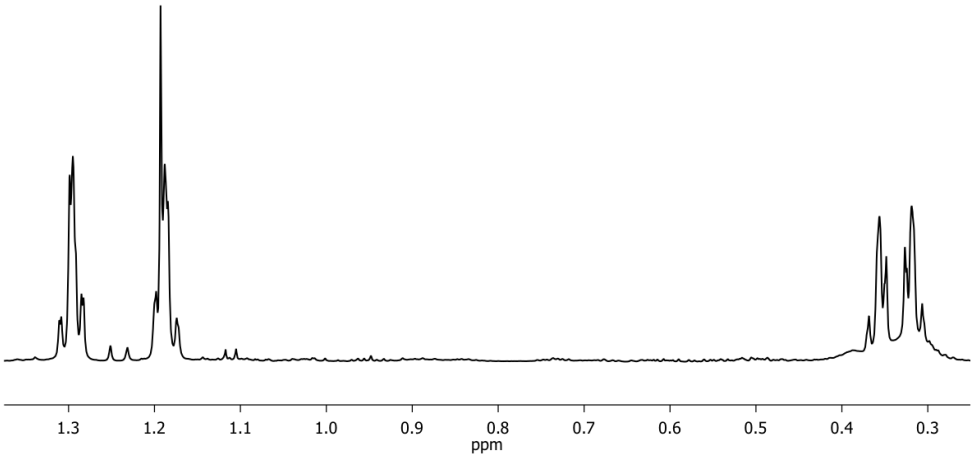

(ii)

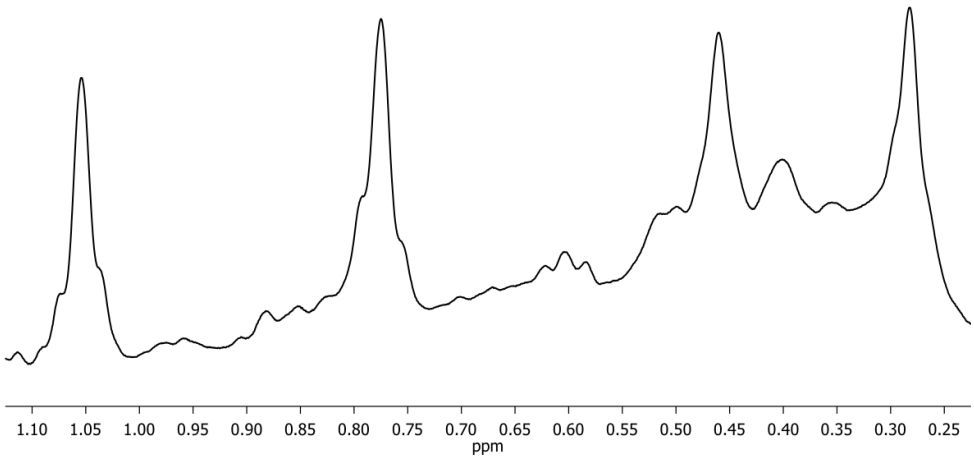

(iii)

Figure 4.3. ^{1}H NMR spectra showing the cyclopropyl peaks for (i) *trans*–[Pt(C(CH$_2$)$_2$C(CH$_2$)$_2$Cl)Cl(SEt$_2$)$_2$] (**32**) (500 MHz, RT, 100 mg/mL, CDCl$_3$), (ii) *cis*–[Pt(C(CH$_2$)$_2$C(CH$_2$)$_2$Cl)Cl(Py)$_2$] (**34a**) (500 MHz, RT, 40 mg/mL, CDCl$_3$) and (iii) *trans*–[Pt(C(CH$_2$)$_2$C(CH$_2$)$_2$Cl)Cl(PTA)$_2$] (**36a**) (300 MHz, RT, 40 mg/mL, CDCl$_3$). * signifies peaks belonging to other species.

the two rings (Figure 4.3). Again, the phosphine complexes were an exception due to the $J_{\text{P–H}}$ couplings. The peaks of the Cl ^{c}Pr ring protons did not have ^{195}Pt satellites, while Pt ^{c}Pr ring protons showed ^{195}Pt coupling, except in **33** (due to overlap of the peaks), **34b** and the phosphine complexes. The *endo* protons had higher $J_{\text{Pt–H}}$ coupling constants (50.8–63.0 Hz) than the *exo* (29.4–37.9 Hz). For **34c**, the magnitudes of $J_{\text{Pt–H}}$ were smaller (29.6 and 19.6 Hz), although the *endo* coupling was still larger than the *exo* coupling. In most cases, the *endo*/*exo* geometry of the rings was confirmed by NOESY correlations (Figure 4.4).

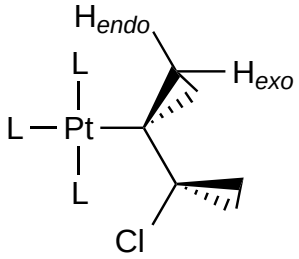

Figure 4.4. Geometry of the *endo*/*exo* protons in β-haloalkyl complexes.

The NMR data of the β-chloroalkyl complex formed from MCP (**34c**) was used to determine the mode of insertion into the Pt–Cl bond. The ^{1}H NMR data showed a singlet peak at 4.13 ppm with $J_{\text{Pt–H}} = 24.6$ Hz and two sharp peaks at 0.52 and 0.32 ppm, with a similar lineshape to the ^{c}Pr CH_2 resonances in the complexes from BCP. The cyclopropyl methylene peaks had $J_{\text{Pt–H}}$ couplings, which were only present in the cyclopropyl ring attached to the metal in the other complexes. The low shifts of the cyclopropyl peaks also indicated that the ^{c}Pr ring was attached to the metal, rather than the methylene. This was supported by the ^{13}C NMR data. There was a peak at -15.6 ppm, with the high field shift indicating that this was the carbon attached to the platinum, although no $^{1}J_{\text{Pt–C}}$ coupling could be found even after running a 20 hr ^{13}C experiment on the 600 MHz NMR instrument due to the low solubility of **34c**. The corresponding resonance in **34b** appeared at -11.09 ppm. There was also a resonance at 76.8 ppm which had an HSQC correlation to the peak in the ^{1}H NMR spectrum at 4.13 ppm due to the carbon attached to the chlorine. The carbon peak was at significantly lower field than that in **34b**, which appeared at 65.9 ppm. Typically, sp^3-cyclopropyl peaks appear at higher field

than sp^3-methylene peaks, indicating that this peak was due to the methylene, and that the cyclopropyl ring was therefore attached to the metal. This was further supported by the ^{31}P NMR spectra of **36c** and **37b**, formed by addition of the phosphines to **34c**. When *trans* to the ^{c}Pr ring in the complexes formed from BCP, the $^1J_{\text{Pt–P}}$ coupling constant was 1522–1654 Hz. In the complexes formed from MCP, $^1J_{\text{Pt–P}}$ was very similar, 1530–1680 Hz. Greater differences would be expected if the methylene was attached to the metal.

Due to the short lifetime of **36a**, ^{13}C NMR data could not be obtained, even when carbon-13 enriched BCP was used. The ^{1}H NMR spectrum showed the same characteristic sharp peaks as the other β-chloroalkyl complexes (Figure 4.3). The chemical shifts were in good agreement with those of **32**–**34c**, with peaks at 0.27, 0.44, 0.76 and 1.03 ppm (Table 4.5). By analogy, the peaks at 0.27 and 0.44 ppm would correspond to those of the ^{c}Pr ring attached to the Pt, while those at 0.76 and 1.03 ppm would correspond to those of the ^{c}Pr ring attached to the Cl. In the ^{31}P NMR spectrum, there was a singlet peak with a $^1J_{\text{Pt–P}}$ coupling constant of 3000 Hz. This indicated that the geometry of the complex was *trans*, as the *cis* complexes had two phosphine environments. The coupling constant was in the range expected for two *trans* phosphines.[181] It was much smaller than the $^1J_{\text{Pt–P}}$ of phosphines *trans* to Cl in *cis* complexes, typically ∼3500 Hz, and 3350 Hz for *cis*–$[PtCl_2(PTA)_2]$ specifically.[181,184]

4.4.4 Computational Studies

Computational models were used in order to determine what structural factors led to the formation of a stable β-chloroalkyl complex. All structures were optimised and frequencies calculated using density functional theory calculations (B3LYP),[154–157] optimised using the def2-TZVP basis set,[158] of triple ζ quality. Complexes with β-chloroalkyl ligands formed from bicyclopropylidene were determined to be stable experimentally, and a number of these were formed (Section 4.4). Complexes were also formed experimentally from methylenecyclopropane, with the cyclopropyl ring directly bound to the metal. These were unstable, decomposing *via* a β-chloride elimination.

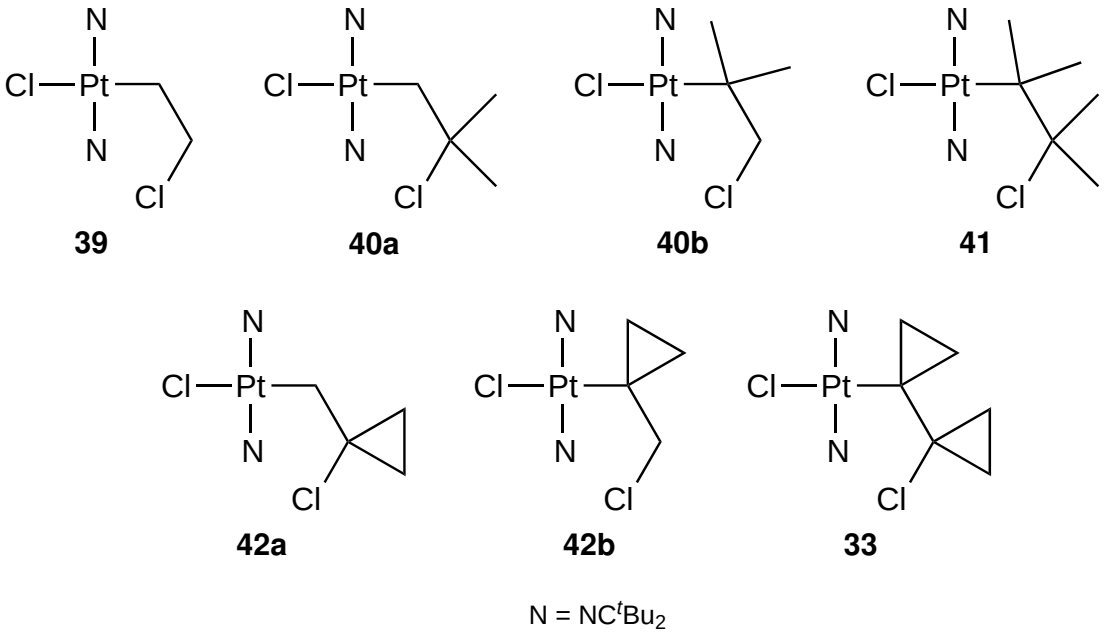

Figure 4.5. Structures of β-chloroalkyl complexes.

There were two potential structural factors that could contribute to the unusual stability of the cyclopropyl β-chloroalkyl complexes. These were the degree of substitution (BCP is tetrasubstituted), and the presence of ^{c}Pr rings. A number of β-chloroalkyl complexes with varying substituents were optimised. These were *trans*–[Pt(CH_2CH_2Cl)Cl($NC^tBu)_2$] (**39**), which had no carbon containing substituents on the β-chloroalkyl ligand, *trans*–[Pt(CH_2CMe_2Cl)Cl($NC^tBu)_2$] (**40a**), disubstituted with methyl groups on the β-carbon, *trans*–[Pt(CMe_2CH_2Cl)Cl($NC^tBu)_2$] (**40b**), disubstituted with methyl groups on the α-carbon, *trans*–[Pt(CMe_2CMe_2Cl)Cl($NC^tBu)_2$] (**41**), tetrasubstituted with methyl groups, *trans*–[Pt($CH_2C(CH_2)_2Cl$)Cl($NC^tBu)_2$] (**42a**), substituted with a ^{c}Pr ring on the β-carbon, *trans*–[Pt($C(CH_2)_2CH_2Cl$)Cl($NC^tBu)_2$] (**42b**), substituted with a ^{c}Pr ring on the α-carbon, and *trans*–[Pt($C(CH_2)_2C(CH_2)_2Cl$)Cl($NC^tBu)_2$] (**33**), substituted with two ^{c}Pr rings (Figure 4.5). Structures were also optimised for the respective *cis*– and *trans*–[$PtCl_2$(L)(NC^tBu)] alkene complexes (L = C_2H_4 (**43**), CH_2CMe_2 (**44**), C_2Me_4 (**45**), MCP (**46**), BCP (**47**), *trans* = **a**, *cis* = **b**), the free alkenes, NC^tBu and *trans*–[$PtCl_2(NC^tBu)_2$].

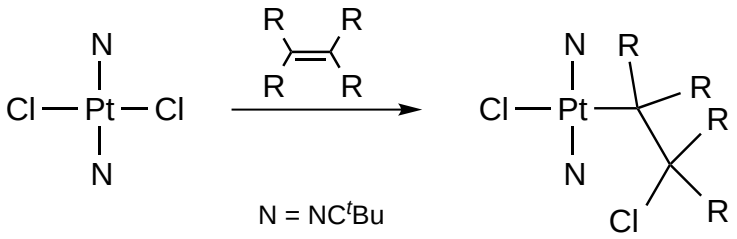

Scheme 4.15. Formation of β-chloroalkyl complexes from *trans*–[$PtCl_2(NC^tBu)_2$].

Table 4.6. Reaction ΔH for the Formation of β-Chloroalkyl Complexes.

Compound		ΔH (kJ mol^{-1})
trans–[$Pt(CH_2CH_2Cl)Cl(NC^tBu)_2$]	**39**	85.1
trans–[$Pt(CH_2CMe_2Cl)Cl(NC^tBu)_2$]	**40a**	111.8
trans–[$Pt(CMe_2CH_2Cl)Cl(NC^tBu)_2$]	**40b**	138.1
trans–[$Pt(CMe_2CMe_2Cl)Cl(NC^tBu)_2$]	**41**	165.4
trans–[$Pt(CH_2C(CH_2)_2Cl)Cl(NC^tBu)_2$]	**42a**	68.3
trans–[$Pt(C(CH_2)_2CH_2Cl)Cl(NC^tBu)_2$]	**42b**	67.0
trans–[$Pt(C(CH_2)_2C(CH_2)_2Cl)Cl(NC^tBu)_2$]	**33**	51.5

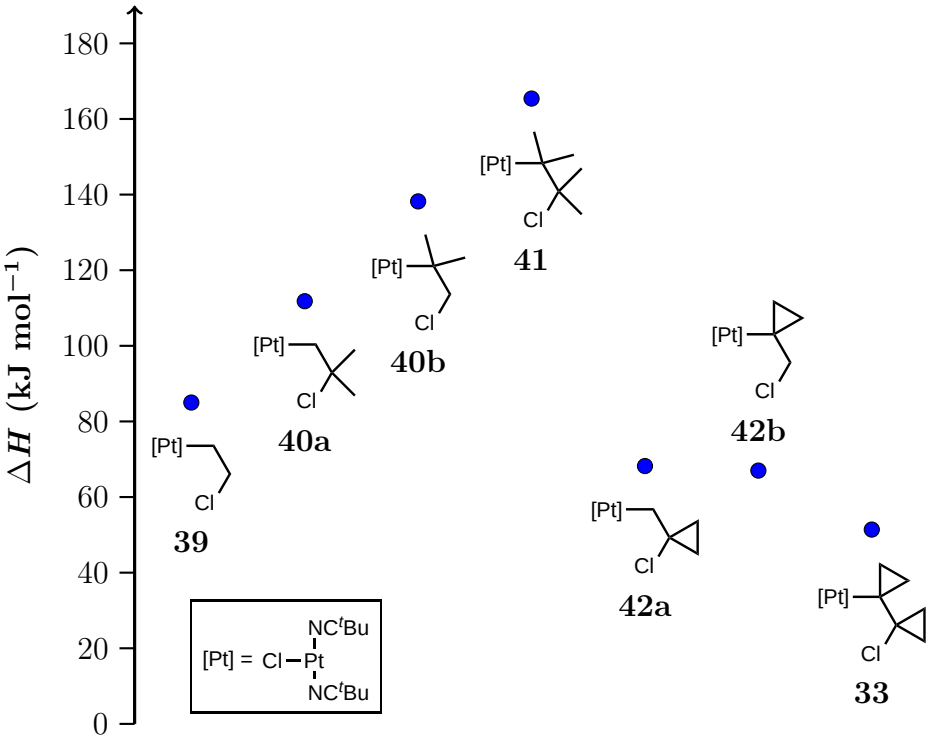

Figure 4.6. Reaction ΔH for the formation of β-chloroalkyl complexes From [$PtCl_2(NC^tBu)_2$].

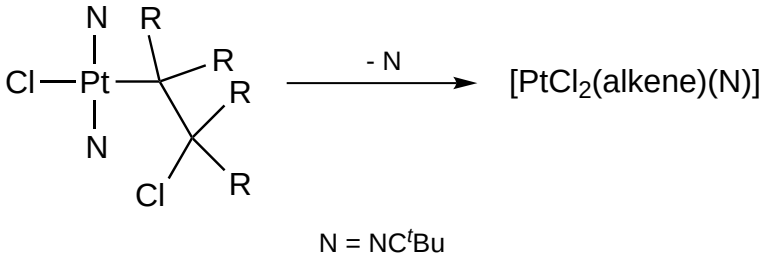

Scheme 4.16. Formation of $[PtCl_2(L)(NC^tBu)]$ *via* β-chloride elimination.

Table 4.7. Reaction ΔH for the Formation of $[PtCl_2(L)(NC^tBu)]$ Through β-Chloride Elimination.

		ΔH (kJ mol^{-1})	
Compound		*trans*	*cis*
trans–$[Pt(CH_2CH_2Cl)Cl(NC^tBu)_2]$	**39**	−80.1	−70.3
trans–$[Pt(CH_2CMe_2Cl)Cl(NC^tBu)_2]$	**40a**	−88.3	−72.2
trans–$[Pt(CMe_2CH_2Cl)Cl(NC^tBu)_2]$	**40b**	−114.5	−98.5
trans–$[Pt(CMe_2CMe_2Cl)Cl(NC^tBu)_2]$	**41**	−113.2	−106.0
trans–$[Pt(CH_2C(CH_2)_2Cl)Cl(NC^tBu)_2]$	**42a**	−66.5	−51.2
trans–$[Pt(C(CH_2)_2CH_2Cl)Cl(NC^tBu)_2]$	**42b**	−65.2	−49.9
trans–$[Pt(C(CH_2)_2C(CH_2)_2Cl)Cl(NC^tBu)_2]$	**33**	−49.4	−38.7

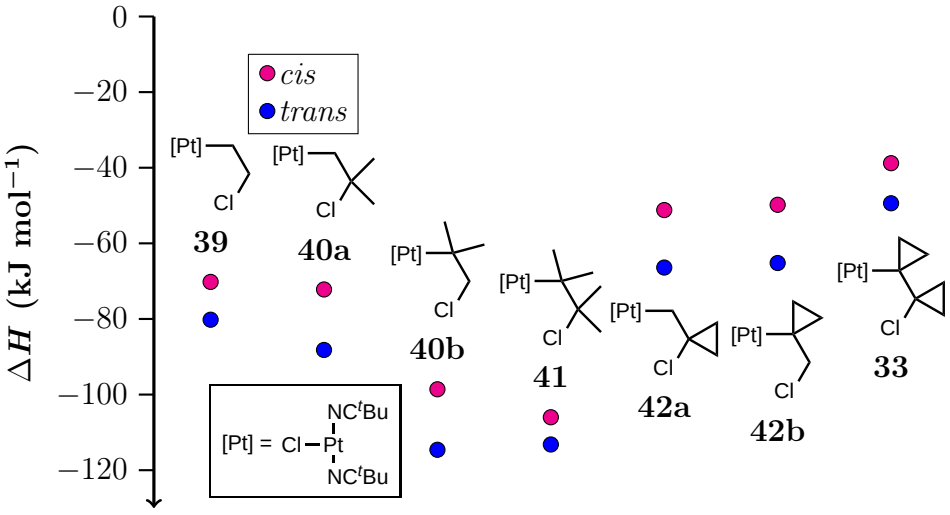

Figure 4.7. Reaction ΔH for the formation of $[PtCl_2(L)(NC^tBu)]$ through β-chloride elimination.

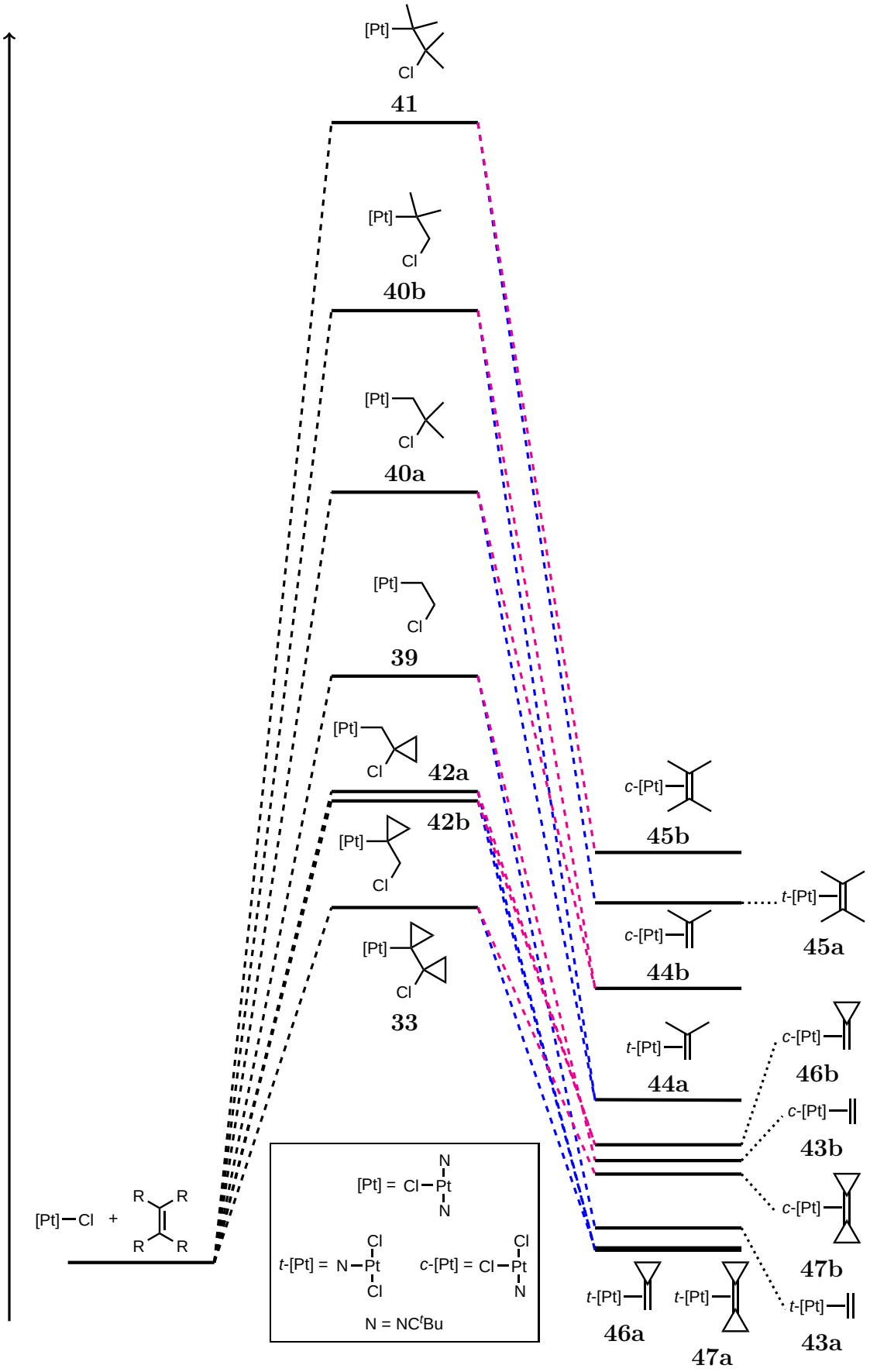

Figure 4.8. Energy diagram for the formation of $[PtCl_2(L)(NC^tBu)]$ from $[PtCl_2(NC^tBu)_2]$ *via* β-chloroalkyl complexes.

The reaction ΔH values for the formation of the β-chloroalkyl complexes from the addition of the appropriate alkene to *trans*–$[PtCl_2(NC^tBu)_2]$ were calculated (Scheme 4.15, Table 4.6, Figures 4.6 and 4.8). This reaction was observed experimentally for BCP, but did not occur with MCP. The reaction ΔH for the decomposition of the β-chloroalkyl complexs *via* β-chloride elimination, forming either the *trans* or *cis* alkene complex $[PtCl_2(L)(NC^tBu)]$ (Scheme 4.16), was also calculated (Table 4.7, Figures 4.7 and 4.8). The species used in the calculations were isolated molecules in the gas phase, so the absolute values of ΔH thus obtained were not necessarily those for the experimental systems. However, the calculated values of reaction ΔH were considered to be accurate indicators of the trends in stability of the complexes, within the limits of the theoretical description. Transition state structures were not calculated, so no kinetic information was obtained.

The reaction ΔH for both the formation from *trans*–$[PtCl_2(NC^tBu)_2]$ and the β-chloride eliminations indicated that the complexes with cyclopropyl ring substituents were the most stable. In the *trans*–$[PtCl_2(NC^tBu)_2]$ reaction, the three ^{c}Pr complexes (**42a**, **42b** and **33**) had the lowest ΔH values, 68.3, 67.0 and 51.5 kJ mol^{-1} respectively, indicating that these reactions were the most likely to occur. The difference between the two monosubstituted ^{c}Pr complexes was small, in favour of the α-substituted complex by 1.3 kJ mol^{-1}. There was a greater difference between the mono- and disubstituted complexes, with **33** 15.5 kJ lower than **42b**. With regard to the β-chloride eliminations, the ΔH values were the highest for the ^{c}Pr substituted complexes (-66.4 and -51.2 kJ mol^{-1} for **42a**, -65.1 and -49.9 kJ mol^{-1} for **42b**, -49.4 and -38.7 kJ mol^{-1} for **33**), indicating that the reactions were less likely to occur and that the β-chloroalkyl complexes were therefore the most stable. The formation of the *trans* alkene complexes was more favourable than the *cis*, with differences of 10.7–15.3 kJ mol^{-1}. Again, the dicyclopropyl complex was more stable than either of the monocyclopropyl complexes and the α-substituted complex was slightly more stable than the β-substituted.

The unsubstituted complex **39** was less stable than the cyclopropyl complexes but more stable than the methyl complexes. For the *trans*–$[PtCl_2(NC^tBu)_2]$ reaction, ΔH

was 85.1 kJ mol^{-1}, while for the β-Cl eliminations, ΔH was -80.1 and -70.2 kJ mol^{-1} for the *trans* and *cis* alkene complexes respectively. The methyl substituted β-chloroalkyl complexes were the least stable in both the *trans*–[$PtCl_2(NC^tBu)_2$] reaction and the β-chloride eliminations. The tetramethyl complex **41** had the highest ΔH for the *trans*–[$PtCl_2(NC^tBu)_2$] reaction (165.4 kJ mol^{-1}), and the lowest for the β-Cl elimination forming the *cis* alkene complex (-106.0 kJ mol^{-1}), indicating that it was the least stable of all the complexes studied. The α-substituted dimethyl complex **40b** had a slightly lower ΔH for the *trans* alkene reaction than **41** (-114.5 *v.s.* -113.2 kJ mol^{-1}), but had a higher ΔH for the *cis* alkene reaction (-98.5 kJ mol^{-1}) and a lower ΔH for the dichloride reaction (138.1 kJ mol^{-1}). The β-substituted dimethyl complex **40a** was more stable than **40b**, with ΔH values of 111.8 kJ mol^{-1} for the dichloride, -88.2 kJ mol^{-1} for the *trans* alkene and -72.2 kJ mol^{-1} for the *cis* alkene reactions. As with the ^{c}Pr substituted complexes, the formation of the *trans* alkene complex was more favourable than the formation of the *cis* alkene complex for all three methyl substituted complexes, with differences of 7.2–16.0 kJ mol^{-1}.

It was evident from the above data that it was the presence of ^{c}Pr rings rather than simply the degree of substitution which determined the stability of the β-chloroalkyl complexes. When substituted with methyl groups, the resulting β-haloalkyl complexes were increasingly unstable with more substitution closer to the metal centre. The opposite trend was observed for ^{c}Pr substitution; it was the complexes with the higher degree of substitution closer to the metal which were more stable. This was in agreement with the experimental observation that complexes formed from BCP were the most stable, while it was the complex with the ^{c}Pr ring in the α-position that was formed from MCP.

Chapter 5

Conclusion

Cyclopropyl rings are an important structural motif. They are found in many biologically active molecules, such as the anti-depressant, tranylcypromine, the molecule responsible for Jamaican vomiting sickness, hypoglycine A, and pyrethroids such as allethrin I, used in RAID flyspray (Figure 5.1).

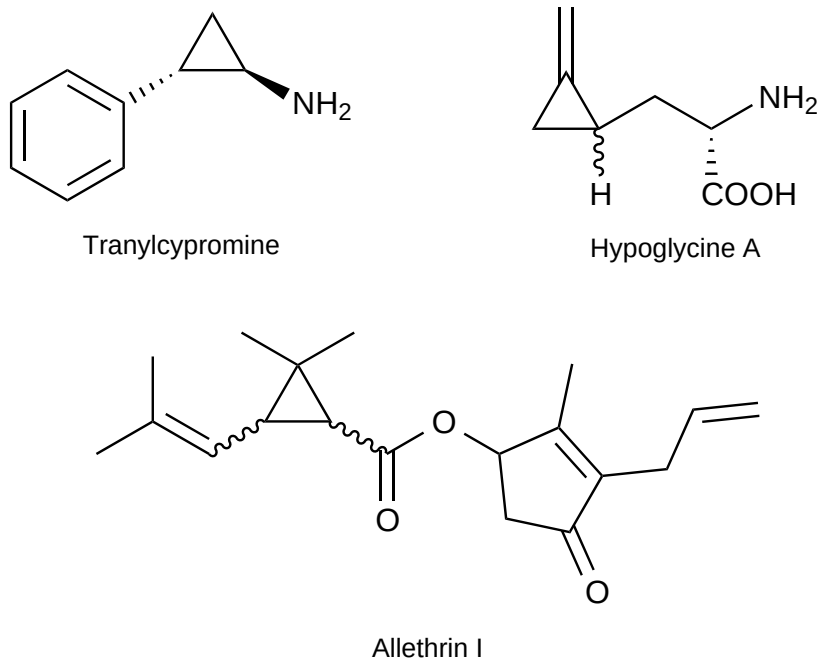

Figure 5.1. Biologically active molecules containing cyclopropyl rings.

Bicyclopropylidene and methylenecyclopropane, alkenes which contain cyclopropyl rings with *exo*-cyclic double-bonds, are useful synthetic precursors, enabling the incorporation of one or even two cyclopropyl rings into a carbon skeleton. Both are have reliable syntheses which enable them to be made in appreciable quantities in a relatively short time. Large amounts of work has been done investigating their reactivity and utility as as reagents for organic chemistry. A significant portion of this has involved the use of transition metal catalysts, particularly those of palladium. Two main modes of reactivity with transition metals have been observed; these are additions across the double-bond, as in reactions with Heck-type catalysts (for examples see Schemes 1.6 and 1.21), and ring-opening, involving cleavage at either the proximal or the distal ring bonds (for examples see Schemes 1.4 and 1.16). Reactions often involve a combination of the two reactivity modes, such as in the domino-Heck-Diels-Alder reactions of BCP.[63,74]

The isolation of transition metal complexes analogous to the proposed intermediates in these reactions has received comparatively little attention. There is one instance of the isolation of an η^3-allyl complex, which resulted from the addition of Pd–Ph across the double bond in a Heck-type reaction.[137] The coordination of MCP and BCP to form η^2-alkene complexes is a likely first step before any reaction takes place. A small handful of such complexes have been isolated, with Ni,[60] Pt,[61] Co[58,59] and Rh[61] for MCP, and Ti[58] and Co[58,59] for BCP.

The objective of this research was to investigate the reactivity of MCP and BCP with platinum, with a particular focus on isolating complexes with ligands derived from these alkenes. The majority of the transition metal chemistry done with these alkenes had involved palladium, while very little work was done with platinum. However, catalytically significant palladium species are transient and therefore difficult to characterise. In contrast, platinum species tend to be more stable, making platinum a useful model for palladium systems. Platinum also has an NMR-active isotope which assists with characterisation.

Initial attempts were made to synthesise homoleptic alkene complexes in order to determine the number of ligands that can coordinate. The typical number of alkene

ligands in complexes such as $[Pt(nb)_3]$ is three;[16] in homoleptic alkyne complexes, the typical number of ligands is two.[187] In BCP, the presence of the cyclopropyl rings increases the s-character of the double-bond carbon orbitals, making the carbons close to sp-hybridised.[29,32,68] This could mean that it would behave more like an alkyne in that only two BCP ligands would coordinate in the homoleptic complex. However, the formation of such complexes was not observed; instead ring-opening reactions occurred.

The synthesis of η^2-alkene complexes was more successful when stabilising auxilliary ligands were used. A range of η^2-BCP and MCP Pt(0) complexes with both mono- and di-phosphine ligands were synthesised, [Pt(L)(P—P)], [Pt(L)(P—S)], $[Pt(C_2H_4)(L)(PR_3)]$ and $[Pt(L)_2(PR_3)]$ (L = η^2-BCP, η^2-MCP; P—P = dppp, dcyppe, dbpe, dbpx; P—S = ^{t}Bu$_2$PCH$_2$(*o*-C$_6$H$_4$)CH$_2$S^{t}Bu; PR_3 = PPh_3, PCy_3), produced by the displacement of an alkene ligand, either ethene or norbornene, from a precursor complex. Platinum(II) complexes $[PtCl_2(L)(L')]$ (L = η^2-BCP, η^2-MCP; L′ = Py, DMSO) were also synthesised, again by displacement of a ligand from a precursor, either ethene or DMSO. These complexes are the first examples of late transition metal complexes of bicyclopropylidene as well as the first bis-methylenecyclopropane complexes of platinum.[79]

The coordinated alkenes proved to be reactive, and both of the reactivity modes observed with other transition metals, namely additions across the double-bond and ring-opening, also occurred with platinum, supporting the formation of η^2-alkene complexes as a first step in TM-catalysed reactions. The alkene ligands underwent reactions with either protons or *in situ* hydrides to produce η^3-allyl complexes. Three different allyl structures were observed in the protonation of [Pt(L)(P—P)] (P—P = dppp, dbpx) , with the relative ratios dependent on both the phosphine auxiliary ligand and the solvent. These allyl structures were the 2-substituted complexes $[Pt(\eta^3\text{-}CH_2C^cPrCH_2)(P—P)]^+$ and $[Pt(\eta^3\text{-}CH_2CMeCH_2)(P—P)]^+$, the 1-methyl substituted complexes with the methyl in the *anti* position $[Pt(\eta^3\text{-}C(CH_2)_2CHCHMe)(P—P)]^+$ and $[Pt(\eta^3\text{-}CH_2CHCHMe)(P—P)]^+$, and the 1-methyl substituted complexes with the methyl in the *syn* position.

Only one allyl structure was produced from the [Pt(L)(P—S)] complexes, the 1-methyl substituted complexes with the methyl in the *anti* position

$[Pt(\eta^3\text{-}C(CH_2)_2CHCHMe)(P—C)]^+$ and $[Pt(\eta^3\text{-}CH_2CHCHMe)(P—C)]^+$. In this case, the coordinated alkene reacted with a hydride generated by *ortho*-metallation of the P—S ligand. Computational models were used to investigate the formation of these various allyl complexes. It was determined that the activation energies for the various reactions had a larger effect than the relative stabilities of the complexes on the final product. The steric bulk of the auxiliary ligand was found to be more important in determining product distributions than the electronic nature of the ligand.

The proposed mechanism for the formation of these allyl complexes involves the addition of Pt–H across the double-bond, followed by cleavage of one of the ring bonds in a cyclopropylmethyl to homoallyl rearrangement.[135] Similar allyl complexes are likely intermediates in other transition metal catalysed reactions, and undergo subsequent reactions with nucleophiles.[38,72,74,137,138] It is likely that the allyl complexes synthesised in this work would also be reactive towards nucleophiles and therefore form the same products observed with palladium systems.

The addition of Pt–H followed by ring-opening in a cyclopropylmethyl to homoallyl rearrangement can also result in the formation of a 1,3-diene.[38,74] With BCP, the diene formed is allylidenecyclopropane, while with MCP it is 1,3-butadiene. Allylidenecyclopropane was produced from BCP with an number of Pt(0) and Pt(II) complexes, while 1,3-butadiene is only formed in the reaction of MCP with $[PtEt_2(COD)]$ as the minor anti-Markovnikov product. The Markovnikov addition of Pt–H across the MCP double-bond is not followed by ring opening. Instead, complexes with 1-methylcyclopropyl ligands are produced, the first stable examples of such complexes.

As allylidenecyclopropane is itself an alkene with a cyclopropyl ring and an *exo*-cyclic double-bond, its coordination chemistry was also explored. Diphosphine complexes $[Pt(ACP)(P—P)]$ ($P—P = Ph_2P(CH_2)_3PPh_2$, $Cy_2P(CH_2)_2PCy_2$, $^tBu_2P(CH_2)_2P^tBu_2$) were synthesised in the same manor as the BCP and MCP analogues, and are the first examples of coordinated ACP. Some of the ACP complexes underwent a rearrangement reaction to form η^2:σ^2-metallacyclopentene complexes, the first instances of the formation of η^2:σ^2-metallacyclopentene complexes from η^2:π-diene complexes, rather than from η^4:π-

diene complexes. This work is the first exploration of the coordination chemistry of allylidenecyclopropane.

Several instances of addition of Pt–Cl across the BCP double-bond were observed. These were not followed by ring-opening. Instead, the addition products were stable β-haloalkyl complexes, *trans*–[Pt(C$(CH_2)_2$C$(CH_2)_2$Cl)Cl(L)$_2$] (L = SEt_2, NC^tBu, Py) and *cis*–[Pt(C$(CH_2)_2$C$(CH_2)_2$Cl)Cl(Py)$_2$]. No *trans* complexes were produced from MCP; only *cis*–[Pt(C$(CH_2)_2CH_2$Cl)Cl(Py)$_2$] was formed. Phosphine complexes were synthesised addition of a phosphine to *cis*–[Pt(C$(CH_2)_2$C$(CH_2)_2$Cl)Cl(Py)$_2$] and *cis*–[Pt(C$(CH_2)_2CH_2$Cl)Cl(Py)$_2$]. The addition of a phosphine to *trans* β-chloroalkyl complexes resulted in β-chloride elimination and the formation of either [$PtCl_2(PR_3)_2$] or [Pt(P—P)$_2$]Cl_2. A short-lived *trans* β-chloroalkyl complex formed with PTA, which was the smallest of the phosphines used. The stability and formation rates of the other phosphine complexes were dependent on the size of the phosphine ligand, with smaller phosphines producing more stable complexes.

These β-chloroalkyl complexes are unusually stable, and are the only reported instances of Pt(II) β-haloalkyl complexes. These are also the only β-haloalkyl complexes formed by insertion into an Pt–X bond, rather than addition of X_2 to an η^2-alkene complex. Computational models of *trans*-[Pt(CR_2CR_2Cl)Cl(NC^tBu)$_2$] (R = CH_2, Me, H) were used to investigate the stability of complexes with different substitution patterns. When substituted with methyl groups, the resulting β-chloroalkyl complexes were increasingly unstable with more substitution closer to the metal centre. The opposite trend was observed for cyclopropyl substitution; it was the complexes with the higher degree of substitution closer to the metal that were more stable. This was in agreement with the experimental observations.

The β-haloalkyl complexes complexes are may have potential in the polymerisation of halogenated monomers such as vinyl chloride.[160–163] The polymerisation reactions currently involve a radical mechanism, which offers limited control of over the polymer structure and can lead to the formation of defects, affecting the stability of the resulting polymer. A mechanism that involves a β-haloalkyl intermediate could lead to more control

over the polymerisation process. However, previous work has been inhibited by very facile β-chloride elimination reactions. This work has shown that the both the substitution of the β-haloalkyl ligands and the nature of the auxiliary ligands affects the stability of such complexes, potentially enabling the further development of these polymerisation reactions.

This work has explored the coordination chemistry of bicyclopropylidene and methylenecyclopropane with platinum. Analogous reactivity to other transition metal systems, particularly palladium, was observed. A number of complexes with ligands derived from BCP and MCP were sythesised. These were η^2-alkene, η^3-allyl, 1-cycloproylmethyl and β-chloroalkyl ligands. Such complexes are not only similar to intermediates in various transition metal catalysed reactions, but are also interesting species in their own rights.

Chapter 6

Experimental

6.1 General Considerations

All reactions were carried out using de-oxygenated solvents and standard Schlenk techniques under either a nitrogen or argon atmosphere, unless stated otherwise. Starting materials were purchased from Sigma-Aldrich and used without further purification unless stated otherwise. Bicyclopropylidene,[67] methylenecyclopropane,[28] $[PtCl_2(dppp)]$,[188] $[Pt(C_2H_4)(dbpx)]$,[83] $[Pt(C_2H_4)(dbpe)]$,[83] $[Pt(C_2H_4)_2(PPh_3)]$,[119] $[Pt(C_2H_4)_2(PCy_3)]$,[119] $[Pt(nb)_3]$,[20] $[Pt(COD)_2]$,[20] $[Pt(C_2H_4)_3]$,[20] $[PtCl_2(SEt_2)_2]$,[178] $[PtCl_2(Py)_2]$,[189] $[PtCl_2(DMSO)_2]$,[190] $[PtCl_2(NC^tBu)_2]$,[191] $[PtMe_2(1,5\text{-hexadiene})]$,[192] and $[PtEt_2(COD)]$[83] were synthesized according to literature methods. The synthesis of dbpx was via the deprotection of dbpx-borane[193] using neat diethylamine, while dcyppe was synthesized by the reaction of cyclopentylmagnesium bromide with 1,2-bis(dichlorophosphino)ethane. Deuterated solvents were purchased from Sigma-Aldrich and stored under a nitrogen atmosphere.

NMR spectra were measured on Varian Unity Inova 300 MHz (300 MHz for ^1H, 121 MHz for ^{31}P, 282 MHz for ^{19}F), Varian Unity Inova 500 MHz (500 MHz for ^1H, 125 MHz for ^{13}C) and Varian DirectDrive 600 MHz (600 MHz for ^1H, 150 MHz for ^{13}C) NMR spectrometers, with chemical shift values δ referenced to the residual solvent peaks for ^1H and $^{13}C\{^1H\}$, to 85% H_3PO_4 for $^{31}P\{^1H\}$ and $CFCl_3$ for ^{19}F. NMR yields were reported for compounds unable to be isolated, and obtained by integration of

the $^{31}P\{^{1}H\}$ or ^{1}H NMR spectra against other species in solution. Elemental analyses were performed by the Campbell Microanalytical Laboratory, University of Otago, New Zealand. Electrospray ionization mass spectra were obtained using a Aglient 6530 Series Q-TOF mass spectrometer or performed by the GlycoSyn QC laboratory at Industrial Research Limited using a Waters Q-TOF Premier Tandem mass spectrometer. Calculated NMR spectra were obtained from gNMR spectral simulation program, version 5.0.6.0, written by P. H. M. Budzelaar, IvorySoft 2006. X-ray diffraction data were collected by the X-ray Crystallograpy Laboratory at the University of Canterbury on a Bruker SMART CCD diffractometer using Mo Kα radiation. Data were reduced using Bruker SAINT software. Absorption correction was performed using the SADABS program. The structures were solved using OLEX2 running SHELXS97 and SHELXL97.[194,195] The positions of all hydrogen atoms were calculated during refinement. Calculations were performed using the Gaussian 09 Revision B.01 program[196,197] and were performed on the Victoria University of Wellington School of Chemical and Physical Sciences' Heisenberg cluster, consisting of eight processing nodes with two 2.53 GHz Xeon X3440 quad-core processors per node and 1 GB of memory per core.

6.2 Chapter Two Experimental

Synthesis of Cyclopropanecarboxylic-*carboxyl*-$^{13}C\{^{1}H\}$ Acid[88]

Magnesium turnings (1.7 g, 0.070 mol) was placed in a 2-neck 100 mL RB flask equipped with a double surface condenser and a dropping funnel and dry stirred overnight. THF (25 mL) was added and bromocyclopropane (5.0 g, 0.413 mol) placed in the dropping funnel. The Mg was activated with 1,2-dibromoethane and heat, and the bromocyclopropane slowly added and the solution stirred for 30 min. Barium carbonate (7.1 g, 0.036 mol, 70% ^{13}C) was placed in a 2-neck 100 mL RB flask equipt with a dropping funnel and a drying tube filled with silica gel attached to a glass tube that vented into a 250 mL flask fitted with a balloon to regulate pressure. This flask was filled with 140 mL of THF and cooled to –78 °C in a dry ice/acetone bath. H_2SO_4 (conc.) was slowly added

onto the $BaCO_3$ while stirring vigorously, with the mouth of the bubbling tube kept above the level of the THF. The $BaCO_3$ was heated to ensure complete reaction. The ^{c}PrMgBr solution was added to the solution of CO_2, and the reaction allowed to warm to room temperature. The reaction mixture was cooled in ice, quenched with H_2SO_4 (25 mL, 4 mol L^{-1}), stirred overnight and filtered. The solution was reduced to ∼50 mL then continuously extracted into Et_2O for 48 hrs. The ether solution was distilled by heating in an oil bath up to 110 °C, adding 5 mL CH_2Cl_2 and continuing until the temperature started to drop. The residue was then distilled under water pump pressure, with the product distilling at 80 °C (745 mg, 19%). ^{1}H NMR (δ, C_6D_6, 500 MHz): 1.60(tt, 8.0, 4.4 Hz, 1H, CH), 1.06(m, 2H, CH_2), 0.93(m, 2H, CH_2). $^{13}C\{^{1}H\}$ NMR (δ, C_6D_6, 125 MHz): 181.5(s, COOH), 13.0(s, CH), 12.9(d, $^{1}J_{C–C}$ = 74.4 Hz, CH), 9.3(s, CH_2).

Synthesis of [Pt(C_2H_4)(dppp)]

[$PtCl_2$(dppp)] (0.455 g, 0.67 mmol) was suspended in ethanol (12.6 mL) under a nitrogen atmosphere. The solution was saturated with ethene and a solution of $NaBH_4$ (2.08 mmol, 10.4 mL, 2 M) in ethanol was added dropwise. The solution was stirred under a flow of ethene for 2 hrs. The supernatant liquid was removed and the pale yellow precipitate washed with water (3 × 6 mL) and ethanol (3 × 6 mL). Benzene (5 mL) was added and the solution dried *in vacuo* to remove water. The product was a yellow crystalline solid (368 mg, 0.58 mmol, 86%). ^{1}H NMR (δ, C_6D_6, 500 MHz): 7.71(m, 8H, *o*-C_6H_5), 7.03(m, 12H, *m*- and *p*-C_6H_5), 2.68(d, 2.7, $J_{Pt–H}$ = 60.0 Hz, 4H, =CH_2), 2.19(m, 4H, P−CH_2), 1.68(m, 2H, CH_2). $^{13}C\{^{1}H\}$ NMR (δ, C_6D_6, 125 MHz): 138.7(m, *i*-C_6H_5), 133.1(m, *o*-C_6H_5), 129.4(s, *p*-C_6H_5), 128.3(s, *m*-C_6H_5), 31.9(t, 25.5, $^{1}J_{Pt–C}$ = 216.0 Hz, =CH_2), 28.9(dd, 14.5, 13.3 Hz, P−CH_2), 21.0(t, 3.8 Hz, CH_2). $^{31}P\{^{1}H\}$ NMR (δ, C_6D_6, 121 MHz): 13.8(s, $^{1}J_{Pt–P}$ = 3340 Hz).

Synthesis of [$PtCl_2$(dcyppe)]

1,2-Bis(dicyclopentylphosphino)ethane (278 mg, 0.76 mmol) was placed in a 50 mL 2-necked round bottom flask fitted with a reflux condenser. $K_2[PtCl_4]$ (314 mg, 0.76 mmol)

was added, followed by EtOH (10 mL) and c. HCl (7 mL). The solution was refluxed overnight, before filtration of the white solid and washing with H_2O (2 × 5 mL) and EtOH (2 × 5 mL). The isolated solid is [$PtCl_2$(dcyppe)] (400 mg, 0.63 mmol, 83%). ^{1}H NMR (δ, $CDCl_3$, 500 MHz): 2.64(m, 4H, P−CH), 2.15(m, 4H, CH_2), 1.92(m, 8H, CH_2), 1.82–1.59(m, 24H, P−CH_2 and CH_2, 125 MHz). ^{13}C{^{1}H} NMR (δ, $CDCl_3$): 36.8(d, 37.8 Hz, P−CH), 29.7(d, 1.5 Hz, CH_2), 29.4(s, CH_2), 26.3(d, 10.1 Hz, CH_2), 25.3(d, 11.6 Hz, CH_2), 22.3(dd, 36.0, 7.8 Hz, P−CH_2). ^{31}P{^{1}H} NMR (δ, $CDCl_3$, 121 MHz): 59.2(s, $^1J_{\text{Pt–P}}$ = 3570 Hz).

Synthesis of [Pt(C_2H_4)(dcyppe)]

Mercury (10.2 g, 0.051 mol) was placed in a Schlenk tube and small pieces of sodium (88 mg, 3.8 mmol) slowly added. When the dissolution was complete, THF (10 mL) was added and the liquid saturated with ethene. [$PtCl_2$(dcyppe)] (248 mg, 0.39 mmol) was added and the reaction stirred for 2 hr. The solution was run through a 1 cm Celite column followed by a 1 cm alumina column and the amalgam was washed with THF (2 × 10 mL). The solvent was removed *in vacuo* yielding a brown solid (116 mg, 0.20 mmol, 51%). ^{1}H NMR (δ, C_6H_6, 500 MHz): 2.38(t, 1.8, $J_{\text{Pt–H}}$ = 58.0 Hz, 4H, =CH_2), 1.97(m, 4H, P−CH), 1.80(m, 8H, CH_2), 1.66–1.50(m, 12H, CH_2), 1.50–1.32(m, 16H, P−CH_2 and CH_2). ^{13}C{^{1}H} NMR (δ, C_6H_6, 125 MHz): 39.3(t, 12.9, $J_{\text{Pt–C}}$ = 49.9 Hz, P−CH), 31.1(t, 4.6, $J_{\text{Pt–C}}$ = 15.2 Hz, CH_2), 30.5(t, 2.9, $J_{\text{Pt–C}}$ = 22.1 Hz, CH_2), 28.7(t, 21.1, $J_{\text{Pt–C}}$ = 17.3 Hz, P−CH_2), 26.4(t, 4.5 Hz, CH_2), 23.2(t, 15.1, $^1J_{\text{Pt–C}}$ = 227.4 Hz, =CH_2). ^{31}P{^{1}H} NMR (δ, C_6H_6, 121 MHz): 75.4(s, $^1J_{\text{Pt–P}}$ = 3170 Hz).

Synthesis of [Pt(BCP)(dppp)] 1a

[Pt(C_2H_4)(dppp)] (0.162 g, 0.28 mmol) was dissolved in toluene (3.5 mL). Bicyclopropylidene (0.052 mL, 0.56 mmol) was added, and the solution stirred for 30 min. The solvent was removed *in vacuo*, yielding an off-white solid ([Pt(BCP)(dppp)], 158 mg, 0.23 mmol, 82%). Crystals of [Pt(BCP)(dppp)] were grown by slow recrystallization from hot toluene. ^{1}H NMR (δ, C_6D_6, 500 MHz): 7.57(m, 8H, *o*-C_6H_5), 7.04(m, 8H, *m*-C_6H_5), 6.98(m, 4H, *p*-

C_6H_5), 2.13(m, 4H, P−CH_2), 1.51(m, 2H, CH_2), 1.29(m, $J_{Pt–H}$= 66.0 Hz, 4H, ^{c}Pr-*endo*), 1.18(d, 4.4, $J_{Pt–H}$ = 37.3 Hz, 4H, ^{c}Pr-*exo*). $^{13}C\{^1H\}$ NMR (δ, C_6D_6, 150 MHz): 136.8(m, *i*-C_6H_5), 132.9(m, *o*-C_6H_5), 129.5(s, *p*-C_6H_5), 128.4(s, *m*-C_6H_5), 34.3(m, $J_{P–C}$ = 73.3, −9.1, $J_{P–P}$ = 24.5, $^1J_{Pt–C}$ = 409.4Hz, =CR_2), 28.5(m, P−CH_2), 20.9(m, CH_2), 8.8(s, $J_{Pt–C}$ = 23.1 Hz, ^{c}Pr). $^{31}P\{^1H\}$ NMR (δ, C_6D_6, 121 MHz): 9.3(s, $^1J_{Pt–P}$ = 2932 Hz). *m/z* = $[M + H]^+$ calcd for $C_{33}H_{35}P_2{}^{194}Pt$ 687.1841; found 687.1849. Anal. Calcd for $C_{33}H_{34}P_2Pt$: C 57.64; H 4.98. Found: C 57.76; H 4.96.

Synthesis of [Pt(BCP)(dcyppe)] 1b

[Pt(C_2H_4)(dcyppe)] (20 mg, 0.034 mmol) was dissolved in C_6D_6 (0.5 mL) and placed in an NMR tube. BCP (3.2 μL, 0.034 mmol) was added and the reaction left overnight. Solution contains 91% [Pt(BCP)(dcyppe)] by $^{31}P\{^1H\}$ NMR. ^{1}H NMR (δ, C_6D_6, 500 MHz): 1.90(m, 4H, P−CH), 1.73(m, 4H, CH_2), 1.63–1.53(m, 18H, CH_2, P−CH_2 and ^{c}Pr), 1.50–1.40(m, 12H, CH_2 and ^{c}Pr), 1.40–1.30(m, 10H, CH_2 and P−CH_2). $^{13}C\{^1H\}$ NMR (δ, C_6D_6, 125 MHz): 39.1(dd, 14.5, 12.1, $J_{Pt–C}$ = 63.0 Hz, P−CH), 33.8(m, $J_{P–C}$ = 66.8, 7.0, $J_{P–P}$ = −59.7, $^1J_{Pt–C}$ = 424.6 Hz, =CR_2), 30.4(t, 2.3, $J_{Pt–C}$ = 19.6 Hz, CH_2), 30.0(t, 7.5, $J_{Pt–C}$ = 11.6 Hz, CH_2), 28.0(t, 41.6, $J_{Pt–C}$ = 14.8 Hz, P−CH_2), 26.2(t, 4.6, CH_2), 10.4(s, $J_{Pt–C}$ = 23.1 Hz, ^{c}Pr). $^{31}P\{^1H\}$ NMR (δ, C_6D_6, 121 MHz): 70.8(s, $^1J_{Pt–P}$ = 2731 Hz).

Synthesis of [Pt(BCP)(dbpe)] 1c

[Pt(C_2H_4)(dbpe)] (20 mg, 0.034 mmol) was dissolved in C_6D_6 (0.5 mL) and placed in an NMR tube. BCP (3.2 μL, 0.034 mmol) was added and the reaction heated at 60 °C for 7 days. Solution contains 80% [Pt(BCP)(dbpe)] by $^{31}P\{^1H\}$ NMR. ^{1}H NMR (δ, C_6D_6, 500 MHz): 1.57(m, 4H, ^{c}Pr), 1.31(m, 8H, P−CH_2 and ^{c}Pr), 1.06(d, 12.0 Hz, 36H, ^{t}Bu). $^{13}C\{^1H\}$ NMR (δ, C_6D_6, 125 MHz): 35.1(t, 9.3, $J_{Pt–C}$ = 49.7 Hz, P−CR_3), 31.8(m, $J_{P–C}$ = 70.5, 4.1, $J_{P–P}$ = 59.5, $^1J_{Pt–C}$ = 428.91 Hz, =CR_2), 29.9(t, 3.5, $J_{Pt–C}$ = 15.9 Hz, CH_3), 26.0(t, 5.1, $J_{Pt–C}$ = 33.7 Hz, P−CH_2), 9.9(s, $J_{Pt–C}$ = 23.7 Hz, ^{c}Pr). $^{31}P\{^1H\}$ NMR (δ, C_6D_6, 121 MHz): 97.4(s, $^1J_{Pt–P}$ = 2798 Hz).

Synthesis of [Pt(BCP)(dbpx)] 1d

[Pt(C_2H_4)(dbpx)] (51 mg, 0.083 mmol) was dissolved in C_6D_6 (0.5 mL) and placed in an NMR tube. BCP (13 μL, 0.14 mmol) was added and the reaction heated at 60 °C for 6 days. Solution contains 98% [Pt(BCP)(dbpx)] by $^{31}P\{^1H\}$ NMR. ^1H NMR (δ, C_6D_6, 500 MHz): 7.14(m, 2H, *o*-C_6H_4), 6.94(m, 2H, *m*-C_6H_4), 3.44(m, 4H, P−CH_2), 1.34(m, $J_{Pt–H}$ = 61.2 Hz, 4H, ^{c}Pr-*endo*), 1.19(d, 12.5 Hz, 36H, ^{t}Bu), 0.99(d, 4.0, $J_{Pt–H}$ = 32.0 Hz, 4H, ^{c}Pr-*exo*). $^{13}C\{^1H\}$ NMR (δ, C_6D_6, 125 MHz): 138.3(s, *i*-C_6H_4), 133.1(s, *o*-C_6H_4), 126.1(s, *m*-C_6H_4), 37.3(m, P−CR_3), 32.0(m, P−CH_2), 30.2(m, CH_3), 29.3(m, $J_{P–C}$ = 78.1, −4.2, $J_{P–P}$ = 21.6, $^1J_{Pt–C}$ = 456.3 Hz, =CR_2), 9.9(s, $J_{Pt–C}$ = 22.5 Hz, ^{c}Pr). $^{31}P\{^1H\}$ NMR (δ, C_6D_6, 121 MHz): 43.3(s, $^1J_{Pt–P}$ = 2983 Hz).

Synthesis of [Pt(MCP)(dppp)] 2a

Pt(C_2H_4)(dppp)] (87 mg, 0.14 mmol) was dissolved in toluene (1 mL). A large excess of methylenecyclopropane was added, and the solution stirred for 30 min. The solvent was removed *in vacuo*, yielding an off-white solid ([Pt(MCP)(dppp)], 79 mg, 0.13 mmol, 92%). ^1H NMR (δ, C_6D_6, 500 MHz): 7.77(t, 9 Hz, 4H, *o*-C_6H_4−P_1), 7.51(t, 8.5 Hz, 4H, *o*-C_6H_4−P_2), 7.05(m, 8H, *m*-C_6H_5), 7.00(m, 4H, *p*-C_6H_4), 2.63(dd, $J_{P–H}$ = 7.7, 4.5, $^2J_{Pt–H}$ = 65.3 Hz, 2H, =CH_2), 2.17(m, 4H, P−CH_2), 1.65(d, 6.5, $J_{Pt–H}$ = 33.0 Hz, 2H, ^{c}Pr-*exo*), 1.59(m, 2H, CH_2), 1.32(d, 9.5, $J_{Pt–H}$ = 82.5 Hz, 2H, ^{c}Pr-*endo*). $^{13}C\{^1H\}$ NMR (δ, C_6D_6, 125 MHz): 138.4(m, *i*-C_6H_4−P_1), 136.9(m, *i*-C_6H_4−P_2), 133.2(m, *o*-C_6H_4−P_1), 132.8(m, *o*-C_6H_4−P_2), 129.4(m, *p*-C_6H_4), 128.4(m, *m*-C_6H_5), 42.7(dd, $J_{P–C}$ = 57.3, 5.0, $^1J_{Pt–C}$ = 455.4 Hz, =CR_2), 28.8(m, P−CH_2), 25.3(dd, $J_{P–C}$ = 36.4, 4.9, $^1J_{Pt–C}$ = 173.4 Hz, =CH_2), 21.0(m, CH_2), 10.1(d, $J_{P–C}$ = 3.8, $J_{Pt–C}$ = 25.9 Hz, ^{c}Pr). $^{31}P\{^1H\}$ NMR (δ, C_6D_6, 121 MHz): 11.8(AB, $^2J_{Pt–P}$ = 41.5, $^1J_{Pt–P}$ = 3275 Hz, P_2 *trans* =CH_2), 11.4(AB, $^2J_{Pt–P}$ = 41.5, $^1J_{Pt–P}$ = 2975 Hz, P_1 *trans* =CR_2). *m/z* = $[M + H]^+$ calcd for $C_{31}H_{33}P_2{}^{194}Pt$ 661.1684; found 661.1678. Anal. Calcd for $C_{31}H_{32}P_2Pt$: C 56.28; H 4.87. Found: C 56.47; H 4.86.

Synthesis of [Pt(MCP)(dcyppe)] 2b

[Pt(C_2H_4)(dcyppe)] (20 mg, 0.034 mmol) was dissolved in C_6D_6 (0.5 mL) and placed in an NMR tube. A large excess of MCP was added and the reaction left at room temperature overnight. Solution contains 100% [Pt(MCP)(dcyppe)] by $^{31}P\{^1H\}$ NMR. ^1H NMR (δ, C_6D_6, 500 MHz): 2.40(dd, 8.5, 4.5, $^2J_{Pt–H}$ = 60.5 Hz, 2H, =CH_2), 1.99–1.89(m, 6H, P−CH and ^{c}Pr), 1.87–1.77(m, 6H, CH_2 and ^{c}Pr), 1.75–1.68(m, 4H, CH_2), 1.6–1.3(m, 28H, P−CH_2 and CH_2). $^{13}C\{^1H\}$ NMR (δ, C_6D_6, 125 MHz): 39.3(dd, 21.6, 4.2, $J_{Pt–C}$ = 43.8 Hz, P−CH), 39.1(dd, 22.5, 4.5, $J_{Pt–C}$ = 53.2 Hz, P−CH), 38.3(dd, 71.0, 8.7, $^1J_{Pt–C}$ = 501.0 Hz, =CR_2), 31.0(d, 8.2, $J_{Pt–C}$ = 15.7 Hz, CH_2), 30.6(d, 5.4, $J_{Pt–C}$ = 16.7 Hz, CH_2), 30.4(d, 5.2, $J_{Pt–C}$ = 22.0 Hz, CH_2), 30.0(d, 14.3, $J_{Pt–C}$ = 10.3 Hz, CH_2), 28.8(m, P−CH_2), 27.6(m, P−CH_2), 26.3(m, CH_2), 22.4(dd, 41.8, 5.6, $^1J_{Pt–C}$ = 168.4 Hz, =CH_2), 12.3(d, 3.9, $J_{Pt–C}$ = 23.4 Hz, ^{c}Pr). $^{31}P\{^1H\}$ NMR (δ, C_6D_6, 121 MHz): 75.0(AB, $^2J_{Pt–P}$ = 62.5, $^1J_{Pt–P}$ = 2751 Hz, P *trans* =CR_2), 70.8(AB, $^2J_{Pt–P}$ = 62.5, $^1J_{Pt–P}$ = 3107 Hz, P *trans* =CH_2).

Synthesis of [Pt(MCP)(dbpe)] 2c

[Pt(C_2H_4)(dbpe)] (20 mg, 0.034 mmol) was dissolved in C_6D_6 (0.5 mL) and placed in an NMR tube. A large excess of MCP was added and the reaction heated at 40 °C overnight. Solution contains 99% [Pt(MCP)(dbpe)] by $^{31}P\{^1H\}$ NMR. ^1H NMR (δ, C_6D_6, 500 MHz): 2.39(dd, 8.4, 4.2, $^2J_{Pt–H}$ = 60.6 Hz, 2H, =CH_2), 1.89(d, 7.2, $J_{Pt–H}$ = 33.6 Hz, 2H, ^{c}Pr-*exo*), 1.79(m, $J_{Pt–H}$ = 60.0 Hz, 2H, ^{c}Pr-endo), 1.30(m, 4H, P−CH_2), 1.10(d, 12.0 Hz, 18H, ^{t}Bu), 1.02(d, 12.0 Hz, 18H, ^{t}Bu). $^{13}C\{^1H\}$ NMR (δ, C_6D_6, 125 MHz): 36.8(dd, 71.9, 8.2, $^1J_{Pt–C}$ = 511.4 Hz, =CR_2), 35.0(dd, 12.2, 4.1 Hz, P−CR_3), 34.9(dd, 13.4, 4.6 Hz, P−CR_3), 30.3(d, 6.4, $J_{Pt–C}$ = 17.7 Hz, CH_3), 29.9(d, 7.0, $J_{Pt–C}$ = 16.2 Hz, CH_3), 26.8(dd, 18.1, 12.2, $J_{Pt–C}$ = 10.4 Hz, P−CH_2), 25.3(dd, 16.9, 14.6, $J_{Pt–C}$ = 14.0 Hz, P−CH_2), 23.5(dd, 42.7, 4.7, $^1J_{Pt–C}$ = 171.6 Hz, =CH_2), 11.8(d, 4.1, $J_{Pt–C}$ = 24.5 Hz, ^{c}Pr). $^{31}P\{^1H\}$ NMR (δ, C_6D_6, 121 MHz): 100.8(AB, $^2J_{Pt–P}$ = 65.7, $^1J_{Pt–P}$ = 2807 Hz, P *trans* =CR_2), 99.2(AB, $^2J_{Pt–P}$ = 65.7, $^1J_{Pt–P}$ = 3167 Hz, P *trans* =CH_2).

Synthesis of [Pt(MCP)(dbpx)] 2d

[Pt(C_2H_4)(dbpx)] (35 mg, 0.057 mmol) was dissolved in C_6D_6 (0.5 mL) and placed in an NMR tube. A large excess of MCP was added and the reaction heated at 60 °C overnight. Solution contains 96% [Pt(MCP)(dbpx)] by $^{31}P\{^1H\}$ NMR. ^1H NMR (δ, C_6D_6, 500 MHz): 7.15(m, 2H, *o*-C_6H_4), 6.92(m, 2H, *m*-C_6H_4), 3.47(m, 4H, P−CH_2), 2.12(t, 6.5, $^2J_{Pt–H}$ = 56.5 Hz, 2H, =CH_2), 1.60(m, 4H, ^{c}Pr), 1.26(d, 12.0 Hz, 18H, ^{t}Bu), 1.17(d, 12.0 Hz, 18H, ^{t}Bu). $^{13}C\{^1H\}$ NMR (δ, C_6D_6, 125 MHz): 138.6(s, *i*-C_6H_4), 138.5(s, *i*-C_6H_4), 133.3(m, *o*-C_6H_4), 126.0(m, *m*-C_6H_4), 37.8(m, P−CR_3), 36.9(dd, 12.9, 3.9, $J_{Pt–C}$ = 45.0 Hz, P−CR_3), 33.6(dd, 72.5, 10.1, $^1J_{Pt–C}$ = 537.6 Hz, =CR_2), 32.5(d, 8.7 Hz, P−CH_2), 32.3(d, 5.3 Hz, P−CH_2), 30.6(d, 5.3, $J_{Pt–C}$ = 16.3 Hz, CH_3), 30.2(d, 6.7, $J_{Pt–C}$ = 15.3 Hz, CH_3), 27.8(dd, 39.4, 5.3, $^1J_{Pt–C}$ = 164.2 Hz, =CH_2), 11.4(d, 2.9, $J_{Pt–C}$ = 25.0 Hz, ^{c}Pr). $^{31}P\{^1H\}$ NMR (δ, C_6D_6, 121 MHz): 49.3(AB, $^2J_{Pt–P}$ = 29.7, $^1J_{Pt–P}$ = 3362 Hz, P *trans* =CH_2), 43.7(AB, $^2J_{Pt–P}$ = 29.7, $^1J_{Pt–P}$ = 3025 Hz, P *trans* =CR_2).

Synthesis of [Pt(ACP)(dppp)] 3a and [$\overline{\text{Pt(CH}_2\text{CH=CHC(CH}_2)_2\text{)}}$(dppp)] 4a

A few crystals of [$PtMe_2$(1,5-hexadiene)] were placed in an NMR tube and $CDCl_3$ (0.5 mL) added. BCP (0.2 mL, 18.7 mmol) was added and the reaction left for 3 days, after which all of the BCP had reacted to form ACP. [Pt(C_2H_4)(dppp)] (30 mg, 0.047 mmol) was placed in an NMR tube and C_6D_6 (0.5 mL) added. A solution of ACP (0.1 mL, 27 mol L^{-1} solution in $CDCl_3$) was added, resulting in the immediate formation of [Pt(ACP)(dppp)]. After several hours, the complex rearranges to form [$\overline{\text{Pt(CH}_2\text{CH=CHC(CH}_2)_2\text{)}}$(dppp)] **4a**. Solution contains 91% [$\overline{\text{Pt(CH}_2\text{CH=CHC(CH}_2)_2\text{)}}$(dppp)] by $^{31}P\{^1H\}$ NMR after 24 hr. **[Pt(ACP)(dppp)] 3a:** ^1H NMR (δ, C_6D_6, 500 MHz): 7.80(t, 8.7 Hz, 2H, *o*-C_6H_5), 7.69(t, 9.0 Hz, 2H, *o*-C_6H_5), 7.54(t, 6.9 Hz, 2H, *o*-C_6H_5), 7.38(t, 8.1 Hz, 2H, *o*-C_6H_5), 7.15–6.96(m, 12H, *m*- and *p*-C_6H_5), 6.47(m, 1H, =CHR), 5.04(m, 1H, =CH_2), 4.69(m, 1H, =CH_2), 3.78(td, 9.3, 3.6, $^2J_{Pt–H}$ = 67.8 Hz, =CHR), 2.40–1.96(m, 4H, P−CH_2), 1.5–1.3(m, 2H, CH_2), 1.3–0.8(m, 4H, ^{c}Pr). $^{31}P\{^1H\}$ NMR (δ, C_6D_6, 121 MHz): 10.3(AB, $^2J_{Pt–P}$ = −39.4, $^1J_{Pt–P}$ = 293 Hz, P *trans* =CHR), 9.7(AB, $^2J_{Pt–P}$ = −39.4, $^1J_{Pt–P}$ = 3003 Hz, P *trans* =CR_2). **[$\overline{\text{Pt(CH}_2\text{CH=CHC(CH}_2)_2\text{)}}$(dppp)] 4a:** ^1H NMR (δ,

C_6D_6, 500 MHz): 7.68(t, 8.0 Hz, 4H, *o*-C_6H_5), 7.58(t, 9.3 Hz, 4H, *o*-C_6H_5), 7.03(m, 12H, *m*- and *p*-C_6H_5), 6.07(dm, 12.0, $J_{Pt–H}$ 97.0 Hz, 1H, =$CHCH_2$), 5.29(t, 5.5, $J_{Pt–H}$ = 86.5 Hz, 1H, =CH−^{c}Pr), 2.85(m, $^2J_{Pt–H}$ = 62.0 Hz, 2H, Pt−CH_2), 2.05(m, 4H, P-CH2), 1.30(m, 2H, CH_2), 0.85(m, $J_{Pt–H}$ = 25.0 Hz, 2H, ^{c}Pr-*exo*), 0.71(d, 7.5, $J_{Pt–H}$ = 55.0 Hz, 2H, ^{c}Pr-*endo*). $^{13}C\{^1H\}$ NMR (δ, C_6D_6, 125 MHz): 154.3(d, 9.6 Hz, $J_{Pt–C}$ = 67.6 Hz, =CH−^{c}Pr), 134.2(m, *o*-C_6H_5), 133.8(m, *o*-C_6H_5), 133.5(m, *i*-C_6H_5), 132.5(m, *i*-C_6H_5), 131.5(m, =$CHCH_2$), 130.1(d, 1.9 Hz, *m*-C_6H_5), 129.9(d, 1.9 Hz, *m*-C_6H_5), 128.6(s, *p*-C_6H_5), 128.4(s, *p*-C_6H_5), 39.3(dd, 83.9, 4.4, $^1J_{Pt–C}$= 450.3 Hz, Pt−CH_2), 32.3(m, Pt−CR_3), 30.5(m, P−CH_2), 27.4(m, P−CH_2), 20.0(s, CH_2), 16.9(s, ^{c}Pr). $^{31}P\{^1H\}$ NMR (δ, C_6D_6, 121 MHz): 2.2(AB, $^2J_{Pt–P}$ = 18.2, $^1J_{Pt–P}$ = 1784 Hz), 1.7(AB, $^2J_{Pt–P}$ = 18.2, $^1J_{Pt–P}$ = 1856 Hz). *m/z* = $[M + H]^+$ calcd for $C_{33}H_{35}P_2{}^{194}Pt$ 687.1841; found 687.1848.

Synthesis of [Pt(ACP)(dcyppe)] 3b and [$\overline{\text{Pt(CH}_2\text{CH=CHC(CH}_2)_2)}$(dcyppe)] 4b

[Pt(C_2H_4)(dcyppe)] (100 mg, 0.170 mmol) was placed in an NMR tube and C_6D_6 (0.5 mL) added. A solution of ACP (0.1 mL, 27 mol L^{-1} solution in $CDCl_3$) was added, resulting in the immediate formation of [Pt(ACP)(dcyppe)] and [$\overline{\text{Pt(CH}_2\text{CH=CHC(CH}_2)_2)}$(dcyppe)]. After 3 hr, the only product is [$\overline{\text{Pt(CH}_2\text{CH=CHC(CH}_2)_2)}$(dcyppe)] **4b**. Solution contains 93% [$\overline{\text{Pt(CH}_2\text{CH=CHC(CH}_2)_2)}$(dcyppe)] by $^{31}P\{^1H\}$ NMR. **[Pt(ACP)(dcyppe)] 3b:** ^1H NMR (δ, C_6D_6, 500 MHz): 6.1(m, 1H, =CHR), 4.9(m, 1H, =CH_2), 4.4(m, 1H, =CH_2), 3.4(m, $^2J_{Pt–H}$ = 62.1 Hz, 1H, =CHR), 2.0–1.2(m, 44H, P−CH_2, cyp and ^{c}Pr). $^{31}P\{^1H\}$ NMR (δ, C_6D_6, 121 MHz): 69.8(AB, $^2J_{Pt–P}$ = −57.7, $^1J_{Pt–P}$ = 3153 Hz, P *trans* =CHR), 68.3(AB, $^2J_{Pt–P}$ = −57.7, $^1J_{Pt–P}$ = 2771 Hz, P *trans* =CR_2). **[$\overline{\text{Pt(CH}_2\text{CH=CHC(CH}_2)_2)}$(dcyppe)] 4b:** ^1H NMR (δ, C_6D_6, 500 MHz): 6.35(m, $J_{Pt–H}$ = 92.4 Hz, 1H, =$CHCH_2$), 5.32(t, 6.0, $J_{Pt–H}$ = 78.0 Hz, 1H, =CH−^{c}Pr), 3.20(m, $^2J_{Pt–H}$= 73.2 Hz, 2H, Pt−CH_2), 2.10(m, 2H, P−CH), 2.01(m, 4H, P−CH and CH_2), 1.81(m, 4H, CH_2), 1.6–1.3(m, 28H, CH_2 and ^{c}Pr-*endo*), 1.24(m, 4H, P−CH_2 and ^{c}Pr-*exo*), 1.11(m, 2H, P−CH_2). $^{13}C\{^1H\}$ NMR (δ, C_6D_6, 125 MHz): 154.0(d, 10.4, $J_{Pt–C}$ = 130.6 Hz, =CH−^{c}Pr), 132.7(dd, 10.4, 4.6 Hz, =$CHCH_2$), 37.2(d, 26.0, $J_{Pt–C}$ = 26.0 Hz,

P−CH), 36.7(d, 21.3, $J_{\text{Pt–C}}$ = 19.2 Hz, P−CH), 33.1(dd, 117.9, 7.0, $^{1}J_{\text{Pt–C}}$ = 959.0 Hz, Pt−CR_3), 31.0(d, 6.4, $J_{\text{Pt–C}}$ = 11.4 Hz, CH_2), 29.5(dd, 89.5, 6.3, $^{1}J_{\text{Pt–C}}$ = 297.1 Hz, Pt−CH_2), 29.4(m, CH_2), 26.6(d, 7.0 Hz, CH_2), 26.4(d, 8.7 Hz, CH_2), 25.8(d, 9.8 Hz, CH_2), 25.7(d, 9.3 Hz, CH_2), 23.4(m, P−CH_2), 22.6(m, P−CH_2), 17.8(s, ^{c}Pr). $^{31}P\{^{1}H\}$ NMR (δ, C_6D_6, 121 MHz): 55.4(s, $^{1}J_{\text{Pt–P}}$ = 1801 Hz), 52.6(s, $^{1}J_{\text{Pt–P}}$ = 1828 Hz).

Synthesis of [Pt(ACP)(dbpe)] 3c

[Pt(C_2H_4)(dbpe)] (100 mg, 0.185 mmol) was dissolved in C_6D_6 (0.5 mL) and placed in an NMR tube. BCP (0.02 mL, 1.87 mmol) was added, and the solution heated at 40 °C for 13 days. Solution contains 88% Pt(ACP)(dbpe)] by $^{31}P\{^{1}H\}$ NMR. ^{1}H NMR (δ, C_6D_6, 500 MHz): 6.20(dt, 16.2, 9.6 Hz, 1H, =CHR), 4.98(m, 1H, =CH_2), 4.64(m, 1H, =CH_2), 3.43(m, $^{2}J_{\text{Pt–H}}$ = 62.0 Hz, 1H, =CHR), 1.9–1.5(m, 6H, P−CH_2 and ^{c}Pr), 1.16(d, 12.5 Hz, 9H, ^{t}Bu), 1.15(d, 12.5 Hz, 9H, ^{t}Bu), 1.03(d, 12.0 Hz, 9H, ^{t}Bu), 1.02(d, 12.5 Hz, 9H, ^{t}Bu), 1.0(m, 2H, ^{c}Pr). $^{13}C\{^{1}H\}$ NMR (δ, C_6D_6, 125 MHz): 147.5(t, $J_{\text{P–C}}$ = 4.6, $J_{\text{P–P}}$ = −34.3, $J_{\text{Pt–C}}$ = 56.4 Hz, =CHR), 102.7(t, $J_{\text{P–C}}$ = 8.6, $J_{\text{P–P}}$ = −25.3, $J_{\text{Pt–C}}$ = 42.9 Hz, =CH_2), 44.7(dd, $J_{\text{P–C}}$ = 38.1, 2.0, $J_{\text{P–P}}$ = −57.7, $^{1}J_{\text{Pt–C}}$ = 165.5 Hz, =CHR), 41.4(m, $J_{\text{P–C}}$ = 70.3, 2.3, $J_{\text{P–P}}$ = 65.8, $^{1}J_{\text{Pt–C}}$ = 533.1 Hz, =CR_2), 36.5(dd, $J_{\text{P–C}}$ = 12.8, 4.6, $J_{\text{P–P}}$ = −27.1, $J_{\text{Pt–C}}$ = 46.8 Hz, P−CR_3), 35.8(dd, $J_{\text{P–C}}$ = 11.5, 5.1, $J_{\text{P–P}}$ = −24.3, $J_{\text{Pt–C}}$ = 44.0 Hz, P−CR_3), 35.5(dd, $J_{\text{P–C}}$ = 13.2, 3.4, $J_{\text{P–P}}$ = −31.2, $J_{\text{Pt–C}}$ = 53.8 Hz, P−CR_3), 34.8(dd, $J_{\text{P–C}}$ = 14.5, 5.4, $J_{\text{P–P}}$ = −31.2, $J_{\text{Pt–C}}$ = 60.0 Hz, P−CR_3), 30.5–29.5(m, CH_3), 26.4(t, 35.8, $J_{\text{Pt–C}}$ = 12.7 Hz, P−CH_2), 25.2(t, 18.0, $J_{\text{Pt–C}}$ = 10.4 Hz, P−CH_2), 10.6(t, $J_{\text{P–C}}$ = 3.3, $J_{\text{P–P}}$ = −10.4, $J_{\text{Pt–C}}$ = 17.7 Hz, ^{c}Pr), 9.5(t, $J_{\text{P–C}}$ = 2.0, $J_{\text{P–P}}$ = −8.9, $J_{\text{Pt–C}}$ = 15.5 Hz, ^{c}Pr). $^{31}P\{^{1}H\}$ NMR (δ, C_6D_6, 121 MHz): 96.4(AB, $^{2}J_{\text{Pt–P}}$ = 62.2, $^{1}J_{\text{Pt–P}}$ = 2848 Hz, P *trans* =CR_2), 96.4(AB, $^{2}J_{\text{Pt–P}}$ = 62.2, $^{1}J_{\text{Pt–P}}$ = 3196 Hz, P *trans* =CHR). m/z = $[M + H]^+$ calcd for $C_{24}H_{49}P_2{}^{194}Pt$ 593.2936; found 593.2946.

Synthesis of [Pt(BCP)(C_2H_4)(PPh_3)] 5a

[Pt(C_2H_4)$_2$(PPh_3)] (20 mg, 0.039 mmol) was dissolved in hexane (2 mL) under an ethene atmosphere. BCP (3.6 μL, 0.34 mmol) was added, and the reaction stirred for 5 min.

The solution was cooled to −78 °C for an hour, after which the supernatant was decanted off, leaving a white solid ([Pt(BCP)(C_2H_4)(PPh_3)], 15 mg, 0.027 mmol, 70%). ^{1}H NMR (δ, C_6D_6, 500 MHz): 7.52(m, 6H, *o*-C_6H_5), 7.00(m, 9H, *m*- and *p*-C_6H_5), 2.71(s, $^2J_{Pt–H}$ = 51.0 Hz, 4H, =CH_2), 1.2–0.8(brs, 8H, ^{c}Pr). ^{13}C{^{1}H} NMR (δ, C_6D_6, 125 MHz): 134.6(d, 43.1, $J_{Pt–C}$ = 25.5 Hz, *i*-C_6H_5), 134.2(d, 12.4, $J_{Pt–C}$ = 18.2 Hz, *o*-C_6H_5), 129.9(d, 2.4 Hz, *m*-C_6H_5), 128.4(s, *p*-C_6H_5), 54.8(d, 2.9, $^1J_{Pt–C}$ = 102.2 Hz, =CH_2), 30.2(d, 16.3, $^1J_{Pt–C}$ = 431.5 Hz, =CR_2), 9.2–6.8(brs, ^{c}Pr). ^{31}P{^{1}H} NMR (δ, C_6D_6, 121 MHz): 23.2(s, $^1J_{Pt–P}$ = 3094 Hz).

Synthesis of [Pt(BCP)(C_2H_4)(PCy_3)] 5b

[Pt(C_2H_4)$_2$(PCy_3)] (63 mg, 0.12 mmol) was dissolved in hexane (3 mL) under an ethene atmosphere. An excess of BCP (0.02 mL, 1.9 mmol) was added, and the solution stirred for 30 min. The solution was reduced to approximately 0.5 mL and cooled to −78 °C. After an hour, the supernatant was decanted, leaving a pale yellow solid ([Pt(BCP)(C_2H_4)(PCy_3)], 53 mg, 0.091 mmol, 76%). ^{1}H NMR (δ, C_6D_6, 500 MHz): 2.68(s, $^2J_{Pt–H}$ = 50.0 Hz, 4H, =CH_2), 2.03(d, 10.0, $J_{Pt–H}$ = 23.0 Hz, 3H, P−CH) 1.86(d, 12.5 Hz, 6H, CH_2), 1.64(d, 11.0 Hz, 6H, CH_2), 1.54(d, 12.5 Hz, 3H, CH_2), 1.35(qm, 13.0 Hz, 6H, CH_2), 1.17–1.05(m, 11H, CH_2 and ^{c}Pr), 1.02(quintt, 13.0, 3.0 Hz, 6H, CH_2). ^{13}C{^{1}H} NMR (δ, C_6D_6, 125 MHz): 50.7(d, 1.9, $^1J_{Pt–C}$ = 101.8 Hz, =CH_2), 36.5(d, 20.6, $J_{Pt–C}$ = 26.0 Hz, P−CH), 30.3(s, $J_{Pt–C}$ = 17.8 Hz, CH_2), 29.1(s, $^1J_{Pt–C}$ = 482.9 Hz, =CR_2), 27.9(d, 10.1 Hz, CH_2), 26.8(s, CH_2), 8.3(brs, $J_{Pt–C}$ = 23.8 Hz, ^{c}Pr). ^{31}P{^{1}H} NMR (δ, C_6D_6, 121 MHz): 25.3(s, $^1J_{Pt–P}$ = 2976 Hz).

Synthesis of [Pt(MCP)(C_2H_4)(PPh_3)] 6a

[Pt(C_2H_4)$_2$(PPh_3)] (10 mg, 0.019 mmol) was dissolved in hexane (1.5 mL) under an ethene atmosphere. An excess of MCP was added, and the solution flushed with C_2H_4 for 5 min. The volume was reduced to ∼0.5 mL, and the solution cooled to −78 °C for an hour. The supernatant was decanted off, leaving pale white crystals. Solution contains 47% [Pt(MCP)(C_2H_4)(PPh_3)] by ^{31}P{^{1}H} NMR. ^{1}H NMR (δ, C_6D_6, 500 MHz): 7.52(m, 6H,

o-C_6H_5), 7.01(m, 9H, *m*- and *p*-C_6H_5), 2.61(s, $^2J_{Pt–H}$ = 56.0 Hz, 4H, C_2H_4 =CH_2), 2.58(d, 6.5, $^2J_{Pt–H}$ = 61.5 Hz, 2H, MCP =CH_2), 1.64(brd, 7.5, $J_{Pt–H}$ = 60.0 Hz, 2H, ^{c}Pr), 1.55(d, 5.5, $J_{Pt–H}$ = 34.0 Hz, 2H, ^{c}Pr). $^{31}P\{^1H\}$ NMR (δ, C_6D_6, 121 MHz): 23.6(s, $^1J_{Pt–P}$ = 3085 Hz).

Synthesis of [Pt(MCP)(C_2H_4)(PCy_3)] 6b

[Pt(C_2H_4)$_2$(PCy_3)] (12 mg, 0.023 mmol) was placed in an NMR tube under an ethene atmosphere, and C_6D_6 (0.5 mL) added. An excess of MCP was added, and the solution flushed with C_2H_4 for 5 min. Solution contains 94% [Pt(MCP)(C_2H_4)(PCy_3)] by $^{31}P\{^1H\}$ NMR. In the presence of excess MCP, [Pt(MCP)$_2$(PCy_3)] forms overnight. ^{1}H NMR (δ, C_6D_6, 500 MHz): 2.52(d, 6.3, $^2J_{Pt–H}$ = 61.2 Hz, 2H, MCP =CH_2), 2.49(s, $^2J_{Pt–H}$ = 48.1 Hz, 4H, C_2H_4 =CH_2), 2.20(m, 3H, P−CH), 1.90(d, 12.0 Hz, 6H, CH_2), 1.7–1.5(m, 9H, CH_2), 1.5–0.9(m, 19H, CH_2 and ^{c}Pr). $^{31}P\{^1H\}$ NMR (δ, C_6D_6, 121 MHz): 28.0(s, $^1J_{Pt–P}$ = 2978 Hz).

Synthesis of [Pt(MCP)$_2$(PPh_3)] 7a

[Pt(C_2H_4)$_2$(PPh_3)] (70 mg, 0.14 mmol) was suspended in hexane (5 mL). An excess of MCP was added, and the reaction stirred for 15 min. Hexane was added to dissolve the remaining solid. The solution was cooled to −78 °C for an hour, after which the supernatant was decanted off, leaving an off-white solid. Solid was 90% [Pt(MCP)$_2$(PPh_3)] **7a**, 10% [Pt(MCP)(C_2H_4)(PPh_3)] **6a**. X-ray quality crystals of [Pt(MCP)$_2$(PPh_3)] were grown by recrystallization from hexane containing a few drops of MCP. ^{1}H NMR (δ, C_6D_6, 500 MHz): 7.52(m, 6H, *o*-C_6H_5), 7.00(m, 9H, *m*- and *p*-C_6H_5), 2.39(d, 4.0, $^2J_{Pt–H}$ = 55.0 Hz, 4H, =CH_2), 1.31(m, 4H, ^{c}Pr). $^{13}C\{^1H\}$ NMR (δ, C_6D_6, 125 MHz): 138.8(d, 39.1, $J_{Pt–C}$ = 26.9 Hz, *i*-C_6H_5), 134.2(m, *o*-C_6H_5), 129.8(d, 2.4Hz, *m*-C_6H_5), 128.4(s, *p*-C_6H_5), 54.1(d, 16.3, $^1J_{Pt–C}$ = 352.9 Hz, =CR_2), 38.9(s, $^1J_{Pt–C}$ = 100.3 Hz, =CH_2), 7.8(s, $J_{Pt–C}$ = 24.5 Hz, ^{c}Pr). $^{31}P\{^1H\}$ NMR (δ, C_6D_6, 121 MHz): 22.3(s, $^1J_{Pt–P}$ = 2932 Hz).

Synthesis of $[Pt(MCP)_2(PCy_3)]$ 7b

$[Pt(C_2H_4)_2(PCy_3)]$ (12mg, 0.023 mmol) was placed in an NMR tube under an ethene atmosphere, and C_6D_6 (0.5 mL) added. A large excess of MCP was added, and Ar bubbled through the solution for 5 min. Solution contains 99% $[Pt(MCP)_2(PCy_3)]$ by $^{31}P\{^1H\}$ NMR. ^1H NMR (δ, C_6D_6, 500 MHz): 2.27(d, 6.0, $^2J_{Pt-H}$ = 50.0 Hz, 4H, $=CH_2$), 2.21(d, 8.5, J_{Pt-H} = 24.0 Hz, 3H, P−CH), 1.88(d, 12.0 Hz, 6H, CH_2), 1.65(dd, 13.0, 2.0 Hz, 6H, CH_2), 1.55(d, 12.0 Hz, 3H, CH_2), 1.47–1.29(m, 11H, CH_2 and ^{c}Pr), 1.13(m, 6H, CH_2), 1.03(m, 6H, CH_2). $^{13}C\{^1H\}$ NMR (δ, C_6D_6, 125 MHz): 48.5(brd, 28.3, $^1J_{Pt-C}$ = 385.6 Hz, $=CR_2$), 36.7(d, 21.1, J_{Pt-C}= 26.9 Hz, P−CH), 32.0(m, $=CH_2$), 30.3(s, J_{Pt-C} = 18.2 Hz, CH_2), 28.0(d, 10.2 Hz, CH_2), 26.9(s, CH_2), 7.2(s, J_{Pt-C} = 25.0 Hz, ^{c}Pr). $^{31}P\{^1H\}$ NMR (δ, C_6D_6): 23.2(s, $^1J_{Pt-P}$= 2695 Hz).

6.3 Chapter Three Experimental

Synthesis of $[Pt(BCP)(^tBu_2PCH_2(o\text{-}C_6H_4)CH_2S^tBu)]$ 8 and $[\overline{Pt(\eta^3\text{-}C(CH_2)_2CHCHMe)(C_6H_3\text{-}o\text{-}CH_2P}^tBu_2\text{-}m\text{-}CH_2S^tBu)]$ (P *trans* ^{c}Pr) 11a and (P *trans* Me) 11b

$[Pt(nb)(^tBu_2PCH_2(o\text{-}C_6H_4)CH_2S^tBu)]$ (30 mg, 0.048 mmol) was placed in a NMR tube and C_6D_6 (0.5 mL) added. Carbon-13 enriched BCP (0.08 mL of a 0.62 mmol/mL sln in C_6D_6, 0.050 mmol, 1.03 eq.) was added, resulting in the immediate formation of $[Pt(BCP)(^tBu_2PCH_2(o\text{-}C_6H_4)CH_2S^tBu)]$ **8**. After an hour, $[\overline{Pt(\eta^3\text{-}C(CH_2)_2CHCHMe)(C_6H_3\text{-}o\text{-}CH_2P}^tBu_2\text{-}m\text{-}CH_2S^tBu)]$ (P *trans* ^{c}Pr) **11a** and $[\overline{Pt(\eta^3\text{-}C(CH_2)_2CHCHMe)(C_6H_3\text{-}o\text{-}CH_2P}^tBu_2\text{-}m\text{-}CH_2S^tBu)]$ (P *trans* Me) **11b** begin to form, reaching 98% completion by $^{31}P\{^1H\}$ NMR after 8 days (85% **11a**, 15% **11b**). **$[Pt(BCP)(^tBu_2PCH_2(o\text{-}C_6H_4)CH_2S^tBu)]$ 8:** ^1H NMR (δ, C_6D_6, 600 MHz): 7.10(d, 7.6 Hz, 1H, o-C_6H_4), 7.06(d, 7.3 Hz, 1H, o-C_6H_4), 7.01(t, 7.4 Hz, 1H, m-C_6H_4), 6.95((t, 7.3 Hz, 1H, m-C_6H_4), 4.11(s, J_{Pt-H} = 28.5 Hz, 2H, S−CH_2), 3.23(d, 8.5, J_{Pt-H} = 17.0 Hz, 2H, P−CH_2), 1.22(s, 9H, S ^{t}Bu), 1.16(d, 12.7 Hz, 18 H, P ^{t}Bu). Data for ^{c}Pr protons could not be obtained. $^{13}C\{^1H\}$ NMR (δ, C_6D_6, 150 MHz): 138.5(s, S i-C_6H_4), 136.1(d,

2.9 Hz, P *i*-C_6H_4), 131.9(d, 2.3 Hz, P *o*-C_6H_4), 131.2(d, 3.5 Hz, S *o*-C_6H_4), 127.2(d, 1.8 Hz, P *m*-C_6H_4), 127.0(d, 2.3 Hz, S *m*-C_6H_4), 49.6(d, 4.0 Hz, S−CR_3), 38.5(d, 2.9, $J_{Pt–C}$ = 32.3 Hz, S−CH_2), 36.2(d, 14.4, $J_{Pt–C}$ = 55.5 Hz, P−CR_3), 29.9(d, 6.4 Hz, P CH_3), 29.8(s, $J_{Pt–C}$ = 12.8 Hz, S CH_3), 28.4(d, 4.6 Hz, P−CH_2), 28.2(d, 78.0, $^1J_{Pt–C}$ = 579.0 Hz, =CR_2 *trans* P), 25.2(d, 5.2, $^1J_{Pt–C}$ = 656.6 Hz, =CR_2 *trans* S), 9.0(brs, ^{c}Pr), 8.7(brs, ^{c}Pr). $^{31}P\{^1H\}$ NMR (δ, C_6D_6, 121 MHz): 54.9(s, $^1J_{Pt–P}$ = 3383 Hz). **[Pt(η^3-C(CH_2)$_2$CHCHMe)(C_6H_3-*o*-$CH_2P^tBu_2$-*m*-CH_2S^tBu)] (P *trans* ^{c}Pr) 11a:** ^{1}H NMR (δ, C_6D_6, 500 MHz): 7.52(t, 4.5, $J_{Pt–H}$ = 59.5 Hz, 1H, Ar-H), 7.10(d, 4.5 Hz, 2H, Ar-H), 4.85(t, 13.5, $J_{Pt–H}$ = 13.0 Hz, 1H, CHMe), 4.54(d, 8.0, $J_{Pt–H}$ = 39.0 Hz, 1H, CH), 3.80(d, 12.5, $J_{Pt–H}$ = 22.0 Hz, 2H, S−CH_2), 3.55(dd, 17.0, 10.0, $J_{Pt–H}$ = 29.0 Hz, 1H, P−CH_2), 3.26(dd, 17.0, 8.0, $J_{Pt–H}$ = 8.0 Hz, 1H, P−CH_2), 1.63(d, 6.5 Hz, 3H, CH_3), 1.56(m, 2H, ^{c}Pr), 1.29(s, 9H, S ^{t}Bu), 1.26(m, 2H, ^{c}Pr), 1.15(d, 13.0 Hz, 9H, P ^{t}Bu), 1.08(d, 13.0 Hz, 9H, P ^{t}Bu). $^{13}C\{^1H\}$ NMR (δ, C_6D_6, 125 MHz): 153.9(d, 2.4, $^1J_{Pt–C}$ = 1192.1, Pt−C), 151.4(d, 15.3, $J_{Pt–C}$ = 72.0 Hz, P *i*-C_6H_4), 136.9(d, 2.9, $J_{Pt–C}$ = 48.9 Hz, Ar), 131.7(d, 12.4, $J_{Pt–C}$ = 59.5 Hz, S *i*-C_6H_4), 126.6(s, $J_{Pt–C}$ = 9.3 Hz, Ar), 126.3(s, Ar), 98.6(d, 4.3, $^1J_{Pt–C}$ = 21.1 Hz, CH), 74.1(s, $^1J_{Pt–C}$ = 32.6 Hz, CHMe), 53.5(d, 76.3, $^1J_{Pt–C}$ = 447.4 Hz, C(CH_2)$_2$), 42.4(s, S−CR_3), 35.7(s, $J_{Pt–C}$ = 13.8 Hz, S−CH_2), 35.4(d, 18.2, $J_{Pt–C}$ = 31.7 Hz, P−CR_3), 34.3(d, 21.1, $J_{Pt–C}$ = 52.3 Hz, P−CR_3), 31.4(d, 33.6, $J_{Pt–C}$ = 89.4 Hz, P−CH_2), 30.9(s, S CH_3), 29.4(d, 4.7, P CH_3), 29.3(d, 5.2, P CH_3), 17.3(s, $J_{Pt–C}$ = 27.9 Hz, CH_3), 7.7(d, 4.3, $J_{Pt–H}$ = 25.9 Hz, ^{c}Pr), 3.7(brs, $J_{Pt–H}$ = 18.0 Hz, ^{c}Pr). $^{31}P\{^1H\}$ NMR (δ, C_6D_6, 121 MHz): 82.0(s, $^1J_{Pt–P}$ = 3141 Hz). **[Pt(η^3-C(CH_2)$_2$CHCHMe)(C_6H_3-*o*-$CH_2P^tBu_2$-*m*-CH_2S^tBu)] (P *trans* Me) 11b:** ^{1}H NMR (δ, C_6D_6, 600 MHz): 8.45(dd, 6.4, 2.3 $J_{Pt–H}$ = 46.7 Hz, 1H, Ar-H), 7.10(d, 4.7 Hz, 2H, Ar-H), 4.82(d, 7.5, $J_{Pt–H}$ = 41.6 Hz, 1H, CH), 4.57(m, 1H, CHMe), 3.82(d, 19.3, $J_{Pt–H}$ = 30.7 Hz, 2H, S−CH_2), 3.66(dd, 17.0, 9.6 Hz, 1H, P−CH_2), 3.33(dd, 17.0, 8.8 Hz, 1H, P−CH_2), 1.65(dd, 6.4, 4.7 Hz, 3H, CH_3), 1.38(m, 2H, ^{c}Pr), 1.29(s, 9H, S ^{t}Bu), 1.26(m, 1H, ^{c}Pr), 1.16(d, 13.6 Hz, 9H, P ^{t}Bu), 1.12(d, 13.6 Hz, 9H, P ^{t}Bu), 1.1(m, 1H, ^{c}Pr). $^{13}C\{^1H\}$ NMR (δ, C_6D_6, 150 MHz): 159.9(d, 2.8, $^1J_{Pt–C}$ = 1043.3, Pt−C), 150.5(d, 13.3, P *i*-C_6H_4), 142.7(d, 2.8, $J_{Pt–C}$ = 41.7 Hz, Ar),

131.8(d, 17.3, $J_{Pt–C}$ = 60.0 Hz, S *i*-C_6H_4), 126.2(s, $J_{Pt–C}$ = 7.1 Hz, Ar), 126.1(s, Ar), 102.8(brs, $^1J_{Pt–C}$ = 7.1 Hz, CH), 84.3(d, 30.1, $^1J_{Pt–C}$ = 130.6 Hz, CHMe), 48.1(s, $^1J_{Pt–C}$ = 202.3 Hz, $C(CH_2)_2$), 42.3(s, S−CR_3), 36.1(d, 23.2, $J_{Pt–C}$ = 63.9 Hz, P−CR_3), 35.9(s, $J_{Pt–C}$ = 12.2 Hz, S−CH_2), 34.3(d, 23.7, $J_{Pt–C}$ = 54.8 Hz, P−CR_3), 33.0(d, 35.3, $J_{Pt–C}$ = 80.8 Hz, P−CH_2), 30.9(s, S CH_3), 29.2(d, 4.1, $J_{Pt–C}$ = 14.0 Hz, P CH_3), 28.7(d, 4.6, $J_{Pt–C}$ = 19.6 Hz, P CH_3), 16.8(d, 4.6, $J_{Pt–C}$ = 41.6 Hz, CH_3), 9.0(s, $J_{Pt–H}$ = 15.0 Hz, ^{c}Pr) 6.6(s, ^{c}Pr). $^{31}P\{^1H\}$ NMR (δ, C_6D_6, 121 MHz): 80.1(s, $^1J_{Pt–P}$ = 3893 Hz). *m/z* = [M^+ calcd for $C_{26}H_{43}P$ ^{194}PtS 613.2468; found 613.2473.

Synthesis of [Pt(MCP)(^{t}Bu$_2$PCH$_2$(*o*-C$_6$H$_4$)CH$_2$S^{t}Bu)] 9 and [Pt(η^3-CH$_2$CHCHMe)(C$_6$H$_3$-*o*-CH$_2$P^{t}Bu$_2$-*m*-CH$_2$S^{t}Bu)] (P *trans* Me) 12a and (P *trans* CH$_2$) 12b

[Pt(nb)(^{t}Bu$_2$PCH$_2$(*o*-C_6H_4)CH_2S^{t}Bu)] (35 mg, 0.056 mmol) was placed in a NMR tube and C_6D_6 (0.5 mL) added. MCP (0.16 mL of a 0.37 mmol/mL sln in C_6D_6, 0.059 mmol, 1.06 eq.) was added, resulting in the immediate formation of [Pt(MCP)(^{t}Bu$_2$PCH$_2$(*o*-C_6H_4)CH_2S^{t}Bu)] (S *trans* ^{c}Pr) **9a** and [Pt(MCP)(^{t}Bu$_2$PCH$_2$(*o*-C_6H_4)CH_2S^{t}Bu)] (P *trans* ^{c}Pr) **9b** (62% **9a**, 38% **9b**, 80% completion by $^{31}P\{^1H\}$ NMR). Overnight, [Pt(η^3-CH_2CHCHMe)(C_6H_3-*o*-CH_2P^{t}Bu$_2$-*m*-CH_2S^{t}Bu)] (P *trans* Me) **12a** and [Pt(η^3-CH_2CHCHMe)(C_6H_3-*o*-CH_2P^{t}Bu$_2$-*m*-CH_2S^{t}Bu)] (P *trans* CH_2) **12b** began to form, reaching 95% completion by $^{31}P\{^1H\}$ NMR after 21 days (63% **12a**, 37% **12b**). **[Pt(MCP)(^{t}Bu$_2$PCH$_2$(*o*-C$_6$H$_4$)CH$_2$S^{t}Bu)] (S *trans* ^{c}Pr) 9a:** ^{1}H NMR (δ, C_6D_6, 600 MHz): 7.12(d, 7.3 Hz, 2H, *o*-C_6H_4), 7.03(t, 7.3 Hz, 1H, *m*-C_6H_4), 6.97((t, 6.1 Hz, 1H, *m*-C_6H_4), 4.19(s, $J_{Pt–H}$ = 26.8 Hz, 2H, S−CH_2), 3.27(d, 8.4, $J_{Pt–H}$ = 14.4 Hz, 2H, P−CH_2), 2.05(d, 8.2, $J_{Pt–H}$ = 52.7 Hz, 2H, =CH_2), 1.45(brs, 2H, ^{c}Pr), 1.37(brs, 2H, ^{c}Pr), 1.34(s, 9H, S ^{t}Bu), 1.25(d, 12.3 Hz, 9H, P ^{t}Bu), 1.17(d, 12.6 Hz, 9H, P ^{t}Bu). $^{13}C\{^1H\}$ NMR (δ, C_6D_6, 150 MHz): 138.9(s, S *i*-C_6H_4), 136.6(d, 3.5 Hz, P *i*-C_6H_4), 132.0(d, 2.3 Hz, P *o*-C_6H_4), 131.4(d, 4.1 Hz, S *o*-C_6H_4), 127.1(d, 1.2 Hz, *m*-C_6H_4), 126.9(d, 2.3 Hz, *m*-C_6H_4), 50.5(d, 4.0 Hz, S−CR_3), 38.8(d, 2.3, $J_{Pt–C}$ = 31.1 Hz, S−CH_2), 37.2(d, 13.9, $J_{Pt–C}$ = 52.6 Hz, P−CR_3), 30.1(s, $J_{Pt–C}$ = 14.5 Hz, S CH_3),

29.8(brd, 6.9, $J_{Pt–C}$ = 29.6 Hz, P CH_3), 28.9(d, 5.2 Hz, P−CH_2), 26.3(d, 38.7, $^1J_{Pt–C}$ = 145.1 Hz, =CH_2), 10.5(d, 1.7, $J_{Pt–C}$ = 30.1 Hz, ^{c}Pr). Data for MCP =CR_2 carbon could not be obtained. $^{31}P\{^1H\}$ NMR (δ, C_6D_6, 121 MHz): 58.8(s, $^1J_{Pt–P}$ = 3870 Hz). **[Pt(MCP)(^{t}Bu$_2$PCH$_2$(*o*-C$_6$H$_4$)CH$_2$S^{t}Bu)] (P *trans* ^{c}Pr) 9b:** ^{1}H NMR (δ, C_6D_6, 600 MHz): 7.14(d, 7.5 Hz, 1H, *o*-C_6H_4), 7.10(d, 7.5 Hz, 1H, *o*-C_6H_4), 7.01(t, 6.6 Hz, 1H, *m*-C_6H_4), 6.96((t, 6.1 Hz, 1H, *m*-C_6H_4), 4.20(s, $J_{Pt–H}$ = 31.4 Hz, 2H, S−CH_2), 3.27(d, 8.4, $J_{Pt–H}$ = 18.8 Hz, 2H, P−CH_2), 2.38(d, 4.2, $J_{Pt–H}$ = 82.1 Hz, 2H, =CH_2), 1.59(m, 2H, ^{c}Pr), 1.50(m, 2H, ^{c}Pr), 1.29(d, 12.3 Hz, 9H, P ^{t}Bu), 1.26(d, 12.0 Hz, 9H, P ^{t}Bu), 1.21(s, 9H, S ^{t}Bu). $^{13}C\{^1H\}$ NMR (δ, C_6D_6, 150 MHz): 138.9(s, S *i*-C_6H_4), 136.5(d, 2.9 Hz, P *i*-C_6H_4), 132.2(d, 1.7 Hz, P *o*-C_6H_4), 131.4(d, 4.0 Hz, S *o*-C_6H_4), 127.0(brs, *m*-C_6H_4), 127.0(d, 2.3 Hz, *m*-C_6H_4), 49.2(d, 4.7 Hz, S−CR_3), 39.5(d, 4.1, $J_{Pt–C}$ = 34.1 Hz, S−CH_2), 36.1(d, 15.1, $J_{Pt–C}$ = 63.0 Hz, P−CR_3), 30.3(brd, 5.2 Hz, $J_{Pt–C}$ = 16.3 Hz, P CH_3), 29.4(s, $J_{Pt–C}$ = 13.8 Hz, S CH_3), 28.9(d, 1.5 Hz, P−CH_2), 25.7(d, 5.7, $^1J_{Pt–C}$ = 270.6 Hz, =CH_2), 10.0(s, $J_{Pt–C}$ = 24.8 Hz, ^{c}Pr). Data for MCP =CR_2 carbon could not be obtained. $^{31}P\{^1H\}$ NMR (δ, C_6D_6, 121 MHz): 55.3(s, $^1J_{Pt–P}$ = 3483 Hz). **[Pt(η^3-CH$_2$CHCHMe)(C$_6$H$_3$-*o*-CH$_2$P^{t}Bu$_2$-*m*-CH$_2$S^{t}Bu)] (P *trans* Me) 12a:** ^{1}H NMR (δ, C_6D_6, 600 MHz): 8.49(t, 7.3, $J_{Pt–H}$ = 55.2 Hz, 1H, Ar-H), 7.1(m, 2H, Ar-H), 4.61(dt, 13.3, 7.7, $J_{Pt–H}$ = 41.9 Hz, 1H, CH), 4.34(m, 1H, CHMe), 3.83(m, 2H, S−CH_2), 3.58(dt, 7.6, 1.2 Hz, 1H, CH_2 *syn*), 3.57(dd, 16.7, 9.1, $J_{Pt–H}$ = 42.5 Hz, 1H, P−CH_2), 3.42(d, 9.1, $J_{Pt–H}$ = 15.4 Hz, 1H, P−CH_2), 2.27(d, 13.2, $J_{Pt–H}$ = 38.1 Hz, 1H, CH_2 *anti*), 1.39(dd, 6.4, 5.6 Hz, 3H, CH_3), 1.29(s, 9H, S ^{t}Bu), 1.16(d, 13.5 Hz, 9H, P ^{t}Bu), 1.09(d, 13.5 Hz, 9H, P ^{t}Bu). $^{13}C\{^1H\}$ NMR (δ, C_6D_6, 150 MHz): 158.4(d, 2.3, $^1J_{Pt–C}$ = 1142.7, Pt−C), 151.0(d, 14.4, $J_{Pt–C}$ = 80.3 Hz, P *i*-C_6H_4), 142.7(d, 3.2, $J_{Pt–C}$ = 52.1 Hz, Ar), 131.9(d, 12.7, $J_{Pt–C}$ = 56.0 Hz, S *i*-C_6H_4), 126.5(s, Ar), 126.2(s, $J_{Pt–C}$ = 8.7 Hz, Ar), 108.2(d, 2.4, $^1J_{Pt–C}$ = 8.4 Hz, CH), 73.4(d, 37.0, $^1J_{Pt–C}$ = 173.4 Hz, CHMe), 42.5(s, $^1J_{Pt–C}$ = 52.0 Hz, CH_2), 42.3(s, S−CR_3), 35.9(s, $J_{Pt–C}$ = 13.8 Hz, S−CH_2), 34.6(d, 22.5, $J_{Pt–C}$ = 54.3 Hz, P−CR_3), 34.1(d, 23.2, $J_{Pt–C}$ = 43.8 Hz, P−CR_3), 32.0(d, 34.7, $J_{Pt–C}$ = 82.6 Hz, P−CH_2), 30.9(s, S CH_3), 29.3(d, 1.7, P CH_3), 29.3(d, 1.7, P CH_3), 15.3(d, 5.2, $J_{Pt–C}$ = 39.9 Hz, CH_3). $^{31}P\{^1H\}$ NMR (δ, C_6D_6, 121 MHz): 84.1(s, $^1J_{Pt–P}$

= 3560 Hz). **[Pt(η^3-$CH_2CHCHMe$)(C_6H_3-*o*-$CH_2P^tBu_2$-*m*-CH_2S^tBu)] (P *trans* CH_2) 12b:** ^{1}H NMR (δ, C_6D_6, 600 MHz): 8.51(d, 7.0, J_{Pt-H} = 58.3 Hz, 1H, Ar-H), 7.1(m, 2H, Ar-H), 4.61(dt, 13.3, 7.7, J_{Pt-H} = 41.9 Hz, 1H, CH), 4.39(quint, 5.1 Hz, 1H, CHMe), 3.83(m, 2H, S−CH_2), 3.6(m, 1H, CH_2 *syn*), 3.51(dd, 9.1, 2.1, J_{Pt-H} = 20.0 Hz, 1H, P−CH_2), 3.39(d, 9.1, J_{Pt-H} = 14.6 Hz, 1H, P−CH_2), 2.92(ddd, 12.9, 9.7, 2.1 Hz, 1H, CH_2 *anti*), 1.29(d, 11.8 Hz, 3H, CH_3), 1.29(s, 9H, S ^{t}Bu), 1.15(d, 13.5 Hz, 9H, P ^{t}Bu), 1.07(d, 13.5 Hz, 9H, P ^{t}Bu). ^{13}C{^{1}H} NMR (δ, C_6D_6, 150 MHz): 155.5(d, 2.4, $^1J_{Pt-C}$ = 1132.8, Pt−C), 151.1(d, 14.5, J_{Pt-C} = 81.0 Hz, P *i*-C_6H_4), 144.5(d, 4.0, J_{Pt-C} = 58.4 Hz, Ar), 131.8(d, 12.8, J_{Pt-C} = 55.3 Hz, S *i*-C_6H_4), 126.3(s, J_{Pt-C} = 7.5 Hz, Ar), 126.0(s, Ar), 108.7(d, 3.4, $^1J_{Pt-C}$ = 11.0 Hz, CH), 62.5(s, $^1J_{Pt-C}$ = 48.6 Hz, CHMe), 53.1(d, 40.4, $^1J_{Pt-C}$ = 182.6 Hz, CH_2), 42.4(s, S−CR_3), 35.8(s, J_{Pt-C} = 13.8 Hz, S−CH_2), 34.8(d, 13.8, J_{Pt-C} = 40.6 Hz, P−CR_3), 34.7(d, 16.1, J_{Pt-C} = 59.0 Hz, P−CR_3), 32.2(d, 34.6, J_{Pt-C} = 82.0 Hz, P−CH_2), 30.9(s, S CH_3), 29.4(d, 5.2, P CH_3), 29.4(d, 4.6, P CH_3), 15.6(s, J_{Pt-C} = 26.6 Hz, CH_3). ^{31}P{^{1}H} NMR (δ, C_6D_6, 121 MHz): 82.0(s, $^1J_{Pt-P}$ = 3590 Hz). *m/z* = $[M + H]^+$ calcd for $C_{24}H_{42}P\ ^{194}PtS$ 583.2299; found 583.2344.

Synthesis of [Pt(MCP)$_2$(^{t}Bu$_2$PCH$_2$(*o*-C_6H_4)CH_2S^tBu)] 10

[Pt(nb)(^{t}Bu$_2$PCH$_2$(*o*-C_6H_4)CH_2S^tBu)] (12 mg, 0.019 mmol) was placed in a NMR tube and C_6D_6 (0.5 mL) added. A large excess of MCP was added, resulting in the immediate formation of **9a**, **9b** and [Pt(MCP)$_2$(^{t}Bu$_2$PCH$_2$(*o*-C_6H_4)CH_2S^tBu)] **10** (40% **9a**, 24% **9b**, 36% **10**, quantitative by ^{31}P{^{1}H} NMR). After an hour, **12a** and **12b** began to form. All of the **10** had reacted after 13 days, and the formation of **12a** and **12b** had reached 91% completion by ^{31}P{^{1}H} NMR after 21 days (63% **12a**, 37% **12b**). ^{1}H NMR (δ, C_6D_6, 600 MHz): 7.1(m, 2H, *o*-C_6H_4), 6.89(t, 7.4 Hz, 1H, *m*-C_6H_4), 6.79((t, 7.5 Hz, 1H, *m*-C_6H_4), 4.29(dd, 10.9, 5.3 Hz, 2H, P−CH_2), 4.24(m, 2H, P−CH_2), 3.96(d, 9.4, J_{Pt-H} = 32.6 Hz, 2H, S−CH_2), 2.49(d, 6.4, J_{Pt-H} = 48.1 Hz, 4H, =CH_2), 1.26(s, 9H, S ^{t}Bu), 1.23(d, 12.3 Hz, 18 H, P ^{t}Bu). Data for ^{c}Pr protons could not be obtained. ^{13}C{^{1}H} NMR (δ, C_6D_6, 150 MHz): 142.0(s, S *i*-C_6H_4), 136.4(d, 5.8 Hz, P *i*-C_6H_4), 131.9(d, 7.5 Hz, Ar), 130.9(s, Ar), 126.8(s, Ar), 48.7(brd, 25.7 Hz, $^1J_{Pt-C}$ = 381.9 Hz, =CR_2), 42.6(s, S−CR_3),

37.8(d, 14.5, $J_{Pt–C}$ = 28.8 Hz, S−CH_2), 35.7(brs, $^1J_{Pt–C}$ = 100.6 Hz, =CH_2), 30.9(s, S CH_3), 30.5(d, 4.0 Hz, P CH_3), 26.5(d, 18.5 Hz, $J_{Pt–C}$ = 30.0 Hz, P−CH_2), 7.2(s, $J_{Pt–C}$ = 25.4 Hz, ^{c}Pr). Data for P−CR_3 carbons could not be obtained. $^{31}P\{^1H\}$ NMR (δ, C_6D_6, 121 MHz): 40.6(s, $^1J_{Pt–P}$ = 2661 Hz).

Synthesis of [Pt(η^3-C$(CH_2)_2$CHCHMe)(dppp)][HC$(SO_2CF_3)_2$] (*anti* Me) 13a[HC$(SO_2CF_3)_2$] and [Pt(η^3-C$(CH_2)_2$CHCHMe)(dppp)][HC$(SO_2CF_3)_2$] (*syn* Me) 13b[HC$(SO_2CF_3)_2$]

[Pt(C_2H_4)(dppp)] (30 mg, 0.047 mmol) was placed in an NMR tube and C_6D_6 (0.5 mL) added. Carbon-13 enriched BCP (0.08 mL of a 0.62 mmol/mL sln in C_6D_6, 0.050 mmol, 1.06 eq.) was added, resulting in the immediate formation of [Pt(^{13}BCP)(dppp)]. After 30 min, the solution was dried *in vacuo* and a solution of $H_2C(SO_2CF_3)_2$ (13 mg, 0.047 mmol) in d_6-acetone (0.5 mL) added. Two new complexes, **13a**[HC$(SO_2CF_3)_2$] and **14a** were formed immediately in a 75:25 ratio by $^{31}P\{^1H\}$ NMR. Overnight, **14a** converted completely to **14b**, while **13a**[HC$(SO_2CF_3)_2$] began to form **13b**[HC$(SO_2CF_3)_2$], stabilising at 27:73 *anti*:*syn* after 2 months. **[Pt(η^3-C$(CH_2)_2$CHCHMe)(dppp)][HC$(SO_2CF_3)_2$] (*anti* Me) 13a[HC$(SO_2CF_3)_2$]:** ^{1}H NMR (δ, d_6-acetone, 600 MHz): 7.9–7.3(m, 20H, Ar-H), 5.40(d, 8.2, $J_{Pt–H}$ = 54.0 Hz, 1H, CH), 4.93(m, 1H, CHMe), 3.80(s, 1H, CHS_2), 3.3–2.9(m, 4H, P−CH_2), 2.3(m, 2H, CH_2), 1.21(m, 1H, ^{c}Pr), 0.88(m, 3H, CH_3), 0.86(m, 1H, ^{c}Pr), 0.37(m, 2H, ^{c}Pr). $^{13}C\{^1H\}$ NMR (δ, d_6-acetone, 150 MHz): 134–129(m, Ar), 122.1(q, $^1J_{F–C}$ = 325.4 Hz, CF_3), 104.2(dd, 3.4, 1.7, CH), 91.2(d, 22.6, $^1J_{Pt–C}$ = 65.9 Hz, CHMe), 66.7(d, 54.3, $^1J_{Pt–C}$ = 252.6 Hz, C$(CH_2)_2$), 55.4(m, CHS_2), 26.3(dd, 37.0, 4.1, $J_{Pt–C}$ = 35.8 Hz, P−CH_2), 25.4(dd, 34.7, 2.3, $J_{Pt–C}$ = 17.2 Hz, P−CH_2), 19.4(s, $J_{Pt–C}$ = 17.3 Hz, CH_2), 15.5(d, 4.1, $J_{Pt–C}$ = 33.2, CH_3), 8.1(d, 4.0, $J_{Pt–C}$ = 16.8 Hz, ^{c}Pr), 4.4(s, $J_{Pt–C}$ = 15.6 Hz, ^{c}Pr). $^{31}P\{^1H\}$ NMR (δ, d_6-acetone, 121 MHz): 1.4(d, 21.2, $^1J_{Pt–P}$ = 3852 Hz, P *trans* CHMe), −2.8(d, 21.2, $^1J_{Pt–P}$ = 3259 Hz, P *trans* ^{c}Pr). ^{19}F NMR (δ, d_6-acetone, 282 MHz): −81.5(brs). **[Pt(η^3-C$(CH_2)_2$CHCHMe)(dppp)][HC$(SO_2CF_3)_2$] (*syn* Me) 13b[HC$(SO_2CF_3)_2$]:** ^{1}H NMR (δ, d_6-acetone, 600 MHz): 7.9–7.3(m, 20H, Ar-H), 5.39(d, 12.5, $J_{Pt–H}$ = 51.0 Hz, 1H, CH), 4.14(m, 1H, CHMe), 3.80(s, 1H, CHS_2),

3.3–2.9(m, 4H, P−CH_2), 2.3(m, 2H, CH_2), 1.38(m, 3H, CH_3), 1.22(m, 1H, ^{c}Pr), 0.65(m, 1H, ^{c}Pr), 0.39(m, 1H, ^{c}Pr), 0.14(m, 1H, ^{c}Pr). $^{13}C\{^1H\}$ NMR (δ, d_6-acetone, 150 MHz): 134–129(m, Ar), 122.1(q, $^1J_{F–C}$ = 325.4 Hz, CF_3), 11.6(dd, 4.1, 1.8, CH), 92.6(d, 21.9, $^1J_{Pt–C}$ = 29.0 Hz, CHMe), 67.1(d, 53.2, $^1J_{Pt–C}$ = 269.3 Hz, $C(CH_2)_2$), 55.4(m, CHS_2), 27.2(dd, 34.7, 2.9, P−CH_2), 25.9(dd, 37.0, 3.5, P−CH_2), 19.7(s, $J_{Pt–C}$ = 13.8 Hz, CH_2), 15.9(d, 2.4, CH_3), 8.6(d, 4.0, $J_{Pt–C}$ = 20.8 Hz, ^{c}Pr), 5.7(s, ^{c}Pr). $^{31}P\{^1H\}$ NMR (δ, d_6-acetone, 121 MHz): 1.0(d, 20.8, $^1J_{Pt–P}$ = 4042 Hz, P *trans* CHMe), −0.41(d, 20.8, $^1J_{Pt–P}$ = 3267 Hz, P *trans* ^{c}Pr). ^{19}F NMR (δ, d_6-acetone, 282 MHz): −81.5(brs). m/z = [M^+ calcd for $C_{33}H_{35}P_2{}^{194}Pt$ 683.1767; found 683.1813.

Synthesis of [Pt(η^3-CH_2CMeCH_2)(dppp)][PhC(SO_2CF_3)$_2$] 15[PhC(SO_2CF_3)$_2$], [Pt(η^3-$CH_2CHCHMe$)(dppp)][PhC(SO_2CF_3)$_2$] (*anti* Me) 16a[PhC(SO_2CF_3)$_2$] and [Pt(η^3-$CH_2CHCHMe$)(dppp)][PhC(SO_2CF_3)$_2$] (*syn* Me) 16b[PhC(SO_2CF_3)$_2$]

[Pt(C_2H_4)(dppp)] (30 mg, 0.047 mmol) was placed in an NMR tube and C_6D_6 (0.25 mL) added. MCP (0.25 mL of a 0.37 mmol/mL sln in C_6D_6, 0.093 mmol, 2 eq.) was added, resulting in the immediate formation of [Pt(MCP)(dppp)]. After 30 min, the solution was dried *in vacuo* and a solution of $H_2C(SO_2CF_3)_2$ (13 mg, 0.047 mmol) in d_6-acetone (0.5 mL) added. Two new complexes, **15**[PhC(SO_2CF_3)$_2$] and **16a**[PhC(SO_2CF_3)$_2$] were formed immediately in a 68:32 ratio by $^{31}P\{^1H\}$ NMR. Overnight, **16a**[PhC(SO_2CF_3)$_2$] began to form **16b**[PhC(SO_2CF_3)$_2$], stabilising at 16:84 *anti*:*syn* after 8 days. **Pt(η^3-CH_2CMeCH_2)(dppp)][PhC(SO_2CF_3)$_2$] 15[PhC(SO_2CF_3)$_2$]:** ^{1}H NMR (δ, d_6-acetone, 600 MHz): 7.7–7.1(m, 25H, Ar-H), 3.56(brs, 2H, CH_2 *syn*), 3.2–2.9(m, 6H, P−CH_2 and CH_2), 2.96(d, 8.5, $J_{Pt–H}$ = 32.0 Hz, 2H, CH_2 *anti*), 1.96(s, $J_{Pt–H}$ = 58.4 Hz, 3H, CH_3). $^{13}C\{^1H\}$ NMR (δ, d_6-acetone, 150 MHz): 136.1(s, Ph), 135.9(t, 3.2, $^1J_{Pt–C}$ = 24.8 Hz, CR_2Me), 134–129(m, Ar), 127.8(s, Ph), 127.7(s, Ph), 123.0(q, $^1J_{F–C}$ = 328.9 Hz, CF_3), 66.4(m, $J_{P–C}$ = 27.5, 1.8, $J_{P–P}$ = 24.6, $^1J_{Pt–C}$ = 85.0 Hz, CH_2), 71.5(sept, $J_{F–C}$ = 3.2, CS_2), 25.6(m, P−CH_2), 24.8(s, $J_{Pt–C}$ = 30.0, CH_3), 20.1(s, $J_{Pt–C}$ = 15.0 Hz, CH_2). $^{31}P\{^1H\}$ NMR (δ, d_6-acetone,

121 MHz): 0.1(s, $^{1}J_{\mathrm{Pt–P}}$ = 3521 Hz). ^{19}F NMR (δ, d_6-acetone, 282 MHz): −78.72(s). **[Pt(η^3-$CH_2CHCHMe$)(dppp)][PhC(SO_2CF_3)$_2$] (*anti* Me) 16a[PhC(SO_2CF_3)$_2$]:** ^{1}H NMR (δ, d_6-acetone, 600 MHz): 7.7–7.1(m, 25H, Ar-H), 5.32(dt, 14.1, 7.6, $J_{\mathrm{Pt–H}}$ = 53.4 Hz, 1H, CH), 4.62(t, 6.2, 1H, CHMe), 3.94(m, 1H, CH_2 *syn*), 3.2–2.9(m, 5H, P−CH_2 and CH_2 *anti*), 2.3–2.2(m, 2H, CH_2), 0.80(m, 3H, CH_3). ^{13}C{^{1}H} NMR (δ, d_6-acetone, 150 MHz): 136.1(s, Ph), 134.4-129.5(m, Ar), 127.8(s, Ph), 127.7(s, Ph), 123.0(q, $^{1}J_{\mathrm{F–C}}$ = 328.9 Hz, CF_3), 113.9(t, 3.2, $^{1}J_{\mathrm{Pt–C}}$ = 16.5 Hz, CH), 83.4(m, $^{1}J_{\mathrm{Pt–C}}$ = 83.7 Hz, CHMe), 60.2(m, $^{1}J_{\mathrm{Pt–C}}$ = 88.0 Hz, CH_2), 71.5(sept, $J_{\mathrm{F–C}}$ = 3.2, CS_2), 25.6(m, P−CH_2), 19.7(s, $J_{\mathrm{Pt–C}}$ = 16.8 Hz, CH_2), 14.1(dd, 2.8, 1.1, $J_{\mathrm{Pt–C}}$ = 23.1, CH_3). ^{31}P{^{1}H} NMR (δ, d_6-acetone, 121 MHz): −1.2(AB, $^{2}J_{\mathrm{Pt–P}}$ = 23.0, $^{1}J_{\mathrm{Pt–P}}$ = 3569 Hz, P *trans* CH_2), −1.2(AB, $^{2}J_{\mathrm{Pt–P}}$ = 23.0, $^{1}J_{\mathrm{Pt–P}}$ = 3625 Hz, P *trans* CHMe). ^{19}F NMR (δ, d_6-acetone, 282 MHz): −78.72(s). **[Pt(η^3-$CH_2CHCHMe$)(dppp)][PhC(SO_2CF_3)$_2$] (*syn* Me) 16b[PhC(SO_2CF_3)$_2$]:** ^{1}H NMR (δ, d_6-acetone, 600 MHz): 7.7–7.1(m, 25H, Ar-H), 5.23(td, 12.7, 7.3, $J_{\mathrm{Pt–H}}$ = 51.5 Hz, 1H, CH), 3.68(m, 1H, CHMe), 3.59(m, 1H, CH_2 *syn*), 3.2–2.9(m, 4H, P−CH_2), 2.54(ddd, 12.7, 10.0, 2.7, 1H, CH_2 *anti*), 2.3-2.1(m, 2H, CH_2), 1.29(m, 3H, CH_3). ^{13}C{^{1}H} NMR (δ, d_6-acetone, 150 MHz): 136.1(s, Ph), 134-129(m, Ar), 127.8(s, Ph), 127.7(s, Ph), 123.0(q, $^{1}J_{\mathrm{F–C}}$ = 328.9 Hz, CF_3), 119.3(t, 3.5, $^{1}J_{\mathrm{Pt–C}}$ = 26.6 Hz, CH), 84.3(d, 27.2, $^{1}J_{\mathrm{Pt–C}}$ = 54.4 Hz, CHMe), 62.3(d, 27.8, $^{1}J_{\mathrm{Pt–C}}$ = 100.1 Hz, CH_2), 71.5(sept, $J_{\mathrm{F–C}}$ = 3.2, CS_2), 26.9(dd, 35.8, 3.5, $J_{\mathrm{Pt–C}}$ = 19.6 Hz, P−CH_2), 25.6(m, P−CH_2), 19.9(s, $J_{\mathrm{Pt–C}}$ = 13.8 Hz, CH_2), 15.9(d, 2.9, $J_{\mathrm{Pt–C}}$ = 3.8, CH_3). ^{31}P{^{1}H} NMR (δ, d_6-acetone, 121 MHz): 1.4(AB, $^{2}J_{\mathrm{Pt–P}}$ = 22.0, $^{1}J_{\mathrm{Pt–P}}$ = 3670 Hz, P *trans* CH_2), −1.8(AB, $^{2}J_{\mathrm{Pt–P}}$ = 22.0, $^{1}J_{\mathrm{Pt–P}}$ = 3693 Hz, P *trans* CHMe). ^{19}F NMR (δ, d_6-acetone, 282 MHz): −78.72(s).

Synthesis of [Pt(η^3-$CH_2C^cPrCH_2$)(dbpx)][HC(SO_2CF_3)$_2$] 17[HC(SO_2CF_3)$_2$]

[Pt(C_2H_4)(dbpx)] (30 mg, 0.049 mmol) was placed in an NMR tube and C_6D_6 (0.5 mL) added. Carbon-13 enriched BCP (0.24 mL of a 0.62 mmol/mL sln in C_6D_6, 0.14 mmol, 3 eq.) was added, and the solution heated at 60 °C for 3 days, forming [Pt(^{13}BCP)(dbpx)] in an 90% yield by ^{31}P{^{1}H} NMR. The solution was dried *in vacuo* and a solution of

$H_2C(SO_2CF_3)_2$ (14 mg, 0.049 mmol) in *d*$_6$-acetone (0.5 mL) added, resulting in the immediate formation of [Pt(η^3-$CH_2C^cPrCH_2$)(dbpx)][$HC(SO_2CF_3)_2$]. ^{1}H NMR (δ, *d*$_6$-acetone, 600 MHz): 7.60(brs, 2H, *o*-C_6H_4), 7.28(brs, 2H, *m*-C_6H_4), 4.81(brs, 2H, CH_2 *syn*), 4.2(br, 4H, P−CH_2), 3.86(brs, 1H, CHS_2), 2.74(d, 8.1, J_{Pt-H} = 41.3 Hz, CH_2 *anti*), 1.44(brm, 37H, ^{t}Bu and CH), 0.93(brm, 2H, ^{c}Pr), 0.87(brm, 2H, ^{c}Pr). $^{13}C\{^1H\}$ NMR (δ, *d*$_6$-acetone, 125 MHz): 136.4(brs, *i*-C_6H_4), 134.2(brs, *o*-C_6H_4), 128.0(s, *m*-C_6H_4), 126.4(s, $^1J_{Pt-C}$ = 44.5 Hz, $CR_2{}^cPr$), 122.2(q, $^1J_{F-C}$ = 325.4 Hz, CF_3), 59.1(m, J_{P-C} = 30.2, −2.1, J_{P-P} = 11.2, $^1J_{Pt-C}$ = 79.8 Hz, CH_2), 55.3(sept, J_{F-C} = 1.2 Hz, CS_2), 40.2(brs, P−CH_2), 39.4(brs, P−CR_3), 30.8(brs, CH_3), 15.6(s, J_{Pt-C} = 24.9 Hz, CH), 8.9(brs, ^{c}Pr). $^{31}P\{^1H\}$ NMR (δ, *d*$_6$-acetone, 121 MHz): 33.9(brs, $^1J_{Pt-P}$ = 3632 Hz), 32.1(brs, $^1J_{Pt-P}$ = 3647 Hz). ^{19}F NMR (δ, *d*$_6$-acetone, 282 MHz): −81.6(brs). *m/z* = [M^+ calcd for $C_{30}H_{53}P_2{}^{194}Pt$ 670.3268; found 670.3256.

Synthesis of [Pt(η^3-CH_2CMeCH_2)(dbpx)][$HC(SO_2CF_3)_2$] 18a[$HC(SO_2CF_3)_2$] and [Pt(η^3-$CH_2CHCHMe$)(dbpx)][$HC(SO_2CF_3)_2$] 18b[$HC(SO_2CF_3)_2$]

[Pt(C_2H_4)(dbpx)] (30 mg, 0.049 mmol) was placed in an NMR tube and C_6D_6 (0.5 mL) added. MCP (0.08 mL of a 1.85 mmol/mL sln in C_6D_6, 0.14 mmol, 3 eq.) was added, and the solution heated at 60 °C for 4 days, forming [Pt(MCP)(dbpx)] in an 83% yield by $^{31}P\{^1H\}$ NMR. The solution was dried *in vacuo* and a solution of $H_2C(SO_2CF_3)_2$ (14 mg, 0.049 mmol) in *d*$_6$-acetone (0.5 mL) added, resulting in the immediate formation of [Pt(η^3-CH_2CMeCH_2)(dbpx)][$HC(SO_2CF_3)_2$] and [Pt(η^3-$CH_2CHCHMe$)(dbpx)][$HC(SO_2CF_3)_2$] in a 58:42 ratio. **[Pt(η^3-CH_2CMeCH_2)(dbpx)][$HC(SO_2CF_3)_2$] 18a[$HC(SO_2CF_3)_2$]:** ^{1}H NMR (δ, *d*$_6$-acetone, 600 MHz): 7.60(brs, 2H, *o*-C_6H_4), 7.28(brs, 2H, *m*-C_6H_4), 4.88(brs, 2H, CH_2 *syn*), 4.2(br, 4H, P−CH_2), 3.77(s, 1H, CHS_2), 2.80(d, 8.4, J_{Pt-H} = 39.4 Hz, CH_2 *anti*), 1.45(brm, 39H, ^{t}Bu and CH_3). $^{13}C\{^1H\}$ NMR (δ, *d*$_6$-acetone, 150 MHz): 136.4(brs, *i*-C_6H_4), 134.2(brs, *o*-C_6H_4), 128.1(s, *m*-C_6H_4), 127.9(m, $^1J_{Pt-C}$ = 56.7 Hz, CR_2Me), 122.2(q, $^1J_{F-C}$ = 326.0 Hz, CF_3), 63.3(m, CH_2), 55.3(m, CS_2), 40.7(brs, P−CR_3),

40.2(brs, P−CH_2), 30.8(brs, CH_3), 21.6(s, $J_{Pt–C}$ = 28.4 Hz, CH). $^{31}P\{^1H\}$ NMR (δ, d_6-acetone, 121 MHz): 33.9(brs, $^1J_{Pt–P}$ = 3572 Hz), 32.4(brs, $^1J_{Pt–P}$ = 3641 Hz). ^{19}F NMR (δ, d_6-acetone, 282 MHz): −81.81(s). **[Pt(η^3-$CH_2CHCHMe$)(dbpx)][$HC(SO_2CF_3)_2$] 18b[$HC(SO_2CF_3)_2$]:** ^1H NMR (δ, d_6-acetone, 600 MHz): 7.60(m, 2H, *o*-C_6H_4), 7.28(m, 2H, *m*-C_6H_4), 6.28(brs, 1H, CHMe), 5.04(dt, 12.2, 7.5 Hz, $J_{Pt–H}$ = 51.9 Hz, 1H, CH), 4.53(m, 1H, CH_2 *syn*), 4.2(br, 4H, P−CH_2), 3.77(brs, 1H, CHS_2), 2.86(ddd, 11.1, 10.0, 2.2, $J_{Pt–H}$ = 34.4 Hz, CH_2 *anti*), 1.45(brm, 39H, ^{t}Bu and CH_3). $^{13}C\{^1H\}$ NMR (δ, d_6-acetone, 150 MHz): 136.4(brs, *i*-C_6H_4), 134.1(brs, *o*-C_6H_4), 128.1(s, *m*-C_6H_4), 122.2(q, $^1J_{F–C}$ = 326.0 Hz, CF_3), 106.8(brs, CH), 84.6(brd, 22.0, $^1J_{Pt–C}$ = 63.7 Hz, CHMe), 55.3(m, CS_2), 51.7(brd, 32.4, $^1J_{Pt–C}$ = 106.9 Hz, CH_2), 40.1(brs, P−CH_2), 39.4(brs, P−CR_3), 30.9(dd, 13.9, 3.5 Hz, CH_3), 30.3(d, 2.9, $J_{Pt–C}$ = 15 Hz, CH_3), 16.5(brs, $J_{Pt–C}$ = 14.5 Hz, CH). $^{31}P\{^1H\}$ NMR (δ, d_6-acetone, 121 MHz): 36.9(d, $^1J_{Pt–P}$ = 3844 Hz). ^{19}F NMR (δ, d_6-acetone, 282 MHz): −81.81(s). *m/z* = [M^+ calcd for $C_{28}H_{51}P_2{}^{194}Pt$ 643.3093; found 643.3089.

6.4 Chapter Four Experimental

Synthesis of [PtEt($C(CH_2)_2CH_3$)(COD)] 27a and [Pt($C(CH_2)_2CH_3$)$_2$(COD)] 27b

[$PtEt_2$(COD)] (20 mg, 0.055 mmol) was placed in an NMR tube and MCP (0.51 mL of a 1.85 mmol/mL solution in C_6D_6, 11 eq.) was added. [PtEt($C(CH_2)_2CH_3$)(COD)] and [Pt($C(CH_2)_2CH_3$)$_2$(COD)] began to form after two hours, ending in a 15:85 ratio by ^1H NMR after 30 days. **[PtEt($C(CH_2)_2CH_3$)(COD)] 27a:** ^1H NMR (δ, C_6D_6, 600 MHz): 4.82(brs, $J_{Pt–H}$ = 33.8 Hz, 2H, =CH), 4.64(brs, $J_{Pt–H}$ = 34.4 Hz, 2H, =CH), 1.96(q, 7.8, $J_{Pt–H}$ = 91.8 Hz, 2H, Et CH_2), 1.85–1.75(m, 8H, COD CH_2), 1.51(t, 7.7, $J_{Pt–H}$ = 74.4 Hz, 3H, Et CH_3), 1.35(s, $J_{Pt–H}$ = 55.9 Hz, 3H, MCP CH_3), 0.73(m, $J_{Pt–H}$ = 66.2 Hz, 2H, ^{c}Pr), 0.42(m, $J_{Pt–H}$ = 46.5 Hz, 2H, ^{c}Pr). $^{13}C\{^1H\}$ NMR (δ, C_6D_6/d_6-acetone, 150 MHz): 101.8(s, $J_{Pt–C}$ = 46.7 Hz, =CH), 98.9(s, $J_{Pt–C}$ = 54.2 Hz, =CH), 31.2(s, $J_{Pt–C}$ = 21.3 Hz, MCP CH_3), 29.8(s, COD CH_2), 29.3(s, COD CH_2), 21.8(s, $J_{Pt–C}$ = 854.8 Hz, Et CH_2),

17.4(s, $J_{Pt–C}$ = 1160.6 Hz, MCP Pt−C), 16.4(s, $J_{Pt–C}$ = 35.2 Hz, Et CH_3), 14.9(s, ^{c}Pr). **[Pt(C(CH_2)$_2$$CH_3$)$_2$(COD)] 27b:** ^{1}H NMR (δ, C_6D_6, 600 MHz): 4.82(brs, $J_{Pt–H}$ = 33.8 Hz, 4H, =CH), 1.85–1.75(m, 8H, COD CH_2), 1.41(s, $J_{Pt–H}$ = 53.5 Hz, 3H, MCP CH_3), 0.86(t, 4.2, $J_{Pt–H}$ = 66.2 Hz, 2H, ^{c}Pr), 0.41(m, $J_{Pt–H}$ = 44.4 Hz, 2H, ^{c}Pr). ^{13}C{^{1}H} NMR (δ, C_6D_6/*d*$_6$-acetone, 150 MHz): 102.0(s, $J_{Pt–C}$ = 43.7 Hz, =CH), 31.5(s, $J_{Pt–C}$ = 21.3 Hz, MCP CH_3), 29.3(s, COD CH_2), 17.2(s, $J_{Pt–C}$ = 1178.5 Hz, MCP Pt−C), 15.9(s, ^{c}Pr).

Synthesis of *trans*–[$PtCl_2$(BCP)(Py)] 28

[$Pt_2Cl_4(C_2H_4)_2$] (50 mg, 0.085 mmol) was placed in an NMR tube and $CDCl_3$ (0.5 mL) added. Pyridine (14 μL, 0.085 mmol) and carbon-13 enriched BCP (0.14 mL of a 0.62 mmol/mL sln in C_6D_6, 0.085 mmol, 1 eq.) were added, resulting in the immediate formation of *trans*–[$PtCl_2$(BCP)(Py)]. Reaction is quantitative by ^{1}H NMR. ^{1}H NMR (δ, $CDCl_3$, 300 MHz): 8.92(dd, 6.6, 1.3, 2H, *o*-H Py), 7.89(tt, 7.8, 1.5, 1H, *p*-H Py), 7.47(td, 6.6, 1.5, 2H, *m*-H Py), 1.58(t, 7.0, $J_{Pt–H}$ = 45.8 Hz, 4H, ^{c}Pr-*endo*), 1.12(t, 7.5, $J_{Pt–H}$ = 29.9 Hz, 4H, ^{c}Pr-*exo*). ^{13}C{^{1}H} NMR (δ, C_6D_6/$CDCl_3$, 150 MHz): 151.6(s, *o*-C Py), 140.1(s, *p*-C Py), 125.5(s, *m*-C Py), 75.3(s, $^1J_{Pt–C}$ = 248.5 Hz, =CR_2), 10.6(s, ^{c}Pr). *m/z* = $[M + H]^+$ calcd for $C_{11}H_{14}Cl_2N$ ^{194}Pt 424.0130; found 424.0136.

Synthesis of *trans*–[$PtCl_2$(MCP)(Py)] 29

[$Pt_2Cl_4(C_2H_4)_2$] (50 mg, 0.085 mmol) was placed in an NMR tube and $CDCl_3$ (0.5 mL) added. Pyridine (14 μL, 0.085 mmol) and MCP (0.09 mL of a 0.92 mmol/mL sln in $CDCl_3$, 0.085 mmol, 1 eq.) were added, resulting in the immediate formation of *trans*–[$PtCl_2$(MCP)(Py)]. Reaction is quantitative by ^{1}H NMR. ^{1}H NMR (δ, $CDCl_3$, 300 MHz): 8.92(d, 5.2, $J_{Pt–H}$ = 33.6 Hz, 2H, *o*-H Py), 7.93(t, 7.6, 1H, *p*-H Py), 7.51(t, 7.0, 2H, *m*-H Py), 5.02(brs, 2H, =CH_2), 1.63(brs, 2H, ^{c}Pr), 1.32(brs, 2H, ^{c}Pr). ^{13}C{^{1}H} NMR (δ, $CDCl_3$, 150 MHz): 151.6(s, *o*-C Py), 140.2(s, *p*-C Py), 125.5(s, *m*-C Py), 91.6(brs, =CR_2), 59.8(brs, =CH_2), 10.2(s, ^{c}Pr). *m/z* = $[M - Cl]^+$ calcd for $C_9H_{11}ClN$ ^{194}Pt 358.0185; found 358.0179.

Synthesis of *cis*–[$PtCl_2$(BCP)(DMSO)] 30

cis–[$PtCl_2(DMSO)_2$] (10 mg, 0.024 mmol) was placed in an NMR tube and $CDCl_3$ (0.5 mL) added. BCP (0.04 mL of a 0.62 mmol/mL solution in C_6D_6, 0.024 mmol) was added, resulting in the formation of *cis*–[$PtCl_2$(BCP)(DMSO)] after 1 hr. Due to the limited solubility of *cis*–[$PtCl_2(DMSO)_2$] in $CDCl_3$, a yield could not be obtained. ^{1}H NMR (δ, $CDCl_3$, 600 MHz): 3.53(s, $J_{Pt–H}$ = 21.2 Hz, 3H, S−CH_3), 1.25(m, 4H, ^{c}Pr), 0.85(m, 4H, ^{c}Pr). ^{13}C{^{1}H} NMR (δ, C_6D_6/$CDCl_3$, 150 MHz): 82.2(s, $^1J_{Pt–C}$ = 251.8 Hz, =CR_2), 44.6(s, S−CH_3), 12.5(s, ^{c}Pr), 11.5(s, ^{c}Pr).

Synthesis of *cis*–[$PtCl_2$(MCP)(DMSO)] 31

cis–[$PtCl_2(DMSO)_2$] (20 mg, 0.047 mmol) was placed in an NMR tube and $CDCl_3$ (0.5 mL) added. MCP (0.05 mL of a 0.92 mmol/mL solution in $CDCl_3$, 0.046 mmol) was added, resulting in the immediate formation of *cis*–[$PtCl_2$(MCP)(DMSO)]. Due to the limited solubility of *cis*–[$PtCl_2(DMSO)_2$] in $CDCl_3$, a yield could not be obtained. ^{1}H NMR (δ, $CDCl_3$, 600 MHz): 4.81(s, $J_{Pt–H}$ = 67.5 Hz, 1H, =CH_2), 4.64(s, $J_{Pt–H}$ = 63.1 Hz, 1H, =CH_2), 3.59(s, $J_{Pt–H}$ = 16.5 Hz, 3H, S−CH_3), 3.45(s, $J_{Pt–H}$ = 14.8 Hz, 3H, S−CH_3), 1.88(dt, 12.0, 8.3, 1H, ^{c}Pr), 1.55(dt, 12.0, 8.3, 1H, ^{c}Pr), 1.38(dt, 9.4, 8.0, 1H, ^{c}Pr), 1.28(td, 9.4, 8.0, 1H, ^{c}Pr). ^{13}C{^{1}H} NMR (δ, $CDCl_3$, 150 MHz): 97.3(s, $^1J_{Pt–C}$ = 277.5 Hz, =CR_2), 67.5(s, $^1J_{Pt–C}$ = 141.0 Hz, =CH_2), 45.5(s, $^1J_{Pt–C}$ = 47.9 Hz, S−CH_3), 44.2(s, $^1J_{Pt–C}$ = 44.0 Hz, S−CH_3), 12.6(s, ^{c}Pr), 11.0(s, ^{c}Pr).

Synthesis of *trans*–[$Pt(C(CH_2)_2C(CH_2)_2Cl)Cl(SEt_2)_2$] 32

[$PtCl_2(SEt_2)_2$] (50 mg, 0.11 mmol) was placed in an NMR tube and $CDCl_3$ (0.5 mL) added. BCP (0.05 mL, 0.53 mmol) was added. After 2 days, *trans*–$Pt(C(CH_2)_2C(CH_2)_2Cl)Cl(SEt_2)_2$] formed. Reaction is quantitative by ^{1}H NMR.^{1}H NMR (δ, $CDCl_3$, 500 MHz): 3.3-2.9(brs, 8H, S−CH_2), 1.37(t, 15 Hz, 12H, CH_3), 0.83(t, 7.0 Hz, 2H, Cl ^{c}Pr), 0.77(t, 7.0 Hz, 2H, Cl ^{c}Pr), 0.36(t, 5.0, $J_{Pt–H}$ = 29.4 Hz, 2H, Pt ^{c}Pr-*exo*), 0.21(t, 5.0, $J_{Pt–H}$ = 63.0 Hz, 2H, Pt ^{c}Pr-*endo*). ^{13}C{^{1}H} NMR (δ, $CDCl_3$, 125 MHz): 57.1(s, Cl−C), 32.2(s, $J_{Pt–C}$ = 17.7 Hz, S−CH_2), 16.4(s, Pt ^{c}Pr), 14.3(s, Cl

^{c}Pr), 13.4(s, $J_{Pt–C}$ = 32.9 Hz, CH_3), −0.4(s, $J_{Pt–C}$ = 1011 Hz, Pt−C). m/z = $[M - Cl]^+$ calcd for $C_{14}H_{28}Cl\,^{194}PtS_2$ 489.0948; found 489.0949.

Synthesis of *trans*–[Pt(C(CH$_2$)$_2$C(CH$_2$)$_2$Cl)Cl(NC^{t}Bu)$_2$] 33

trans–[$PtCl_2(NC^tBu)_2$] (10 mg, 0.026 mmol) was was placed in an NMR tube and $CDCl_3$ (0.5 mL) added. BCP (2.4 μL, 0.026 mmol) was added, resulting in the formation of *trans*–[$Pt(C(CH_2)_2C(CH_2)_2Cl)Cl(NC^tBu)_2$] after 2 days. Reaction is quantitative by ^{1}H NMR. ^{1}H NMR (δ, $CDCl_3$, 500 MHz): 1.44(s, 18H, ^{t}Bu), 1.03(t, 6.3 Hz, 2H, Cl ^{c}Pr), 0.73(t, 6.3 Hz, 2H, Cl ^{c}Pr), 0.30(m, 4H, Pt ^{c}Pr). ^{13}C{^{1}H} NMR (δ, $CDCl_3$, 125 MHz): 122.1(s, $J_{Pt–C}$ = 349 Hz, N≡C), 55.2(s, Cl−C), 30.2(s, CR_3), 27.9(s, Me), 15.8(s, Cl ^{c}Pr), 14.7(s, Pt ^{c}Pr), 0.0(s, $J_{Pt–C}$ = 953 Hz, Pt−C).

Synthesis of *trans*–[Pt(C(CH$_2$)$_2$C(CH$_2$)$_2$Cl)Cl(Py)$_2$] 34a

trans–[$PtCl_2(Py)_2$] (20 mg, 0.047 mmol) was placed in an NMR tube and $CDCl_3$ (0.5 mL) added. BCP (4.4 μL, 0.047 mmol) was added. Overnight, *trans*–[$Pt(C(CH_2)_2C(CH_2)_2Cl)Cl(Py)_2$] forms, ending up as 30% of the species in solution. ^{1}H NMR (δ, $CDCl_3$, 600 MHz): 9.04(dd, 6.6, 1.2, $J_{Pt–H}$ = 39.7 Hz, 4H, *o*-Py), 7.41(tt, 7.9, 1.6 Hz, 2H, *p*-Py), 6.98(td, 6.6, 0.9 Hz, 4H, *m*-Py), 0.41(t, 6.4 Hz, 2H, Cl ^{c}Pr-*exo*), −0.03(td, 4.1, 1.2, $J_{Pt–H}$ = 37.9 Hz, 2H, Pt ^{c}Pr-*exo*), −0.15(t, 4.1, 1.2, $J_{Pt–H}$ = 50.8 Hz, 2H, Pt ^{c}Pr-*endo*), −0.25(t, 6.4 Hz, 2H, Cl ^{c}Pr-*endo*). ^{13}C{^{1}H} NMR (δ, $CDCl_3$, 150 MHz): 153.7(s, *o*-Py), 136.7(s, *p*-Py), 124.9(s, *m*-Py), 56.2(s, Cl−C), 13.1(s, Pt ^{c}Pr), 12.9(s, Cl ^{c}Pr), 1.1(s, $J_{Pt–C}$ = 1202 Hz, Pt−C).

Synthesis of *cis*–[Pt(C(CH$_2$)$_2$C(CH$_2$)$_2$Cl)Cl(Py)$_2$] 34b

[$Pt_2Cl_4(C_2H_4)_2$] (20 mg, 0.034 mmol) was placed in an NMR tube and $CDCl_3$ (0.5 mL) added. Pyridine (11 μL, 0.137 mmol, 4 eq.) and BCP (6.4 μL, 0.068 mmol, 2 eq.) were added, resulting in the immediate formation of paritally soluble yellow *cis*–[$Pt(C(CH_2)_2C(CH_2)_2Cl)Cl(Py)_2$]. Reaction is quantitative by ^{1}H NMR. ^{1}H NMR (δ, $CDCl_3$, 500 MHz): 9.46(d, 6.0 Hz, 2H, *o*-H *cis*-Py), 8.87(d, 5.0 Hz, 2H, *o*-H *trans*-Py),

8.28(t, 8.0 Hz, 1H, *p*-H *cis*-Py), 7.83(t, 7.5 Hz, 2H, *m*-H *cis*-Py), 7.62(t, 8.0 Hz, 1H, *p*-H *trans*-Py), 7.18(t, 6.5 Hz, 2H, *m*-H *trans*-Py), 1.34(t, 6.5 Hz, 2H, Cl ^{c}Pr-*endo*), 1.05(t, 6.5 Hz, 2H, Cl ^{c}Pr-*exo*), 0.50(t, 4.8 Hz, 2H, Pt ^{c}Pr-*endo*), 0.36(t, 4.8 Hz, 2H, Pt ^{c}Pr-*exo*). $^{13}C\{^1H\}$ NMR (δ, $CDCl_3$, 125 MHz): 151.3(s, *o*-C *trans*-Py), 146.5(s, *o*-C *cis*-Py), 144.4(s, *p*-C *cis*-Py), 136.5(s, *p*-C *trans*-Py), 126.1(s, *m*-C *cis*-Py), 124.5(s, *m*-C *trans*-Py), 65.9(s, Cl−C), 15.0(s, Pt ^{c}Pr), 11.1(s, Cl ^{c}Pr), −11.1(s, J_{Pt-C} = 970 Hz, Pt−C). *m/z* = $[M - Cl]^+$ calcd for $C_{16}H_{18}ClN_2{}^{194}Pt$ 467.0785; found 467.0791.

Synthesis of *cis*–[Pt(C(CH$_2$)$_2$CH$_2$Cl)Cl(Py)$_2$] 34c

$[Pt_2Cl_4(C_2H_4)_2]$ (20 mg, 0.034 mmol) was placed in an NMR tube and d_6-acetone(0.5 mL) added. Pyridine (11 μL, 0.137 mmol, 4 eq.) and MCP (0.07 mL of a 0.92 mmol/mL solution in $CDCl_3$, 0.068 mmol, 2 eq.) were added, resulting in the immediate formation of sparingly soluble yellow *cis*–$[Pt(C(CH_2)_2CH_2Cl)Cl(Py)_2]$. Reaction is quantitative by ^1H NMR. ^1H NMR (δ, d_6-acetone, 600 MHz): 9.50(d, 5.6, J_{Pt-H} = 81.9 Hz, 2H, *o*-H *cis*-Py), 8.91(dt, 4.7, 1.8 Hz, 2H, *o*-H *trans*-Py), 8.54(td, 7.7, 1.4 Hz, 1H, *p*-H *cis*-Py), 8.08(t, 6.9 Hz, 2H, *m*-H *cis*-Py), 7.82(tt, 7.6, 1.8 Hz, 1H, *p*-H *trans*-Py), 7.31(ddd, 7.6, 5.0, 1.4 Hz, 2H, *m*-H *trans*-Py), 4.13(s, J_{Pt-H} = 24.6 Hz, 2H, Cl−CH_2), 0.52(td, 5.0, 1.5, J_{Pt-H} = 29.6 Hz, 2H, Pt ^{c}Pr-*endo*), 0.32(td, 5.0, 1.5, J_{Pt-H} = 19.6 Hz, 2H, Pt ^{c}Pr-*exo*). $^{13}C\{^1H\}$ NMR (δ, d_6-acetone, 150 MHz): 153.5(s, *o*-C *trans*-Py), 151.1(s, *o*-C *cis*-Py), 138.8(s, *p*-C *trans*-Py), 136.3(s, *p*-C *cis*-Py), 126.4(s, *m*-C *trans*-Py), 124.0(s, *m*-C *cis*-Py), 76.8(s, Cl−C), 14.3(s, Pt ^{c}Pr), −15.6(s, Pt−C). *m/z* = $[M - Cl]^+$ calcd for $C_{14}H_{16}ClN_2{}^{194}Pt$ 437.0597; found 437.0601.

Synthesis of [Pt(dppp)$_2$]Cl$_2$ 35a

$[PtCl_2(SEt_2)_2]$ (50 mg, 0.11 mmol) was placed in an NMR tube and $CDCl_3$ (0.5 mL) added. BCP (0.05 mL, 0.54 mmol) was added, resulting in the formation of *trans*–$[Pt(C(CH_2)_2C(CH_2)_2Cl)Cl(SEt_2)_2]$ (**32**) after 5 days. The solution was frozen in liquid N_2, and a solution of dppp (90 mg, 0.22 mmol) in $CDCl_3$ (0.5 mL) added. X-ray quality crystals of $[Pt(dppp)_2]Cl_2$ formed as the solution warmed to RT.

Synthesis of *trans*–[Pt(C(CH$_2$)$_2$C(CH$_2$)$_2$Cl)Cl(PTA)$_2$] 36a

[PtCl$_2$(SEt$_2$)$_2$] (50 mg, 0.11 mmol) was placed in an NMR tube and CDCl$_3$ (0.5 mL) added. BCP (0.05 mL, 0.53 mmol) was added. After 2 days, *trans*–Pt(C(CH$_2$)$_2$C(CH$_2$)$_2$Cl)Cl(SEt$_2$)$_2$] formed and the solvent was removed *in vacuo*. PTA (40 mg, 0.25 mmol) was dissolved in CDCl$_3$ (0.5 mL) and added to the NMR tube., resulting in the immediate formation of *trans*–[Pt(C(CH$_2$)$_2$C(CH$_2$)$_2$Cl)Cl(PTA)$_2$]. After ∼1 hr, the complex had decomposed to form *cis*–[PtCl$_2$(PTA)$_2$] and BCP. Due to the insolubility of *cis*–[PtCl$_2$(PTA)$_2$], a yield was not obtained.^{1}H NMR (δ, CDCl$_3$, 600 MHz): 4.45(m, 12H, N−CH$_2$), 4.31(dd, 47.4, 14.4, 12H, P−CH$_2$), 1.03(t, 6.0 Hz, 2H, Cl ^{c}Pr), 0.76(t, 6.0 Hz, 2H, Cl ^{c}Pr), 0.44(s, 2H, Pt ^{c}Pr), 0.27(s, 2H, Pt ^{c}Pr). ^{31}P{^{1}H} NMR (δ, CDCl$_3$, 121 MHz): −59.2(s, $^1J_{\text{Pt–P}}$ = 3000 Hz).

Synthesis of *cis*–[Pt(C(CH$_2$)$_2$C(CH$_2$)$_2$Cl)Cl(PTA)$_2$] 36b

[Pt$_2$Cl$_4$(C$_2$H$_4$)$_2$] (30 mg, 0.051 mmol) was placed in an NMR tube and CDCl$_3$ (0.3 mL) added. Pyridine (16.5 μL, 0.21 mmol, 4 eq.) and BCP (0.25 mL of a 0.62 mmol/mL solution in C$_6$D$_6$, 0.153 mmol, 3 eq.) were added, resulting in the immediate formation of *cis*–[Pt(C(CH$_2$)$_2$C(CH$_2$)$_2$Cl)Cl(Py)$_2$]. The solvent was removed *in vacuo* and PTA (48 mg of a sample containing 10% PTA oxide, ∼6 eq.) in CDCl$_3$ (0.5 mL) added. A large amount of *cis*–[PtCl$_2$(PTA)$_2$] was formed, as well as *cis*–[Pt(C(CH$_2$)$_2$C(CH$_2$)$_2$Cl)Cl(PTA)$_2$]. Relative amounts could not be calculated due to the insolubility of *cis*–[PtCl$_2$(PTA)$_2$].. ^{1}H NMR (δ, CDCl$_3$, 600 MHz): 4.7–4.1(m, 24H, N−CH$_2$ and P−CH$_2$), 1.69(dt, 11.2, 6.7 Hz, 1H, Cl ^{c}Pr), 1.31(dt, 10.2, 7.1 Hz, 1H, Cl ^{c}Pr), 0.92(m, 2H, Cl ^{c}Pr and Pt ^{c}Pr), 0.85(dt, 10.9, 6.2 Hz, 1H, Cl ^{c}Pr), 0.80(m, 1H, Pt ^{c}Pr), 0.49(m, 1H, Pt ^{c}Pr), 0.27(m, 1H, Pt ^{c}Pr). ^{13}C{^{1}H} NMR (δ, CDCl$_3$, 150 MHz): 72.8(m, N−CH$_2$), 72.2(d, 9.2 Hz, N−CH$_2$), 64.8(s, Cl−C), 53.5(dd, 23.3, 2.4 Hz, P−CH$_2$), 51.9(d, 14.7 Hz, P−CH$_2$), 16.7(s, Cl ^{c}Pr), 15.7(s, Cl ^{c}Pr), 15.5(dd, 121.8, 8.6, $^1J_{\text{Pt–C}}$ = 809.1 Hz, Pt−C), 13.4(s, Pt ^{c}Pr), 8.7(d, 3.7 Hz, Pt ^{c}Pr). ^{31}P{^{1}H} NMR (δ, CDCl$_3$, 121 MHz): −57.9(d, 15.6, $^1J_{\text{Pt–P}}$ = 3949 Hz, *trans* Cl), −65.8(d, 15.6, $^1J_{\text{Pt–P}}$ = 1522 Hz, $J_{\text{P–C}}$ = 121.5 Hz, *trans* ^{c}Pr). m/z = [M + K]$^+$ calcd for C$_{18}$H$_{32}$Cl$_2$KN$_6$P$_2$^{194}Pt 699.0804; found 699.0784.

Synthesis of *cis*–[Pt(C(CH$_2$)$_2$CH$_2$Cl)Cl(PTA)$_2$] 36c

[$Pt_2Cl_4(C_2H_4)_2$] (30 mg, 0.051 mmol) was placed in an NMR tube and MCP (0.17 mL of a 0.92 mmol/mL solution in $CDCl_3$, 0.153 mmol, 3 eq.) and pyridine (16.5 μL, 0.21 mmol, 4 eq.) added, resulting in the immediate formation of *cis*–[Pt(C(CH$_2$)$_2$CH$_2$Cl)Cl(Py)$_2$]. PTA (48 mg of a sample containing 10% PTA oxide, ∼6 eq.) in $CDCl_3$ (0.3 mL) was added. A large amount of *cis*–[$PtCl_2$(PTA)$_2$] was formed, as well as *cis*–[Pt(C(CH$_2$)$_2$CH$_2$Cl)Cl(PTA)$_2$] (50% of species in solution). After 5 days, all of the *cis*–[Pt(C(CH$_2$)$_2$CH$_2$Cl)Cl(PTA)$_2$] had decomposed to form *cis*–[$PtCl_2$(PTA)$_2$]. $^{31}P\{^1H\}$ NMR (δ, $CDCl_3$, 121 MHz): −58.9(d, 14.9, $^1J_{Pt–P}$ = 3884 Hz, *trans* Cl), −65.8(d, 14.9, $^1J_{Pt–P}$ = 1530 Hz, *trans* ^{c}Pr).

Synthesis of *cis*–[Pt(C(CH$_2$)$_2$C(CH$_2$)$_2$Cl)Cl(dppp)] 37a

[$Pt_2Cl_4(C_2H_4)_2$] (30 mg, 0.051 mmol) was placed in an NMR tube and $CDCl_3$ (0.3 mL) added. Pyridine (16.5 μL, 0.21 mmol, 4 eq.) and BCP (0.25 mL of a 0.62 mmol/mL solution in C_6D_6, 0.153 mmol, 3 eq.) were added, resulting in the immediate formation of *cis*–[Pt(C(CH$_2$)$_2$C(CH$_2$)$_2$Cl)Cl(Py)$_2$]. The solvent was removed *in vacuo* and dppp (42 mg, 0.102 mmol) in $CDCl_3$ (0.5 mL) added. *cis*–[Pt(C(CH$_2$)$_2$C(CH$_2$)$_2$Cl)Cl(dppp)] (85%) and *cis*–[$PtCl_2$(dppp)] (11%) formed immediately. ^1H NMR (δ, $CDCl_3$, 600 MHz): 7.86(t, 8.4 Hz, 4H, Ar), 7.53(t, 9.0 Hz, 4H, Ar), 7.37(m, 4H, Ar), 7.2(m, 8H, Ar), 4.47(brs, 1H, P−CH_2), 3.41(t, 13.8 Hz, 1H, P−CH_2), 2.51(m, 2H, P−CH_2), 2.28(m, 1H, CH_2), 1.05(m, 2H, CH_2 and Cl ^{c}Pr), 0.71(m, 1H, Cl ^{c}Pr), 0.48(m, 2H, Cl ^{c}Pr and Pt ^{c}Pr), 0.35(m, 1H, Pt ^{c}Pr), 0.20(m, 1H, Pt ^{c}Pr), −0.46(m, 1H, Cl ^{c}Pr), −1.22(m, 1H, Pt ^{c}Pr). $^{13}C\{^1H\}$ NMR (δ, $CDCl_3$, 150 MHz): 134.3(d, 10.0 Hz, Ar), 133.5(d, 9.6 Hz, Ar), 132.9(d, 10.0 Hz, Ar), 130.6(d, 13.8 Hz, Ar), 128.8(m, Ar), 128.5(d, 9.5 Hz, Ar), 128.1(d, 11.2 Hz, Ar), 127.0(d, 10.6 Hz, Ar), 63.6(s, Cl−C), 28.5(dd, 39.3, 5.9 Hz, P−CH_2), 22.8(d, 29.2 Hz, P−CH_2), 18.8(m, CH_2), 17.1(s, Cl ^{c}Pr), 15.6(dd, 124.5, 6.8, $^1J_{Pt–C}$ = 789.4 Hz, Pt−C), 13.3(s, Pt ^{c}Pr), 12.2(s, Cl ^{c}Pr), 6.1(d, 3.2 Hz, Pt ^{c}Pr). $^{31}P\{^1H\}$ NMR (δ, $CDCl_3$, 121 MHz): −1.8(d, 25.9, $^1J_{Pt–P}$ = 1654 Hz, *trans* ^{c}Pr), −2.7(d, 25.9, $^1J_{Pt–P}$ = 4133 Hz, *trans* Cl).

Synthesis of *cis*–[Pt(C(CH$_2$)$_2$CH$_2$Cl)Cl(dppp)] 37b

[$Pt_2Cl_4(C_2H_4)_2$] (30 mg, 0.051 mmol) was placed in an NMR tube and MCP (0.17 mL of a 0.92 mmol/mL solution in $CDCl_3$, 0.153 mmol, 3 eq.) and pyridine (16.5 μL, 0.21 mmol, 4 eq.) added, resulting in the immediate formation of *cis*–[Pt(C(CH$_2$)$_2$CH$_2$Cl)Cl(Py)$_2$]. Dppp (42 mg, 0.102 mmol) in $CDCl_3$ (0.3 mL) was added. *cis*–[Pt(C(CH$_2$)$_2$CH$_2$Cl)Cl(dppp)] (58%), *cis*–[$PtCl_2$(dppp)] (26%) and [Pt(dppp)$_2$]Cl_2 (16%) formed immediately. The *cis*–[Pt(C(CH$_2$)$_2$CH$_2$Cl)Cl(dppp)] decomposed to form *cis*–[$PtCl_2$(dppp)] overnight. $^{31}P\{^1H\}$ NMR (δ, $CDCl_3$, 121 MHz): 0.4(d, 25.2, $^1J_{Pt–P}$ = 4051 Hz, *trans* Cl), 0.2(d, 25.2, $^1J_{Pt–P}$ = 1684 Hz, *trans* ^{c}Pr).

Synthesis of *cis*–[Pt(C(CH$_2$)$_2$C(CH$_2$)$_2$Cl)Cl(PPh$_3$)$_2$] 38a

[$Pt_2Cl_4(C_2H_4)_2$] (30 mg, 0.051 mmol) was placed in an NMR tube and $CDCl_3$ (0.3 mL) added. Pyridine (16.5 μL, 0.21 mmol, 4 eq.) and BCP (0.25 mL of a 0.62 mmol/mL solution in C_6D_6, 0.153 mmol, 3 eq.) were added, resulting in the immediate formation of *cis*–[Pt(C(CH$_2$)$_2$C(CH$_2$)$_2$Cl)Cl(Py)$_2$]. The solvent was removed *in vacuo* and PPh_3 (54 mg, 0.204 mmol) in $CDCl_3$ (0.5 mL) added. [Pt(C(CH$_2$)$_2$C(CH$_2$)$_2$Cl)Cl(Py)(PPh$_3$)] (70%) and *cis*–[$PtCl_2$(PPh$_3$)$_2$] (30%) formed immediately. After an hour, *cis*–[Pt(C(CH$_2$)$_2$C(CH$_2$)$_2$Cl)Cl(PPh$_3$)$_2$] began to form, ending up as 53% *cis*–[Pt(C(CH$_2$)$_2$C(CH$_2$)$_2$Cl)Cl(PPh$_3$)$_2$], 8.5% [Pt(C(CH$_2$)$_2$C(CH$_2$)$_2$Cl)Cl(Py)(PPh$_3$)] (70%) and 30% *cis*–[$PtCl_2$(PPh$_3$)$_2$] after 4 days. **[Pt(C(CH$_2$)$_2$C(CH$_2$)$_2$Cl)Cl(Py)(PPh$_3$)] 38b:** $^{31}P\{^1H\}$ NMR (δ, $CDCl_3$, 121 MHz): 10.8(s, $^1J_{Pt–P}$ = 4738 Hz). ***cis*–[Pt(C(CH$_2$)$_2$C(CH$_2$)$_2$Cl)Cl(PPh$_3$)$_2$] 38a:** ^1H NMR (δ, $CDCl_3$, 600 MHz): 8–7(m, 8H, Ar), 1.34(m, 1H, Cl ^{c}Pr), 0.85(m, 1H, Cl ^{c}Pr), 0.77(m, 1H, Pt ^{c}Pr), 0.69(m, 1H, Cl ^{c}Pr), 0.57(m, 1H, Pt ^{c}Pr), −0.41(m, 1H, Cl ^{c}Pr), −0.85(m, 1H, Pt ^{c}Pr). $^{13}C\{^1H\}$ NMR (δ, $CDCl_3$, 150 MHz): 134.7(m, Ar), 133.6(d, 18.4 Hz, Ar), 128.9–127.6(m, Ar), 63.3(s, Cl−C), 19.2(s, Cl ^{c}Pr), 15.8(d, 4.3 Cl ^{c}Pr), 15.7(dd, 126.7, 8.0, $^1J_{Pt–C}$ = 797.7 Hz, Pt−C), 13.3(s, Pt ^{c}Pr), 8.1(d, 3.7 Hz, Pt ^{c}Pr). $^{31}P\{^1H\}$ NMR (δ, $CDCl_3$, 121 MHz): 22.7(d, 15.6, $^1J_{Pt–P}$ = 1646 Hz, *trans* ^{c}Pr), 16.7(d, 15.6, $^1J_{Pt–P}$ = 4490 Hz, *trans* Cl). m/z = $[M - Cl]^+$ calcd for $C_{42}H_{38}ClP_2{}^{194}Pt$ 835.1783; found

838.1785.

Synthesis of *cis*–[Pt(C(CH$_2$)$_2$CH$_2$Cl)Cl(Py)(PPh$_3$)] 38c

[$Pt_2Cl_4(C_2H_4)_2$] (30 mg, 0.051 mmol) was placed in an NMR tube and MCP (0.17 mL of a 0.92 mmol/mL solution in $CDCl_3$, 0.153 mmol, 3 eq.) and pyridine (16.5 μL, 0.21 mmol, 4 eq.) added, resulting in the immediate formation of *cis*–[Pt(C(CH$_2$)$_2$CH$_2$Cl)Cl(Py)$_2$]. PPh_3 (54 mg, 0.204 mmol) in $CDCl_3$ (0.3 mL) was added. [Pt(C(CH$_2$)$_2$CH$_2$Cl)Cl(Py)(PPh$_3$)] (32%) and *cis*–[$PtCl_2(PPh_3)_2$] (30%) formed immediately, with the [Pt(C(CH$_2$)$_2$CH$_2$Cl)Cl(Py)(PPh$_3$)] decomposing to form *cis*–[$PtCl_2(PPh_3)_2$] over 4 hours. $^{31}P\{^1H\}$ NMR (δ, $CDCl_3$, 121 MHz): 13.5(s, $^1J_{Pt–P}$ = 4661 Hz).

Appendix A

NMR Spectra

A.1 Chapter Two

[Pt(BCP)(dppp)] (1a)

^{1}H NMR spectrum – Figures A.1 and A.2, pages 162 and 163

^{13}C{^{1}H} NMR spectrum – Figures A.4 and A.5, pages 164 and 165

^{31}P{^{1}H} NMR spectrum – Figure A.3, page 163

[Pt(MCP)(dppp)] (2a)

^{1}H NMR spectrum – Figures A.6 and A.7, pages 166 and 167

^{13}C{^{1}H} NMR spectrum – Figures A.8–A.10, pages 168–170

^{31}P{^{1}H} NMR spectrum – Figure A.11, page 170

[Pt($CH_2CH{=}CHC(CH_2)_2$)(dppp)] (4a)

^{1}H NMR spectrum – Figures A.12–A.14, pages 171–173

^{13}C{^{1}H} NMR spectrum – Figures A.16–A.19, pages 174–177

^{31}P{^{1}H} NMR spectrum – Figure A.15, page 173

$[Pt(MCP)_2(PPh_3)]$ (7a)

^{1}H NMR spectrum – Figures A.20 and A.21, pages 178 and 179

$^{13}C\{^{1}H\}$ NMR spectrum – Figures A.22–A.24, pages 180–182

$^{31}P\{^{1}H\}$ NMR spectrum – Figure A.25, page 182

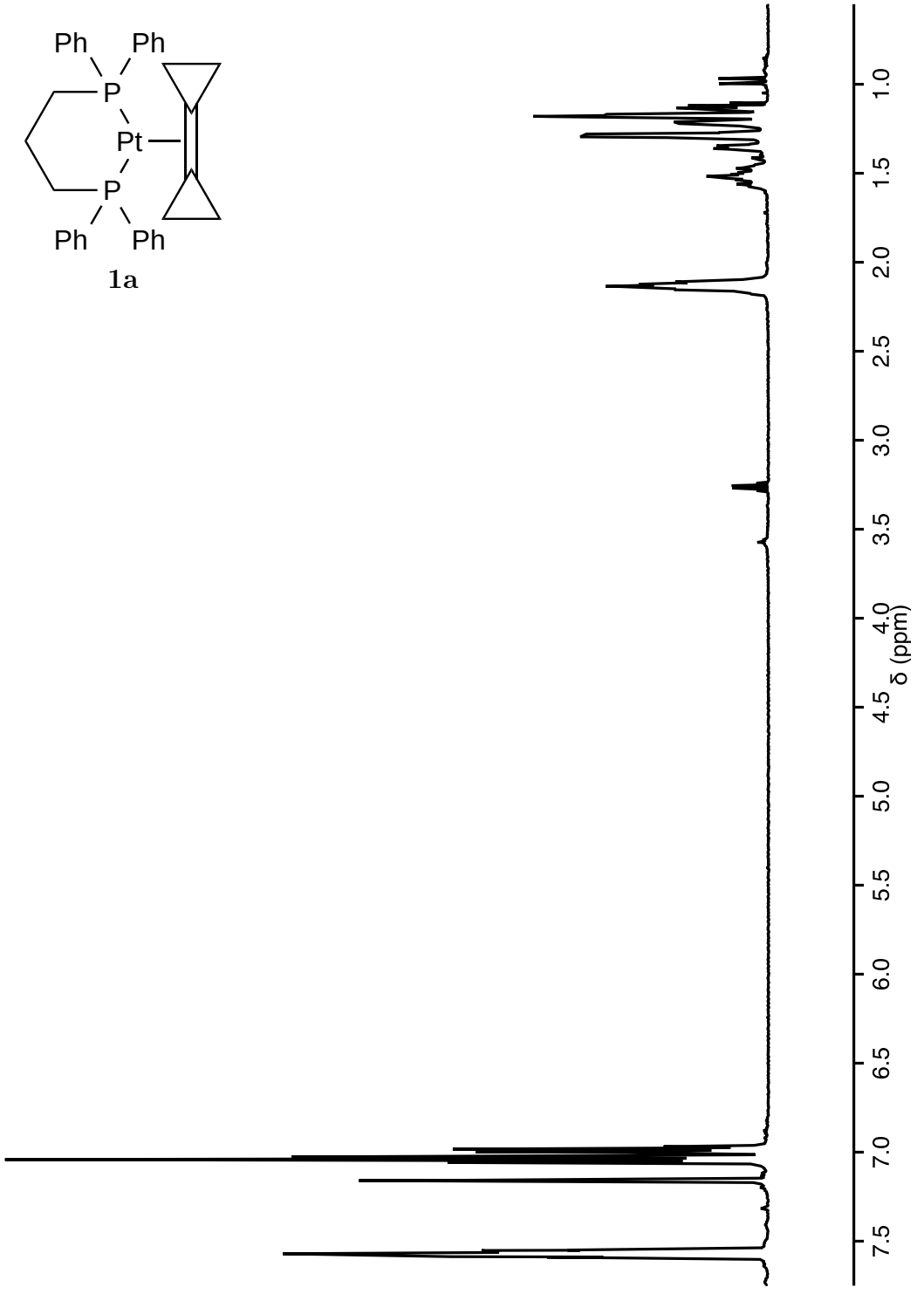

Figure A.1. ^{1}H NMR spectrum of [Pt(BCP)(dppp)] (**1a**) (600 MHz, RT, 40 mg/mL, C_6D_6).

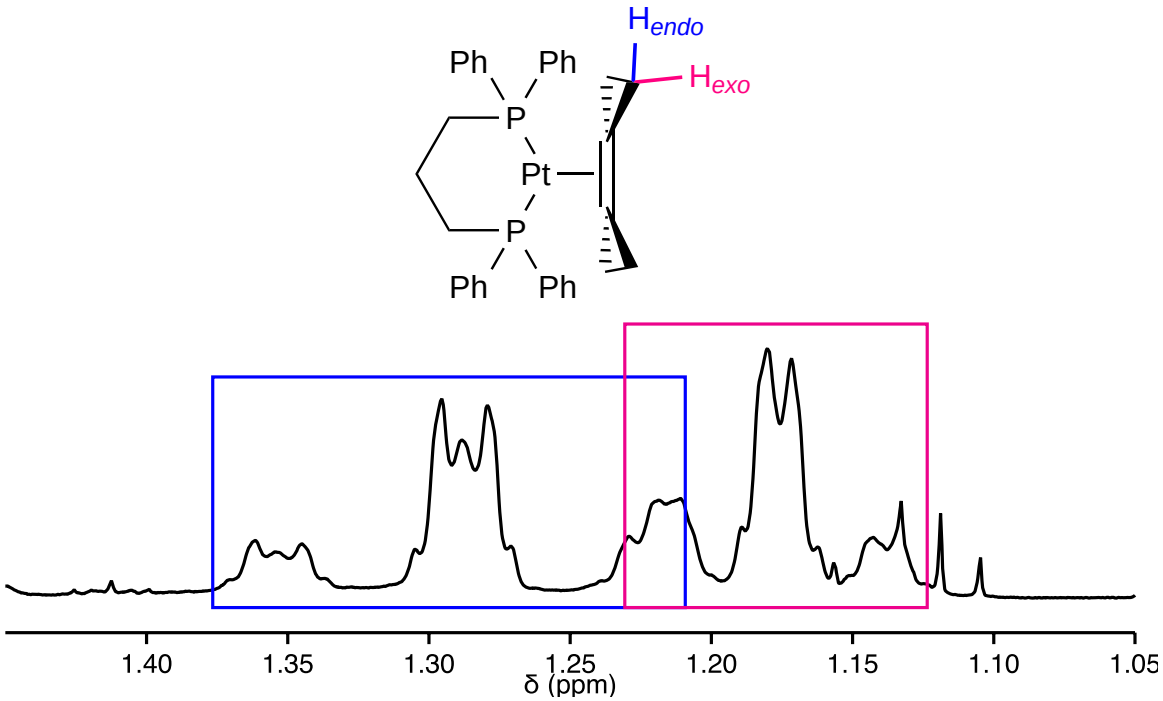

Figure A.2. Expanded ^{1}H NMR spectrum of [Pt(BCP)(dppp)] (**1a**) (600 MHz, RT, 40 mg/mL, C_6D_6).

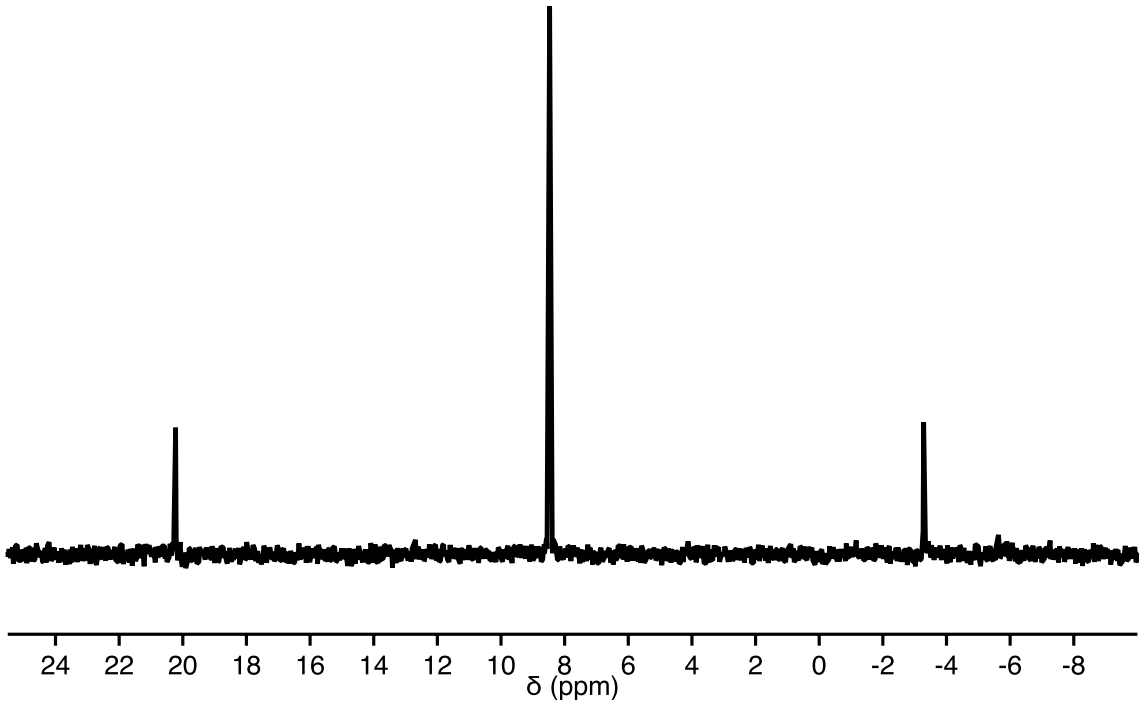

Figure A.3. ^{31}P{^{1}H} NMR spectrum of [Pt(BCP)(dppp)] (**1a**) (121 MHz, RT, 40 mg/mL, C_6D_6).

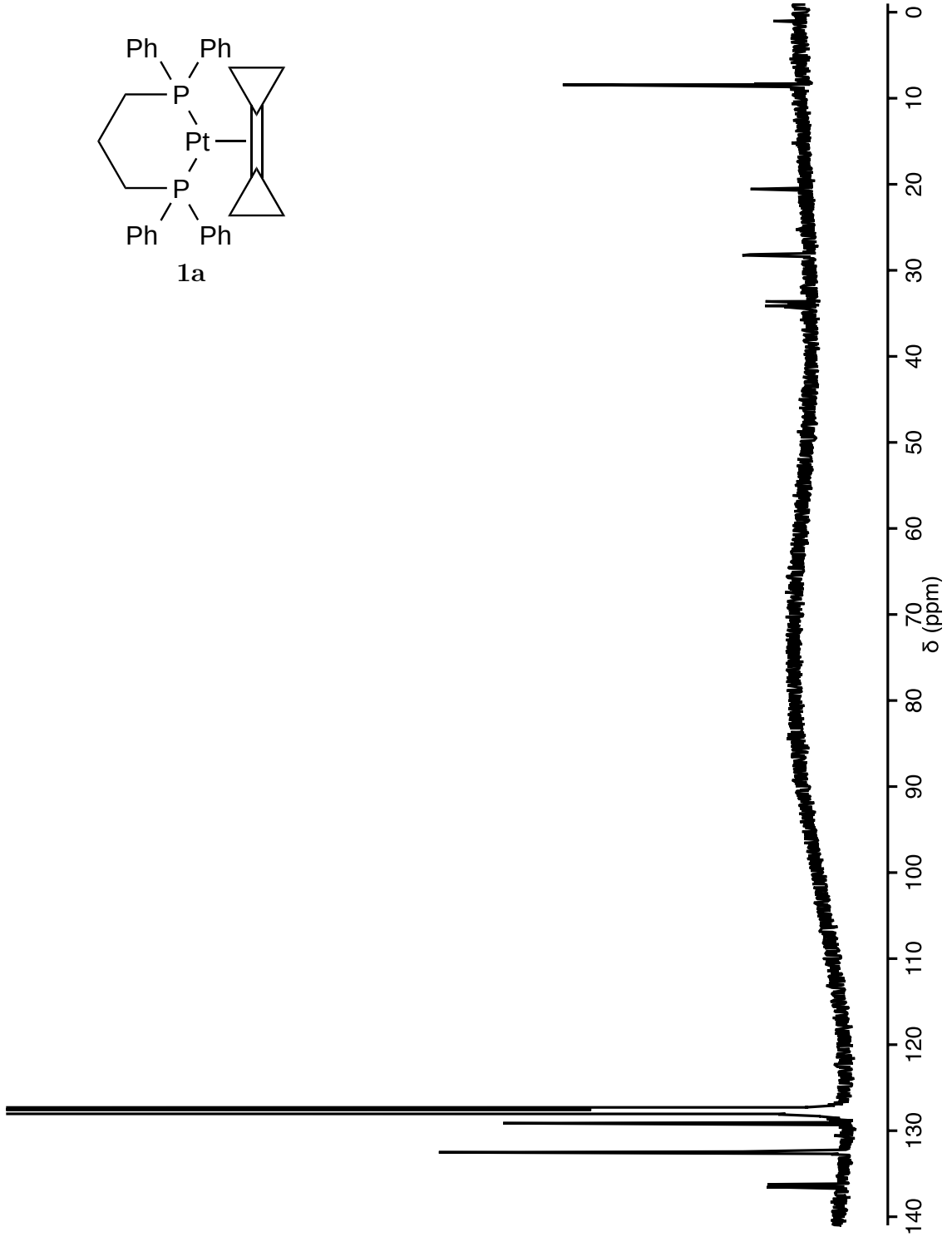

Figure A.4. $^{13}C\{^{1}H\}$ NMR spectrum of [Pt(BCP)(dppp)] (**1a**) (150 MHz, RT, 40 mg/mL, C_6D_6).

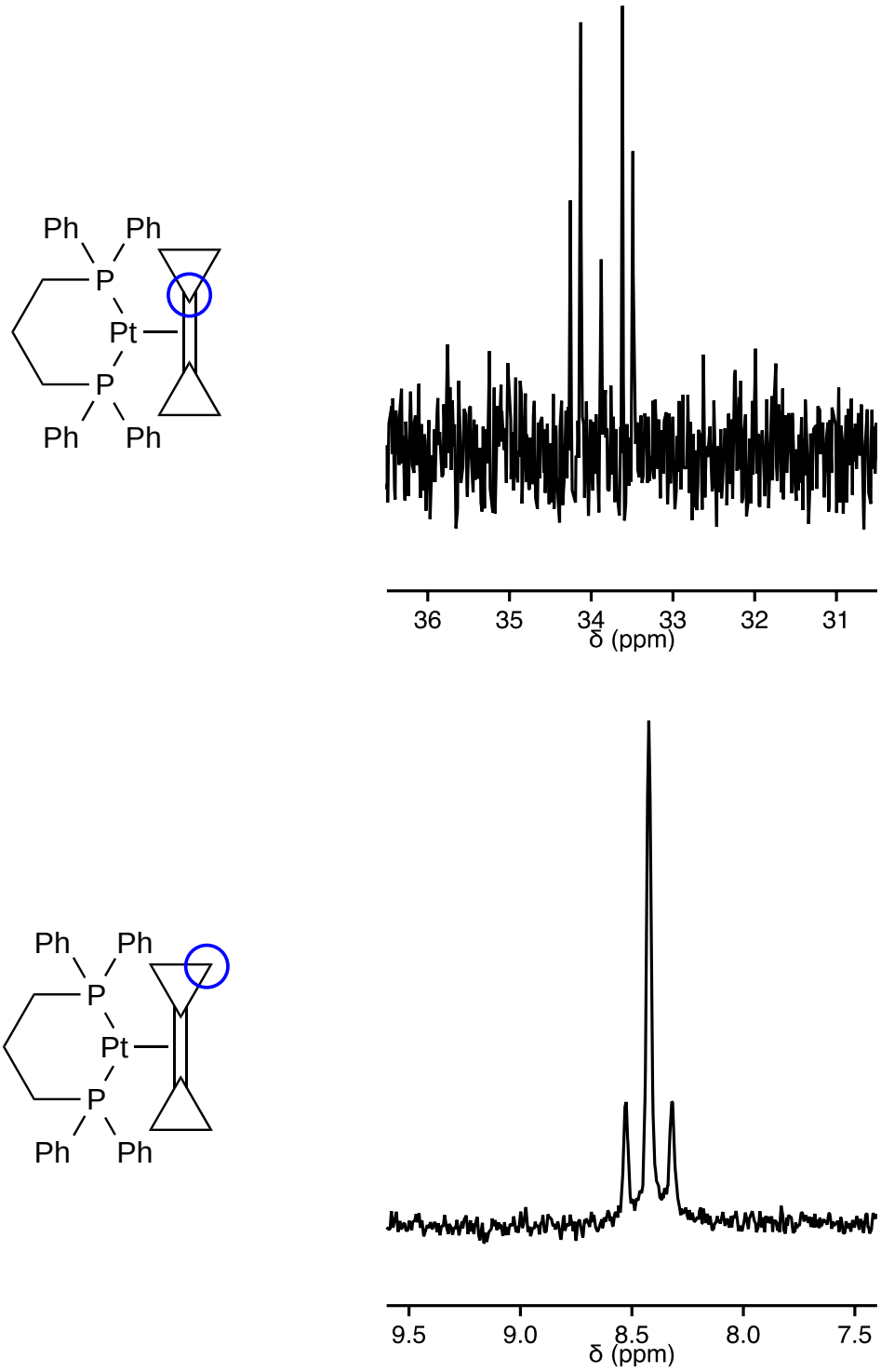

Figure A.5. Expanded $^{13}C\{^{1}H\}$ NMR spectrum of [Pt(BCP)(dppp)] (**1a**) (150 MHz, RT, 40 mg/mL, C_6D_6).

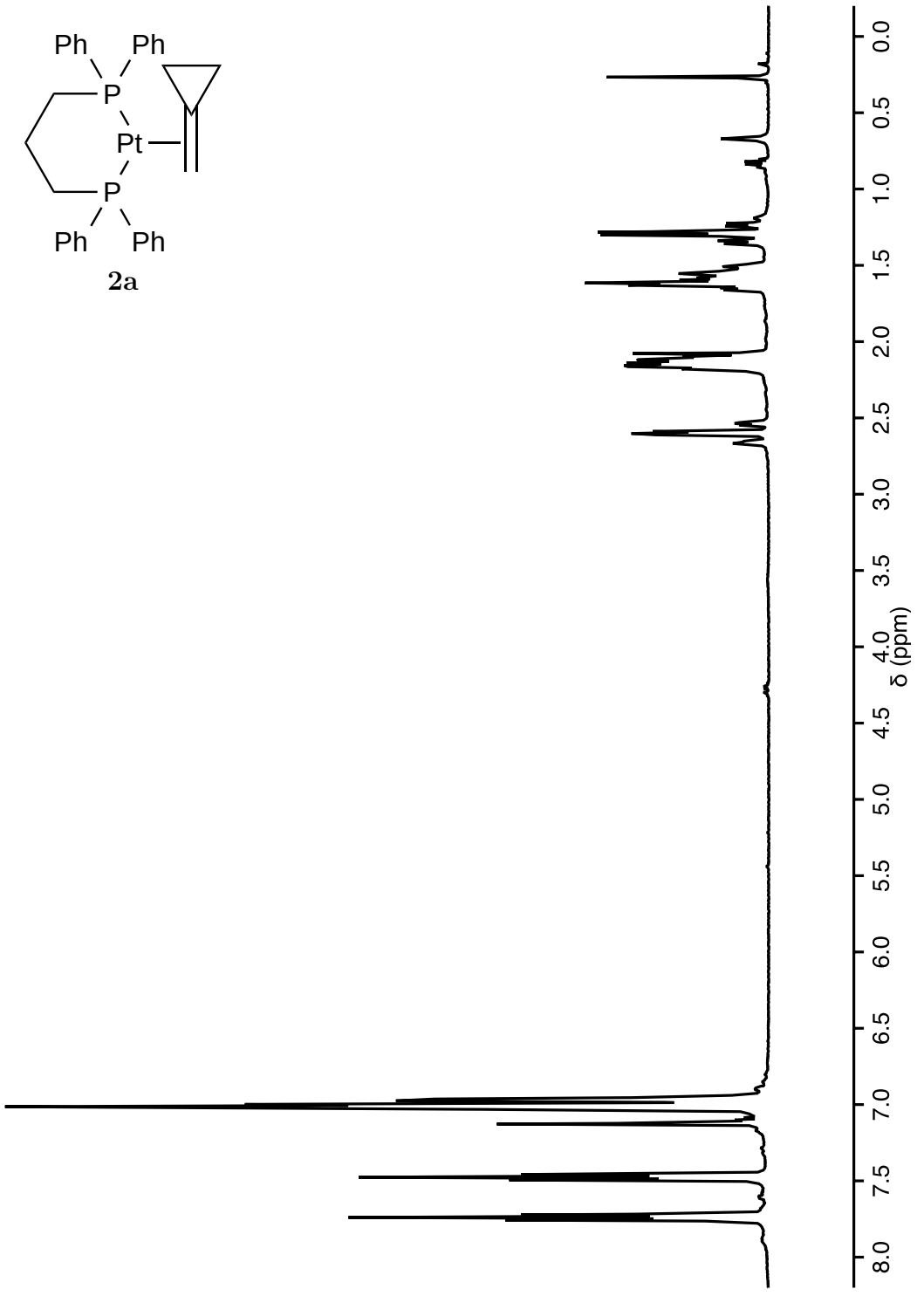

Figure A.6. ^{1}H NMR spectrum of [Pt(MCP)(dppp)] (**2a**) (500 MHz, RT, 40 mg/mL, C_6D_6).

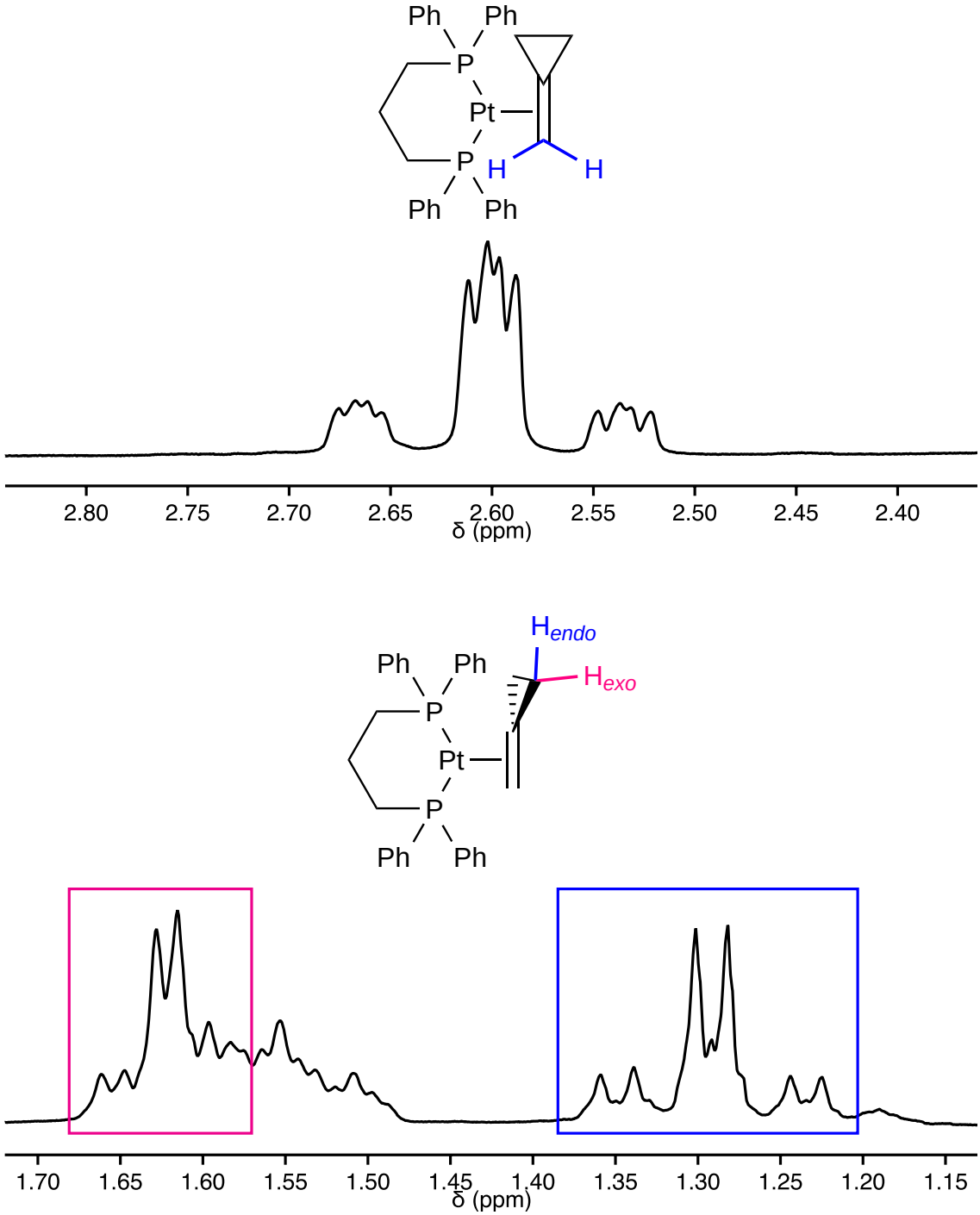

Figure A.7. Expanded ^{1}H NMR spectrum of [Pt(MCP)(dppp)] (**2a**) (500 MHz, RT, 40 mg/mL, C_6D_6).

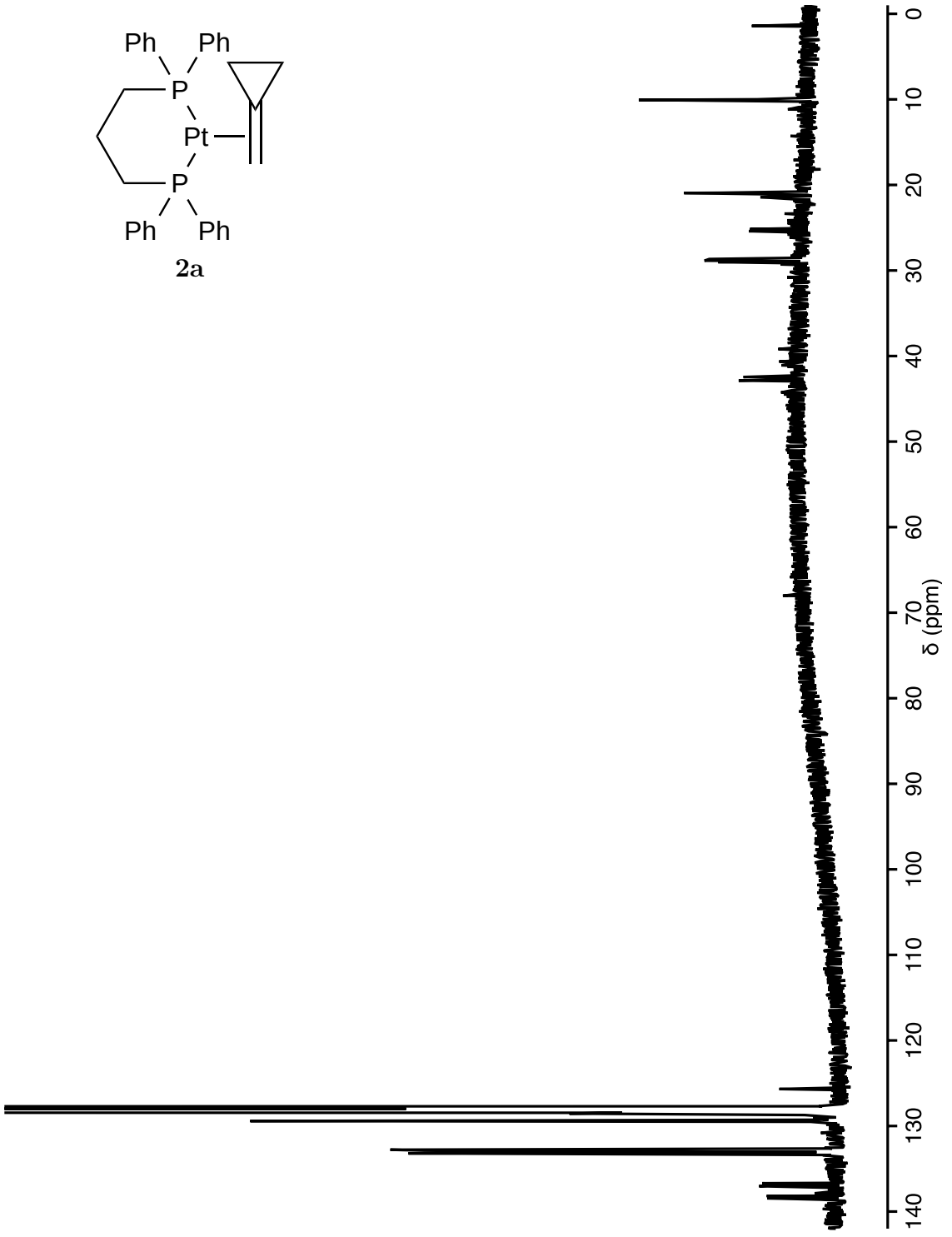

Figure A.8. $^{13}C\{^{1}H\}$ NMR spectrum of [Pt(MCP)(dppp)] (**2a**) (125 MHz, RT, 40 mg/mL, C_6D_6).

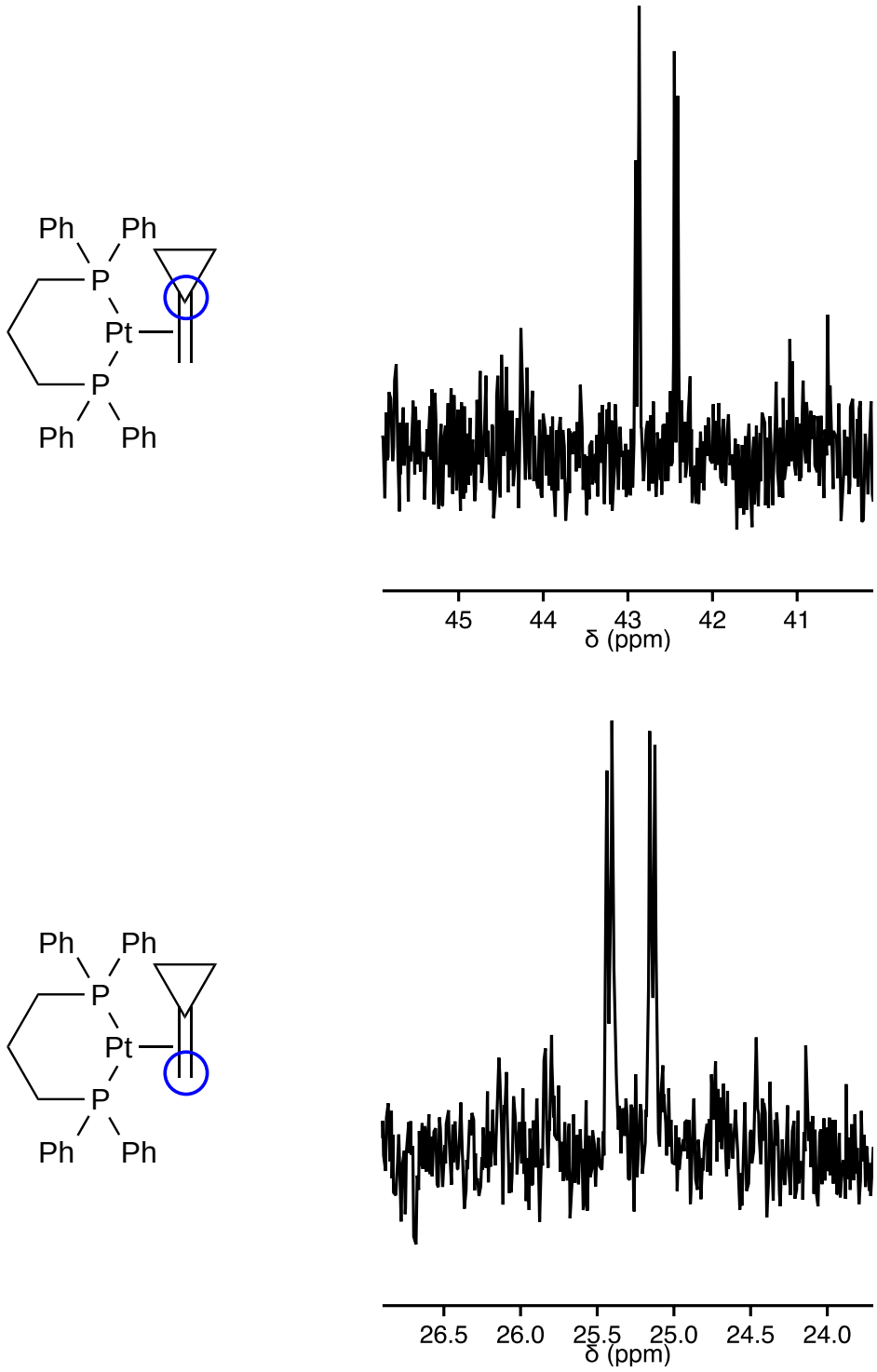

Figure A.9. Expanded $^{13}C\{^{1}H\}$ NMR spectrum of [Pt(MCP)(dppp)] (**2a**) (125 MHz, RT, 40 mg/mL, C_6D_6).

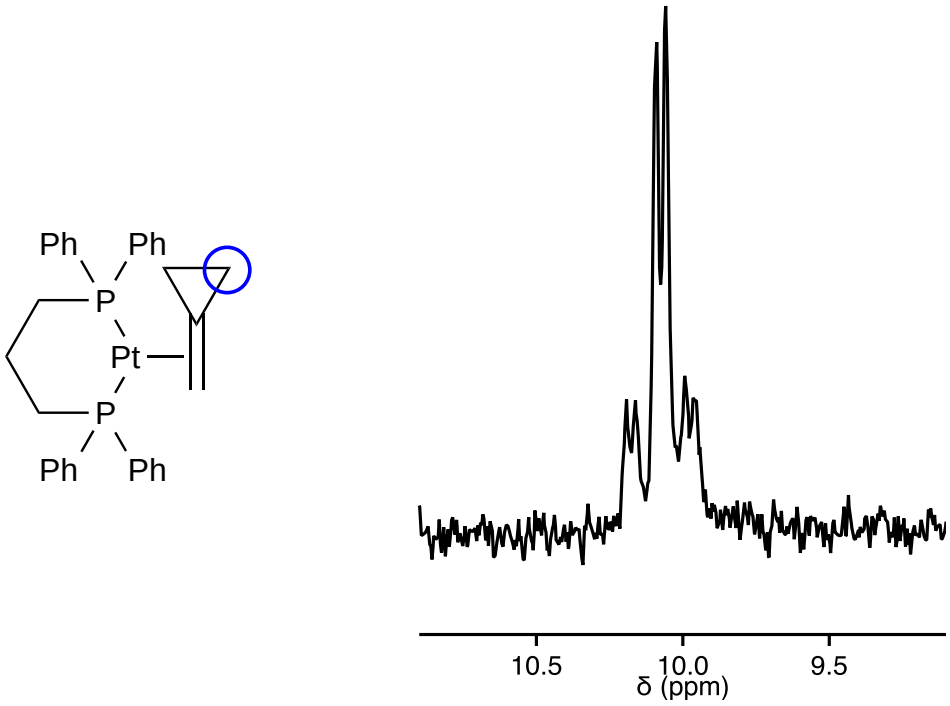

Figure A.10. Expanded $^{13}C\{^{1}H\}$ NMR spectrum of [Pt(MCP)(dppp)] (**2a**) (125 MHz, RT, 40 mg/mL, C_6D_6).

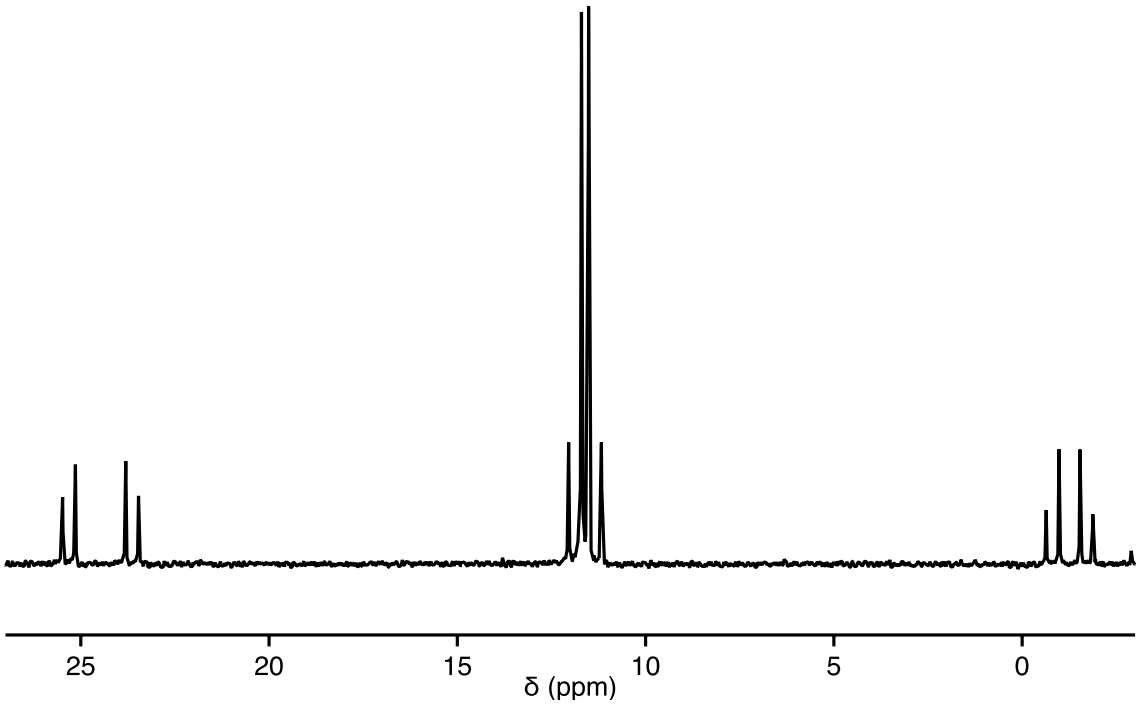

Figure A.11. $^{31}P\{^{1}H\}$ NMR spectrum of [Pt(MCP)(dppp)] (**2a**) (121 MHz, RT, 40 mg/mL, C_6D_6).

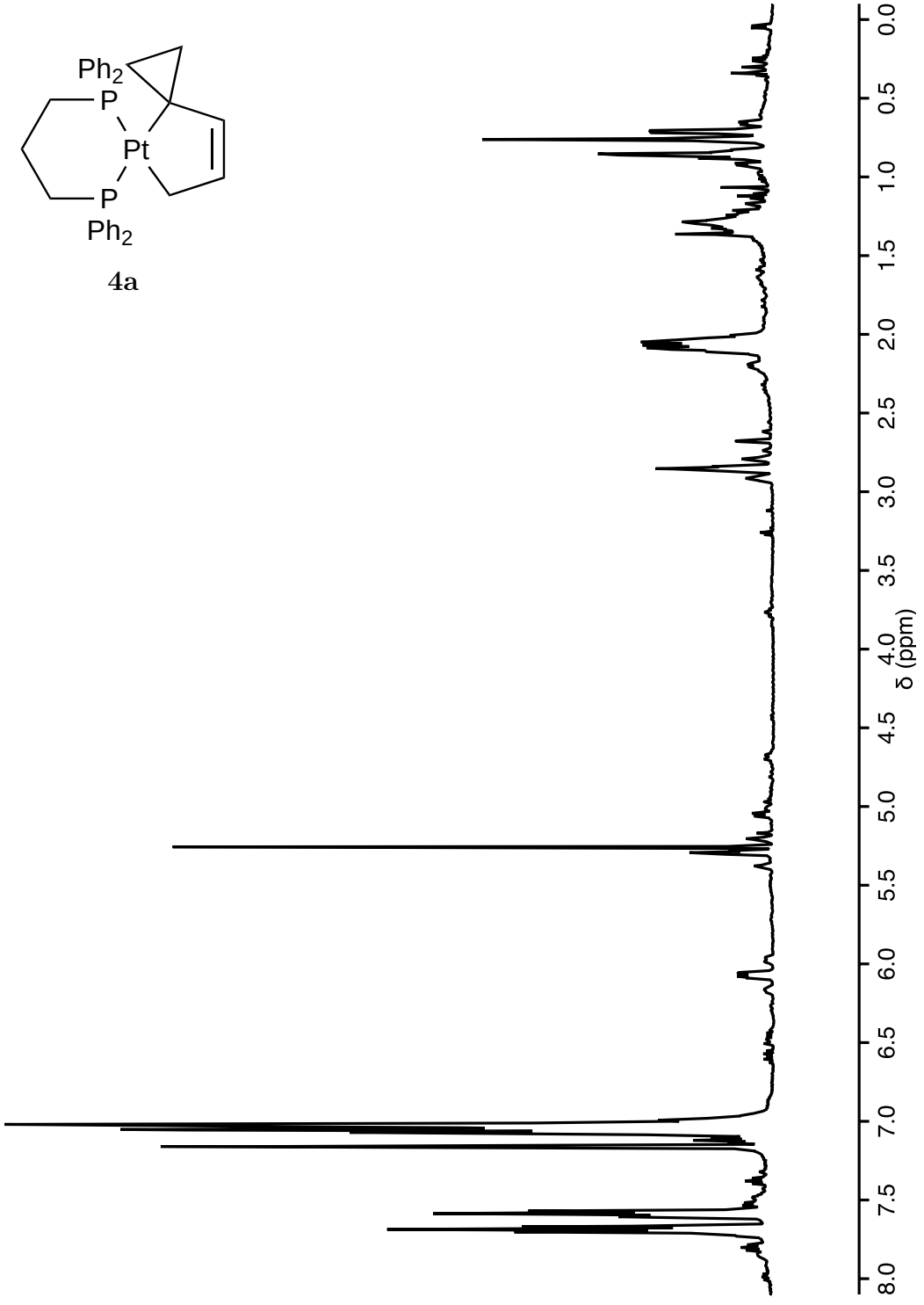

Figure A.12. ^{1}H NMR spectrum of [Pt($CH_2CH{=}CHC(CH_2)_2$)(dppp)] (**4a**) (500 MHz, RT, 40 mg/mL, C_6D_6).

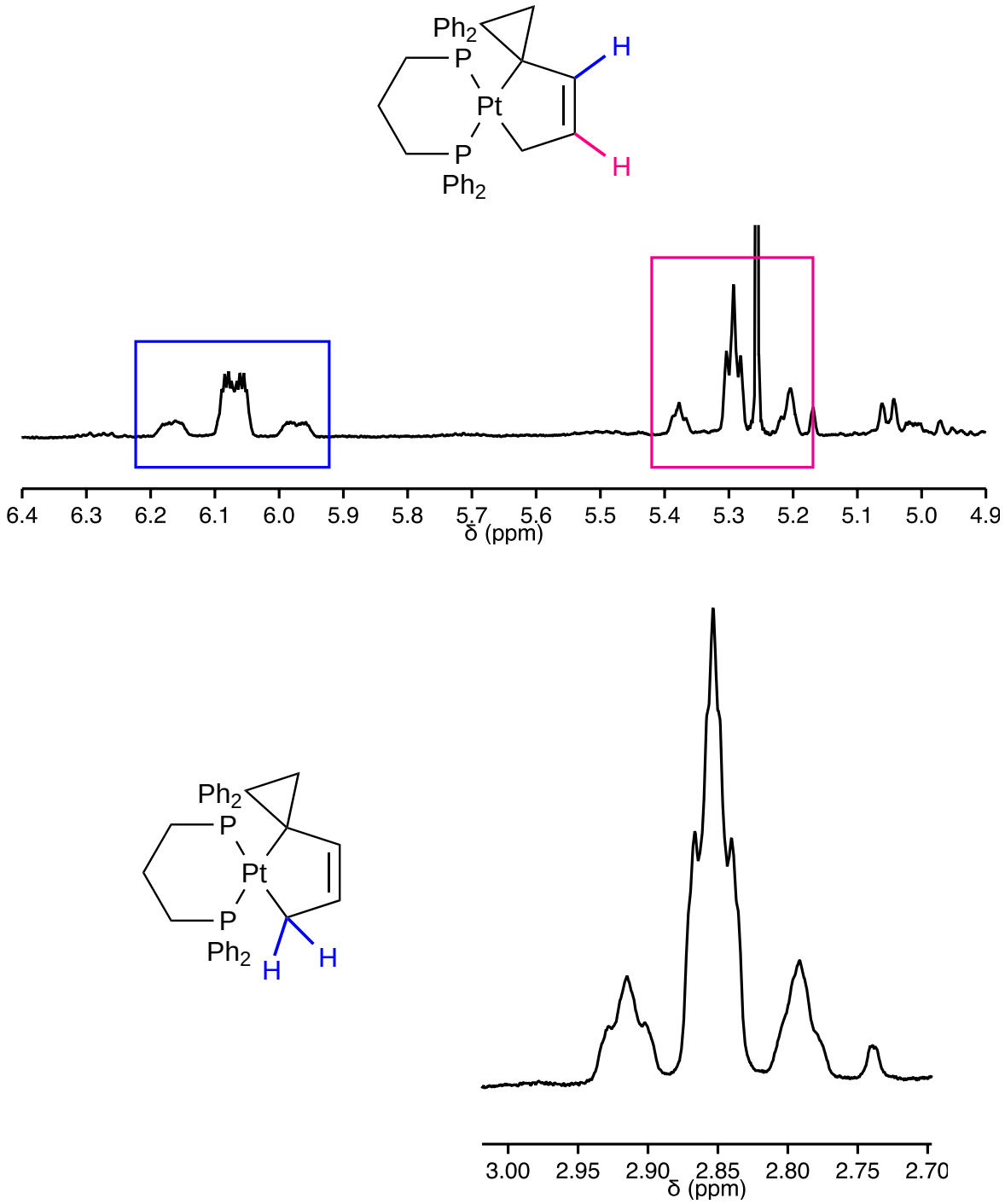

Figure A.13. Expanded ^{1}H NMR spectrum of [Pt($CH_2CH{=}CHC(CH_2)_2$)(dppp)] (**4a**) (500 MHz, RT, 40 mg/mL, C_6D_6).

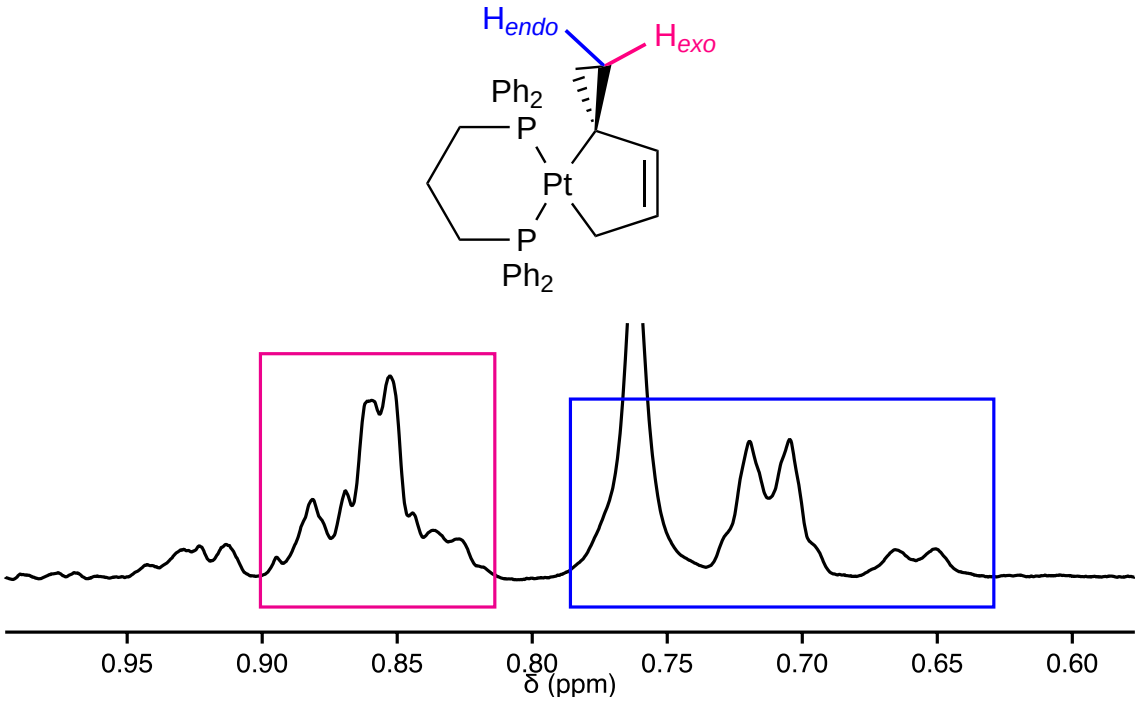

Figure A.14. Expanded ^{1}H NMR spectrum of [Pt(CH$_2$CH=CHC(CH$_2$)$_2$)(dppp)] (**4a**) (500 MHz, RT, 40 mg/mL, C$_6$D$_6$).

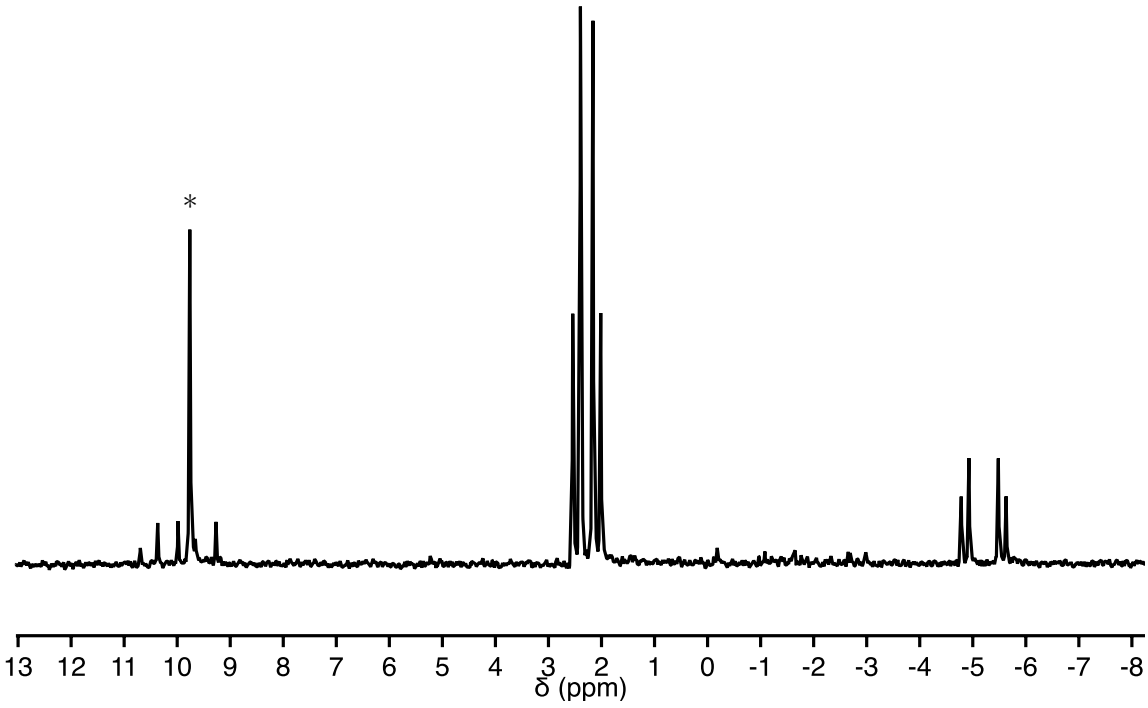

Figure A.15. ^{31}P{^{1}H} NMR spectrum of [Pt(CH$_2$CH=CHC(CH$_2$)$_2$)(dppp)] (**4a**) (121 MHz, RT, 40 mg/mL, C$_6$D$_6$). * signifies peaks belonging to other species.

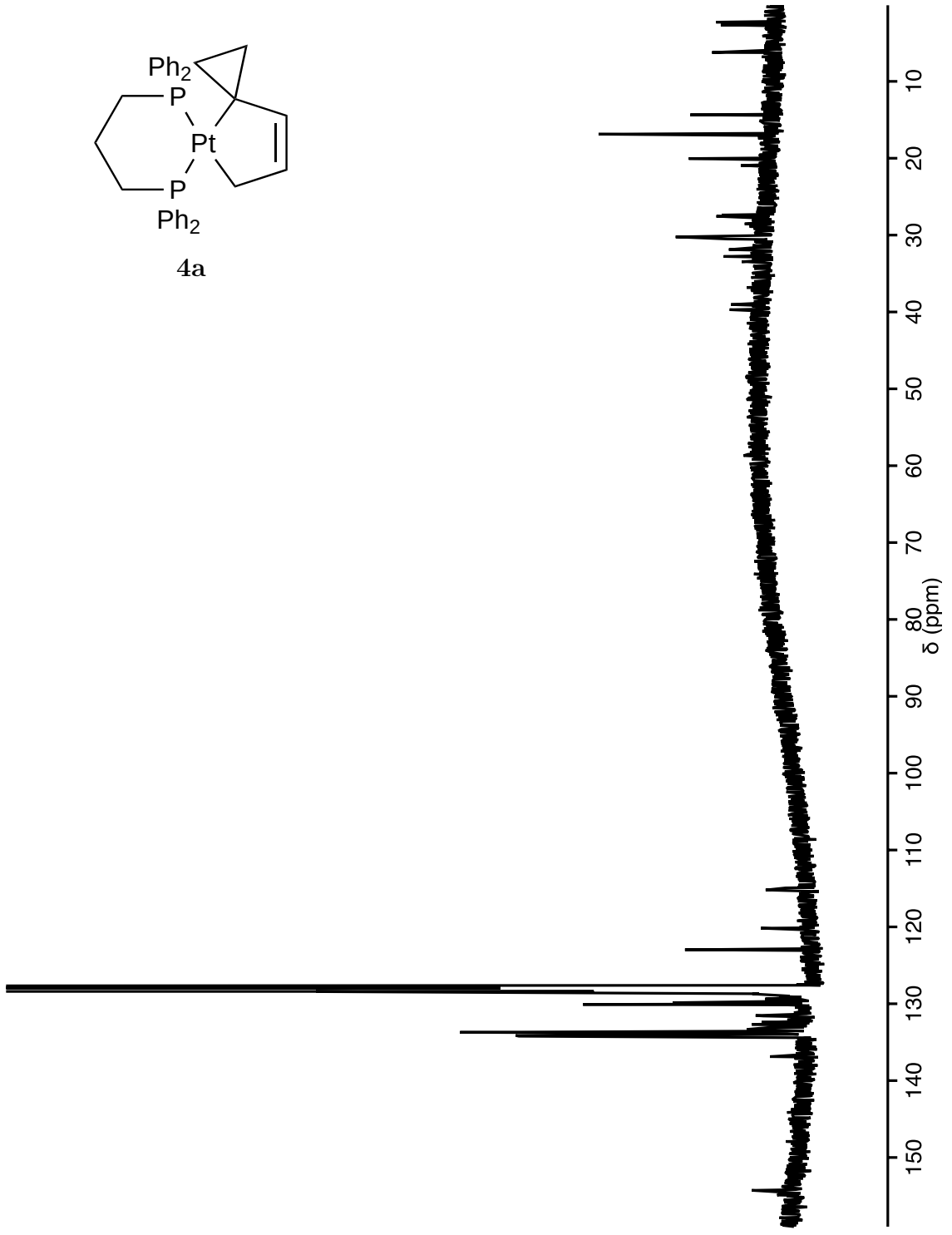

Figure A.16. $^{13}C\{^{1}H\}$ NMR spectrum of [Pt($CH_2CH{=}CHC(CH_2)_2$)(dppp)] (**4a**) (125 MHz, RT, 40 mg/mL, C_6D_6).

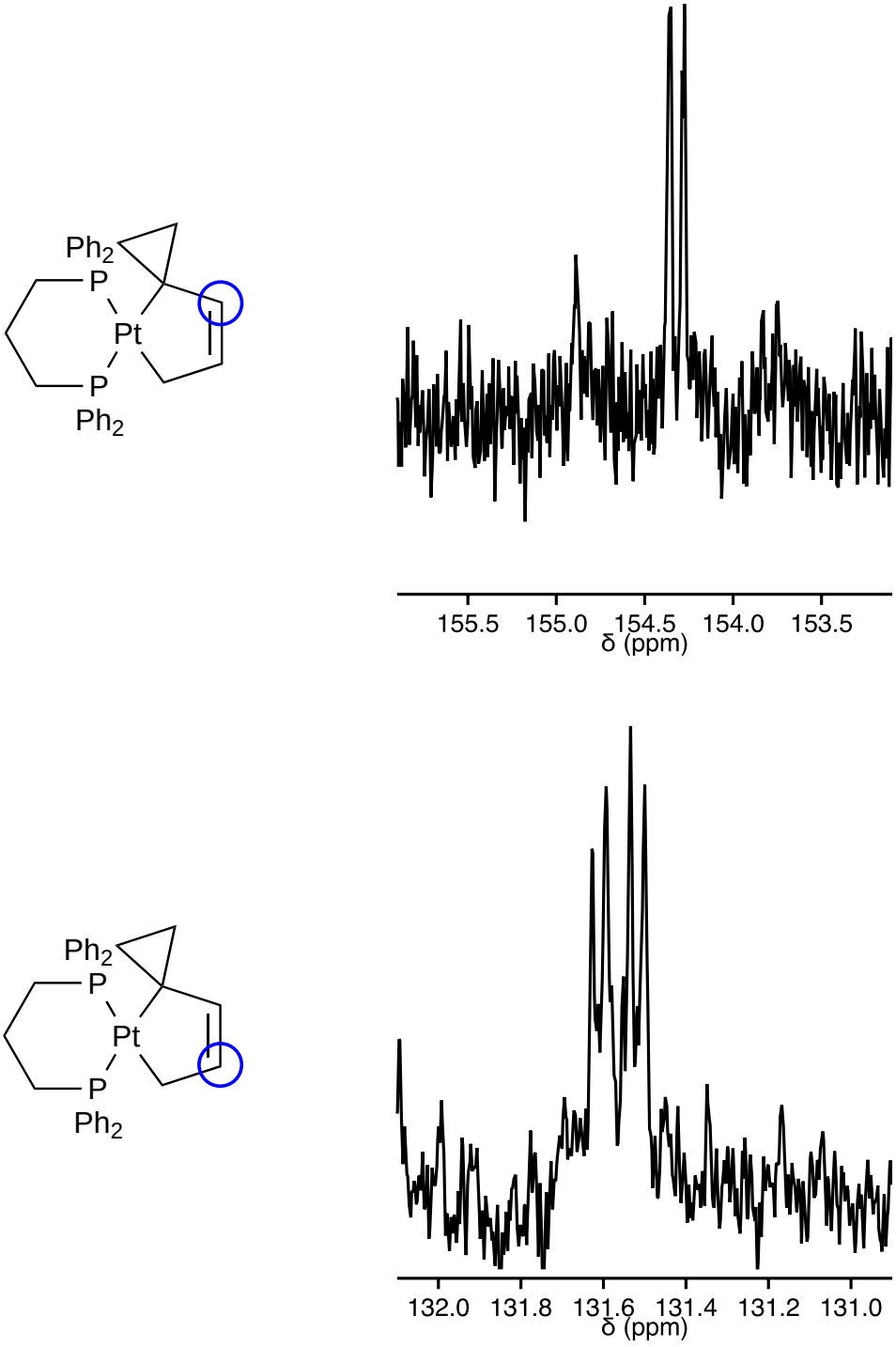

Figure A.17. Expanded $^{13}C\{^{1}H\}$ NMR spectrum of [Pt($CH_2CH{=}CHC(CH_2)_2$)(dppp)] (**4a**) (125 MHz, RT, 40 mg/mL, C_6D_6).

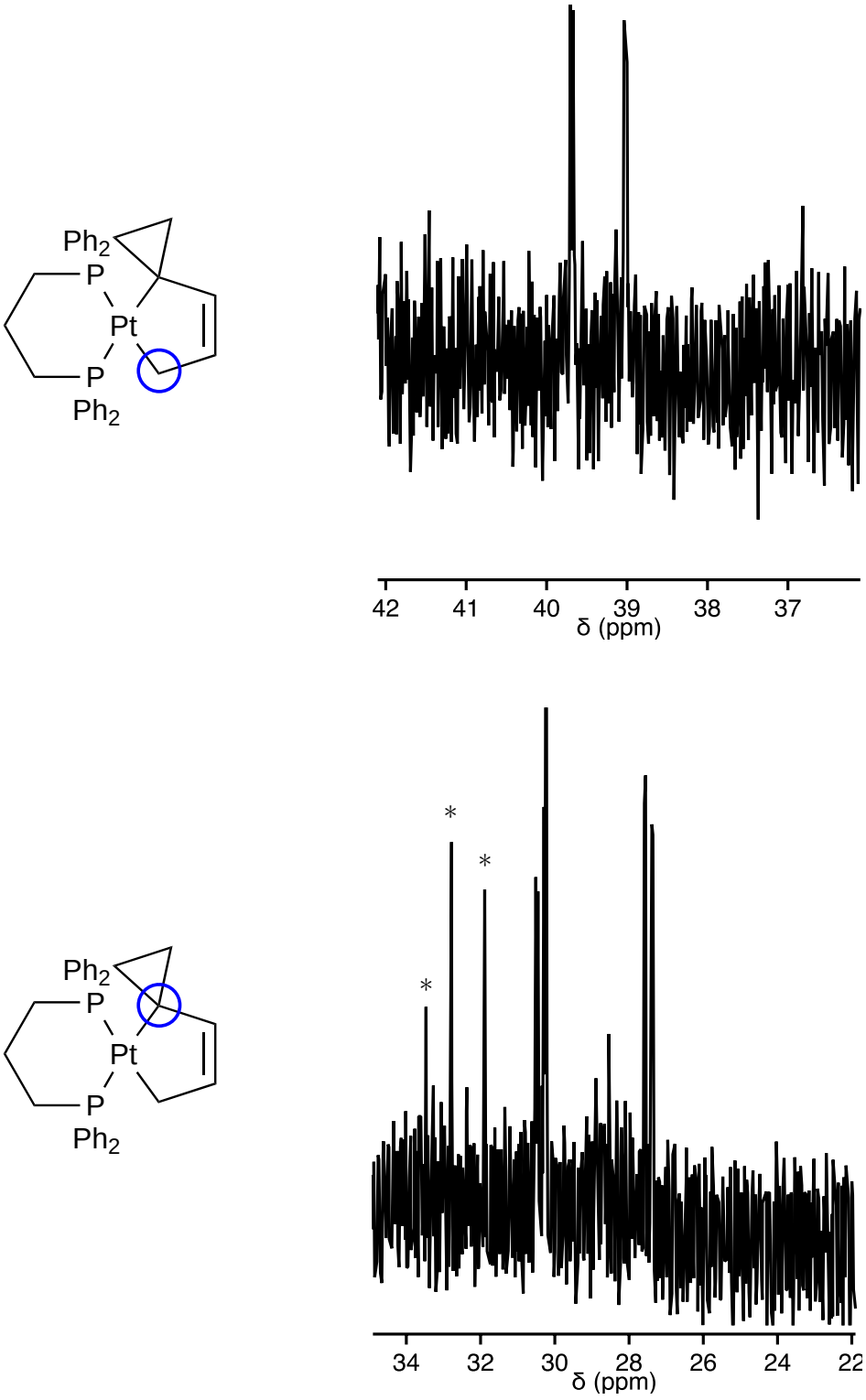

Figure A.18. Expanded $^{13}C\{^{1}H\}$ NMR spectrum of [Pt($CH_2CH{=}CHC(CH_2)_2$)(dppp)] (**4a**) (125 MHz, RT, 40 mg/mL, C_6D_6).* signifies peaks belonging to other species

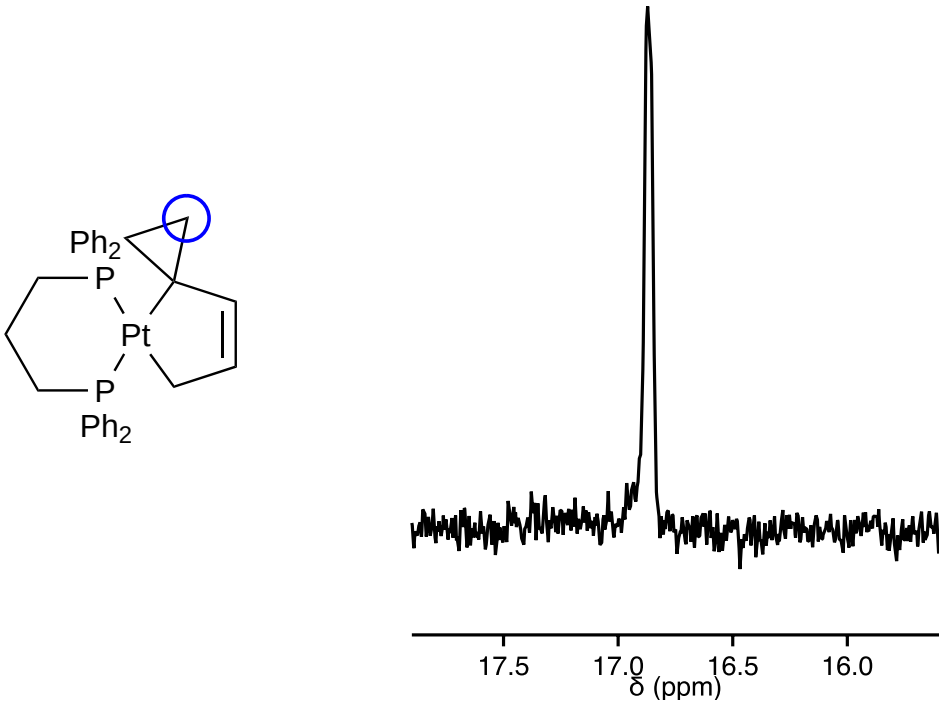

Figure A.19. Expanded $^{13}C\{^{1}H\}$ NMR spectrum of [Pt($CH_2CH{=}CHC(CH_2)_2$)(dppp)] (**4a**) (125 MHz, RT, 40 mg/mL, C_6D_6).

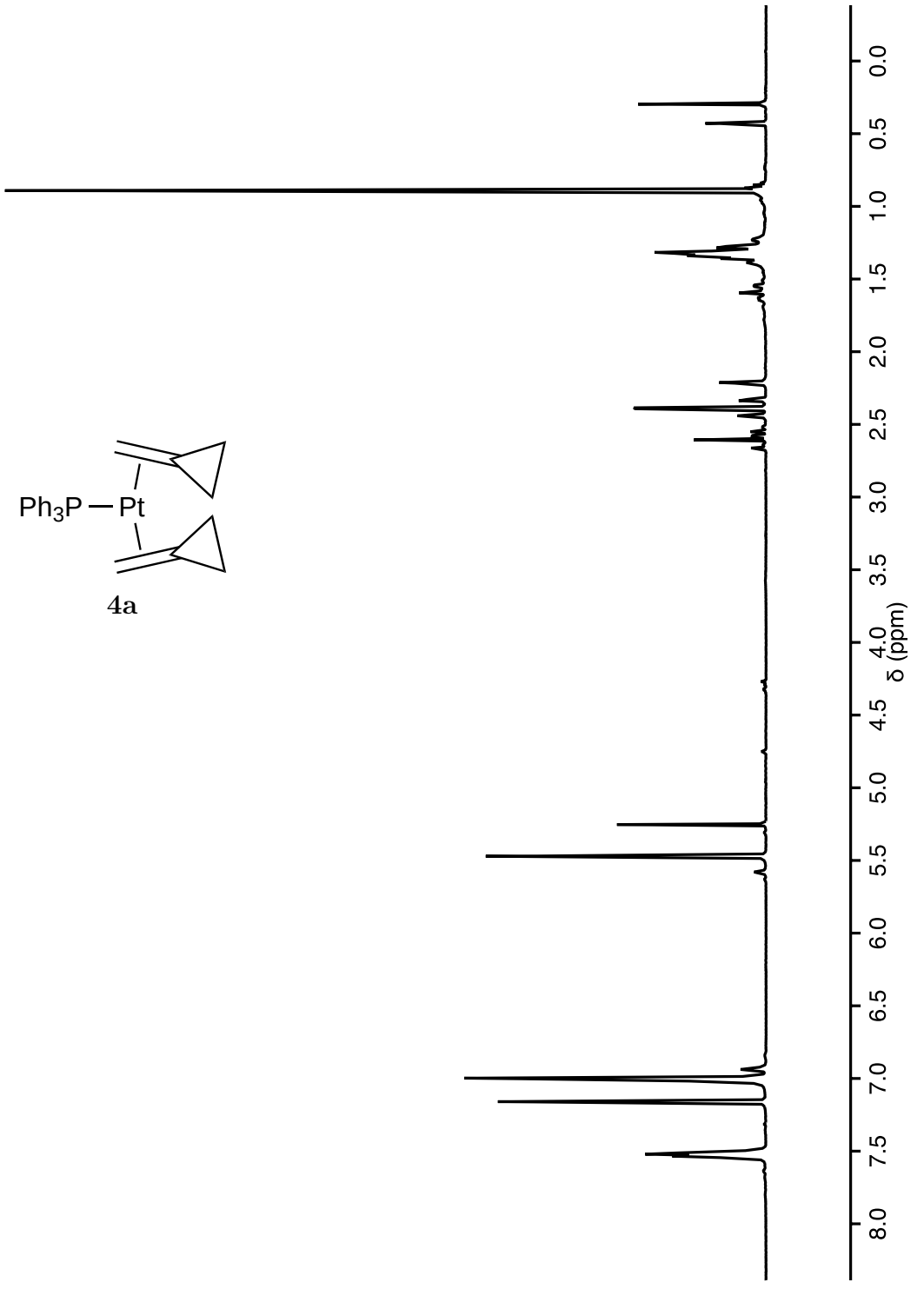

Figure A.20. ^{1}H NMR spectrum of [Pt(MCP)$_2$(PPh$_3$)] (**7a**) (500 MHz, RT, 40 mg/mL, C_6D_6).

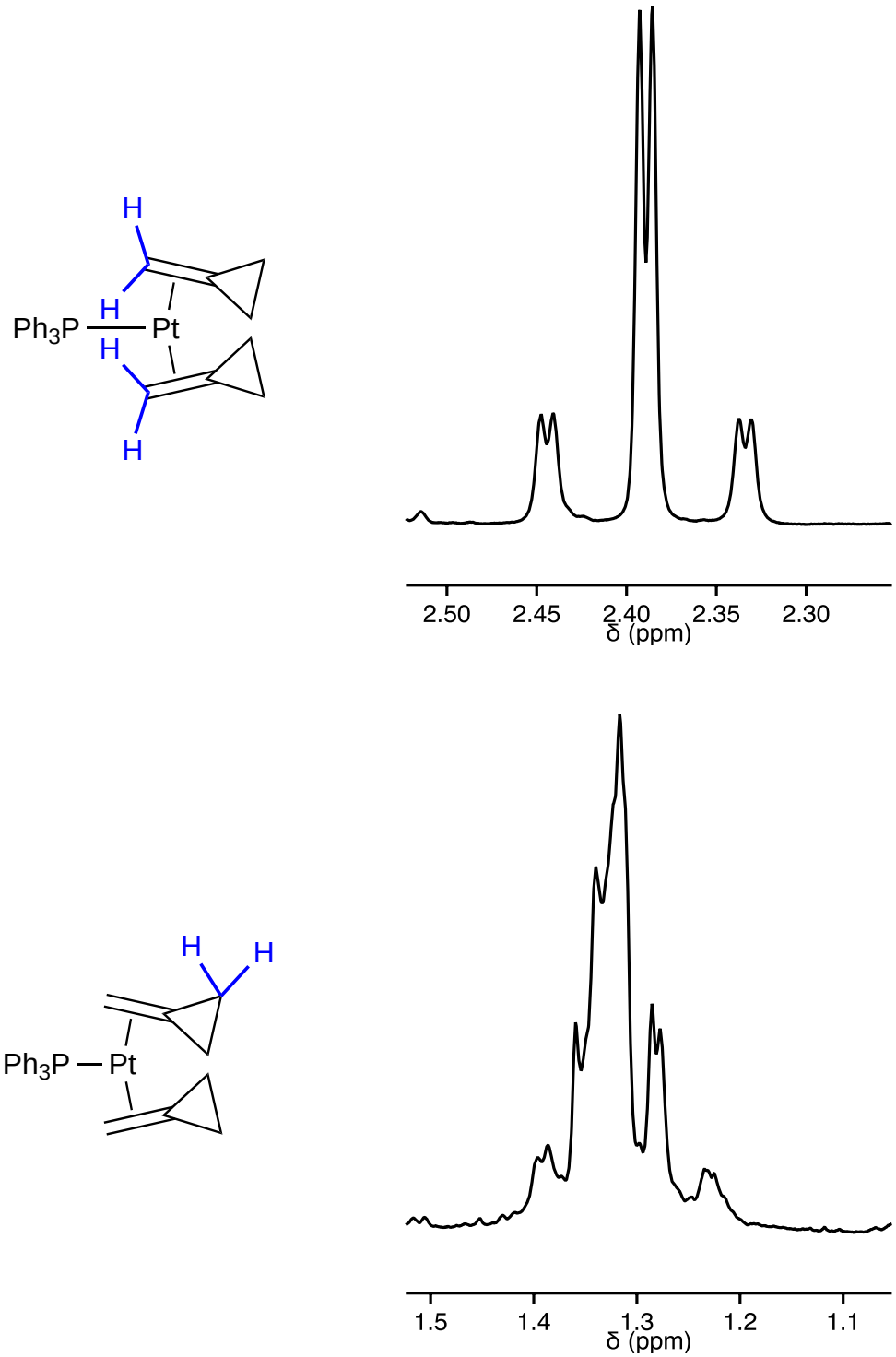

Figure A.21. Expanded ^{1}H NMR spectrum of [Pt(MCP)$_2$(PPh$_3$)] (**7a**) (500 MHz, RT, 40 mg/mL, C_6D_6).

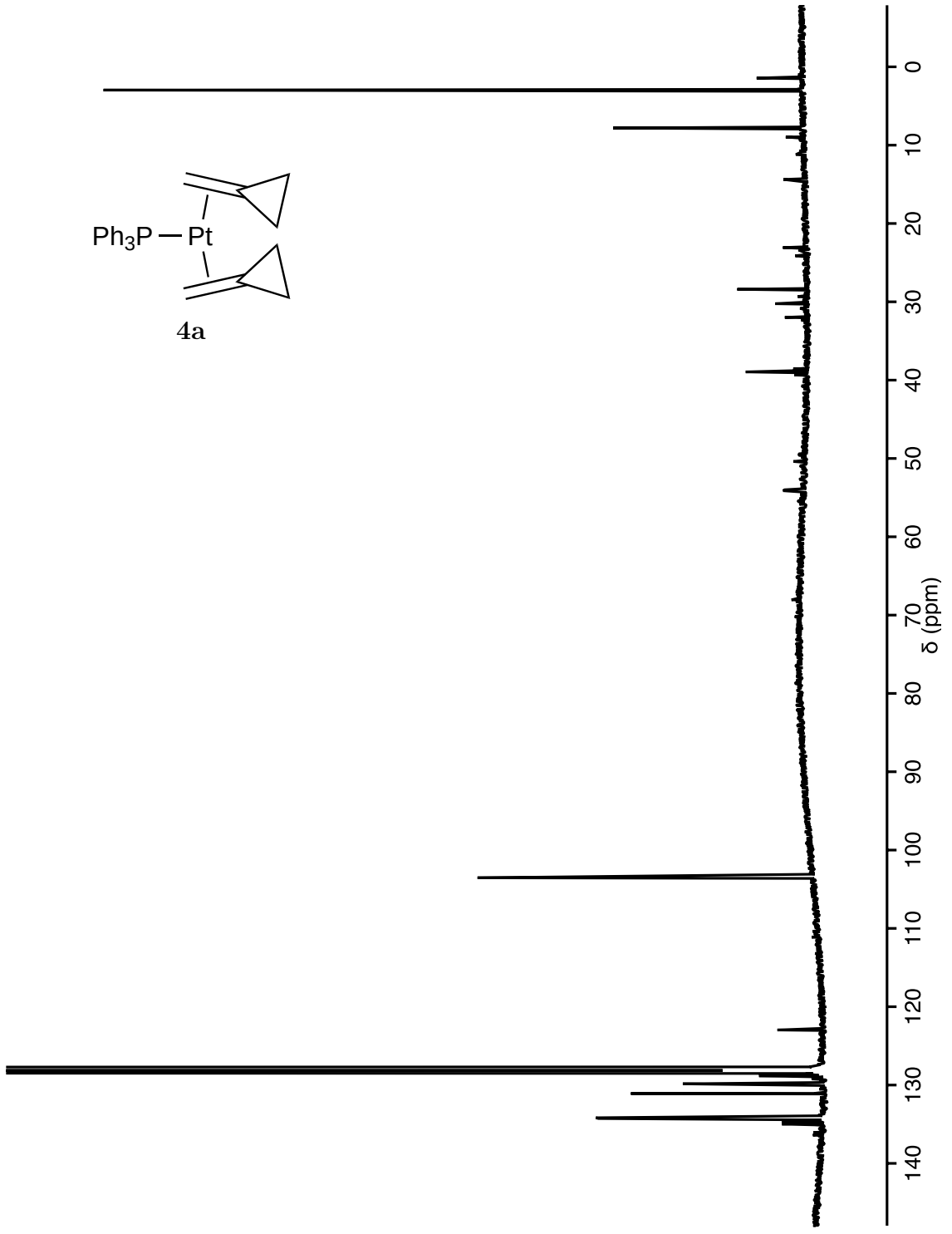

Figure A.22. $^{13}C\{^{1}H\}$ NMR spectrum of [Pt(MCP)$_2$(PPh$_3$)] (**7a**) (125 MHz, RT, 40 mg/mL, C_6D_6).

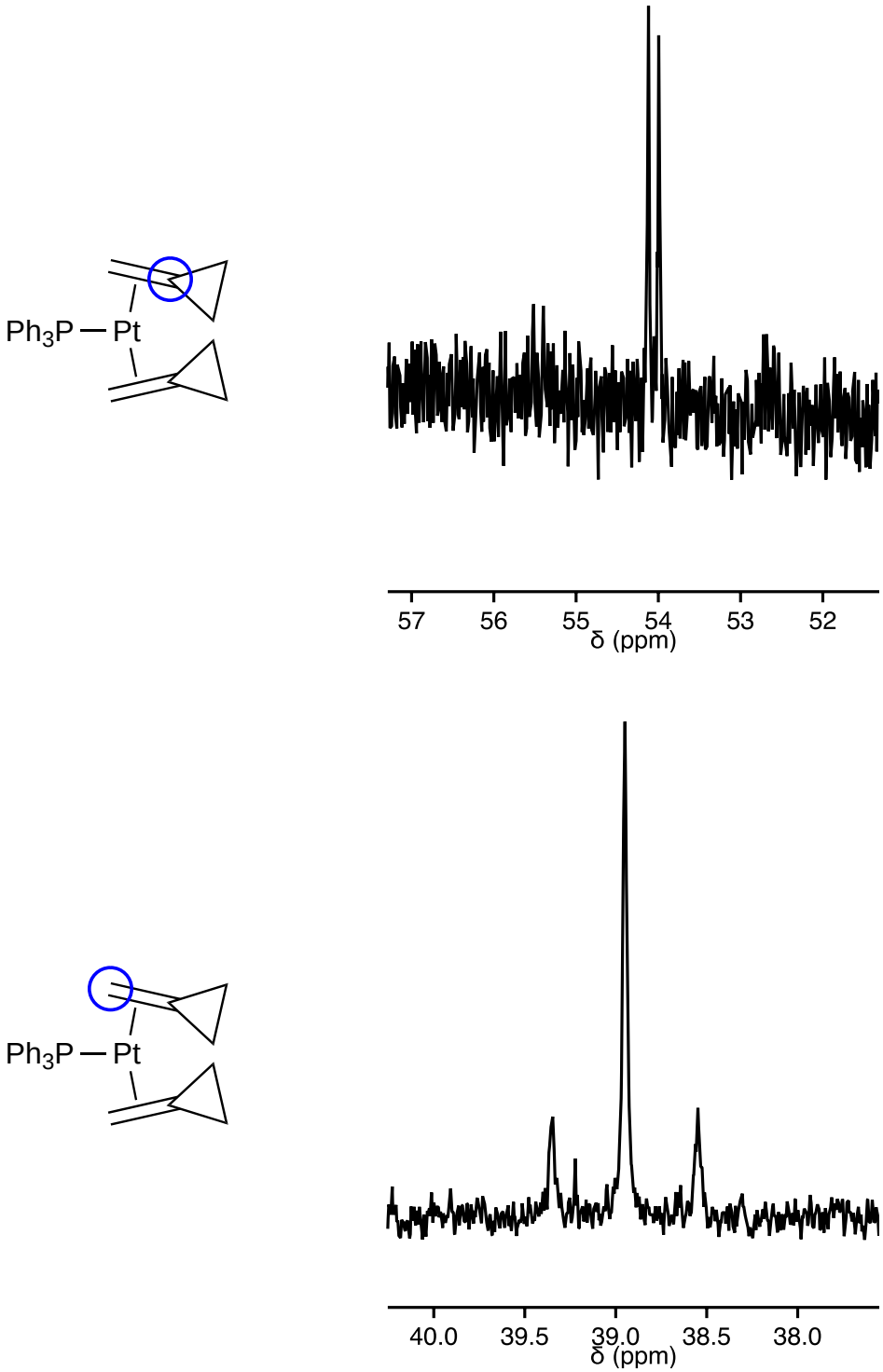

Figure A.23. Expanded $^{13}C\{^{1}H\}$ NMR spectrum of $[Pt(MCP)_2(PPh_3)]$ (**7a**) (125 MHz, RT, 40 mg/mL, C_6D_6).

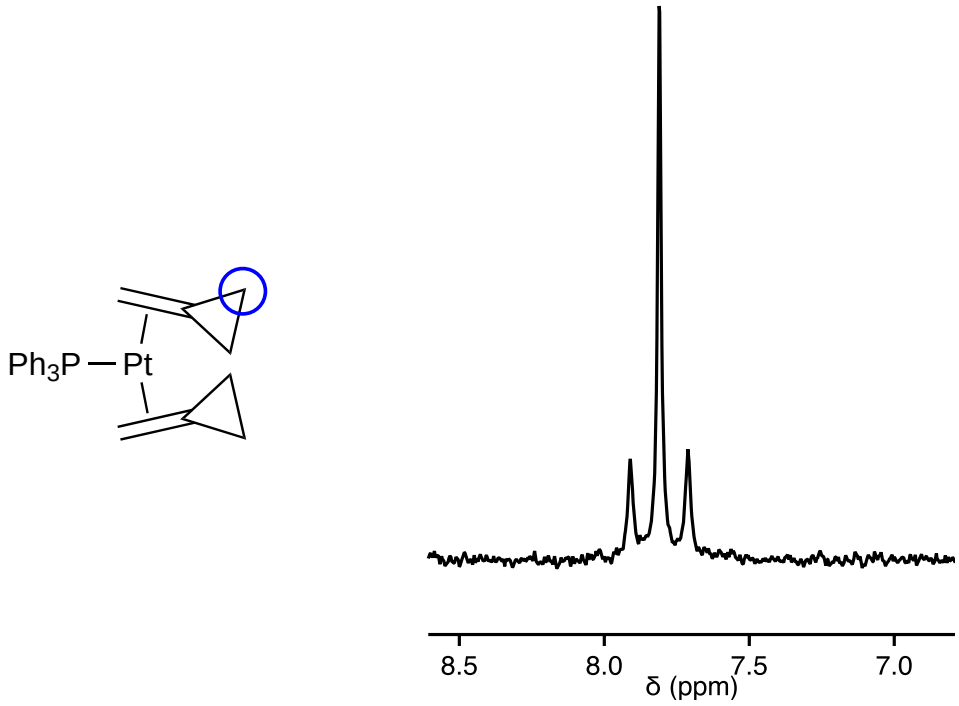

Figure A.24. Expanded $^{13}C\{^{1}H\}$ NMR spectrum of $[Pt(MCP)_2(PPh_3)]$ (**7a**) (125 MHz, RT, 40 mg/mL, C_6D_6).

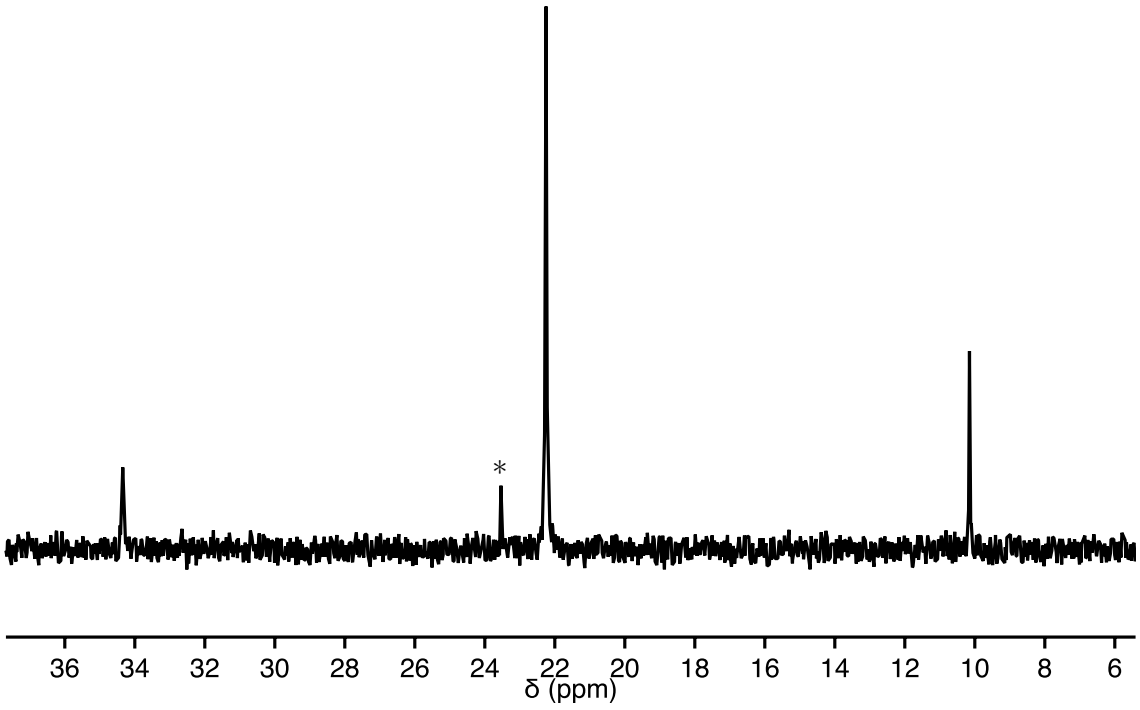

Figure A.25. $^{31}P\{^{1}H\}$ NMR spectrum of $[Pt(MCP)_2(PPh_3)]$ (**7a**) (121 MHz, RT, 40 mg/mL, C_6D_6). * signifies peaks belonging to other species.

A.2 Chapter Three

[Pt(η^3-C(CH_2)$_2$CHCHMe)(C_6H_3-*o*-$CH_2P^tBu_2$-*m*-CH_2S^tBu)] (11a and 11b)

^{1}H NMR spectrum – Figures A.26 and A.27, pages 185 and 186

^{13}C{^{1}H} NMR spectrum – Figures A.28–A.31, pages 187–190

HMBC spectrum – Figures A.32 and A.33, pages 191 and 192

COSY spectrum – Figure A.34, page 192

^{31}P{^{1}H} NMR spectrum – Figure A.35, page 193

[Pt(η^3-C(CH_2)$_2$CHCHMe)(dppp)][$HC(SO_2CF_3)_2$] (*anti* Me) (13a[$HC(SO_2CF_3)_2$]) and [Pt(η^3-C(CH_2)$_2$CHCHMe)(dppp)][$HC(SO_2CF_3)_2$] (*syn* Me) (13b[$HC(SO_2CF_3)_2$])

^{1}H NMR spectra – Figures A.36–A.39, pages 194–197

^{13}C{^{1}H} NMR spectrum – Figures A.40–A.43, pages 198–201

HMBC spectrum – Figures A.44 and A.45, pages 202 and 203

COSY spectrum – Figure A.46, page 203

^{31}P{^{1}H} NMR spectra – Figures A.47 and A.48, pages 204 and 205

[Pt(η^3-CH_2CMeCH_2)(dppp)][$PhC(SO_2CF_3)_2$] (15[$PhC(SO_2CF_3)_2$]), [Pt(η^3-$CH_2CHCHMe$)(dppp)][$PhC(SO_2CF_3)_2$] (*anti* Me) (16a[$PhC(SO_2CF_3)_2$]) and [Pt(η^3-$CH_2CHCHMe$)(dppp)][$PhC(SO_2CF_3)_2$] (*syn* Me) (16b[$PhC(SO_2CF_3)_2$])

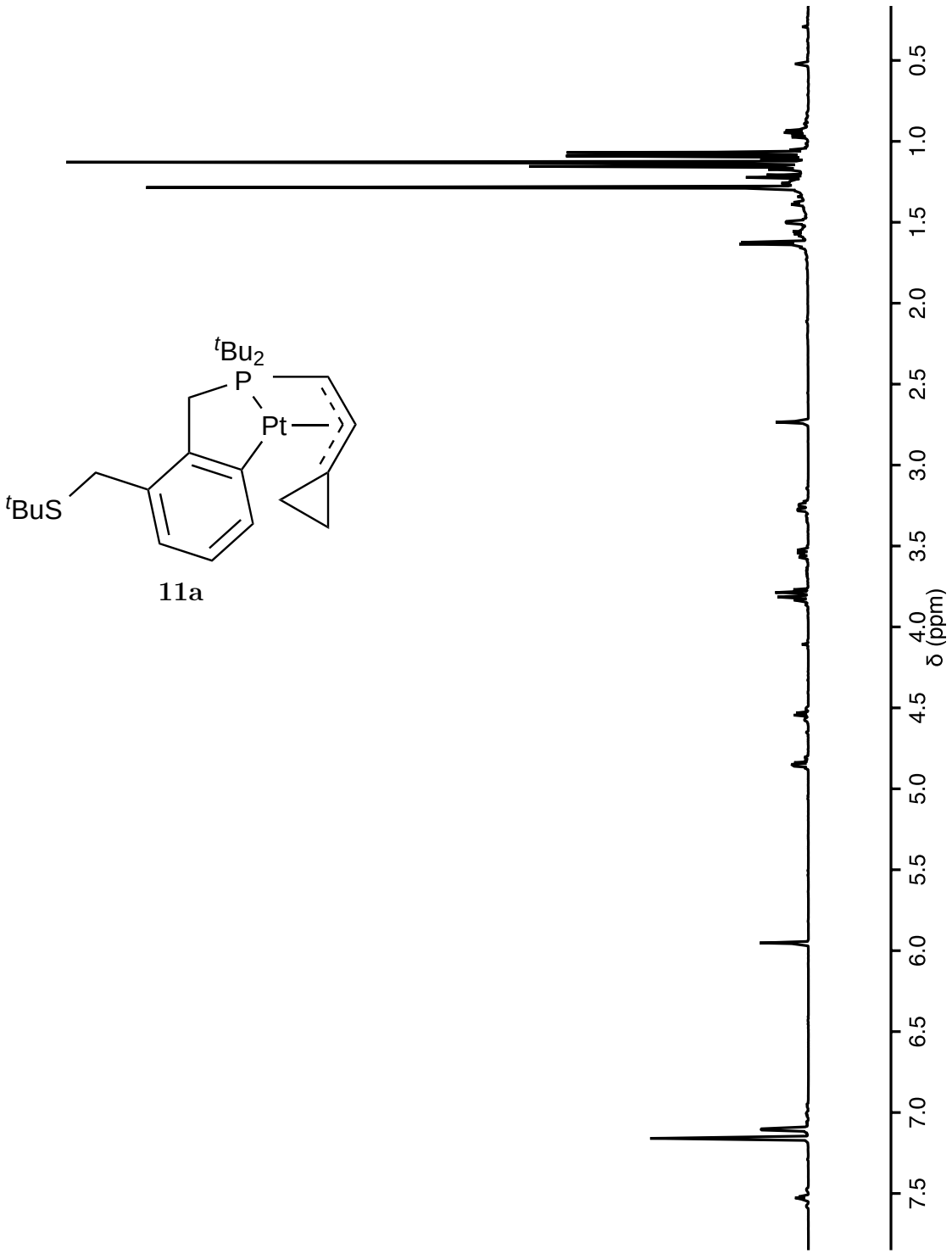

Figure A.26. ^{1}H NMR spectrum of $[Pt(\eta^3\text{-}C(CH_2)_2CHCHMe)(C_6H_3\text{-}o\text{-}CH_2P^tBu_2\text{-}m\text{-}CH_2S^tBu)]$ (**11a**) (600 MHz, RT, 40 mg/mL, C_6D_6).

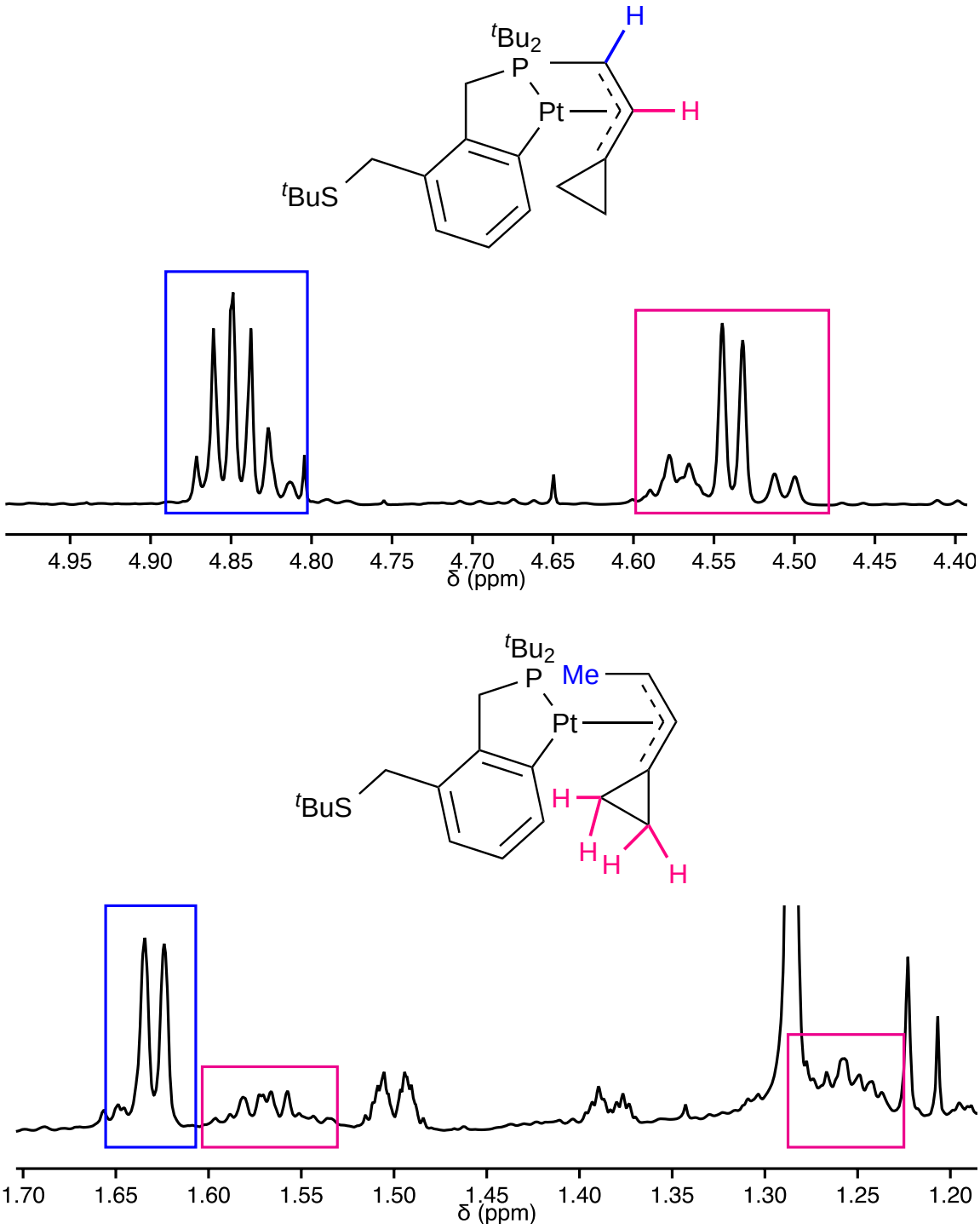

Figure A.27. Expanded ^{1}H NMR spectrum of [Pt(η^3-C(CH$_2$)$_2$CHCHMe)(C$_6$H$_3$-*o*-CH$_2$P^{t}Bu$_2$-*m*-CH$_2$S^{t}Bu)] (**11a**) (600 MHz, RT, 40 mg/mL, C$_6$D$_6$).

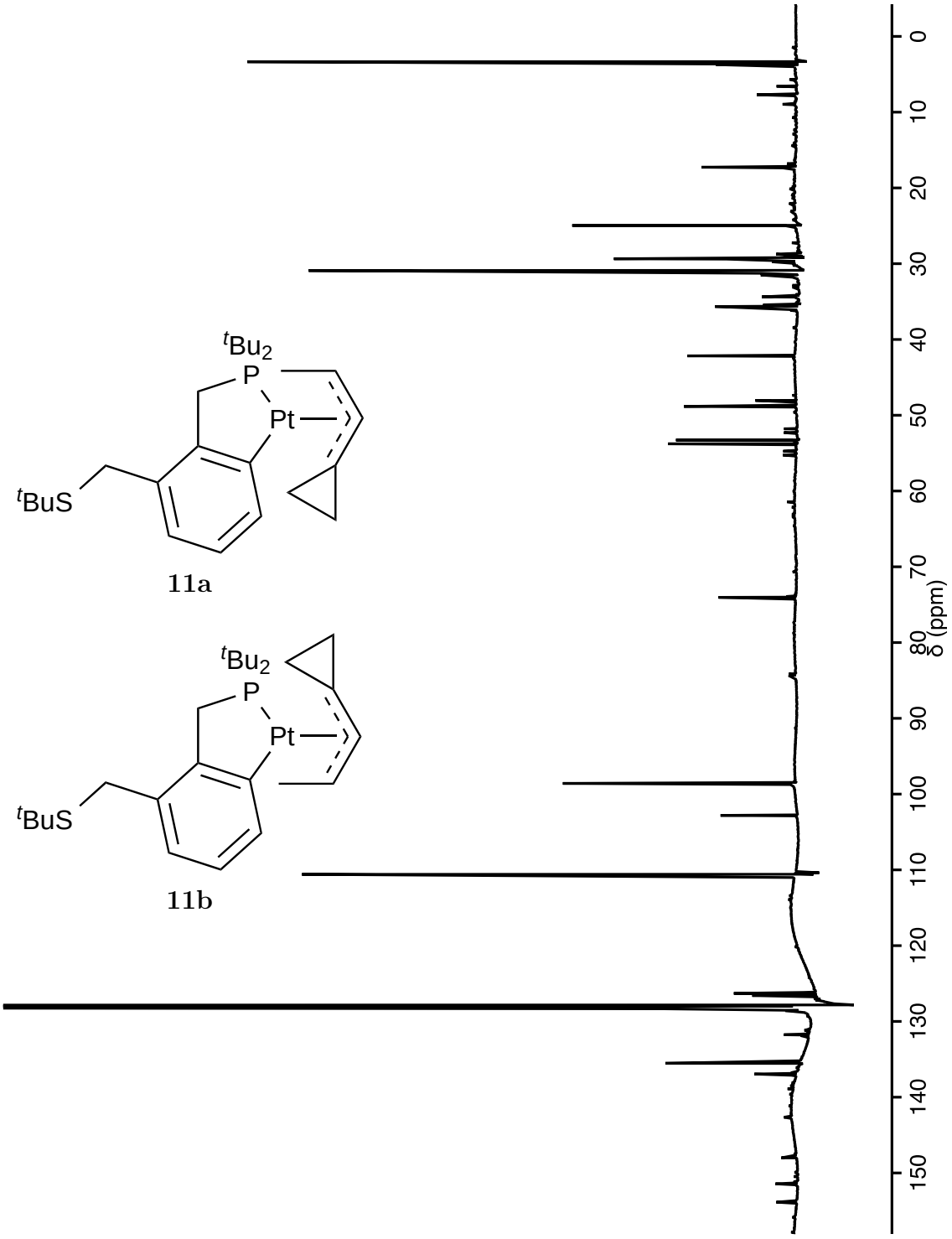

Figure A.28. $^{13}C\{^{1}H\}$ NMR spectrum of carbon-13 enriched [Pt(η^3-C$(CH_2)_2$CHCHMe)(C_6H_3-*o*-$CH_2P^tBu_2$-*m*-CH_2S^tBu)] (**11a** and **11b**) (150 MHz, RT, 40 mg/mL, C_6D_6).

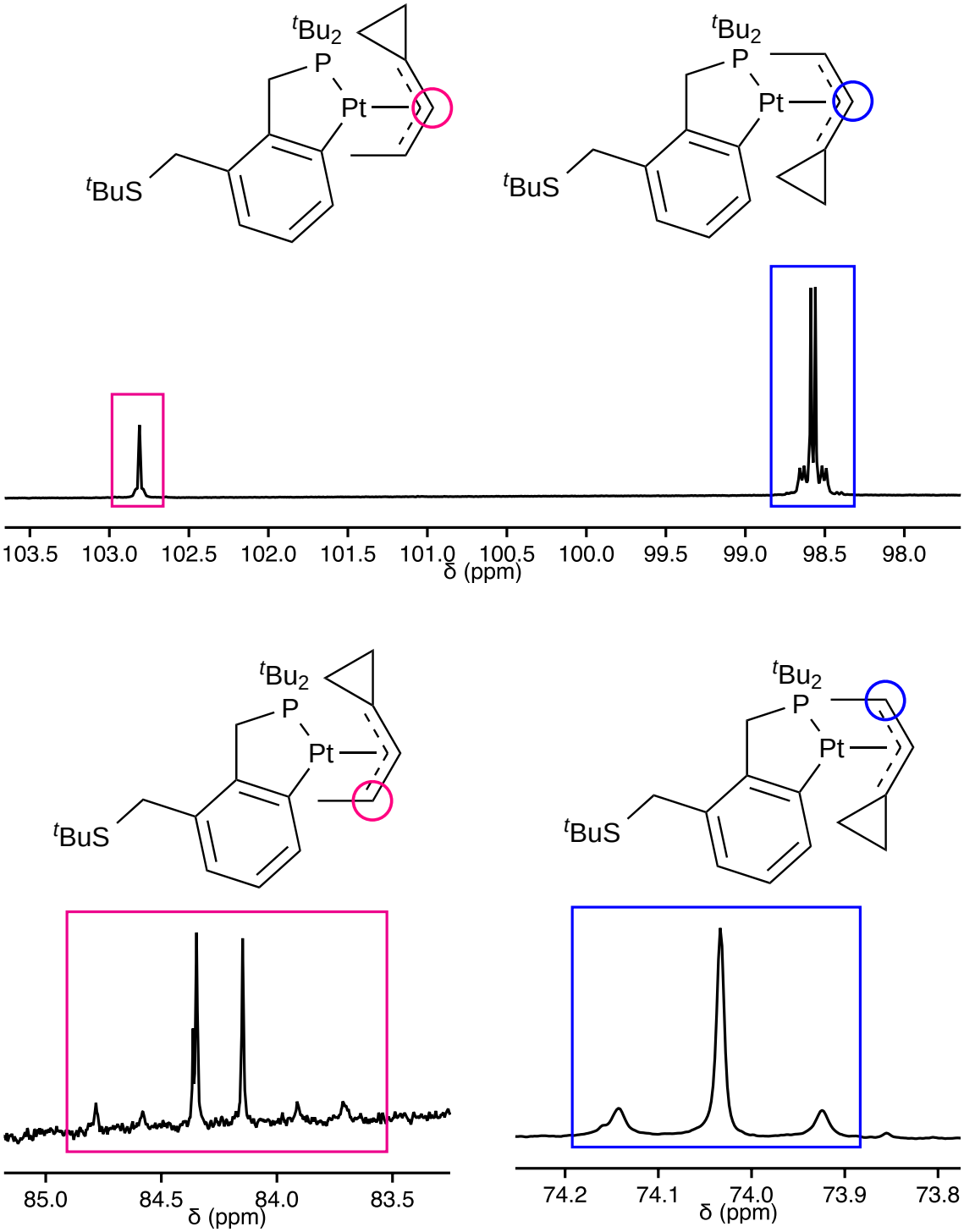

Figure A.29. Expanded $^{13}C\{^{1}H\}$ NMR spectrum of carbon-13 enriched [Pt(η^3-C$(CH_2)_2$CHCHMe)(C_6H_3-*o*-$CH_2P^tBu_2$-*m*-CH_2S^tBu)] (**11a** and **11b**) (150 MHz, RT, 40 mg/mL, C_6D_6).

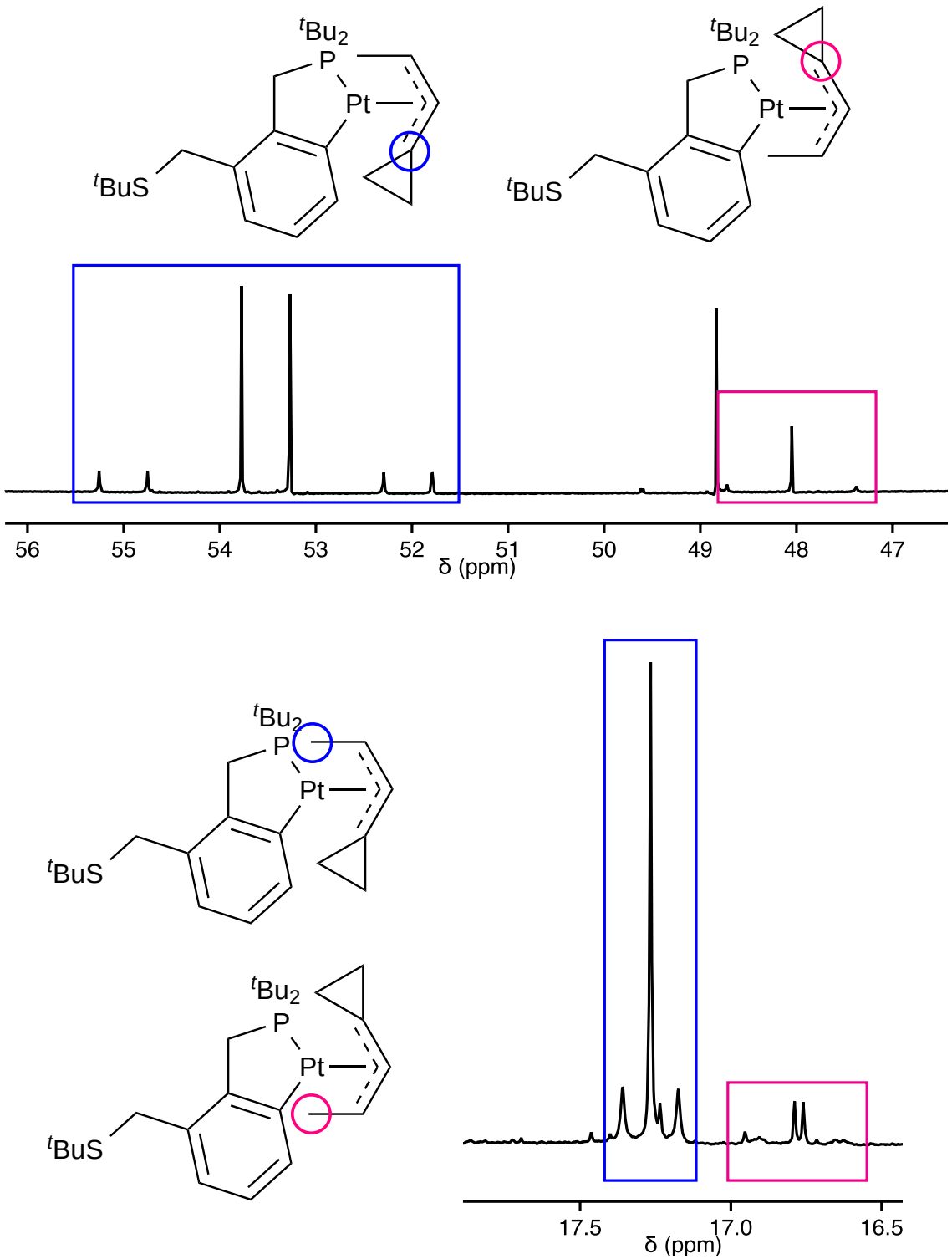

Figure A.30. Expanded $^{13}C\{^{1}H\}$ NMR spectrum of carbon-13 enriched [Pt(η^3-C(CH_2)$_2$CHCHMe)(C_6H_3-*o*-$CH_2P^tBu_2$-*m*-CH_2S^tBu)] (**11a** and **11b**) (150 MHz, RT, 40 mg/mL, C_6D_6).

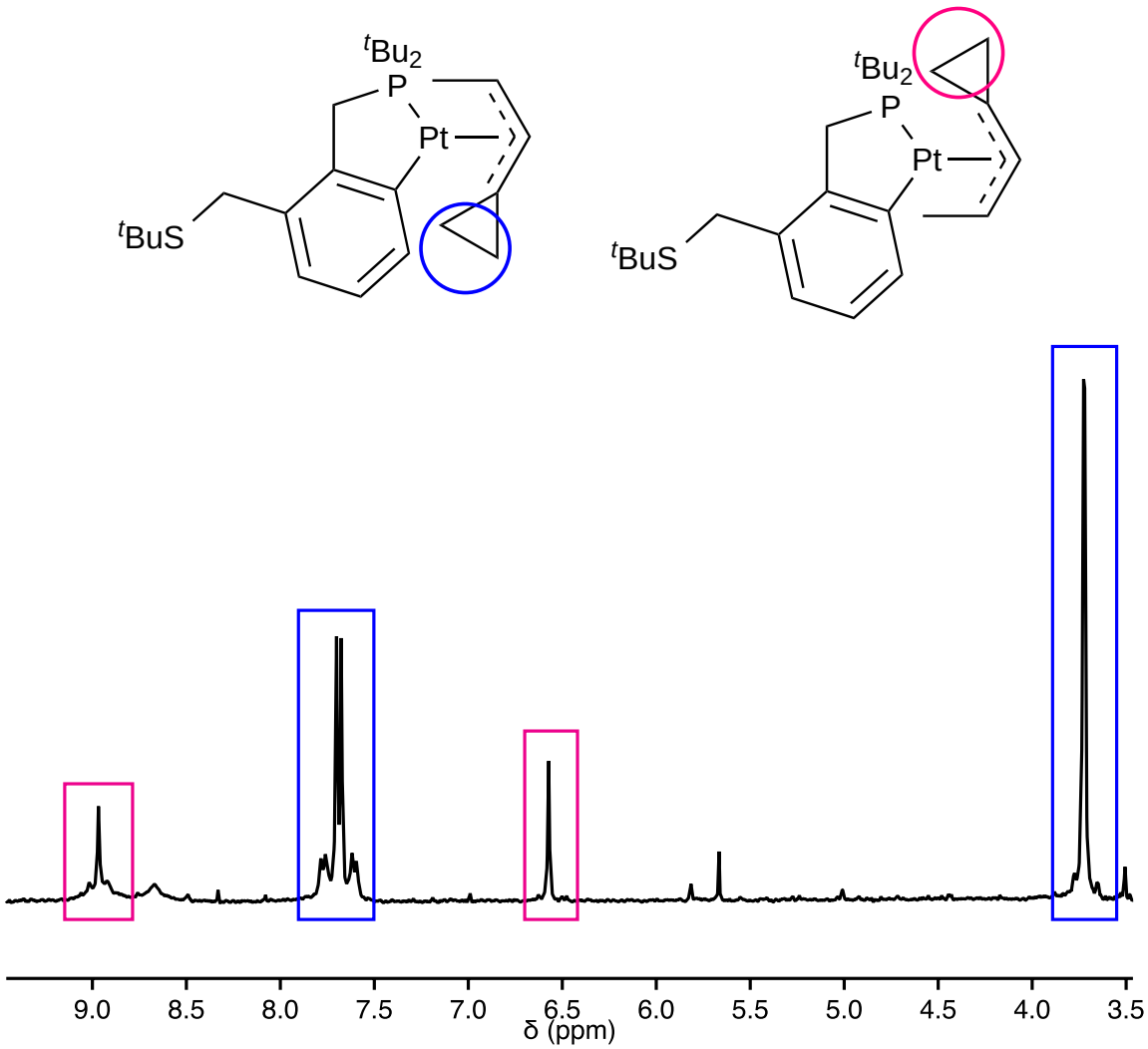

Figure A.31. Expanded $^{13}C\{^{1}H\}$ NMR spectrum of carbon-13 enriched [Pt(η^3-C$(CH_2)_2$CHCHMe)(C_6H_3-*o*-$CH_2P^tBu_2$-*m*-CH_2S^tBu)] (**11a** and **11b**) (150 MHz, RT, 40 mg/mL, C_6D_6).

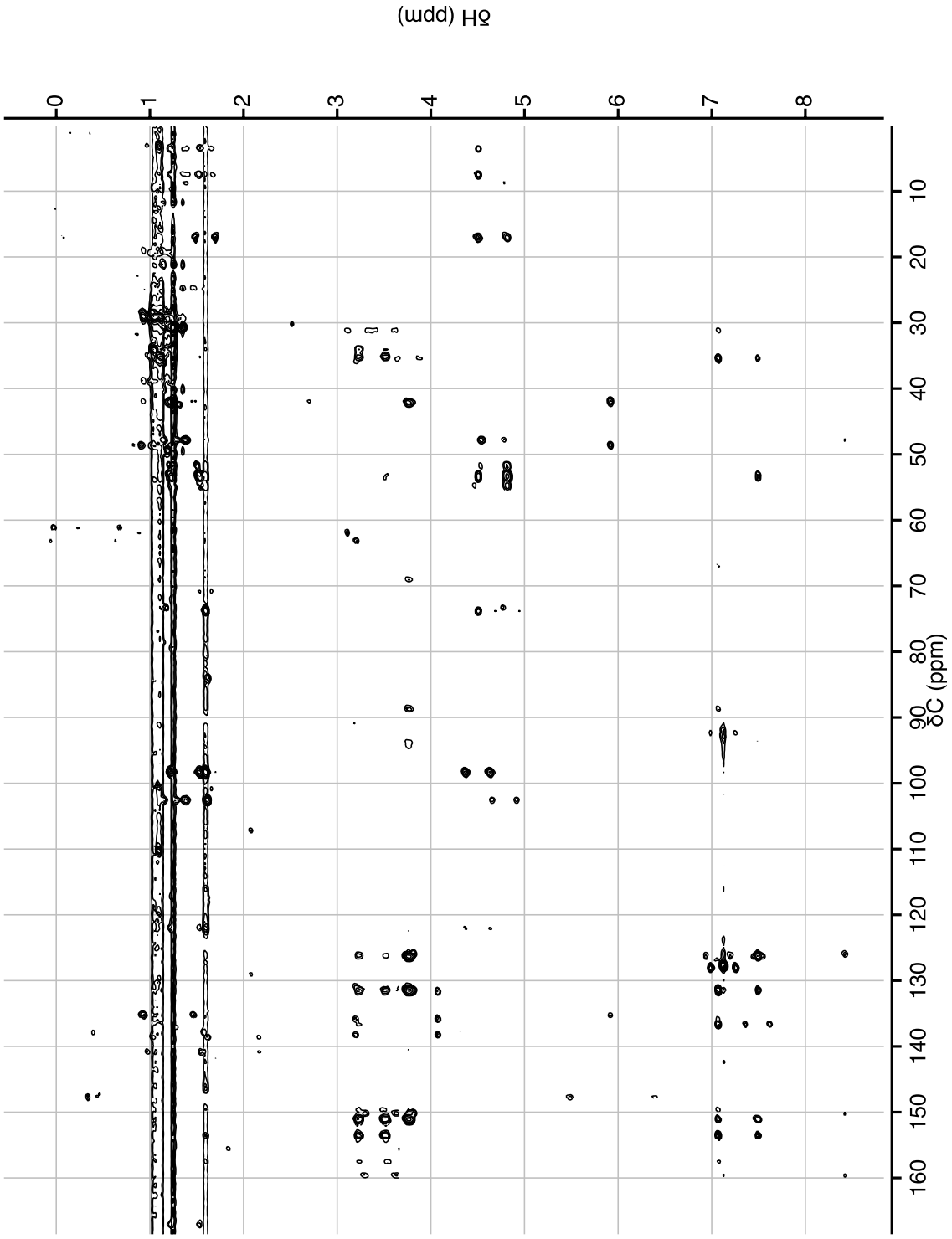

Figure A.32. HMBC spectrum of carbon-13 enriched [Pt(η^3-C(CH$_2$)$_2$CHCHMe)(C$_6$H$_3$-*o*-CH$_2$P^{t}Bu$_2$-*m*-CH$_2$S^{t}Bu)] (**11a** and **11b**) (600/150 MHz, RT, 40 mg/mL, C$_6$D$_6$). Some residual one bond coupling is present.

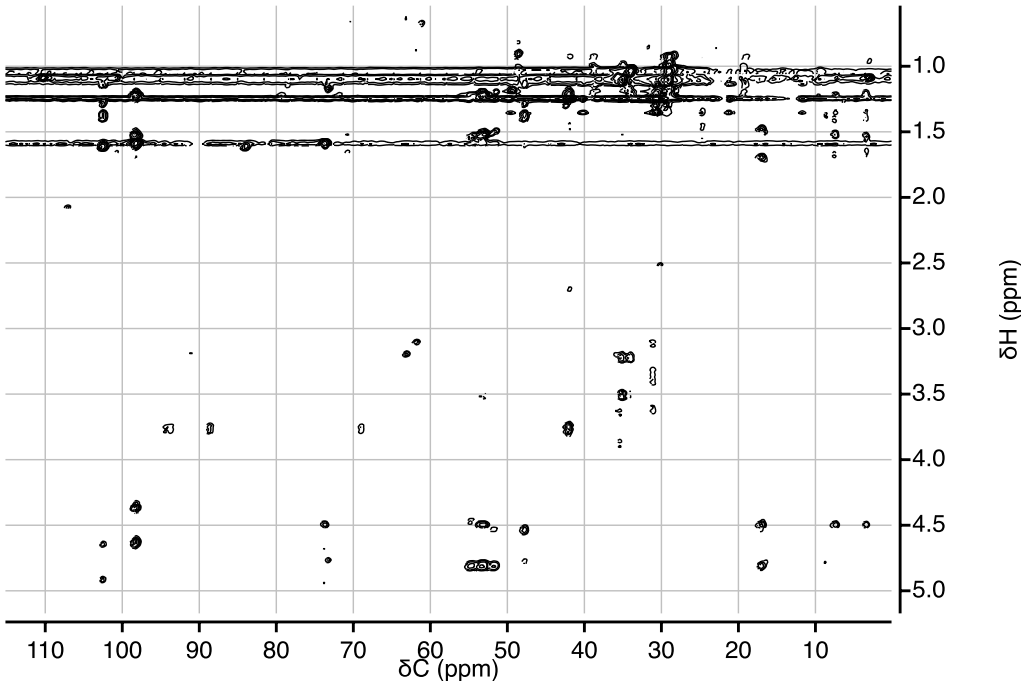

Figure A.33. Expanded HMBC spectrum of carbon-13 enriched [Pt(η^3-C$(CH_2)_2$CHCHMe)(C_6H_3-*o*-$CH_2P^tBu_2$-*m*-CH_2S^tBu)] (**11a** and **11b**) (600/150 MHz, RT, 40 mg/mL, C_6D_6). Some residual one bond coupling is present.

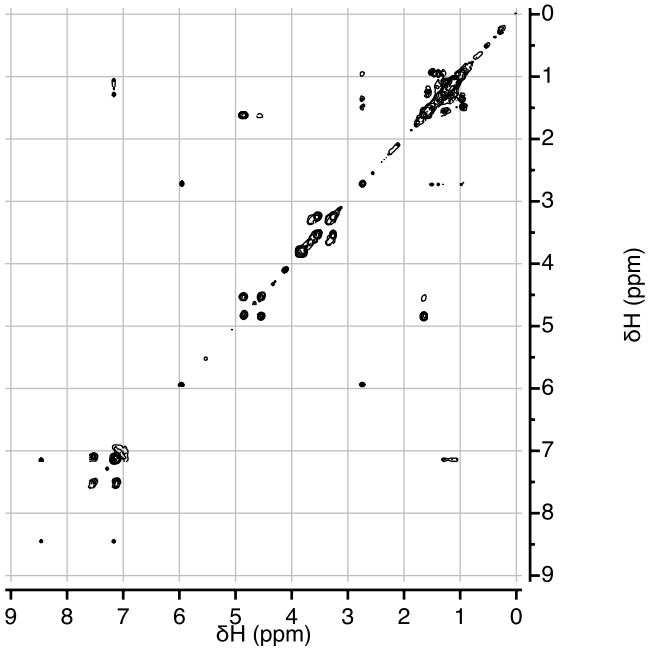

Figure A.34. COSY spectrum of [Pt(η^3-C$(CH_2)_2$CHCHMe)(C_6H_3-*o*-$CH_2P^tBu_2$-*m*-CH_2S^tBu)] (**11a** and **11b**) (600 MHz, RT, 40 mg/mL, C_6D_6).

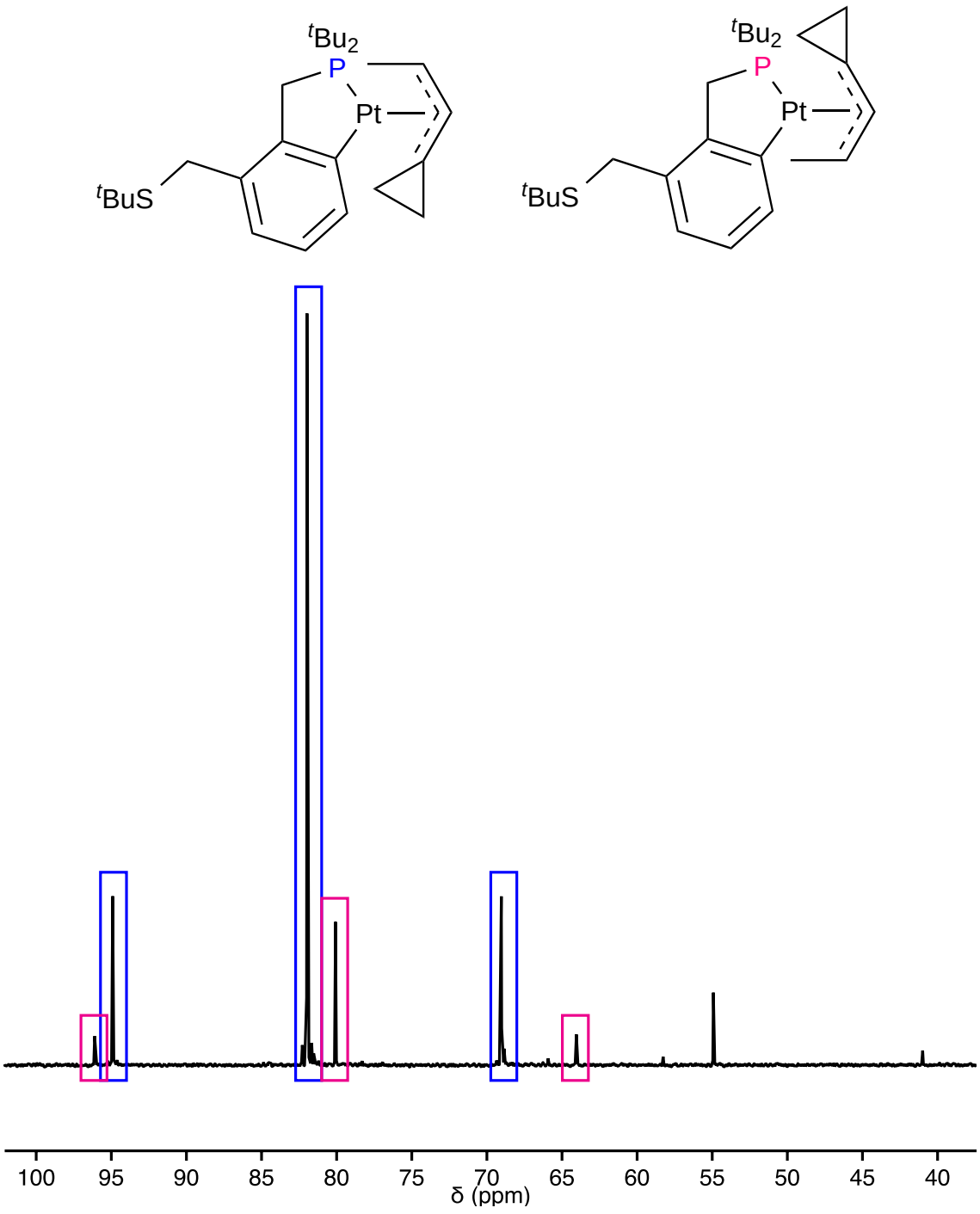

Figure A.35. $^{31}P\{^{1}H\}$ NMR spectrum of [Pt(η^3-C(CH_2)$_2$CHCHMe)(C_6H_3-*o*-$CH_2P^tBu_2$-*m*-CH_2S^tBu)] (**11a** and **11b**) (121 MHz, RT, 40 mg/mL, C_6D_6).

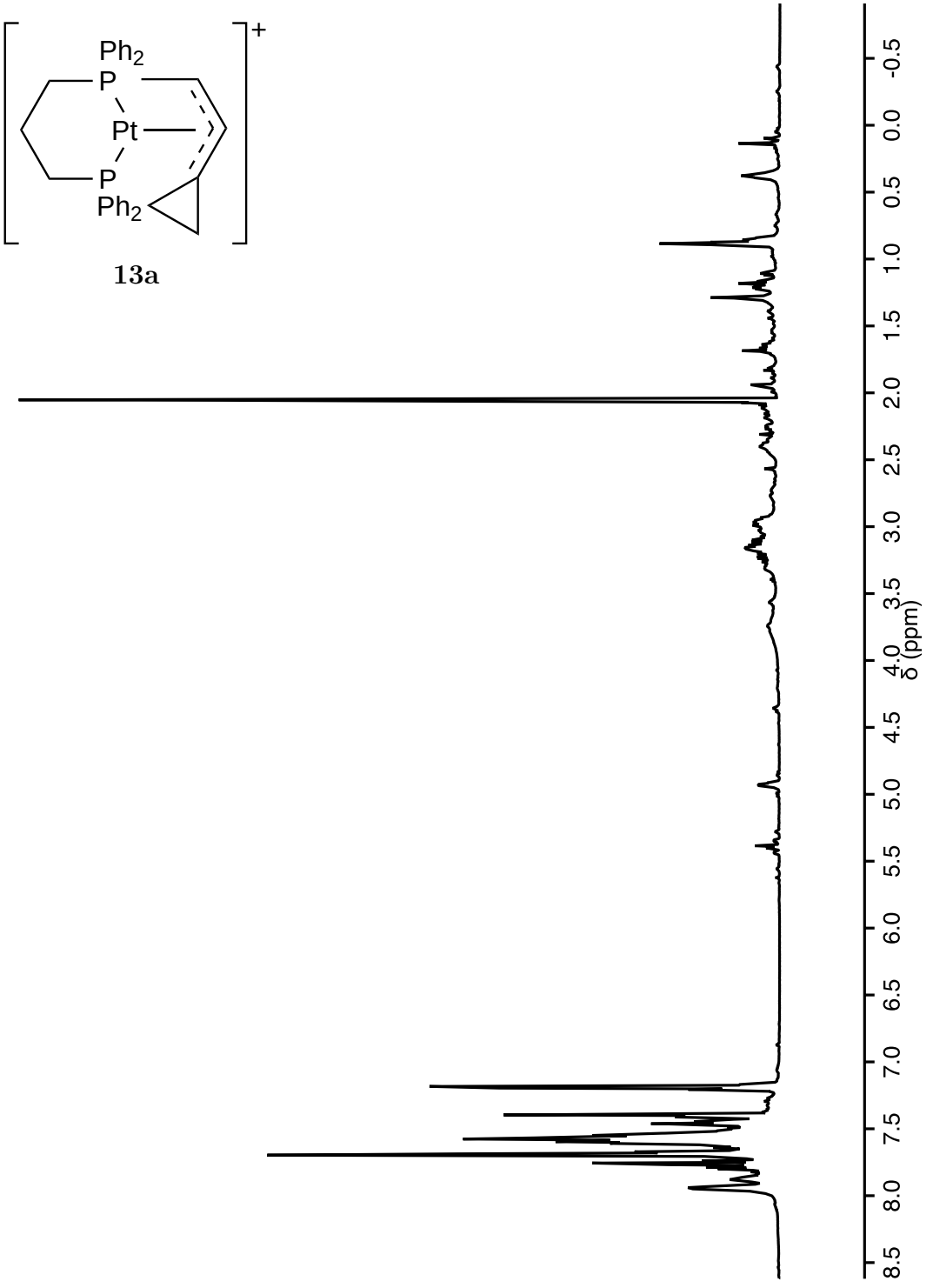

Figure A.36. ^{1}H NMR spectrum of [Pt(η^3-C$(CH_2)_2$CHCHMe)(dppp)][HC$(SO_2CF_3)_2$] (*anti* Me) (**13a**[HC$(SO_2CF_3)_2$]) (600 MHz, RT, 40 mg/mL, d_6-acetone).

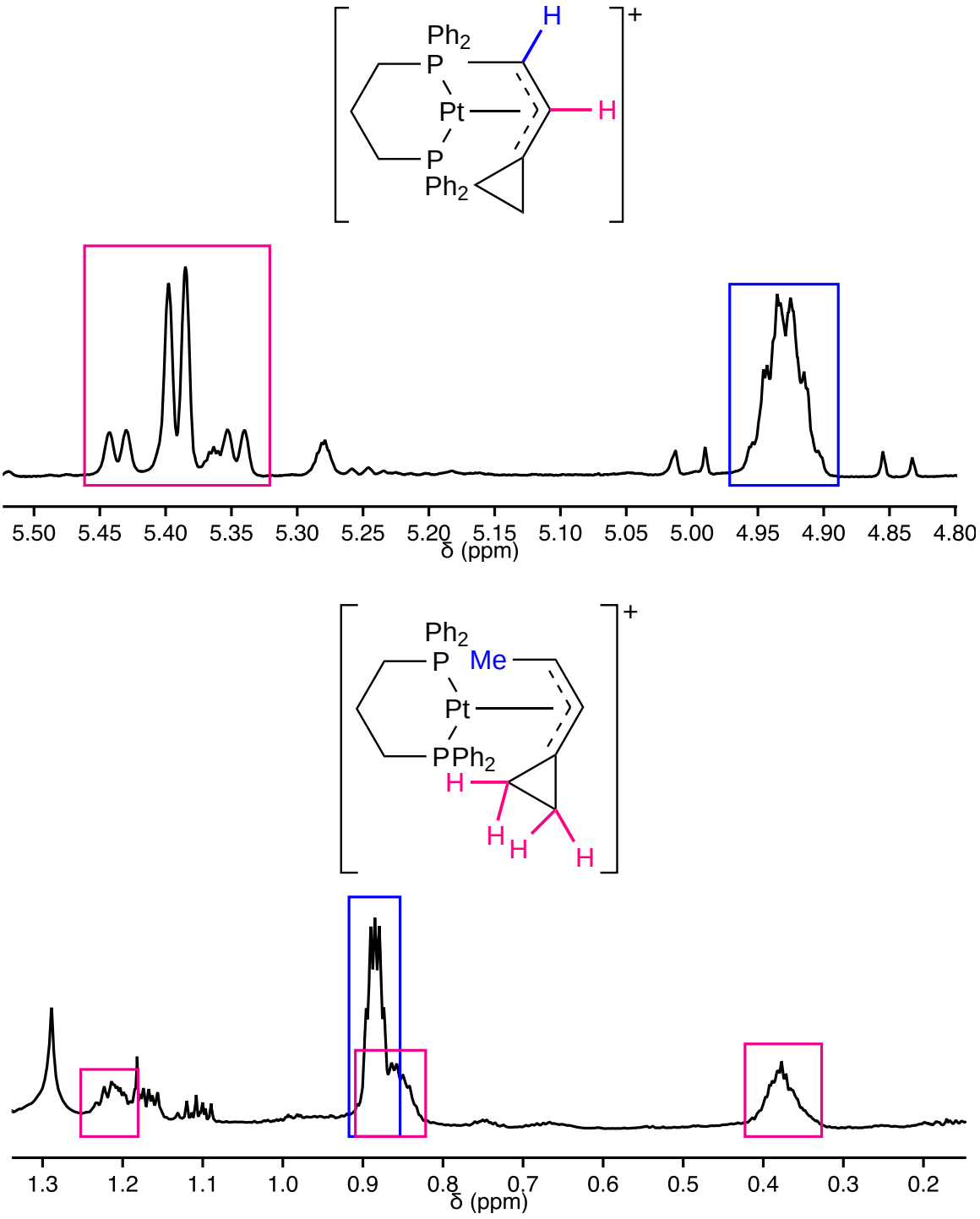

Figure A.37. Expanded ^{1}H NMR spectrum of [Pt(η^3-C$(CH_2)_2$CHCHMe)(dppp)][HC$(SO_2CF_3)_2$] (*anti* Me) (**13a**[HC$(SO_2CF_3)_2$]) (600 MHz, RT, 40 mg/mL, d_6-acetone).

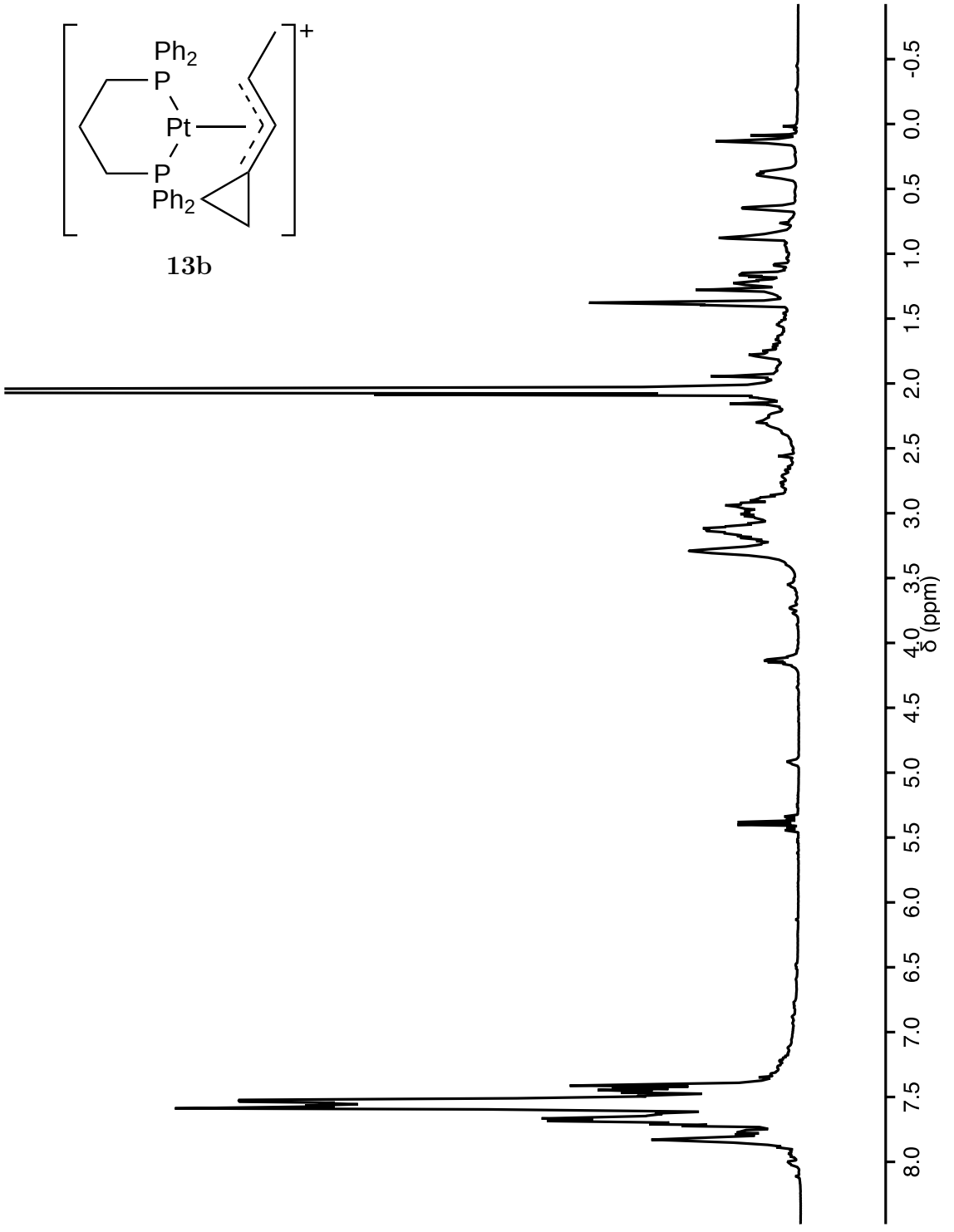

Figure A.38. ^{1}H NMR spectrum of [Pt(η^3-C$(CH_2)_2$CHCHMe)(dppp)][HC$(SO_2CF_3)_2$] (*syn* Me) (**13b**[HC$(SO_2CF_3)_2$]) (600 MHz, RT, 40 mg/mL, d_6-acetone).

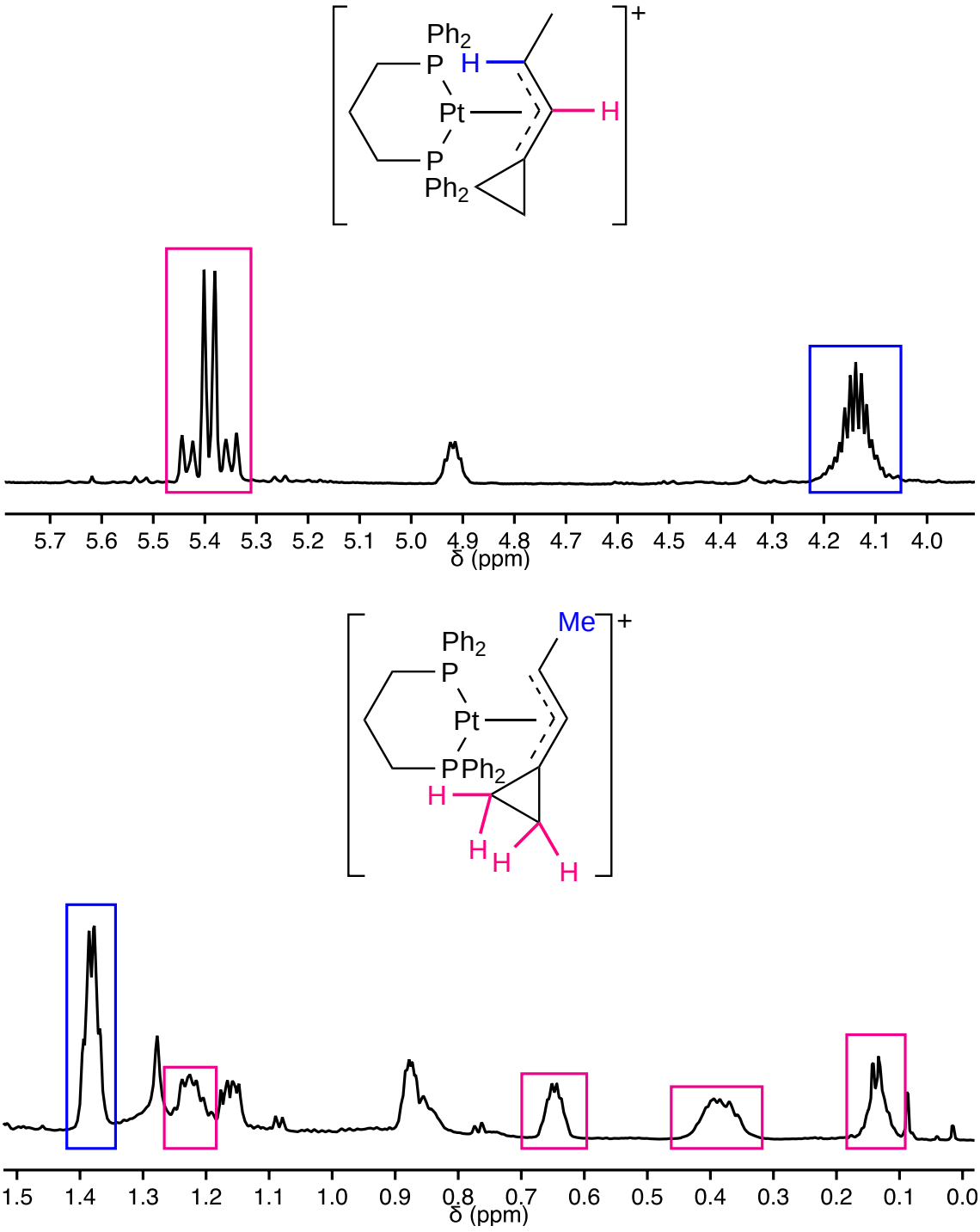

Figure A.39. Expanded ^{1}H NMR spectrum of [Pt(η^3-C$(CH_2)_2$CHCHMe)(dppp)][HC$(SO_2CF_3)_2$] (*syn* Me) (**13b**[HC$(SO_2CF_3)_2$]) (600 MHz, RT, 40 mg/mL, d_6-acetone).

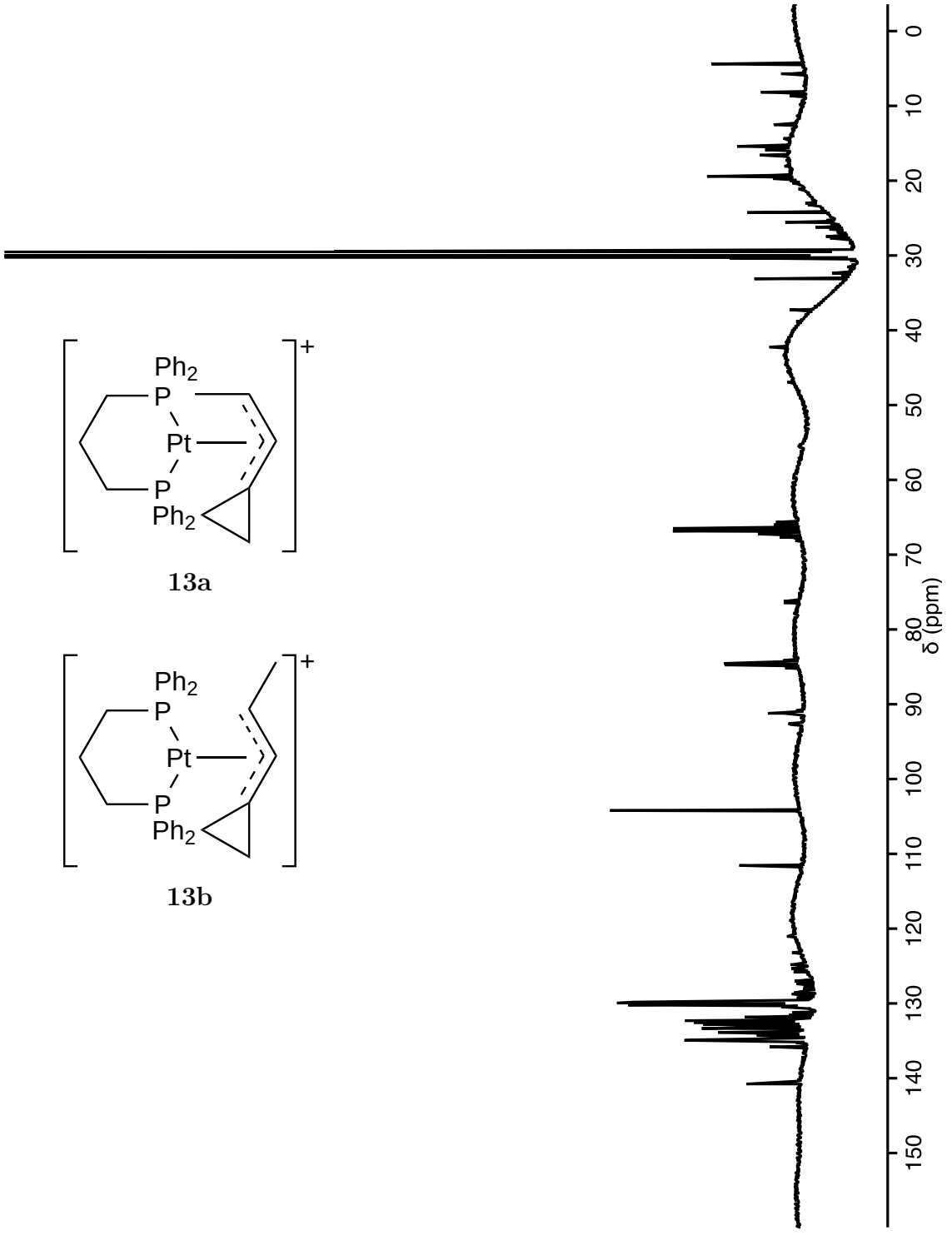

Figure A.40. $^{13}C\{^{1}H\}$ NMR spectrum of carbon-13 enriched [Pt(η^3-C$(CH_2)_2$CHCHMe)(dppp)][HC$(SO_2CF_3)_2$] (**13a**[HC$(SO_2CF_3)_2$] and **13b**[HC$(SO_2CF_3)_2$]) (150 MHz, RT, 40 mg/mL, *d*$_6$-acetone).

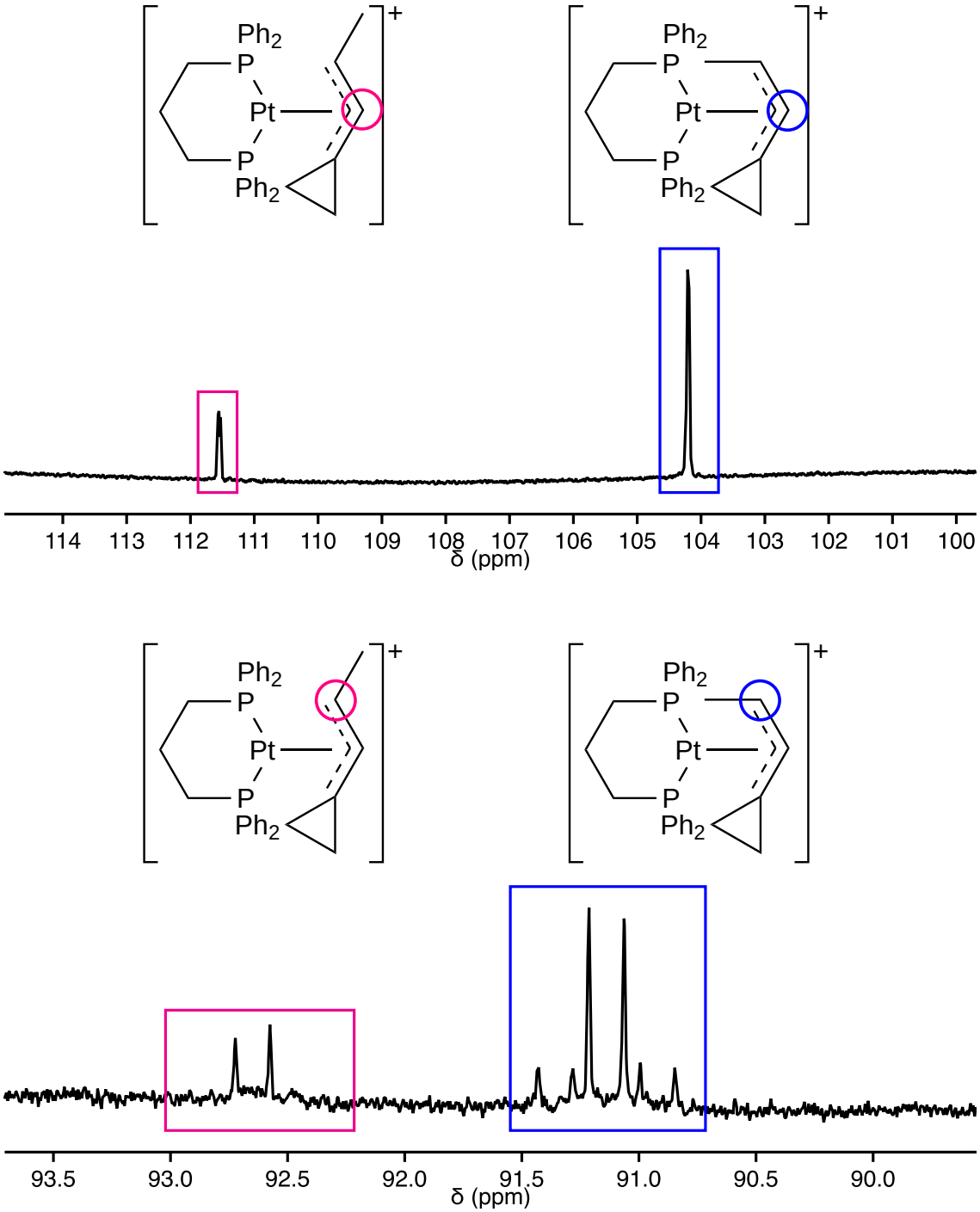

Figure A.41. Expanded $^{13}C\{^{1}H\}$ NMR spectrum of carbon-13 enriched $[Pt(\eta^3\text{-}C(CH_2)_2CHCHMe)(dppp)][HC(SO_2CF_3)_2]$ (**13a**$[HC(SO_2CF_3)_2]$ and **13b**$[HC(SO_2CF_3)_2]$) (150 MHz, RT, 40 mg/mL, d_6-acetone).

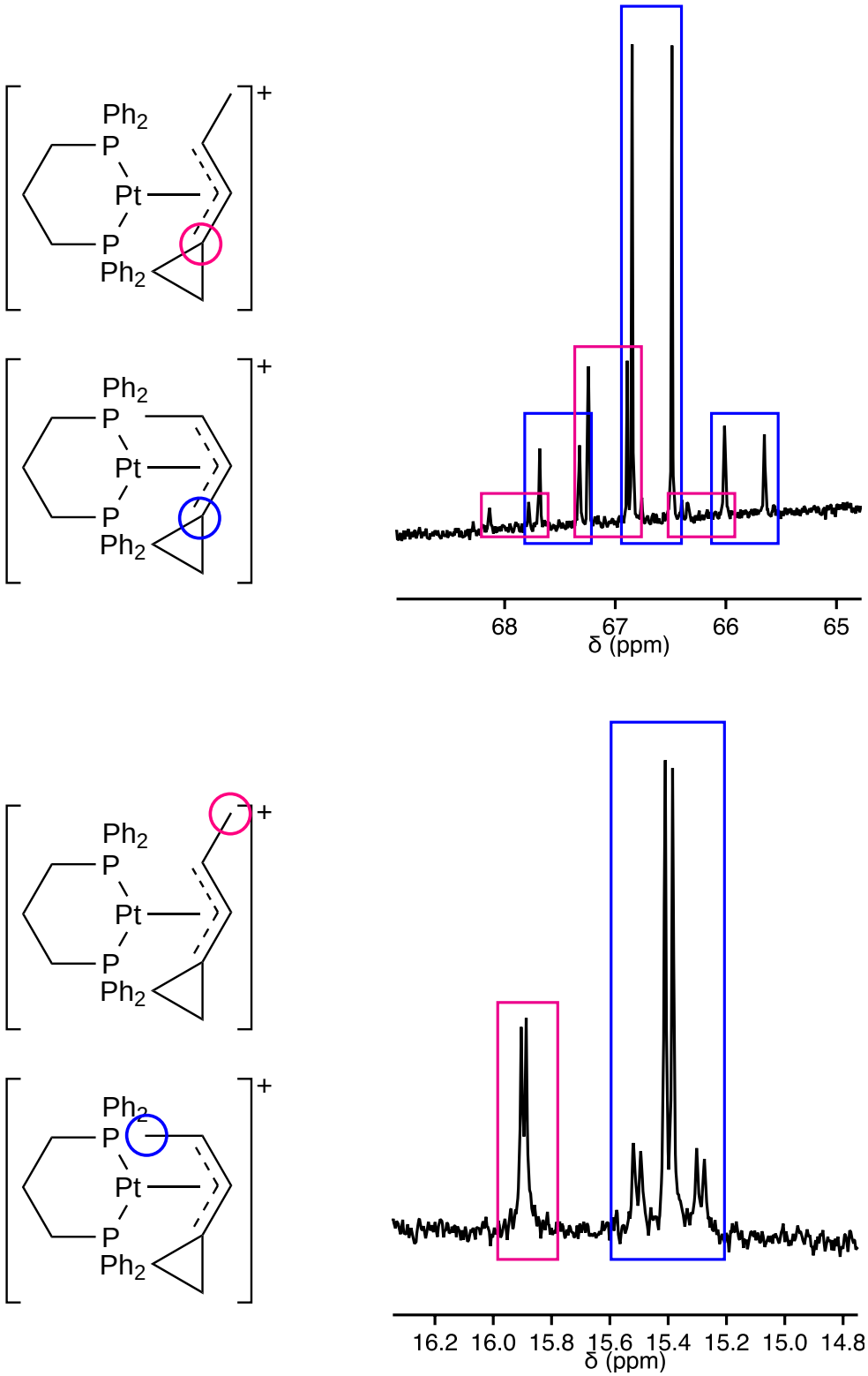

Figure A.42. Expanded $^{13}C\{^{1}H\}$ NMR spectrum of carbon-13 enriched [Pt(η^3-C$(CH_2)_2$CHCHMe)(dppp)][HC$(SO_2CF_3)_2$] (**13a**[HC$(SO_2CF_3)_2$] and **13b**[HC$(SO_2CF_3)_2$]) (150 MHz, RT, 40 mg/mL, d_6-acetone).

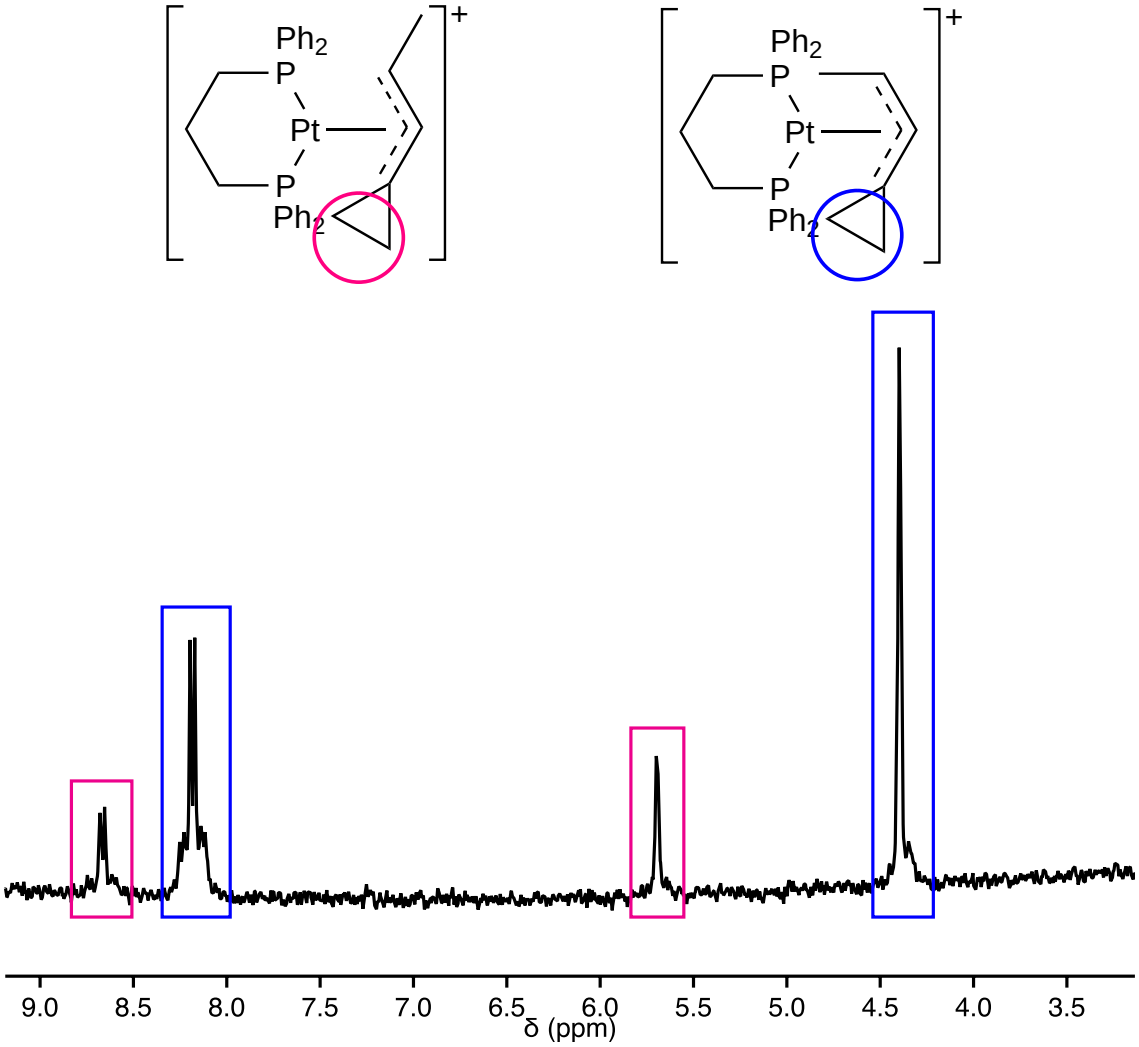

Figure A.43. Expanded $^{13}C\{^{1}H\}$ NMR spectrum of carbon-13 enriched [Pt(η^3-C(CH_2)$_2$CHCHMe)(dppp)][$HC(SO_2CF_3)_2$] (**13a**[$HC(SO_2CF_3)_2$] and **13b**[$HC(SO_2CF_3)_2$]) (150 MHz, RT, 40 mg/mL, d_6-acetone).

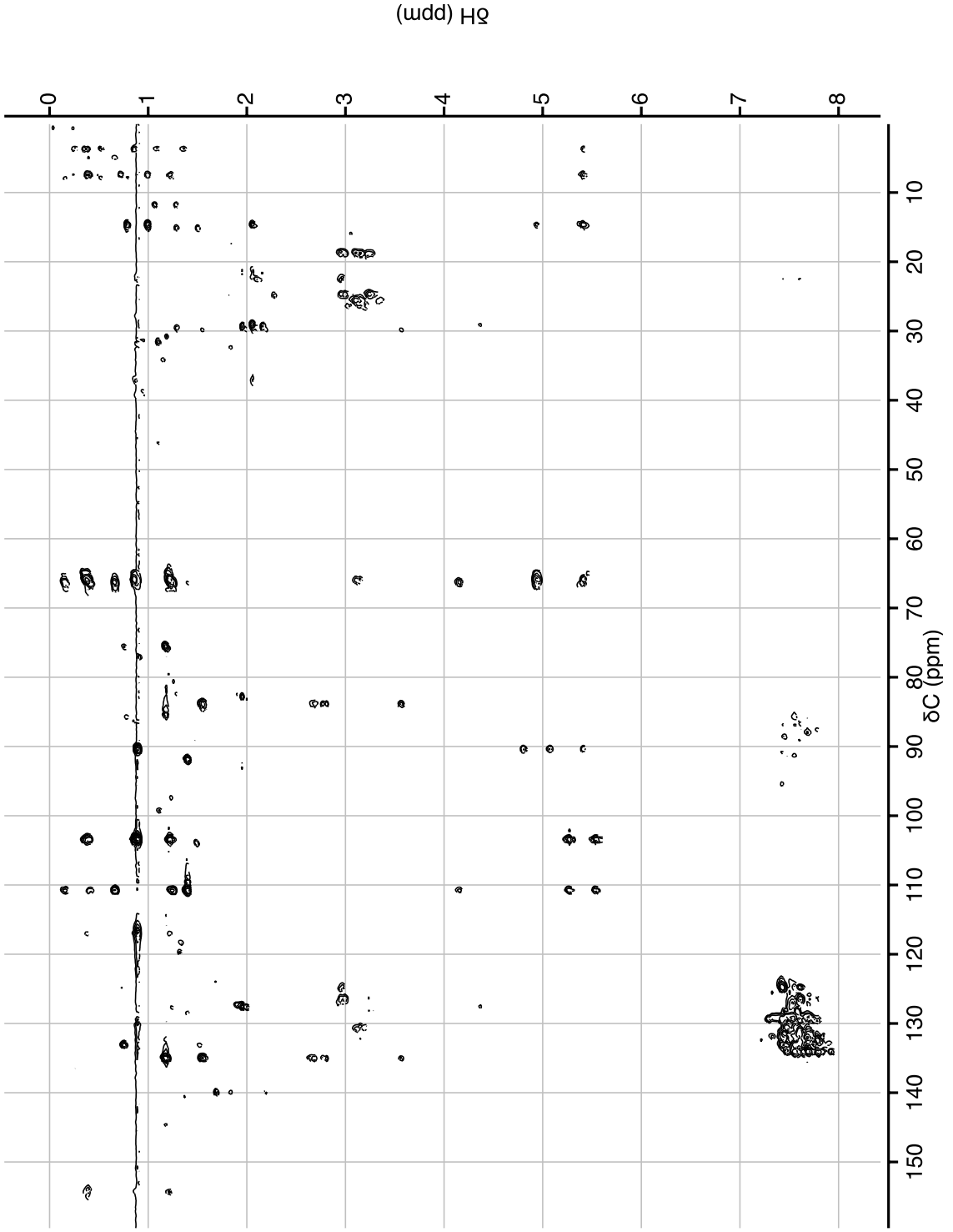

Figure A.44. HMBC spectrum of carbon-13 enriched $[Pt(\eta^3\text{-}C(CH_2)_2CHCHMe)(dppp)][HC(SO_2CF_3)_2]$ (**13a**$[HC(SO_2CF_3)_2]$ and **13b**$[HC(SO_2CF_3)_2]$) (600/150 MHz, RT, 40 mg/mL, d_6-acetone). Some residual one bond coupling is present.

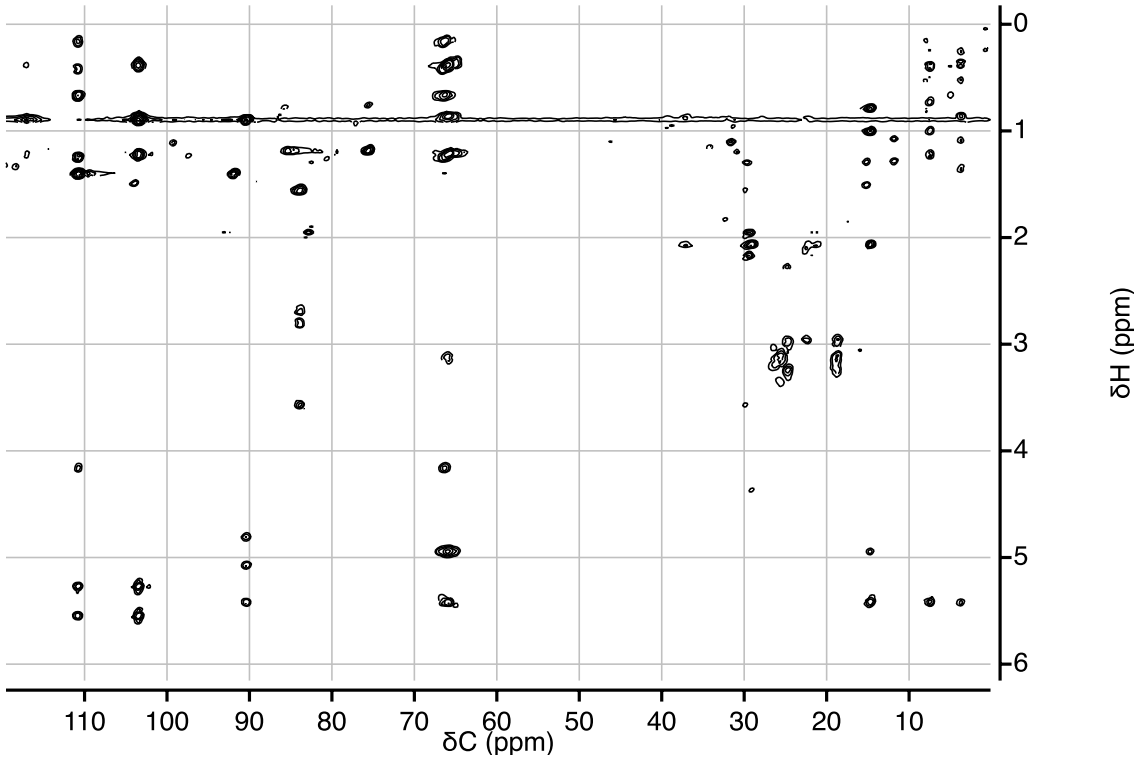

Figure A.45. Expanded HMBC spectrum of carbon-13 enriched [Pt(η^3-C(CH_2)$_2$CHCHMe)(dppp)][HC(SO_2CF_3)$_2$] (**13a**[HC(SO_2CF_3)$_2$] and **13b**[HC(SO_2CF_3)$_2$]) (600/150 MHz, RT, 40 mg/mL, d_6-acetone). Some residual one bond coupling is present.

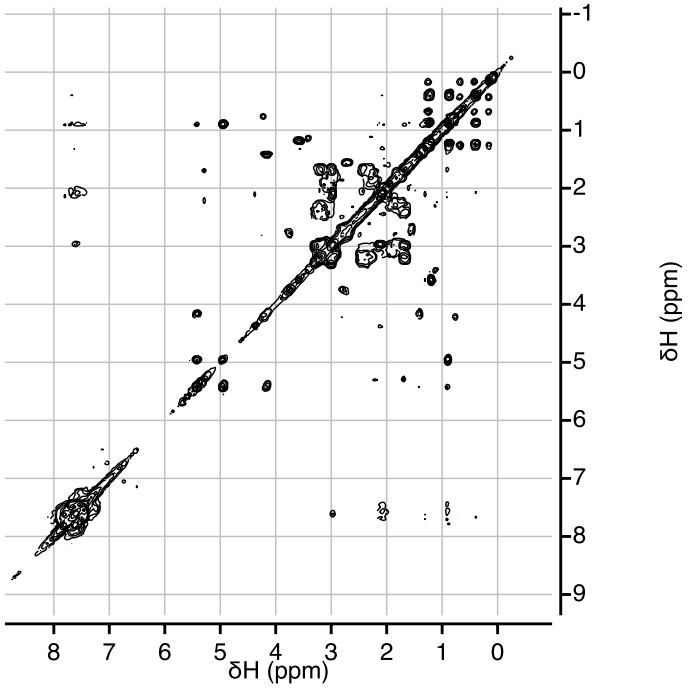

Figure A.46. COSY spectrum of carbon-13 enriched [Pt(η^3-C(CH_2)$_2$CHCHMe)(dppp)][HC(SO_2CF_3)$_2$] (**13a**[HC(SO_2CF_3)$_2$]) (150 MHz, RT, 40 mg/mL, d_6-acetone).

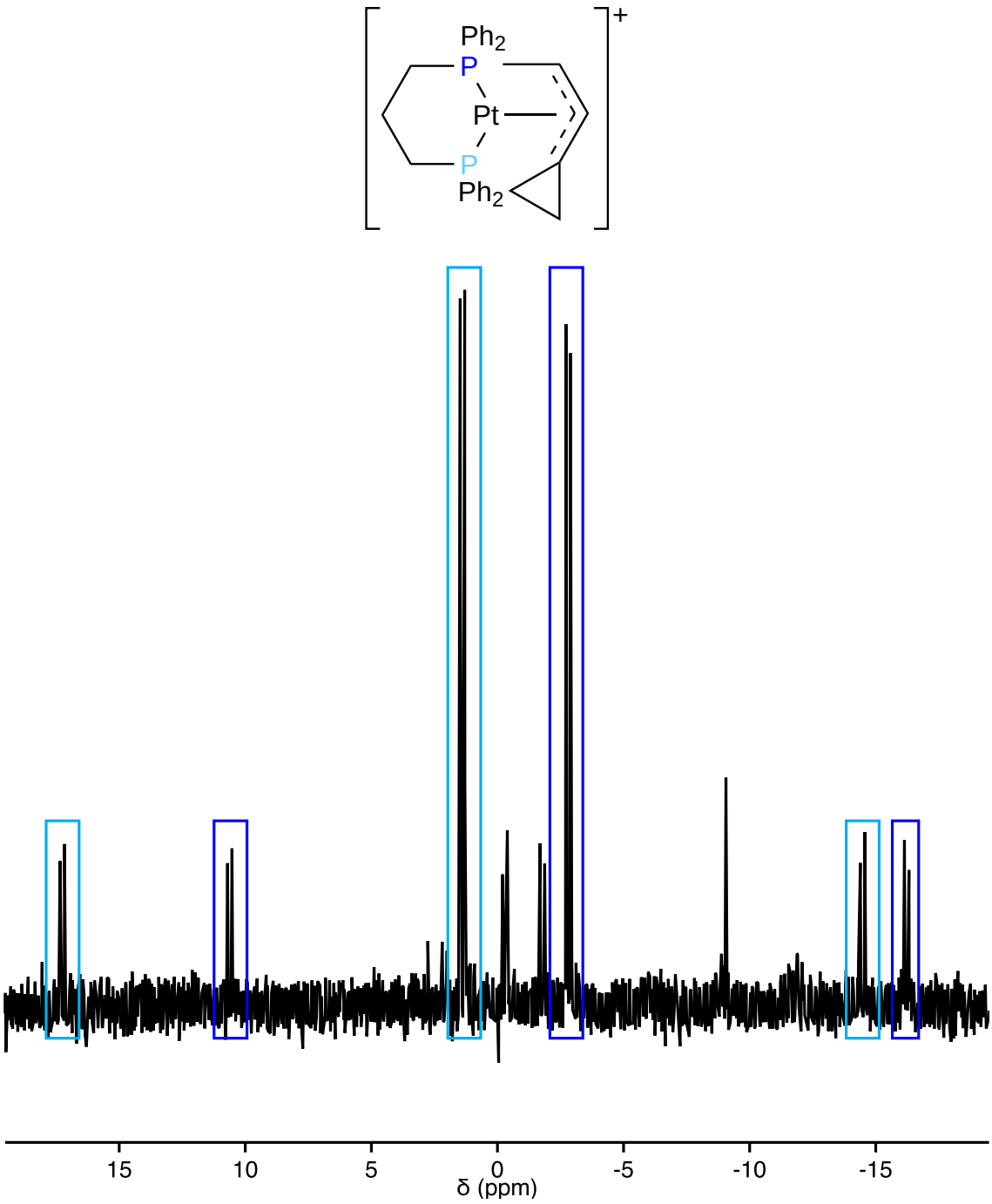

Figure A.47. $^{31}P\{^{1}H\}$ NMR spectrum of $[Pt(\eta^3\text{-}C(CH_2)_2CHCHMe)(dppp)][HC(SO_2CF_3)_2]$ (**13a**$[HC(SO_2CF_3)_2]$) (121 MHz, RT, 40 mg/mL, d_6-acetone).

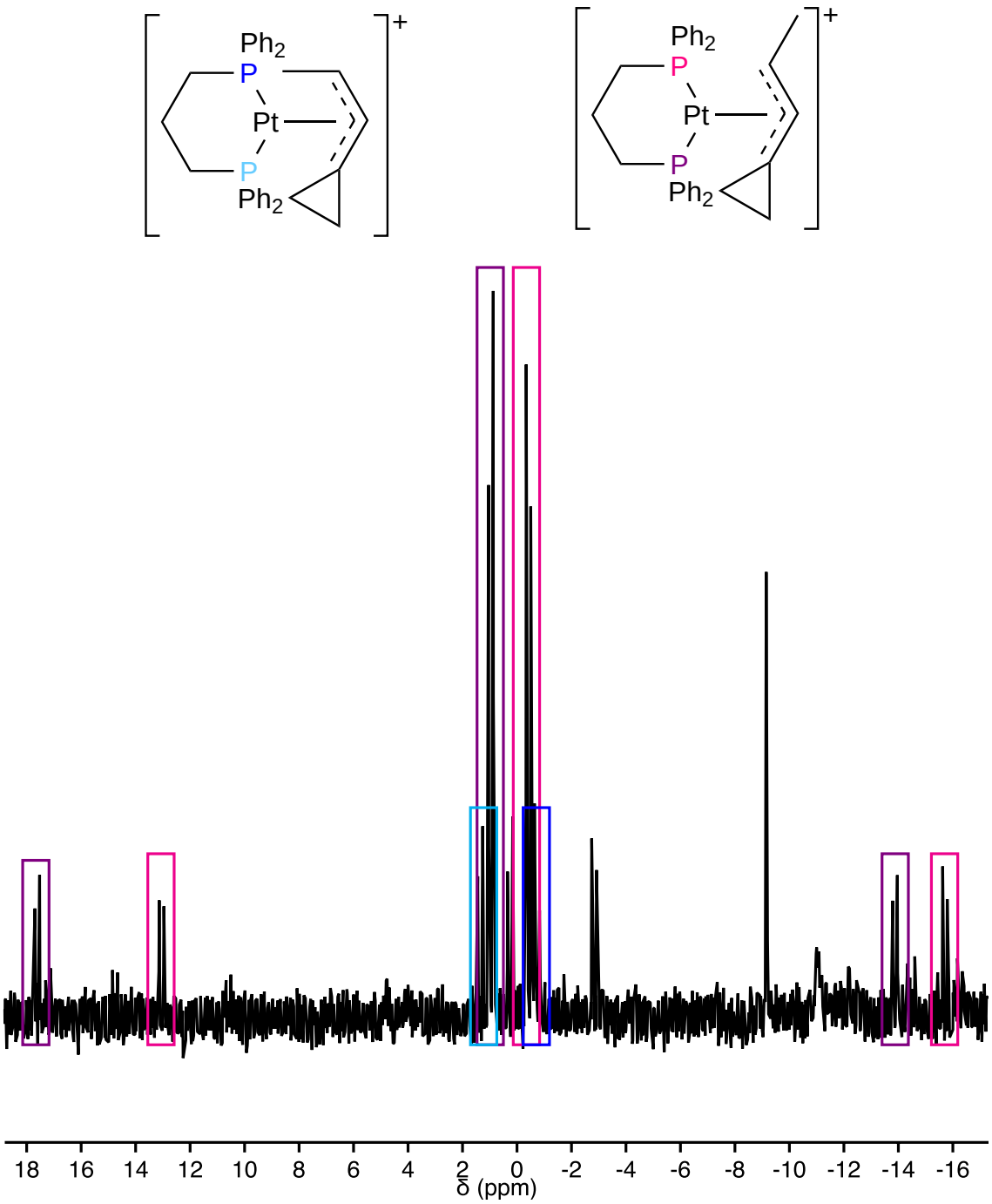

Figure A.48. $^{31}P\{^{1}H\}$ NMR spectrum of $[Pt(\eta^3\text{-}C(CH_2)_2CHCHMe)(dppp)][HC(SO_2CF_3)_2]$ (**13a**$[HC(SO_2CF_3)_2]$ and **13b**$[HC(SO_2CF_3)_2]$) (121 MHz, RT, 40 mg/mL, d_6-acetone).

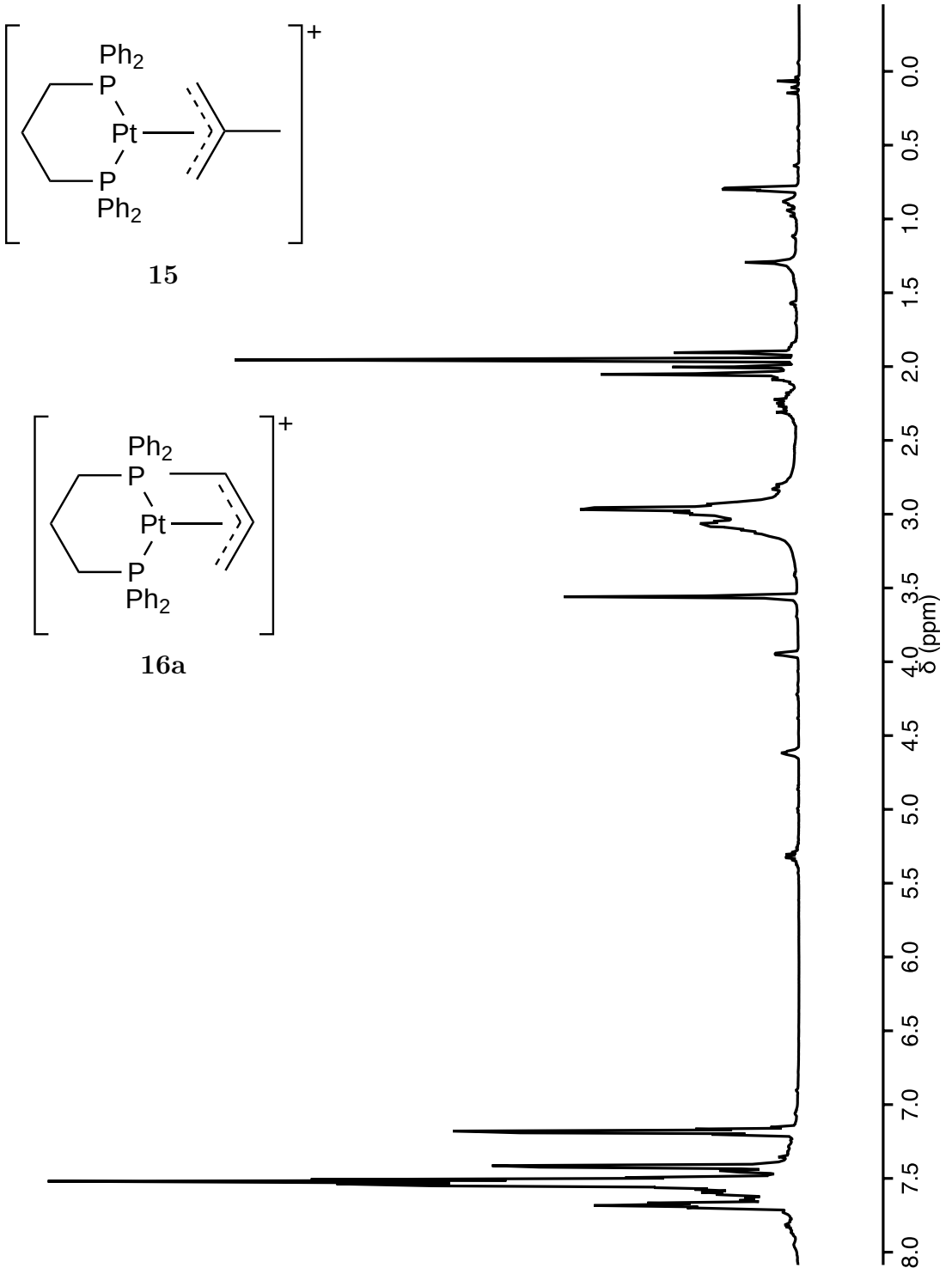

Figure A.49. ^{1}H NMR spectrum of [Pt(η^3-CH_2CMeCH_2)(dppp)][PhC(SO_2CF_3)$_2$] (**15**[PhC(SO_2CF_3)$_2$]) and [Pt(η^3-$CH_2CHCHMe$)(dppp)][PhC(SO_2CF_3)$_2$] (*anti* Me) (**16a**[PhC(SO_2CF_3)$_2$]). (600 MHz, RT, 40 mg/mL, d_6-acetone).

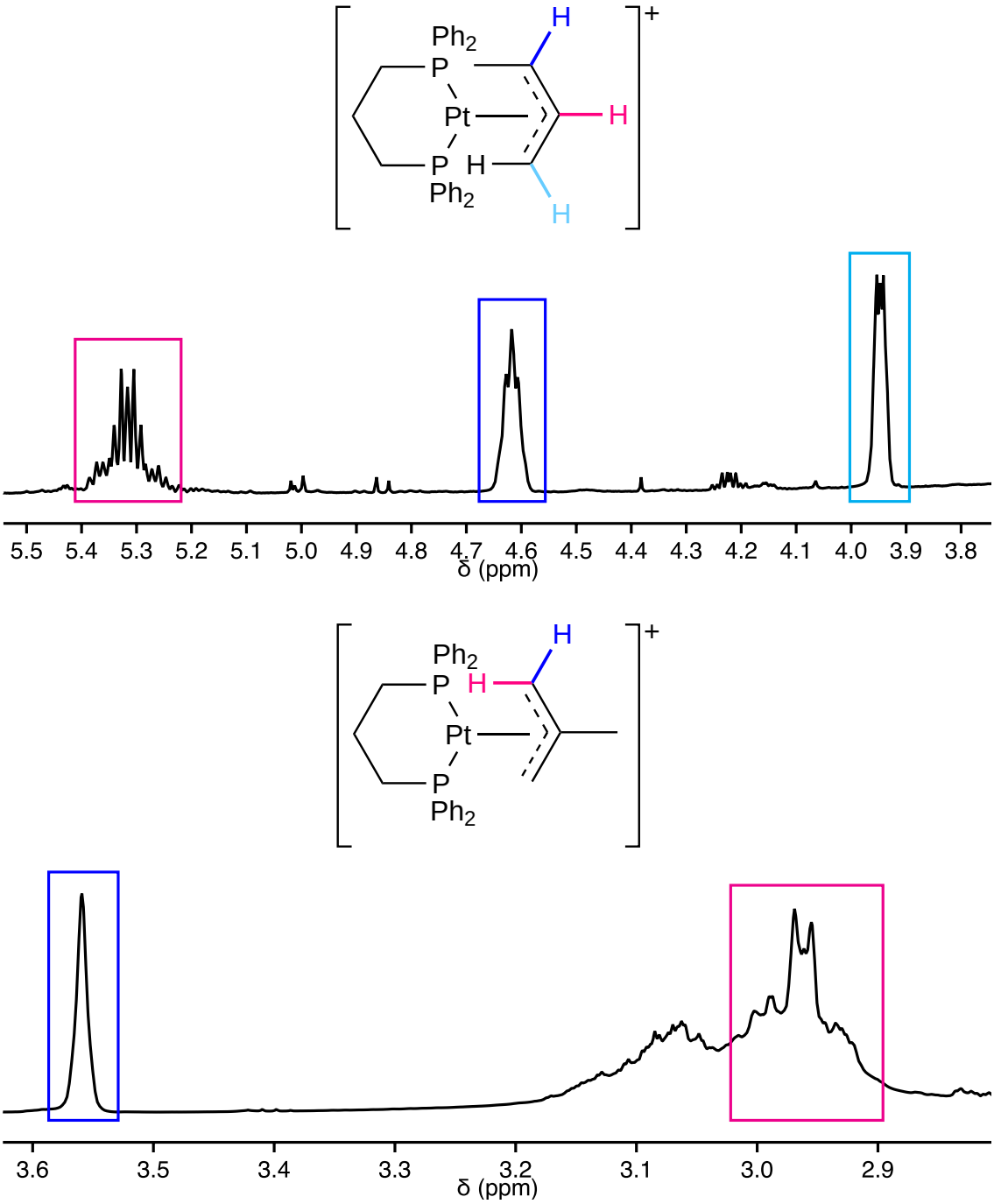

Figure A.50. Expanded ^{1}H NMR spectrum of $[Pt(\eta^3\text{-}CH_2CMeCH_2)(dppp)][PhC(SO_2CF_3)_2]$ (**15**$[PhC(SO_2CF_3)_2]$) and $[Pt(\eta^3\text{-}CH_2CHCHMe)(dppp)][PhC(SO_2CF_3)_2]$ (*anti* Me) (**16a**$[PhC(SO_2CF_3)_2]$). (600 MHz, RT, 40 mg/mL, d_6-acetone).

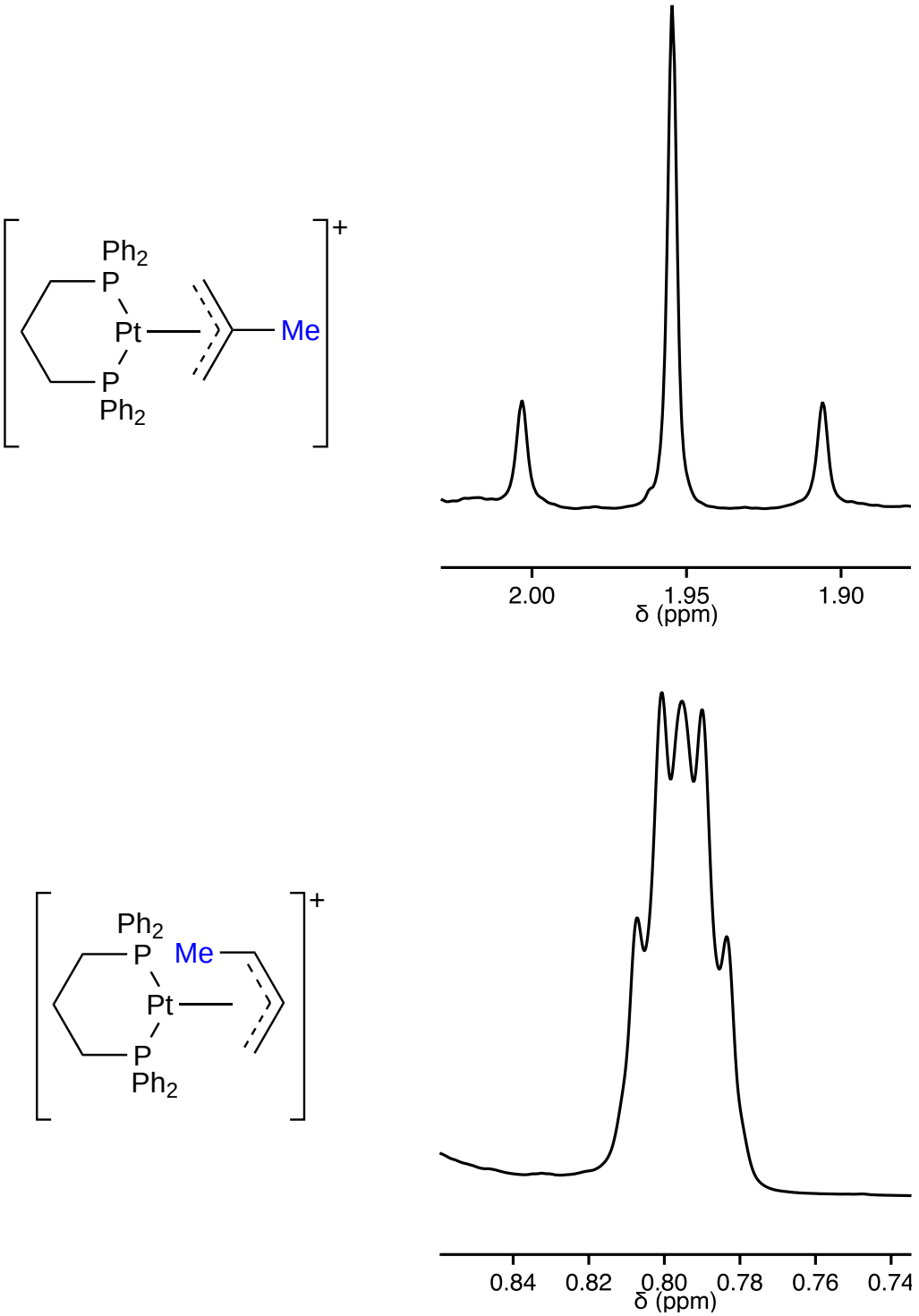

Figure A.51. Expanded ^{1}H NMR spectrum of $[Pt(\eta^3\text{-}CH_2CMeCH_2)(dppp)][PhC(SO_2CF_3)_2]$ (**15**$[PhC(SO_2CF_3)_2]$) and $[Pt(\eta^3\text{-}CH_2CHCHMe)(dppp)][PhC(SO_2CF_3)_2]$ (*anti* Me) (**16a**$[PhC(SO_2CF_3)_2]$). (600 MHz, RT, 40 mg/mL, d_6-acetone).

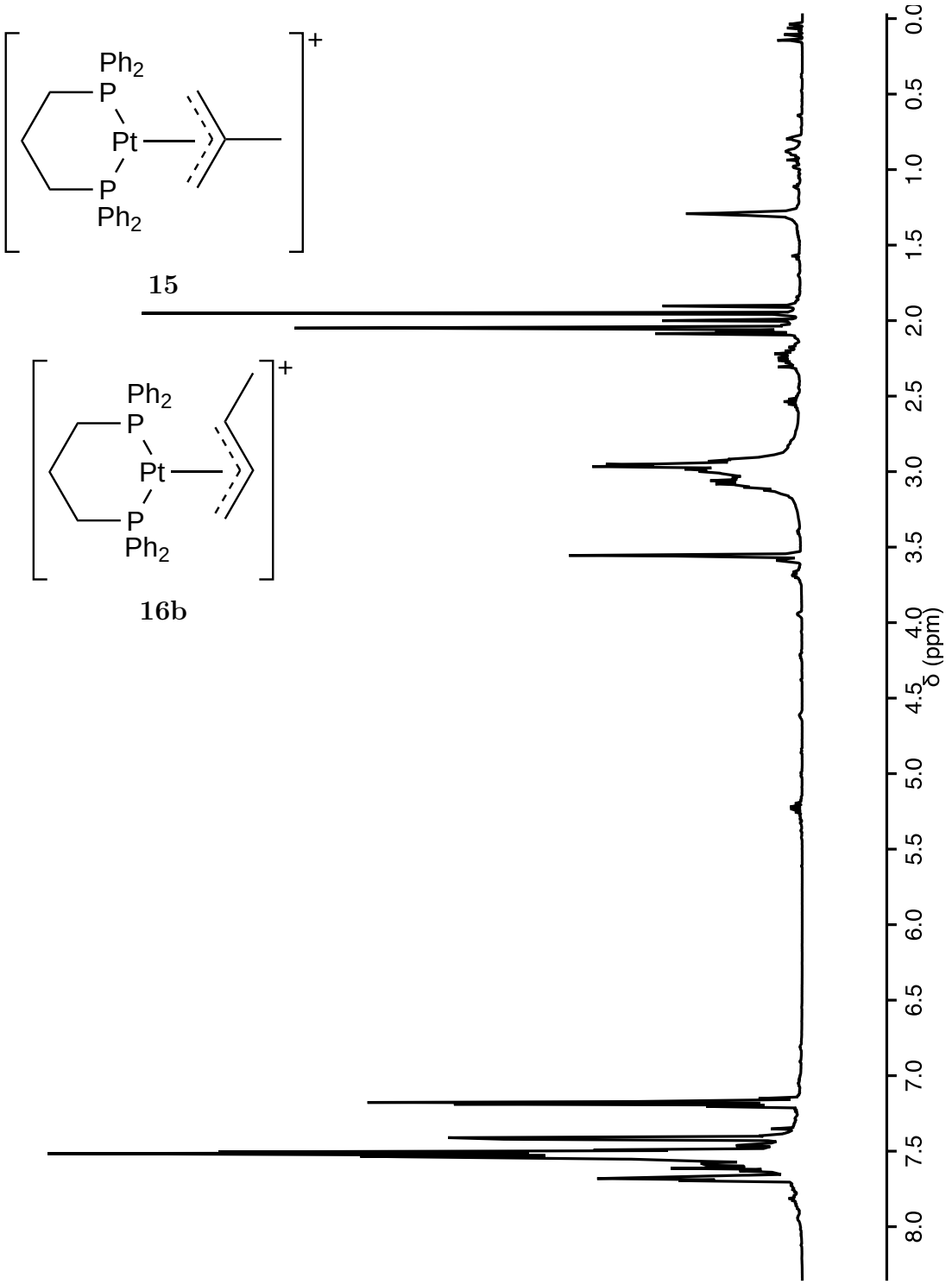

Figure A.52. ^{1}H NMR spectrum of [Pt(η^3-CH_2CMeCH_2)(dppp)][PhC(SO_2CF_3)$_2$] (**15**[PhC(SO_2CF_3)$_2$]) and [Pt(η^3-$CH_2CHCHMe$)(dppp)][PhC(SO_2CF_3)$_2$] (*syn* Me) (**16b**[PhC(SO_2CF_3)$_2$]). (600 MHz, RT, 40 mg/mL, d_6-acetone).

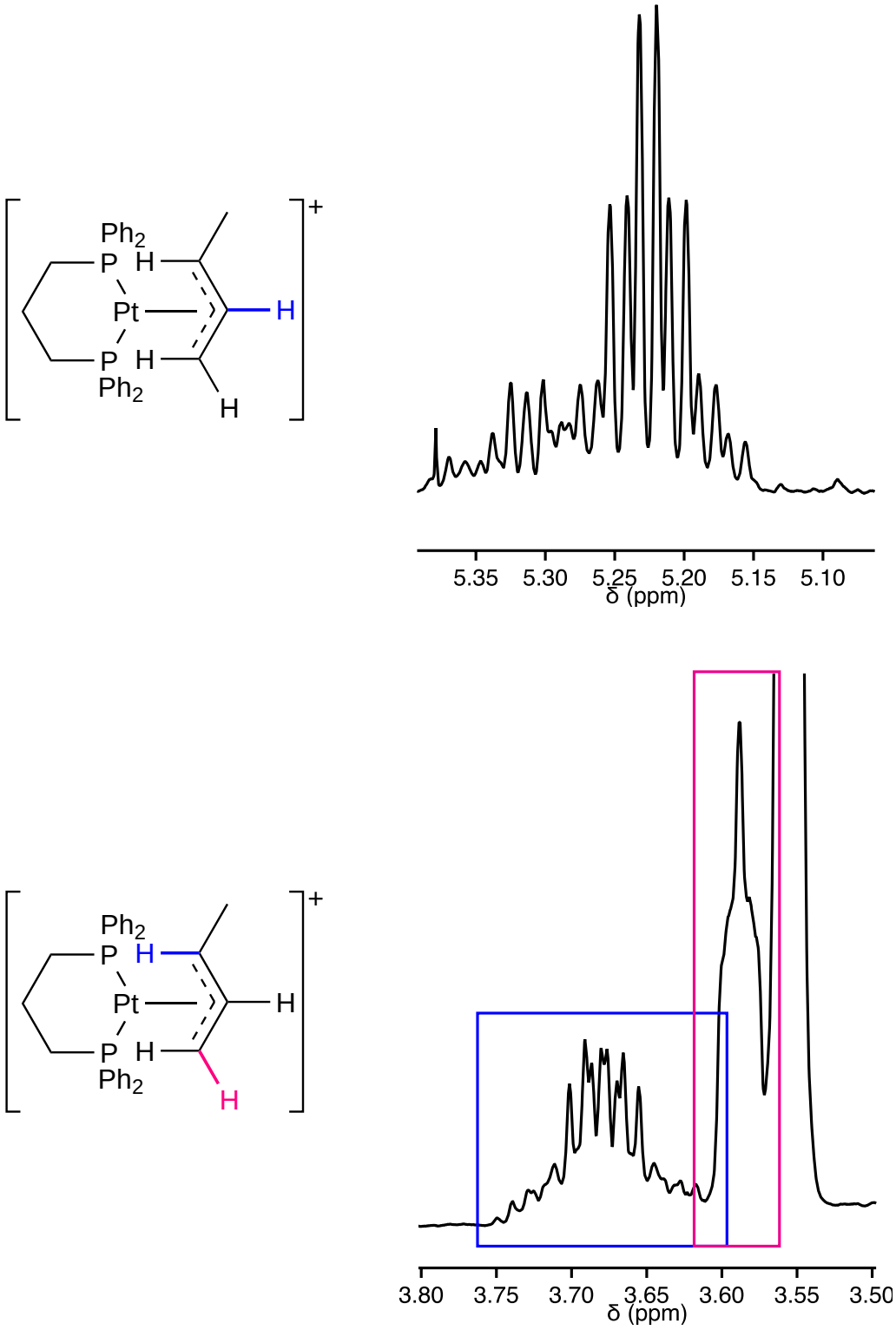

Figure A.53. Expanded ^{1}H NMR spectrum of $[Pt(\eta^3\text{-}CH_2CMeCH_2)(dppp)][PhC(SO_2CF_3)_2]$ (**15**$[PhC(SO_2CF_3)_2]$) and $[Pt(\eta^3\text{-}CH_2CHCHMe)(dppp)][PhC(SO_2CF_3)_2]$ (*syn* Me) (**16b**$[PhC(SO_2CF_3)_2]$). (600 MHz, RT, 40 mg/mL, d_6-acetone).

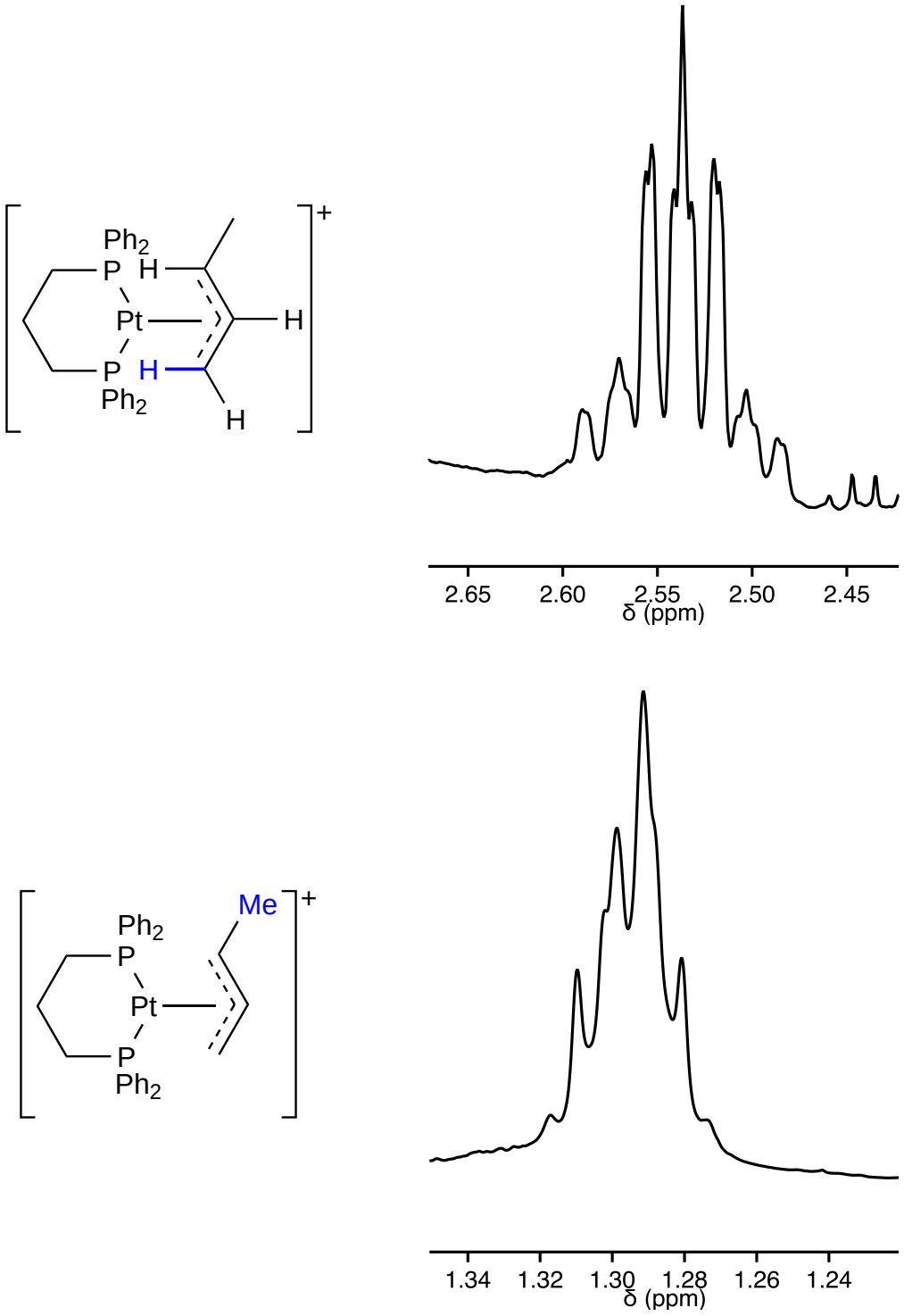

Figure A.54. Expanded ^{1}H NMR spectrum of $[Pt(\eta^3\text{-}CH_2CMeCH_2)(dppp)][PhC(SO_2CF_3)_2]$ (**15**$[PhC(SO_2CF_3)_2]$) and $[Pt(\eta^3\text{-}CH_2CHCHMe)(dppp)][PhC(SO_2CF_3)_2]$ (*syn* Me) (**16b**$[PhC(SO_2CF_3)_2]$). (600 MHz, RT, 40 mg/mL, d_6-acetone).

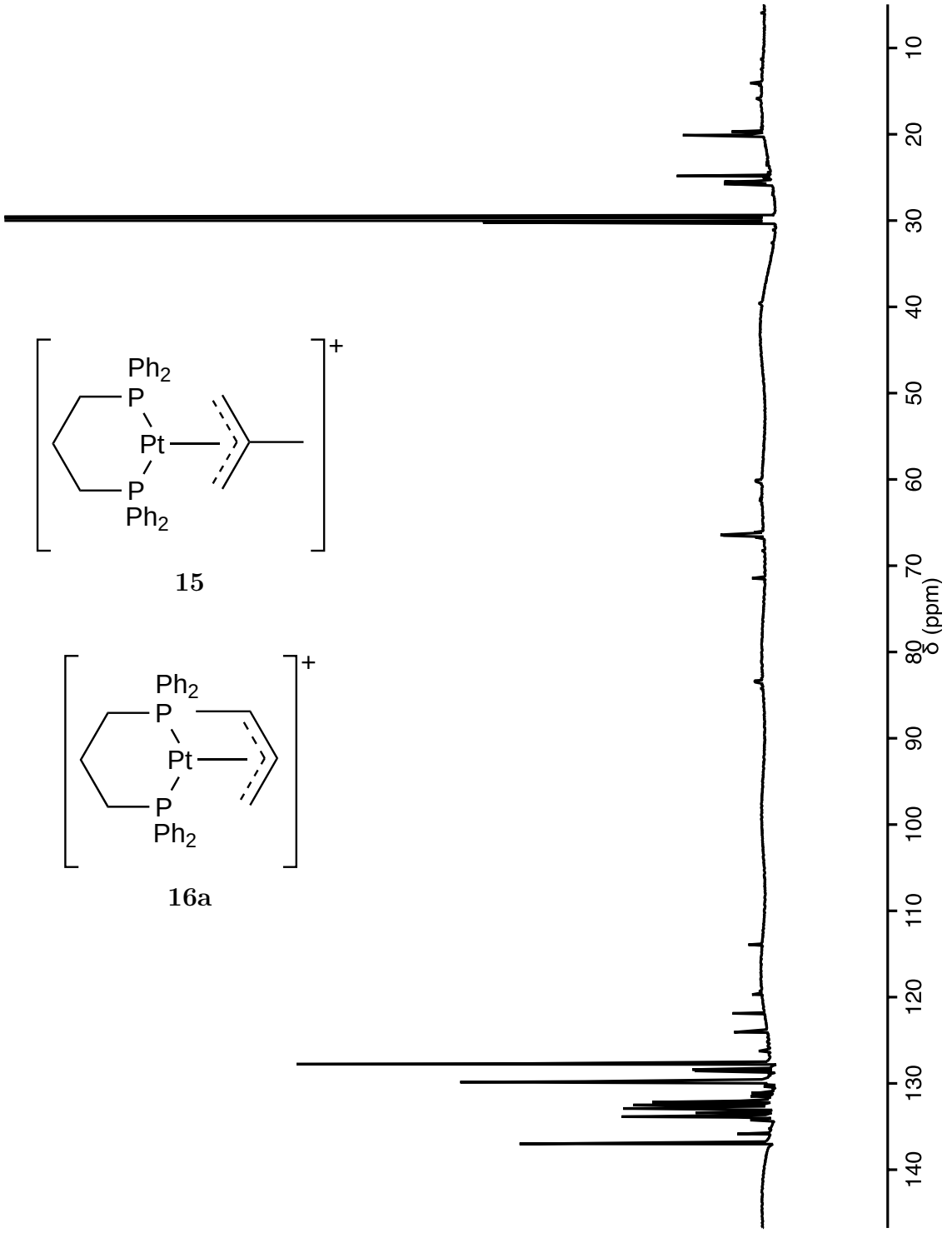

Figure A.55. $^{13}C\{^{1}H\}$ NMR spectrum of [Pt(η^3-CH_2CMeCH_2)(dppp)][$PhC(SO_2CF_3)_2$] (**15**[$PhC(SO_2CF_3)_2$]) and [Pt(η^3-$CH_2CHCHMe$)(dppp)][$PhC(SO_2CF_3)_2$] (*anti* Me) (**16a**[$PhC(SO_2CF_3)_2$]). (150 MHz, RT, 40 mg/mL, d_6-acetone).

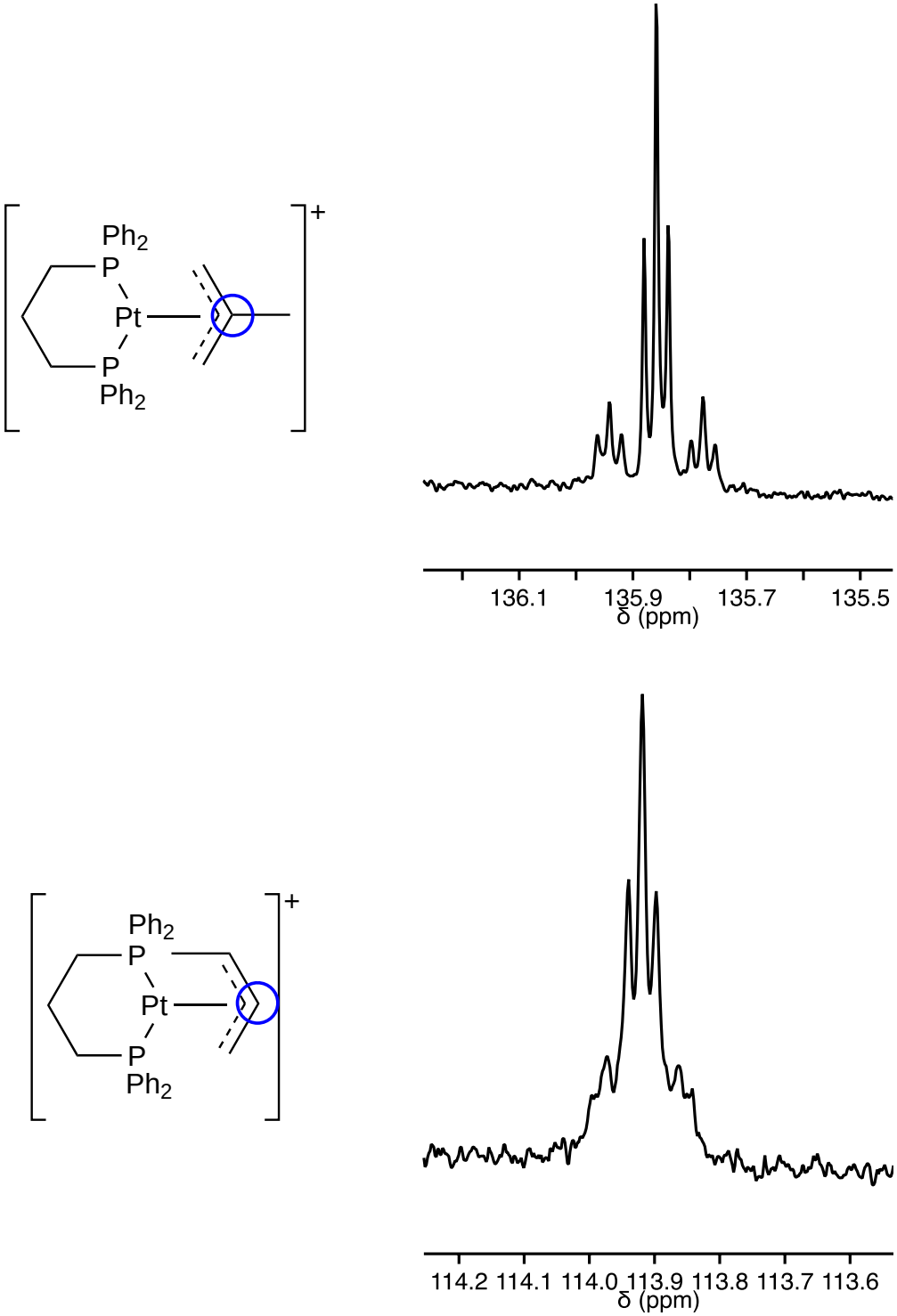

Figure A.56. Expanded $^{13}C\{^{1}H\}$ NMR spectrum of $[Pt(\eta^3\text{-}CH_2CMeCH_2)(dppp)][PhC(SO_2CF_3)_2]$ (**15**$[PhC(SO_2CF_3)_2]$) and $[Pt(\eta^3\text{-}CH_2CHCHMe)(dppp)][PhC(SO_2CF_3)_2]$ (*anti* Me) (**16a**$[PhC(SO_2CF_3)_2]$). (150 MHz, RT, 40 mg/mL, d_6-acetone).

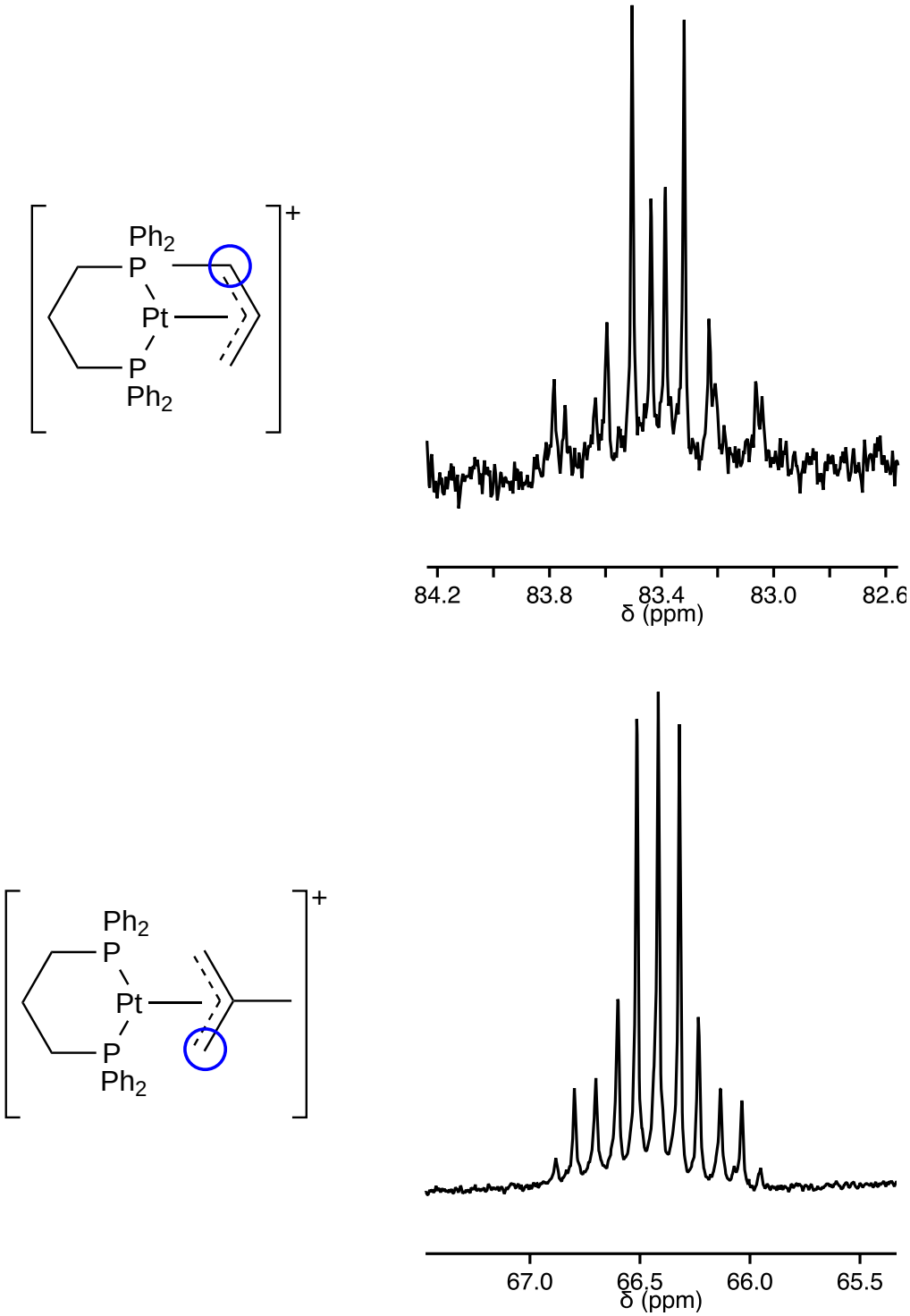

Figure A.57. Expanded $^{13}C\{^{1}H\}$ NMR spectrum of $[Pt(\eta^3\text{-}CH_2CMeCH_2)(dppp)][PhC(SO_2CF_3)_2]$ (**15**$[PhC(SO_2CF_3)_2]$) and $[Pt(\eta^3\text{-}CH_2CHCHMe)(dppp)][PhC(SO_2CF_3)_2]$ (*anti* Me) (**16a**$[PhC(SO_2CF_3)_2]$). (150 MHz, RT, 40 mg/mL, d_6-acetone).

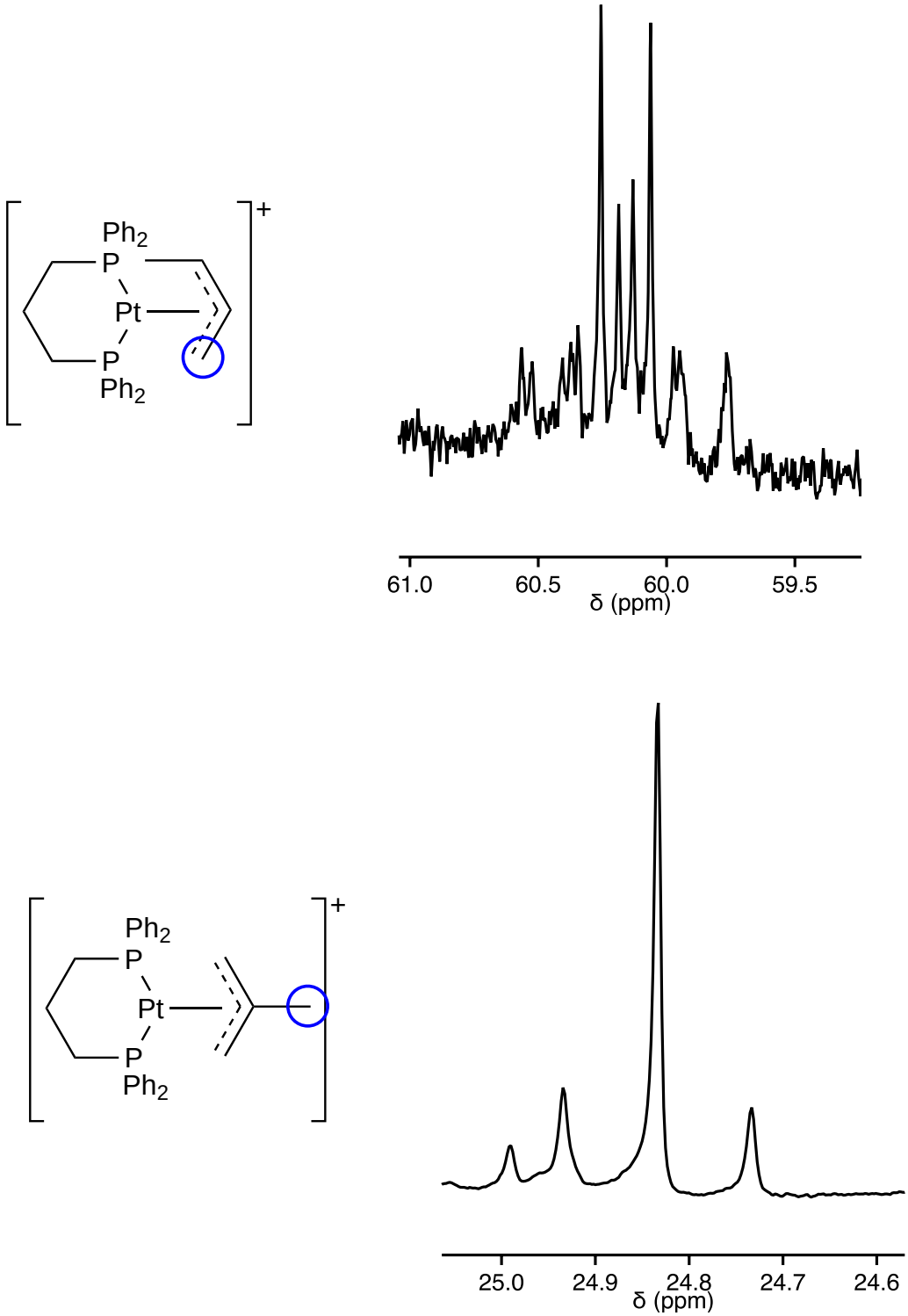

Figure A.58. Expanded $^{13}C\{^{1}H\}$ NMR spectrum of $[Pt(\eta^3\text{-}CH_2CMeCH_2)(dppp)][PhC(SO_2CF_3)_2]$ (**15**$[PhC(SO_2CF_3)_2]$) and $[Pt(\eta^3\text{-}CH_2CHCHMe)(dppp)][PhC(SO_2CF_3)_2]$ (*anti* Me) (**16a**$[PhC(SO_2CF_3)_2]$). (150 MHz, RT, 40 mg/mL, d_6-acetone).

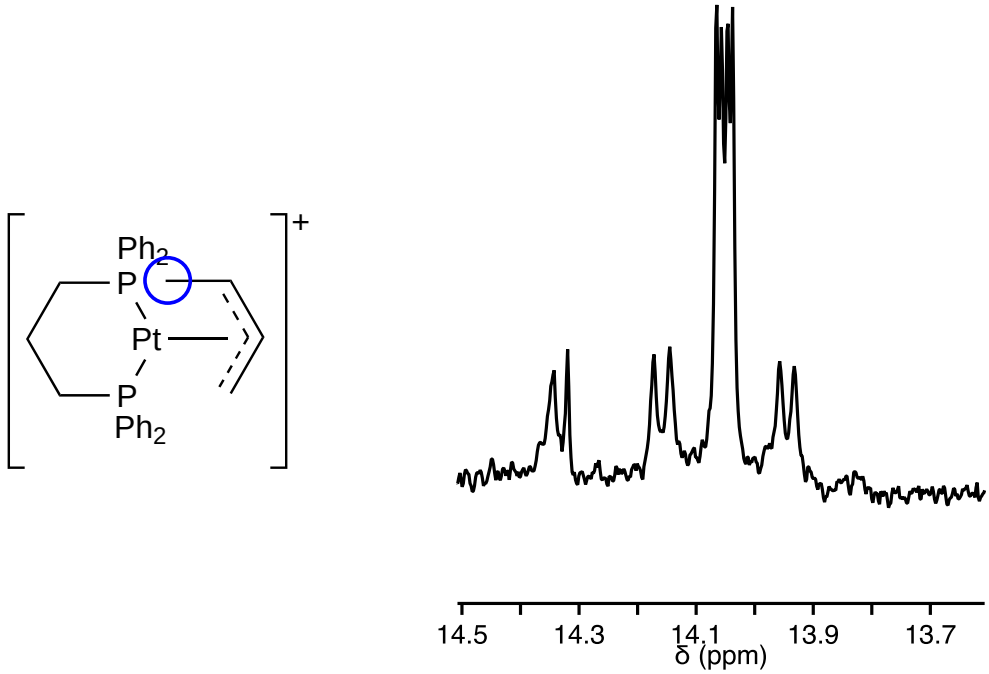

Figure A.59. Expanded $^{13}C\{^{1}H\}$ NMR spectrum of $[Pt(\eta^3\text{-}CH_2CMeCH_2)(dppp)][PhC(SO_2CF_3)_2]$ (**15**$[PhC(SO_2CF_3)_2]$) and $[Pt(\eta^3\text{-}CH_2CHCHMe)(dppp)][PhC(SO_2CF_3)_2]$ (*anti* Me) (**16a**$[PhC(SO_2CF_3)_2]$). (150 MHz, RT, 40 mg/mL, d_6-acetone).

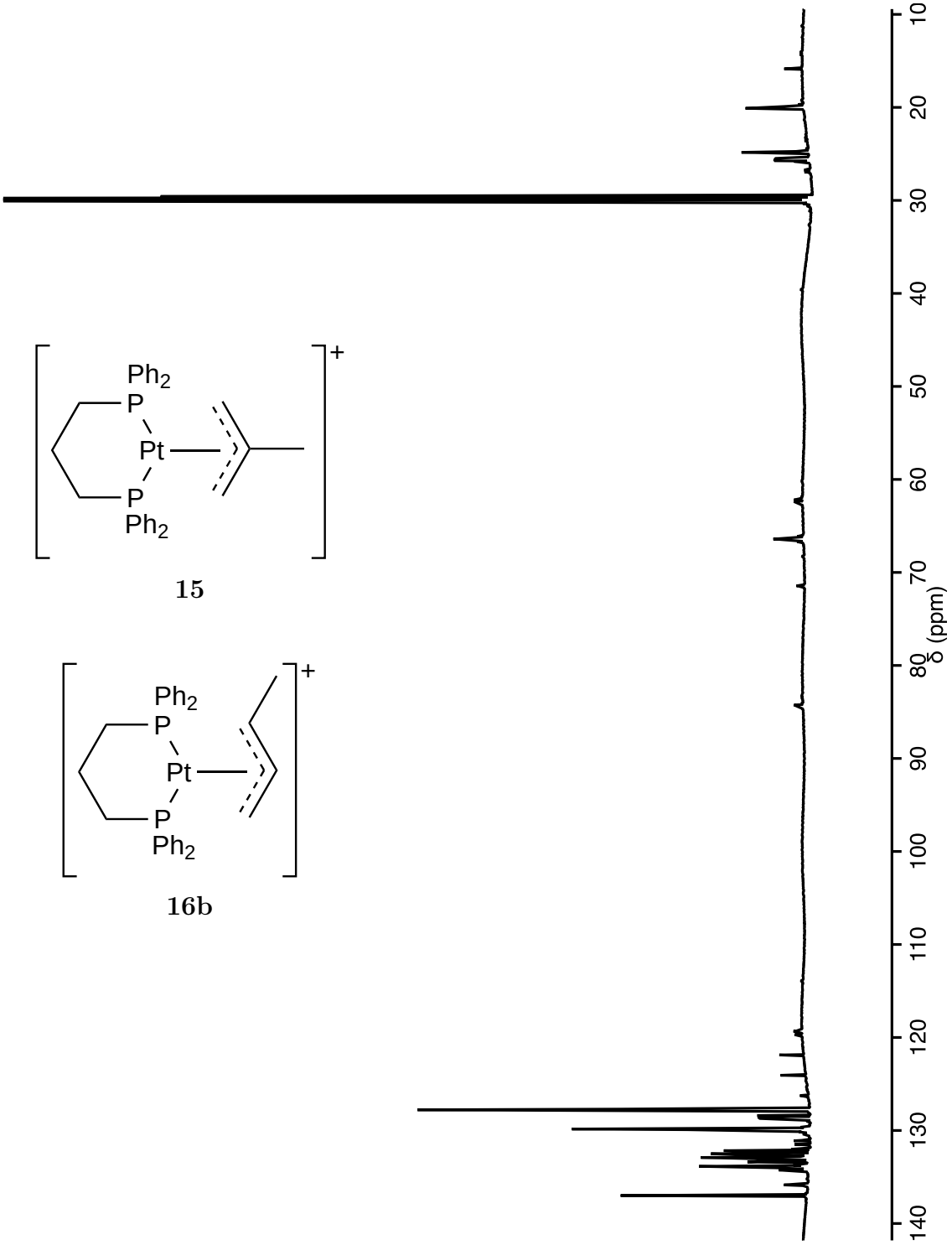

Figure A.60. $^{13}C\{^{1}H\}$ NMR spectrum of [Pt(η^3-CH_2CMeCH_2)(dppp)][$PhC(SO_2CF_3)_2$] (**15**[$PhC(SO_2CF_3)_2$]) and [Pt(η^3-$CH_2CHCHMe$)(dppp)][$PhC(SO_2CF_3)_2$] (*syn* Me) (**16b**[$PhC(SO_2CF_3)_2$]). (150 MHz, RT, 40 mg/mL, d_6-acetone).

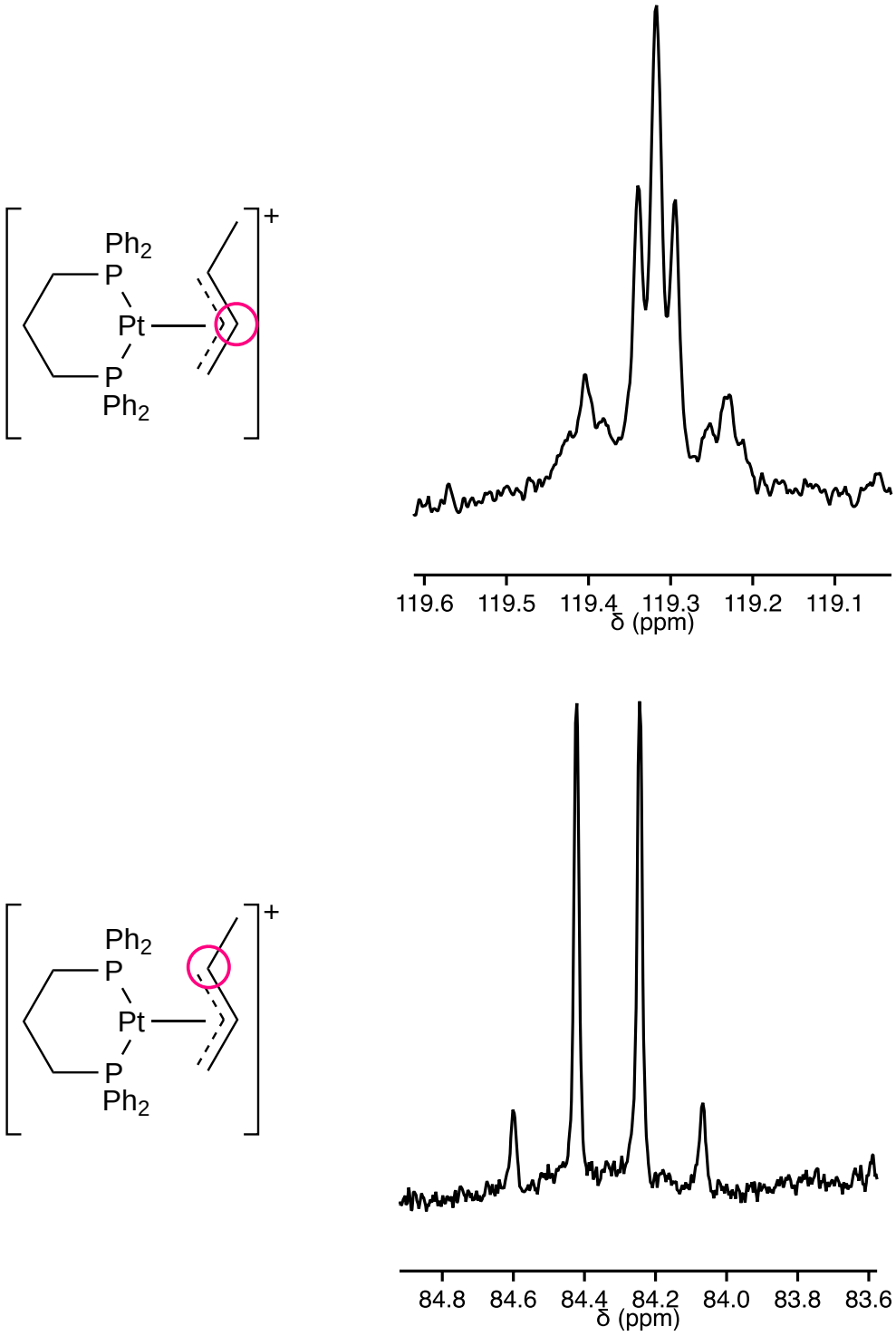

Figure A.61. Expanded $^{13}C\{^{1}H\}$ NMR spectrum of $[Pt(\eta^3\text{-}CH_2CMeCH_2)(dppp)][PhC(SO_2CF_3)_2]$ (**15**$[PhC(SO_2CF_3)_2]$) and $[Pt(\eta^3\text{-}CH_2CHCHMe)(dppp)][PhC(SO_2CF_3)_2]$ (*syn* Me) (**16b**$[PhC(SO_2CF_3)_2]$). (150 MHz, RT, 40 mg/mL, d_6-acetone).

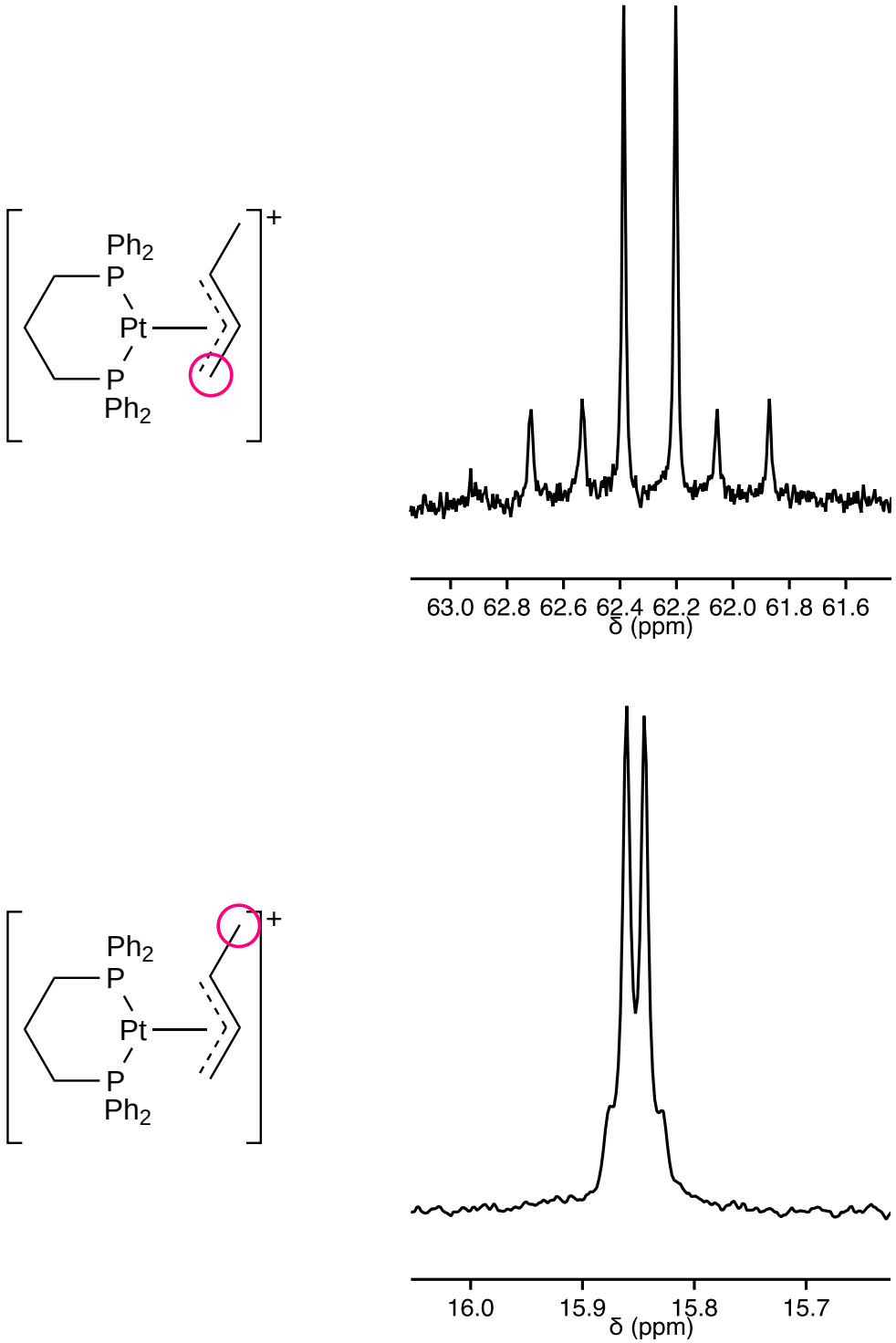

Figure A.62. Expanded $^{13}C\{^{1}H\}$ NMR spectrum of $[Pt(\eta^3\text{-}CH_2CMeCH_2)(dppp)][PhC(SO_2CF_3)_2]$ (**15**$[PhC(SO_2CF_3)_2]$) and $[Pt(\eta^3\text{-}CH_2CHCHMe)(dppp)][PhC(SO_2CF_3)_2]$ (*syn* Me) (**16b**$[PhC(SO_2CF_3)_2]$). (150 MHz, RT, 40 mg/mL, d_6-acetone).

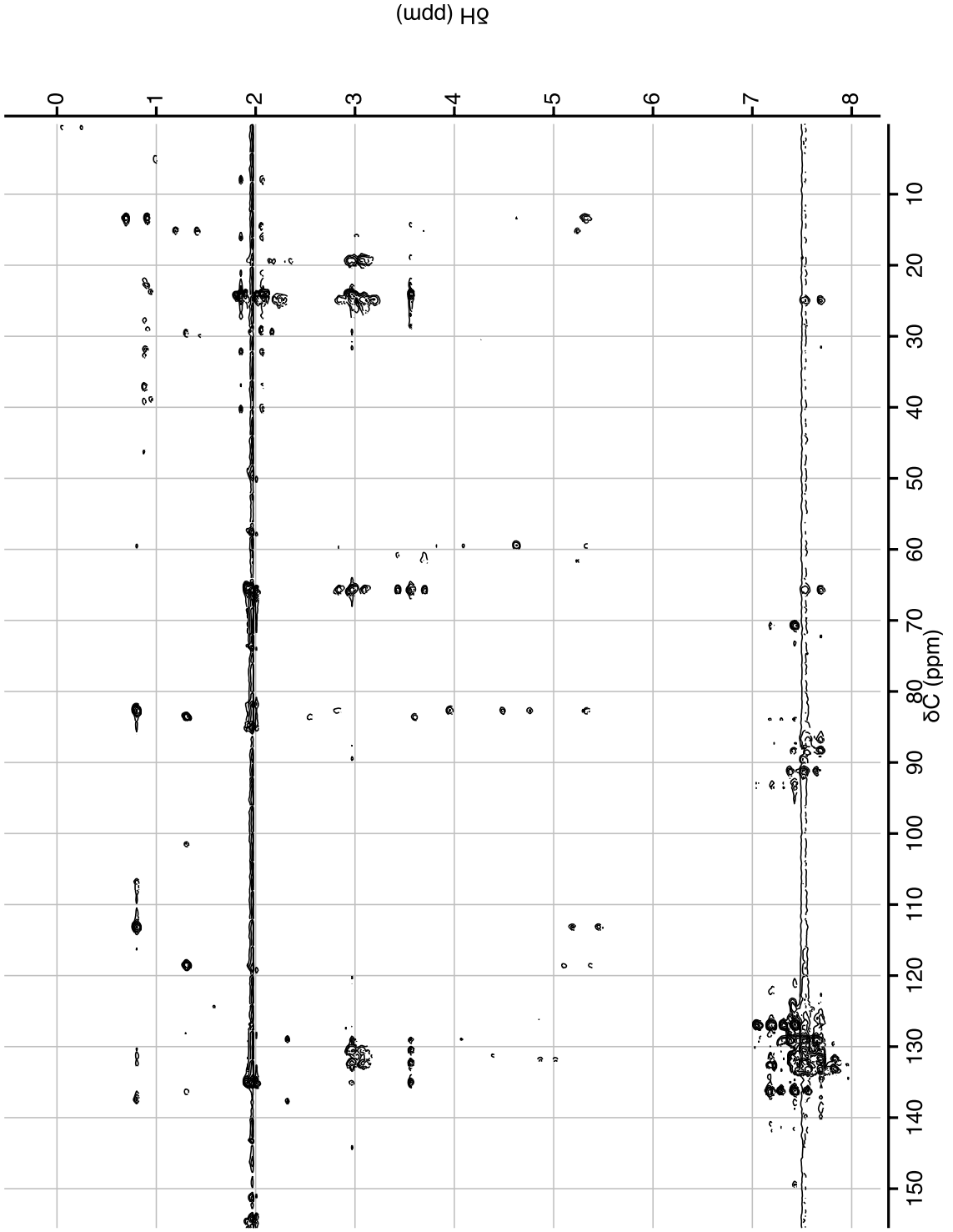

Figure A.63. HMBC spectrum of [Pt(η^3-CH_2CMeCH_2)(dppp)][$PhC(SO_2CF_3)_2$] (**15**[$PhC(SO_2CF_3)_2$]) and [Pt(η^3-$CH_2CHCHMe$)(dppp)][$PhC(SO_2CF_3)_2$] (*anti* Me) (**16a**[$PhC(SO_2CF_3)_2$]). (600/150 MHz, RT, 40 mg/mL, d_6-acetone). Some residual one bond coupling is present.

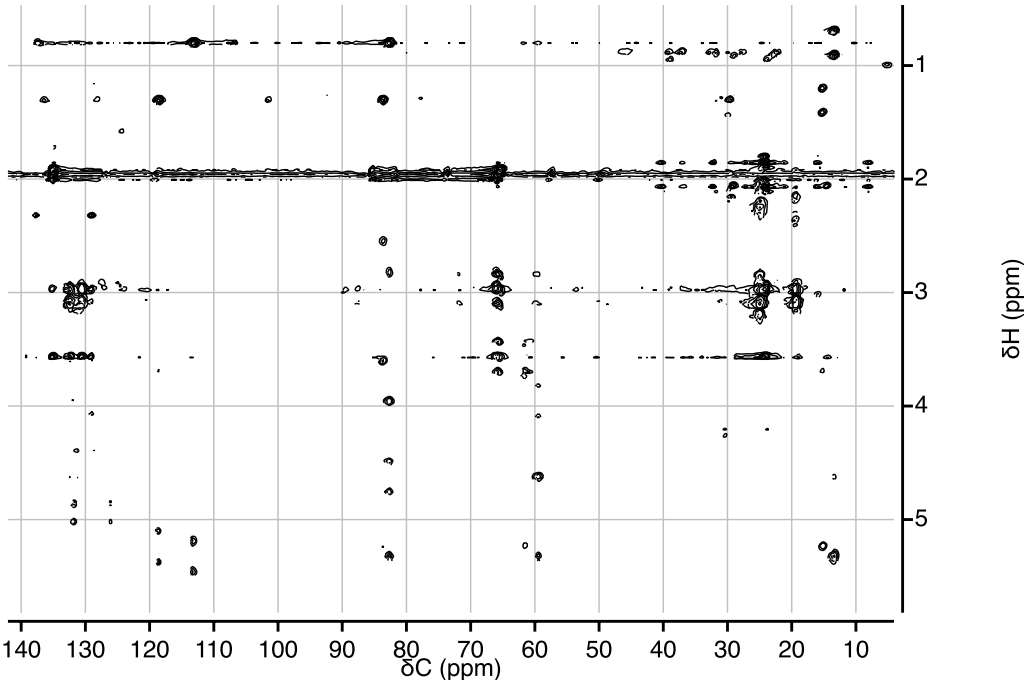

Figure A.64. Expanded HMBC spectrum of [Pt(η^3-CH_2CMeCH_2)(dppp)][$PhC(SO_2CF_3)_2$] (**15**[$PhC(SO_2CF_3)_2$]) and [Pt(η^3-$CH_2CHCHMe$)(dppp)][$PhC(SO_2CF_3)_2$] (*anti* Me) (**16a**[$PhC(SO_2CF_3)_2$]). (150 MHz, RT, 40 mg/mL, d_6-acetone). Some residual one bond coupling is present.

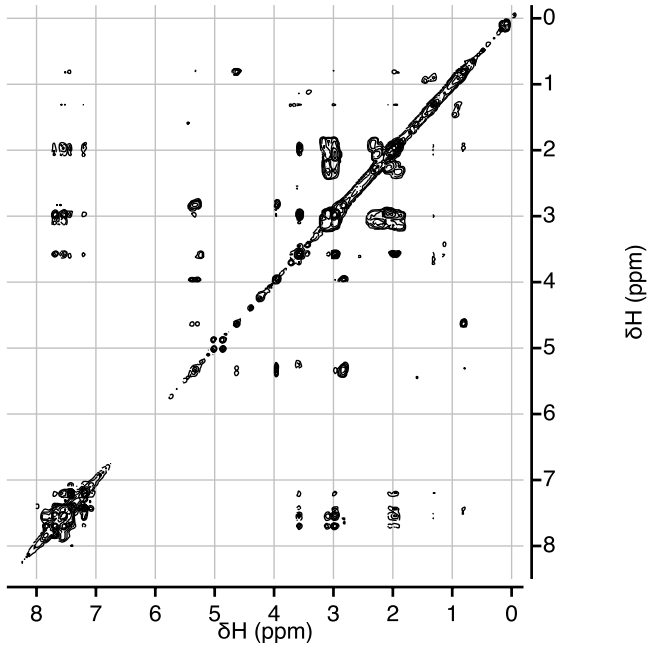

Figure A.65. COSY spectrum of carbon-13 enriched[Pt(η^3-CH_2CMeCH_2)(dppp)][$PhC(SO_2CF_3)_2$] (**15**[$PhC(SO_2CF_3)_2$]) and [Pt(η^3-$CH_2CHCHMe$)(dppp)][$PhC(SO_2CF_3)_2$] (*anti* Me) (**16a**[$PhC(SO_2CF_3)_2$]). (150 MHz, RT, 40 mg/mL, d_6-acetone).

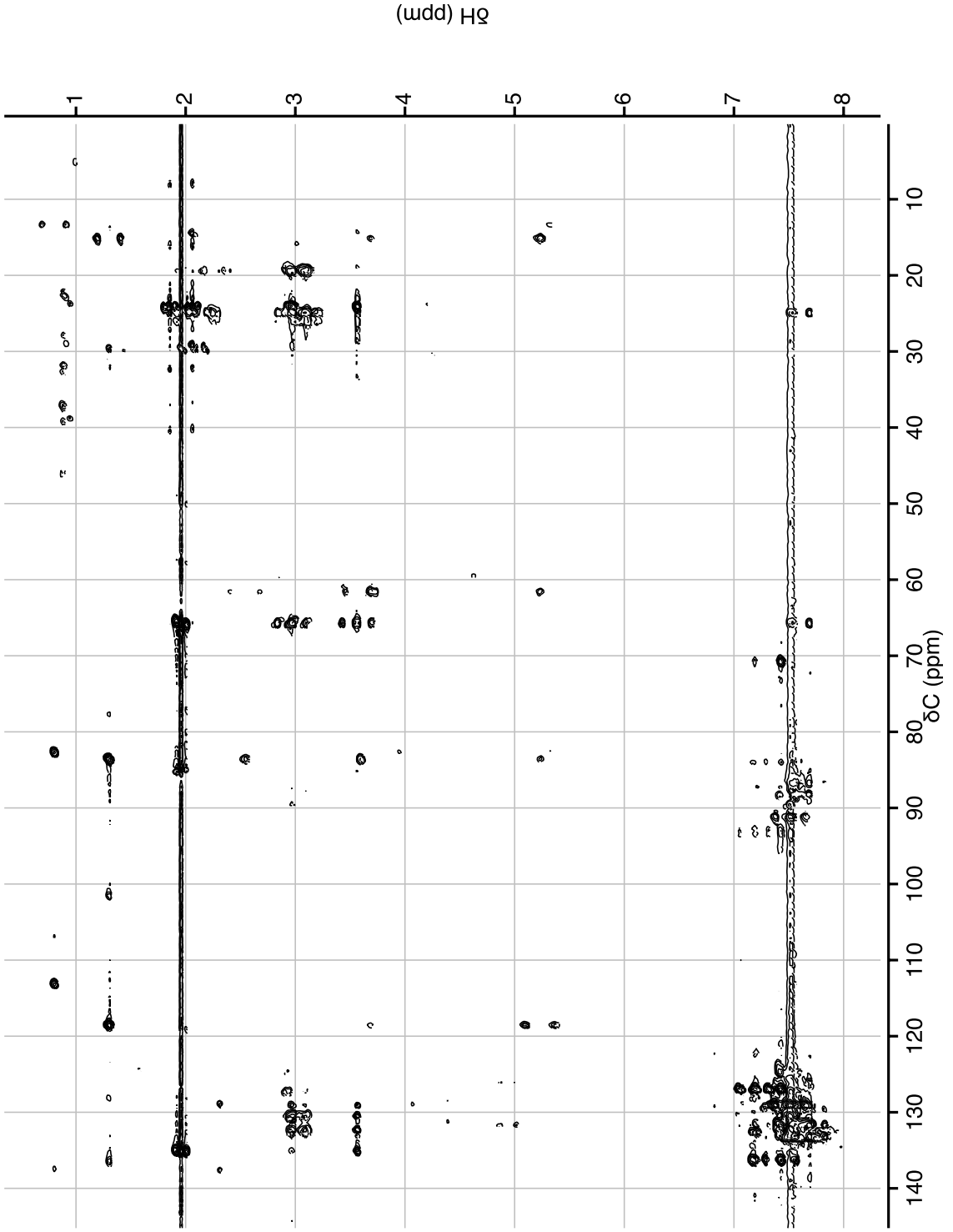

Figure A.66. HMBC spectrum of [Pt(η^3-CH_2CMeCH_2)(dppp)][$PhC(SO_2CF_3)_2$] (**15**[$PhC(SO_2CF_3)_2$]) and [Pt(η^3-$CH_2CHCHMe$)(dppp)][$PhC(SO_2CF_3)_2$] (*syn* Me) (**16b**[$PhC(SO_2CF_3)_2$]). (600/150 MHz, RT, 40 mg/mL, d_6-acetone). Some residual one bond coupling is present.

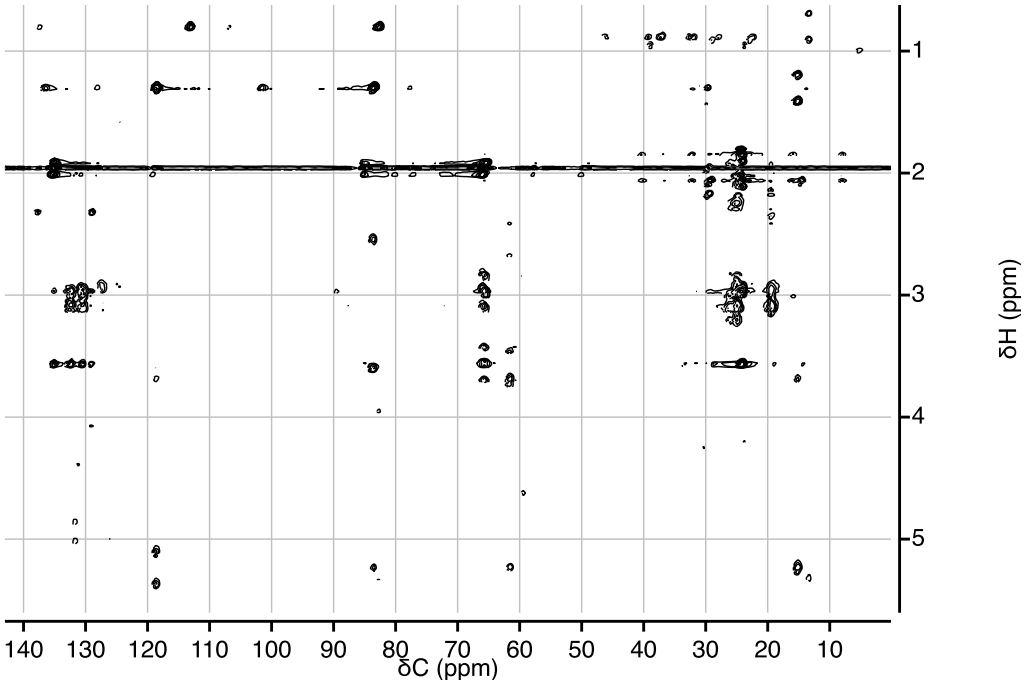

Figure A.67. Expanded HMBC spectrum of [Pt(η^3-CH_2CMeCH_2)(dppp)][$PhC(SO_2CF_3)_2$] (**15**[$PhC(SO_2CF_3)_2$]) and [Pt(η^3-$CH_2CHCHMe$)(dppp)][$PhC(SO_2CF_3)_2$] (*syn* Me) (**16b**[$PhC(SO_2CF_3)_2$]). (150 MHz, RT, 40 mg/mL, d_6-acetone). Some residual one bond coupling is present.

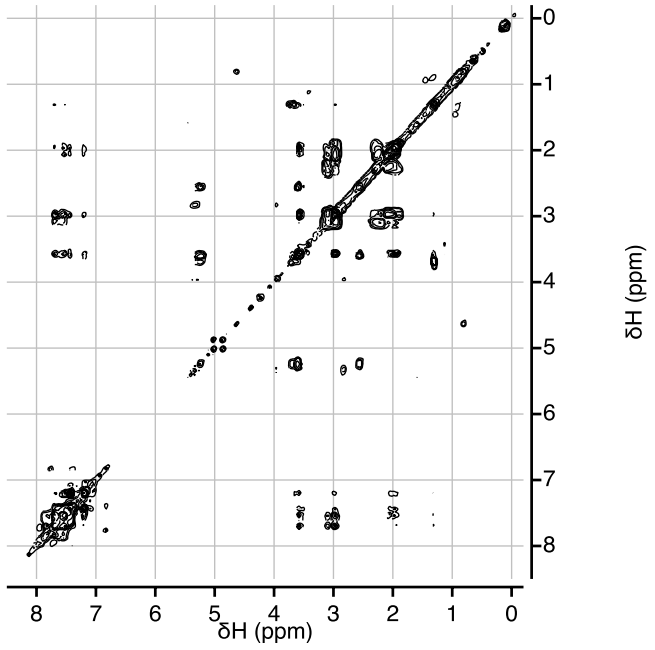

Figure A.68. COSY spectrum of carbon-13 enriched[Pt(η^3-CH_2CMeCH_2)(dppp)][$PhC(SO_2CF_3)_2$] (**15**[$PhC(SO_2CF_3)_2$]) and [Pt(η^3-$CH_2CHCHMe$)(dppp)][$PhC(SO_2CF_3)_2$] (*syn* Me) (**16b**[$PhC(SO_2CF_3)_2$]). (150 MHz, RT, 40 mg/mL, d_6-acetone).

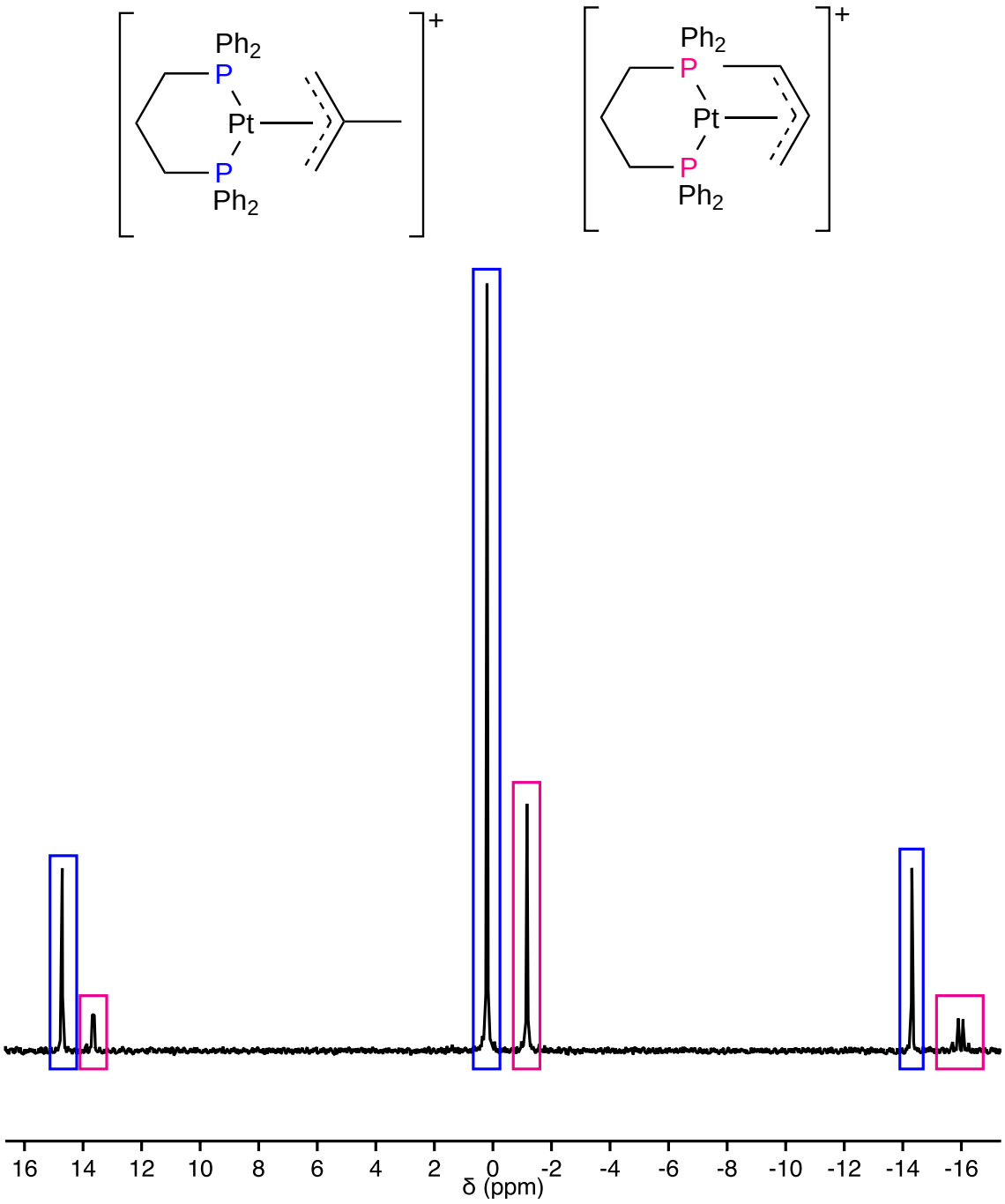

Figure A.69. $^{31}P\{^{1}H\}$ NMR spectrum of [Pt(η^3-CH_2CMeCH_2)(dppp)][$PhC(SO_2CF_3)_2$] (**15**[$PhC(SO_2CF_3)_2$]) and [Pt(η^3-$CH_2CHCHMe$)(dppp)][$PhC(SO_2CF_3)_2$] (*anti* Me) (**16a**[$PhC(SO_2CF_3)_2$]). (150 MHz, RT, 40 mg/mL, d_6-acetone).

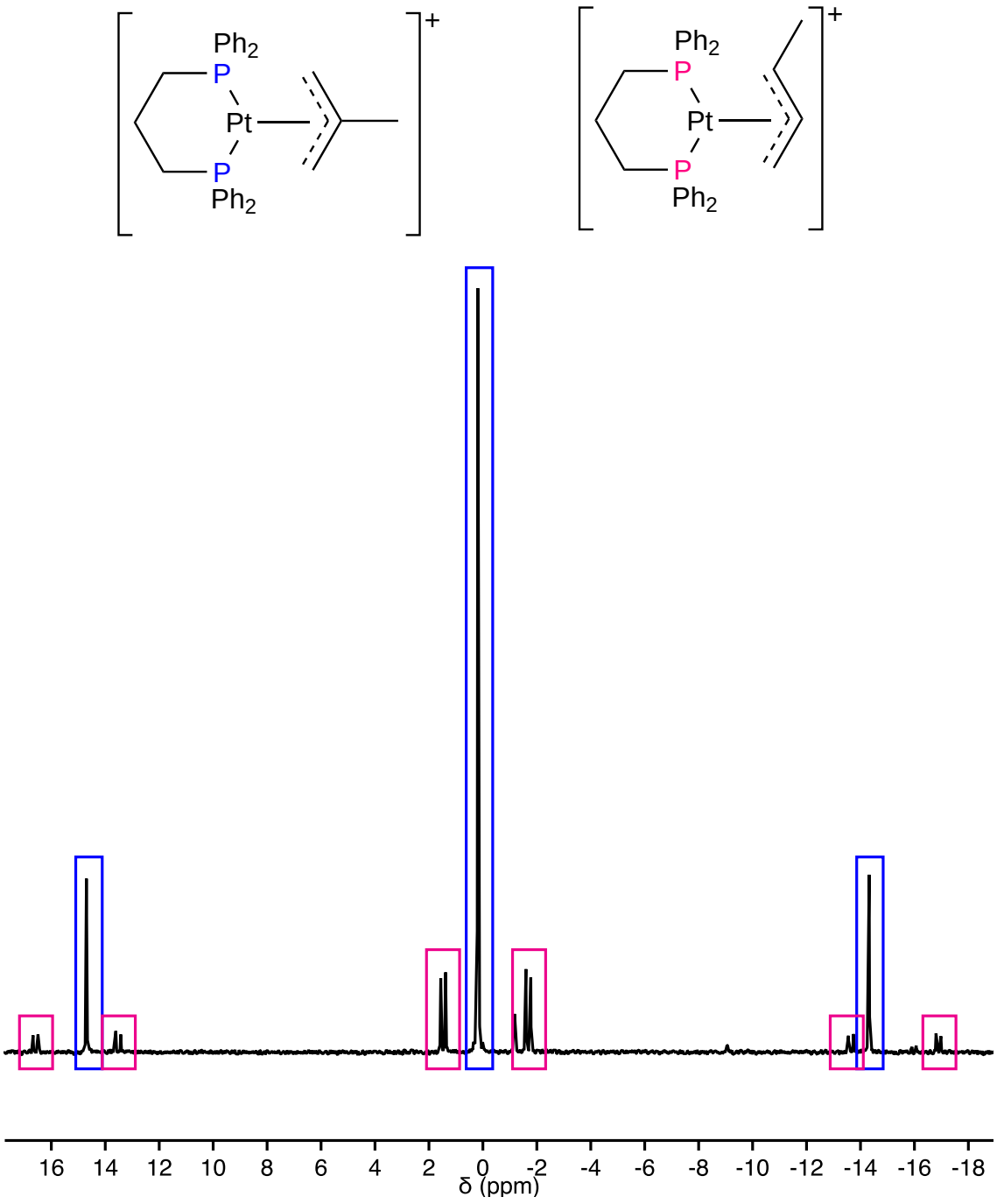

Figure A.70. $^{31}P\{^{1}H\}$ NMR spectrum of [Pt(η^3-CH_2CMeCH_2)(dppp)][$PhC(SO_2CF_3)_2$] (**15**[$PhC(SO_2CF_3)_2$]) and [Pt(η^3-$CH_2CHCHMe$)(dppp)][$PhC(SO_2CF_3)_2$] (*syn* Me) (**16b**[$PhC(SO_2CF_3)_2$]). (150 MHz, RT, 40 mg/mL, d_6-acetone).

A.3 Chapter Four

[PtEt(C(CH$_2$)$_2$CH$_3$)(COD)] (27a) and [Pt(C(CH$_2$)$_2$CH$_3$)$_2$(COD)] (27b)

Trans–[PtCl$_2$(BCP)(Py)] (28)

Trans–[Pt(C(CH$_2$)$_2$C(CH$_2$)$_2$Cl)Cl(SEt$_2$)$_2$] (32)

Cis–[Pt(C(CH$_2$)$_2$C(CH$_2$)$_2$Cl)Cl(Py)$_2$] (34b)

Cis–[Pt(C(CH$_2$)$_2$C(CH$_2$)$_2$Cl)Cl(dppp)] (37a)

^{1}H NMR spectrum – Figures A.97 and A.98, pages 251 and 252

^{13}C{^{1}H} NMR spectrum – Figures A.99–A.101, pages 253–255

HMBC spectrum – Figures A.102 and A.103, pages 256 and 257

COSY spectrum – Figure A.104, pages 257

^{31}P{^{1}H} NMR spectrum – Figure A.105, page 258

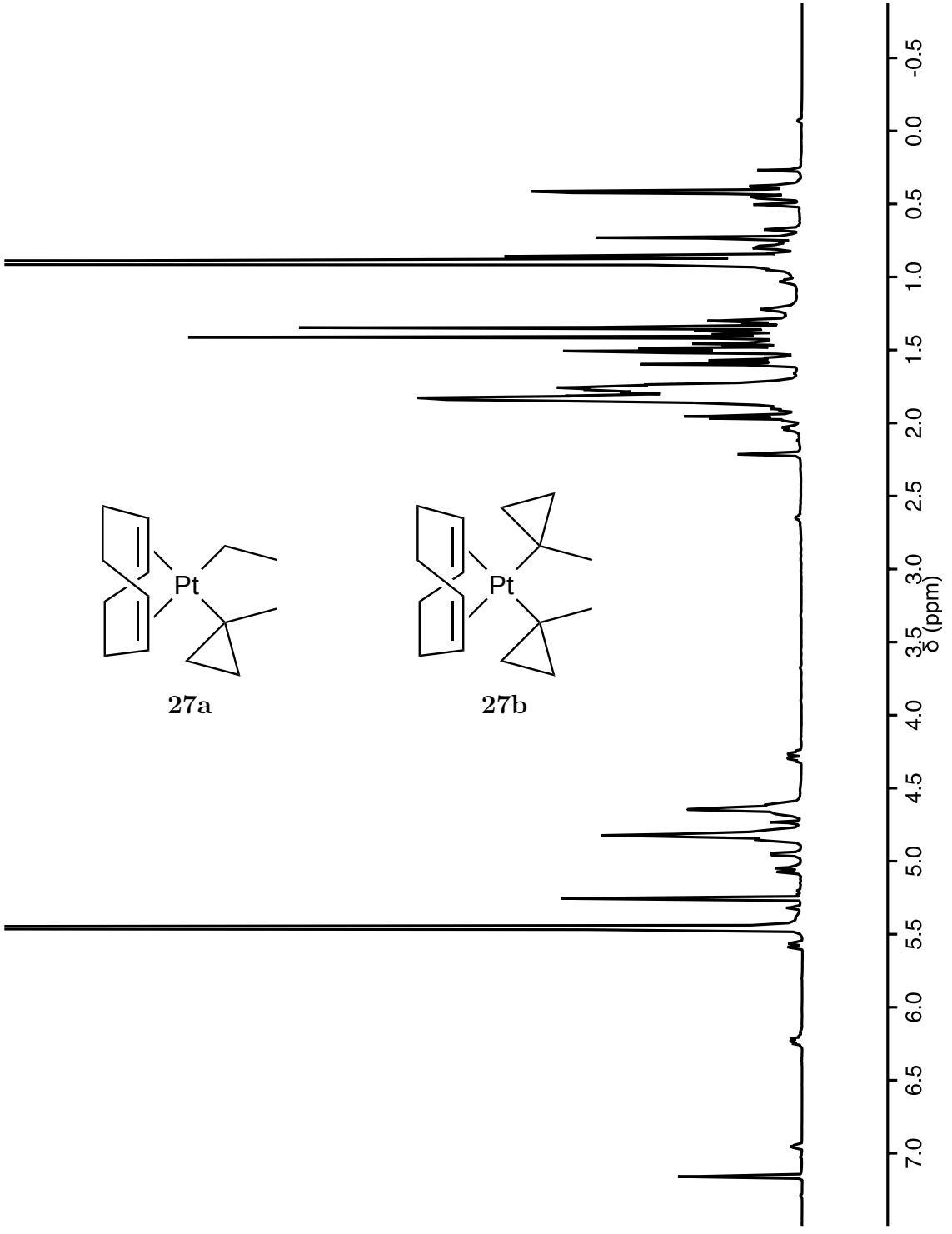

Figure A.71. ^{1}H NMR spectrum of [PtEt(C$(CH_2)_2CH_3$)(COD)] (**27a**) and [Pt(C$(CH_2)_2CH_3)_2$(COD)] (**27b**) (600 MHz, RT, 40 mg/mL, C_6D_6).

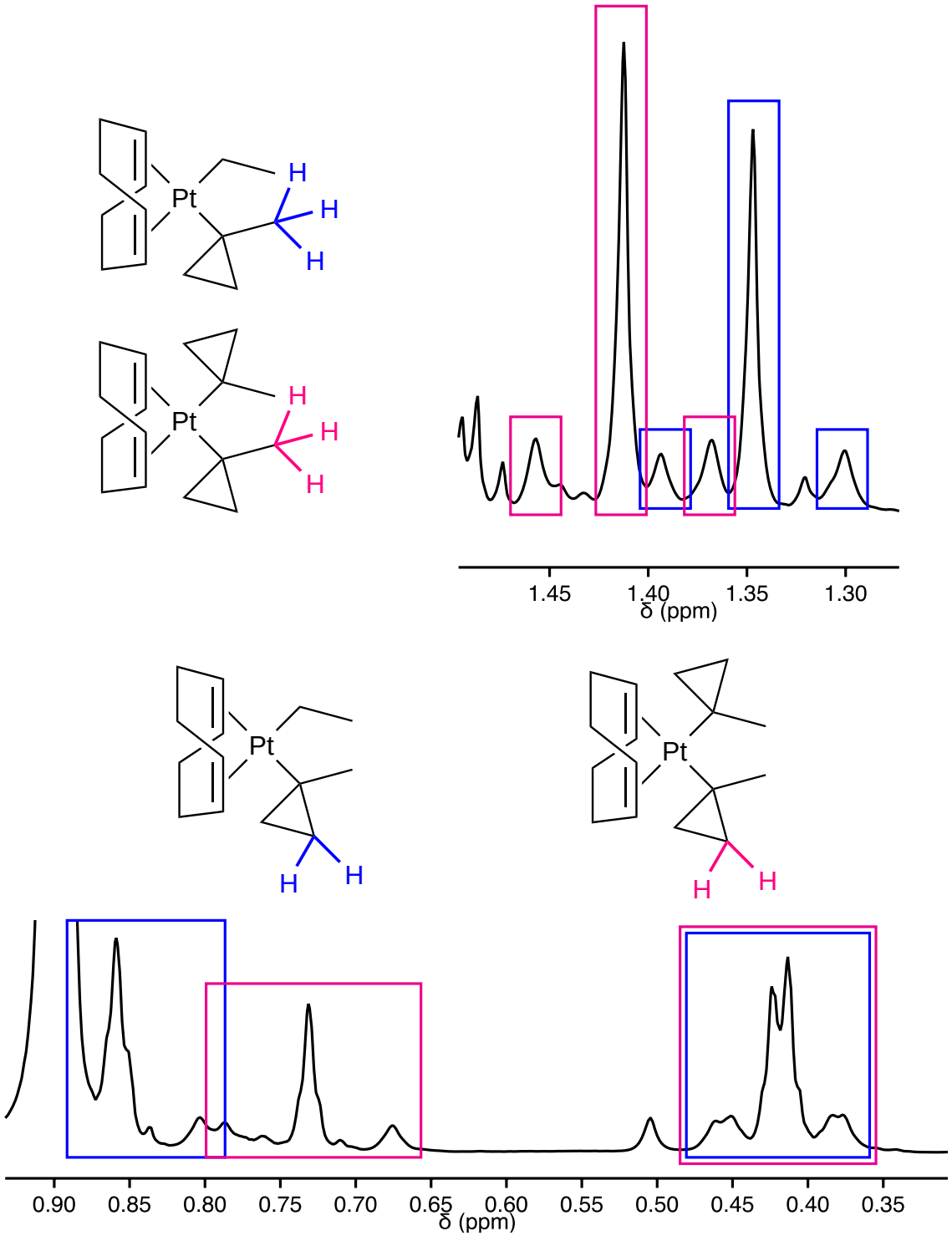

Figure A.72. Expanded ^{1}H NMR spectrum of [PtEt(C$(CH_2)_2CH_3$)(COD)] (**27a**) and [Pt(C$(CH_2)_2CH_3)_2$(COD)] (**27b**) (600 MHz, RT, 40 mg/mL, C_6D_6).

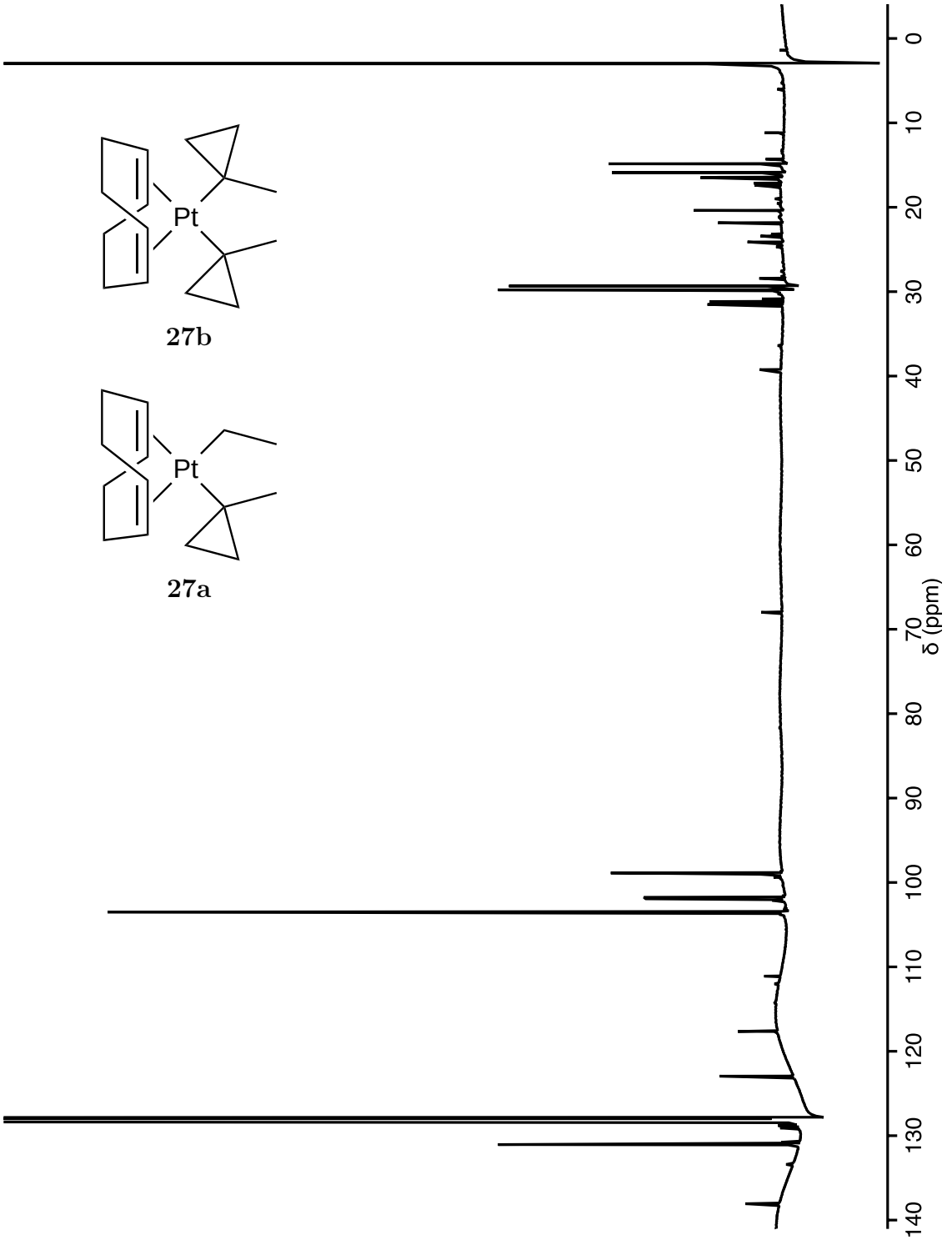

Figure A.73. $^{13}C\{^{1}H\}$ NMR spectrum of $[PtEt(C(CH_2)_2CH_3)(COD)]$ (**27a**) and $[Pt(C(CH_2)_2CH_3)_2(COD)]$ (**27b**) (150 MHz, RT, 40 mg/mL, C_6D_6).

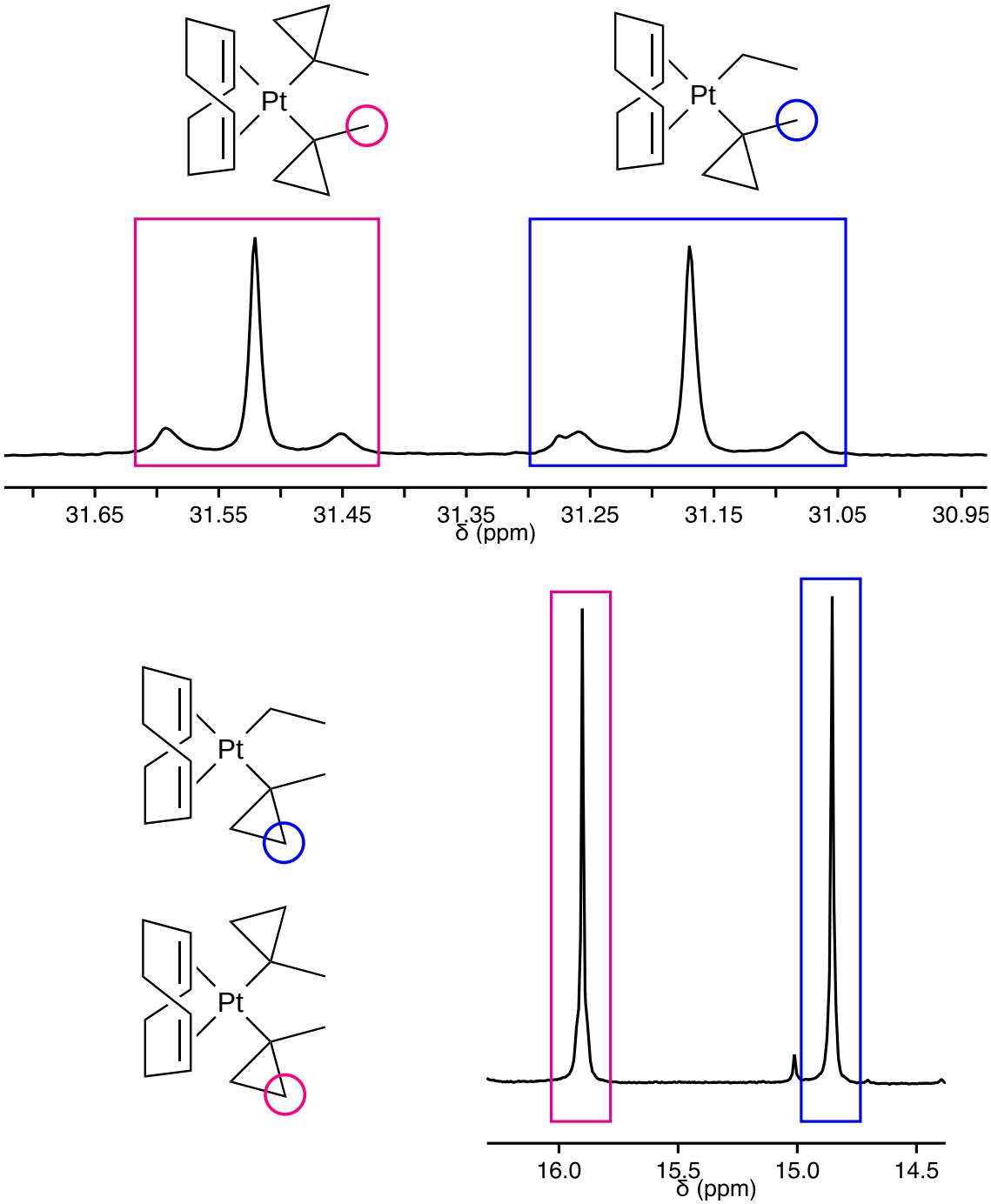

Figure A.74. Expanded $^{13}C\{^{1}H\}$ NMR spectrum of [PtEt($C(CH_2)_2CH_3$)(COD)] (**27a**) and [Pt($C(CH_2)_2CH_3$)$_2$(COD)] (**27b**) (150 MHz, RT, 40 mg/mL, C_6D_6).

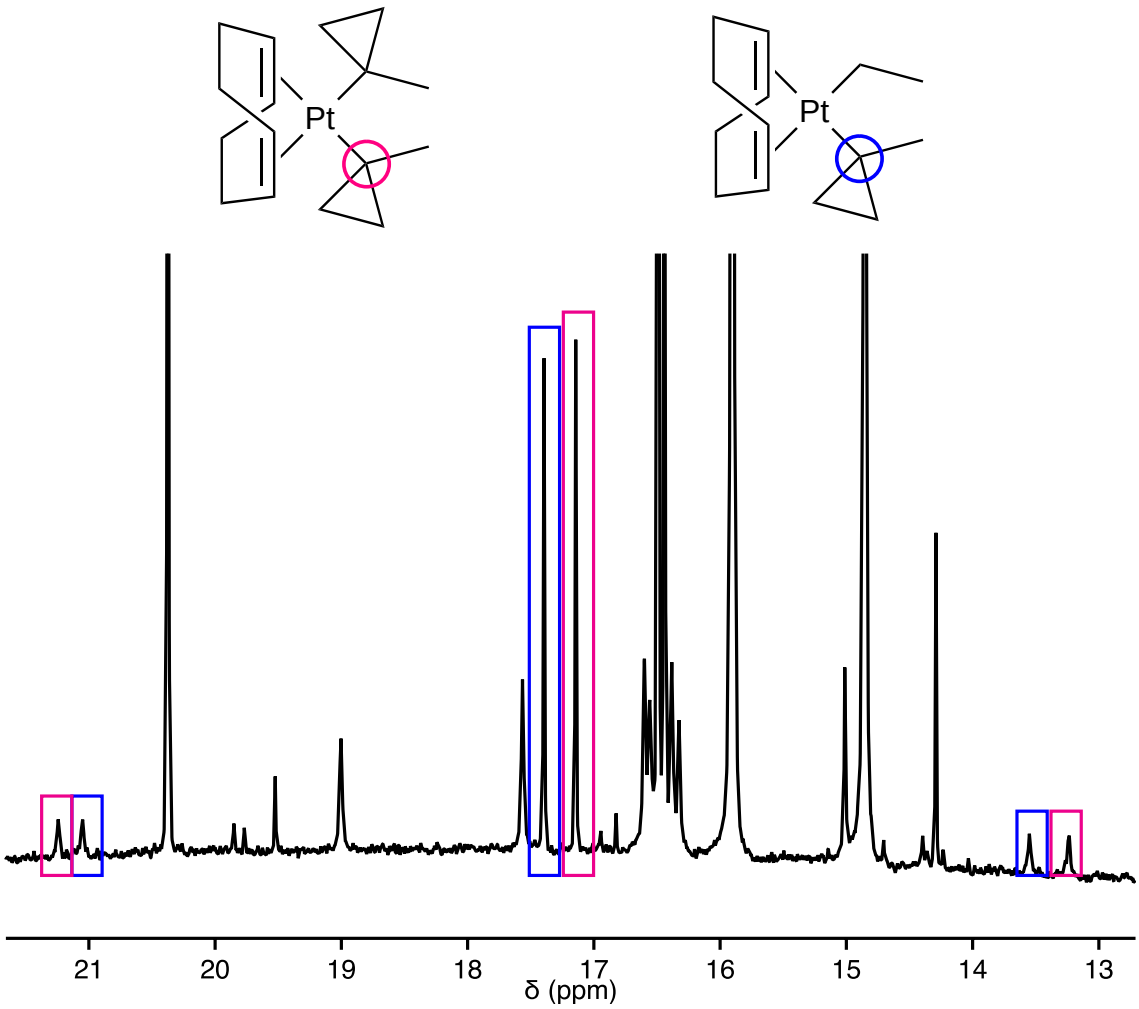

Figure A.75. Expanded $^{13}C\{^{1}H\}$ NMR spectrum of [PtEt($C(CH_2)_2CH_3$)(COD)] (**27a**) and [Pt($C(CH_2)_2CH_3$)$_2$(COD)] (**27b**) (150 MHz, RT, 40 mg/mL, C_6D_6).

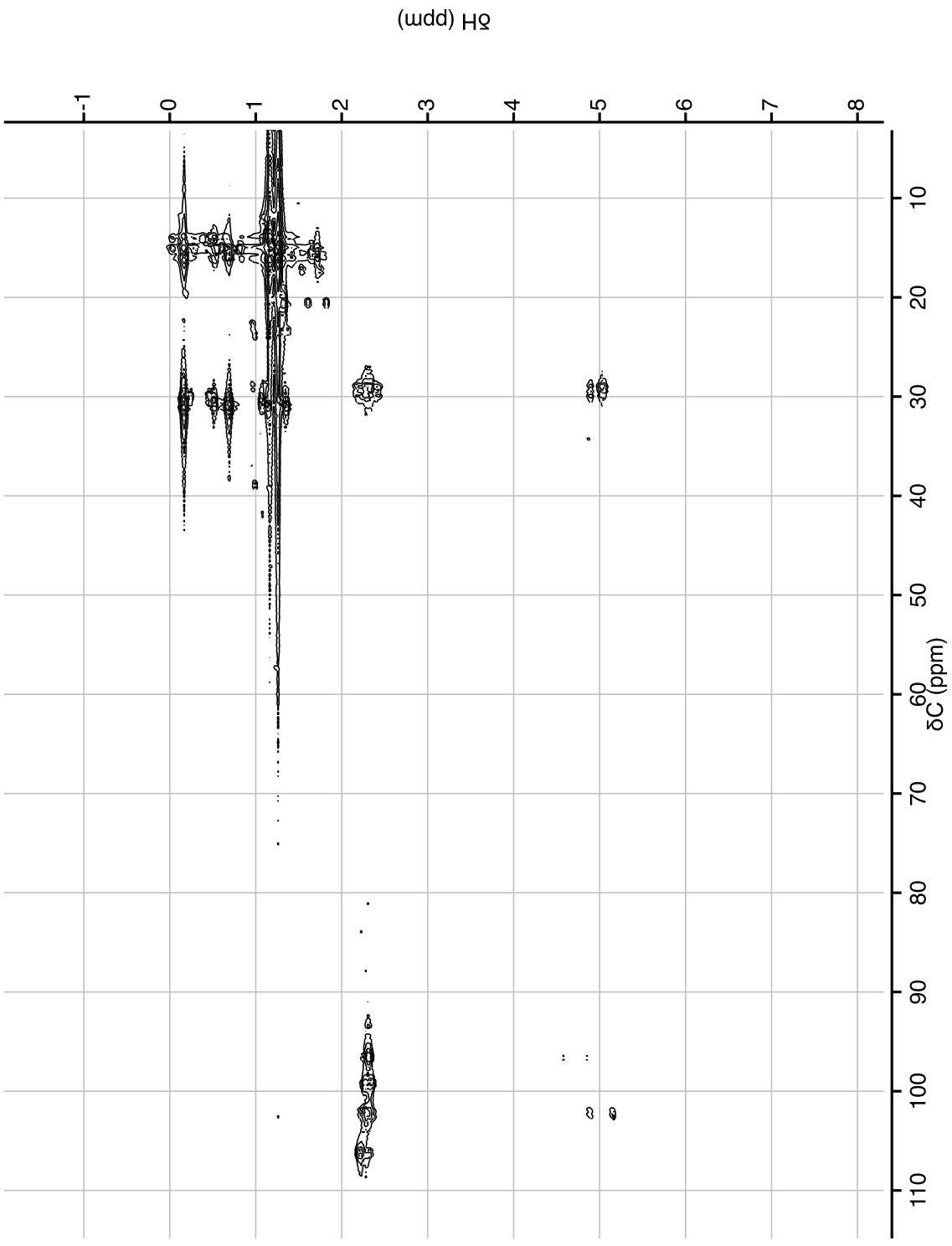

Figure A.76. HMBC spectrum of [PtEt(C$(CH_2)_2CH_3$)(COD)] (**27a**) and [Pt(C$(CH_2)_2CH_3)_2$(COD)] (**27b**) (600/150 MHz, RT, 40 mg/mL, C_6D_6). Some residual one bond coupling is present.

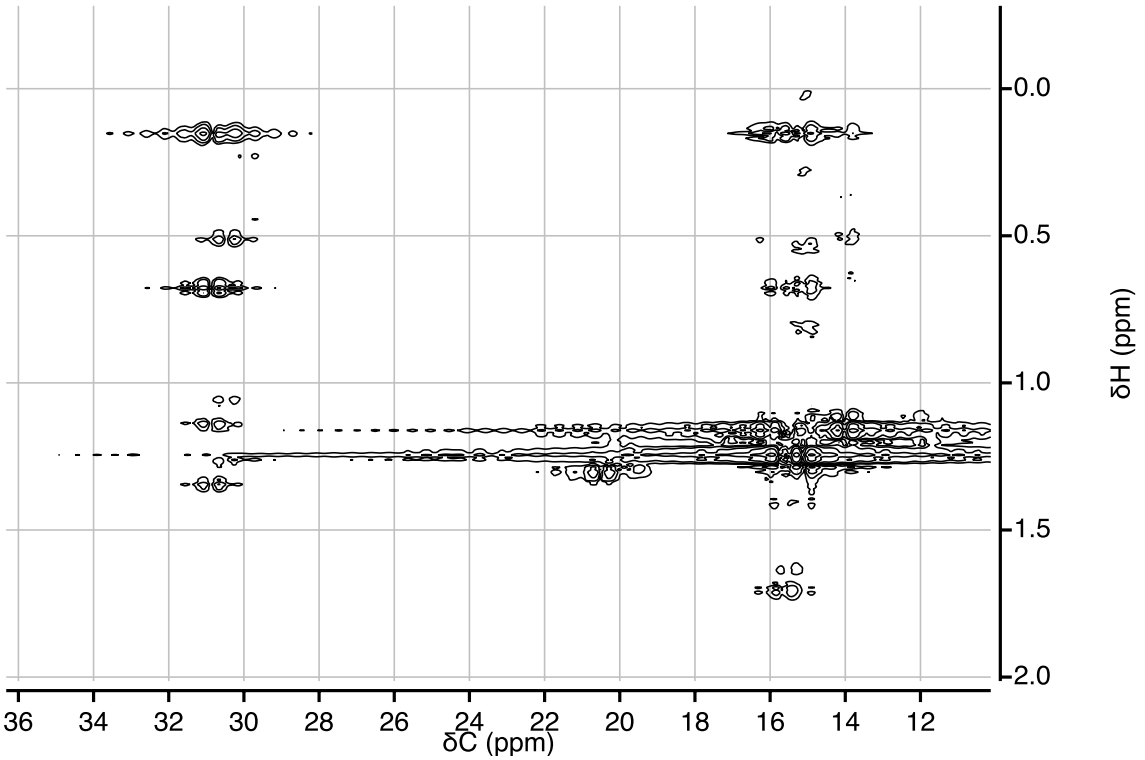

Figure A.77. Expanded HMBC spectrum of [PtEt(C$(CH_2)_2CH_3$)(COD)] (**27a**) and [Pt(C$(CH_2)_2CH_3)_2$(COD)] (**27b**) (600/150 MHz, RT, 40 mg/mL, C_6D_6). Some residual one bond coupling is present.

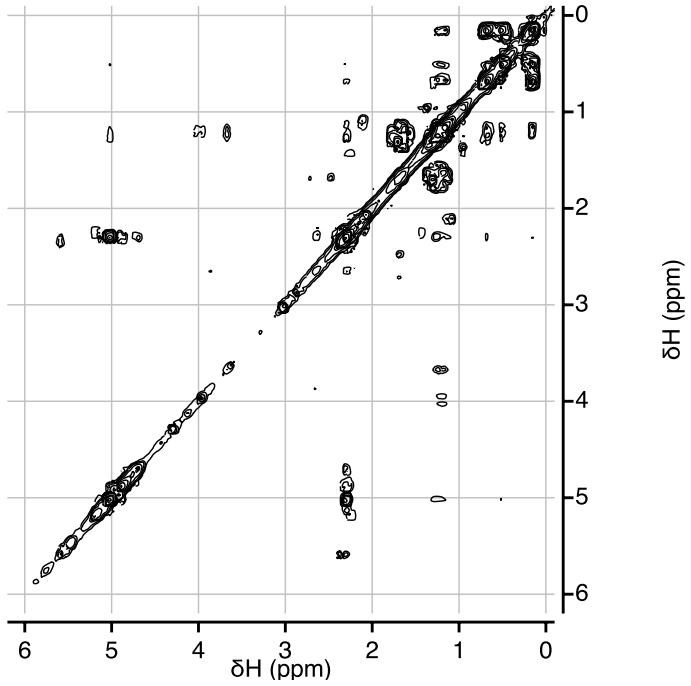

Figure A.78. COSY spectrum of [PtEt(C$(CH_2)_2CH_3$)(COD)] (**27a**) and [Pt(C$(CH_2)_2CH_3)_2$(COD)] (**27b**) (600 MHz, RT, 40 mg/mL, C_6D_6).

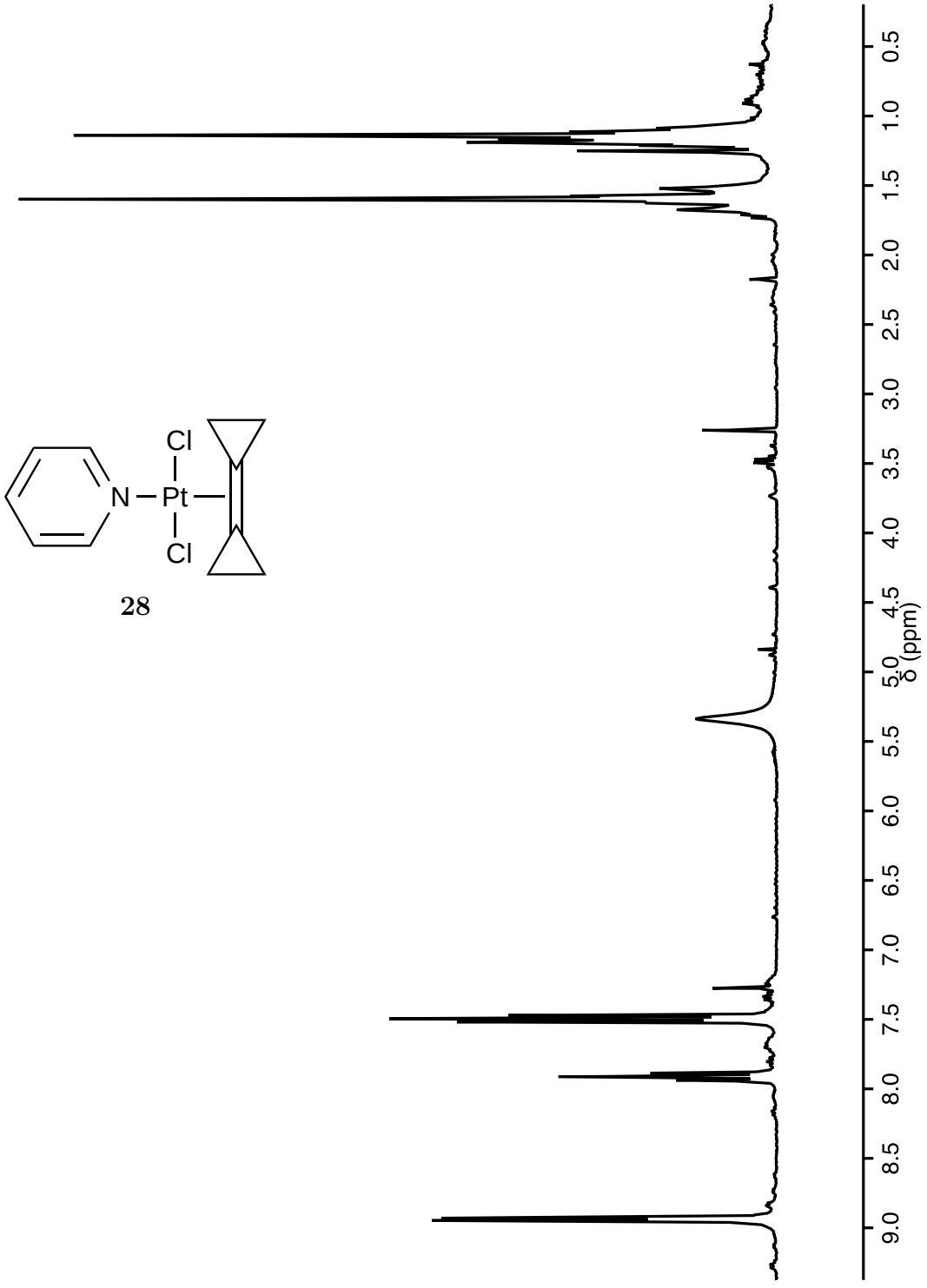

Figure A.79. ^{1}H NMR spectrum of *trans*–[$PtCl_2$(BCP)(Py)] (**28**) (300 MHz, RT, 100 mg/mL, $CDCl_3$).

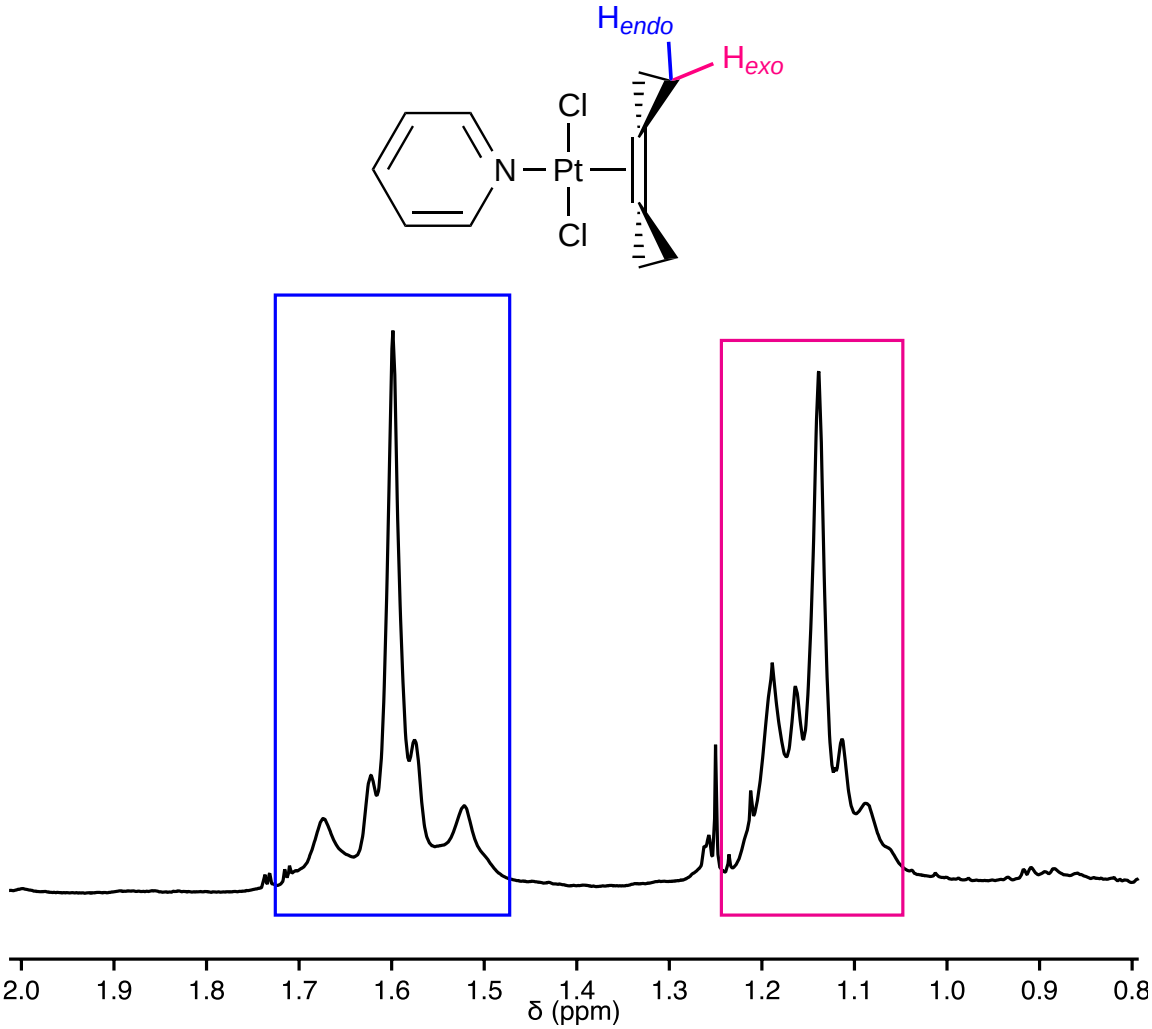

Figure A.80. Expanded ^{1}H NMR spectrum of *trans*–[$PtCl_2$(BCP)(Py)] (**28**) (300 MHz, RT, 100 mg/mL, $CDCl_3$).

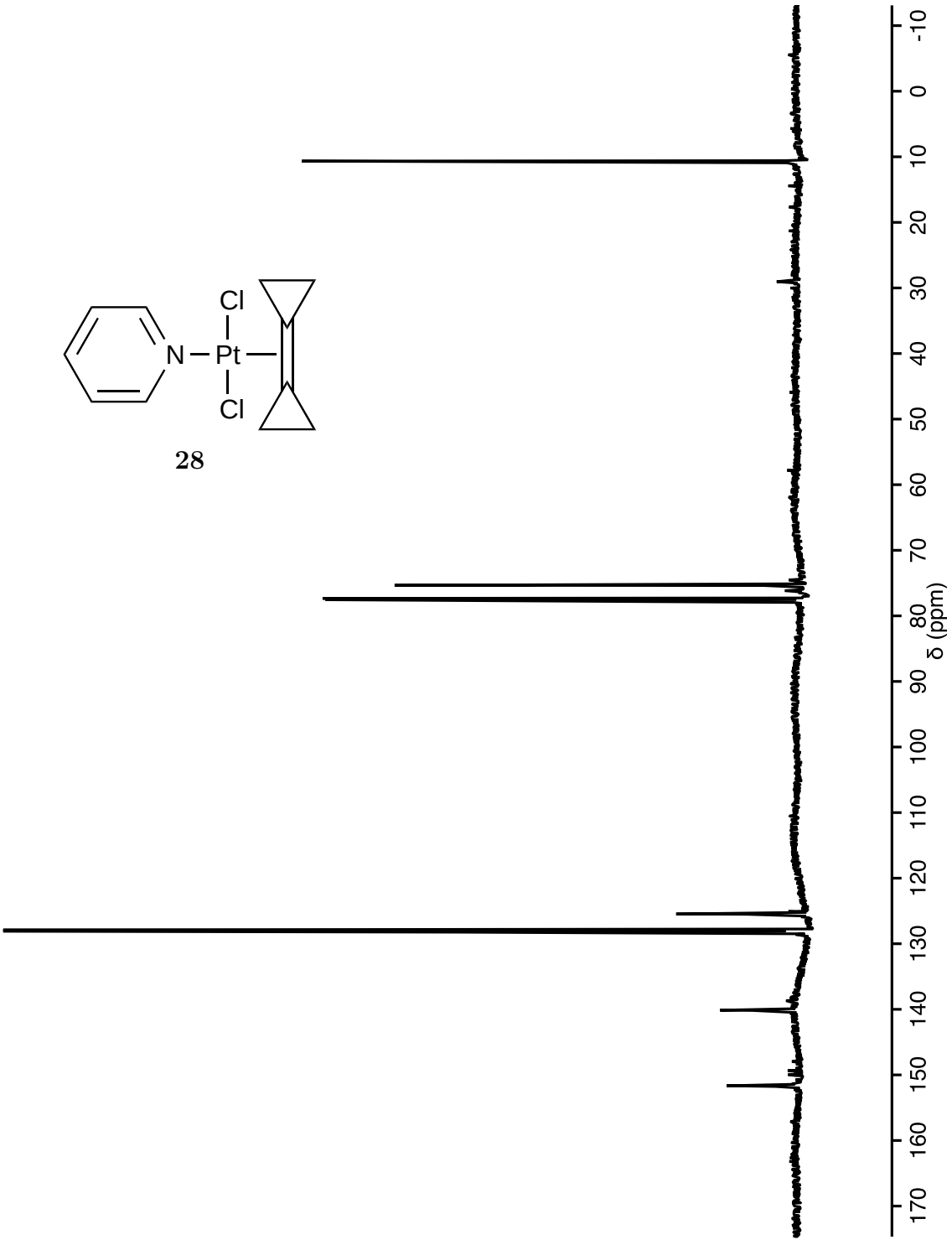

Figure A.81. $^{13}C\{^{1}H\}$ NMR spectrum of carbon-13 enriched *trans*–$[PtCl_2(BCP)(Py)]$ (**28**) (150 MHz, RT, 100 mg/mL, $CDCl_3$).

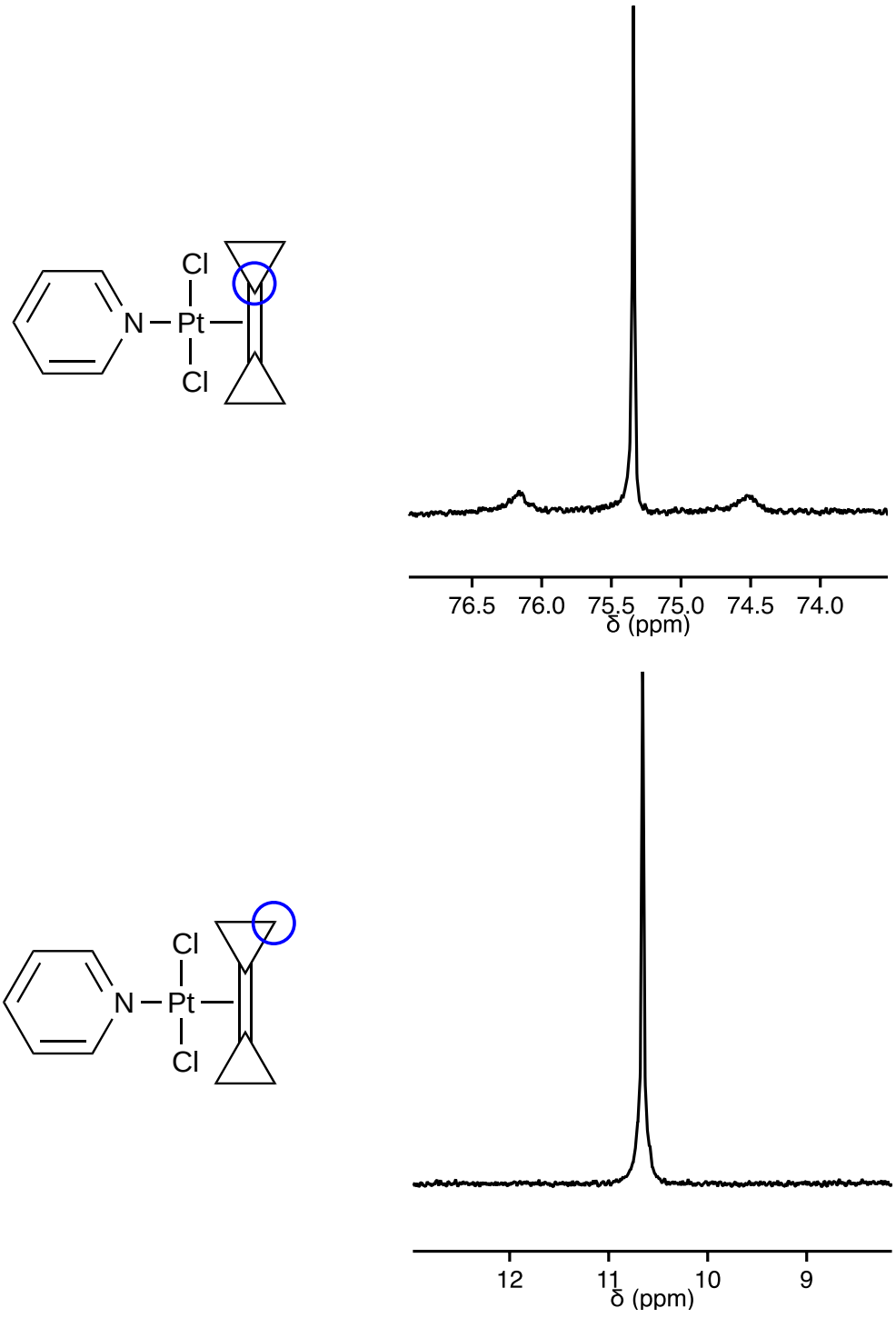

Figure A.82. Expanded $^{13}C\{^{1}H\}$ NMR spectrum of carbon-13 enriched *trans*–[$PtCl_2$(BCP)(Py)] (**28**) (150 MHz, RT, 100 mg/mL, $CDCl_3$).

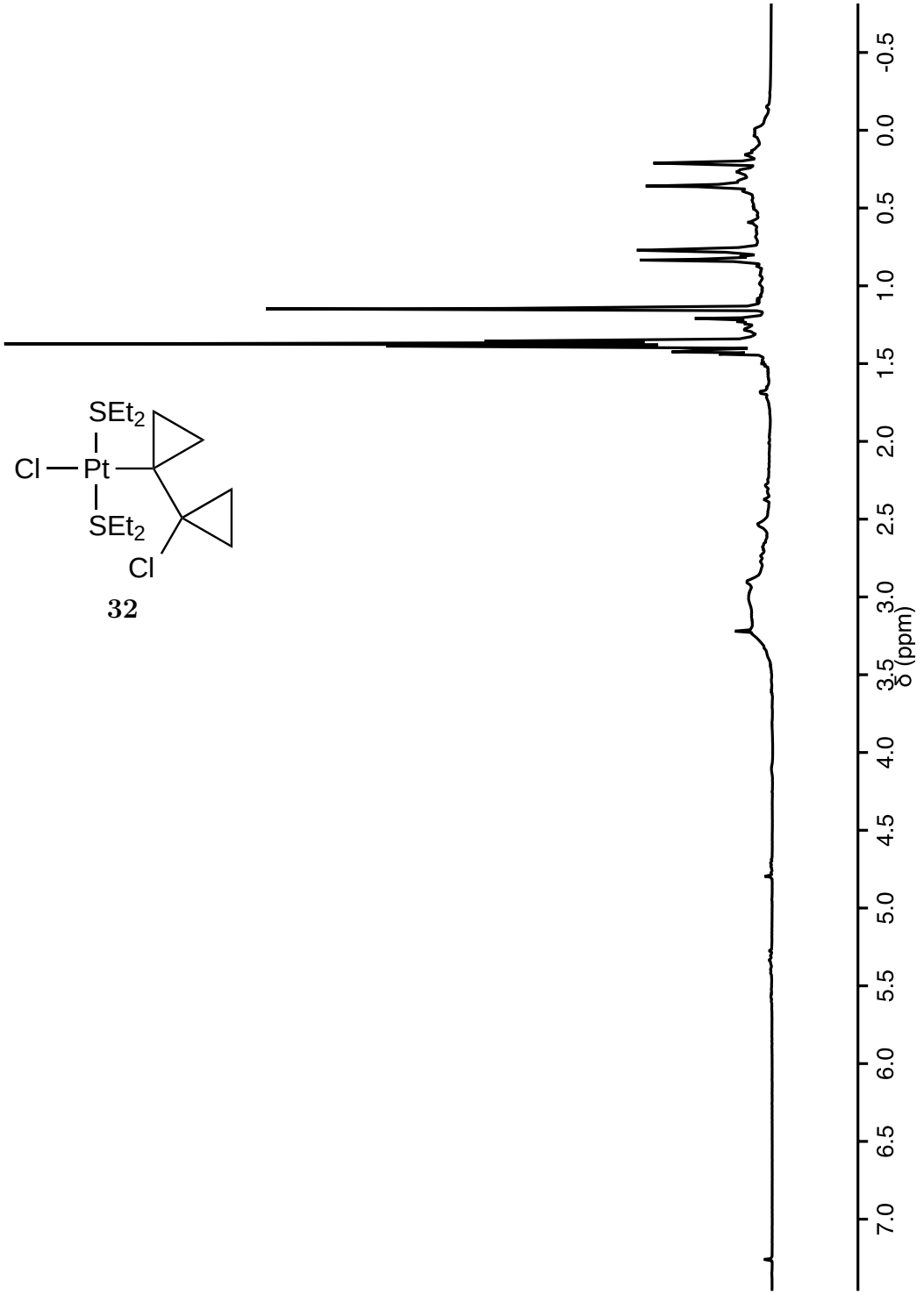

Figure A.83. ^{1}H NMR spectrum of *trans*–[Pt(C(CH$_2$)$_2$C(CH$_2$)$_2$Cl)Cl(SEt$_2$)$_2$] (**32**) (500 MHz, RT, 100 mg/mL, CDCl$_3$).

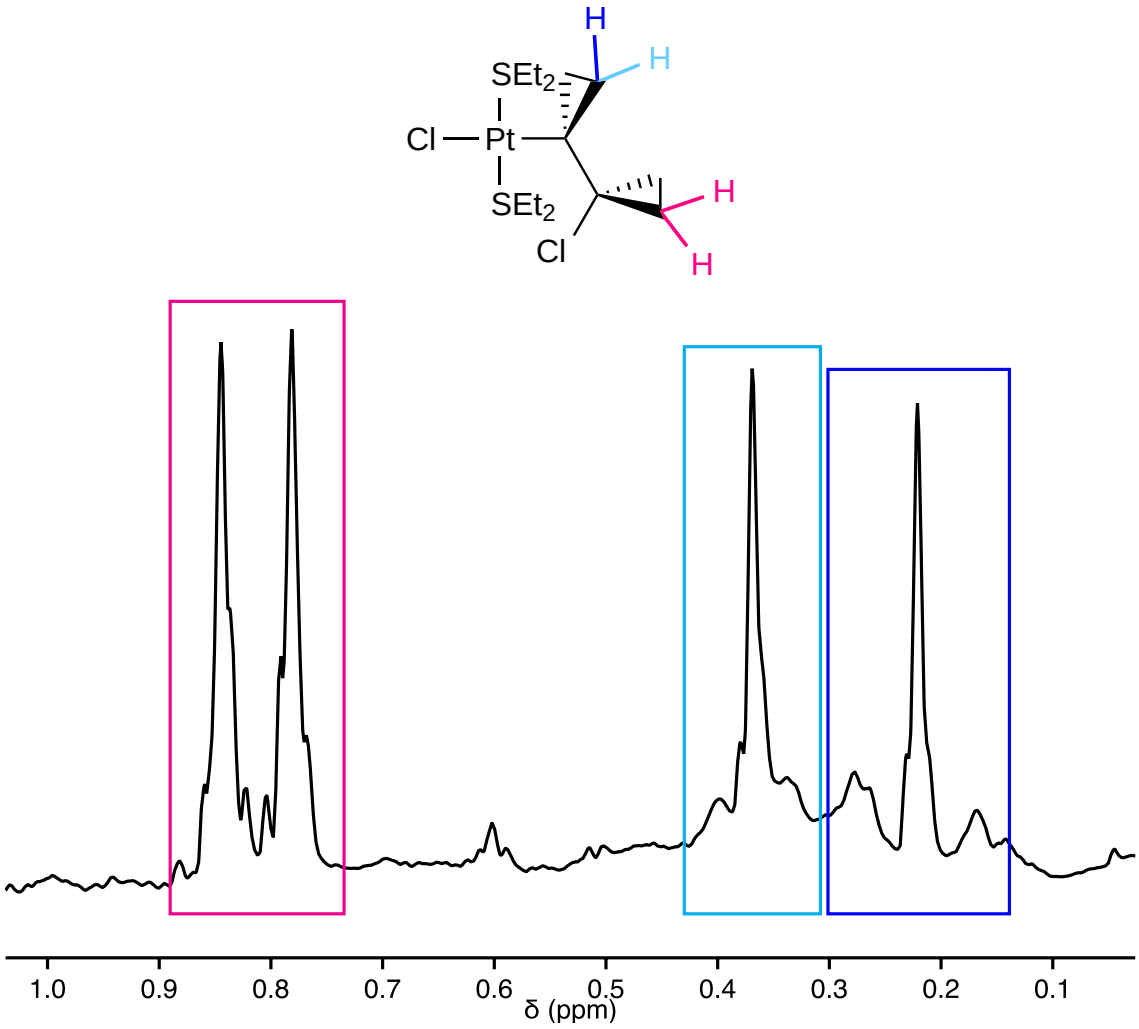

Figure A.84. Expanded ^{1}H NMR spectrum of *trans*–[Pt(C(CH$_2$)$_2$C(CH$_2$)$_2$Cl)Cl(SEt$_2$)$_2$] (**32**) (500 MHz, RT, 100 mg/mL, CDCl$_3$).

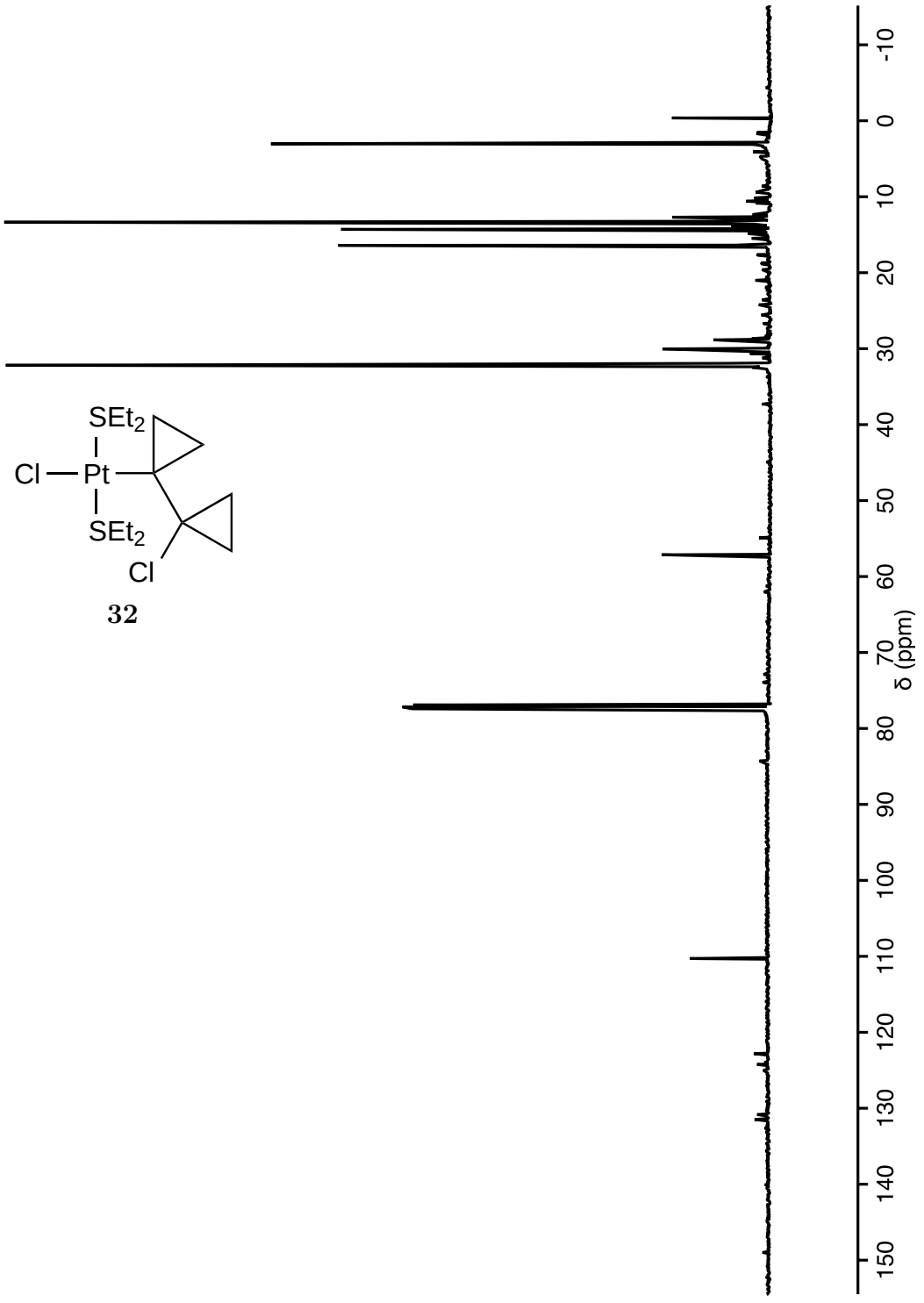

Figure A.85. $^{13}C\{^{1}H\}$ NMR spectrum of *trans*–[$Pt(C(CH_2)_2C(CH_2)_2Cl)Cl(SEt_2)_2$] (**32**) (125 MHz, RT, 100 mg/mL, $CDCl_3$).

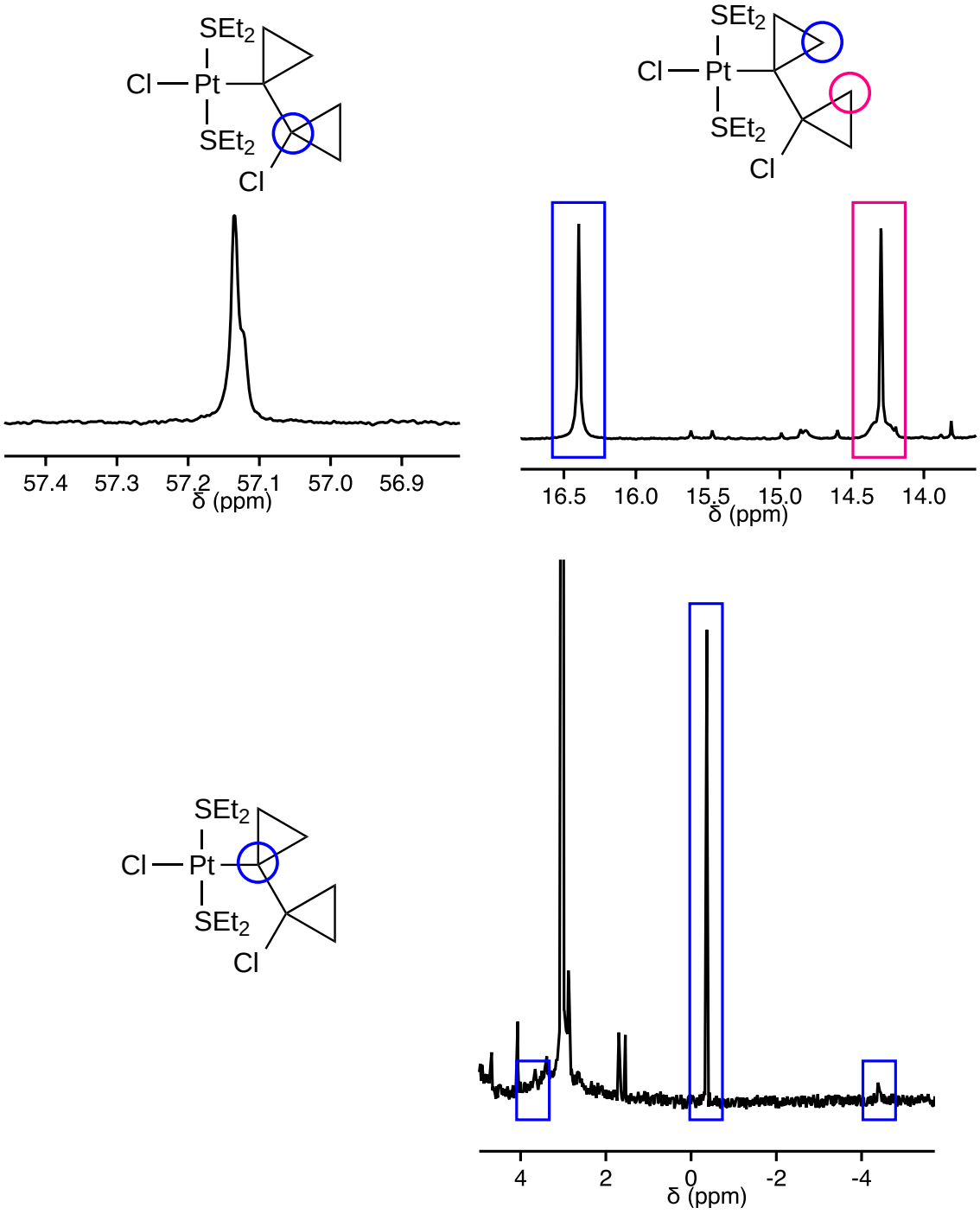

Figure A.86. Expanded $^{13}C\{^{1}H\}$ NMR spectrum of *trans*–[Pt(C(CH$_2$)$_2$C(CH$_2$)$_2$Cl)Cl(SEt$_2$)$_2$] (**32**) (125 MHz, RT, 100 mg/mL, $CDCl_3$).

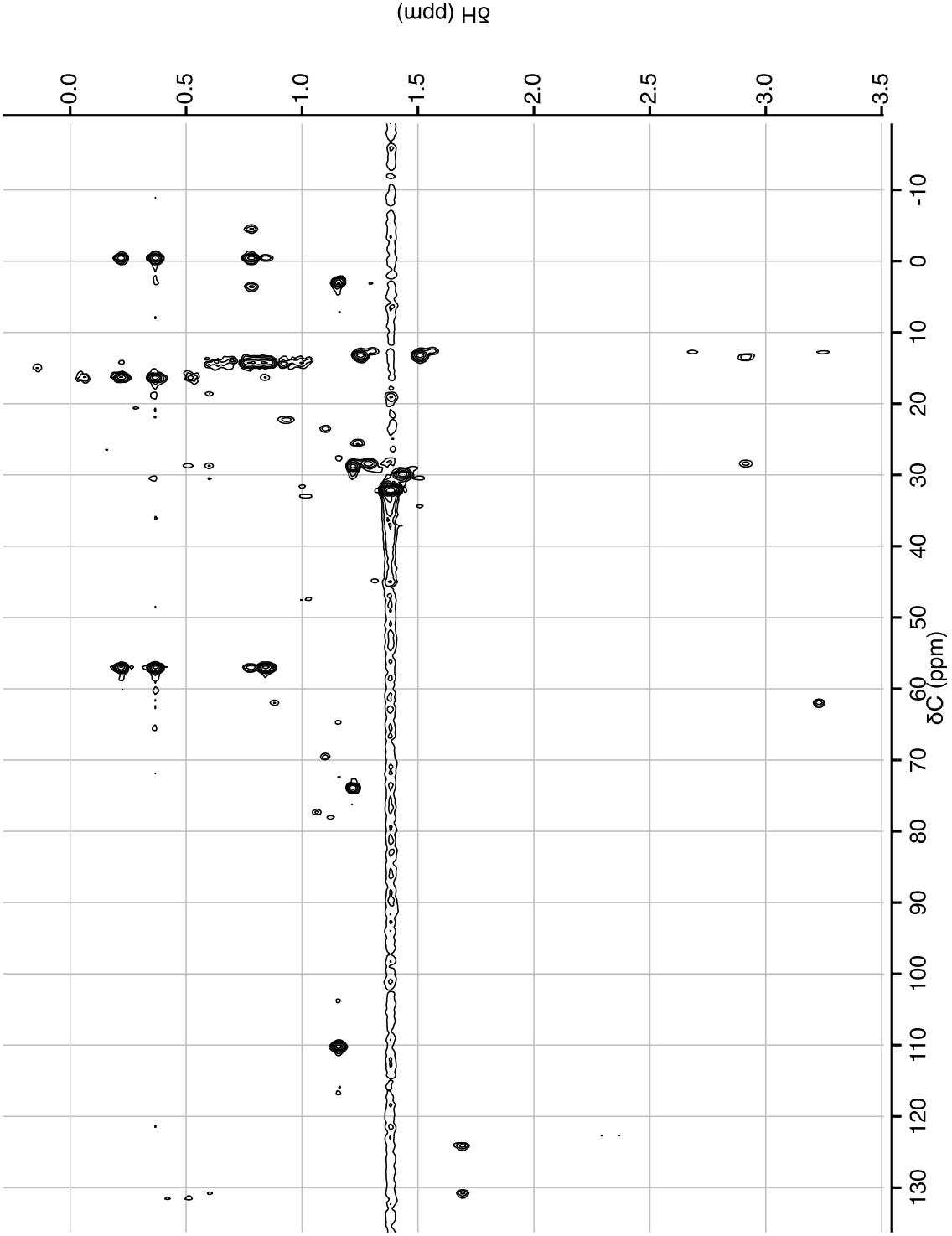

Figure A.87. HMBC spectrum of *trans*–[Pt(C$(CH_2)_2$C$(CH_2)_2$Cl)Cl$(SEt_2)_2$] (**32**) (500/125 MHz, RT, 100 mg/mL, $CDCl_3$).

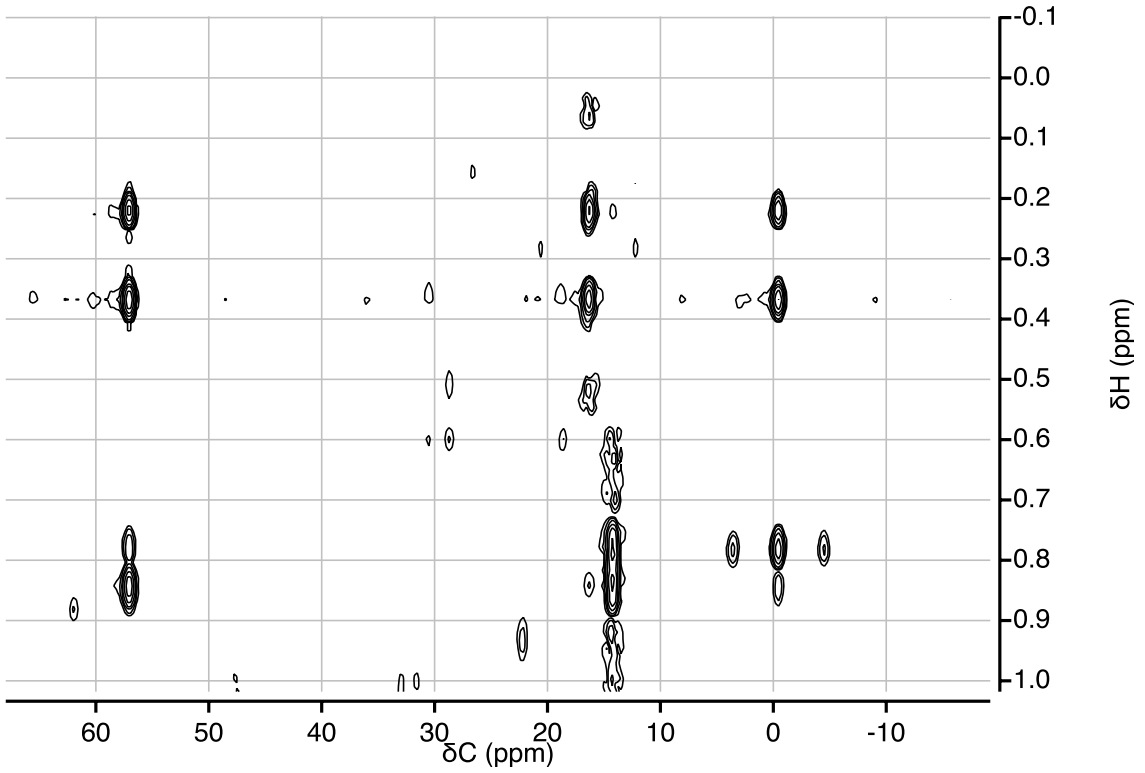

Figure A.88. Expanded HMBC spectrum of *trans*–[Pt(C(CH_2)$_2$C(CH_2)$_2$Cl)Cl(SEt_2)$_2$] (**32**) (500/125 MHz, RT, 100 mg/mL, $CDCl_3$).

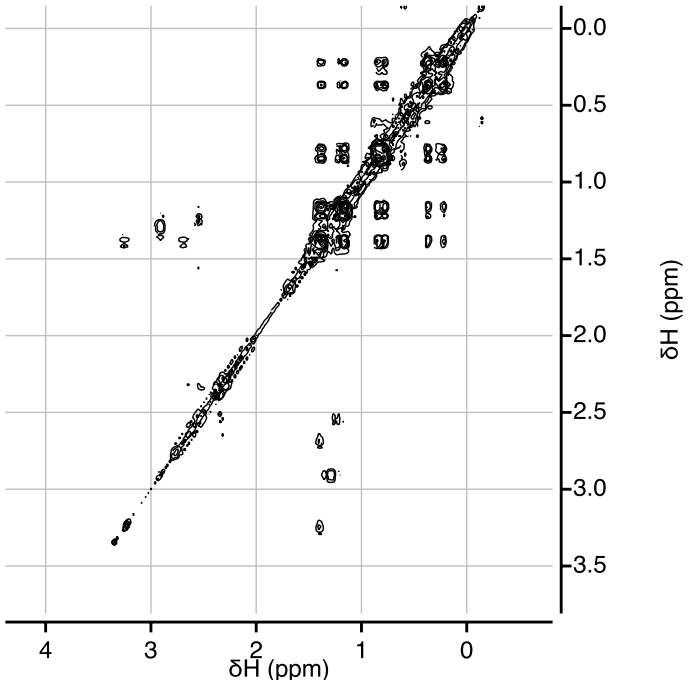

Figure A.89. COSY spectrum of *trans*–[Pt(C(CH_2)$_2$C(CH_2)$_2$Cl)Cl(SEt_2)$_2$] (**32**) (500 MHz, RT, 100 mg/mL, $CDCl_3$).

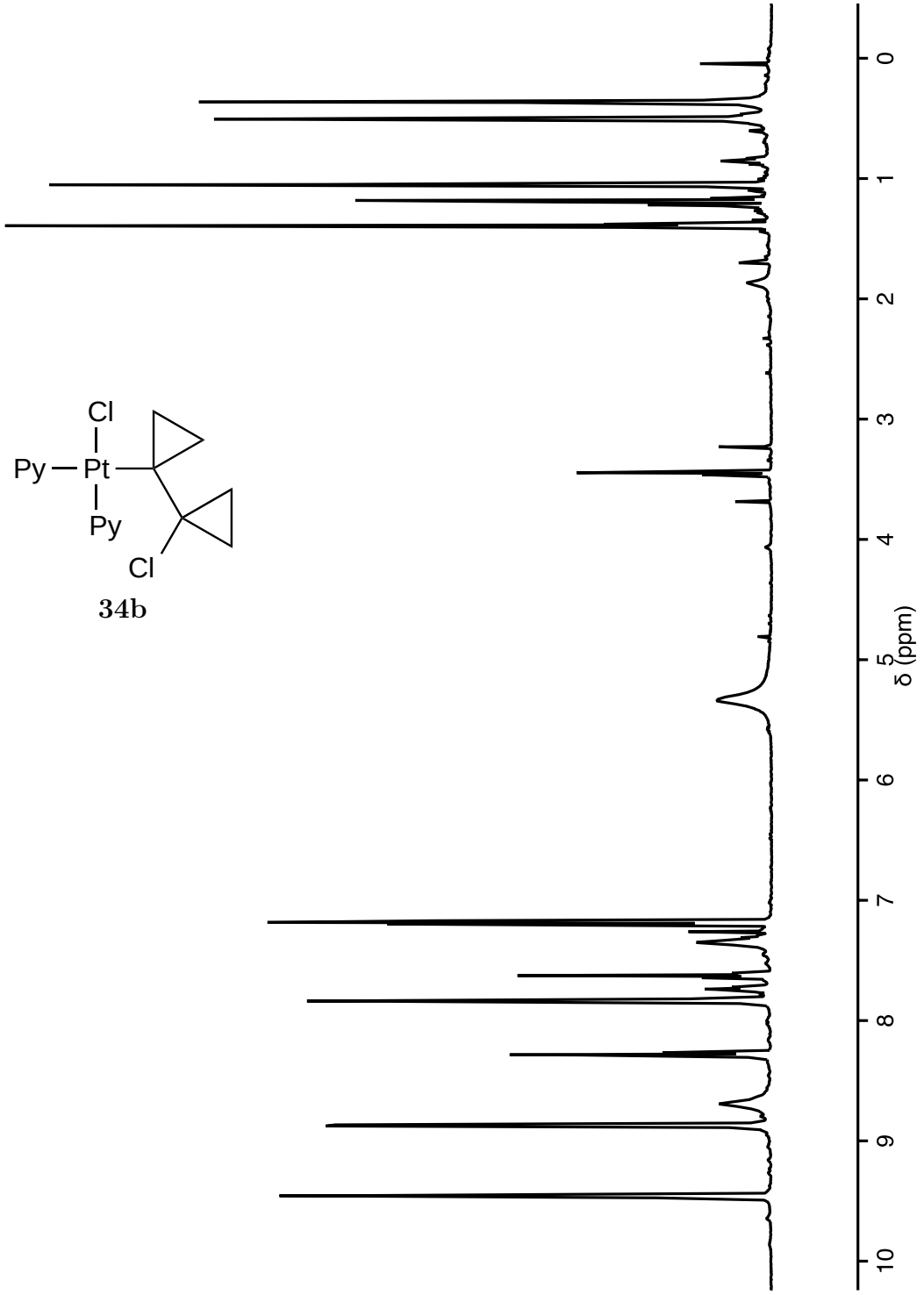

Figure A.90. ^{1}H NMR spectrum of *cis*–[Pt(C(CH$_2$)$_2$C(CH$_2$)$_2$Cl)Cl(Py)$_2$] (**34b**) (500 MHz, RT, 40 mg/mL, $CDCl_3$).

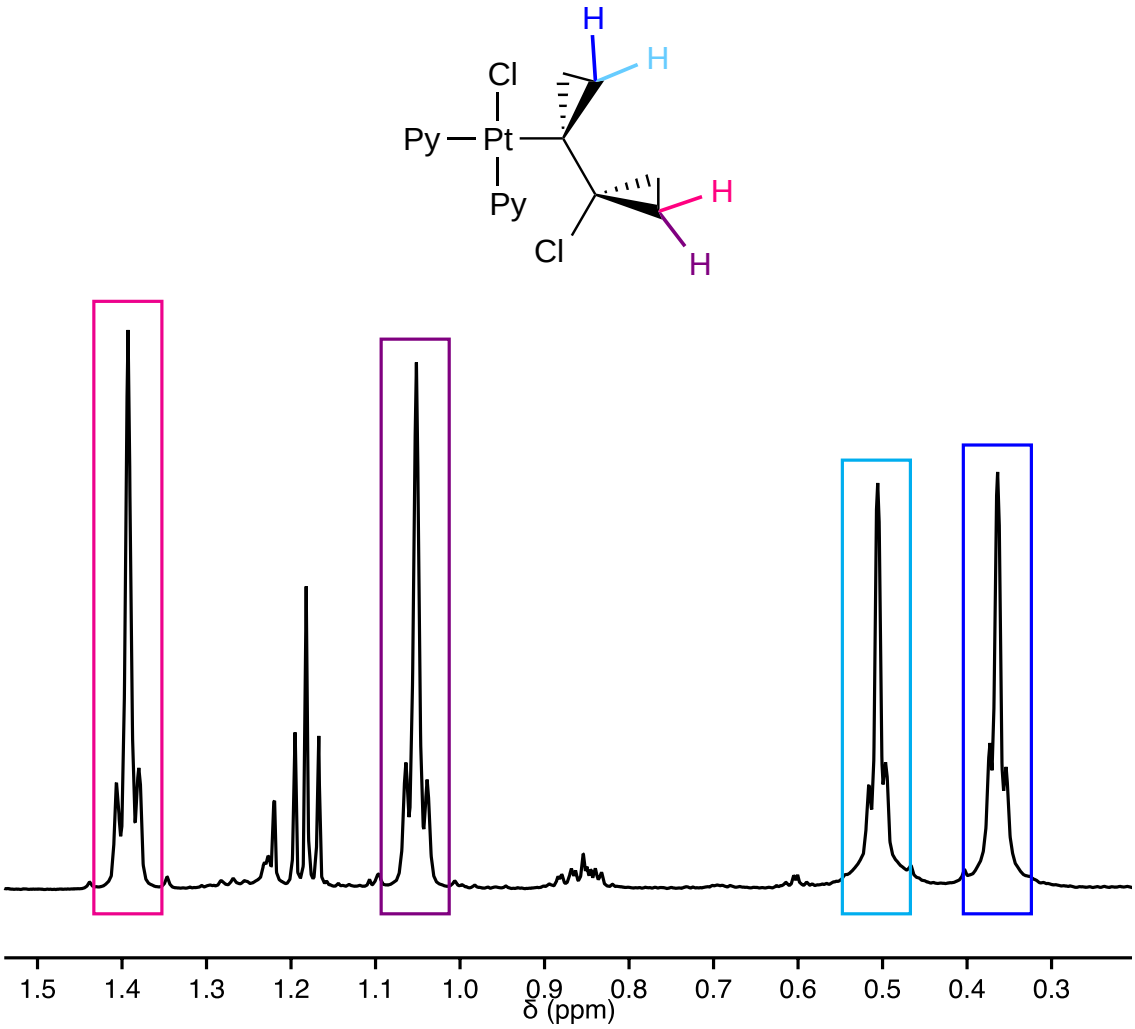

Figure A.91. Expanded ^{1}H NMR spectrum of *cis*–[Pt(C(CH$_2$)$_2$C(CH$_2$)$_2$Cl)Cl(Py)$_2$] (**34b**) (500 MHz, RT, 40 mg/mL, CDCl$_3$).

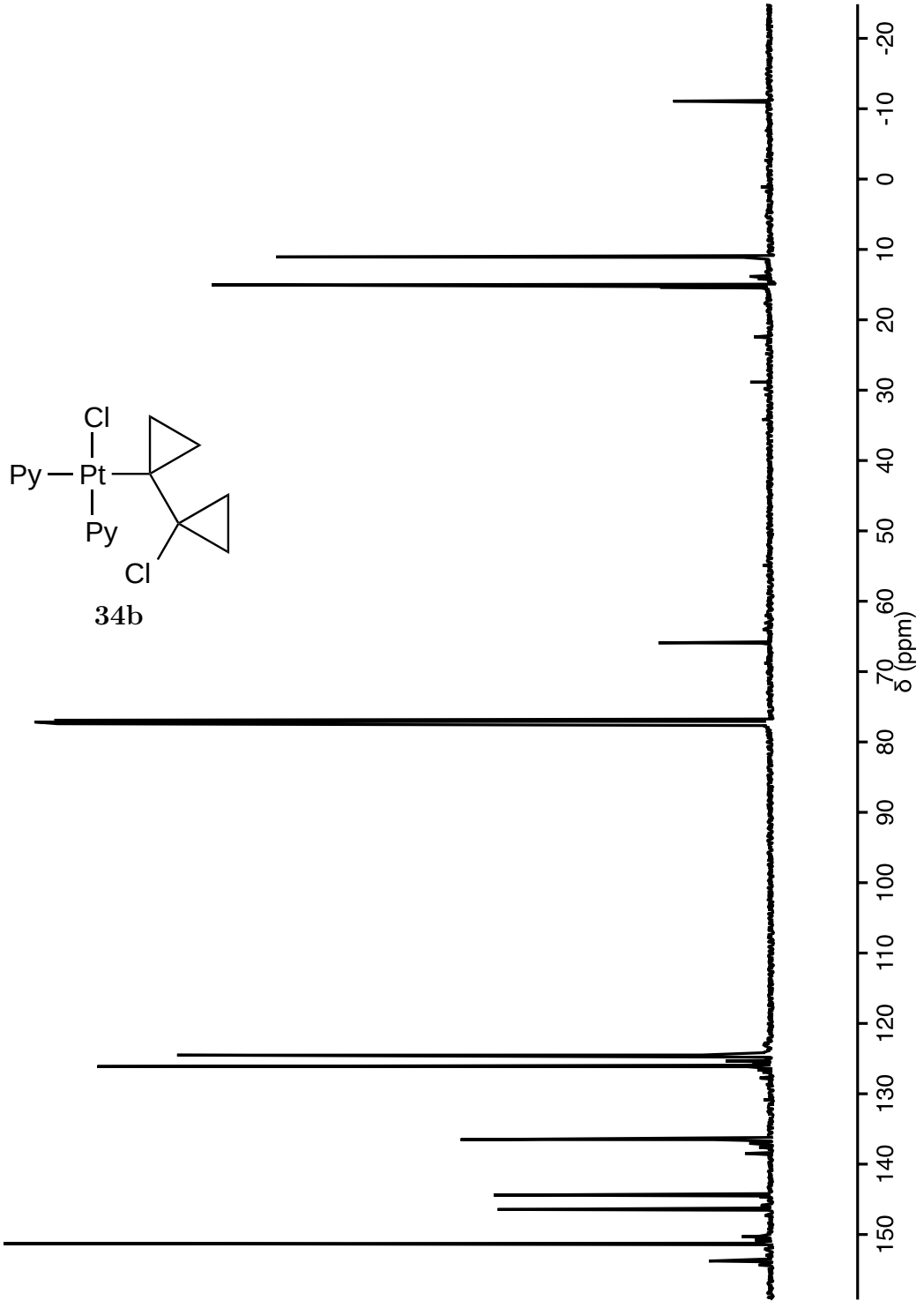

Figure A.92. $^{13}C\{^{1}H\}$ NMR spectrum of *cis*–[Pt(C(CH$_2$)$_2$C(CH$_2$)$_2$Cl)Cl(Py)$_2$] (**34b**) (125 MHz, RT, 40 mg/mL, $CDCl_3$).

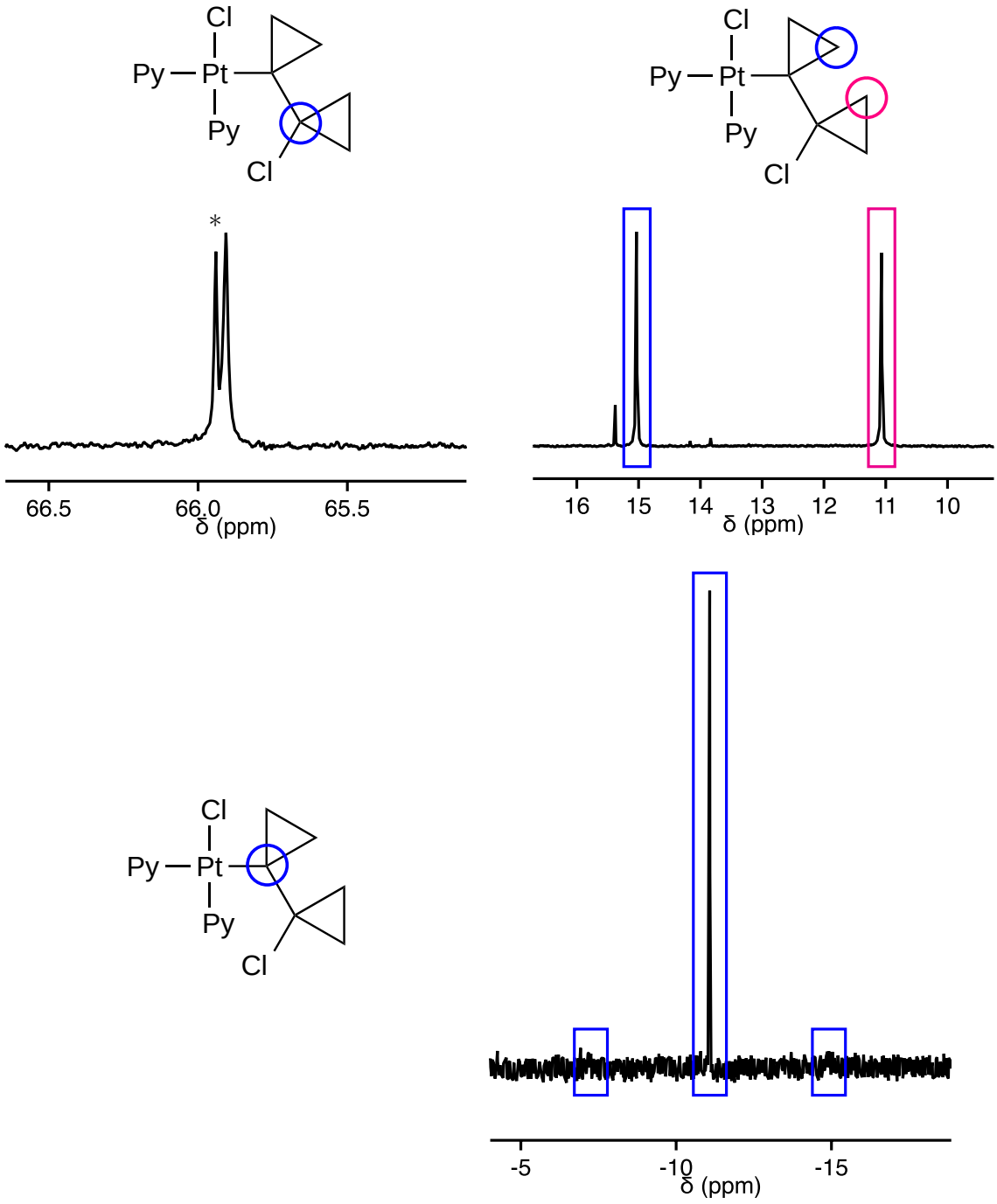

Figure A.93. Expanded $^{13}C\{^{1}H\}$ NMR spectrum of *cis*–[Pt(C(CH$_2$)$_2$C(CH$_2$)$_2$Cl)Cl(Py)$_2$] (**34b**) (125 MHz, RT, 40 mg/mL, $CDCl_3$).* signifies peaks belonging to other species.

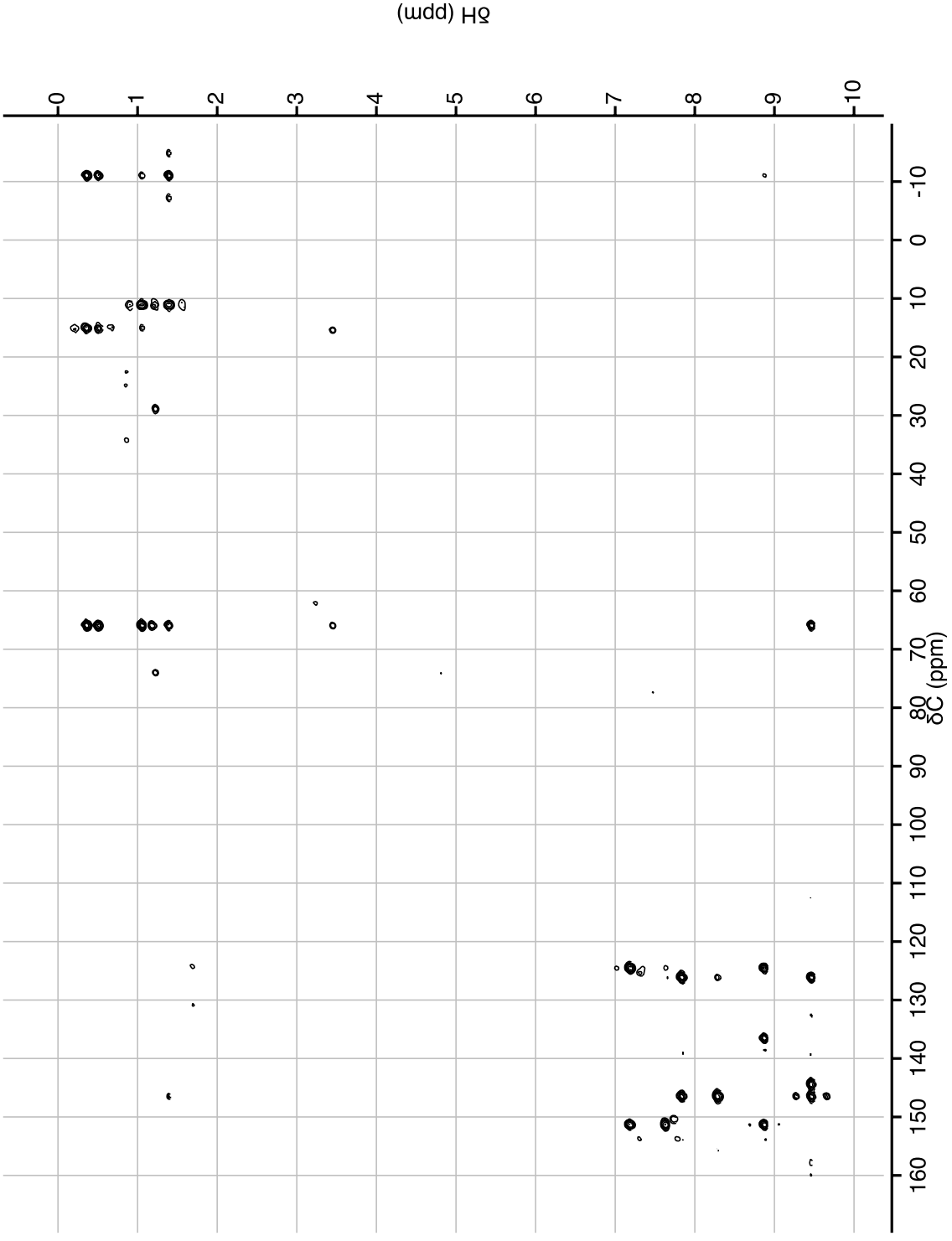

Figure A.94. HMBC spectrum of *cis*–[Pt(C(CH_2)$_2$C(CH_2)$_2$Cl)Cl(Py)$_2$] (**34b**) (500/125 MHz, RT, 40 mg/mL, $CDCl_3$).

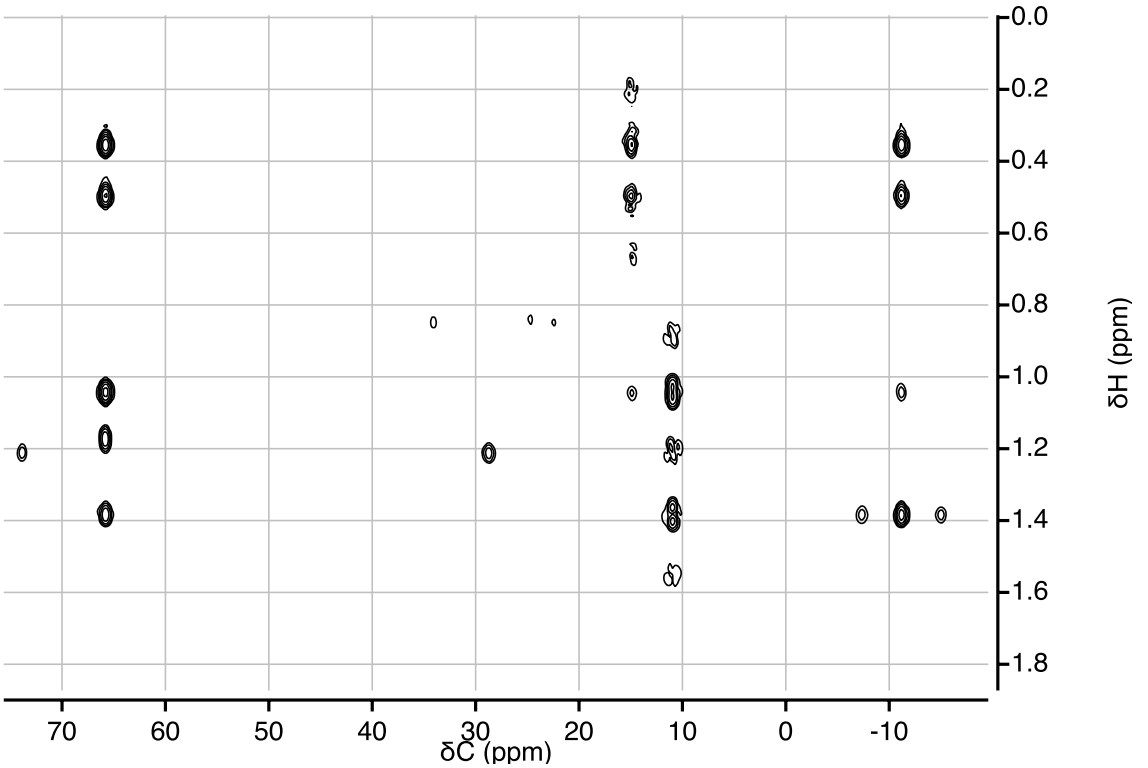

Figure A.95. Expanded HMBC spectrum of *cis*–[Pt(C$(CH_2)_2$C$(CH_2)_2$Cl)Cl$(Py)_2$] (**34b**) (500/125 MHz, RT, 40 mg/mL, $CDCl_3$).

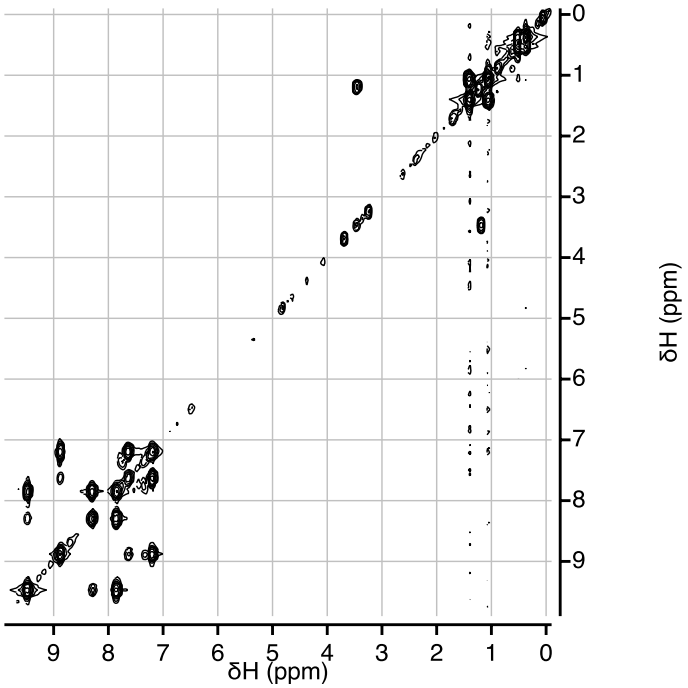

Figure A.96. COSY spectrum of *cis*–[Pt(C$(CH_2)_2$C$(CH_2)_2$Cl)Cl$(Py)_2$] (**34b**) (500 MHz, RT, 40 mg/mL, $CDCl_3$).

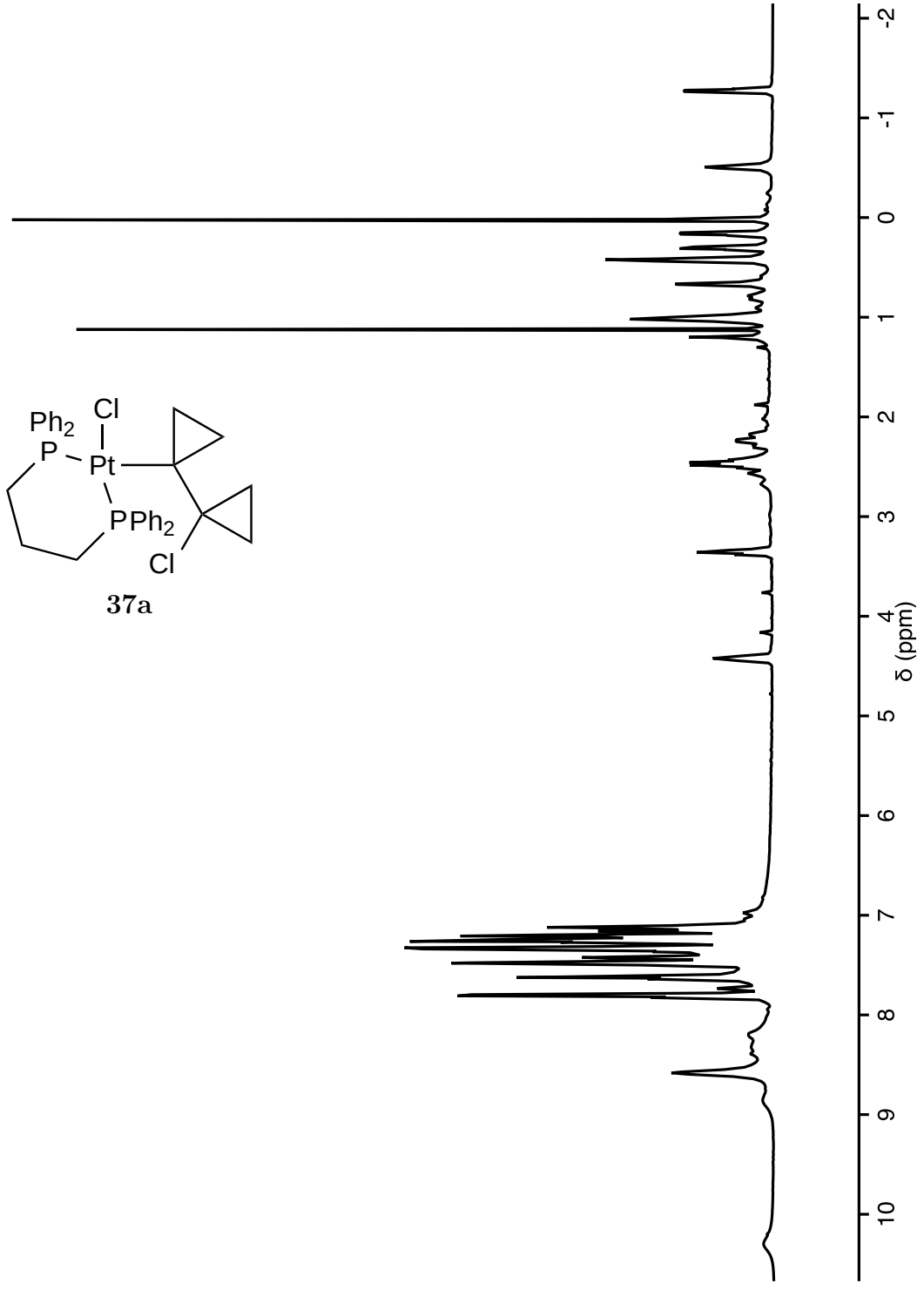

Figure A.97. ^{1}H NMR spectrum of *cis*–[Pt(C(CH$_2$)$_2$C(CH$_2$)$_2$Cl)Cl(dppp)] (**37a**) (600 MHz, RT, 40 mg/mL, CDCl$_3$).

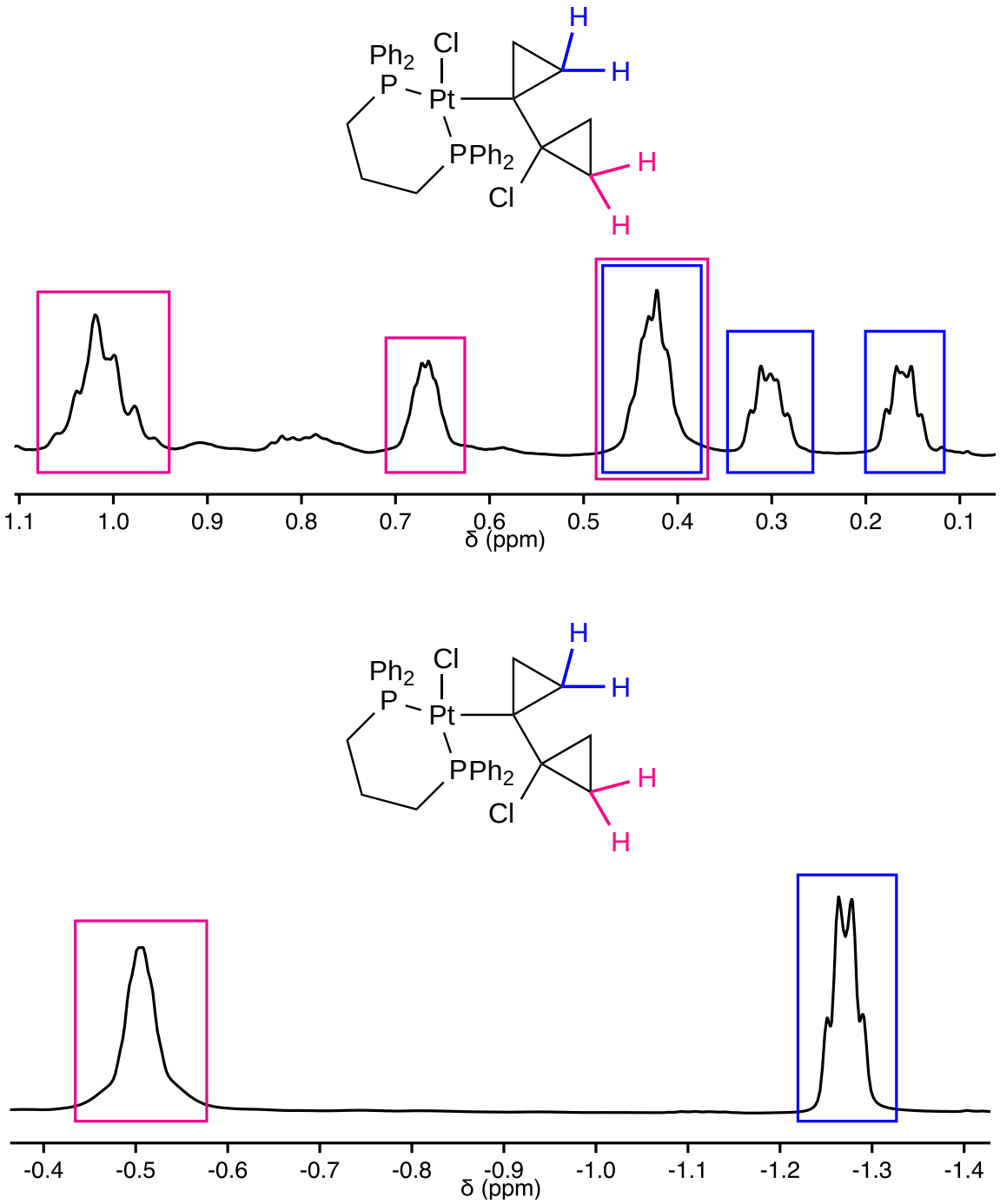

Figure A.98. Expanded ^{1}H NMR spectrum of *cis*–[Pt(C(CH$_2$)$_2$C(CH$_2$)$_2$Cl)Cl(dppp)] (**37a**) (600 MHz, RT, 40 mg/mL, CDCl$_3$).

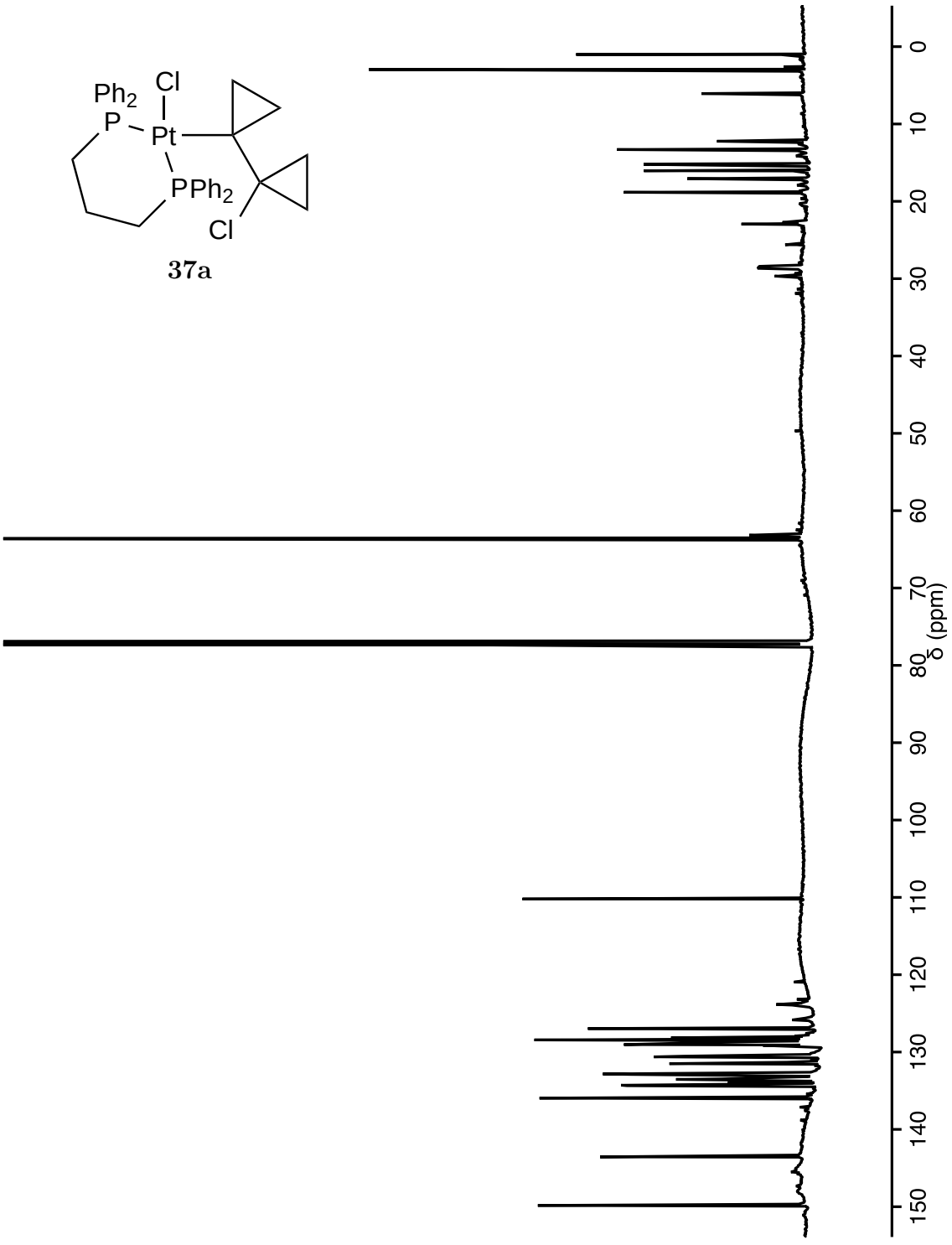

Figure A.99. $^{13}C\{^{1}H\}$ NMR spectrum of carbon-13 enriched *cis*–[Pt($C(CH_2)_2C(CH_2)_2Cl$)Cl(dppp)] (**37a**) (150 MHz, RT, 40 mg/mL, $CDCl_3$).

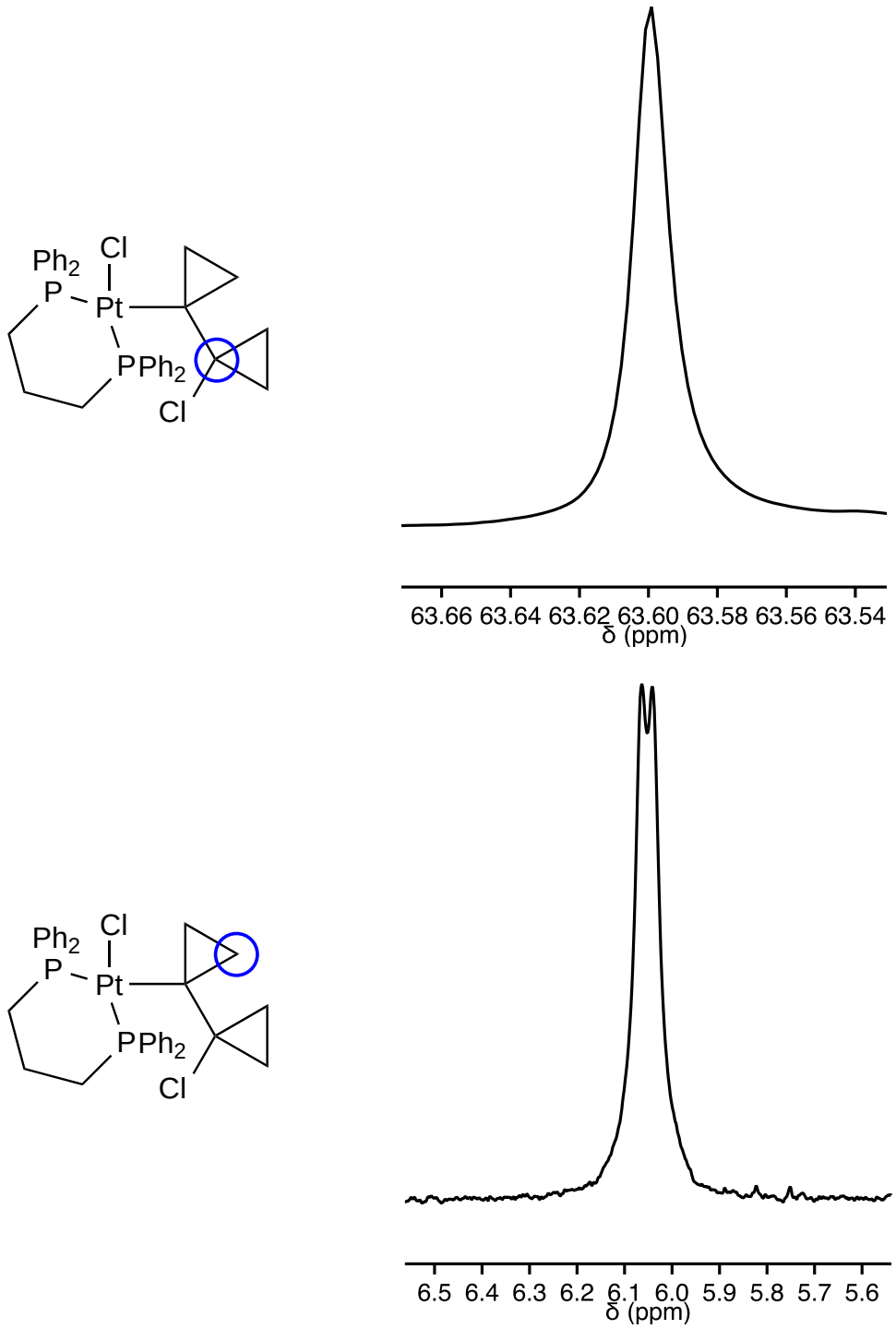

Figure A.100. Expanded $^{13}C\{^{1}H\}$ NMR spectrum of carbon-13 enriched *cis*–[Pt($C(CH_2)_2C(CH_2)_2Cl$)Cl(dppp)] (**37a**) (150 MHz, RT, 40 mg/mL, $CDCl_3$).

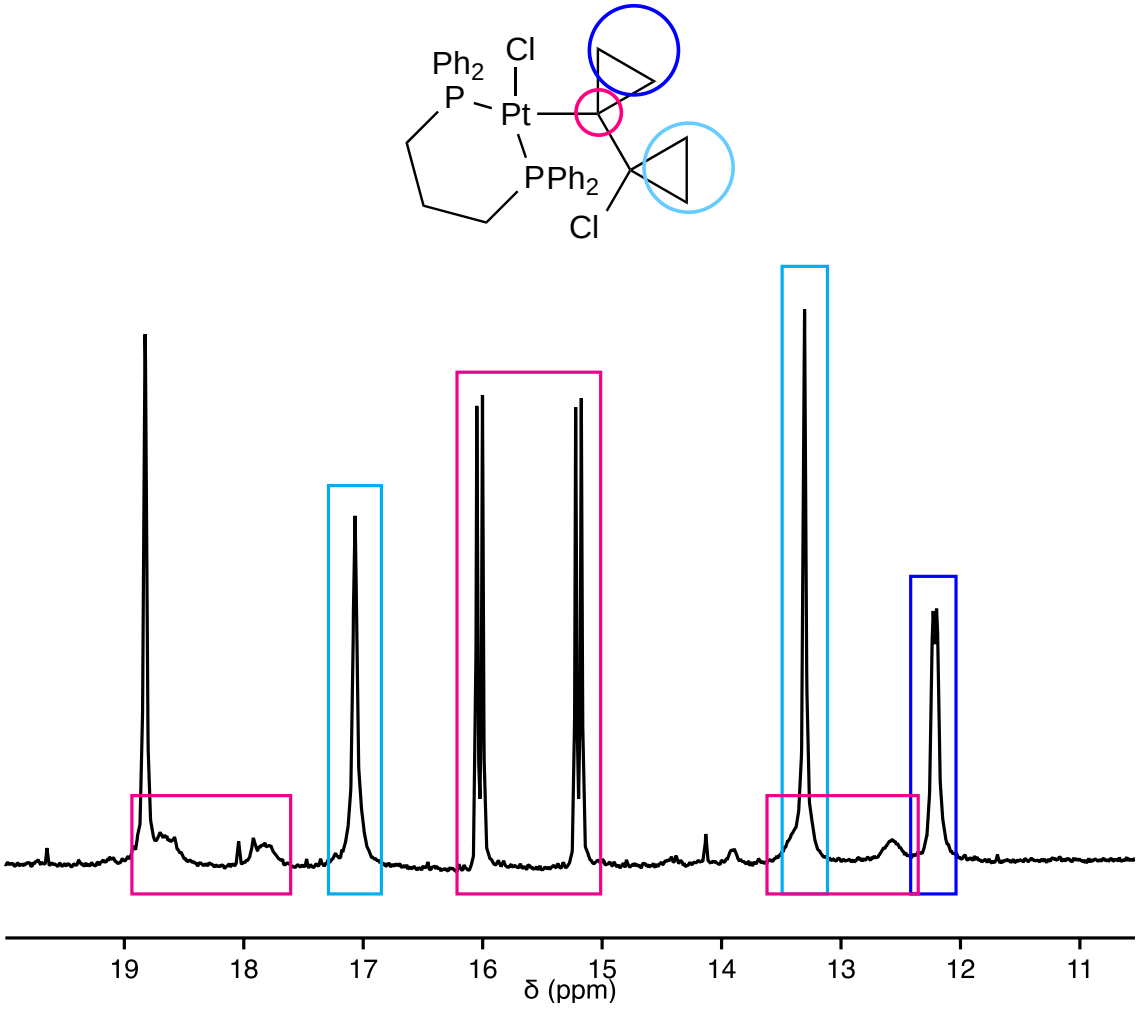

Figure A.101. Expanded $^{13}C\{^{1}H\}$ NMR spectrum of carbon-13 enriched *cis*–[Pt($C(CH_2)_2C(CH_2)_2Cl$)Cl(dppp)] (**37a**) (150 MHz, RT, 40 mg/mL, $CDCl_3$).

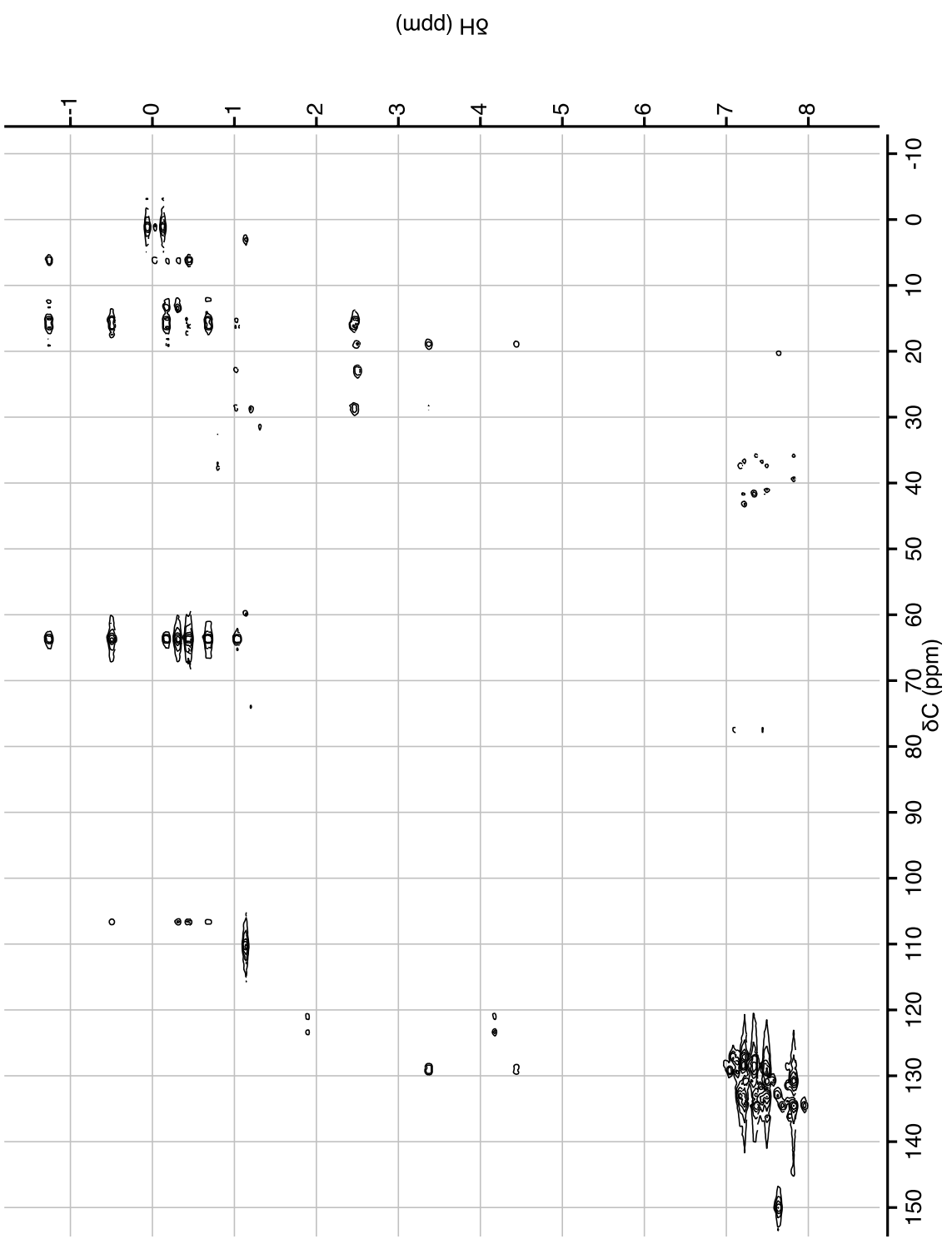

Figure A.102. HMBC spectrum of carbon-13 enriched *cis*–[Pt(C(CH_2)$_2$C(CH_2)$_2$Cl)Cl(dppp)] (**37a**) (600/150 MHz, RT, 40 mg/mL, $CDCl_3$). Some residual one bond coupling is present.

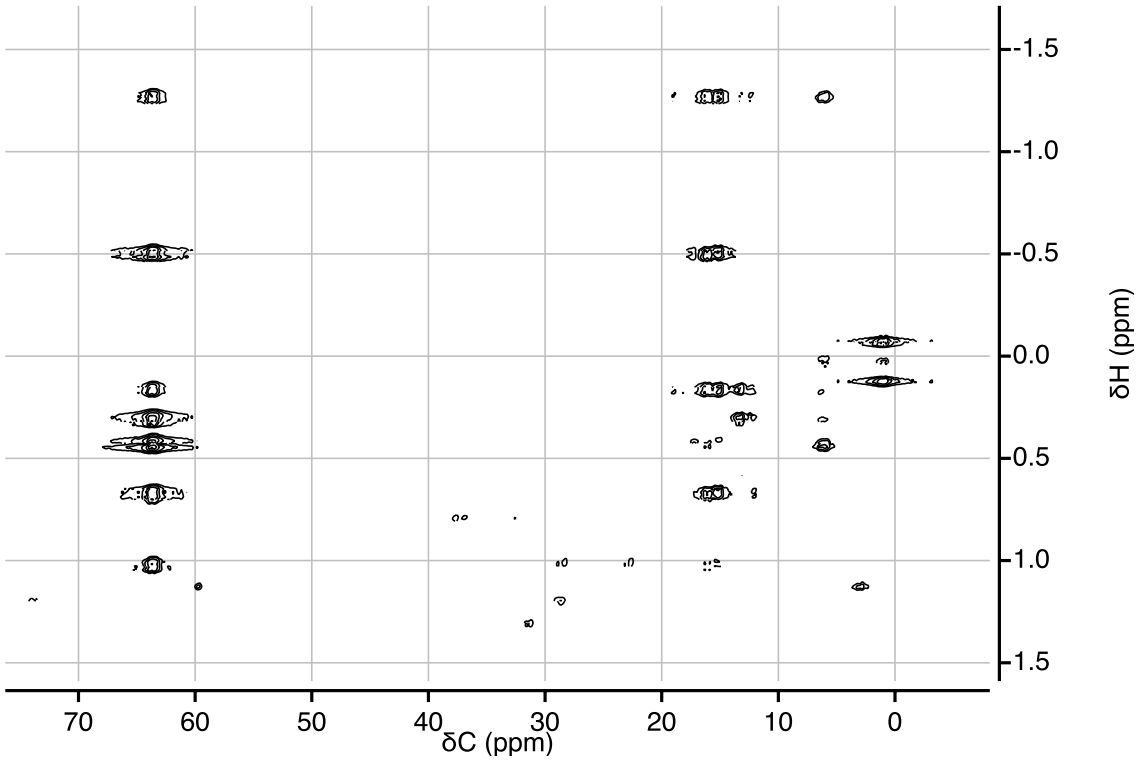

Figure A.103. Expanded HMBC spectrum of carbon-13 enriched *cis*–[Pt($C(CH_2)_2C(CH_2)_2Cl$)Cl(dppp)] (**37a**) (600/150 MHz, RT, 40 mg/mL, $CDCl_3$). Some residual one bond coupling is present.

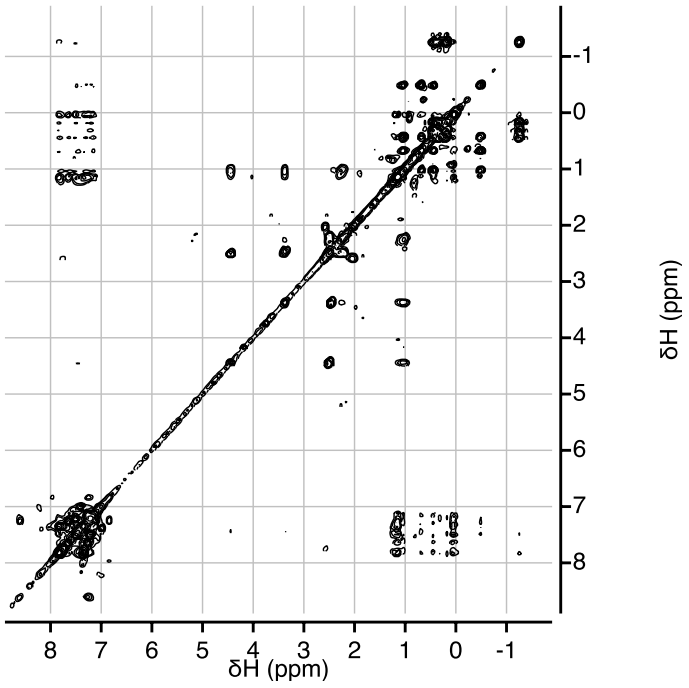

Figure A.104. COSY spectrum of carbon-13 enriched *cis*–[Pt($C(CH_2)_2C(CH_2)_2Cl$)Cl(dppp)] (**37a**) (600 MHz, RT, 40 mg/mL, $CDCl_3$).

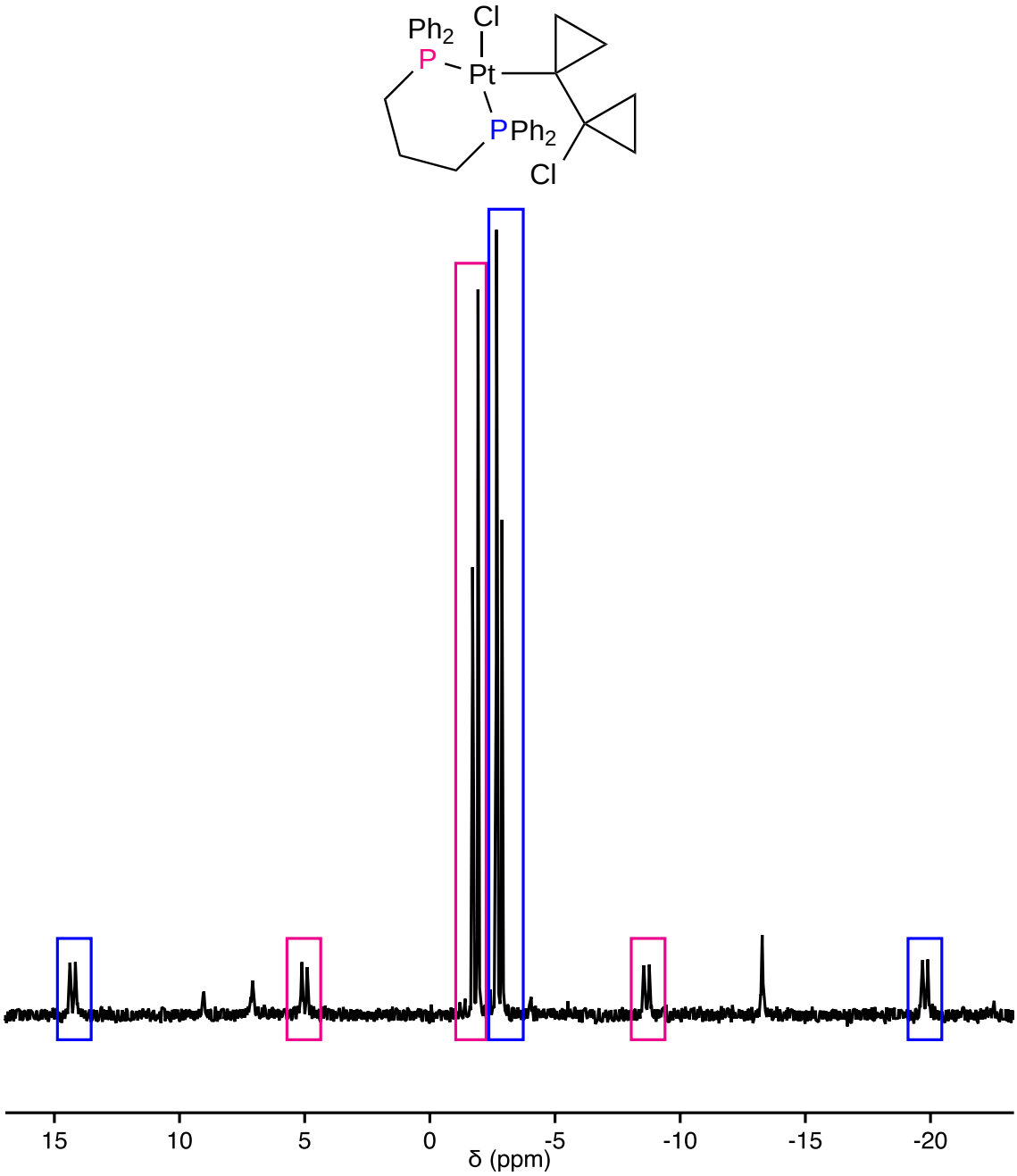

Figure A.105. $^{31}P\{^{1}H\}$ NMR spectrum of *cis*–[Pt(C$(CH_2)_2$C$(CH_2)_2$Cl)Cl(dppp)] (**37a**) (150 MHz, RT, 40 mg/mL, $CDCl_3$).

References

1. Kurosawa, H.; Ikeda, I. *J. Organomet. Chem.* **1992**, *428*, 289–301.
2. Hartley, F. R. *Chem. Rev.* **1969**, *69*, 799–844.
3. Wunderlich, J. A.; Mellor, D. P. *Acta Crystallogr.* **1953**, *7*, 130.
4. Dewar, M. J. S. *Bull. Soc. Chim. Fr.* **1951**, C71–C79.
5. Chatt, J.; Duncanson, L. A. *J. Chem. Soc.* **1953**, 2939–2947.
6. Frenking, G.; Frohlich, N. *Chem. Rev.* **2000**, *100*, 717–774.
7. Mingos, D. M. P. *J. Organomet. Chem.* **2001**, *635*, 1–8.
8. Johnson, J. B.; Rovis, T. *Angew. Chem., Int. Ed.* **2008**, *47*, 840–871.
9. Tolman, C. A. *J. Am. Chem. Soc.* **1974**, *96*, 2780–2789.
10. Fürstner, A.; Davies, P. W. *Angew. Chem., Int. Ed.* **2007**, *46*, 3410–3449.
11. Casey, C. P.; Lee, T.-Y.; Tunge, J. A.; Carpenetti, D. W. *J. Am. Chem. Soc.* **2001**, *123*, 10762–10763.
12. Casey, C. P.; Tunge, J. A.; Lee, T.-Y.; Fagan, M. A. *J. Am. Chem. Soc.* **2003**, *125*, 2641–2651.
13. Stoebenau, E. J.; Jordan, R. F. *J. Am. Chem. Soc.* **2006**, *128*, 8162–8175.
14. Joy, J. R.; Orchin, M. *J. Am. Chem. Soc.* **1959**, *81*, 310–311.
15. Tolman, C. A. *Organometallics* **1983**, *2*, 614–621.
16. Green, M.; Howard, J. A. K.; Spencer, J. L.; Stone, F. G. A. *J. Chem. Soc., Dalton Trans.* **1977**, 271–277.
17. Denning, R. G.; Venanzi, L. M. *J. Chem. Soc.* **1963**, 3241–3247.
18. Garcia, L. M.; Shupack, S. I.; Orchin, M. *Inorg. Chem.* **1962**, *1*, 893–896.
19. Chatt, J.; Shaw, B. L.; Williams, A. A. *J. Chem. Soc.* **1962**, 3269–3270.
20. Spencer, J. L. *Inorg. Synth.* **1979**, *19*, 213–218.
21. Fitton, P.; McKeon, J. E. *Chem. Commun.* **1968**, 4–6.
22. Otto, S.; Roodt, A.; Elding, L. I. *Inorg. Chem. Commun.* **2006**, *9*, 764–766.

23. Scherer, W.; Eickerling, G.; Shorokhov, D.; Gullo, E.; McGrady, G. S.; Sirsch, P. *New J. Chem.* **2006**, *30*, 309–312.

24. Howard, J. A. K. *Acta Crystallogr., Sect. B* **1982**, *B38*, 2896–2898.

25. Galano, A.; Alvarez-Idaboy, J. R.; Vivier-Bunge, A. *Theor. Chem. Acc.* **2007**, *118*, 597–606.

26. Gragson, J. T.; Greenlee, K. W.; Derfer, J. M.; Boord, C. E. *J. Am. Chem. Soc.* **1953**, *75*, 3344–3347.

27. Köster, R.; Arora, S.; Binger, P. *Angew. Chem., Int. Ed. Engl.* **1969**, *8*, 205–206.

28. Salaun, J.; Champion, J.; Conia, J. M. *Org. Synth.* **1977**, *57*, 36–40.

29. Laurie, V. W.; Stigliani, W. M. *J. Am. Chem. Soc.* **1970**, *92*, 1485–1488.

30. de Boer, J. S. A. M.; Stam, C. H. *Recl. Trav. Chim. Pays-Bas* **1993**, *112*, 635–638.

31. Skancke, A.; Boggs, J. E. *J. Mol. Struct.* **1978**, *50*, 173–182.

32. Traetteberg, M.; Simon, A.; Peters, E.-M.; De Meijere, A. *J. Mol. Struct.* **1984**, *118*, 333–343.

33. Bieri, G.; Burger, F.; Heilbronner, E.; Maier, J. P. *Helv. Chim. Acta* **1977**, *60*, 2213–2233.

34. Bertie, J. E.; Norton, M. G. *Can. J. Chem.* **1970**, *48*, 3889–3902.

35. Aihara, J. *Bull. Chem. Soc. Jpn.* **1980**, *53*, 3404–3407.

36. Rol, N. C.; Clague, A. D. H. *Org. Magn. Res.* **1981**, *16*, 187–194.

37. de Meijere, A.; Kozhushkov, S. *Eur. J. Org. Chem.* **2000**, 3809–3822.

38. Nakamura, I.; Yamamoto, Y. *Adv. Synth. Catal.* **2002**, *344*, 111–129.

39. Noyori, R.; Odagi, T.; Takaya, H. *J. Am. Chem. Soc.* **1970**, *92*, 5780–5781.

40. Trost, B. M. *Angew. Chem., Int. Ed. Engl.* **1986**, *25*, 1–20.

41. Suzuki, T.; Fujimoto, H. *Inorg. Chem.* **2000**, *39*, 1113–1119.

42. Yamago, S.; Nakamura, E. *J. Chem. Soc., Chem. Commun.* **1988**, 1112–1113.

43. Lautens, M.; Ren, Y.; Delanghe, P. H. M. *J. Am. Chem. Soc.* **1994**, *116*, 8821–8822.

44. Bräse, S.; de Meijere, A. *Angew. Chem., Int. Ed. Engl.* **1995**, *34*, 2545–2547.

45. Weintz, H.-J.; Binger, P. *Tetrahedron Lett.* **1985**, *26*, 4075–4078.

46. Nakamura, I.; Oh, B. H.; Saito, S.; Yamamoto, Y. *Angew. Chem., Int. Ed.* **2001**, *40*, 1298–1300.

47. Oh, B. H.; Nakamura, I.; Saito, S.; Yamamoto, Y. *Tetrahedron Lett.* **2001**, *42*, 6203–6205.

48. Fournet, G.; Balme, G.; Gore, J. *Tetrahedron* **1988**, *44*, 5809–5820.

49. Fournet, G.; Balmea, G.; Barieux, J. J.; Gore, J. *Tetrahedron* **1988**, *44*, 5821–5832.

50. Lautens, M.; Meyer, C.; Lorenz, A. *J. Am. Chem. Soc.* **1996**, *118*, 10676–10677.

51. Chatani, N.; Takeyasu, T.; Hanafusa, T. *Tetrahedron Lett.* **1988**, *29*, 3979–3982.

52. Ishiyama, T.; Momota, S.; Miyaura, N. *Synlett* **1999**, 1790–1792.

53. Suginome, M.; Matsuda, T.; Ito, Y. *J. Am. Chem. Soc.* **2000**, *122*, 11015–11016.

54. Barnes, S. G. *J. Chem. Soc., Chem. Commun.* **1980**, 267–268.

55. Noyori, R.; Yamakawa, M.; Takaya, H. *Tetrahedron Lett.* **1978**, *19*, 4823–4826.

56. Trost, B. M.; Chan, D. M. T. *J. Am. Chem. Soc.* **1980**, *102*, 6359–6361.

57. Fischer, H.; Bidell, W.; Hofmann, J. *J. Chem. Soc., Chem. Commun.* **1990**, 858–859.

58. Foerstner, J.; Kozhushkov, S.; Binger, P.; Wedemann, P.; Noltemeyer, M.; de Meijere, A.; Butenschön, H. *Chem. Commun.* **1998**, 239–240.

59. Kozhushkov, S. I.; Foerstner, J.; Kakoschke, A.; Stellfeldt, D.; Yong, L.; Wartchow, R.; de Meijere, A.; Butenschön, H. *Chem. Eur. J.* **2006**, *12*, 5642–5647.

60. Isaeva, L. S.; Peganova, T. A.; Petrovskii, P. V.; Furman, D. B.; Zotova, S. V.; Kudryashev, A. V.; Bragin, O. V. *J. Organomet. Chem.* **1983**, *258*, 367–372.

61. Green, M.; Howard, J. A. K.; Hughes, R. P.; Kellett, S. C.; Woodward, P. *J. Chem. Soc., Dalton Trans.* **1975**, 2007–2014.

62. Kashiwagi, T.; Yasuoka, N.; Kasai, N.; Kukudo, M. *J. Chem. Soc. D* **1969**, 317–318.

63. Molander, G. A. *Pure Appl. Chem.* **2000**, *72*, 1745–1756.

64. Le Perchec, P.; Conia, J. M. *Tetrahedron Lett.* **1970**, *11*, 1587–1588.

65. de Meijere, A. *Chem. Ber.* **1974**, *107*, 1702–1713.

66. de Meijere, A.; Kozhushkov, S. I.; Spaeth, T.; Zefirov, N. S. *J. Org. Chem.* **1993**, *58*, 502–505.

67. de Meijere, A.; Kozhushkov, S.; Spaeth, T. *Org. Synth.* **2002**, *78*, 142–151.

68. Gleiter, R.; Haider, R.; Conia, J.-M.; Barnier, J.-P.; De Meijere, A.; Weber, W. *J. Chem. Soc., Chem. Commun.* **1979**, 130–132.

69. Brammer, C. N.; Nelson, D. J.; Li, R. *Tetrahedron Lett.* **2007**, *48*, 3237–3241.

70. de Meijere, A. *Angew. Chem., Int. Ed. Engl.* **1979**, *18*, 809–826.

71. de Meijere, A.; Erden, I.; Weber, W.; Kaufmann, D. *J. Org. Chem.* **1988**, *53*, 152–161.

72. Binger, P.; Kozhushkov, S. I.; Wedemann, P.; de Meijere, A. *Eur. J. Org. Chem.* **1998**, 113–119.

73. Oishi, Y.; Sakamoto, E.; Fujimoto, H. *Inorg. Chem.* **1996**, *35*, 231–238.

74. Nüske, H.; Bräse, S.; Kozhushkov, S. I.; Noltemeyer, M.; Es-Sayed, M.; de Meijere, A. *Chem. Eur. J.* **2002**, *8*, 2350–2369.

75. Kaufmann, D.; de Meijere, A. *Tetrahedron Lett.* **1979**, *20*, 779–782.

76. de Meijere, A.; Nüske, H.; Es-Sayed, M.; Labahn, T.; Schroen, M.; Bräse, S. *Angew. Chem., Int. Ed.* **1999**, *38*, 3669–3672.

77. Pohlmann, T.; de Meijere, A. *Org. Lett.* **2000**, *2*, 3877–3879.

78. Butenschön, H.; Kettenbach, R. T.; Krüger, C. *Angew. Chem., Int. Ed. Engl.* **1992**, *31*, 1066–1068.

79. Hoyte, S. A.; Spencer, J. L. *Organometallics* **2011**, *30*, 5415–5423.

80. Blue, E. D.; Davis, A.; Conner, D.; Gunnoe, T. B.; Boyle, P. D.; White, P. S. *Journal of the American Chemical Society* **2003**, *125*, 9435–9441.

81. Fanjul, T.; Eastham, G.; Floure, J.; Forrest, S. J. K.; Haddow, M. F.; Hamilton, A.; Pringle, P. G.; Orpen, A. G.; Waugh, M. *Dalton Trans.* **2012**, *42*, 100.

82. Tolman, C. A. *Chem. Rev.* **1977**, *77*, 313–348.

83. Carr, N.; Mole, L.; Orpen, A. G.; Spencer, J. L. *J. Chem. Soc., Dalton Trans.* **1992**, 2653–2662.

84. Carmichael, D.; Hitchcock, B.; Nixon, J. F.; Pidcock, A. *J. Chem. Soc., Chem. Commun.* **1988**, 1554–1556.

85. Tulip, T. H.; Yamagata, T.; Yoshida, T.; Wilson, R. D.; Ibers, J. A.; Otsuka, S. *Inorg. Chem.* **1979**, *18*, 2239–2250.

86. Head, R. A. *Inorg. Synth.* **1990**, *28*, 132–135.

87. Rao, C. G. *Org. Prep. Proced. Int.* **1980**, *12*, 225–228.

88. Renk, E.; Shafer, P. R.; Graham, W. H.; Mazur, R. H.; Roberts, J. D. *J. Am. Chem. Soc.* **1961**, *83*, 1987–1989.

89. Eraker, J.; Roemming, C. *Acta Chem. Scand.* **1967**, *21*, 2721–2726.

90. Asker, K. A.; Hitchcock, P. B.; Moulding, R. P.; Seddon, K. R. *Inorg. Chem.* **1990**, *29*, 4146–4148.

91. Saito, S.; Tando, K.; Kabuto, C.; Yamamoto, Y. *Organometallics* **2000**, *19*, 3740–3743.

92. Zhang, K.; Hu, J.; Chan, K. C.; Wong, K. Y.; Yip, H. K. J. *Eur. J. Inorg. Chem.* **2007**, *2007*, 384–393.

93. Appleton, T. G.; Clark, H. C.; Manzer, L. E. *Coord. Chem. Rev.* **1973**, *10*, 335–422.

94. Godleski, S. A.; Gundlach, K. B.; Valpey, R. S. *Organometallics* **1985**, *4*, 296–302.

95. Nicolaides, A.; Smith, J. M.; Kumar, A.; Barnhart, D. M.; Borden, W. T. *Organometallics* **1995**, *14*, 3475–3485.

96. Uddin, J.; Dapprich, S.; Frenking, G.; Yates, B. F. *Organometallics* **1999**, *18*, 457–465.

97. Yates, B. F. *J. Organomet. Chem.* **2001**, *635*, 142–152.

98. Hersh, W. H. *J. Chem. Educ.* **1997**, *74*, 1485–1489.

99. Ault, A. *J. Chem. Educ.* **1970**, *47*, 812–818.

100. Yasuda, H.; Nakamura, A. *Angew. Chem., Int. Ed. Engl.* **1987**, *26*, 723–742.

101. Erker, G.; Krueger, C.; Mueller, G. In *Adv. Organomet. Chem.*; Elsevier, 1985; Vol. 24, pp 1–39.

102. Mashima, K.; Kaidzu, M.; Nakayama, Y.; Nakamura, A. *Organometallics* **1997**, *16*, 1345–1348.

103. Murakami, M.; Itami, K.; Ito, Y. *Organometallics* **1999**, *18*, 1326–1336.

104. Hitchcock, P. B.; Mason, R. *Chem. Commun.* **1967**, 242–243.

105. Hunt, R. L.; Roundhill, D. M.; Wilkinson, G. *J. Chem. Soc. A* **1967**, 982–984.

106. Wakatsuki, Y.; Aoki, K.; Yamazaki, H. *J. Chem. Soc., Dalton Trans.* **1986**, 1193–1199.

107. Gausing, W.; Wilke, G. *Angew. Chem., Int. Ed. Engl.* **1981**, *20*, 186–187.

108. Roundhill, D. M.; Lawson, D. N.; Wilkinson, G. *J. Chem. Soc. A* **1968**, 845–849.

109. Hughes, R. P.; Rose, P. R.; Rheingold, A. L. *Organometallics* **1993**, *12*, 3109–3117.

110. Murakami, M.; Itami, K.; Ito, Y. *J. Am. Chem. Soc.* **1996**, *118*, 11672–11673.

111. Bleeke, J. R.; Haile, T.; Chiang, M. Y. *Organometallics* **1991**, *10*, 19–21.

112. Bleeke, J. R.; Behm, R. *J. Am. Chem. Soc.* **1997**, *119*, 8503–8511.

113. Paneque, M.; Poveda, M. L.; Salazar, V.; Gutierrez-Puebla, E.; Monge, A. *Organometallics* **2000**, *19*, 3120–3126.

114. Paneque, M.; Poveda, M. L.; Rendón, N. *Eur. J. Inorg. Chem.* **2011**, *2011*, 19–33.

115. Barker, G. K.; Green, M.; Howard, J. A. K.; Spencer, J. L.; Stone, F. G. A. *J. Chem. Soc., Dalton Trans.* **1978**, 1839–1847.

116. Barrau, J.; Rima, G.; El Amraoui, T. *Organometallics* **1998**, *17*, 607–614.

117. Mashima, K.; Sugiyama, H.; Kanehisa, N.; Kai, Y.; Yasuda, H.; Nakamura, A. *J. Am. Chem. Soc.* **1994**, *116*, 6977–6978.

118. Zhao, L.; de Meijere, A. *Adv. Synth. Catal.* **2006**, *248*, 2484–2492.

119. Harrison, N. C.; Murray, M.; Spencer, J. L.; Stone, F. G. A. *J. Chem. Soc., Dalton Trans.* **1978**, 1337–1342.

120. Van Nes, G. J. H.; Vos, A. *Acta Crystallogr., Sect. B* **1979**, *35*, 2593–2601.

121. Howard, J. A. K.; Mitrprachachon, P.; Roy, A. *J. Organomet. Chem.* **1982**, *235*, 375–381.

122. Lentz, D.; Bach, A.; Buschmann, J.; Luger, P.; Messerschmidt, M. *Chem. Eur. J.* **2004**, *10*, 5059–5066.

123. Allan, K. M. Unpublished work.

124. Mmongoyo, J. A.; Mgani, Q. A.; Mdachi, S. J. M.; Pogorzelec, P. J.; Cole-Hamilton, D. J. *Eur. J. Lipid Sci. Technol.* **2012**, *114*, 1183–1192.

125. Núñez Magro, A. A.; Eastham, G. R.; Cole-Hamilton, D. J. *Dalton Trans.* **2009**, 4683.

126. Rucklidge, A. J.; Morris, G. E.; Slawin, A. M.; Cole-Hamilton, D. J. *Helv. Chim. Acta* **2006**, *89*, 1783–1800.

127. Tooze, R. P.; Eastham, G. R.; Whiston, K.; Wang, X. L. *Process for the Carbonylation of Ethylene and Catalyst System for Use Therein*, Patent Application, 1996, WO 1996/019434 A1.

128. Eastham, G. R.; Tooze, R. P.; Heaton, B. T.; Iggo, J. A.; Whyman, R.; Zacchini, S. *Chem. Commun.* **2000**, 609–610.

129. Wiester, M. J.; Braunschweig, A. B.; Yoo, H.; Mirkin, C. A. *Inorg. Chem.* **2010**, *49*, 7188–7196.

130. Oliveri, C. G.; Gianneschi, N. C.; Nguyen, S. T.; Mirkin, C. A.; Stern, C. L.; Wawrzak, Z.; Pink, M. *J. Am. Chem. Soc.* **2006**, *128*, 16286–16296.

131. Rosen, M. S.; Spokoyny, A. M.; Machan, C. W.; Stern, C.; Sarjeant, A.; Mirkin, C. A. *Inorg. Chem.* **2011**, *50*, 1411–1419.

132. Spokoyny, A. M.; Machan, C. W.; Clingerman, D. J.; Rosen, M. S.; Wiester, M. J.; Kennedy, R. D.; Stern, C. L.; Sarjeant, A. A.; Mirkin, C. A. *Nature Chem.* **2011**, *3*, 590–596.

133. Carr, N.; Dunne, B. J.; Orpen, A. G.; Spencer, J. L. *J. Chem. Soc., Chem. Commun.* **1988**, 926.

134. Phillips, R.; Puddephatt, R. *J. Organomet. Chem.* **1977**, *136*, C52–C54.

135. Phillips, R. L.; Puddephatt, R. J. *J. Chem. Soc., Dalton Trans.* **1978**, 1736–1739.

136. Noyori, R.; Takaya, H. *J. Chem. Soc. D* **1969**, 525–525.

137. Nüske, H.; Noltemeyer, M.; de Meijere, A. *Angew. Chem., Int. Ed.* **2001**, *40*, 3411–3413.

138. Yucel, B.; Arve, L.; de Meijere, A. *Tetrahedron* **2005**, *61*, 11355–11373.

139. Jones, N. L.; Ibers, J. A. *Organometallics* **1982**, *1*, 326–330.

140. Hahn, C. *Chem. Eur. J.* **2004**, *10*, 5888–5899.

141. Clark, H. C.; Kurosawa, H. *Inorg. Chem.* **1973**, *12*, 357–362.

142. Kurosawa, H.; Yoshida, G. *J. Organomet. Chem.* **1976**, *120*, 297–311.

143. Boag, N. M.; Green, M.; Spencer, J. L.; Stone, F. G. A. *J. Chem. Soc., Dalton Trans.* **1980**, 1200–1207.

144. Sano, M.; Nakamura, Y. *J. Chem. Soc., Dalton Trans.* **1991**, 417–424.

145. Carturan, G.; Belluco, U.; Del Pra, A.; Zanotti, G. *Inorg. Chim. Acta* **1979**, *33*, 155–160.

146. Koppel, I. A.; Koppel, J.; Pihl, V.; Leito, I.; Mishima, M.; Vlasov, V. M.; Yagupolskii, L. M.; Taft, t. l. R. W. *J. Chem. Soc., Perkin Trans. 2* **2000**, 1125–1133.

147. Kütt, A.; Rodima, T.; Saame, J.; Raamat, E.; Mäemets, V.; Kaljurand, I.; Koppel, I. A.; Garlyauskayte, R. Y.; Yagupolskii, Y. L.; Yagupolskii, L. M.; Bernhardt, E.; Willner, H.; Leito, I. *J. Org. Chem.* **2011**, *76*, 391–395.

148. Tsutsumi, H.; Sunada, Y.; Shiota, Y.; Yoshizawa, K.; Nagashima, H. *Organometallics* **2009**, *28*, 1988–1991.

149. Cavallo, L.; Macchioni, A.; Zuccaccia, C.; Zuccaccia, D.; Orabona, I.; Ruffo, F. *Organometallics* **2004**, *23*, 2137–2145.

150. Cooper, D. G.; Powell, J. *Inorg. Chem.* **1976**, *15*, 1959–1968.

151. Chisholm, M. H.; Clark, H. C.; Manzer, L. E.; Stothers, J. B. *J. Am. Chem. Soc.* **1972**, *94*, 5087–5089.

152. Fanjul, T.; Eastham, G.; Haddow, M. F.; Hamilton, A.; Pringle, P. G.; Orpen, A. G.; Turner, T. P. W.; Waugh, M. *Catal. Sci. Tech.* **2012**, *2*, 937.

153. Fanjul, T.; Eastham, G.; Fey, N.; Hamilton, A.; Orpen, A. G.; Pringle, P. G.; Waugh, M. *Organometallics* **2010**, *29*, 2292–2305.

154. Becke, A. D. *J. Chem. Phys.* **1993**, *98*, 5648–5652.

155. Lee, C.; Yang, W.; Parr, R. G. *Phys. Rev. B* **1988**, *37*, 785–789.

156. Vosko, S. H.; Wilk, L.; Nusair, M. *Can. J. Phys.* **1980**, *58*, 1200–1211.

157. Stephens, P. J.; Devlin, F. J.; Chabalowski, C. F.; Frisch, M. J. *J. Phys. Chem.* **1994**, *98*, 11623–11627.

158. Weingend, F.; Ahlrichs, R. *Phys. Chem. Chem. Phys.* **2005**, *7*, 3297–3305.

159. Bryndza, H. E. *J. Chem. Soc., Chem. Commun.* **1985**, 1696.

160. Stockland, R. A.; Foley, S. R.; Jordan, R. F. *J. Am. Chem. Soc.* **2003**, *125*, 796–809.

161. Stockland, R.; Jordan, R. *J. Am. Chem. Soc.* **2000**, *122*, 6315–6316.

162. Foley, S. R.; Stockland, R. A.; Shen, H.; Jordan, R. F. *J. Am. Chem. Soc.* **2003**, *125*, 4350–4361.

163. Boone, H. W.; Athey, P. S.; Mullins, M. J.; Philipp, D.; Muller, R.; Goddard, W. A. *J. Am. Chem. Soc.* **2002**, *124*, 8790–8791.

164. von Schenck, H.; Strömberg, S.; Zetterberg, K.; Ludwig, M.; Åkermark, B.; Svensson, M. *Organometallics* **2001**, *20*, 2813–2819.

165. Philipp, D. M.; Muller, R. P.; Goddard, W. A.; Storer, J.; McAdon, M.; Mullins, M. *J. Am. Chem. Soc.* **2002**, *124*, 10198–10210.

166. Zhao, H.; Ariafard, A.; Lin, Z. *Organometallics* **2006**, *25*, 812–819.

167. Friedrich, H. B.; Moss, J. R. *Adv. Organomet. Chem.* **1991**, *33*, 235–290.

168. Halpern, J.; Jewsbury, R. *J. Organomet. Chem.* **1979**, *181*, 223–232.

169. Fanizzi, F.; Maresca, L.; Pacifico, C.; Natile, G.; Lanfranchi, M.; Tiripicchio, A. *Eur. J. Inorg. Chem.* **1999**, *1999*, 1351–1358.

170. Deeming, A. J.; Shaw, B. L. *J. Chem. Soc. A* **1971**, 376.

171. Schmidt, E. K. G. *J. Organomet. Chem.* **1980**, *204*, 393–403.

172. Burns, R. J.; Bulkowski, P. B.; Stevens, S. C. V.; Baird, M. C. *J. Chem. Soc., Dalton Trans.* **1974**, 415.

173. Churchill, M. R.; Fennessey, J. P. *Inorg. Chem.* **1967**, *6*, 1213–1220.

174. Hensley, D. W.; Stewart, R. P., Jr *Inorg. Chem.* **1978**, *17*, 905–910.

175. Hughes, R. P.; Sweetser, J. T.; Tawa, M. D.; Williamson, A.; Incarvito, C. D.; Rhatigan, B.; Rheingold, A. L.; Rossi, G. *Organometallics* **2001**, *20*, 3800–3810.

176. Hughes, R. P.; Overby, J. S.; Williamson, A.; Lam, K.-C.; Concolino, T. E.; Rheingold, A. L. *Organometallics* **2000**, *19*, 5190–5201.

177. King, R. B.; Bond, A. *J. Am. Chem. Soc.* **1974**, *96*, 1334–1338.

178. Albrecht, M.; Gossage, R.; Lutz, M.; Spek, A.; van Koten G, *Chem. Eur. J.* **2000**, *6*, 1431–1445.

179. Roulet, R.; Barbey, C. *Helv. Chim. Acta* **1973**, *56*, 2179–2186.

180. Al-Najjar, I.; Green, M. *J. Chem. Soc., Chem. Commun.* **1977**, 212–213.

181. Al-Najjar, I. M. *Inorg. Chim. Acta* **1987**, *128*, 93–104.

182. Anderson, G. K.; Davies, J. A.; Schoeck, D. J. *Inorg. Chim. Acta* **1983**, *76*, L251–L252.

183. Anderson, B. G.; Hoyte, S. A.; Spencer, J. L. In press.

184. Darensbourg, D. J.; Decuir, T. J.; Stafford, N. W.; Robertson, J. B.; Draper, J. D.; Reibenspies, J. H.; Kathó, A.; Joó, F. *Inorg. Chem.* **1997**, *36*, 4218–4226.

185. Meij, A. M. M.; Otto, S.; Roodt, A. *Inorg. Chim. Acta* **2005**, *358*, 1005–1011.

186. Rigamonti, L.; Rusconi, M.; Manassero, C.; Manassero, M.; Pasini, A. *Inorg. Chim. Acta* **2010**, *363*, 3498–3505.

187. Boag, N. M.; Green, M.; Grove, D. M.; Howard, J. A. K.; Spencer, J. L.; Stone, F. G. A. *J. Chem. Soc., Dalton Trans.* **1980**, 2170.

188. Slack, D. A.; Baird, M. C. *Inorg. Chim. Acta* **1977**, *24*, 277–280.

189. Kauffman, G. B. *Inorg. Synth.* **1963**, *7*, 249–253.

190. Price, J.; Williamson, A.; Schramm, R.; Wayland, B. *Inorg. Chem.* **1971**, *11*, 1280–1284.

191. Fraccarollo, D.; Bertani, R.; Mozzon, M.; Belluco, U.; Michelin, R. A. *Inorg. Chim. Acta* **1992**, *201*, 15–22.

192. Vaughan, T. F.; Koedyk, D. J.; Spencer, J. L. *Organometallics* **2011**, *30*, 5170–5180.

193. Allan, K. M.; Spencer, J. L. *Tetrahedron Lett.* **2009**, *50*, 834–835.

194. Dolomanov, O. V.; Bourhis, L. J.; Gildea, R. J.; Howard, J. A. K.; Puschmann, H. J. *J. Appl. Crystallogr.* **2009**, *42*, 339–341.

195. Sheldrick, G. M. *Acta Crystallogr., Sect. A* **2008**, *64*, 112–122.

196. Frisch, M. J. et al. *Gaussian 09 Revision B.01*, Gaussian Inc. Wallingford CT, 2009.

197. Glendening, E. D.; Reed, A. E.; Carpenter, J. E.; Weinhold, F. *NBO Version 3.1, E. D.*